



# La neuroinflammation "invisible" dans les atteintes cérébrales aigue et chronique

Antoine Drieu

## ► To cite this version:

Antoine Drieu. La neuroinflammation "invisible" dans les atteintes cérébrales aigue et chronique. Médecine humaine et pathologie. Normandie Université, 2018. Français. NNT: 2018NORMC422 . tel-02148964v1

HAL Id: tel-02148964

<https://theses.hal.science/tel-02148964v1>

Submitted on 6 Jun 2019 (v1), last revised 6 Jun 2019 (v2)

**HAL** is a multi-disciplinary open access archive for the deposit and dissemination of scientific research documents, whether they are published or not. The documents may come from teaching and research institutions in France or abroad, or from public or private research centers.

L'archive ouverte pluridisciplinaire **HAL**, est destinée au dépôt et à la diffusion de documents scientifiques de niveau recherche, publiés ou non, émanant des établissements d'enseignement et de recherche français ou étrangers, des laboratoires publics ou privés.



Normandie Université

## THÈSE

**Pour obtenir le diplôme de doctorat**

**Spécialité ASPECTS MOLECULAIRES ET CELLULAIRES DE LA BIOLOGIE**

**Préparée au sein de l'Université de Caen Normandie**

### **La neuroinflammation "invisible" dans les atteintes cérébrales aigue et chronique**

**Présentée et soutenue par  
Antoine DRIEU**

**Thèse soutenue publiquement le 05/12/2018  
devant le jury composé de**

M. ADAM DENES	Directeur de recherche, Université de Budapest	Rapporteur du jury
Mme ANNA-MARIA PLANAS	Directeur de recherche, IIBB-CSIC Barcelone - Espagne	Rapporteur du jury
Mme CARINE ALI	Professeur des universités, UNIVERSITE CAEN NORMANDIE	Président du jury
Mme BRITTA ENGELHARDT	Directeur de recherche, Université de Berne Suisse	Membre du jury
M. BRUNO GONZALEZ	Directeur de recherche, UNIVERSITE ROUEN NORMANDIE	Membre du jury
Mme MARINA RUBIO GOMEZ	Ingénieur HDR, UNIVERSITE CAEN NORMANDIE	Directeur de thèse

**Thèse dirigée par MARINA RUBIO GOMEZ, Physiopathologie et imagerie des troubles neurologiques**



UNIVERSITÉ  
CAEN  
NORMANDIE

 497  
NBISE  
Normande de Biologie Intégrative,  
Santé, Environnement

 Inserm  
La science pour la santé  
From science to health

Un merci tout particulier à Florian et Hervé, les parrains (ou parents, sait-on jamais) de mes futurs enfants.

Un grand merci à Carine, tu as toujours été présente pour moi (et pour tous les autres d'ailleurs), on s'est bien marrés à Bordeaux, on s'est bien marrés tout court.

Un grand merci à Marina, qui a réussi à me supporter pendant autant de temps, j'ai adoré ma thèse en très grande partie grâce à toi. Tu m'as laissé donner mon avis, tu étais à l'écoute, et tu m'as toujours poussé à en faire plus. C'est grâce à toi que tout ce travail a été aussi abouti. Je te souhaite le meilleur pour la suite.

Merci à Tesla, ton gros bidou va me manquer quand je serai aux States.

Merci à toi, Barbara (tu notes, tu es après Tesla).

Et enfin, un grand merci à ma famille, sans vous je ne serai rien. Je vous dois tout, et j'ai une dette de temps de présence que je vais rembourser un jour, promis.

## Liste des abréviations

ACM : artère cérébrale moyenne

APC : cellule présentatrice d'antigène

APP : précurseur du peptide béta amyloïde

AQP4 : aquaporine 4

ATP : adénosine triphosphate

AVC : accident vasculaire cérébral

BAM : macrophages associés à la bordure des vaisseaux sanguins

BHE : barrière hémato-encéphalique

BSL : barrière sang-LCS

CAM : molécule d'adhésion cellulaire

CCI : impact cortical contrôlé

CD : cluster de différenciation

CPM : macrophage des plexus choroïdes

CSF : facteur stimulant la colonie

CSPG : protéoglycane chondroïtine-sulfate

DAI : dommage axonal diffus

DAMP : motifs moléculaires associés aux dégâts

DC : cellule dendritique

DSC : débit sanguin cérébral

DPA : *N,N*-diéthyl-2-[4-(2-fluoroéthoxy)phényl]-5,7-diméthylpyrazolo[1,5-*a*]pyrimidine-3-acétamide

EC : cellule endothéliale

FPI : blessure par percussion fluidique

GFAP : protéine acide fibrillaire gliale

HTA : hypertension artérielle

Iba1 : ionized calcium-binding adaptor molecule 1

ICAM-1 : molécule d'adhésion cellulaire intercellulaire-1

IFN : interféron

IL : interleukine

IL-1-RA : récepteur antagoniste à l'IL-1

iNOS : synthase de l'oxyde nitrique inducible

IRM : imagerie par résonance magnétique

LCS : liquide cérébrospinal

LPS : lipopolysaccharide

MAPK : protéine kinase activée par le mitogène

MCP-1 : protéine chimio-attractante des monocytes-1

MHC : complexe majeur d'histocompatibilité

MM : macrophage des méninges

MPIO : microparticule d'oxyde de fer

MPO : myélopéroxydase

mTBI : traumatisme crânien léger

MTBI : traumatisme crânien modéré

NADPH : nicotinamide adénine dinucléotide phosphate

NEP (1-40) : antagoniste des récepteurs Nogo (1-40)

NFL : ligue de football nationale

Nf-κB : facteur nucléaire κB

NLR : récepteur de type Nod

NMDA : récepteur N-méthyl-D-aspartate

NO : monoxyde d'azote

NSE : énolase spécifique des neurones

OMS : organisation mondiale de la santé

PAMP : motifs moléculaires associés aux pathogènes

PBBI : blessure par pénétration d'objets ballistiques

PBS : tampon phosphate salin

PECAM-1 : molécule d'adhésion cellulaire plaquettes endothélium-1

PRR : Récepteur de reconnaissance de motifs moléculaires

PVM : macrophage périvasculaire

S100 $\beta$  : protéine 100 bêta se liant au calcium

SNC : système nerveux central

STAT-3 : activateur de transcription et de transduction du signal-3

sTBI : traumatisme crânien sévère

TBI : traumatisme crânien

TEP : tomographie par émission de positons

TGF : facteur de croissance transformant

TLR : récepteur de type Toll

TNF : facteur de nécrose tumorale

tPA : activateur tissulaire du plasminogène

TSPO : protéine translocatrice

USPIO : nanoparticules d'oxyde de fer

VCAM-1 : molécule d'adhésion cellulaire vasculaire-1

YFP : protéine fluorescente dans le jaune



## Table des matières

INTRODUCTION .....	5
1. La réaction inflammatoire .....	7
I. Généralités .....	7
1. Historique .....	7
2. Définition.....	8
II. Les acteurs cellulaires de l'inflammation .....	8
1. Immunité innée .....	9
2. Immunité adaptative .....	10
3. Controverse : l'immunité entraînée .....	11
4. Cellules endothéliales.....	14
5. Cytokines et chimioamines.....	15
III. Inflammation aiguë et inflammation chronique .....	17
1. Inflammation aiguë .....	17
2. Inflammation chronique.....	18
Résumé.....	19
2. Cas de l'inflammation cérébrale.....	21
I. Barrière hématoencéphalique .....	21
1. Historique .....	21
2. Description .....	21
3. Dysfonctionnement de la BHE.....	24
II. Immunité résidente du SNC .....	25
1. Cellules microgliales .....	25
a. Historique .....	25
b. Description .....	27
c. Rôles .....	29
2. Macrophages périvasculaires .....	31
a. Historique .....	31
b. Description .....	32
c. Rôles .....	33
3. Autres cellules immunitaires résidentes du SNC.....	34
a. Macrophages des méninges et des plexus choroïdes .....	34

b.	Lymphocytes.....	35
c.	Cellules dendritiques .....	36
	Résumé.....	39
3.	L'inflammation dans le cadre de l'accident vasculaire cérébral ischémique .....	41
I.	Généralités sur l'accident vasculaire cérébral.....	41
1.	Historique .....	41
2.	Définition.....	41
II.	Traitements de l'AVC approuvés en clinique .....	42
1.	Traitements pharmacologique.....	42
2.	Traitements mécanique .....	43
III.	Physiopathologie de l'AVC.....	44
1.	Excitotoxicité .....	45
2.	Dépolarisations envahissantes .....	46
3.	Apoptose .....	46
4.	Réaction inflammatoire .....	46
a.	Réaction de l'immunité résidente .....	47
b.	Réaction endothéliale.....	50
c.	Recrutement des leucocytes .....	50
d.	Réparation tissulaire et cicatrice gliale.....	51
IV.	Les différents modèles expérimentaux d'AVC .....	52
1.	Modèle monofilament.....	52
2.	Modèle d'électrocoagulation .....	55
3.	Modèle de photothrombose .....	56
4.	Modèles thromboemboliques.....	57
	Résumé.....	59
5.	Existe-t-il une réponse inflammatoire chez les patients atteints d'AVC ? .....	61
6.	Vers de nouvelles thérapies pour l'AVC : traitements ciblant la réponse inflammatoire.....	63
a.	Traitements ciblant les effets de l'IL-1 .....	63
b.	Traitements ciblant les cellules microgliales.....	63
c.	Traitements ciblant les macrophages résidents.....	64
d.	Traitements ciblant l'activation endothéliale et l'infiltration des leucocytes.....	64
7.	Les facteurs de risque d'AVC .....	66
4.	Cas particulier de la consommation d'alcool .....	67

I.	Généralités .....	70
1.	Historique .....	70
2.	Quelques chiffres.....	70
II.	Consommation d'alcool et inflammation.....	71
1.	Inflammation systémique.....	71
2.	Inflammation cérébrale .....	73
III.	Y-a-t-il une seule origine aux pathologies causées par l'alcool ? .....	75
5.	L'inflammation dans le cadre des traumatismes crâniens.....	77
I.	Généralités .....	79
1.	Historique .....	79
2.	Epidémiologie .....	80
a.	Définition .....	80
b.	Quelques chiffres.....	81
c.	Facteurs de risque .....	82
II.	Physiopathologie .....	83
1.	Une physiopathologie proche de l'AVC ischémique .....	83
2.	Modèles expérimentaux.....	83
a.	Diversité.....	83
b.	Description .....	84
3.	Dommage axonal diffus.....	88
4.	Réaction inflammatoire .....	88
a.	Cellules résidentes.....	88
b.	Recrutement des leucocytes .....	97
III.	Essais cliniques .....	98
	Résumé .....	101
	OBJECTIVES.....	103
	RESULTATS.....	104
1.	Study 1: Spatio-temporal profile of inflammatory responses in a thromboembolic stroke model	
	105	
2.	Study 2: Review of the literature of anti-inflammatory treatments in stroke .....	135
3.	Study 3: Impact of chronic alcohol consumption on ischemic stroke.....	153
4.	Study 4: Perivascular macrophages mediate the aggravating effect of inflammatory priming on	
	ischemic stroke.....	199
5.	Study 5: How to detect invisible lesion induced by a single mTBI .....	227

DISCUSSION .....	257
I.    What is the role of the inflammatory response after stroke? .....	259
II.   Does leukocyte infiltration determine lesion volume? .....	259
III.  Inflammatory priming, a status to be taken into account.....	260
1.  Visualization methods .....	263
2.  New approaches.....	266
IV.  PVM as priming regulator?.....	267
1.  Role of PVM on leukocyte infiltration .....	268
2.  Prospects .....	269
a.  Scavenger role of PVM in brain pathologies .....	269
b.  Role of PVM on leukocyte infiltration in other brain pathologies .....	272
V.   General conclusion .....	274
Références bibliographiques .....	275
Annexes .....	303

# INTRODUCTION



# 1. La réaction inflammatoire

## I. Généralités

### 1. Historique

L'inflammation a été décrite dès l'époque égyptienne dans le papyrus d'Ebers autour du 16<sup>ème</sup> siècle avant JC. On y parle de glandes lymphatiques purulentes, de *carbuncle* (mieux connu sous le nom d'anthrax). Il y est également conseillé de laisser cicatriser les blessures pour les faire guérir. Il a y 2 000 ans Celsus décrit l'inflammation par 4 manifestations : *rubor* (rougeur), *calor* (chaleur), *tumor* (gonflement) et *dolor* (douleur). Ce n'est qu'en 1958 que Rudolf Virchow ajouta à ces 4 manifestations une cinquième : l'impotence fonctionnelle (Figure 1).

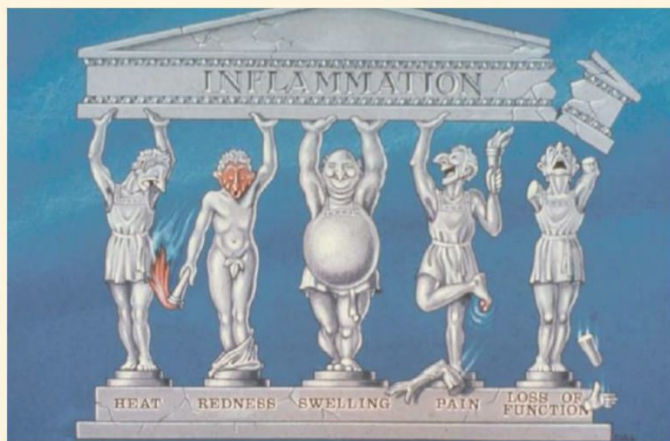


Figure 1 : les signes cardinaux de l'inflammation. De gauche à droite : heat (chaleur), redness (rougeur), swelling (gonflement), pain (douleur), loss of function (impotence fonctionnelle). D'après (Lawrence et al., 2002).

Virchow affirma que l'inflammation était la conséquence d'une consommation excessive de nourriture provenant du sang par les cellules, rendant la cellule hypertrophique ou dégénérée et formant ainsi une tumeur inflammatoire. Cette théorie est appelée la théorie « cellulaire ». Cette théorie était controversée par Julius Cohnheim (1839-1884) et ses confrères, qui pensaient que l'inflammation prenait place dans les vaisseaux sanguins : ce qu'il se passait à l'extérieur des vaisseaux était seulement un effet secondaire. C'est la théorie « vasculaire ». La théorie vasculaire de Cohnheim a été confirmée par Julius Arnold (1835-1915) avec la découverte du phénomène de diapédèse en 1875. De plus, en 1890, une autre équipe a mis en évidence que l'injection d'anticorps dans le sang protégeait du téton. En 1882, Elie Metchnikoff (1845-1916) a découvert le principe de la phagocytose. Il travaillait dans un laboratoire de biologie marine sur des larves d'étoiles de mer. En insérant une épine de rosier dans les larves (elles sont transparentes, dépourvues de système nerveux et de vaisseaux sanguins), il a observé des cellules se mobilisant autour de l'épine et ainsi découvert le principe de phagocytose (traduction grecque de « manger les cellules »), confirmant donc la théorie cellulaire de Virchow. Mais lors de ces travaux, Metchnikoff observa également le phénomène de diapédèse chez des espèces pourvues de vaisseaux sanguins, qu'il décrit dans son manuscrit « leçons sur la pathologie comparée de l'inflammation » en 1892. Les deux théories étaient donc complémentaires. Il est intéressant de noter que la théorie « cellulaire », d'origine française, était opposée à la théorie « vasculaire » d'origine allemande, et ce durant les années 1870, en pleine guerre franco-allemande.

A la suite de ces découvertes, Sir Henry Dale (1875-1968) ouvrit un nouveau champ d'investigations en découvrant que des phénomènes biologiques pouvaient être régulés par la formation, synthèse ou libération de médiateurs

moléculaires. C'est d'ailleurs à Henry Dale que l'on doit la découverte de l'acétylcholine, décrite un peu plus tard comme neurotransmetteur par Otto Loewi (1873-1961) en 1921. Suite à cela, beaucoup de travaux ont permis la découverte de nombreuses molécules assimilées à la réaction inflammatoire comme la bradykinine, les prostaglandines...

## 2. Définition

Une définition concise de l'inflammation est difficile à donner. Par exemple, voici une définition de l'inflammation par Rocha e Silva (1978) : « phénomène multi-médié où tous les médiateurs vont et viennent à un moment approprié pour jouer leurs rôles en augmentant la perméabilité vasculaire, attirant les leucocytes, produisant une douleur, un œdème local et une nécrose, dans laquelle la prédominance de l'un d'entre eux serait fortuite ou dépendant de ses capacités spécifiques à produire des symptômes, directement ou indirectement, soit en potentialisant la réaction soit en libérant d'autres agents » (Rocha e Silva, 1978). Plus brièvement, l'inflammation est une réaction du système immunitaire suite à une agression externe ou interne. Elle a trois principales fonctions : i) éliminer la cause de l'agression, ii) nettoyer le tissu endommagé et iii) initier la réparation tissulaire. Elle fait intervenir plusieurs acteurs, allant des cellules immunitaires résidentes (macrophages, cellules dendritiques...), aux cellules immunitaires de la circulation sanguine (neutrophiles, lymphocytes, monocytes...) ainsi qu'à des médiateurs chimiques comme les cytokines, les chimiokines et le système du complément.

## II. Les acteurs cellulaires de l'inflammation

Globalement, les cellules immunitaires peuvent être catégorisées en deux groupes. L'immunité innée fait intervenir des cellules comme les macrophages et les neutrophiles, qui ont une réponse non spécifique face au pathogène, à savoir le relargage de cytokines/chimiokines, et la phagocytose des débris. Le deuxième groupe, *a contrario* du premier, est l'immunité adaptative : leur réponse, *stricto sensu*, est globalement de détecter la nature exacte de l'antigène, puis de produire des anticorps spécifiques ciblant cet antigène. Cette réaction permet l'amplification de la réaction inflammatoire.

## 1. Immunité innée

L'immunité innée est une réponse très rapide. Elle permet de contenir l'agression en phagocytant les débris ou l'agent pathogène. De plus, les cellules de l'immunité innée vont produire des médiateurs de l'inflammation comme des cytokines/chimiokines, afin d'amplifier la réaction et de recruter plus de leucocytes provenant de la circulation sanguine.

Les premières cellules impliquées dans l'immunité innée sont les cellules résidentes, vu qu'elles sont les plus proches du lieu de l'agression. Les macrophages vont venir phagocytter l'agent pathogène, ou les débris cellulaires, afin de ralentir la progression de l'infection ou de la blessure (Murray et al., 2014; Xue et al., 2014). Les mastocytes, eux, vont produire de grandes quantités de médiateurs chimiques, dont le plus connu est l'histamine responsable des réactions allergiques. L'histamine va entraîner une vasodilatation et une augmentation de la perméabilité des vaisseaux sanguins à proximité (Wernersson and Pejler, 2014). Ceci va permettre le recrutement des leucocytes circulants, qui vont pouvoir s'accrocher à la paroi des vaisseaux, puis migrer vers le tissu lésé par diapédèse (Figure 2). En plus de ces deux types cellulaires, les cellules dendritiques (DC), ou présentatrices d'antigène, surveillent constamment le tissu. En cas de dommage, elles phagocytent l'agent pathogène puis sont capables de présenter l'antigène aux lymphocytes (D'Agostino et al., 2012).

Le processus de diapédèse est complexe (Vestweber, 2015). Tout d'abord, les cellules endothéliales (EC pour *endothelial cells*) formant la paroi des vaisseaux sanguins vont s'activer grâce aux signaux envoyés par l'immunité résidente. Une fois activées, les EC vont exprimer à leur surface des molécules d'adhésion (ou CAMs pour *cell adhesion molecules*) comme les sélectines (E et P), VCAM-1 (pour *vascular cell adhesion molecule-1*), ICAM-1 (pour *intercellular adhesion molecule-1*) et PECAM-1 (pour *platelet endothelial cell adhesion molecule-1*). Les sélectines permettent le roulement (de l'anglais *rolling*), VCAM-1 et ICAM-1 l'adhésion, et enfin PECAM-1 le passage des leucocytes dans le tissu lésé/infecté (Figure 2).

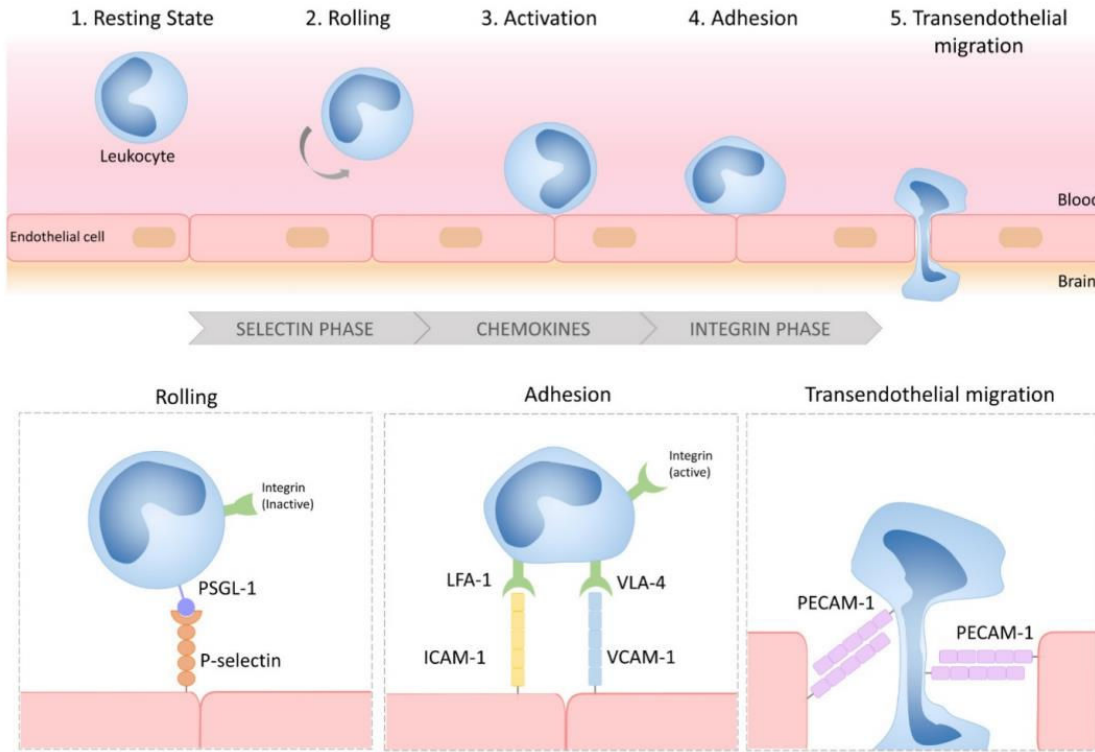


Figure 2 : Diapédèse leucocytaire. Suite à leur roulement, les leucocytes adhèrent à la paroi des vaisseaux sanguins puis migrent dans le tissu lésé/infecté par transmigration (entre les cellules endothéliales). D'après (Gauberti et al., 2018).

Les cellules immunitaires de la circulation sanguine sont principalement des lymphocytes (entre 50 et 80%), puis des neutrophiles (15-40%) et des monocytes (1-15%). Une fois infiltrés, les neutrophiles vont sécréter le contenu de leurs granulations, très riches en facteurs inflammatoires comme des cytokines/chimiokines, ainsi que des facteurs du complément (Lacy, 2006). Les monocytes infiltrés vont, quant à eux, se différencier en macrophages et ainsi participer au nettoyage des débris/agents infectieux. Enfin, les lymphocytes vont reconnaître l'antigène, et sécréter des anticorps ciblant cet antigène : c'est l'immunité adaptative qui débute.

## 2. Immunité adaptative

L'immunité adaptative intervient un peu plus tardivement dans la réaction inflammatoire, et n'est nécessaire que si l'immunité innée n'est pas suffisante pour combattre l'agression. Pour intervenir, l'immunité innée doit d'abord passer l'endothélium (voir ci-dessus), puis aller reconnaître l'antigène. Pour cela, des cellules spécialisées dans la présentation d'antigène (ou DC

pour *dendritic cells*) sont d'ores et déjà sur le lieu de l'agression (D'Agostino et al., 2012). Elles ont au préalable phagocyté l'agent pathogène, et présenté à leur surface une petite partie de l'agent, un antigène. Les lymphocytes vont se rapprocher des DC puis reconnaître spécifiquement cet antigène. Ici, deux cas de figure se présentent : soit l'agent pathogène est intracellulaire, soit extracellulaire. Dans le premier cas, les antigènes sont situés sur la paroi de la cellule infectée : les lymphocytes T vont alors reconnaître cet antigène et vont détruire la cellule infectée. Dans le cadre d'un pathogène extracellulaire, ce sont les lymphocytes B qui agissent : une fois l'antigène reconnu, les lymphocytes B vont se multiplier, se transformer en plasmocytes et produire une grande quantité d'anticorps, qui viennent se fixer sur l'antigène *via* leur domaine hypervariable. Les anticorps vont alors pouvoir activer le complément, et se fixer aux cellules phagocytaires par leur domaine constant. Dans les deux cas, après reconnaissance de l'antigène, les lymphocytes, en se multipliant (par mitose), vont soit orchestrer la réaction inflammatoire, soit être stockés sous forme de lymphocytes « mémoire ». En effet, dans le corps, on compte autant de lymphocytes différents que d'antigènes ; autrement dit, chaque lymphocyte est spécialisé d'un antigène, d'où le concept de mémoire de l'immunité (Romani, 2004).

Les lymphocytes ne sont pas les seules cellules immunitaires concernées par l'immunité adaptative. En effet, des souris déficientes en lymphocytes (B et T) ont tout de même montré une hypersensibilité à l'exposition à un pathogène pendant au moins quatre semaines (O'Leary et al., 2006). Il a été montré dans cette étude que les cellules *natural killers* pouvaient, à elles seules, déclencher cette hypersensibilité. Pour étayer leur propos, les auteurs ont montré que l'injection de *natural killers* chez des souris déficientes en lymphocytes et en *natural killers* permettait de retrouver cette hypersensibilité (O'Leary et al., 2006).

### 3. Controverse : l'immunité entraînée

Il est intéressant de noter que contrairement à l'immunité adaptative, l'immunité innée était considérée jusque là comme aspécifique, c'est-à-dire qu'elle va répondre de la même manière contre n'importe quelle agression. En d'autres termes, il n'existe pas de mémoire de l'immunité innée.

En vérité, cette notion est à revoir. En effet, de récentes études parlent désormais de mémoire de l'immunité innée ou d'immunité entraînée (Netea et al., 2016) (Figure 3).

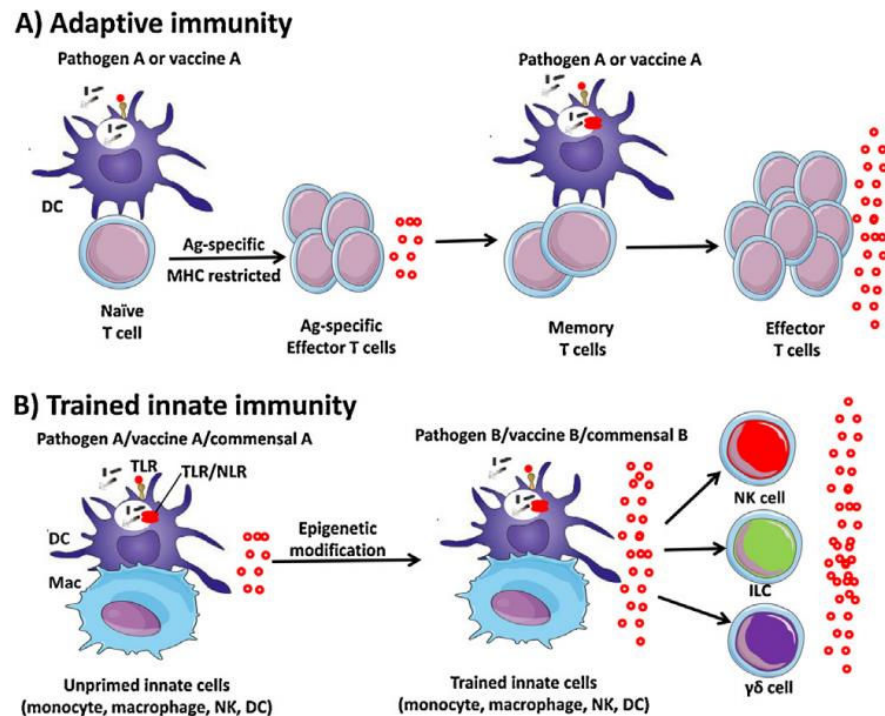


*Figure 3 : Concept de « l'immunité entraînée » ou mémoire de l'immunité innée. (A) L'immunité adaptative. Les lymphocytes reconnaissent l'antigène présenté par la cellule dendritique (DC), puis se multiplient en lymphocytes effecteurs spécifiques de l'antigène détecté. (B) L'immunité innée entraînée (ou trained immunity). Les DC présentent l'antigène aux cellules myéloïdes (monocytes, macrophages, Natural Killers) et entraînent des modifications épigénétiques de ces cellules. Suite à une deuxième exposition, ou à une exposition à un autre pathogène, les cellules myéloïdes ont une réponse conditionnée à la première exposition, rendant la réaction plus effective. D'après (Gardiner and Mills, 2016).*

Cette théorie a vu le jour grâce à des expériences sur des plantes et des invertébrés, qui sont tous deux des organismes déficients en immunité adaptative. Toutefois, ces organismes développent une résistance suite à une deuxième infection du même agent pathogène (Durrant and Dong, 2004). Suite à cela, des expériences ont été réalisées chez des souris infectées par le champignon *Candida albicans* (Quintin et al., 2012). Suite à une première infection en faible dose par *C. albicans*, les animaux ont subi sept jours plus tard une deuxième infection à dose létale : les animaux ayant été infectés la première fois ont survécu. Pour s'affranchir de l'effet de l'immunité

adaptative sur la survie des souris, les auteurs ont réalisé la même expérience chez des souris transgéniques déficiences en lymphocytes ( $Rag1^{-/-}$ ) : les souris ont également survécu, sans différence significative avec le groupe possédant des lymphocytes (Quintin et al., 2012).

Les monocytes/macrophages peuvent également être entraînés. Cette découverte a été associée à la découverte de récepteurs présents à la surface des monocytes/macrophages : les récepteurs de reconnaissance de motifs moléculaires (ou PRR pour *pattern recognition receptors*). Les PRR permettent la reconnaissance de motifs moléculaires associés aux pathogènes (ou PAMP pour *pathogen-associated molecular pattern*) et de motifs moléculaires associés aux dégâts (ou DAMP pour *danger-associated molecular pattern*) (Kawai and Akira, 2010). Il existe plusieurs PRR, dont les récepteurs de type Nod (ou NLR pour *nod-like receptors*) et les récepteurs de type Toll (TLR). La fixation de l'agent pathogène au PRR entraîne une cascade d'événements intracellulaires menant à une translocation de Nf- $\kappa$ B (pour *nuclear factor-  $\kappa$ B*) du cytosol vers le noyau cellulaire. Nf- $\kappa$ B est un facteur de transcription permettant la production de cytokines pro-inflammatoires comme les interleukines (IL) IL-1 $\beta$ , IL-6 ou le facteur de nécrose tumorale (ou TNF pour *tumor necrosis factor*) par les monocytes/macrophages et par les DC, aboutissant au recrutement des leucocytes périphériques (provenant de la circulation sanguine) (Lawrence, 2016).

Il s'avère que contrairement aux lymphocytes, qui se divisent et conservent leur spécificité antigénique, les monocytes/macrophages et DC ne conservent pas ce pouvoir ; ils peuvent toutefois subir des modifications épigénétiques leur conférant une réaction modifiée suite à un deuxième contact avec un agent pathogène (Saeed et al., 2014). Ces cellules peuvent alors réagir selon trois modes différents : elles peuvent i) devenir tolérantes, comme c'est le cas lors de l'exposition prolongées à de faibles doses d'endotoxine (Shi et al., 2011) ; elles peuvent également ii) être hyper-réactives (Dobrovolskaia and Vogel, 2002) ; elles peuvent enfin iii) être immunsuppressives, en adoptant un phénotype anti-inflammatoire (Hotchkiss et al., 2013) (Figure 4).

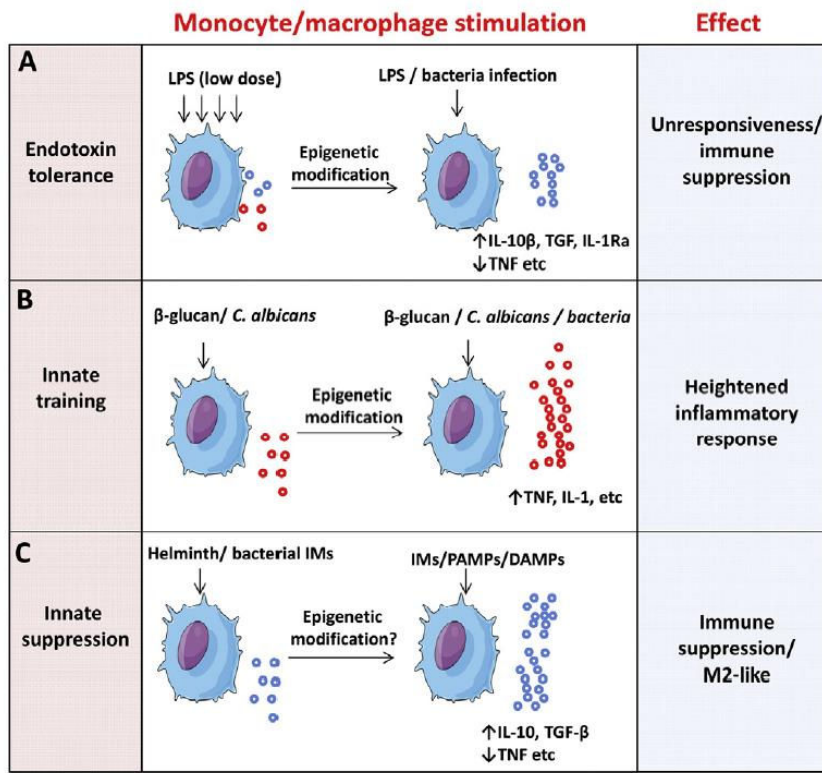


Figure 4 : Différentes stimulations induisant différents types de mémoire de l'immunité innée. (A) Suite à une exposition prolongée à de faibles doses de LPS, les monocytes/macrophages ne répondent plus à une stimulation ultérieure. (B) Une exposition à un pathogène entraîne une réponse exacerbée à une deuxième stimulation au même pathogène. (C) Une exposition à un pathogène entraîne une immunosuppression des monocytes/macrophages à la suite d'une stimulation par d'autres agents. D'après (Gardiner and Mills, 2016).

#### 4. Cellules endothéliales

Les EC forment la barrière qui sépare le compartiment sanguin des tissus. En condition physiologique, elles permettent le passage d'oxygène et de nutriments. Suite à un dommage vasculaire, les EC vont s'activer et produire une grande quantité de CAM permettant ainsi le recrutement de leucocytes sur le lieu de l'agression et donc le bon déroulement de la réaction inflammatoire (Figure 2) :

- Les sélectines (E et P) sont produites constitutionnellement par les EC. Elles sont stockées dans des vésicules : les corps de Weibel Palade. Une fois les EC activées, ces vésicules vont être adressées à la surface, permettant ainsi le roulement des leucocytes contre la paroi des EC. Ainsi, des souris déficientes en P-sélectine ont moins

- d'infiltration de cellules immunitaires (notamment de neutrophiles) dans un modèle de péritonite (Yang et al., 2000).
- VCAM-1 (ou CD106 pour *cluster of differentiation 106*) et ICAM-1 (ou CD54 pour *cluster of differentiation 54*) sont des CAM qui ne sont pas exprimées constitutivement, contrairement aux sélectines. Les EC expriment VCAM-1 et ICAM-1 suite à une exposition à des cytokines/chimiokines comme le TNF ou l'IL-1 $\beta$ . Ces CAM sont responsables de l'adhésion des leucocytes à la paroi des vaisseaux. Il a d'ailleurs été montré qu'il y avait moins de leucocytes adhérents chez des souris déficientes en ICAM-1 (Simon et al., 2014). Il faut noter qu'ICAM-1 n'est pas seulement exprimée par les EC, mais aussi par des neutrophiles et par certains macrophages comme les cellules de Kupffer (les macrophages résidents du foie) (Essani et al., 1995) et par les cellules microgliales (macrophages résidents du cerveau) (Hailer et al., 1997).
  - PECAM-1 est, quant à elle, impliquée dans la transmigration des leucocytes du compartiment sanguin vers le tissu agressé. Une étude a montré que chez des souris déficientes en PECAM-1 il n'y avait pas de différence dans le nombre de leucocytes adhérents à la paroi des vaisseaux sanguins suite à une stimulation par injection de cytokines pro-inflammatoires telles qu'IL-1 $\beta$  et TNF. Toutefois, dans cette même étude il a été montré que le nombre de leucocytes qui transmigraient était significativement moins important après injection d'IL-1 $\beta$  (Thompson et al., 2001). Il faut noter que PECAM-1 est également exprimée par les leucocytes (monocytes/macrophages, *natural killers*, lymphocytes, neutrophiles) ainsi que par les plaquettes (Marelli-Berg et al., 2013).

## 5. Cytokines et chimiokines

Le recrutement des cellules immunitaires provenant de la circulation vers le tissu endommagé/infecté s'établit par contacts chimiques émanant des cellules immunitaires résidentes. En effet, les macrophages résidents, ainsi que les cellules dendritiques vont émettre des médiateurs de l'inflammation, appelées cytokines et chimiokines, qui vont passer dans la

circulation sanguine et ainsi alerter les leucocytes circulants d'une agression locale. De plus, ces cytokines/chimiokines vont activer les EC, qui vont produire des CAM nécessaires à la diapédèse des leucocytes dans le compartiment tissulaire.

Les cytokines (du grec *cyto kinos*, littéralement : cellule en mouvement) sont des petites molécules produites par les cellules immunitaires pour amplifier la réaction inflammatoire ; elles permettent de favoriser le recrutement des cellules immunitaires provenant de la circulation sanguine (Turner et al., 2014). Cette famille de protéines regroupe les IL, l'interféron (IFN), le TNF, le facteur de croissance transformant (TGF pour *transforming growth factor*) et d'autres facteurs stimulants comme le CSF-1 (ou M-CSF pour *macrophage colony stimulating factor*) ou le CSF-2 (ou GM-CSF pour *granulocyte/macrophage colony stimulating factor*). Ces molécules permettent le contrôle régulé de la réaction inflammatoire : certaines sont pro-inflammatoires comme l'IL-1 $\beta$ , l'IL-6 ou le TNF ; d'autres sont anti-inflammatoires comme l'IL-10 ou le TGF- $\beta$ .

Les chimiokines sont en fait une sous-famille de cytokines. Elles sont spécialisées dans l'attraction chimique des cellules immunitaires : on appelle ce phénomène le chimiotactisme (Proost et al., 1996; Sokol and Luster, 2015). De plus, elles peuvent modifier l'état d'activation des cellules immunitaires. Elles sont constituées de quatre résidus cystéines, et sont classées en quatre catégories selon l'arrangement de leurs deux cystéines en position N-terminale. On peut citer par exemple CX3CL1 (les C correspondent aux cystéines), ou fractalkine, qui est exprimée en condition physiologique par les neurones. On peut également citer CCL2, principalement retrouvée dans la littérature sous le nom de MCP-1 (pour *monocyte chemoattractant protein-1*), dont le récepteur CCR2 est exprimé par les monocytes/macrophages, ainsi que par les lymphocytes et les basophiles (Griffith et al., 2014).

### III. Inflammation aiguë et inflammation chronique

Il est important de noter que les réactions inflammatoires peuvent être séparées en deux grandes catégories : l'inflammation aiguë, comme par exemple une griffure ; et l'inflammation chronique comme les maladies auto-immunes (par exemple, la maladie de Crohn), la cirrhose hépatique ou la tuberculose. Dans les deux cas, les acteurs de l'inflammation interviennent, mais il est avéré que la réaction inflammatoire diffère entre les deux catégories.

#### 1. Inflammation aiguë

Trois phases vont s'enchaîner lors d'une inflammation aiguë :

- La phase d'initiation : les cellules résidentes vont s'activer (les macrophages, les mastocytes et les DC), phagocytter le pathogène ou des débris puis libérer des cytokines/chimiokines pro-inflammatoires dans la circulation sanguine environnante.
- S'en suit la phase d'amplification de la réaction inflammatoire avec l'activation des EC et le recrutement des cellules immunitaires provenant de la circulation sanguine. Les cellules majoritairement recrutées ici sont des neutrophiles, qui vont venir sécréter leurs granulations, constituées de facteurs inflammatoires comme des cytokines/chimiokines, des facteurs du complément (Lacy, 2006; Ricklin et al., 2018). Ceci permettra d'amplifier la réaction, notamment le recrutement des macrophages nécessaires à l'étape suivante de réparation tissulaire.
- Enfin, la dernière phase consiste en la résolution de l'inflammation et la réparation du tissu endommagé, notamment par l'action des macrophages. Les fibroblastes vont fabriquer du tissu, tandis que les EC, avec l'aide des macrophages, vont participer à la formation de nouveaux vaisseaux sanguins (angiogenèse).

Si cette réaction inflammatoire (innée) n'est pas suffisante, les DC vont migrer dans les ganglions lymphatiques voisins et présenter l'antigène aux lymphocytes : c'est l'intervention de l'immunité adaptative.

## 2. Inflammation chronique

Si la cause de la réaction inflammatoire aiguë persiste, l'inflammation devient chronique. Les cellules deviennent hyperactives, des cytokines/chimiokines sont régulièrement sécrétées, et des phases de dégradation/réparation tissulaires s'effectuent continuellement. De plus, contrairement à une inflammation aiguë normale, des lymphocytes peuvent être impliqués, ceci formant une réponse adaptative exacerbée.

L'inflammation chronique peut prendre place lors de maladies chroniques comme les maladies neurodégénératives, les maladies auto-immunes, les maladies auto-inflammatoires. Généralement, ces maladies sont progressives, avec peu de signes d'inflammation apparents (absence des signes cardinaux), qui peuvent durer dans le temps et qui font intervenir l'immunité adaptative (lymphocytes).

## Résumé

**La réaction inflammatoire est un phénomène complexe, pouvant être aigu ou bien chronique, et faisant intervenir un nombre très important d'acteurs cellulaires et moléculaires. Ces réactions doivent être finement orchestrées afin de combattre l'agression tissulaire. Sinon, la réaction dégénère et peut entraîner une réaction inflammatoire exacerbée.** Il est intéressant de noter que la réaction inflammatoire, et notamment le recrutement de leucocytes provenant de la circulation sanguine, connaît une exception. Plus précisément, un organe du corps humain est particulièrement protégé/isolé du reste du corps par différentes barrières : le cerveau.



## 2. Cas de l'inflammation cérébrale

### I. Barrière hématoencéphalique

#### 1. Historique

Paul Ehrlich (1854-1915), en injectant du bleu de trypan dans la circulation sanguine, avait remarqué qu'il retrouvait ce colorant dans tous les organes sauf dans le cerveau. Pour appuyer cette idée, son étudiant Edwin Goldmann (1862-1913) avait injecté du bleu de trypan mais dans le liquide cérébrospinal (LCS) chez le chien (Saunders et al., 2014). Cette fois, le cerveau était coloré, mais pas le reste du corps. Ces expériences ont démontré que le cerveau possèdait une barrière qui le séparait du reste du corps : la barrière hémato-encéphalique (BHE) (Liddelow, 2011) (Figure 5).

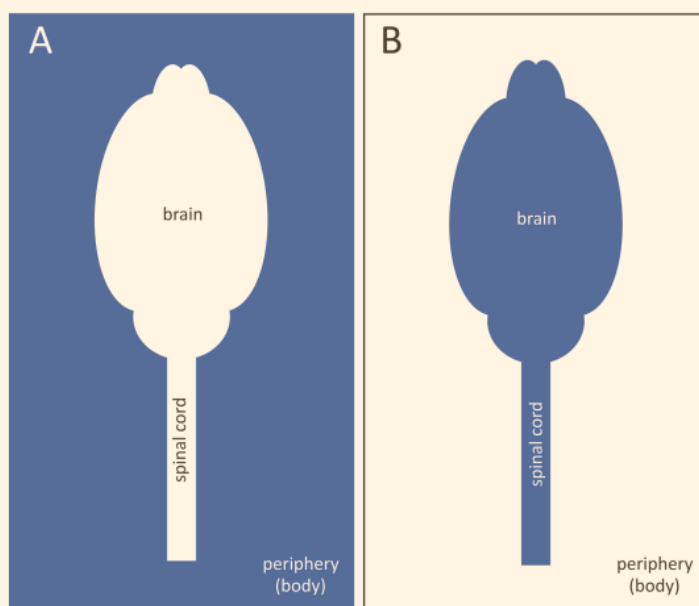


Figure 5 : Démonstration de l'existence de la barrière hémato-encéphalique par Ehrlich et Goldmann. (A) Une injection dans la circulation sanguine du bleu trypan résulte en la coloration du corps entier excepté le SNC. (B) Une injection dans le LCS résulte en la coloration du SNC et non du reste du corps.

Dès lors, beaucoup de scientifiques se sont intéressés à l'existence de cette BHE. Désormais, nous savons qu'il existe non pas une mais plusieurs barrières au niveau du SNC, différenciées par leur localisation, leur composition et par les compartiments qui la forment (Liddelow, 2011).

#### 2. Description

La barrière hémato-encéphalique (BHE), à proprement parlée, est localisée au niveau des vaisseaux sanguins cérébraux et sépare le tissu de la circulation sanguine. Elle est constituée d'EC

formant la lame basale, des pieds astrocytaires formant la lame basale gliale ou *glia limitans*. De plus, un espace est situé entre les deux lames basales : l'espace périvasculaire, contenant du liquide cérébrospinal (LCS). La particularité des capillaires formant la BHE est qu'ils ne sont pas fenêtrés : les EC sont reliées entre-elles par des jonctions serrées, rendant alors les capillaires imperméables.

La barrière sang-LCS sépare (BSL), comme son nom l'indique, le LCS des vaisseaux sanguins. Elle est située au niveau des plexus choroïdes, situés dans les ventricules cérébraux. Contrairement à la BHE, les capillaires qui forment la BSL sont dits fenêtrés, ce qui permet le passage de solutés du sang vers le LCS.

La barrière LCS-encéphalique se situe sur la paroi des ventricules cérébraux ainsi qu'au niveau de l'espace sous-arachnoïdien. La barrière au niveau de la paroi des ventricules n'est présente qu'au cours du développement embryonnaire : les jonctions serrées (*jonctions strap*) entre les cellules ependymaires disparaissent. Les jonctions serrées au niveau de la membrane arachnoïdienne permettent la formation de la barrière. Les vaisseaux sanguins de l'espace sous-arachnoïdien sont également fenêtrés (Liddelow, 2011) (Figure 6).

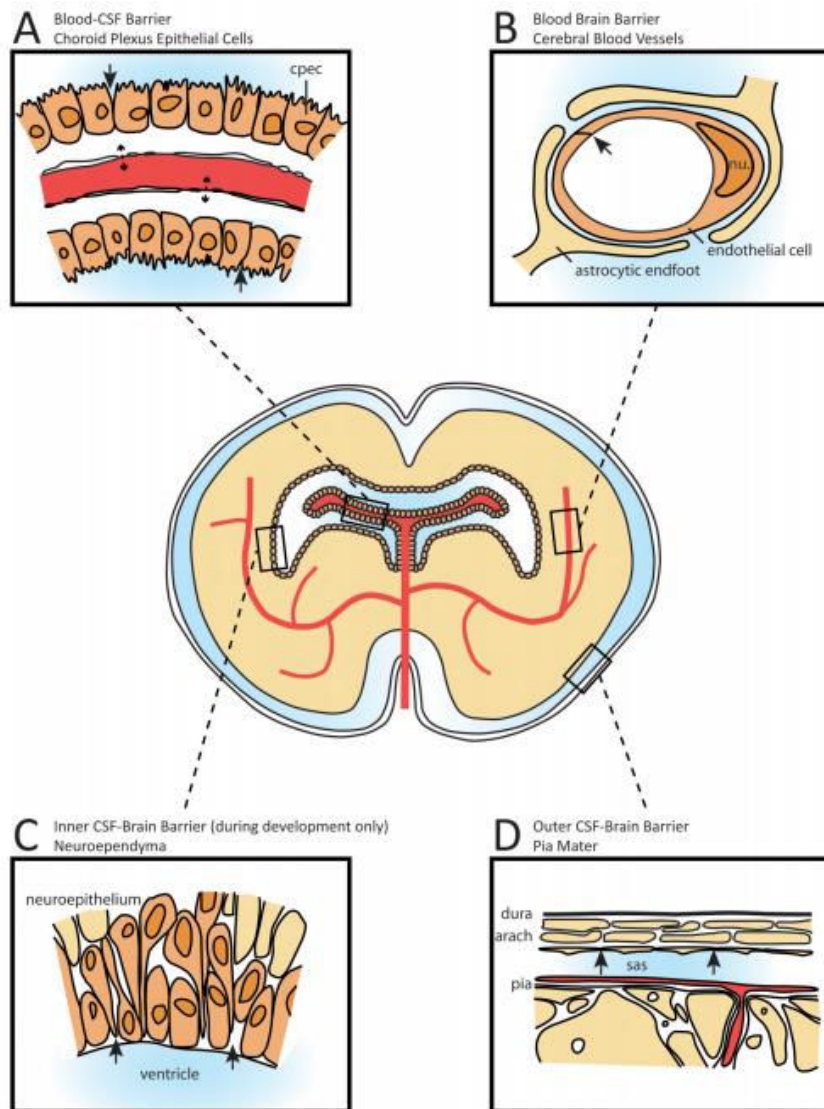
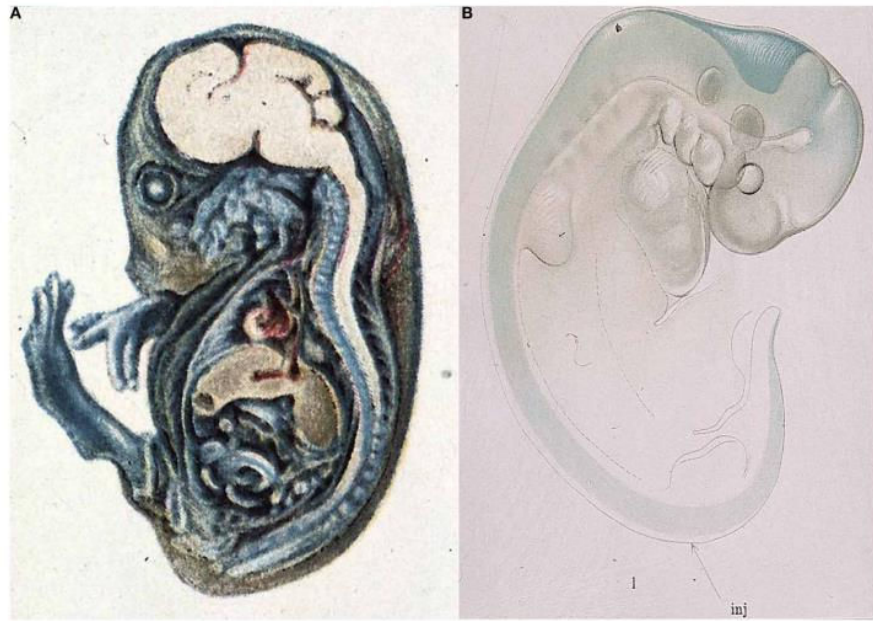


Figure 6 : Les différentes barrières du SNC. (A) Barrière sang-LCS (Blood-CSF barrier). (B) BHE (Blood-Brain barrier) à proprement parlée. (C) Barrière LCS-encéphalique (CSF-Brain barrier) au niveau des cellules épendymaires bordant les ventricules cérébraux. Il faut noter que cette barrière n'a d'existence que durant le développement embryonnaire. (D) Barrière LCS-encéphalique (CSF-Brain barrier) au niveau de l'espace sous-arachnoïdien. D'après (Liddelow, 2011).

Ces barrières sont fonctionnelles dès le développement du SNC. En effet, Georges Wislocki (1892-1956) a procédé à une injection de bleu de trypan dans la circulation sanguine chez l'embryon de cobaye (*guinea pig*) et a montré que le colorant ne passait pas dans le SNC. De plus, LH Weed a procédé à une injection de bleu de Prusse dans le canal de la moelle épinière chez l'embryon de cochon : le colorant restait cloitré dans le SNC (Saunders et al., 2014) (Figure 7).



*Figure 7 : La BHE est d'ores et déjà fonctionnelle chez l'embryon. (A) Une injection de bleu de trypan dans la circulation sanguine ne passe pas dans le SNC. (B) Une injection dans le canal de la moelle épinière (flèche marquée « inj ») ne passe pas dans la circulation sanguine et reste dans le SNC. D'après (Saunders et al., 2014).*

### 3. Dysfonctionnement de la BHE

Il est de plus en plus établi que les maladies neurodégénératives sont associées à des troubles vasculaires. Ces troubles vasculaires sont décrits dans la maladie d'Alzheimer (Sweeney et al., 2015), la sclérose latérale amyotrophique (Winkler et al., 2013), la maladie de Parkinson (Korcyn, 2015) ou encore la maladie de Huntington (Drouin-Ouellet et al., 2015). D'ailleurs il a été montré que des troubles vasculaires pouvant aboutir à une accumulation de protéines neurotoxiques, de fibrinogène, de plasmine etc... étaient à l'origine de maladies neurodégénératives (Iadecola, 2013). Il a par ailleurs été montré que certaines démences étaient liées à des lésions cérébrales discrètes et multiples chez des patients atteints d'hypertension (le majeur facteur de risque vasculaire) (Hachinski et al., 1974). D'autres pathologies d'origine vasculaire sont à l'origine de troubles cérébraux, comme la maladie d'Alexander, la calcification primaire du cerveau, la microcéphalie, les malformations cérébrales caverneuses, le syndrome de De Vivo (Zhao et al., 2015).

Il est important de noter que même si le dysfonctionnement de la BHE conduit à des maladies neurodégénératives, parfois même létales, son ouverture peut être également bénéfique pour le SNC. En effet, l'ouverture transitoire de la BHE permet l'ancrage des leucocytes provenant de la circulation et leur diapédèse au sein du tissu cérébral lésé (Iadecola and Anrather, 2011). Ces leucocytes permettent une réparation tissulaire rapide et efficace.

## II. Immunité résidente du SNC

### 1. Cellules microgliales

#### a. Historique

La neuroglie, ou l'ensemble des cellules gliales du SNC, a été caractérisée pour la première fois par Rudolf Virchow (1821-1902) en 1846. Contrairement aux neurones, elles sont qualifiées de « gluantes » (d'où le terme « glie » qui vient du grec « *gloios* » signifiant gluant) et permettent de soutenir le tissu neuronal d'où le terme neuroglie (la glue des neurones). C'est ensuite Franz Nissl (1860-1919) et William Ford Robertson (1867-1923) qui ont pour la première fois différencié les cellules microgliales des autres cellules « neurogliales » dans les années 1880. De plus, Victor Babes (1854-1926) a, lui, découvert les changements morphologiques des cellules microgliales, alors appelées « cellules en bâtonnet », lors de l'observation d'un cas de rage en 1897. Santiago Ramon y Cajal (1852-1934) nomma ces cellules le « troisième élément », faisant référence aux neurones et astrocytes constituant les deux premiers éléments. C'est Nicolas Achucarro (1880-1918), un collaborateur de Santiago Ramon y Cajal, qui s'intéressa de plus près aux cellules microgliales en perfectionnant les méthodes de fixation des tissus de Cajal. Achucarro étant mort précocement d'un lymphome qu'il a lui-même diagnostiqué (il avait 38 ans), Pio del Rio Hortega (1882-1945), un étudiant de Cajal, continua les travaux d'Achucarro et attribua l'appellation « cellules microgliales » dans le début des années 1920. Pour l'anecdote, les cellules microgliales peuvent également répondre à l'appellation de « cellules de Hortega » (Figure 8).

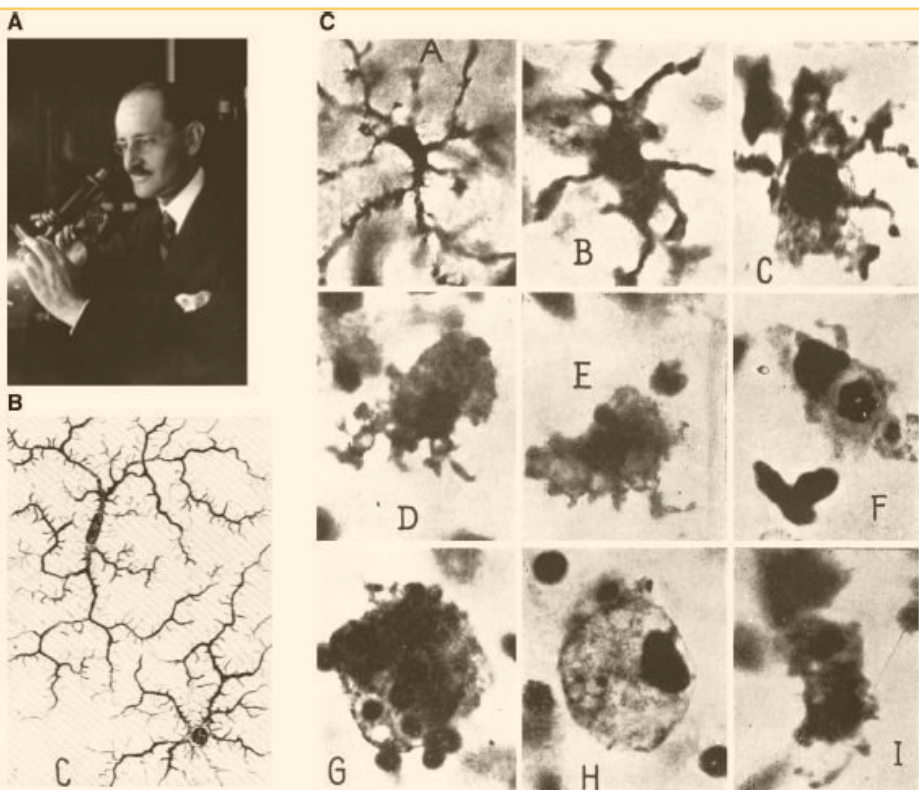


Figure 8 : Découverte des cellules microgliales. (A) Pio del Rio Hortega (1882-1945). (B) Cellules microgliales au repos dessinées/photographiées par Hortega. (C) Evolution de l'activité phagocytaire de la microglie. (A) repos, (B) prolongements plus petits, corps plus large, (C) cellule hypertrophique avec pseudopodes, (D et E) forme amiboïde avec pseudopodes, (F) microglie ayant phagocyté des leucocytes, (G) microglie ayant phagocyté des érythrocytes (H) cellule riche en lipides, (I) microglie en division mitotique.

Dès lors, avec les avancées technologiques en termes de culture cellulaire et de microscopie, bon nombre d'études ont caractérisé les cellules microgliales, que ce soit en condition physiologique ou pathologique. En effet, il est par exemple désormais rendu possible d'étudier la dynamique des changements morphologiques de la microglie chez un animal vivant par l'intermédiaire de la microscopie intravitaire multiphotonique chez des souches de souris transgéniques (Krabbe et al., 2017) (Figure 9).

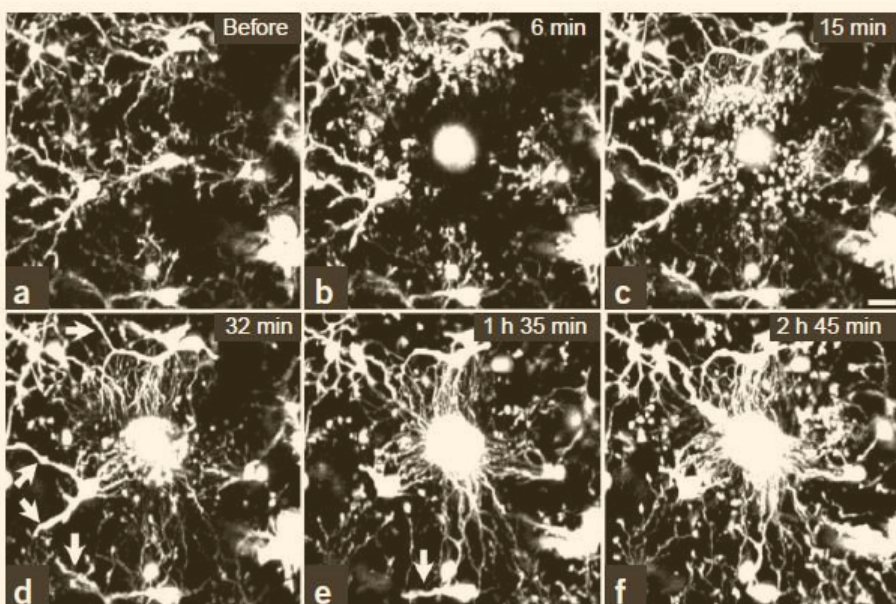


Figure 9: Dynamique des cellules microgliales après lésion laser sous microscope biphotonique. (A) microglie au repos, puis 6min (B), 15min (C), 32min (D), 1h35min (E), 2h45min (F) après induction de la lésion. D'après (Krabbe et al., 2017).

b. Description

Les cellules microgliales sont considérées comme les principales cellules immunitaires résidentes du cerveau. Elles sont en grand nombre (environ 10-15% des cellules du SNC) et couvrent tout le territoire du SNC (Lawson et al., 1992). On peut les distinguer des autres cellules résidentes (macrophages périvasculaires, des méninges et des plexus choroïdes) de par leur localisation, qui leur permet d'entrer en contact avec les autres cellules du SNC, notamment les neurones. Ainsi, il a été montré que les cellules microgliales pouvaient avoir un rôle sur la plasticité synaptique : une déficience en récepteurs spécifiques sur les cellules microgliales empêche l'englobement de bourgeons synaptiques durant le développement cérébral, pouvant ainsi causer des troubles (Reshef et al., 2017) (Figure 10).

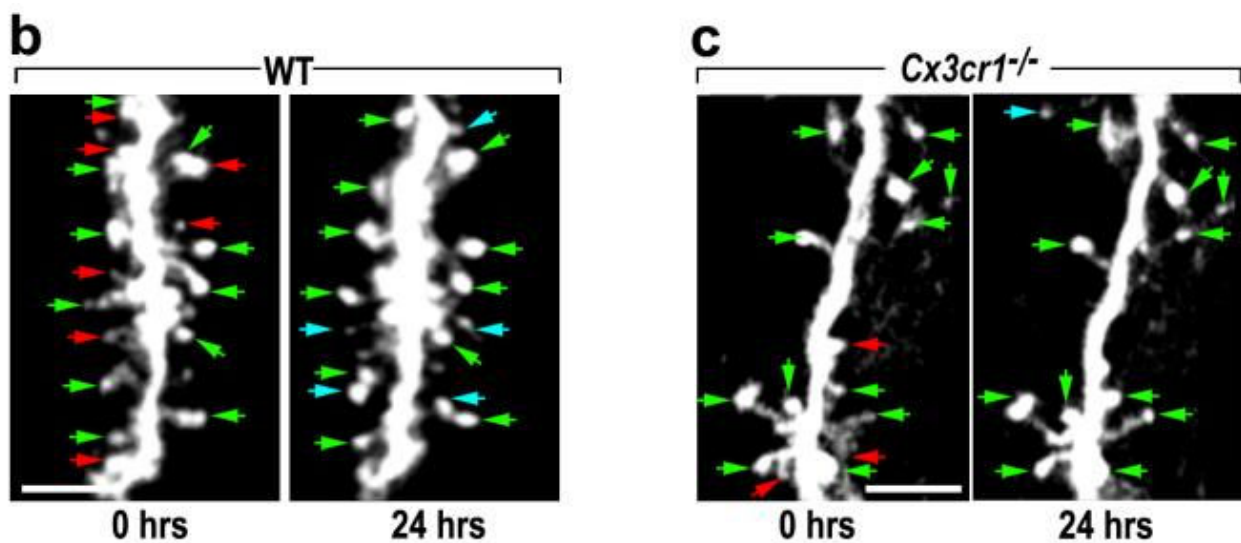


Figure 10: La plasticité synaptique est dépendante des cellules microgliales. (B) Chez une souris saine non transgénique, des synapses se forment (flèches bleues), restent (flèches vertes) ou sont éliminées (flèches rouges) en 24h. (C) Chez une souris déficiente en CX3CR1, un récepteur présent à la surface des cellules microgliales, les synapses sont moins éliminées (moins de flèches rouges), et peu sont nouvellement formées (moins de flèches bleues). D'après (Reshef et al., 2017).

Les cellules microgliales ont une origine mésenchymale (en provenance du sac vitellin ou *yolk sac*), contrairement aux monocytes circulants par exemple, qui ont une origine ectodermale. De plus elles ont une longue durée de vie, et un *turnover* très lent, se faisant par renouvellement local (en anglais, *self-renewal*) (Goldmann et al., 2016; Saijo and Glass, 2011).

Ces cellules sont capables de changer de forme en cas de stimulus : on parle de phénotypes ou d'état d'activation (Saijo and Glass, 2011). En condition physiologique, la microglie possède de nombreux embranchements (ou ramifications), et surveille son environnement en appliquant sans cesse des contacts cellulaires avec les autres cellules environnantes. Par exemple, en condition physiologique les neurones produisent de la fractalkine (ou CX3CL1, L pour ligand), une molécule dont la microglie possède le récepteur (ou CX3CR1, R pour récepteur). En cas d'atteinte, CX3CL1 n'est plus exprimée par les neurones et la microglie s'active (Cardona et al., 2006). Selon la nature du stimulus, et selon la cinétique, la microglie possède un large panel d'états d'activation ou phénotypes, dont les extrêmes sont les phénotypes pro- (M1) et anti-inflammatoire (M2) (Perego et al., 2011; Pisanu et al., 2014). Cette notion M1-M2 est de plus en plus désuète car estimée trop simpliste, elle permet néanmoins d'avoir une notion générale de l'état pro- ou anti-inflammatoire et ainsi élaborer d'éventuels traitements forçant un *switch* de phénotype de la microglie (Drieu et al., 2017; Hanisch and Kettenmann, 2007). Lors de son activation, la microglie adopte également des changements morphologiques : en effet, selon le phénotype, elle peut soit présenter ses nombreuses ramifications (microglie branchée), jusqu'à complètement perdre ses prolongements et devenir ronde (ou appelée microglie amibioïde) (Perry et al., 2010) (Figure 11). De plus, elle est capable de secréter des médiateurs de l'inflammation comme des IL, des chimiokines, du TNF ou du TGF- $\beta$  (Girard et al., 2013). Ces médiateurs sont destinés à recruter les autres cellules immunitaires sur le site du dommage et ainsi favoriser la réaction inflammatoire (Iadecola and Anrather, 2011).

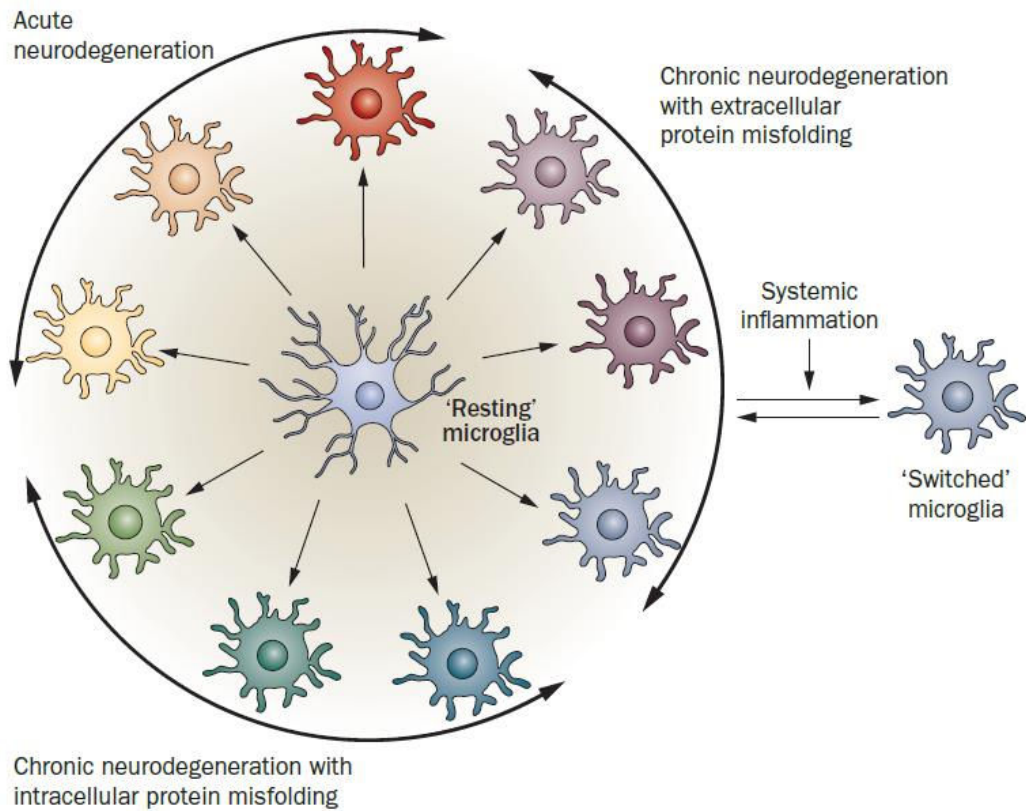


Figure 11 : Les cellules microgliales possèdent une multitude de phénotypes, qui sont exprimés en fonction du type de stimulus. D'après (Perry et al., 2010).

### c. Rôles

Les travaux d'Hortega ont pointé différents rôles potentiels des cellules microgliales. Il avait proposé que les cellules microgliales i) apparaissaient dans le cerveau au cours du développement cérébral, ii) qu'elles pouvaient se déplacer dans le tissu *via* des réseaux de fibres ou en suivant les vaisseaux sanguins, iii) qu'elles pouvaient changer de forme, iv) qu'elles étaient réparties uniformément dans tout le cerveau, avec très peu de variabilité, v) qu'elles occupaient un territoire qui leur était propre. Il s'avère que toutes les suppositions d'Hortega se sont vérifiées et sont d'ailleurs toujours d'actualité. Leur principal rôle reste toutefois de combattre une infection ou de nettoyer le système nerveux central (SNC) ayant subi une lésion (Hanisch and Kettenmann, 2007). Elles sont pour cela capables de phagocytter les débris (Brown and Neher,

2014), d'englober des synapses (Reshef et al., 2017), de présenter des antigènes (Greter et al., 2015) et de promouvoir la cicatrice gliale avec l'aide des astrocytes (Silver and Miller, 2004).

En plus de tous ces rôles plutôt attribués à des stimuli aigus, la microglie peut aussi jouer un rôle dans le cadre d'une inflammation chronique. En effet, plusieurs groupes s'accordent sur le fait qu'en cas de maladies neurodégénératives comme la maladie d'Alzheimer ou une infection à prions, la microglie adopte un autre phénotype considéré comme « légèrement activé » ou « silencieux ». On retrouve régulièrement dans la littérature le terme de *priming*, faisant référence à un processus latent, silencieux mais qui, suite à un deuxième stimulus aigu, provoque une réponse exacerbée des cellules microgliales. Ce concept de *priming* a été démontré dans un modèle expérimental de maladie à prions (Hughes et al., 2010). Pour cela, les auteurs ont injecté des billes de latex inertes dans l'hippocampe de souris saines ainsi qu'à des souris ayant été exposées à un prion. Quelques heures après l'injection des billes, seules les cellules microgliales des souris infectées ont phagocyté celles-ci, prouvant ainsi que ces cellules, même en étant morphologiquement identiques à celles d'une souris saine, répondent de manière exacerbée à un stimulus (Hughes et al., 2010) (Figure 12).

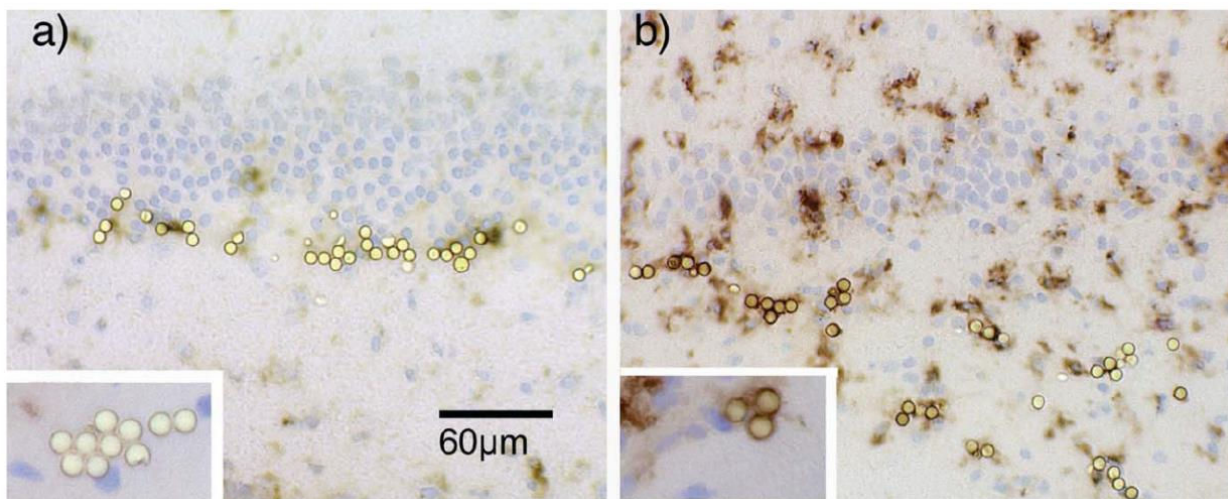


Figure 12: Concept du priming microglial. Suite à une infection à prions, les cellules microgliales phagocytent les billes de latex (image de droite), contrairement aux cellules microgliales d'une souris saine (image de gauche). Les cellules microgliales ont été marquées avec le marqueur de phagocytose CD68. D'après (Hughes et al., 2010).

Plus généralement, le concept de *priming* a été validé dans le contexte des maladies neurodégénératives (Perry and Holmes, 2014). Cet état « d'activation » serait dû à une

accumulation de protéines mal conformées. C'est à se demander si le seul fait de vieillir pourrait mener à un état de *priming* microglial (Von Bernhardi et al., 2015).

## 2. Macrophages périvasculaires

### a. Historique

Les macrophages périvasculaires (ou PVM pour *perivascular macrophages*) ont été, contrairement aux cellules microgliales, découverts que très récemment. Après avoir été décrits comme des « cellules perivasculaires fluorescentes » par Fleischhauer en 1964 (Fleischhauer, 1964), puis comme des « cellules microgliales péricytiques » par Mori et Leblond en 1969 (Mori and Leblond, 1969), c'est Masao Mato qui a réalisé le plus d'expériences de caractérisation de ces cellules. Il les nomma alors « cellules périthéliales granulaires fluorescentes » en 1980 (Mato et al., 1980) (Figure 13). Les PVM ont alors été nommés « cellules de Mato ».

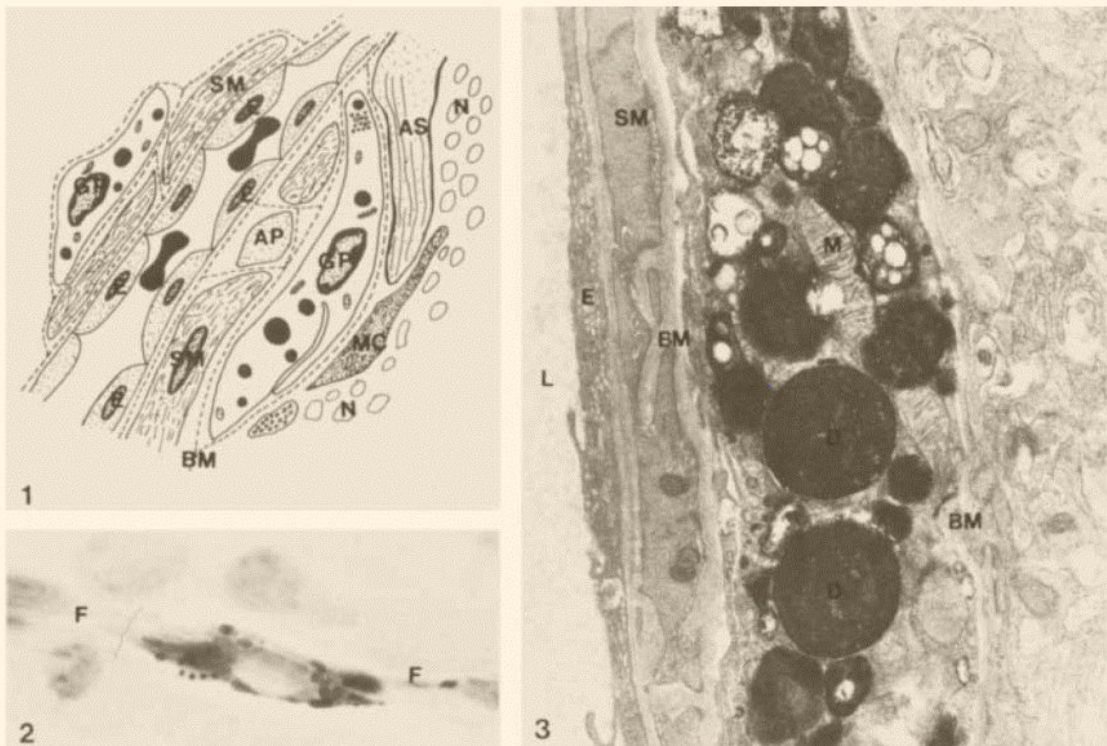


Figure 13 : Description des cellules de Mato (1980 ; maintenant nommées macrophages périvasculaires). Ici la cellule de Mato est indiquée par GP pour Granular Pericytic cell. (1) Schéma représentant la localisation des cellules de Mato. (2) Les PVM peuvent phagocytter des colorants (ici, de la peroxydase). (3) Image de microscopie électronique dévoilant de nombreuses granulations (en gris foncé) dans un PVM.

Puis, en 1986, c'est Hickey et Kimura qui les renommèrent « cellules microgliales périvasculaires » (Hickey and Kimura, 1988). Enfin, Graeber et collaborateurs, en 1989, les nommèrent cellules périvasculaires ED-2 positives (Graeber et al., 1989) : ED-2, ou autrement appelé CD163 (pour *cluster of differentiation 163*) correspond à un récepteur *scavenger* (en français, éboueur) découvert par Jan Krejsek et collaborateurs en 1987 (Onofre et al., 2009; Zwadlo et al., 1987). Toutes ces dénominations vont dans le sens d'une localisation périvasculaire, d'une cellule plutôt volumineuse contenant des granules autofluorescents, et ayant un rôle d'éboueur du cerveau.

### b. Description

Maxime Durant-Fardel a révélé l'existence d'un espace situé entre les vaisseaux sanguins et le tissu cérébral : l'espace périvasculaire (*Traité du ramollissement du cerveau*, 1843). Ce concept a été étudié en détail par Virchow (1851) puis par Charles-Philippe Robin en 1859, d'où l'autre nom donné aux espaces périvasculaires : l'espace de Virchow-Robin (Kisler et al., 2017) (Figure 14). Il s'avère que PVM, comme leur nom l'indique, sont localisés dans l'espace périvasculaire. Au vu de leur emplacement stratégique au sein du SNC, les PVM seraient pressentis pour avoir des rôles dans la communication entre les différents compartiments.

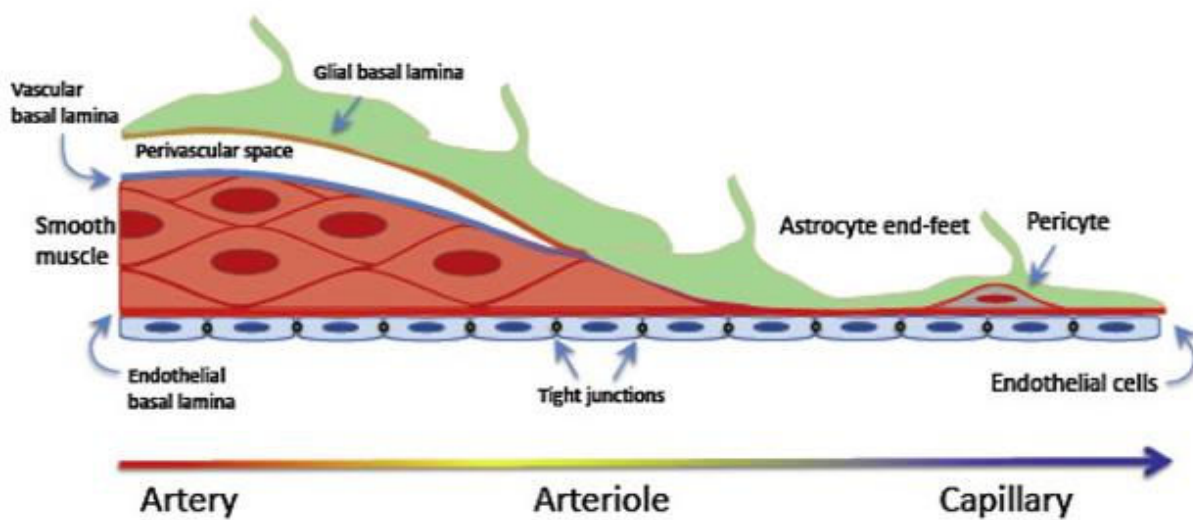
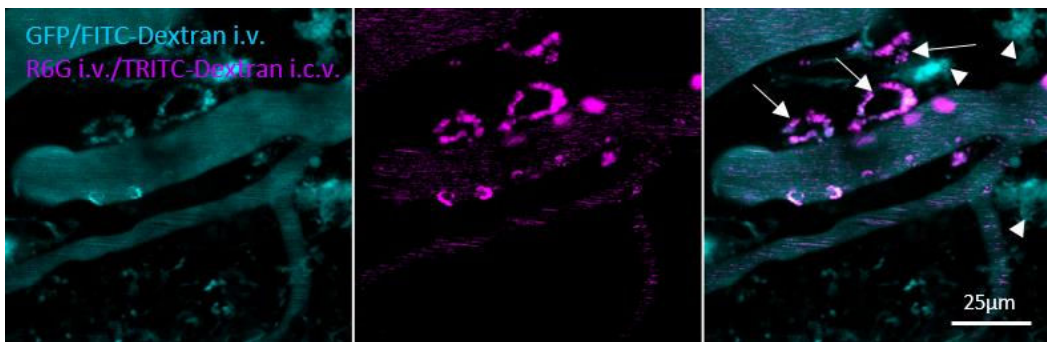


Figure 14 : Schéma représentant l'espace périvasculaire (ou espace de Virchow-Robin). Il faut noter que les deux lames basales (vasculaire et gliale) fusionnent au niveau des capillaires : il n'y a donc plus d'espace périvasculaire autour des capillaires. D'après (Kisler et al., 2017).

Leur origine est mésenchymale (*yolk sac*), tout comme les cellules microgliales (Goldmann et al., 2016). Comme la microglie, les PVM sont des cellules à longue durée de vie, et leur *turnover* se fait lentement, tout le long de la vie de l'individu (Bechmann et al., 2001a). Contrairement à la microglie, le turnover des PVM se ferait par le recrutement de monocytes provenant de la circulation sanguine (Soulas et al., 2009). Ils sont peu nombreux comparativement aux autres cellules du SNC, et sont répartis autour des artères, artéries, veinules et veines. Les PVM ne sont pas retrouvés autour des capillaires de par l'absence d'espace périvasculaire. Ce sont des grosses cellules pouvant présenter des prolongements, mais généralement de forme allongée au vu du

manque d'espace qui leur est conféré. Les PVM possèdent des granules à lysosomes leur permettant de nettoyer les déchets du SNC. Une étude a montré que le peptide bêta amyloïde était retrouvé en grande quantité dans les PVM dans un modèle murin de la maladie d'Alzheimer (Park et al., 2017). Cette capacité de phagocytose des PVMs est utilisée pour les marquer à l'aide de fluorophores injectés dans les ventricules cérébraux (Bechmann et al., 2001b) (Figure 15). Par le biais de la même méthode il est possible de les dépléter, par injection de liposomes contenant du clodronate, une substance pro-apoptotique (Polfliet et al., 2001).



*Figure 15: L'injection d'un dextran dans les ventricules permet la visualisation des PVM in vivo. Les PVM marqués au TRITC-dextran (flèches) sont en dehors des vaisseaux sanguins marqués au FITC-dextran, sont distinguables des leucocytes provenant de la circulation sanguine marqués à la rhodamine-6G, et de la microglie marquée à la GFP (têtes de flèche). Travaux réalisés au laboratoire.*

### c. Rôles

Les PVM n'ayant été décrits que récemment, leurs rôles physiopathologiques sont encore mal connus. Toutefois, comme dit précédemment, la communauté scientifique s'accorde sur le fait de leur rôle de *scavenger*, ne serait-ce que par l'expression de récepteurs *scavengers* (CD163, CD206) à leur surface. Néanmoins, des études récentes pointent un effet modérateur des PVMs dans le cadre de pathologies chroniques comme l'hypertension artérielle (HTA) chronique (Faraco et al., 2016), la maladie d'Alzheimer (Park et al., 2017), la sclérose en plaques (Polfliet et al., 2002) et très récemment dans l'accident vasculaire cérébral ou AVC (Pedragosa et al., 2018). Pour information, l'HTA concerne une personne sur quatre dans le monde, la maladie d'Alzheimer, 48 millions de personnes en 2015, et la sclérose en plaques, 2,3 millions en 2013 : il est donc essentiel de mieux comprendre et caractériser le(s) rôle(s) des PVM.

### 3. Autres cellules immunitaires résidentes du SNC

#### a. Macrophages des méninges et des plexus choroïdes

Les macrophages des méninges (MM pour *meningeal macrophages*) et des plexus choroïdes (CPM pour *choroid plexus macrophages*), comme leur nom l'indique, sont situés respectivement au niveau des méninges, qui enveloppent le cerveau, et au niveau des plexus choroïdes, situés dans des ventricules cérébraux (Prinz et al., 2017) (Figure 16). Ces deux types cellulaires proviennent du sac vitellin, tout comme les cellules microgliales et les PVM (Goldmann et al., 2016). Toutefois, il a été montré que les CPM ont une durée de vie plus courte que les autres macrophages résidents, et que leur *turnover* se fait *via* le recrutement de monocytes circulants. En effet, après avoir marqués les macrophages résidents à la YFP, une molécule fluorescente, durant le développement, seuls les CPM n'étaient plus YFP positifs à l'âge adulte, contrairement aux autres macrophages résidents (Goldmann et al., 2016).

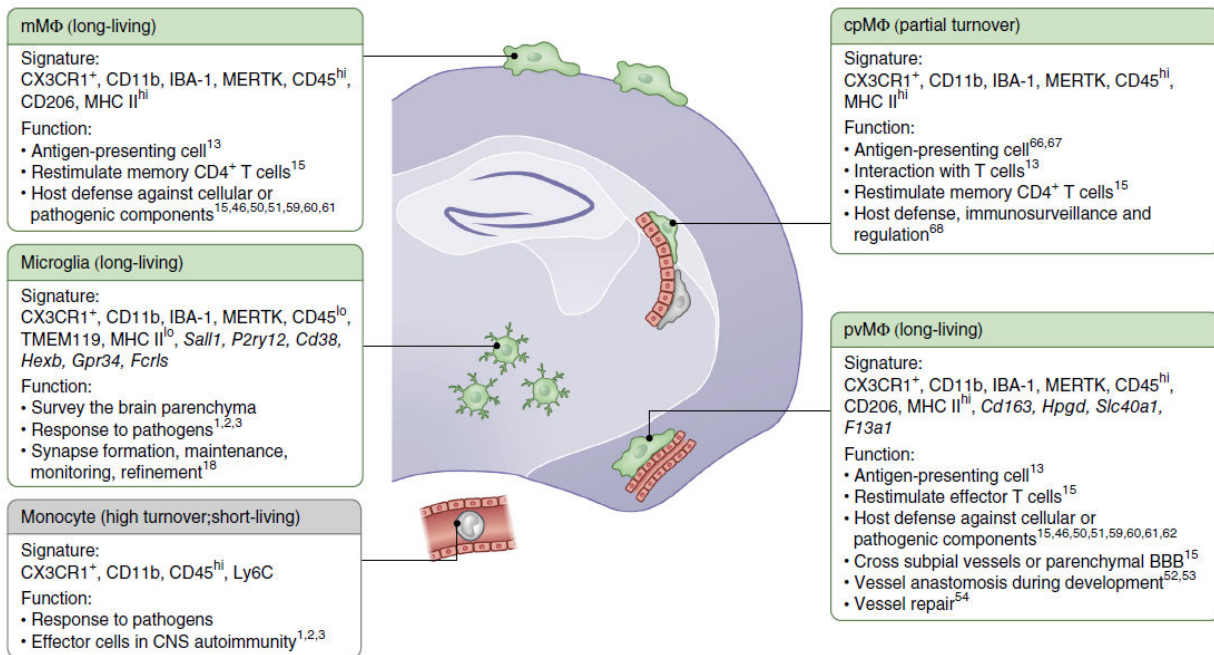


Figure 16 : Illustration des différentes populations de macrophages au sein du SNC. Il faut noter que seules les cellules microgliales font partie intégrante du tissu cérébral. Les macrophages périvasculaires (ici notés *pvMΦ*), les macrophages des plexus choroïdes (*cpMΦ*) et les macrophages des méninges (*mMΦ*) sont les autres types de macrophages rencontrés dans le SNC. D'après (Prinz et al., 2017).

Les rôles des CPM et des MM sont principalement la présentation d'antigènes, l'interaction avec les lymphocytes, ainsi que la défense de l'organisme (Prinz et al., 2017).

*b. Lymphocytes*

Il était convenu que le cerveau sain était totalement protégé du système immunitaire *via* la présence de la barrière hémato-encéphalique. Toutefois, cette notion paraît moins claire de par le fait que quelques lymphocytes ont été retrouvés dans le parenchyme cérébral en condition physiologique (Anthony et al., 2003). De plus, la barrière biologique formée au niveau des plexus choroïdes n'est pas aussi imperméable que la BHE, permettant un dialogue constant entre système immunitaire et cerveau. D'ailleurs, quelques lymphocytes sont retrouvés dans le stroma des plexus choroïdes en condition physiologique (Deczkowska et al., 2016). De plus, des lymphocytes sont retrouvés dans la circulation du LCS, ce qui suggère qu'il y a une constante surveillance du SNC par les lymphocytes (Kleine, 2015).

De manière intéressante, des souris déplétées en lymphocytes T (ce sont des souris SCID pour *severe combined immunodeficiency*) ont une neurogenèse amoindrie par rapport à des souris saines : ceci apporte une preuve supplémentaire que le système immunitaire peut jouer un rôle dans le fonctionnement du SNC (Ziv et al., 2006) (Figure 17).

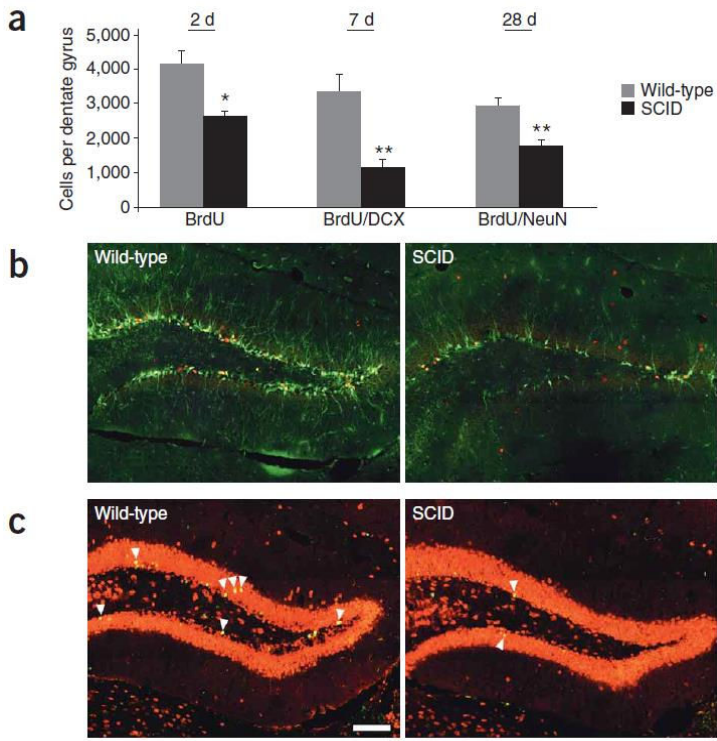
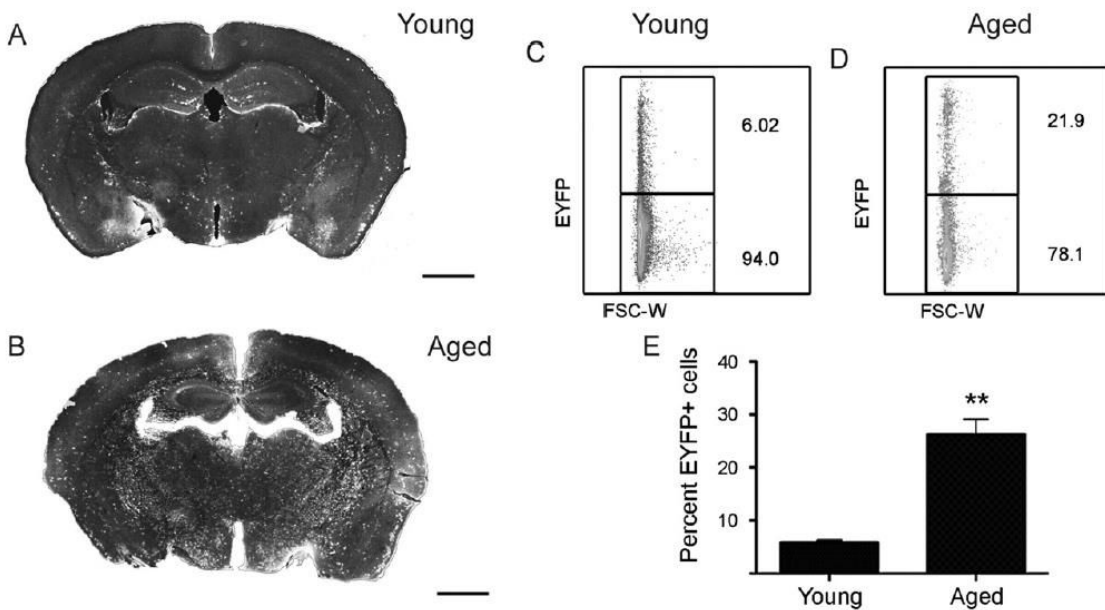


Figure 17: La neurogenèse est compromise chez des souris déplétées en lymphocytes (SCID) comparativement aux souris saines (wild-type). (A) Quantification à 2, 7 et 28 jours après la première injection d'un marqueur de prolifération cellulaire (BrdU) du nombre de cellules nouvellement formées ( $BrdU^+$ ), co-marquées avec soit un marquage de neurogenèse (double-cortine, DCX), soit un marqueur neuronal (NeuN). (B) Images représentatives du co-marquage BrdU/DCX (DCX en vert) chez une souris saine (à gauche) et chez une souris SCID (à droite). (C) Images représentatives du co-marquage BrdU/NeuN (NeuN en rouge) chez une souris saine (à gauche) et chez une souris SCID (à droite). Les flèches indiquent la présence de co-marquage. D'après (Ziv et al., 2006).

### c. Cellules dendritiques

Les DC sont spécialisées dans la présentation d'antigènes : elles sont d'ailleurs parfois renommées cellules présentatrices d'antigène (ou APC, de *antigen presenting cells*). Les DC sont classiquement détectées par deux comarquages dans le SNC : elles sont doublement positives pour CD11c et le complexe majeur d'histocompatibilité-2 ou CMH-II (ou MHC-II pour *major histocompatibility complex-II*) (Gottfried-Blackmore et al., 2009). Chez des souris saines, elles ne sont pas détectables dans le parenchyme cérébral. Néanmoins, elles sont retrouvées en faible nombre dans l'espace périvasculaire, les méninges et les plexus choroïdes (McMenamin, 1999). Dans le cadre de l'ischémie cérébrale, le nombre de DC augmente dès une heure après la survenue de l'AVC, puis leur nombre augmente continuellement jusqu'à atteindre un pic à 6 jours (Kostulas et al., 2002). De manière intéressante, la microglie adopte elle aussi un phénotype de cellule présentatrice d'antigène suite à l'AVC : le nombre de cellules OX62<sup>+</sup> (marqueur de DC) également marquées avec OX42<sup>+</sup> (plus communément connu sous le nom de CD11b, un

marqueur de cellules microgliales/macrophages) augmente jusqu'à également atteindre un pic à 6 jours (Kostulas et al., 2002). De plus, les DC sont associées à une production de cytokines pro-inflammatoires, suggérant un rôle fonctionnel des DC dans les processus physiopathologiques liés à la survenue d'un AVC. Dans une autre étude il a été montré que les DC étaient capables de présenter des antigènes aux lymphocytes T dans le cadre d'une infection par *Listeria* (Hayashi et al., 2009). Enfin, une autre étude a évoqué que les DC pouvaient avoir un rôle dans le processus de vieillissement : en effet, des DC sont retrouvées en nombre significativement plus important dans le cerveau des souris âgées par comparaison à des souris jeunes adultes (Kaunzner et al., 2012) (Figure 18).



*Figure 18 : Accumulation de cellules dendritiques (DC) dans le cerveau de souris âgées. (A) Image de microscopie d'une coupe de cerveau d'une souris jeune (young). Les points blancs sont des cellules EYFP<sup>+</sup> (positives pour le marqueur CD11c fluorescent dans le jaune). (B) Même type d'image mais chez une souris âgée (aged): on constate de visu plus de points blancs dans le cerveau d'une souris âgée, correspondant à une accumulation de DC CD11c<sup>+</sup>. (C) et (D) Quantification du nombre de cellules EYFP<sup>+</sup> chez les souris jeunes (C) et âgées (D) : 6,02% des cellules sont EYFP<sup>+</sup> chez les souris jeunes ; 21,9% chez les souris âgées. (E) Pourcentage de cellules EYFP<sup>+</sup> par rapport au nombre de cellules EYFP<sup>-</sup> chez les souris jeunes et âgées. D'après (Kaunzner et al., 2012).*



## Résumé

La réaction inflammatoire est un phénomène complexe faisant intervenir les cellules immunitaires résidentes du tissu lésé, et les cellules immunitaires provenant de la circulation sanguine. Les acteurs de l'inflammation peuvent être scindés en deux catégories. Tout d'abord, l'immunité innée permet de limiter l'étendue de la lésion/infection et d'amplifier la réaction inflammatoire *via* des médiateurs comme les cytokines/chimiokines. L'immunité adaptative, majoritairement représentée par les lymphocytes, cible spécifiquement l'agent pathogène pour le dégrader par les lymphocytes tueurs ; l'agent pathogène est aussi mémorisé par les lymphocytes mémoire afin d'améliorer la réaction inflammatoire en cas d'une nouvelle atteinte par ce même agent pathogène.

Le cas de l'inflammation cérébrale est différent d'autres régions du corps du fait de la présence de la BHE. Il est toutefois possible que cette BHE soit endommagée, ceci permettant l'infiltration des cellules immunitaires au sein du parenchyme cérébral. De plus certaines études ont montré qu'en condition physiologique l'ouverture de la BHE serait dynamique en fonction de nombreux facteurs comme le cycle du sommeil, l'âge ou encore la composition de la flore intestinale (Keaney and Campbell, 2015). De plus, il existe des régions cérébrales dépourvues de BHE où le trafic de cellules immunitaires est rendu possible, même en condition physiologique (Engelhardt and Ransohoff, 2005; Ziv et al., 2006). Ceci va à l'encontre de précédents travaux concernant le statut « privilégié » du SNC qui serait protégé du système immunitaire périphérique. Mais ceci prouve l'existence d'un véritable lien entre la périphérie et le SNC *via* les cellules immunitaires.



### 3. L'inflammation dans le cadre de l'accident vasculaire cérébral ischémique

#### I. Généralités sur l'accident vasculaire cérébral

##### 1. Historique

C'est sans le savoir qu'Hippocrate (environ 460-380 avant JC) avait introduit la notion d'AVC en décrivant la condition d'apoplexie, une maladie qu'il a caractérisée par une perte de conscience qui s'ensuit d'une mort soudaine de l'individu. L'apoplexie ayant été caractérisée par l'arrêt de la perfusion sanguine par Claude Galien (129-216), puis à un saignement interne de l'organe, on peut penser que l'apoplexie décrite par Hippocrate correspondait en fait à une hémorragie cérébrale. En fait, Jacob Wepfer (1620-1695) a montré que, suite à une apoplexie, quelque chose empêchait la venue du sang dans le cerveau : dans certains cas, il y avait un saignement (c'est l'AVC hémorragique), et dans d'autres cas, les vaisseaux sanguins étaient bouchés (c'est l'AVC ischémique). Les premières chirurgies visant à déboucher les artères ont vu le jour au début du 19<sup>ème</sup> siècle et ont été menées par Amos Twitchell (1781-1850). Plus précisément, Amos Twitchell avait postulé qu'il fallait retirer le cholestérol au niveau de la paroi artérielle car il favorisait la survenue de l'apoplexie : cette technique est toujours utilisée de nos jours, sous le nom d'endarterectomie carotidienne. Avec l'apparition de nouvelles techniques d'imagerie comme l'angiographie (1927), inventée par Egas Moniz (1874-1955), les méthodes de détection des apoplexies se perfectionnaient. Pour l'anecdote, Moniz a aussi inventé la lobotomie (il a reçu le prix Nobel en 1949 pour cette invention), qu'il voulait utiliser comme moyen de traitement contre l'homosexualité. Son prix Nobel ne lui a pas été destitué.

En 1928, l'apoplexie cérébrale devient « accident vasculaire cérébral », et est séparé en deux catégories, ischémique ou hémorragique. Le premier traitement médicamenteux de l'AVC voit le jour en 1976 : Henry Barnett (1922-2016) a découvert que l'aspirine pouvait empêcher la formation des caillots chez les populations à risque, et éviter la formation de nouveaux caillots chez des patients ayant auparavant subi un AVC.

En 1994, l'imagerie par résonance magnétique (inventée par Paul Lauterbur et Peter Mansfield en 1971) devient l'imagerie diagnostique de référence des AVC.

##### 2. Définition

L'AVC est défini comme « l'apparition et l'installation soudaine de signes cliniques localisés ou globaux de dysfonction cérébrale sans autre cause apparente qu'une origine vasculaire ».

On distingue deux types d'AVC. L'AVC hémorragique correspond à une rupture d'un vaisseau sanguin cérébral entraînant une extravasation du sang au niveau du tissu cérébral. Ce type d'AVC intervient dans 20% des cas. L'AVC ischémique, qui intervient dans 80% des cas, correspond à une interruption du flux sanguin par obstruction d'un vaisseau sanguin cérébral par un caillot (thrombus ou embole).

D'après l'organisation mondiale de la santé (OMS), 15 millions de personnes par an subissent un AVC dans le monde. De ces 15 millions, 5 millions de personnes sont mortes et 5 millions sont handicapées à vie. L'AVC est d'ailleurs la première cause de handicap acquis chez l'adulte, et, de surcroît, la seconde cause de mortalité et de démence dans les pays développés (toujours d'après l'OMS). Par exemple, aux Etats-Unis, un AVC arrive toutes les quarante secondes, et une personne meurt d'un AVC toutes les 4 minutes (selon *l'American Stroke Association*). En France, cette pathologie touche environ 130 000 personnes par an, dont environ 60 000 décès. Les personnes âgées de plus de 65 ans sont les plus majoritairement concernées par cette pathologie ; toutefois, un quart des personnes ayant subi un AVC ont moins de 55 ans.

## II. Traitements de l'AVC approuvés en clinique

### 1. Traitement pharmacologique

De nos jours, le seul traitement médicamenteux validé pour le traitement de l'AVC ischémique est l'injection intraveineuse de l'activateur tissulaire du plasminogène ou tPA (pour *tissue-type plasminogen activator*) (National Institute of Neurological Disorders and Stroke rt-PA Stroke Study Group, 1995). Le fait est qu'en réalité peu de patients sont éligibles pour la fibrinolyse : environ 5% seulement des patients atteints d'AVC ischémiques sont traités au tPA (Goldstein, 2016). Ce traitement possède plusieurs limites : la fenêtre thérapeutique est courte (<4,5 heures), le risque hémorragique est augmenté, la mortalité est aussi augmentée, et le taux de reperfusion est assez faible (seulement 1/3 des patients ont une reperfusion complète).

**Ce maigre choix de traitement pharmacologique contraste avec plus de 1000 molécules déjà testées qui ont montré un effet bénéfique dans les modèles expérimentaux d'occlusion mécanique de l'ACM. Cet échec dans la translation de la paillasse à la clinique montre qu'il est essentiel d'étudier la physiopathologie de l'AVC dans d'autres modèles expérimentaux**, en choisissant un modèle qui se rapproche au plus près de la réalité clinique, afin de pouvoir trouver des traitements de l'AVC. Pour cette raison, depuis quelques années, des nouveaux modèles expérimentaux d'AVC ont été développés et ont cherché à créer des vrais caillots au sein des artères cérébrales *via* l'injection de thrombine directement dans l'ACM (Orset et al., 2007, 2016),

l'application de chlorure de fer (Karatas et al., 2011) ou par photothrombose (Labat-gest and Tomasi, 2013).

## 2. Traitement mécanique

En plus de la thrombolyse médicamenteuse réalisée par injection intraveineuse de tPA, depuis 2016 le retrait mécanique du thrombus est devenu aussi traitement de référence (Bracard et al., 2016). Ce thrombus peut soit être aspiré par succion, soit retiré à l'aide d'un filament au bout duquel est fixé un *stent* ou un *coil* : c'est la thrombectomie mécanique (Figure 19). Le filament est inséré par voie fémorale, remonte dans le cœur puis passe par l'aorte et enfin arrive au niveau des principales artères qui irriguent le cerveau (Raychev and Saver, 2012). Les patients qui peuvent bénéficier de la thrombectomie mécanique sont ceux dont l'occlusion artérielle se produit uniquement sur les grosses artères à la base du cerveau, par souci d'accessibilité (Lapergue et al., 2018).

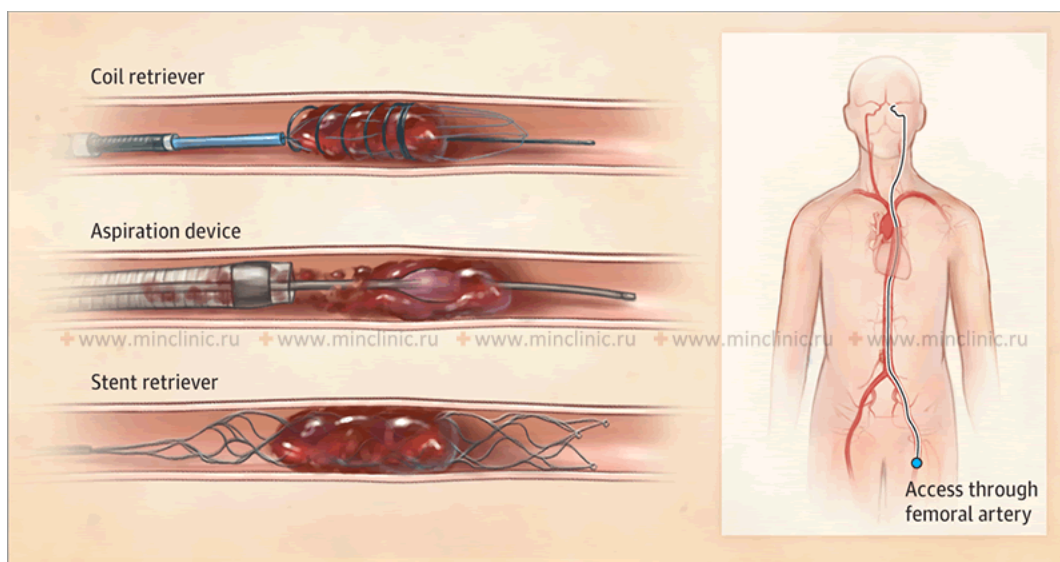


Figure 19 : Thrombectomie mécanique, soit par aspiration, soit à l'aide d'un coil ou d'un stent.

La thrombectomie mécanique peut être associée à la thrombolyse par tPA. Une étude de cas a montré des effets bénéfiques de cette association lors d'une large occlusion (Cobb et al., 2017). L'essai clinique THRACE a montré i) qu'il n'y avait pas d'effet sur la mortalité du double traitement et que ii) cela permettait une meilleure récupération fonctionnelle (Bracard et al., 2016; Morelli

et al., 2017). Une récente méta-analyse a montré que le double traitement permettait une meilleure récupération fonctionnelle, une meilleure recanalisation de l'artère, ainsi qu'une diminution significative de la mortalité comparé à la seule thrombolyse par tPA (Mistry et al., 2017). Une autre étude a confirmé ces résultats dans le cadre d'occlusions proximales de l'ACM (Lobsien et al., 2016).

Concernant la fenêtre thérapeutique, une étude récente a montré que contrairement à la fibrinolyse par tPA, la thrombectomie mécanique conservait des effets bénéfiques au-delà de 6h après la survenue de l'AVC (Vidale et al., 2018).

En France, 1 222 personnes étaient concernées par la thrombectomie mécanique en 2011 ; elles étaient 2918 en 2015, et de 4589 en 2016. Toutefois il faut rappeler que cette intervention n'est que très peu pratiquée pour le moment : elle se fait pratiquer par des neuroradiologues interventionnels (ils étaient 140 en France en 2016), dans des centres de neuroradiologie interventionnelle (37 centres en France en 2016). De plus, la thrombectomie ne peut être pratiquée que lors d'AVC survenant sur de gros vaisseaux. **Il est donc nécessaire de trouver de nouvelles cibles thérapeutiques pouvant couvrir un nombre plus important de patients.**

### III. Physiopathologie de l'AVC

Pour trouver des nouvelles cibles thérapeutiques pouvant couvrir un nombre plus important de patients qui ne peuvent pas être traités ni par tPA ni par thrombectomie, il faut connaître la physiopathologie de l'AVC. A ce jour, il est généralement accepté que les mécanismes participant à la physiopathologie de l'AVC sont l'excitotoxicité, les dépolarisations envahissantes, l'apoptose et l'inflammation (Dirnagl et al., 1999) (Figure 20).

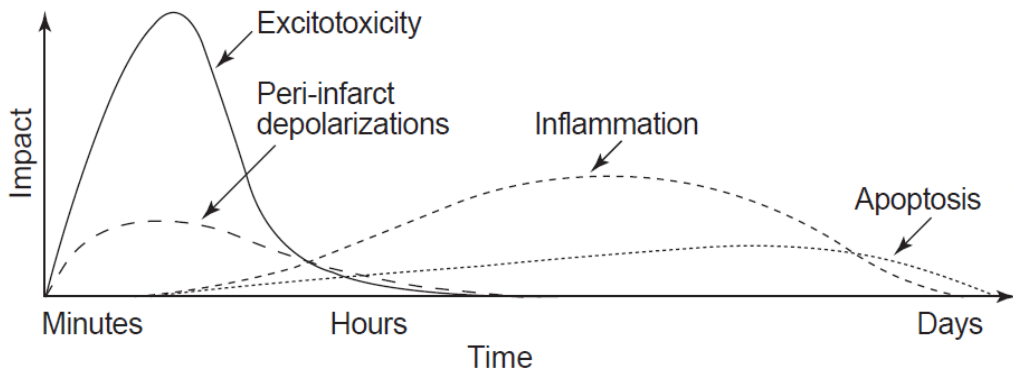


Figure 20 : Cascade des événements suite à la survenue d'un AVC ischémique. Quelques minutes seulement après la survenue de l'AVC, les neurones du core de l'ischémie meurent par excitotoxicité. Ceci a pour conséquences des vagues de dépolarisation des neurones autour de la lésion, puis une entrée des neurones en apoptose. Enfin, l'inflammation prend place, et se maintient dans le temps. D'après (Dirnagl et al., 1999).

## 1. Excitotoxicité

Suite à la survenue de l'AVC, les neurones avoisinant le vaisseau obstrué sont en souffrance. En effet, les neurones ne possèdent pas de réserves énergétiques, ils ont donc besoin d'un apport constant en oxygène et nutriments. De fait de l'obstruction, il n'y a plus d'apport en oxygène et nutriments : les neurones se meurent. Ce stress hyper-active les neurones : ils vont alors produire en grandes quantités un neurotransmetteur excitateur qu'est le glutamate. Le glutamate va se fixer sur les récepteurs N-méthyl-D-aspartate (ou NMDA) du compartiment post-synaptique entraînant une trop grande entrée d'ions calcium ( $\text{Ca}^{2+}$ ). Les ions  $\text{Ca}^{2+}$  en excès vont alors activer des enzymes capables de dégrader les structures cellulaires comme l'ADN ou le cytosquelette, menant à la mort du neurone : c'est le phénomène d'excitotoxicité. Ce phénomène a été décrit dans les années 50 par Hayashi : il avait remarqué qu'une trop forte quantité de glutamate pouvait entraîner des crises d'épilepsie. L'excitotoxicité a été également décrite dans d'autres pathologies comme les traumatismes crâniens et de la moelle épinière, ou comme dans la maladie d'Alzheimer.

## 2. Dépolarisations envahissantes

Le phénomène d'excitotoxicité a pour conséquence une très importante augmentation de concentration en glutamate dans le tissu lésé par l'ischémie. De ce fait, le glutamate en excès va venir activer les neurones voisins, qui, du fait de leur sensibilité au glutamate, vont également s'hyperactiver, et donc produire de plus en plus de glutamate. Ce phénomène s'étend au tissu non lésé, qui devient alors lui aussi en souffrance : c'est le phénomène de dépolarisations envahissantes (on parle aussi de dépression envahissante ou de *spreading depression*). De manière intéressante, il a été montré que les ondes de dépolarisation pouvaient réverbérer dans les cerveaux des gyrencéphales, amplifiant *de facto* l'effet délétère des dépolarisations envahissantes (Santos et al., 2014). Les phénomènes de dépolarisations envahissantes sont responsables de la formation de l'œdème cytotoxique (Dreier et al., 2015).

## 3. Apoptose

L'entrée massive des ions  $\text{Ca}^{2+}$  a d'autres conséquences que l'entrée de glutamate *via* les récepteurs NMDA. En effet, les ions  $\text{Ca}^{2+}$  vont également agir sur le fonctionnement des mitochondries : ils vont s'y accumuler, entraînant la formation de dérivés réactifs de l'oxygène, et un arrêt de la production d'adénosine triphosphate (ou ATP). De plus, l'entrée de  $\text{Ca}^{2+}$  s'accompagne d'un déséquilibre ionique, menant à un gonflement de la mitochondrie (œdème). La mitochondrie étant en souffrance, elle va libérer les ions  $\text{Ca}^{2+}$ , et les radicaux libres oxygénés, qui vont aboutir au déclenchement de la mort programmée de la cellule *via* l'activation des caspases : c'est le phénomène d'apoptose (Kristián and Siesjö, 1996).

## 4. Réaction inflammatoire

La réponse inflammatoire est un processus mis en place dès les premiers instants et perdure dans le temps, ce qui en fait une **cible thérapeutique intéressante, puisque potentiellement modifiable à tout temps**. Un schéma de la réaction inflammatoire déclenchée par l'AVC ischémique est présenté dans la Figure 21.

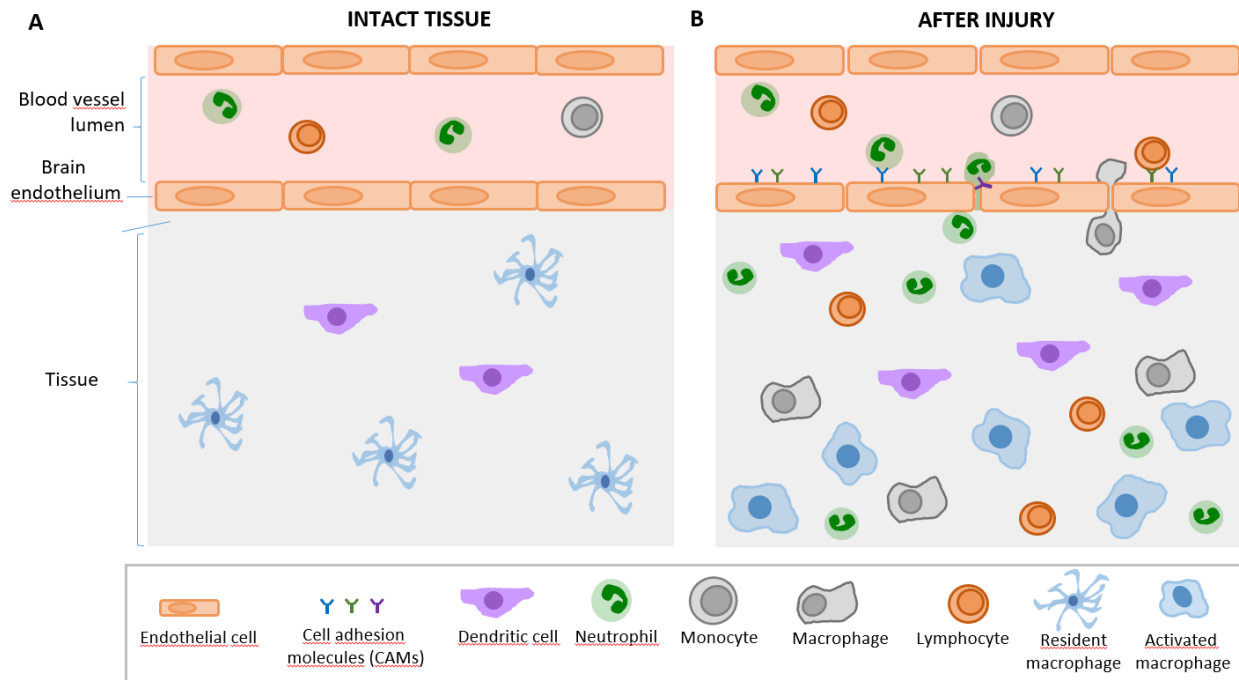


Figure 21 : Schéma résumant les cellules immunitaires impliquées lors de la réaction inflammatoire. (A) Au sein du tissu sain se dressent les macrophages et les cellules dendritiques, qui surveillent constamment si le tissu n'est pas endommagé. (B) En cas de dommage, les macrophages et les cellules dendritiques s'activent, phagocytent des débris et sécrètent des cytokines/chimiokines pro-inflammatoires menant à l'activation des cellules endothéliales locales et au recrutement des leucocytes (neutrophiles et monocytes) provenant de la circulation sanguine. Ce recrutement se fait par diapédèse grâce aux molécules d'adhésion exprimées à la paroi des cellules endothéliales. Si cette réaction n'est pas suffisante, les lymphocytes vont également être recrutés

#### a. Réaction de l'immunité résidente

##### Cellules microgliales

Comme expliqué précédemment, les cellules microgliales font partie de l'immunité résidente du cerveau. Elles jouent un rôle de sentinelle en condition physiologique, surveillant constamment l'activité du tissu cérébral. Dans le cadre de l'ischémie cérébrale, les cellules microgliales sentent la souffrance neuronale par plusieurs moyens. Comme déjà évoqué précédemment, les neurones en souffrance arrêtent de produire la fractalkine (ou CX3CL1), une chimiokine normalement continuellement exprimée et captée par les cellules microgliales *via* leurs récepteurs CX3CR1. De plus, les neurones expriment de la phosphatidylsérine à leur surface (elle est normalement

contenue dans le corps cellulaire) lorsqu'ils entrent en apoptose : la phosphatidylsérine est alors détectée par les cellules microgliales qui expriment son récepteur (Napoli and Neumann, 2009). Enfin, les neurones en souffrance sont capables de produire du TNF, qui est une cytokine pro-inflammatoire pouvant interagir avec les récepteurs de type Toll, aussi exprimés par les cellules microgliales (Janelsins et al., 2008).

Les cellules microgliales, suite à l'ischémie, peuvent adopter différents phénotypes, passant d'un état « au repos » à un état « activé ». Comme discuté précédemment, il existe deux états d'activation principaux (même si c'est un peu caricatural) : les cellules microgliales peuvent être plutôt pro- ou plutôt anti-inflammatoires. Le phénotype dépend de la cinétique de la réaction inflammatoire, et donc de la présence de telle ou telle cellule immunitaire ainsi que des cytokines/chimiokines exprimées. En effet, si l'on observe un taux élevé de cytokines pro-inflammatoires comme par exemple le TNF libéré par les neurones en souffrance, les cellules microgliales vont adopter un profil pro-inflammatoire : elles vont alors produire un grand nombre de cytokines pro-inflammatoires et des dérivés réactifs de l'oxygène, permettant le recrutement des leucocytes provenant de la circulation sanguine (Benakis et al., 2015). De plus, elles vont développer une morphologie amiboïde, caractéristique des macrophages : ce changement morphologique s'accompagne d'une augmentation de CD68, un marqueur de phagocytose (Perego et al., 2011) (Figure 22). La microglie exprime également Ym1 (ou *chitinase-3-like protein 3*), qui joue un rôle dans le chimiotactisme des lymphocytes. De plus, elles expriment du CD206, le récepteur au mannose, qui a un rôle de *scavenger* (Galea et al., 2005). Enfin, en plus d'exprimer CD11b (comme toutes les cellules myéloïdes) les cellules microgliales peuvent, comme le présage l'expression d'Ym1, présenter des antigènes : elles expriment alors CD11c, comme les DC (Caravagna et al., 2018).

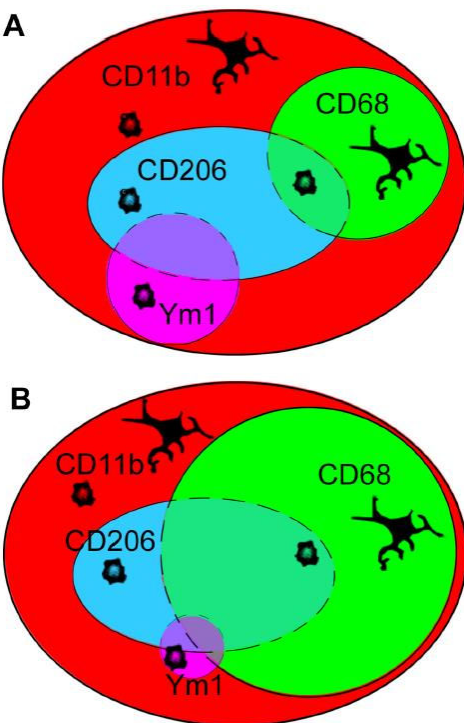


*Figure 22 : Les différentes expressions moléculaires de la microglie (A) 24h et (B) 7 jours après un AVC ischémique. Il est important de noter que cette étude se base sur un modèle expérimental d'ischémie cérébrale permanente : le modèle d'électrocoagulation de l'ACM. D'après (Perego et al., 2011).*

Enfin, en plus de changer de morphologie et de phénotype, les cellules microgliales sont capables de proliférer dans le cadre de l'ischémie cérébrale. En effet il a été montré dans divers modèles expérimentaux (transitoires et permanents) que la microglie, dès les premières 24 heures, était retrouvée en plus grand nombre dans l'hémisphère ipsilatéral (Gelderblom et al., 2009; Zhou et al., 2013).

### *Macrophages*

Le rôle des autres macrophages résidents du cerveau (à savoir les PVM, les CPM et les MM) dans le cadre de l'ischémie cérébrale sont peu connus. Il a été montré que les plexus choroïdes étaient une voie clé du passage des lymphocytes dans le cadre de l'AVC ischémique (Llovera et al., 2017). Du fait de leur interaction connue avec les lymphocytes (Hickey and Kimura, 1988), il est possible que les CPM soient responsables, du moins en partie, de cette infiltration. Pour continuer dans cette idée, il a été montré que les CPM exprimaient CD11c, un marqueur reflétant la capacité à

présenter des antigènes aux lymphocytes (Chinnery et al., 2010), même ceci n'a jamais été prouvé. Le rôle des MM dans l'AVC est mal connu. Il a été montré qu'un autre type cellulaire au niveau des méninges pouvait avoir un rôle délétère dans l'ischémie cérébrale : les mastocytes (Arac et al., 2014).

*b. Réaction endothéliale*

Comme il a été précédemment décrit, les EC au niveau cérébral forment des jonctions serrées entre elles pour former la BHE, empêchant le passage des leucocytes dans le tissu cérébral en condition physiologique. Même si cette notion est à prendre avec beaucoup de précautions (Engelhardt and Ransohoff, 2005), il en est de fait qu'en conditions pathologiques comme dans le cadre de l'AVC, cette BHE devient perméable, permettant ainsi l'infiltration des leucocytes par migration transendothéliale (Gauberti et al., 2013; Montagne et al., 2012). Les EC, suite à l'AVC, et parallèlement à l'activation des cellules microgliales, vont alors s'activer : les jonctions serrées se rétractent, et les premières molécules d'adhésion cellulaire (les sélectines) sont exprimées à leur surface. S'en suit l'adhésion des leucocytes *via* les molécules d'adhésion VCAM-1 et ICAM-1 (Deddens et al., 2017; Gauberti et al., 2013). Enfin, la transmigration des leucocytes à travers les EC se fait *via* PECAM-1 (Muller, 2002).

*c. Recrutement des leucocytes*

Il est intéressant de noter que la dynamique de la réaction inflammatoire suite à l'AVC dépend du modèle expérimental étudié. Selon si le modèle est transitoire ou permanent, ou selon sous quel abord la chirurgie est pratiquée (branche distale ou proximale de l'ACM), la réaction inflammatoire est différente, tout comme le volume de lésion et les régions cérébrales lésées.

Les neutrophiles sont les premiers leucocytes circulants recrutés dans le cadre de l'AVC. Leur principal rôle est de libérer leurs granulations riches en médiateurs de l'inflammation pour amplifier la réaction inflammatoire. Un débat existe sur la localisation des neutrophiles dans le tissu cérébral : en effet, certaines études montrent qu'ils se situent directement dans le tissu

(Gelderblom et al., 2009; Zhou et al., 2013) ; d'autres montrent qu'ils se restreignent dans l'espace périvasculaire (Enzmann et al., 2013).

Les lymphocytes sont recrutés quelques jours après la survenue de l'AVC ischémique. Ils participent au nettoyage des débris cellulaires et à la production de cytokines/chimiokines promouvant l'infiltration de macrophages. Il a été récemment proposé que la principale voie d'entrée des lymphocytes dans le tissu lésé ne serait pas la voie transendothéliale nommée précédemment, mais à travers les plexus choroïdes (Llovera et al., 2017). En effet dans l'étude de Llovera et collaborateurs, la photothrombose des plexus choroïdes provoquait une diminution du nombre de lymphocytes infiltrés dans le tissu lésé 5 jours après l'ischémie cérébrale.

Les monocytes circulants vont être recrutés à des phases tardives au même titre que les lymphocytes (Garcia-Bonilla et al., 2016; Wattananit et al., 2016). Ils vont permettre le nettoyage des débris cellulaires et la réparation tissulaire. Empêcher la venue des macrophages ne semble pas bénéfique dans le cadre de l'AVC ischémique, du moins dans les modèles expérimentaux.

#### *d. Réparation tissulaire et cicatrice gliale*

La réparation tissulaire comprend la neurogenèse, la formation de nouvelles dendrites (dendritogenèse), la prolifération d'oligodendrocytes ainsi que le renouvellement de la matrice extracellulaire (Peruzzotti-Jametti et al., 2014). La réparation tissulaire fait intervenir les astrocytes, dont l'expression de la protéine acide fibrillaire gliale (ou GFAP pour *glial fibrillary acid protein*) augmente fortement. Cette protéine sert de matrice/soutien aux cellules nouvellement formées. D'autres molécules sont également fortement exprimées lors de la réparation tissulaire : c'est par exemple le cas des molécules de la matrice extracellulaire comme les protéoglycans chondroïtine-sulfate (ou CSPG pour *chondroitin-sulfate proteoglycans*).

En plus de la réparation du tissu cérébral, il y a également formation de nouveaux vaisseaux sanguins : c'est l'angiogenèse. Cette angiogenèse est médiée par l'immunité innée, et notamment par les monocytes/macrophages (Liu et al., 2016). De plus, les macrophages, ainsi que la microglie, produisent des cytokines anti-inflammatoires comme le TGF- $\beta$  et de l'IL-10, suite à la

phagocytose des débris cellulaires (Denes et al., 2007; Schilling et al., 2005). Le TGF- $\beta$  va supprimer l'inflammation en inhibant la production de lymphocytes *helper* tout en facilitant le recrutement de lymphocytes mémoire (Taylor et al., 2006). L'IL-10 est produite par les cellules immunitaires, et notamment par les lymphocytes mémoire : elle a des propriétés neuroprotectrices et également anti-inflammatoires (Liesz et al., 2009).

## IV. Les différents modèles expérimentaux d'AVC

**Il est très important de noter que, historiquement, deux modèles ont été utilisés dans la recherche préclinique sur les AVC : ce sont les modèles d'occlusion mécanique de l'ACM (transitoire ou permanente), ou bien l'occlusion permanente par électrocoagulation de l'ACM. C'est donc grâce à ces modèles que beaucoup de cibles thérapeutiques ont été identifiées. Malheureusement, mis à part le tPA, aucun traitement testé jusqu'à aujourd'hui n'a montré un clair effet bénéfique en clinique, malgré des résultats prometteurs mis en évidence dans la recherche préclinique. Au vue de cet échec dans la translation vers la clinique, d'autres modèles expérimentaux ont été développés dans les dernières années : les modèles thromboemboliques par photothrombose et le modèle thrombine en sont les principaux.**

### 1. Modèle monofilament

Ce modèle consiste en l'insertion d'un filament de nylon dans la carotide interne, que l'on fait remonter jusqu'au niveau de la bifurcation de l'ACM, qui est alors occlue à sa base. Le temps d'occlusion peut être soit transitoire et varier de 30 minutes à 90 minutes (Gelderblom et al., 2009; Zhou et al., 2013), soit le filament peut être laissé de manière permanente (Chu et al., 2014; Pedragosa et al., 2018). Généralement la lésion comprend le cortex, le thalamus et le striatum, ce qui correspond à un volume de lésion important (entre 40 et 70mm<sup>3</sup>).

Dans les cas d'occlusion transitoire, ce modèle induit une réaction inflammatoire assez légère, qui se traduit par une infiltration mineure de leucocytes à des temps tardifs et une légère, voire

une absence dans certains cas (Gelderblom et al., 2009), de réactivité des cellules microgliales (Zhou et al., 2013).

Dans une étude utilisant le modèle monofilament, il a été montré que l’occlusion permanente de l’ACM (le monofilament a été laissé sur place) entraînait une aggravation de la réaction inflammatoire comparativement à une occlusion transitoire (1 heure) (Figure 23).

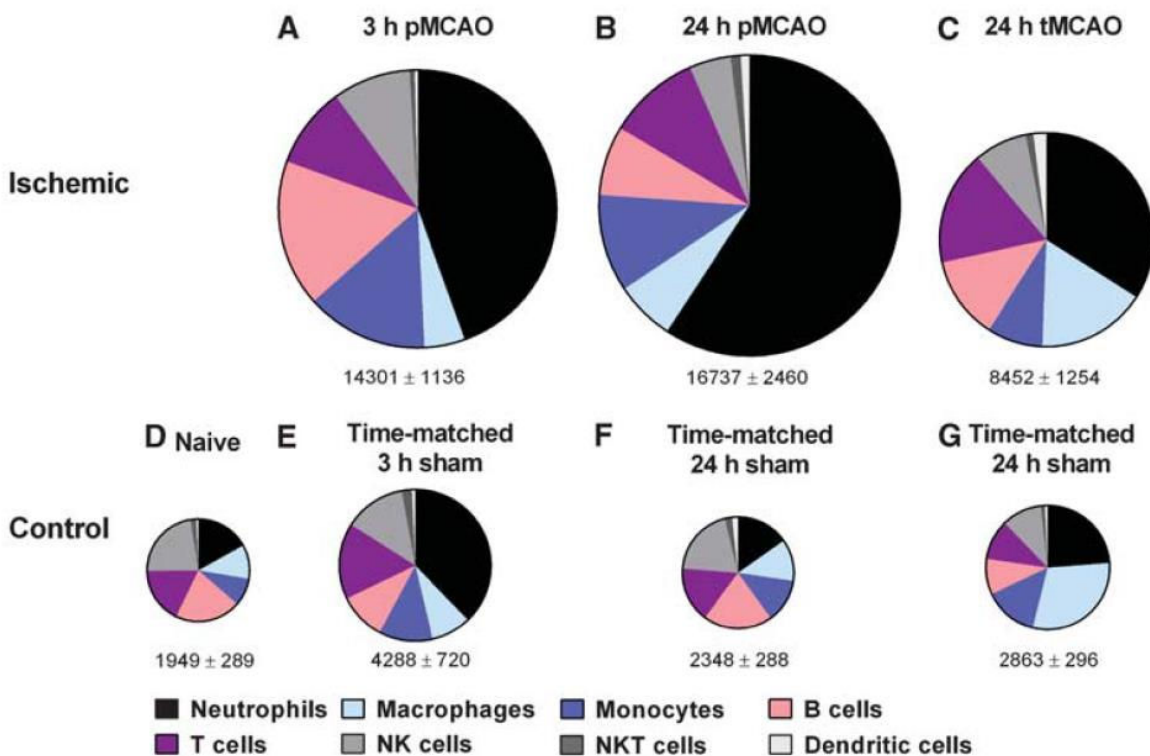


*Figure 23 : Inflammation cérébrale après l’occlusion (transitoire ou permanente) de l’ACM dans le modèle monofilament, (A) 3h, (B) 24h après occlusion permanente, et (C) 24h après occlusion transitoire (1h) de l’ACM. (D) souris contrôle, (E-G) souris témoin-opérées. D’après (Chu et al., 2014).*

Toutefois, il est important de noter que dans ce modèle, la fibrinolyse par tPA est délétère, ce qui ne correspond pas à la réalité clinique (Wang et al., 1998). De plus, il a été démontré que 70% du volume de lésion est dû en fait à la formation de microthromboses secondaires au retrait du monofilament (Gauberti et al., 2014; Pham et al., 2010) (Figure 24).

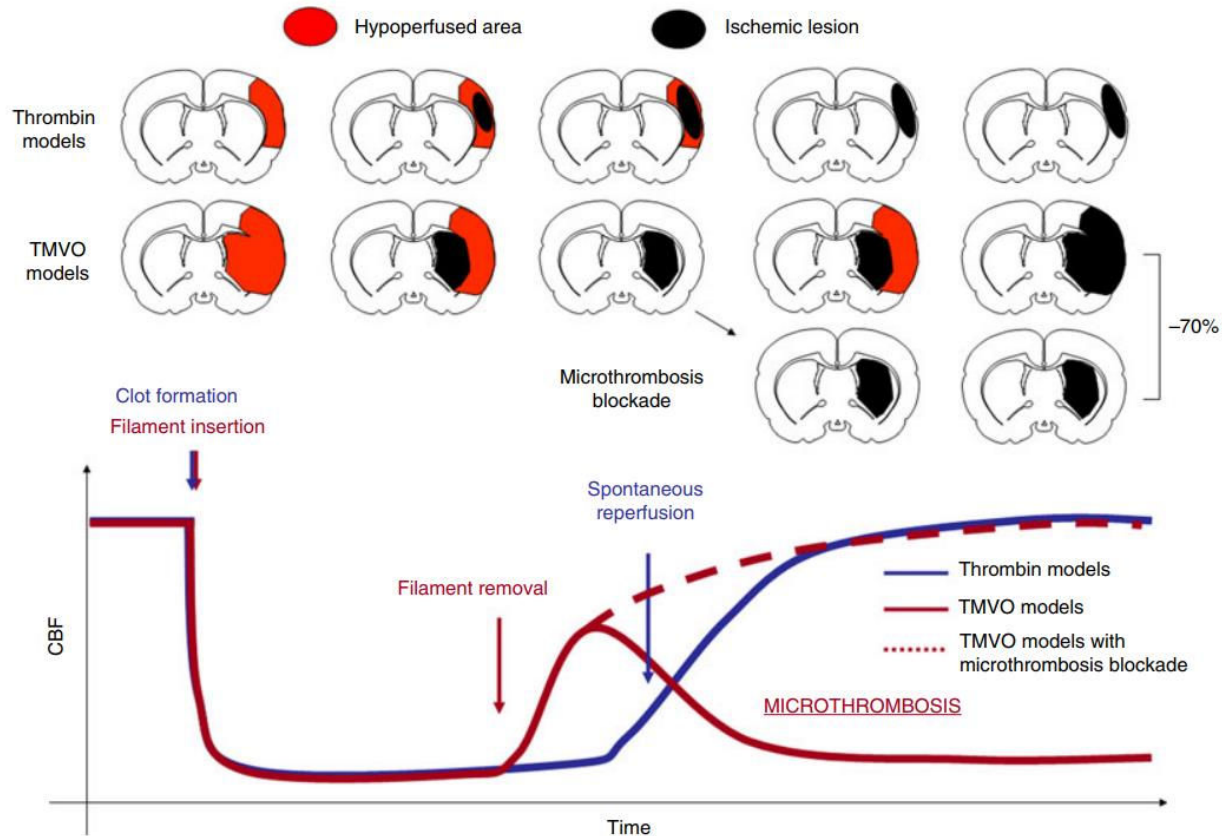


Figure 24 : Les microthromboses secondaires sont responsables de 70% du volume de lésion final dans le modèle monofilament. Il n'y a pas de microthrombose secondaire dans le modèle thrombine D'après (Gauberti et al., 2014).

Il faut noter que lors de la rétraction du filament, les phénomènes inflammatoires observés peuvent être associés aux phénomènes d'ischémie/reperfusion, et non pas *stricto sensu* à la mort neuronale induite par l'ischémie. Il paraîtrait cohérent d'associer ce modèle (transitoire) à la thrombectomie mécanique, puisque lors des deux pratiques un filament est inséré de manière transitoire. De plus, la thrombectomie mécanique induit également une reperfusion immédiate et brutale. Toutefois il n'a pas été montré chez les patients d'effet délétère de la reperfusion, ce qui est probablement dû à une meilleure circulation collatérale et à la présence d'anastomoses, et aussi la taille de la lésion, plus petite proportionnellement chez l'humain par rapport aux souris.

## 2. Modèle d'electrocoagulation

Ce modèle consiste en l'occlusion permanente de l'ACM à l'aide de forceps situés de part et d'autre de l'ACM. Une stimulation électrique provoque l'electrocoagulation de l'ACM, puis l'ACM est coupée pour éviter toute récanalisation éventuelle. Une craniotomie est nécessaire afin de découvrir l'ACM. Ce modèle expérimental n'induit pas de présence de zone péri-lésionnelle. La lésion est plus petite que dans le modèle de monofilament (autour de 25mm<sup>3</sup>), et se cantonne à la zone corticale (). La réaction inflammatoire décrite dans ce modèle est en revanche plus importante que dans le modèle monofilament, en termes de nombre de cellules immunitaires infiltrées, et aussi en termes de réaction des cellules microgliales (Zhou et al., 2013). Cette réaction inflammatoire est aussi exacerbée lorsque l'on regarde le niveau d'expression des cytokines pro-inflammatoires comme l'IL-1, de TNF, d'IFN ainsi que des molécules d'adhésion comme ICAM-1 et VCAM-1 (Zhou et al., 2013).

L'étude de Zhou et collaborateurs montre qu'il ne semble pas y avoir de corrélation entre volume de lésion et réaction inflammatoire dans les modèles expérimentaux : la réaction inflammatoire est plus importante dans le modèle d'électrocoagulation que dans le modèle monofilament, alors que le volume de lésion est plus important dans le modèle monofilament (Zhou et al., 2013) (Figure 25). Ceci suggère que **la réaction inflammatoire n'a pas l'air de dépendre du volume de lésion, mais plutôt du modèle expérimental d'AVC utilisé.**

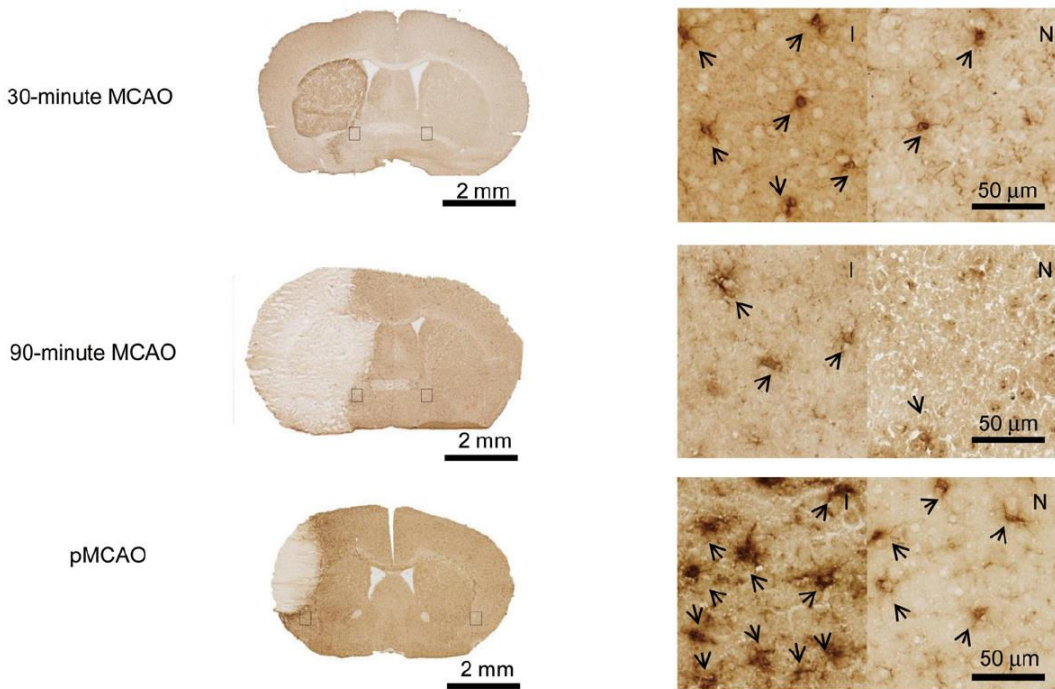


*Figure 25 : Absence de corrélation entre volume de lésion et réaction inflammatoire. Le marqueur Iba1 (microglie) montre une forte augmentation du nombre de cellules microgliales dans le modèle d'électrocoagulation du côté ipsilatéral, qui est plus faible dans le modèle transitoire d'occlusion par monofilament. D'après (Zhou et al., 2013).*

Il est également possible que l'absence de reperfusion dans le modèle d'électrocoagulation soit responsable de l'augmentation de la réaction inflammatoire. Dans cette idée, il est intéressant de noter qu'une étude d'occlusion mécanique permanente de l'ACM (où le monofilament est laissé sur place de façon permanente), a montré une aggravation de la réaction inflammatoire comparativement à une occlusion transitoire (1 heure), avec cette fois-ci une lésion plus importante chez les animaux dont l'ACM a été occlue de façon permanente (Chu et al., 2014).

### 3. Modèle de photothrombose

L'ischémie par photothrombose repose sur le principe d'un composé chimique, le rose Bengal, qui réagit à la lumière, et forme un caillot lorsque la source de lumière se situe sur le bord du crâne, tandis que le rose Bengal a préalablement été injecté par voie intraveineuse. Cette manipulation induit un AVC de petite taille (autour de  $10-15\text{mm}^3$ , selon la zone illuminée), sans

apparition de zone péri-lésionnelle. Il a été montré dans ce modèle qu'il y avait infiltration de monocytes (préalablement marqués avec des USPIO pour *ultrasmall particles of iron oxyde*) en IRM (Oude Engberink et al., 2008), ainsi qu'une infiltration de lymphocytes et d'une augmentation du niveau de cytokines pro-inflammatoires jusqu'à 14 jours après la survenue de l'AVC (Feng et al., 2017).

#### 4. Modèles thromboemboliques

Plusieurs modèles thromboemboliques existent. Un caillot préalablement formé (par du sang autologue ou hétérologue) peut être dirigé jusqu'à la base de l'ACM à l'aide d'un filament (Lehmann et al., 2014). Un caillot peut aussi se former en appliquant sur l'artère du chlorure de fer ou d'aluminium (Bonnard and Hagemeyer, 2015).

Un autre modèle d'ischémie thromboembolique a été développé dans notre laboratoire (Orset et al., 2007). La même approche est utilisée que dans le modèle d'électrocoagulation, mais cette fois-ci l'ACM n'est pas électrocoagulée mais, à l'aide d'une micropipette, de la thrombine est injectée directement dans l'ACM, provoquant ainsi localement la cascade de la coagulation et la formation d'un caillot riche en fibrine (Le Behot et al., 2014). L'ACM recanalise spontanément dans les 24 premières heures, et une lésion est d'ores et déjà établie dès 2h30 après la chirurgie (Lemarchand et al., 2015). A 24 heures, la lésion est majoritairement corticale et bien définie, ressemblant à une lésion obtenue par électrocoagulation de l'ACM. **La différence majeure entre les deux modèles est la présence d'une zone péri-lésionnelle dans le modèle thromboembolique, qui peut être sauvée par fibrinolyse au tPA (Orset et al., 2007, 2016).**

Durant ma thèse j'ai étudié la réaction inflammatoire de manière longitudinale dans ce modèle ; ces résultats font l'objet d'un article en cours de préparation (ETUDE 1).



## Résumé

De nombreuses études expérimentales se sont focalisées sur la réaction inflammatoire induite par l'AVC, afin d'identifier de potentielles cibles thérapeutiques visant à moduler la réaction inflammatoire (Macrez et al., 2011). Le fait est que dans tous les modèles expérimentaux existe une réaction inflammatoire. Cependant, la réaction inflammatoire varie en termes d'acteurs, de cinétique et d'amplitude de la réponse inflammatoire en fonction du modèle expérimental utilisé.

Lorsque l'on synthétise l'ensemble de résultats obtenus en préclinique, trois concepts semblent émerger :

- L'occlusion permanente de l'ACM par electrocoagulation induit une forte réaction inflammatoire
- Le modèle d'occlusion mécanique (transitoire ou permanente) de l'ACM provoque une réponse inflammatoire moins forte que le modèle d'electrocoagulation
- La réaction inflammatoire n'est pas forcement proportionnelle au volume de lésion : la lésion est de grande taille dans le modèle d'occlusion mécanique transitoire, alors que la réaction inflammatoire est faible.



## 5. Existe-t-il une réponse inflammatoire chez les patients atteints d'AVC ?

Comme il a été précédemment décrit, la survenue d'un AVC induit indubitablement une réponse inflammatoire cérébrale, du moins chez l'animal. Même s'il manque clairement des données démontrant l'existence d'une réaction inflammatoire post-AVC chez l'humain, et même suite aux nombreux échecs des stratégies thérapeutiques visant à moduler la réaction inflammatoire, de nombreux indices, dont des échantillons humains post-mortem, font entrevoir l'existence d'une telle réaction chez l'humain. Par exemple, CD68, un marqueur de phagocytose, est surexprimé post-AVC chez l'humain, comme l'indiquent des coupes de cerveau post-mortem (Rodhe et al., 2016).

De nouvelles avancées en termes d'imagerie permettent d'imager la neuroinflammation chez l'humain. La tomographie par émission de positons (TEP) permet la détection de l'activation microgliale *via* la fixation d'un radiotraceur aux mitochondries exprimées par les cellules microgliales en cas d'activation (Liu et al., 2014). Plus précisément, les radiotraceurs vont se lier au TSPO (pour *translocator protein*) exprimé à la surface des mitochondries des cellules microgliales, uniquement et spécifiquement lors d'un état d'activation. Le TSPO n'étant pas ou infiniment peu exprimé à l'état basal, il permet de marquer spécifiquement l'inflammation puisqu'il est fortement exprimé suite à l'activation microgliale (Liu et al., 2014) (Figure 26).

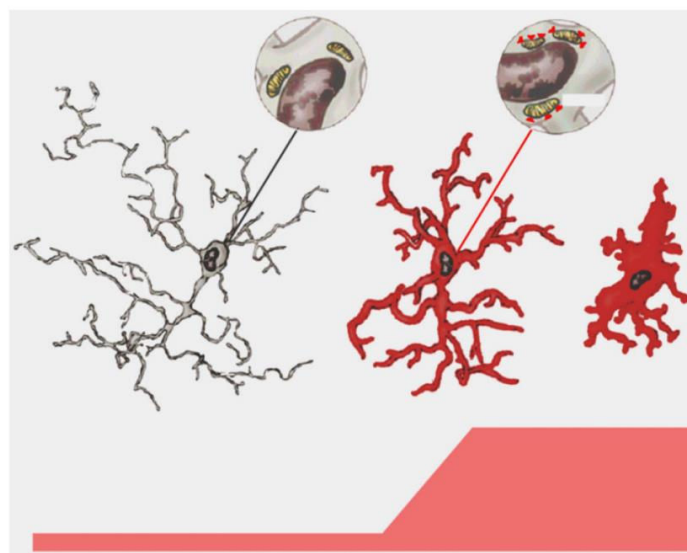


Figure 26 : Le TSPO est surexprimé par les cellules microgliales suite à leur activation. D'après (Liu et al., 2014).

Dès lors, de nombreux radiotraceurs ont vu le jour, dont les plus connus sont le [<sup>14</sup>C]-PK11195 et le [<sup>18</sup>F]-DPA. Cette perspective a permis la visualisation de l'activation microgliale dans l'AVC chez l'humain (Price et al., 2006; Thiel and Heiss, 2011; Weinstein et al., 2010) (Figure 27).

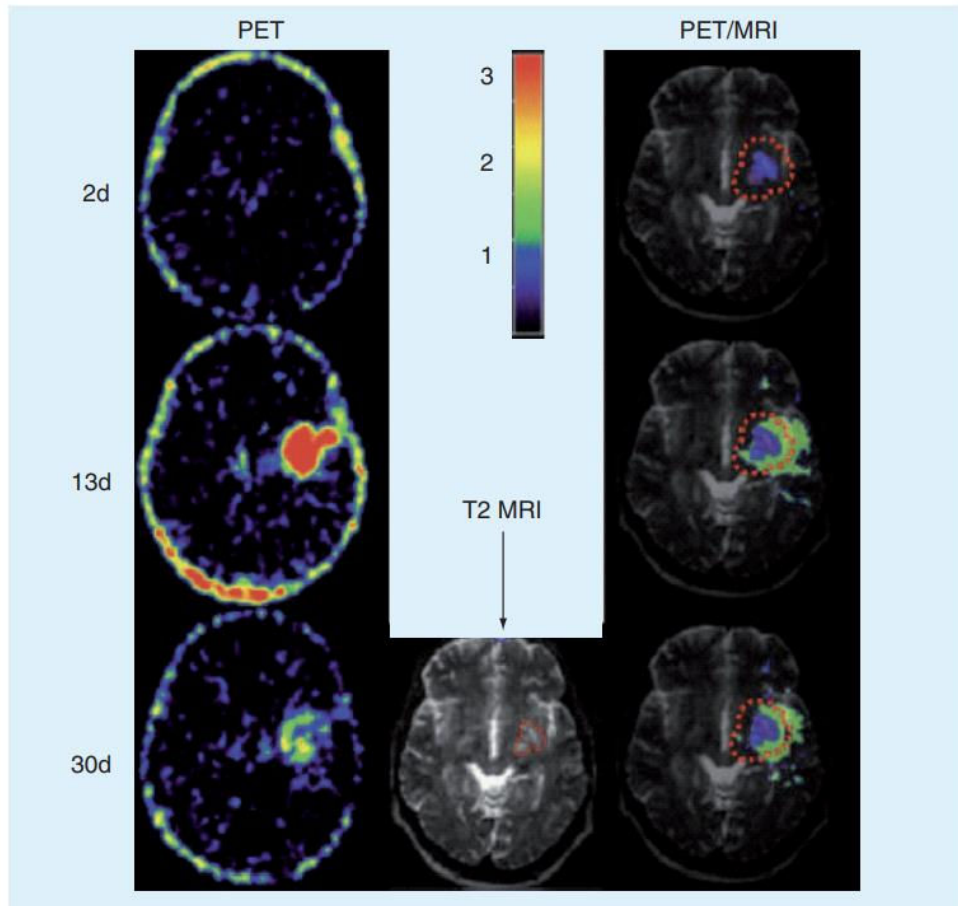


Figure 27 : Imagerie TEP de l'activation microgliale 2, 13 et 30 jour après un AVC chez l'humain. Ici, le radiotraceur utilisé est le [<sup>14</sup>C]-PK11195. D'après (Weinstein et al., 2010).

En plus de l'activation microgliale, des cellules immunitaires provenant de la circulation sanguine sont capables de traverser la BHE, et infiltrer le tissu cérébral en souffrance. Des neutrophiles infiltrés ont d'ailleurs été retrouvés chez des patients ayant subi un AVC au niveau de la zone infarcie (Perez-de-Puig et al., 2015), ainsi que des lymphocytes (Doyle et al., 2015).

## 6. Vers de nouvelles thérapies pour l'AVC : traitements ciblant la réponse inflammatoire

### a. Traitements ciblant les effets de l'IL-1

Une méta-analyse a montré que l'administration d'IL-1-RA, un récepteur antagoniste de l'IL-1, était associée avec une diminution du volume de lésion (Banwell et al., 2009). Néanmoins, un essai clinique de phase II n'a montré aucun effet bénéfique de l'administration sous-cutanée d'IL1-RA sur la récupération post-AVC (Smith et al., 2018).

### b. Traitements ciblant les cellules microgliales

Une étude a montré que la lésion ischémique était significativement plus importante chez des souris dont les cellules microgliales ont été déplétées que chez des souris contrôles ischémierées, traduisant un effet global protecteur des cellules microgliales dans l'AVC ischémique (Szalay et al., 2016).

Des études ont montré que faire varier le phénotype microglial du stade pro- au stade anti-inflammatoire pouvait être protecteur dans le cadre de l'ischémie cérébrale. La minocycline est un antibiotique capable de détruire les cytokines/chimiokines pro-inflammatoires ainsi que les caspases responsables de la mort neuronale par apoptose (Morimoto et al., 2005; Wang et al., 2002; Xu et al., 2004). Dès lors, cette molécule agit sur le phénotype microglial en penchant la balance du côté anti-inflammatoire. Il a aussi été montré qu'il était possible de *switcher* la microglie de phénotype pro-inflammatoire vers un état anti-inflammatoire en injectant de l'IL-33 (une cytokine anti-inflammatoire) dans les ventricules cérébraux (Yang et al., 2017). [Durant ma thèse j'ai d'ailleurs rédigé un commentaire dans le \*Journal of Neurosciences\* sur cette étude \(Drieu et al., 2017\)](#).

En clinique, deux études cliniques ont suggéré que la minocycline pouvait être une cible thérapeutique envisageable car elle n'entraînait pas d'effets indésirables dans le cadre de l'AVC ischémique (Lampl et al., 2007; Padma Srivastava et al., 2012), toutefois son effet bénéfique sur

le volume de lésion ischémique n'a pas encore été démontré à grande échelle (Kohler et al., 2013).

*c. Traitements ciblant les macrophages résidents*

Le rôle des autres macrophages résidents du cerveau (à savoir les PVM, les CPM et les MM) dans le cadre de l'ischémie cérébrale sont peu connus. Toutefois, une très récente étude a montré que leur déplétion par injection intracérébroventriculaire de liposomes contenant du clodronate permettait une diminution des facteurs de chimiotactisme et une diminution de l'infiltration de neutrophiles granulocytes, et ce malgré une absence d'effet sur le volume de lésion dans un modèle d'occlusion permanente par monofilament (Pedragosa et al., 2018).

*d. Traitements ciblant l'activation endothéiale et l'infiltration des leucocytes*

Beaucoup d'études ont ciblé les CAM dans le cadre de l'AVC et ont même mené à des essais cliniques. Aucun changement de volume de lésion ischémique n'a été retrouvé chez des souris déficientes en P-sélectine comparativement à des souris sauvages, et ce malgré une protection de la BHE et une réduction drastique du nombre de neutrophiles infiltrés chez les souris déficientes en P-sélectine (Jin et al., 2010). Aucun changement de volume de lésion n'a non plus été retrouvé chez des souris déficientes en ICAM-1 (Enzmann et al., 2018). Un anticorps ciblant ICAM-1, l'enlimomab, a montré des effets bénéfiques sur le volume de lésion et l'adhésion leucocytaire dans des modèles expérimentaux (Bowes et al., 1995) ; toutefois il n'a pas d'effet bénéfique en clinique, il aurait même des effets délétères (Enlimomab Acute Stroke Trial Investigators, 2001).

De manière intéressante, le blocage de l'adhésion des neutrophiles via l'utilisation d'un anticorps anti CD11/CD18 a montré des effets bénéfiques sur le volume de lésion seulement dans un modèle expérimental d'ischémie transitoire (Prestigiacomo et al., 1999), et non dans les modèles d'ischémie permanente (Garcia et al., 1996; Jiang et al., 1998).

Certaines études relatent d'une augmentation du volume de lésion en cas de déplétion en lymphocytes (Liesz et al., 2009, 2013), tandis qu'une autre étude a montré une diminution du volume de lésion (Kleinschnitz et al., 2013). Il a été montré dans plusieurs études qu'une diminution du nombre de lymphocytes circulants était protectrice dans des modèles expérimentaux d'AVC ischémique (Becker et al., 2001; Liesz et al., 2011; Neumann et al., 2015). Dans une autre étude, une diminution du nombre de lymphocytes infiltrés n'a pas montré d'influence sur le volume de lésion (Llovera et al., 2017). Au niveau clinique, le fingolimod, une molécule qui inhibe la transmigration des lymphocytes dans le tissu cérébral et qui est déjà utilisée dans la sclérose en plaques, a fait l'objet d'essais cliniques dans le cadre de l'AVC (Zhu et al., 2015). Dans cette étude, les patients ayant été traités au fingolimod en association avec le tPA ont des lésions plus petites, une inflammation réduite et une meilleure récupération à 90 jours comparés aux patients traités au tPA seulement. Un essai clinique de phase II utilisant le fingolimod en combinaison avec le tPA est en cours.

Une étude visant à dépléter les monocytes circulants n'a montré aucun effet sur le volume de lésion ischémique (Schmidt et al., 2017). De manière intéressante, une récente étude a montré qu'un transfert adoptif de monocytes de souris préconditionnées à une faible dose de lipopolysaccharides (LPS) était neuroprotecteur chez des souris naïves subissant un AVC, démontrant ainsi i) un rôle potentiel des monocytes dans le devenir de l'AVC ischémique (Garcia-Bonilla et al., 2018) et ii) un rôle du phénotype inflammatoire des cellules immunitaires circulantes dans l'AVC ischémique.

L'essai clinique ACTION, qui consiste en l'administration de natalizumab, une molécule empêchant l'adhésion des leucocytes à la paroi des vaisseaux sanguins, n'a pas montré de réduction du volume de lésion. Cette étude a toutefois été récemment reconduite dans le cadre d'un autre essai clinique ACTION II, visant à étudier l'effet du natalizumab sur la récupération fonctionnelle post-AVC.

Pendant ma thèse, j'ai participé à la rédaction d'une revue sur les traitements immunomodulateurs pour le traitement de l'AVC, qui a été récemment publiée dans *Therapeutic Advances in Neurological Disorders* (Drieu et al., 2018).

## 7. Les facteurs de risque d'AVC

Il est intéressant de noter que le statut inflammatoire pré-AVC (comme par exemple des patients ayant une infection systémique) est à la fois un facteur de risque de faire un AVC et également un potentiel facteur aggravateur sur le devenir de l'AVC, comme par exemple l'exacerbation du volume de lésion (Macrez et al., 2011). Il est également important de noter que 90% des AVC sont associés aux 10 principaux facteurs de risque de faire un AVC (Figure 28) (O'Donnell et al., 2010).

Hypercholestéromie	<b>2</b>
Sténose carotidienne asymptomatique	<b>2</b>
Diabète	<b>1,8-6</b>
Excès de poids	<b>1,8-2,4</b>
Alcool >5verres/jours	<b>1,6-2,4</b>
Nicotine/Tabac	<b>1,5-3</b>
Hypertension Artérielle	<b>1,4-4</b>
Substitution hormonale post ménopause	<b>1,4</b>

Figure 28 : tableau représentatif des principaux facteurs de risque de faire un AVC.

Les facteurs de risque de faire un AVC peuvent être rangés en deux catégories. Les facteurs non modifiables sont l'âge, le genre, l'éthnie, et l'historique familial. Les facteurs modifiables sont l'hypertension artérielle chronique, les maladies cardiaques, le diabète, ainsi que la cigarette ou la consommation d'alcool (Deoke et al., 2012; Siegler et al., 2013).

## 4. Cas particulier de la consommation d'alcool

Il faut noter que la consommation d'alcool est en effet un cas particulier. Une consommation modérée d'alcool (entre 1 et 4 verres par jour) diminue le risque de faire un AVC, tandis qu'une consommation plus importante (supérieure à 5 verres par jour) augmente le risque de faire un AVC. La relation entre consommation d'alcool et risque d'AVC ischémique suit donc une allure de courbe en J (Sacco et al., 1999) (Figure 29).

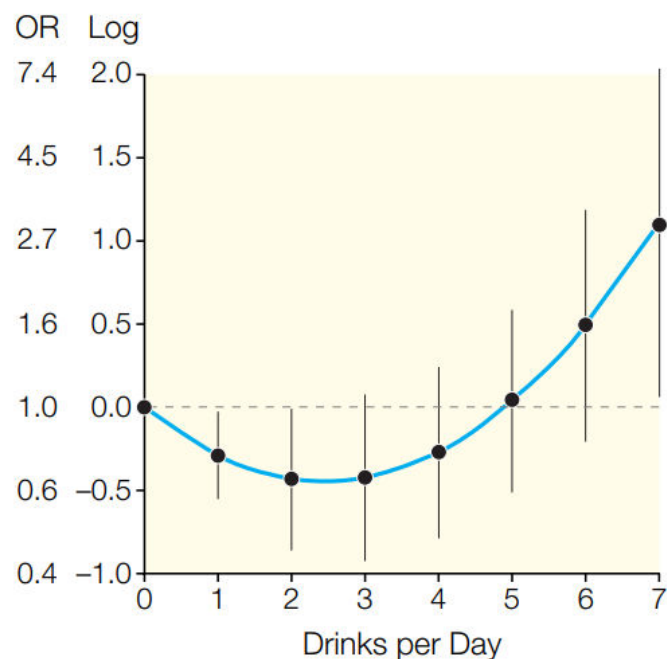
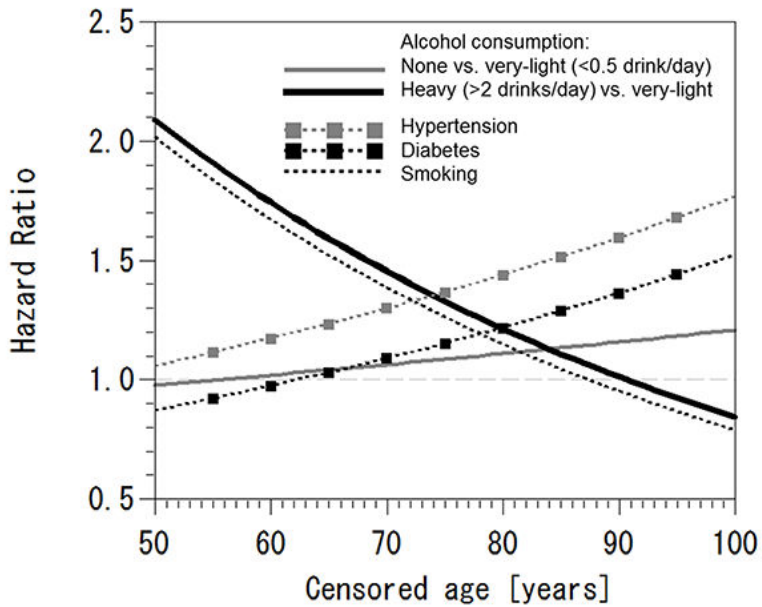


Figure 29 : Relation entre consommation d'alcool et risque de faire un AVC. D'après (Sacco et al., 1999)

Il a été récemment publié une méta-analyse réalisée sur plus de 11000 jumeaux où il est montré un important effet âge dans le risque d'AVC : avant 75 ans, la consommation de plus de 2 verres d'alcool par jour augmente le risque d'AVC de manière plus importante que l'hypertension et le diabète, et diminue de 5 ans l'âge moyenne des victimes d'AVC (Figure 30) (Kadlecová et al., 2015).



*Figure 30 : Variation du poids de divers facteurs de risque d'AVC (consommation d'alcool, hypertension et diabète) en fonction de l'âge. D'après (Kadlecová et al., 2015).*

De manière intéressante, en plus d'être un facteur de risque de faire un AVC, la consommation d'alcool peut aggraver les lésions : une étude a d'ailleurs démontré cet effet aggravateur de l'alcool chez l'homme (Ducroquet et al., 2013). Une étude réalisée dans notre laboratoire a montré que la consommation d'alcool était responsable de l'augmentation du volume de lésion ischémique chez la souris (Lemarchand et al., 2015) (Figure 31). De plus, dans cette étude, il a été montré que la thrombolyse par tPA n'était plus bénéfique sur le volume de lésion chez les souris chroniquement exposées à l'alcool, ceci ayant été attribué à un déficit de sa clairance par le foie (Lemarchand et al., 2015).

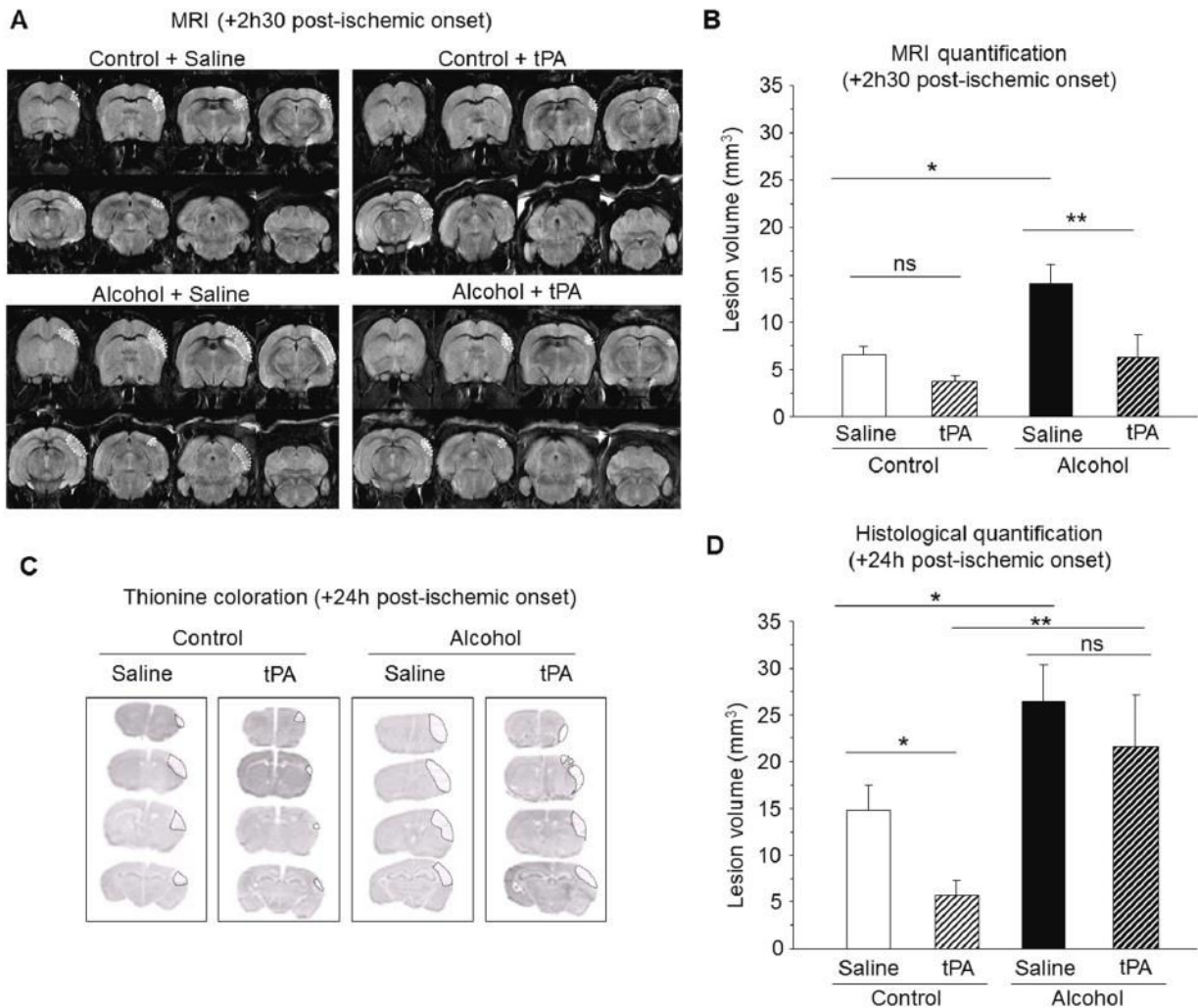


Figure 31 : L'exposition prolongée à l'alcool aggrave les lésions ischémiques chez la souris. (A) IRM représentatives 2h30 après la survenue de l'AVC chez des animaux contrôles ou exposés chroniquement (6 semaines) à l'alcool, avec ou sans traitement au tPA. (B) Quantification du volume de lésion 2h30 après l'AVC. (C) Coloration à la thionine 24h après l'AVC. (D) Quantification du volume de lésion 24h après l'AVC. D'après (Lemarchand et al., 2015).

Suite à cette étude, nous avons voulu comprendre en quoi l'exposition prolongée à l'alcool pouvait contribuer à l'augmentation du volume de lésion. Pour cela, nous avons réalisé une étude translationnelle focalisée sur la réponse inflammatoire pré et post-ischémique chez des patients et des rongeurs (**étude n°3**). Cette étude est actuellement en cours de soumission.

## I. Généralités

### 1. Historique

La dépendance à l'alcool existe depuis que l'alcool existe. Et l'alcool existe depuis... longtemps. Dans l'Egypte ancienne, le hiéroglyphe « repas » était représenté par du pain et de la bière ; l'alcool était d'ailleurs considéré comme la boisson des dieux. Les sumériens brassaient leur bière (4<sup>ème</sup> millénaire avant JC), qui s'appelait *sikaru* (pain liquide). L'alcool était par ailleurs monnaie d'échange dans certains pays (contre des esclaves par exemple). On peut citer comme autre fait historique le fait que Dionysos était considéré comme le dieu de l'ivresse (de la vigne, du vin et ses excès) ou plus récemment, qu'Attila est mort des suites d'un syndrome de Mallory-Weiss (une perforation de la paroi au niveau de la jonction entre l'œsophage et l'estomac, dont la cause principale de survenue est la consommation chronique d'alcool). L'alcoolisation de masse apparaît en même temps que la révolution industrielle (et des transports) au cours du 19<sup>ème</sup> siècle. Ce n'est que vers la fin du siècle qu'il n'est pas bien vu d'être en état d'ivresse en public. En France, un décret établi en 1956 change le verre d'alcool donné pendant les repas au collège contre un verre de lait sucré.

Les troubles associés à une consommation excessive d'alcool ont déjà été explorés dans l'Histoire. Le grec Agapios a décrit ces états en 1647, qui associe la toxicité de l'alcool à des troubles du système nerveux et du corps dans son intégralité, comprenant des crises d'épilepsie et des hémorragies internes. Christoph Hufeland (1762-1836) parle lui de dipsomanie (*dipso* veut dire soif en grec), et non pas d'alcoolisme (1819). Certaines associations américaines anti-alcools voient le jour dès le milieu du 16<sup>ème</sup> siècle : elles répondent au nom de ligue de tempérance. Le mouvement prit de l'ampleur au 19<sup>ème</sup> siècle. En 1826 fut fondée la société américaine de tempérance, visant à promulguer la modération de la prise d'alcool. Puis le mouvement changea et revendiquait cette fois-ci non pas une modération mais une prohibition de la prise d'alcool. En 1855, 12 Etats étaient « secs », où une loi (loi du Maine et 1851) interdisait la vente d'alcool excepté pour raison médicale. Le 18<sup>ème</sup> amendement des Etats-Unis est validé, où il est introduit la prohibition de la production et vente de boissons alcoolisées. Cet amendement a pour conséquence une marginalisation du commerce de l'alcool (ou marché noir de l'alcool). Al Capone a par exemple bien profité du marché noir de l'alcool pour s'enrichir (à Chicago autour des années 1920). C'est en 1933 sous l'égide du Président Roosevelt que le 21<sup>ème</sup> amendement a été déposé, qui a eu pour but d'abroger le 18<sup>ème</sup> amendement et donc d'autoriser la consommation d'alcool. Pour l'anecdote, c'est le seul amendement de la constitution des Etats-Unis qui a abrogé un amendement préexistant.

Il est important de noter que jusqu'au milieu du 20<sup>ème</sup> siècle, l'espérance de vie était faible, et donc on ne connaissait pas l'impact de la consommation à long terme de l'alcool chez l'individu. C'est avec l'amélioration des conditions de vie et donc parallèlement de l'augmentation de l'espérance de vie que le mésusage de l'alcool a pris de l'ampleur et est devenu un phénomène de société : c'est la deuxième cause de décès évitable en France après la consommation de tabac.

### 2. Quelques chiffres

D'après l'OMS, le mésusage de l'alcool est responsable de 3,3 millions de morts par an (ce qui correspond à environ 6% des décès). Dans le monde une personne âgée de plus de 15 ans consomme en moyenne 6,2L d'alcool pur par an. Toutefois « seulement » 38% de la population mondiale consomme de l'alcool : donc les consommateurs boivent environ 17L d'alcool pur par an en moyenne. Le nombre est sûrement sous-estimé puisqu'environ 25% de la consommation

d'alcool n'est pas mesurée (car la consommation à la maison et le marché noir ne sont pas comptabilisés). Toujours d'après l'OMS, 16% des personnes âgées de plus de 15 ans sont considérées comme ayant un trouble de mésusage de l'alcool.

## II. Consommation d'alcool et inflammation

### 1. Inflammation systémique

Il est d'ores et déjà établi que la consommation d'alcool engendre un statut inflammatoire systémique, notamment au niveau hépatique (Farkas and Kemény, 2013; Louvet and Mathurin, 2015). Il a également été montré que les atteintes hépatiques pouvaient avoir des répercussions cérébrales (D'Mello and Swain, 2017). Des auteurs ont d'ailleurs montré que des patients atteints d'hépatite C montraient des signes dépressifs ainsi qu'une élévation du taux plasmatique de cytokines pro-inflammatoires telles que l'IL-1 $\beta$  et le TNF (Loftis et al., 2008). L'encéphalopathie hépatique est une maladie se traduisant par une inflammation systémique et par une augmentation importante de la concentration plasmatique en ammoniac (hyperammonémie) induisant une intoxication cérébrale et la formation d'un œdème cytotoxique accompagné d'une augmentation de la pression intracrânienne (Felipo, 2013). De manière intéressante de nombreuses pathologies hépatiques, dont certaines, précédemment citées, peuvent découler d'une consommation chronique d'alcool (Beier and McClain, 2010).

Un des mécanismes proposé est que l'alcool dégrade la paroi intestinale, ayant pour conséquence une translocation du LPS vers la circulation sanguine. Des études ont d'ailleurs démontré cette hypothèse chez la souris (Yan et al., 2011), ainsi que chez l'humain (Leclercq et al., 2014). Le LPS est capable d'interagir avec les PRR (les récepteurs de reconnaissance de motifs moléculaires) des macrophages résidents du foie : les cellules de Kupffer. Ces cellules vont alors produire des cytokines pro-inflammatoires, *via* la voie NF- $\kappa$ B, passant dans le cerveau et induire une cascade inflammatoire responsable des dommages cérébraux (Miller et al., 2005). Il est d'ores et déjà prouvé qu'une inflammation systémique pouvait entraîner une réponse inflammatoire cérébrale, qui peut d'ailleurs perdurer. Une étude a montré qu'une seule injection intrapéritonéale de LPS

induisait une augmentation du taux de TNF au niveau sanguin, hépatique et cérébral. De manière intéressante, la concentration de TNF cérébral (et pas sanguine ni hépatique) reste augmentée jusqu'à 10 mois après l'injection de LPS (Qin et al., 2007) (Figure 32).

On peut alors penser que l'alcool, via la translocation de LPS de la paroi intestinale vers la circulation sanguine, peut induire une inflammation cérébrale chronique. Une étude a montré que l'injection intrapéritonéale de LPS induisait une ouverture de la BHE (Singh et al., 2007). Dans cette même étude, les auteurs ont aussi montré que la consommation chronique d'alcool seule induisait une ouverture de la BHE.

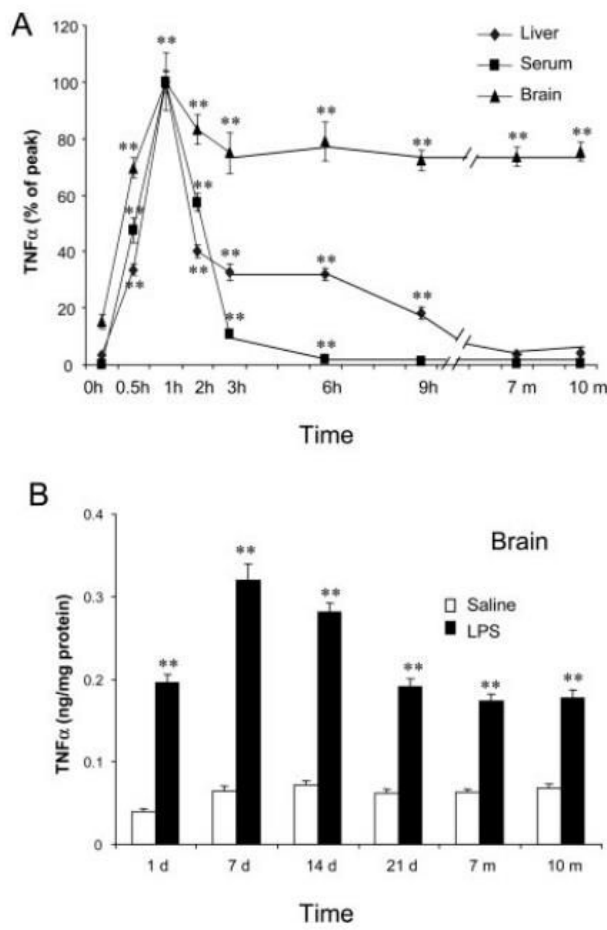


Figure 32 : Une seule injection intrapéritonéale de LPS (5mg/kg) entraîne une augmentation du taux de TNF dans le cerveau jusqu'à dix mois post-injection. (A) Pourcentage de TNF retrouvé dans le foie, le sérum et le cerveau de 30min à 10 mois après injection intrapéritonéale de LPS. (B) Concentration cérébrale de TNF dans le cerveau 1, 7, 14, 21 jours puis 7 et 10 mois après une seule injection intrapéritonéale de LPS ou de sérum physiologique (saline). D'après (Qin et al., 2007).

## 2. Inflammation cérébrale

La molécule d'éthanol étant très petite, et totalement miscible dans les solutions hydrophiles et lipophiles, elle peut aisément traverser la BHE, et avoir des effets directs sur le SNC. Tout comme pour les cellules de Kupffer hépatiques, l'alcool, *via* la voie NF-κB, va activer les cellules microgliales qui vont produire des cytokines et déclencher la réaction inflammatoire par la voie d'activation des récepteurs TLR4 (Alfonso-Loeches et al., 2010; Lippai et al., 2013a).

De manière intéressante, l'inflammation chronique, contrairement à un stress aigu, peut également amener à une production de cytokines anti-inflammatoires. Ainsi il a été montré par le groupe de Colm Cunningham que les cellules microgliales exprimaient significativement plus de TGF-β dans le contexte d'une inflammation chronique lors d'une maladie de prions (Cunningham et al., 2002). Dans cette idée, la microglie produit également plus de TGF-β dans un modèle murin de la maladie d'Alzheimer, sans pour autant produire plus de cytokines pro-inflammatoires (Gomez-Nicola and Perry, 2015). Dans un modèle expérimental d'alcoolisation prolongée, les cellules microgliales sont plus nombreuses, et produisent plus d'IL-1β, une cytokine pro-inflammatoire (Pradier et al., 2018). Cet effet est retrouvé après 6 mois d'exposition, et est accentué après 12 mois d'exposition à l'alcool (Figure 33).

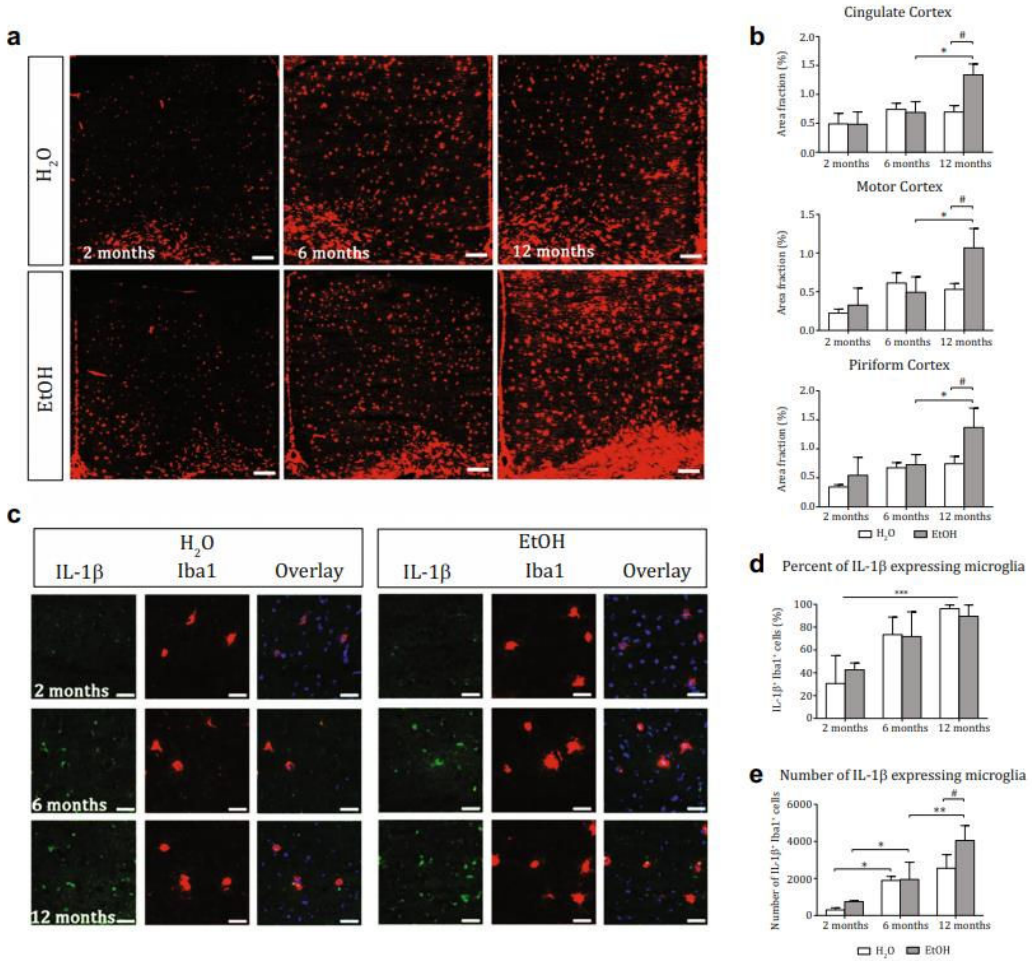


Figure 33 : Effet de la durée de consommation chronique d'alcool sur les cellules microgliales au niveau du cortex chez la souris. (A) Images représentatives de la microglie (marquée par Iba1 en rouge) chez des souris exposées à l'eau (groupe H<sub>2</sub>O) ou à l'alcool (groupe EtOH) pendant 2, 6 et 12 mois. (B) Quantification du nombre de cellules Iba1 positives dans le cortex cingulaire, moteur et pyriforme aux différents temps. (C) Images représentatives du comarquage IL-1 $\beta$  (en vert) et Iba1 (en rouge) dans les deux groupes et aux différents temps. (D) Pourcentage du nombre de cellules doublement positives pour IL-1 $\beta$  et Iba1 sur le nombre total de cellules Iba1 positives. (E) Quantification du nombre de cellules doublement positives pour IL-1 $\beta$  et Iba1. D'après (Pradier et al., 2018).

La voie TLR4 n'est pas la seule voie possible d'induction de neuroinflammation par la consommation d'alcool. L'inflammasome est une réponse intracellulaire induite par un stimulus inflammatoire, qui aboutit à l'activation de certains récepteurs spécifiques provenant de la famille des PRR, les NLR situés dans le cytoplasme des cellules immunitaires. Suite au stimulus ces récepteurs s'assemblent et s'oligomérisent pour donner le complexe de l'inflammasome. Son principal rôle est de favoriser la production de cytokines pro-inflammatoires par la cellule, via

notamment l'activation de la cascade de la caspase-1. Il a été montré que l'augmentation d'IL-1 $\beta$  au niveau cérébral après consommation chronique d'alcool était en fait due à une altération de l'inflamasome (Lippai et al., 2013b).

La consommation d'alcool semble également jouer un rôle dans la production de fractalkine par les neurones. En effet, l'alcool induirait une forte réduction de la production de fractalkine, entraînant *de facto* l'activation des cellules microgliales (Kane and Drew, 2016).

### III. Y-a-t-il une seule origine aux pathologies causées par l'alcool ?

Nous avons vu précédemment que l'exposition prolongée à l'alcool entraînait une inflammation à long terme au niveau cérébral. Toutefois, il est important d'ajouter que l'alcool ne touche pas que le cerveau. La prise chronique de l'alcool induit, en plus des dommages cérébraux, des dommages hépatiques (de la fibrose allant jusqu'à la cirrhose), rénaux, du tube digestif et des poumons. La défaillance de ces organes peut accentuer les dommages cérébraux et déclencher des pathologies : on peut citer par exemple l'encéphalopathie hépatique, qui est un cas courant chez les patients alcoolo-dépendants. On ne peut donc pas affirmer que la réaction inflammatoire provoquée dans les différents modèles d'exposition à l'alcool est seulement due aux effets directs de l'alcool sur le cerveau. Une étude a par exemple montré qu'une ligature du canal biliaire provoquant une inflammation hépatique, entraînait une activation des cellules microgliales, et une augmentation du nombre de leucocytes présents à la paroi des vaisseaux sanguins cérébraux (D'Mello et al., 2009, 2013).



## 5. L'inflammation dans le cadre des traumatismes crâniens

Nous avons voulu étudier les conséquences à long terme d'une réaction inflammatoire au niveau cérébral dans une autre pathologie ciblant uniquement le cerveau, à savoir le traumatisme crânien (TBI pour *traumatic brain injury*).

Après une revue de la littérature, nous nous sommes aperçus que la plupart des études expérimentales utilisaient des modèles animaux mimant des TBI sévères, qui, dans la plupart des cas, pouvaient entraîner une perte de tissu cérébral (Keskin et al., 2017) (Figure 34).

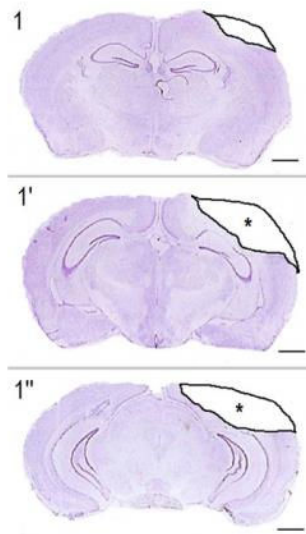


Figure 34 : Images représentatives de la perte de tissu cérébral après un TBI (coloration au créosyl violet pour voir la mort neuronale). Les chiffres représentent un changement de coupe. D'après (Keskin et al., 2017).

Or, en France, sur 150 000 nouveaux cas de TBI par an, « seulement » 10% sont considérés comme sévères. Nous avons donc choisi de modéliser un TBI ayant une portée plus importante : à savoir que 80 à 90% des TBI sont dits légers. Par léger, il faut entendre que les patients TBI légers (plus tard appelés mTBI pour *mild TBI*) n'ont pas de lésion cérébrale détectée en IRM par une

séquence pondérée en T2 (où l'on recherche la présence d'œdème) ni en séquence pondérée en T2\* (où l'on recherche la présence d'hémorragie). De manière intéressante, 30 à 50% de ces patients souffrent, malgré l'absence de signe clinique en imagerie, de déficits mnésiques, de vertiges ou de problèmes locomoteurs. Nous avons donc voulu essayer de comprendre quelle était la nature des troubles dont souffraient les patients atteints de mTBI. Ces travaux que j'ai réalisés pendant ma thèse nous ont appris que, même en l'absence de lésion en imagerie classique, le mTBI provoquait une réaction inflammatoire qui se maintenait à des temps tardifs chez la souris (au moins jusqu'à 3 semaines après la survenue du mTBI). Cette étude a abouti à la rédaction d'un article qui est en cours de préparation (**étude n°5**).

## I. Généralités

### 1. Historique

Le cas le plus connu de traumatisme crânien est certainement celui de Phineas Gage (1823-1860). Cet homme était contremaître des chemins de fer aux Etats-Unis. En 1848, alors qu'il préparait de la poudre pour faire exploser un rocher, le bourroir (ou la barre à mine) est venu heurter le rocher, créant une étincelle, ce qui a déclenché une explosion. Ce même bourroir a traversé la boîte crânienne de Gage (Figure 35).

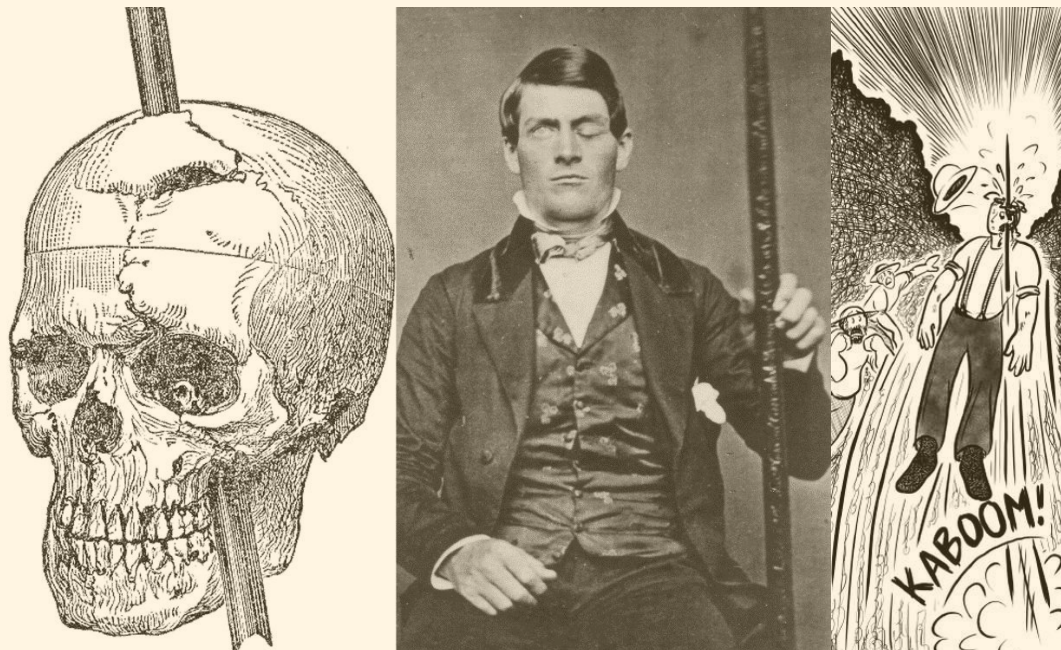


Figure 35 : Phineas Gage (1823-1860) (au centre), et la représentation du bourroir (qu'il tient dans sa main gauche) traversant sa boîte crânienne (à gauche). A droite, une illustration de l'accident.

Quelques minutes seulement après l'accident, Gage s'est relevé et arrivait à marcher avec de l'aide. John Harlow (1819-1907), le médecin sur place, n'a d'abord pas cru Gage, qui était capable de lui décrire la scène de l'accident. Puis Gage a vomi, ce qui a poussé dehors une petite partie de son cerveau (30 grammes) en dehors de la boîte crânienne (son médecin l'a cru après avoir constaté cela). Après avoir nettoyé la plaie, Harlow garda Gage en observation. Gage est passé par tous les états durant sa convalescence : coma, paralysie, pertes de mémoire... entrecoupés de périodes rationnelles. La plaie s'étant infectée, Harlow retira le pus (250ml). Par la suite, l'état de santé de Gage alla de mieux en mieux : il a pu recommencer à voyager pour retrouver sa famille, puis à travailler dans une ferme. Gage est mort en 1860 d'un état de mal épileptique. Ce cas clinique est très intéressant car il a ouvert un débat sur la régionalisation des fonctions cérébrales. En effet, Gage, d'après ses proches, avait changé son comportement : il était devenu instable mentalement, d'humeur changeante (il aura changé souvent de travail) et asocial. Il était en fait atteint ce que l'on appelle maintenant le syndrome frontal.

Les cas de traumatismes crâniens (et de leur traitement) ont été référencés bien avant dans l'Histoire. En effet, des cerveaux datant du néolithique ont été retrouvés avec des marques caractéristiques de trépanation, ce qui en fait la plus vieille chirurgie dont il existe des preuves physiques. Elle était probablement destinée à faire baisser l'hypertension intracrânienne. Il a été montré que les « chirurgiens » de l'époque s'entraînaient au geste de trépanation des crânes de vaches également trépanés ont été découverts. Une étude a montré que sur 130 crânes trépanés retrouvés dans une grotte, que 70% des « patients » avaient survécu (le trou était rebouché). Il a été décrit

plusieurs types de traumatismes crâniens suivant les symptômes dans le papyrus d'Edwin Smith datant d'environ -1600 avant JC. La trépanation est encore à l'heure actuelle un moyen de soulager l'hypertension intracrânienne induite par un traumatisme crânien : elle est plus communément appelée craniotomie décompressive. Le volet crânien est retiré puis « stocké » dans la paroi abdominale du patient jusqu'à repos du volet. Pour l'anecdote, certaines personnes pratiquent la trépanation à des fins pseudoscientifiques pour augmenter leur volume cérébral et le métabolisme cérébral : c'est le cas par exemple de Bart Huges (1934-2004) en 1965, qui a influencé Joseph Mellen dans l'écriture de son livre *Bore Hole* (de traduction littérale puits de forage). Joseph Mellen a vécu avec Amanda Feilding pendant 30 ans ; cette femme est connue pour s'être également auto-trépanée. Son hypothèse scientifique était que le fait d'avoir le cerveau comprimé par la boîte crânienne empêchait de ressentir tout le pouvoir des battements du cœur dans le cerveau, ce que pouvaient sentir les nouveau-nés qui n'avaient pas le crâne totalement fermé. Les nouveau-nés avaient alors un état de conscience supérieur avant que les os du crâne ne fusionnent. Son auto-trépanation a été filmée en direct par Mellen, ce qui a donné un film intitulé *Heartbeat in the Brain* paru en 1970 (Figure 36).



Figure 36 : Images provenant du film *Heartbeat in the Brain*, où l'on voit Amanda Feilding s'auto-trépanner.

Après le cas Phineas Gage, beaucoup de cas de troubles comportementaux ont pu être associés à des cas de traumatismes crâniens. L'avènement des avancées technologiques comme le scanner et l'IRM, notamment les séquences de diffusion, permettent de diagnostiquer plus aisément les traumatismes crâniens. Néanmoins, il n'y a à ce jour aucun traitement cliniquement valable pour traiter les traumatismes crâniens.

## 2. Épidémiologie

### a. Définition

Le TBI est décrit comme un dommage cérébral induit par une force mécanique externe. Les TBI peuvent être rangés en deux catégories : les TBI pénétrants (un objet qui s'insère, par exemple) et les non pénétrants (chute, par exemple). De plus, le devenir du TBI est déterminé par deux

mécanismes bien distincts : le choc primaire, sans visée thérapeutique mais plutôt préventive, et le choc secondaire, qui correspond aux répercussions à long terme du choc initial. Le choc primaire correspond aux réponses immédiates du tissu suite au choc externe : la contusion du tissu, les hémorragies, ou les dommages axonaux sont des exemples de conséquences immédiates du TBI. A cela s'ajoutent les conséquences secondaires au choc, à savoir les cascades métaboliques, cellulaires et moléculaires pouvant amener à la mort cellulaire, aux dommages cérébraux à long terme et à l'atrophie cérébrale. Ce sont ces événements secondaires qui sont la cible thérapeutique des TBI. Néanmoins, et comme dans le cas de l'AVC, malgré le succès de molécules dans l'évolution du TBI dans les modèles expérimentaux, aucune molécule n'a montré d'effet positif dans les essais cliniques (Schouten, 2007).

b. *Quelques chiffres*

En France, c'est 150 000 personnes qui sont concernées (référencées) par les TBI par an. De ces 150 000, environ 80-90% auront subi un mTBI. Ce type de TBI est associé à une absence de perte de connaissance et de lésion visible en imagerie, malgré une survenue évidente d'un TBI. Pour ce qui est des 10-20% restants, il existe deux cas de figure : soit le TBI est modéré (ou MTBI pour *moderate TBI*) soit il est sévère ou grave (ou sTBI pour *severe TBI*). Le coma est étroitement lié avec la survenue d'un sTBI. En ce qui concerne le MTBI, il peut y avoir perte de conscience pendant quelques minutes et/ou fracture. Cinquante pourcent des cas graves décèdent ou gardent des handicaps sévères. Dans les deux cas, il peut y avoir des séquelles sensori-motrices et/ou cognitives.

Une proportion importante de patients atteints de mTBI conserve à long terme des symptômes comme des difficultés de concentration, des maux de tête, des troubles de la mémoire : on appelle ce phénomène syndrome post-commotionnel persistant. Ces troubles peuvent persister au-delà d'une année. Une récente étude a montré que 53% des patients conservaient des infirmités 5 à 7 ans après la survenue d'un TBI (Whitnall et al., 2006).

Il a également été montré que 53% des patients atteints de TBI développaient des syndromes dépressifs, contre 6,7% de la population générale, soit environ 8 fois plus (Bombardier et al., 2010).

### c. Facteurs de risque

Les TBI sont la première cause de mortalité et de morbidité chez les individus âgés de moins de 45 ans (Langlois et al., 2006). Les jeunes enfants, les adolescents et les personnes âgées sont les personnes les plus à risque. L'âge moyen pour les hommes est de 27 ans ; il est de 32 ans pour les femmes. Deux fois plus d'hommes sont touchés que de femmes.

Il faut noter qu'environ la moitié des TBI est due à un mésusage de la consommation d'alcool (en combinant les personnes victimes et les personnes potentiellement coupables de TBI à autrui comme par exemple lors d'accidents de la route ou de violence) (Kolakowsky-Hayner et al., 1999) (Figure 37).

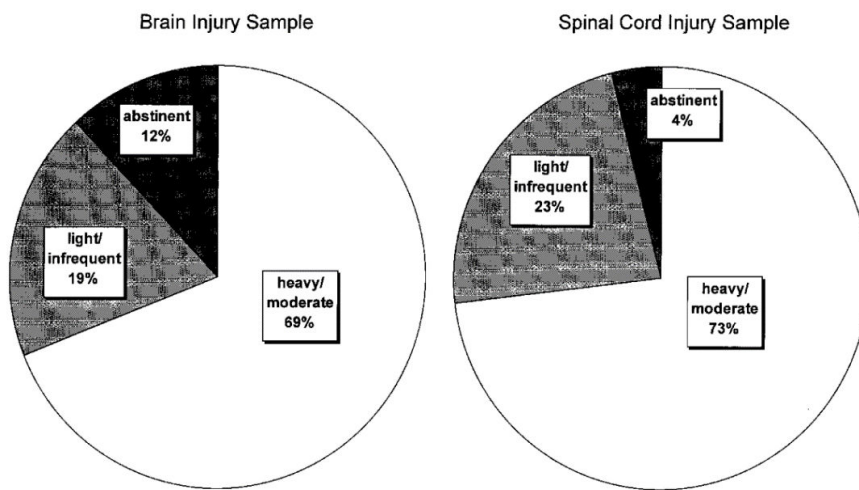


Figure 37 : 69% des personnes ayant subi un TBI et 73% des personnes ayant un traumatisme de la moelle épinière ont un trouble de l'usage de l'alcool. D'après (Kolakowsky-Hayner et al., 1999).

Il existe beaucoup de causes de TBI, mais, pour 70% des cas environ, ce sont les conséquences d'accidents de la voie publique. On peut également énumérer comme causes : les accidents du travail, du sport et domestiques (chutes) ainsi que les agressions/violences.

Il est important en pratique hospitalière d'évaluer le score clinique des patients atteints de TBI : pour cela, Teasdale et Jennet ont créé une échelle neurologique appelée l'échelle de Glasgow en 1974. Cette échelle est toujours valable de nos jours pour évaluer l'état de conscience d'un patient.

## II. Physiopathologie

### 1. Une physiopathologie proche de l'AVC ischémique

La physiopathologie du TBI se rapproche fortement de celle de l'AVC ischémique (se référer à la partie du manuscrit concernée). D'ailleurs, le choc secondaire au TBI est souvent la survenue d'une baisse du débit sanguin cérébral (DSC) accompagné d'une souffrance tissulaire importante, ce qui mime une ischémie cérébrale. Les processus de cytotoxicité, de mort cellulaire par apoptose et l'inflammation sont également mis en œuvre lors de la survenue d'un TBI. Toutefois, on peut noter quelques différences. Classiquement, une zone ischémie hypoperfusée correspond à des valeurs de DSC comprises entre 5 et 8ml par 100g par minute. Les valeurs retrouvées pour les patients atteints de TBI avoisinent plutôt des valeurs autour de 15ml par 100g par minute (Cunningham et al., 2005). De plus, d'autres événements accompagnent les événements ischémiques suite à un TBI : les forces de cisaillement dues au choc, la pression intracrânienne élevée, d'éventuels événements hémorragiques suite à une fracture (Werner and Engelhard, 2007). Un autre événement s'accompagne de la survenue d'un TBI : le traumatisme axonal. En effet, sous le coup de forces de tension, compression, torsion, les grandes projections axonales projetant dans la substance blanche sont atteintes et des troubles du transport axonal surviennent, notamment suite à la dégradation de la myéline. Enfin, la majeure différence qui existe entre le TBI et l'AVC réside dans la cause : un AVC est d'origine vasculaire, et non un traumatisme crânien. Il est d'ailleurs établi que lors d'un TBI les vaisseaux sanguins sont épargnés (sauf lors de cas de TBI sévères avec hémorragie), alors que les axones des neurones sont, eux, endommagés (Blumbergs et al., 1995). Tous ces événements font de la physiopathologie du TBI un phénomène très complexe, qui n'est pas encore entièrement défini dans sa globalité.

### 2. Modèles expérimentaux

#### a. Diversité

Il est important de noter que, du fait de l'existence de différentes modalités/différents degrés de TBI, il existe un nombre très important de modèles expérimentaux (dont la majorité est pratiquée sur des rongeurs) de TBI. Il est d'autant plus difficile de comprendre les mécanismes physiopathologiques du TBI au vu de sa grande variabilité visible en clinique, et, de fait, de la grande variabilité de modèles expérimentaux existants. Pour résumer, il existe deux grandes catégories, au sein desquelles une multitude de modèles expérimentaux coexistent : les TBI focaux, que l'on peut résumer à une percussion locale du crâne ou directement du cerveau (dans la majorité des cas) ; et les TBI diffus, qui sont réalisés par des mouvements d'accélération/décélération et de percussions. Il faut entendre par cela que chaque modèle répondant à une question scientifique ne peut pas avoir une portée thérapeutique globale en clinique au vu de la grande disparité de cas de TBI chez les patients, ainsi que de la grande disparité des modèles expérimentaux en préclinique. Il est toutefois admis que lors d'un TBI, il y a i) dommage de la BHE accompagné d'un dommage neuronal, ii) une dysfonction mitochondriale, iii) une activation astrocytaire et iv) une réaction inflammatoire cérébrale (Zetterberg and Blennow, 2016) (Figure 38).

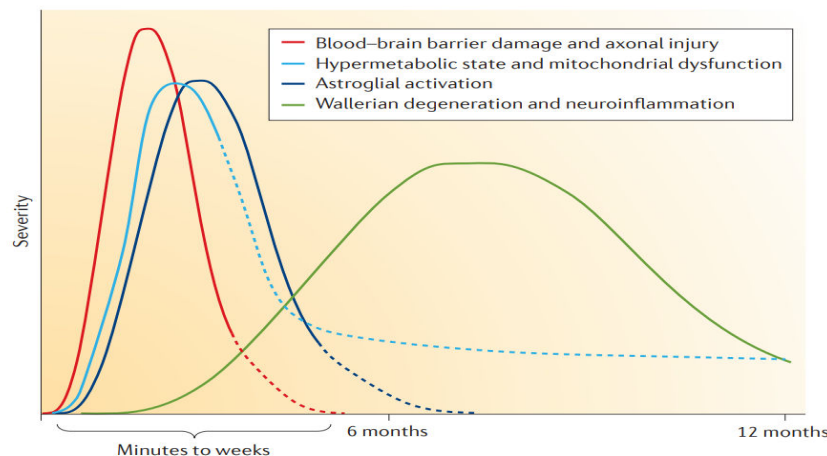


*Figure 38 : Consensus sur la physiopathologie du TBI. Suite au TBI, il y a dommage endothérial et tissulaire, suivi d'une dysfonction mitochondriale. Dans le même temps, les astrocytes s'activent, participant à la réaction inflammatoire qui peut perdurer dans le temps. D'après (Zetterberg and Blennow, 2016).*

#### b. Description

Cinq grands types de modèles expérimentaux de TBI sont pratiqués majoritairement dans les études précliniques (Figure 39) :

- Le modèle de percussion fluidique (ou FPI pour *fluid percussion injury*). La percussion fluidique se fait par un pendule qui vient frapper un piston rempli d'eau, ce qui génère un courant de pression fluidique directement au contact du cerveau de l'animal. La force de pression dépend du balancement du pendule. Cette opération peut être réalisée sur le haut du crâne ou latéralement. Cette percussion a pour conséquences un déplacement et/ou une déformation du tissu cérébral, dépendant de la pression induite par le pendule (McIntosh et al., 1989).
- Le modèle d'impact cortical contrôlé (ou CCI pour *controlled cortical impact*). L'impact est cette fois-ci réalisé à l'aide d'un impacteur pneumatique ou électromagnétique directement sur la dure-mère. Cette opération peut entraîner un hématome, une concussion, une rupture de la BHE voire même un coma suite à la déformation du cortex. Les dommages cérébraux peuvent s'étendre à l'hippocampe et au thalamus (Hall et al., 2005). Le gros avantage de cette technique est le contrôle des paramètres de l'impact comme la profondeur, la vitesse et le temps d'impact.
- Le modèle mimant une pénétration d'objets balistiques (ou PBBI pour *penetrating ballistic-like brain injury*). Contrairement aux autres modèles expérimentaux de TBI, le PBBI, du fait de la pénétration à grande vitesse d'un projectile dans le tissu cérébral, créé une cavité dans le cerveau, d'une taille supérieure à la taille du projectile. Cette technique peut causer des dommages de la matière grise et de la matière blanche, des hématomes, des crises d'épilepsie ainsi que des dépressions corticales envahissantes : tous ses phénomènes pouvant avoir lieu de manière dépendante de la trajectoire du projectile. Ces événements se traduisent par des troubles moteurs et cognitifs, dont l'amplitude est corrélée à la sévérité du PBBI (Shear et al., 2010, 2011).
- Le modèle du poids (ou *weight-drop model*). Ce modèle consiste à exposer le crâne (ou le cerveau directement) à un poids lâché librement au-dessus de la zone à impacter. La sévérité de ce modèle dépend de la masse du poids ainsi que de la hauteur à laquelle il est lâché. L'inconvénient principal de ce modèle est la grande variabilité dans la sévérité de la blessure, mais il est facile à produire, peu coûteux, et reproduit bien les cas cliniques (Feeney et al., 1981; Marmarou et al., 1994).

- Le modèle d'explosion (ou *blast injury*). Ce modèle expérimental a vu le jour suite aux nombreux cas de militaires ayant eu comme diagnostic un TBI après avoir été exposés à une explosion, sans pour autant de blessure. Ce modèle consiste à placer l'animal dans un tube fermé à une extrémité, et d'induire un choc *via* une explosion ou une surpression d'air au niveau de cette extrémité. L'onde de choc produit des dommages axonaux diffus, l'apparition d'œdèmes cérébraux, de l'hyperémie et des vasospasmes ainsi qu'une augmentation de la pression intracrânienne (Reneer et al., 2011). De manière intéressante, les animaux ayant été protégés par une veste en Kevlar ont montré une diminution significative de diminution de la mortalité ainsi qu'un amoindrissement du dommage axonal : ceci prouve que le TBI induit par explosion/surpression d'air peut avoir des effets systémiques potentiellement responsables du devenir à long terme du TBI (DeWitt and Prough, 2009).

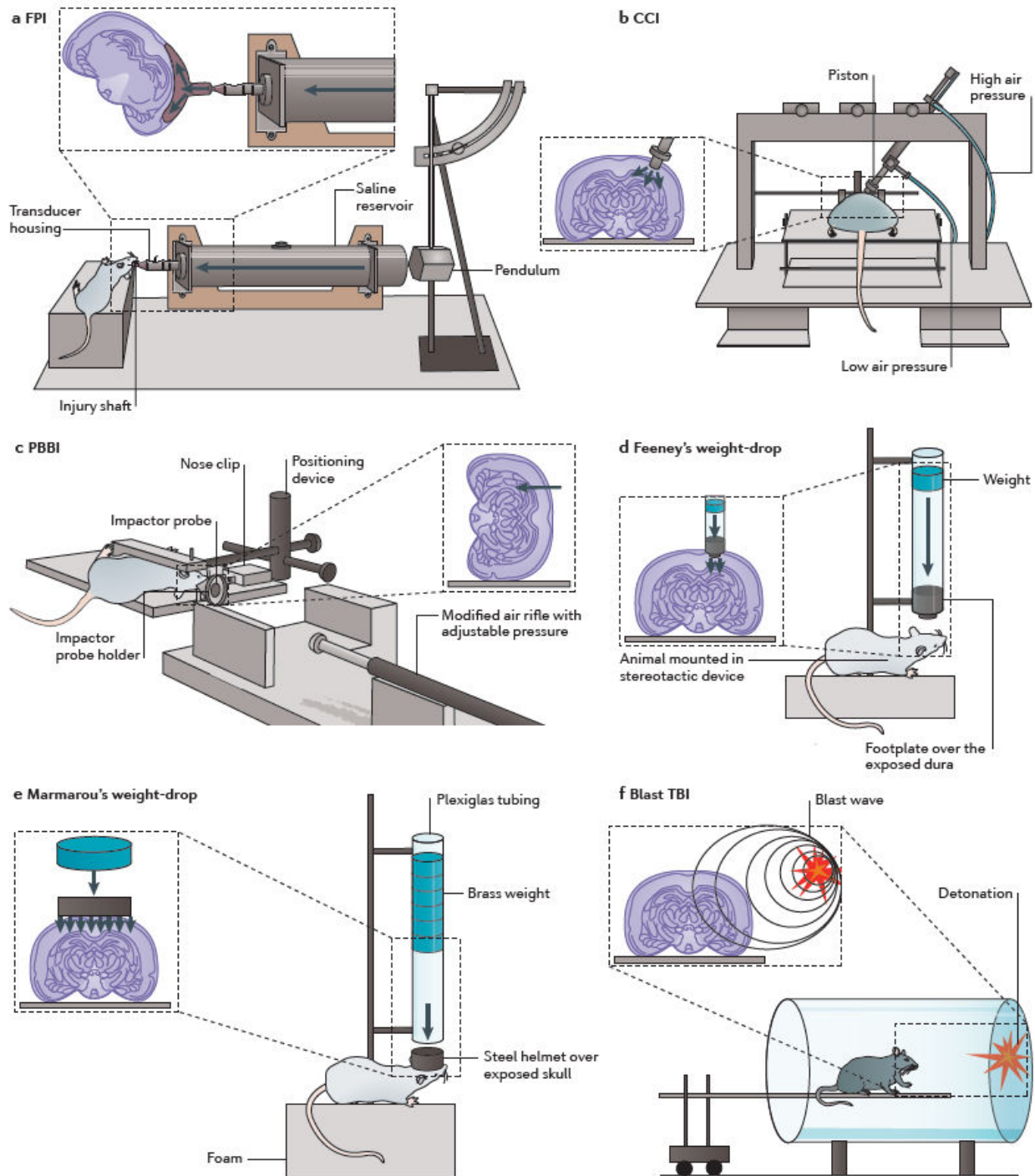


Figure 39 : Principaux modèles expérimentaux de TBI. (A) Percussion fluidique, (B) Impact cortical contrôlé, (C) Pénétration d'objets balistiques, (D) modèle du poids de Feeney, (E) modèle du poids de Mamarou, (F) modèle d'explosion. D'après (Xiong et al., 2013).

### 3. Dommage axonal diffus

Les neurones sont des cellules peu élastiques, notamment fragiles au niveau de leur axone. Ils sont donc sensibles à des chocs externes comme lors de la survenue d'un TBI. D'ailleurs, les neurones présentent à leur surface des mécanorécepteurs, qui, comme leur nom l'indique, sont sensibles aux chocs mécaniques externes. Dès lors, suite au choc, les axones des neurones sont en souffrance, amenant le neurone à secréter des cytokines, à produire en grande quantité du glutamate provoquant alors les phénomènes d'excitotoxicité et d'apoptose neuronales. On appelle ce phénomène dommage axonal (ou DAI pour *diffuse axonal injury*). Il est intéressant de noter que dans des modèles expérimentaux ainsi que chez des patients atteints de mTBI, il a été montré qu'en l'absence de mort neuronale persistaient tout de même des déficits cognitifs post-traumatiques, et qu'ils étaient probablement dus à des dommages axonaux (Browne et al., 2011; Lipton et al., 2008; Niogi et al., 2008; Rubovitch et al., 2011).

### 4. Réaction inflammatoire

#### a. Cellules résidentes

##### *Oligodendrocytes*

Les oligodendrocytes sont, entre autres, responsables de la formation de la gaine de myéline. Cette gaine de myéline se situe autour des axones des neurones et joue le rôle d'amplificateur de la conduction de l'influx nerveux. La gaine de myéline est précieuse pour le bon fonctionnement neuronal. Une dysfonction/dommage de la myéline peut conduire à des troubles neurodégénératifs : on peut citer par exemple le cas la sclérose en plaques qui est une maladie auto-immune où le système immunitaire s'attaque à la gaine de myéline, entraînant des pertes de fonctions sensori-motrices importantes dans les phases de poussées de la maladie.

Des études ont montré que la myéline était aussi endommagée dans le cadre du TBI (Armstrong et al., 2016; Mierzwa et al., 2015). De manière intéressante, ces dommages axonaux sont chroniques (Figure 40).

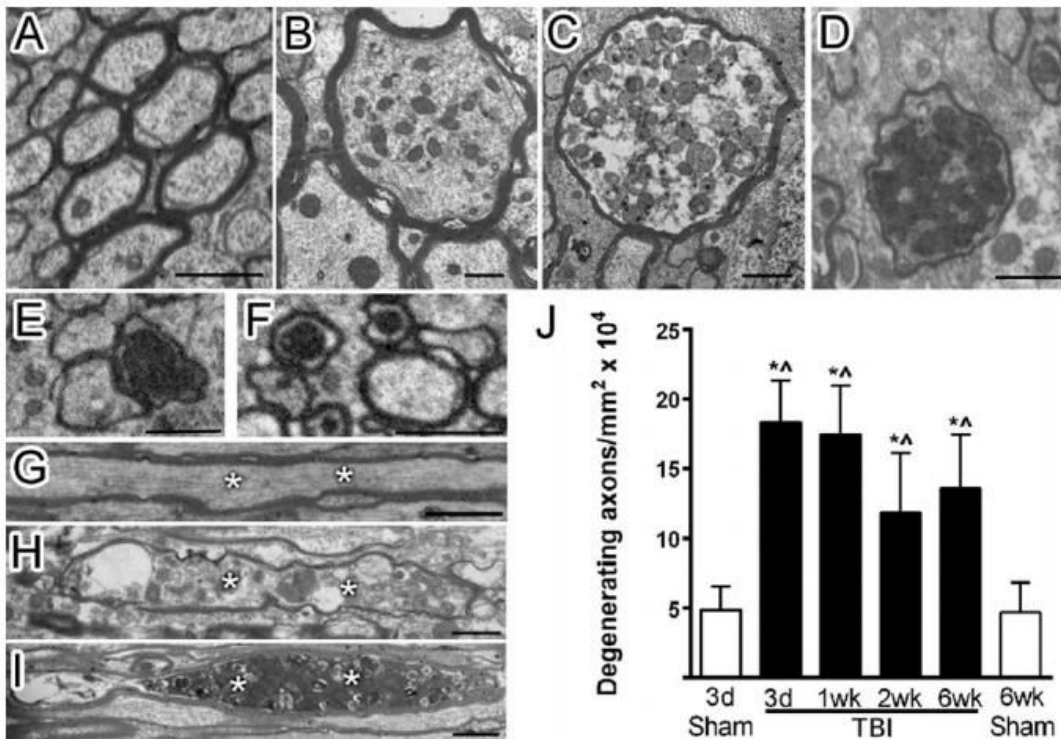


*Figure 40 : Etude de la dégénérescence axonale en microscopie électronique suite à la survenue d'un mTBI. (A) Axones d'un animal Sham (témoin opéré n'ayant pas subi le mTBI). (B) à (D) : accumulation de diverses vésicules dans le corps axonal suite au mTBI. (E) Axone à cytoplasme dense. (F) Gonflement des mitochondries. (G) Chez un animal sham, la structure de l'axone est uniforme, contrairement à un animal mTBI en (H) et (I) où l'on peut voir une accumulation de vésicules (astérisques). (J) Quantification de la dégénérescence axonale montrant que 6 semaines après le mTBI la dégénérescence axonale persiste. D'après (Mierzwa et al., 2015).*

Il a été montré dans différents modèles de TBI (percussions fluidiques latérale et centrale) que suite au TBI il y avait perte de myéline (ou démyélinisation), en plus d'une apoptose des oligodendrocytes et d'une prolifération des précurseurs d'oligodendrocytes (Flygt et al., 2013). De plus, dans cette étude, il a été observé une accumulation d'APP, un précurseur du peptide bêta amyloïde : ceci sous-entend que soit le trafic neuronal est perturbé, soit la clairance des déchets est perturbée, soit les deux.

Une étude a montré qu'une injection intraveineuse de NEP (1-40), un antagoniste des récepteurs Nogo, une molécule issue des produits de dégradation de la myéline, permettait de modifier le phénotype des cellules microgliales vers un phénotype anti-inflammatoire : ceci pourrait supposer une meilleure dégradation des déchets et donc une meilleure récupération/réparation tissulaire suite au mTBI (Ziebell et al., 2017).

### *Astrocytes*

Les astrocytes, tout comme les axones des neurones, ont des structures relativement rigides. A leur surface, les astrocytes expriment des mécanorécepteurs, qui sont donc sensibles à des gradients de pression mécanique se produisant lors d'un TBI, ceci aboutissant à leur activation (Bowman et al., 1992). Une autre hypothèse plus convenue est l'activation astrocytaire suite à la souffrance neuronale : les neurones produisent alors des cytokines pro-inflammatoires activant *de facto* les astrocytes ainsi que les autres cellules immunitaires résidentes telles que la microglie et les macrophages.

La réponse astrocytaire à un TBI est multipotente (Figure 41) : il a été montré que les astrocytes pouvaient, en cas de stress physique, internaliser en excès des ions  $\text{Na}^+$  et  $\text{Ca}^{2+}$  (Floyd et al., 2005), libérer de l'ATP (Neary et al., 2005) ainsi que des molécules vasoactives comme l'endothéline-1 (qui est vasoconstrictrice) (Ostrow et al., 2011). Une autre conséquence de la survenue du TBI sur l'activation astrocytaire est l'augmentation significative de l'expression des filaments intermédiaires. Les principaux filaments intermédiaires exprimés par les astrocytes sont le GFAP, la vimentine et la nestine ; tous les trois sont plus exprimés suite à un TBI ou alors après un AVC (Li and Chopp, 1999; Liu et al., 2014).

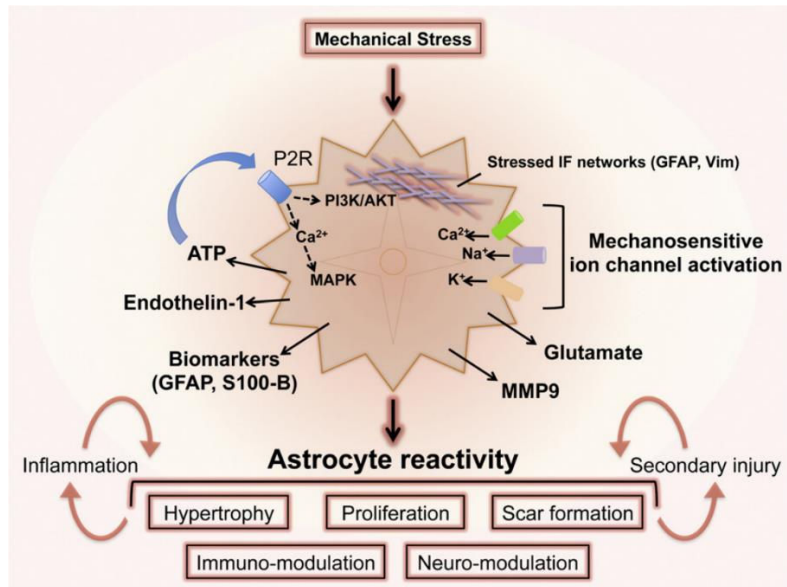


Figure 41 : Réactivité astrocytaire dans le cadre du TBI. Suite au stress mécanique, les astrocytes répondent de façon exhaustive sous différentes formes : ils peuvent s'hypertrophier, proliférer, participer à la réaction immunitaire, moduler la réponse neuronale, et participer à la réparation tissulaire. D'après (Burda et al., 2016).

Le modèle proposé par Burda et collaborateurs sur le rôle des astrocytes dans le TBI est le suivant : i) les forces mécaniques dues à la survenue du TBI entraîne une libération d'ATP par les cellules mécano-sensibles comme les neurones et les astrocytes. ii) La libération d'ATP par les astrocytes induit une entrée massive d'ions Ca<sup>2+</sup> (et Na<sup>+</sup>) dans leur cytoplasme. iii) La cascade d'événements de la vague calcique astrocytaire implique une activation des astrocytes ainsi que le recrutement des cellules immunitaires locales comme la microglie, qui, de surcroit, s'active suite à la vague calcique et suite au contact de l'ATP libéré par les cellules en souffrance (Burda et al., 2016).

Les astrocytes peuvent réguler la réponse inflammatoire associée au TBI. En effet, les astrocytes sont capables de produire des cytokines/chimiokines, ainsi que des DAMPs qui vont interagir avec les PRR des cellules immunitaires. De manière intéressante, les astrocytes expriment également à leur surface des PRR (Gorina et al., 2010) : ceci sous-tend que les astrocytes peuvent produire des cytokines comme le TNF via la cascade PRR-Nf-κB, ce mécanisme étant le même que les cellules microgliales.

Les astrocytes participent à la cicatrisation du tissu lésé : c'est le phénomène de cicatrice gliale. Une étude a montré que chez des souris déficientes en GFAP, la réaction inflammatoire induite

par un TBI perdurait et était amplifiée : plus de cellules immunitaires infiltreraient le cerveau, la BHE était perméable plus longtemps, et les dommages neuronaux étaient exacerbés (Bush et al., 1999). Une autre étude a montré qu'*in vitro* les astrocytes étaient incapables de ségrégérer les leucocytes s'ils étaient déficients en STAT-3 (pour *signal transducer and activator of transcription-3*) (Wanner et al., 2013) (Figure 42).

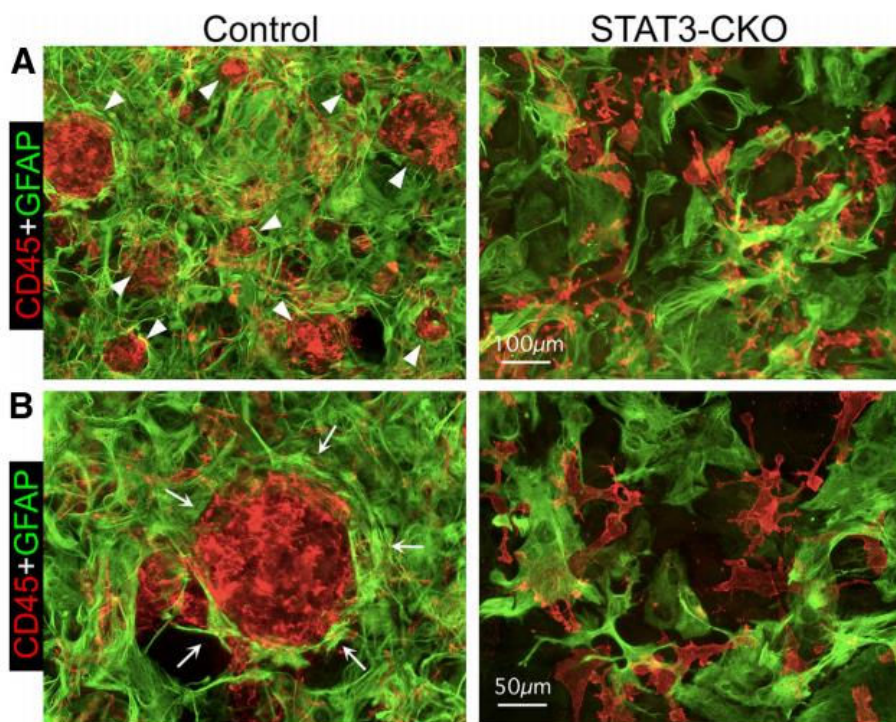
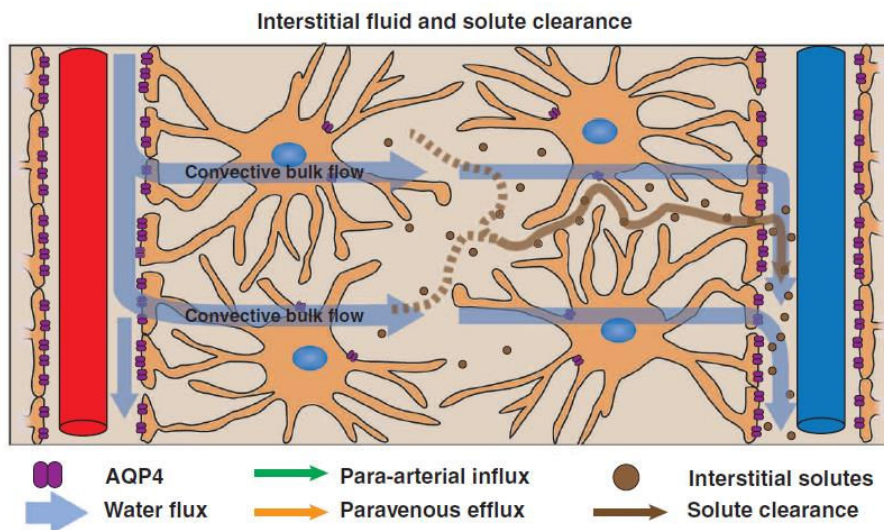


Figure 42 : Cicatrice gliale *in vitro* dans une condition contrôle (panels de gauche) et dans une condition où les astrocytes sont déficients en STAT-3 (panels de droite). Les astrocytes sont marqués avec GFAP (en vert), les leucocytes avec CD45 (en rouge). Chez les astrocytes contrôle, on peut remarquer une ségrégation des leucocytes, alors que les leucocytes sont répartis de manière anarchique chez les astrocytes déficients en STAT-3. D'après (Wanner et al., 2013).

Les astrocytes pourraient indirectement participer à l'évaluation de la sévérité du TBI *via* le dosage de molécules dans la circulation sanguine. En effet, des marqueurs sanguins pourraient indiquer la sévérité du TBI, et donc permettre d'adapter les traitements en fonction de la concentration plasmatique de ces marqueurs. De manière intéressante, les principaux marqueurs plasmatiques, à savoir le S100 $\beta$  et le GFAP, sont exprimés par les astrocytes. Une étude a proposé que le passage de ces molécules du tissu cérébral vers le compartiment sanguin puisse se faire par l'intermédiaire du système « glymphatique », le système lymphatique du cerveau (Plog et al., 2015). Le système glymphatique est un système de clairance des déchets cérébraux par

l'intermédiaire d'échanges fluidiques : le LCS provenant des espaces de Virchow-Robin péri-artériels passerait (passivement ou activement) dans le tissu cérébral, emmenant avec lui les déchets, puis serait évacué dans le système péri-veineux où les déchets soit repasseraient dans la circulation sanguine, soit se dirigeaient vers les ganglions lymphatiques et seraient libérés au niveau de la lame criblée sous forme de mucosités. Ce système a été nommé glymphatique en référence au système lymphatique et aux cellules gliales (« glie » « lymphatique »), qui semblent jouer un rôle prépondérant dans l'établissement d'un tel système car ils possèdent à leur surface des canaux à eau appelés aquaporines, notamment l'aquaporine 4 (ou AQP4) participant au bon établissement du système glymphatique (Iliff et al., 2012) (Figure 43). D'ailleurs, des souris déficientes en AQP4 ont un système glymphatique défectueux, ce qui semble jouer un rôle important dans le TBI. En effet, la quantité des marqueurs GFAP et S100 $\beta$  est significativement réduite chez les souris déficientes en AQP4, contrairement à des souris naïves ayant elles aussi subi un TBI (Plog et al., 2015). Une étude a d'ailleurs montré indirectement que le système de clairance des molécules du parenchyme cérébral était altéré : en effet, suite à un TBI modéré a été observée une accumulation de peptide bêta amyloïde (Tajiri et al., 2013).



*Figure 43 : Représentation du système glymphatique, le système lymphatique cérébral. Un flux de LCS (water flux) diffuse dans le compartiment tissulaire en provenance de l'espace de Virchow-Robin. Durant son passage, il transporte les déchets vers l'espace péri-veineux où il est ensuite évacué vers les ganglions lymphatiques ou dans la circulation sanguine. D'après (Iliff et al., 2012).*

## *Cellules microgliales*

Les cellules microgliales ont un rôle prépondérant dans la physiopathologie du TBI, à savoir que ce sont les premières cellules immunitaires impliquées, et donc participent activement au devenir de la réaction inflammatoire induite par le TBI. Il s'avère que lors d'un TBI léger (en l'absence de lésion classique), les cellules microgliales activées n'acquièrent pas de phénotype amiboïde comme on pourrait s'attendre : elles acquièrent plutôt un phénotype *primé* (voir le paragraphe « *priming microglial* »).

Il faut savoir qu'en plus d'être une cause majeure de mortalité et de morbidité dans le monde, le TBI augmente aussi l'incidence de développer des séquelles neuropsychiatriques comme la dépression, les détériorations cognitives, et peut même être un facteur de risque de développer *à posteriori* des maladies neurodégénératives (Bombardier et al., 2010). Il s'avère que la microglie *primée*, étant donc chroniquement activée, apparaît être un candidat de choix dans l'étude des conséquences à long terme de la survenue d'un TBI : lorsqu'elle est *primée*, la microglie a un seuil d'activation plus faible et suite à un deuxième challenge, elle devient hyperactive (Norden and Godbout, 2013).

Les cellules microgliales sont capables d'interagir avec les neurones, en jouant par exemple un rôle dans la plasticité synaptique (Figure 10). Dès lors on peut penser que ces cellules vont jouer un rôle dans la plasticité synaptique des neurones dont l'axone a été endommagé suite au TBI. D'ailleurs, une réponse classique du SNC en cas de traumatisme est de détruire les synapses des axones des neurones en souffrance. Il a été montré que des cellules MHC I positives (pour *major histocompatibility complex I*) venaient s'agglomérer autour des neurones ayant été axotomisés, majoritairement des cellules microgliales (Blinzinger and Kreutzberg, 1968).

Les cellules microgliales augmentent rapidement leur niveau d'expression en Iba1 et CD68 (des marqueurs classiques de l'activation microgliale) dans un modèle de FPI (Bachstetter et al., 2013). Leur morphologie n'est toutefois pas amiboïde : elles sont plutôt hypertrophiées. Ce modèle ayant pour conséquence une augmentation d'IL-1 $\beta$ , TNF et CD14 au niveau hippocampique et cortical et ce, dès 4h, est corrélé avec l'état d'activation de la microglie. De manière intéressante,

des souris dont les cellules microgliales ont été déplétées en p38 $\alpha$  MAPK (une protéine kinase permettant la production de cytokines par les cellules microgliales) étaient protégées suite au FPI. Les mêmes résultats ont été démontrés avec non pas des souris déplétées mais sous traitement d'un inhibiteur de p38 $\alpha$  MAPK (Bachstetter et al., 2011). Dans ce modèle, seules des médiateurs pro-inflammatoires ont montré des signes significatifs d'élévation. Ce n'est pas le cas dans un modèle focal de TBI où l'on retrouve aussi des médiateurs pro-inflammatoires comme CD11b, mais également de l'IL-10, du TGF- $\beta$  et de l'arginase qui persistent jusqu'à 5 jours après le CCI (Wang et al., 2013). De plus, la minocycline, qui diminue l'activation microgliale, a montré des effets bénéfiques dans les modèles d'explosion/surpression (Kovesdi et al., 2012) et du poids (Homsi et al., 2010).

Il est nécessaire d'ajouter que la microglie n'a pas que des effets délétères. En effet, il a été montré que les cellules microgliales avaient un rôle protecteur dans un type de lésion hippocampique : suite à la lésion, les auteurs ont montré une augmentation de la mort neuronale chez des souris déplétées en cellules microgliales (Rice et al., 2015). Il a également été montré un rôle neuroprotecteur des cellules microgliales dans l'AVC (Szalay et al., 2016).

Tous les mécanismes précédemment décrits concernent la partie aigue post-traumatique. L'activation microgliale peut toutefois persister dans le temps, et c'est d'ailleurs le cas suite au TBI. En effet, une élévation de CD68, MHC II et de NAPDH oxydase (un complexe d'enzymes responsables de la formation de dérivés réactifs de l'oxygène) par les cellules microgliales a été démontrée jusqu'à un mois après un FPI (Ziebell et al., 2012), et même jusqu'à un an après la survenue d'un CCI (Loane et al., 2014). Dans une autre étude utilisant le modèle FPI, les cellules microgliales sont toujours actives un mois après le FPI. Leur morphologie et leur état d'activation suggèrent un *priming* microglial (Fenn et al., 2014). Pour confirmer le *priming* microglial, un challenge inflammatoire systémique par injection de LPS a été effectué : il a induit une exagération de la production de cytokines pro-inflammatoires (IL-1 $\beta$  et TNF) spécifiquement par les cellules microgliales, ce qui est typiquement retrouvé en cas de *priming* microglial. De plus, les cellules microgliales TBI+LPS ont un périmètre plus important (elles sont plus longues), et une enveloppe convexe (une quantification de la forme arrondie) plus grande que chez des souris TBI sans exposition systémique au LPS (Muccigrosso et al., 2016) (Figure 44). Il est important de noter

que malgré tous ces changements, le nombre de cellules microgliales totales n'a pas varié si l'on compare par rapport aux souris contrôles ayant subi le FPI : autrement dit, le *priming* microglial ne coïncide pas avec une augmentation du nombre de cellules, mais bien avec un état d'activation modéré (les cellules ne sont pas phagocytaires ou amiboïdes, comme lors d'état d'activation sévère).

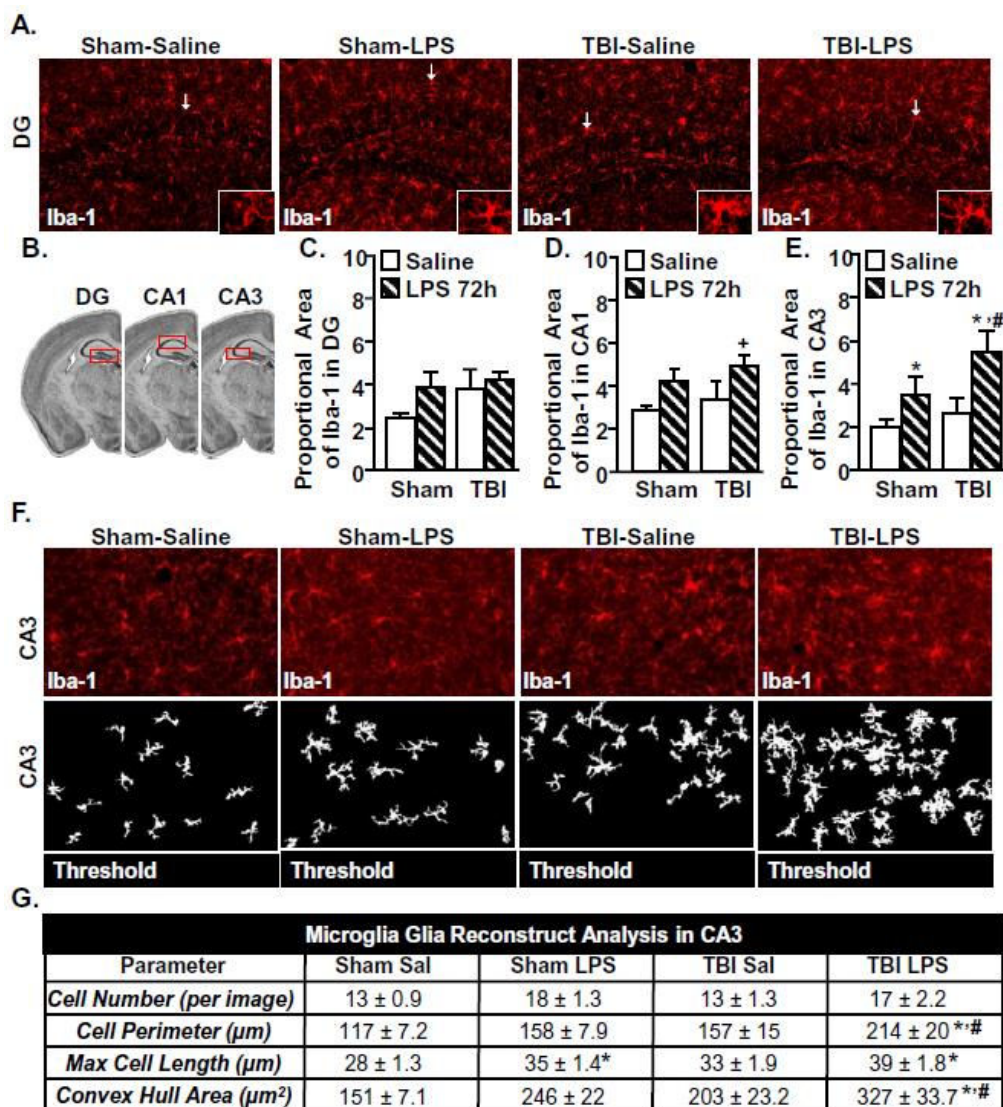


Figure 44 : Priming microglial dans l'hippocampe 1 mois après la survenue d'un TBI (modèle FPI). (A) Images représentatives des cellules microgliales (marquage Iba1 en rouge) chez des animaux témoins opérés (sham) et ayant subi un FPI avec ou sans exposition à un agent pathogène (LPS) au niveau du gyrus denté de l'hippocampe (DG). (B) Localisation des structures hippocampiques d'intérêt pour les quantifications. DG= gyrus denté (dentate gyrus) ; CA=corne d'ammon. (C-E) Quantifications de l'aire d'Iba1 dans DG, (D) CA1 et (E) CA3. (F) Images représentatives des cellules microgliales dans la zone CA3 et le seuillage (images en noir et blanc) respectives. (G) Quantification du nombre de cellules, le périmètre, la longueur maximale et l'enveloppe convexe des cellules microgliales. D'après (Muccigrosso et al., 2016).

### *Autres macrophages résidents*

Pour l'heure il n'existe pas de données de la littérature concernant un rôle potentiel des PVM, CPM et MM dans la physiopathologie du TBI. Une étude immunohistochimique de CD163, un marqueur commun des macrophages, a été réalisée dans un modèle expérimental du poids afin de mesurer l'infiltration de macrophages. La quantification indique une forte augmentation du nombre de cellules CD163 positives jusqu'à au moins quatre jours après la survenue du TBI (Zhang et al., 2012). Il est donc possible que les PVM puissent jouer un rôle dans la physiopathologie du TBI. Toutefois, ce marquage n'a pas été retrouvé que dans les espaces périvasculaires, mais également dans le tissu cérébral, ce qui indique une probable infiltration de monocytes circulants. On ne peut donc pas conclure de l'implication des PVM dans cette étude (Zhang et al., 2012).

#### *b. Recrutement des leucocytes*

Les études s'intéressant à l'infiltration leucocytaire suite à la survenue d'un TBI sont rares. Dans ces études, les modèles expérimentaux utilisés sont plutôt invasifs, et l'on observe donc une infiltration importante de cellules immunitaires au sein du parenchyme cérébral. Une étude a par exemple montré une infiltration de monocytes *via* les plexus choroïdes vers le tissu lésé dans un modèle expérimental de CCI chez le rat (Szmydynger-Chodobska et al., 2012). Si l'on regarde plus précisément la méthode chirurgicale aboutissant au CCI, on constate que le cône d'impact est inséré de 3mm en profondeur au sein du parenchyme, sachant que les animaux ont auparavant subi une craniotomie. Une autre étude s'est intéressée au blocage de l'entrée des neutrophiles dans un modèle de CCI sévère chez la souris : en utilisant du mannitol (utilisé en routine en clinique pour diminuer la pression intracrânienne en cas d'œdème cérébral), l'infiltration de neutrophiles était significativement amoindrie 32h après le CCI (Kumasaka et al., 2014). Une autre étude a également montré une infiltration de neutrophiles suite à un TBI, cette fois-ci dans un modèle du poids (Carlos et al., 1997). Cette infiltration de neutrophiles est accompagnée d'une augmentation de la production d'E-sélectine et ICAM-1, des molécules d'adhésion nécessaires

pour le recrutement des neutrophiles à la surface des cellules endothéliales des vaisseaux sanguins cérébraux.

### III. Essais cliniques

Malgré le bénéfice de certaines molécules dans le cadre de recherches précliniques, aucun traitement efficace de la phase aiguë du traumatisme crânien n'est applicable en clinique.

La progestérone paraissait pourtant être un candidat idéal. Ce traitement a d'abord été découvert de manière fortuite : une étude a montré que les femelles rat pseudo-gestantes (c'est à dire par stimulation mécanique du vagin pendant 10s) avaient une meilleure récupération fonctionnelle et un œdème cérébral amoindri suite à la survenue d'un TBI (modèle d'aspiration par succion d'une partie du tissu cérébral) comparé à des rats femelles en cycle normal (Attella et al., 1987). Parallèlement, beaucoup d'études se sont intéressées au caractère neuroprotecteur de la progestérone, et notamment dans le traumatisme crânien (Wei and Xiao, 2013). La progestérone est une molécule anti-apoptotique, capable aussi de réduire l'expression de l'AQP4, et d'améliorer l'imperméabilité de la BHE. De plus, elle a des propriétés anti-inflammatoires car elle réduit la production de cytokines pro-inflammatoires en agissant sur le facteur de transcription Nf-κB. Après deux essais cliniques de phase II concluants (Wright et al., 2007; Xiao et al., 2008), deux essais cliniques de phase III ont vu le jour, mais n'ont pas montré d'effet bénéfiques de l'administration aigüe de progestérone suite à un TBI sévère (Skolnick et al., 2014; Wright et al., 2014) (Figure 45).

D'autres molécules ont été testées dans le cadre du traitement du TBI. La cyclosporine A est une molécule qui va empêcher la perméabilisation de la membrane mitochondriale, visant ainsi à limiter l'apoptose et la libération d'ATP dans l'espace extracellulaire. Elle a permis de réduire le volume de lésion dans un modèle de CCI (Sullivan et al., 2000). Toutefois les essais cliniques de phase II ne sont pas très concluants, montrant seulement un effet au niveau du métabolisme chez des patients atteints de TBI sévère (Mazzeo et al., 2008). Ce non-effet peut s'expliquer par le faible pouvoir pénétrant de la cyclosporine A au sein du parenchyme cérébral, qu'elle a une courbe dose-réponse biphasique et qu'elle peut avoir un effet immunosuppresseur si elle est

exposée de manière chronique (Margulies et al., 2009). Les statines ont également fait l'objet d'études expérimentales en tant que traitement du TBI. Elles ont des propriétés neuroprotectrices, anti-inflammatoires, anti-excitotoxiques, anti-apoptotiques et favorisent la neurogenèse (Loane and Faden, 2010). Leurs effets ont été démontrés également dans le TBI, notamment leur effet anti-inflammatoire : elles réduisent la production de facteurs pro-inflammatoires, limitent l'activité des cellules gliales et préservent l'intégrité de la BHE (Chen et al., 2009, 2007; Lu et al., 2004). Un essai clinique de phase II a montré un effet bénéfique des statines (Rosuvastatine) dans l'amnésie et la désorientation après un TBI chez les patients (Tapia-Perez et al., 2008).

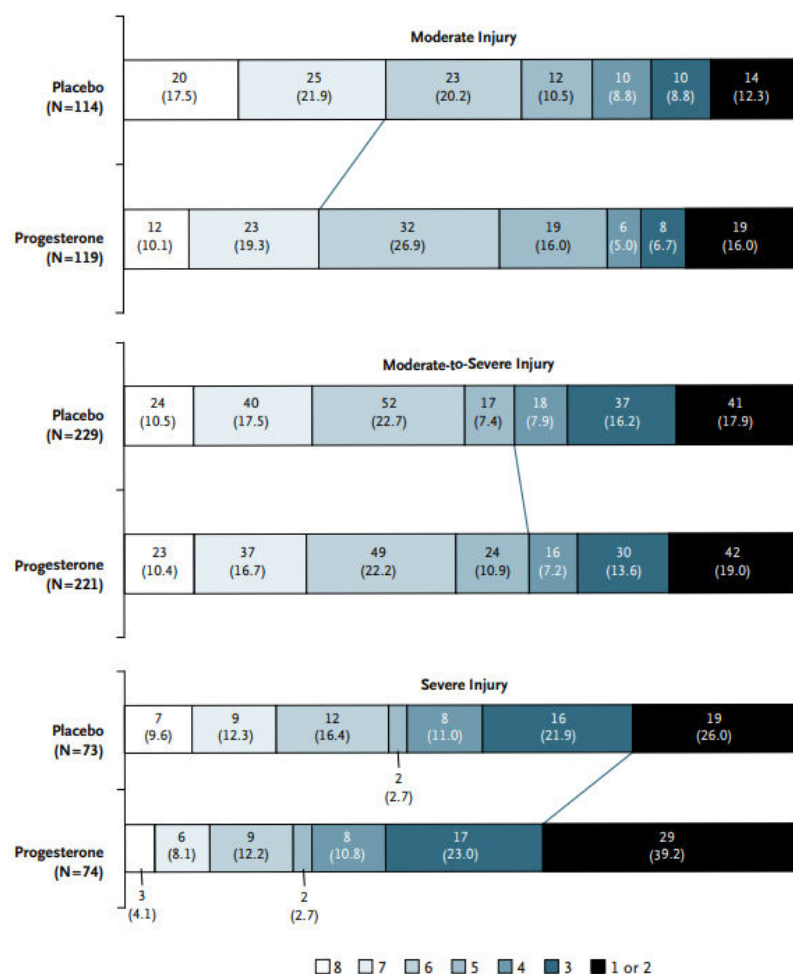


Figure 45 : Résultats de l'essai Clinique PROTECT III. La progestérone n'a pas d'effet bénéfique quelle que soit la sévérité du TBI. 1=décès ; 2=état végétatif ; 3/4=déficits sévères ; 5/6=déficits légers, 7/8=bonne récupération.  
D'après (Wright et al., 2014).

Le seul traitement semblant avoir des effets positifs directs sur le TBI est l’oxygénothérapie hyperbare. Le but de cette thérapie est d’endiguer le choc secondaire du TBI à savoir une chute de l’apport en oxygène au tissu cérébral suite à la réduction du DSC. Cette réduction a pour conséquence une conversion du métabolisme cérébral d’un mode aérobie à un mode anaérobie inefficace, pouvant causer la mort cellulaire. Une étude (Daly et al., 2018) a référencé 20 études précliniques et seulement une d’entre elles a montré un effet négatif de l’oxygénothérapie hyperbare (Tinianow et al., 2000). Toutefois cette étude est critiquée car les auteurs utilisaient des très fortes doses d’O<sub>2</sub>, pouvant alors favoriser la formation de dérivés réactifs de l’oxygène. Six essais cliniques de phase II aussi été référencés dans cette étude : elles ont montré une utilité potentielle de l’oxygénothérapie hyperbare sur le TBI, notamment dans l’abaissement de la pression intracrânienne et dans l’amélioration du métabolisme de l’oxygène (Lin et al., 2008; Prakash et al., 2012; Rockswold et al., 1992, 2001, 2010, 2013). Un autre essai clinique de phase II est en cours : HOBIT (pour *Hyperbaric Oxygen Brain Injury Treatment trial*).

## Résumé

Il est essentiel de mieux comprendre la physiopathologie du TBI pour pouvoir enfin traiter les patients. Les essais cliniques sont malheureusement inefficaces, probablement à cause d'une très grande variabilité de TBI chez les patients. Cette variabilité est également très problématique dans les études précliniques car il existe un très grand nombre de modèles expérimentaux.

L'inflammation joue un rôle important dans le choc primaire ainsi que dans le choc secondaire. Une étude clinique montré un effet bénéfique de la minocycline dans le cadre du TBI. Du moins, dans la réduction de l'activation microgliale, car elle n'a toutefois pas montré d'effet positif dans la récupération fonctionnelle : elle a même montré un effet pro-neurodégénératif (Scott et al., 2018). Ceci soutient un rôle positif de l'activation microgliale dans l'inflammation à long terme engendrée par le TBI.

Nous avons mis en place dans notre laboratoire un nouveau modèle de mTBI que nous avons caractérisé par une absence de lésion cérébrale par imagerie classique, mais avec toutefois une réaction inflammatoire importante, notamment parenchymateuse, allant du cortex jusqu'à l'hippocampe. De manière intéressante, cette réaction inflammatoire s'intensifie (notamment au niveau du cortex) au cours du temps, et est détectable par des techniques d'autoradiographie. Ceci pourrait indiquer que l'on pourrait détecter *in vivo* l'inflammation induite par un mTBI par tomographie par émission de positons (TEP), prouvant ainsi aux patients atteints de mTBI qu'il existe, en effet, une réaction non physiologique potentiellement responsable de l'émergence des troubles dont ils souffrent. **Ces travaux ont permis l'élaboration d'un article en cours de préparation.**



# OBJECTIVES

The inflammatory response is an important part of the physiopathology of brain injury. Brain inflammatory reaction is, in some cases, relatively difficult to detect. Furthermore, inflammation could be related to cerebral deficits, even if no abnormality is detected on conventional imaging (MRI or CT-scan).

The objectives of this thesis were to extensively describe inflammatory responses that occur after a variety of brain injuries, such as ischemic stroke, mild traumatic brain injury and chronic alcohol consumption by using new imaging techniques, and detecting original targets that could modulate inflammatory reactions.

More precisely, the objectives are:

- 1) To describe the inflammatory responses after thromboembolic stroke model;
- 2) To discuss the anti-inflammatory treatments on stroke, from clinical and preclinical points of view;
- 3) To describe the inflammatory priming caused by chronic alcohol consumption and the consequences on stroke;
- 4) To develop a new model of mild TBI to longitudinally study the inflammatory responses and behavioral deficits provoked by this new model of mild TBI.

# RESULTATS

# 1. Study 1: Spatio-temporal profile of inflammatory responses in a thromboembolic stroke model

As described in the introduction, the **poor clinical relevance of experimental models of stroke** has been suggested as a main contributor to the dichotomy between promising experimental results and unsuccessful clinical trials testing immunomodulatory molecules for ischemic stroke. Most of the preclinical studies on the inflammatory responses triggered after ischemic stroke have been performed in models in which the middle cerebral artery (MCA) is permanently or transitorily occluded respectively by electrocoagulation or by a monofilament.

In this study, **we have investigated the inflammatory responses to stroke in an experimental model closer to the human pathology**, consisting on the direct injection of thrombin in the MCA which leads to the *in situ* formation of a fibrin-rich clot. **This model shares two important characteristics with the human pathology:** (i) mice can recanalize progressively and spontaneously within 24 hours after MCA occlusion, as in the case of a significant proportion of untreated stroke patients, and (ii) tPA-induced thrombolysis is beneficial when administered early after stroke onset ([Macrez et al., 2011](#); [Orset et al., 2007, 2016](#)).

We have compared the inflammatory reactions in this thromboembolic stroke model (TESM) to the “classical” experimental models of stroke. Our data show that the timing of inflammatory responses triggered by the TESM is quite similar to that observed in the permanent electrocoagulation model of the MCA, and is very different from that observed in the transient mechanical vascular occlusion models. **We propose the use of this clinically relevant experimental model to test immunomodulatory drugs before the translation to clinical trials.**



## **Spatio-temporal profile of inflammatory responses in a thromboembolic stroke model**

**Authors:** Antoine Drieu<sup>1</sup>, Camille Brodin<sup>1</sup>, Damien Levard<sup>1</sup>, Denis Vivien, PhD<sup>2</sup>, Marina Rubio, PhD<sup>1\*</sup>

### **Affiliations:**

<sup>1</sup> Normandie Univ, UNICAEN, INSERM, UMR-S U1237, Physiopathology and Imaging of Neurological Disorders, 14000 Caen, France

<sup>2</sup> CHU de Caen Normandy, Department of Clinical Research, 14000 Caen, France

\*To whom correspondence should be addressed: [rubio@cyceron.fr](mailto:rubio@cyceron.fr)

Cover title: Inflammation in thromboembolic stroke

Key Words: inflammation, ischemic stroke, leukocytes, microglia, experimental models

## **Abstract**

Inflammation has been proposed as a critical contributor to the pathophysiology of ischemic stroke. Nevertheless, clinical trials on stroke using immunomodulatory treatments have shown limited beneficial effects. In order to improve translational research in this field of research, it is mandatory to propose clinically relevant experimental models of stroke and to better characterize the inflammatory processes involved in the pathophysiology of stroke. Here, we characterized the inflammatory processes occurring in a clinically relevant stroke model consisting in the *in situ* injection of thrombin in the middle cerebral artery (MCA). Similar to clinical conditions, in this experimental model MCA spontaneously recanalizes within 24 hours after stroke onset more than 70% of mice. Magnetic resonance imaging and histological follow-up study to characterize the innate and adaptive immune responses to ischemic stroke was performed from early stages (six hours) up to 5 days after stroke onset. This model of stroke induces inflammatory reactions including (i) an early, long-lasting microglial response; (ii) neutrophil infiltration from 48 hours after stroke; and (iii) a late (after 48 hours) lymphocyte and blood-derived macrophage infiltration accompanied by fibrin(ogen) deposits at the lesion site. Our results suggest that this clinically relevant model should be used to test immunomodulatory drugs before the translation to clinical trials.

## **Introduction**

Ischemic stroke is the second leading cause of death and the first cause of acquired long-term disability worldwide. Every two seconds, someone in the world have a stroke ([stroke.org.uk](http://stroke.org.uk)). Ischemic stroke (80-85% of strokes) is described as the sudden interruption of blood flow in a particular brain region leading to rapid neuronal death [1]. Stroke is envisioned to be a multiphasic process involving excitotoxicity, apoptosis and inflammation [2]. In spite of promising results in experimental models of stroke, any of the treatments targeting these mechanisms have shown a clear beneficial effect in clinical practice. Indeed, the only successful and approved therapies for ischemic stroke nowadays are thrombolysis [i.e., the intravenous injection of tissue-type plasminogen activator (tPA)] within 4.5 hours after stroke onset [3] and thrombectomy (i.e., the mechanical removal of the clot) up to 24 hours after stroke onset [4].

The poor clinical relevance of experimental models of stroke has been suggested as a main contributor to the dichotomy between promising experimental results and unsuccessful clinical trials testing immunomodulatory molecules for ischemic stroke [5]. Although the majority of stroke patients show spontaneous and progressive arterial recanalization, most of the preclinical studies on the inflammatory responses triggered after ischemic stroke have been performed in models in which the middle cerebral artery (MCA) is permanently or transitorily occluded respectively by electrocoagulation or by a monofilament. In the case of transient mechanical occlusions, recanalization of the artery is sudden and associated to ischemic/reperfusion injuries [6]. Kinetics, localization, and intensity of the inflammatory responses differ among these models [7–9]. In an attempt to develop a more clinically relevant model of ischemic stroke, we conceived in the past years a new model of thromboembolic stroke in mice consisting in the injection of thrombin directly into the middle cerebral artery (MCA). This model leads to the formation of a fibrin-rich

clot in the lumen of the MCA [10,11]. Similar to clinical results [12–14], in this experimental model tissue-type plasminogen activator is able to reduce ischemic volume when injected early after stroke onset but not when injected late [10,15,16]. Also similar to the human pathology, in this experimental model the MCA spontaneously and progressively recanalizes in more than 70% of mice 24 hours after MCAo. The goal of this study is to describe the time-course inflammatory responses triggered after stroke onset in this clinically relevant experimental model of ischemic stroke.

## **Material and Methods**

### *Animals*

Studies were conducted in male Swiss mice (age 12 weeks, weight 35-45g). Mice were housed with food and water *ad libitum* access. All experiments were performed following the ARRIVE guidelines ([www.nc3rs.org.uk](http://www.nc3rs.org.uk)), including blind analyses of the samples.

### *Thromboembolic stroke model*

Mice were placed in a stereotaxic device, a small craniotomy was performed, the dura was excised, and the middle cerebral artery (MCA) was exposed. A pipette was introduced into the lumen of the MCA and 1 µL of purified murine alpha-thrombin (1 UI; Enzyme Research Labs) was pneumatically injected to induce the *in situ* formation of a clot. The pipette was removed 10 minutes after, when the clot had stabilized. Cerebral blood flow was monitored before and up to 30 min after MCA occlusion (MCAo).

### *Magnetic Resonance Imaging*

Mice were deeply anesthetized with 5% isoflurane and maintained with 1.5-2% isoflurane 30%O<sub>2</sub>/70%N<sub>2</sub>O during the acquisitions. Experiments were carried out on a Pharmascan 7T (Bruker, Germany). T2-weighted images were acquired using a multislice multiecho sequence: TE/TR 33 ms/2500 ms. Lesion sizes were quantified on these images using ImageJ software. T2\*-weighted sequences were used to control if animals underwent hemorrhages events. Two dimensional time-of-flight angiographies (TE/TR 12 ms/7 ms) were acquired and analyses of the MCA angiogram were also performed to control the recanalization status of the MCA. The angiographic score is inspired on the TIMI grade flow scoring. Score 0 refers to the absence of any antegrade flow beyond the MCA. Score 1 is incomplete filling of the distal bed. Score 2 is almost complete filling of the distal territory. Score 3 is complete filling of the distal territory.

### *Molecular imaging of infiltrated macrophages*

Two hundred microliters of naked Micro-sized particles of iron oxide (MPIOs) (diameter 1.08 mm) (Invitrogen) were gently injected into the caudal vein one day before thrombin injection. Three-dimensional T2\*-weighted gradient echo imaging of flow compensation (spatial resolution 70mm<sup>3</sup> isotropic), TE/TR 13.2ms/200ms and a flip angle of 21° was performed to detect MPIOs. T2\*-MRI acquisitions were performed every day starting from 1 day post MCAo. Signal void quantification was performed by using image threshold and results presented as MPIOs-induced signal void on the contralateral cortex divided by the signal void on the structure of interest in percent. Images were analyzed by Fiji software.

#### *Immunohistochemistry*

For all groups, mice were deeply anesthetized and transcardially perfused with cold heparinized saline (15 mL) followed by 100 mL of fixative (PBS 0.1 M. pH 7.4 containing 2% paraformaldehyde and 0.2% picric acid). Brains were post-fixed (18 hours; 4°C) and cryoprotected (sucrose 20% in PBS; 24 hours; 4°C) before freezing in Tissue-Tek (Miles Scientific, Naperville, IL, USA). Cryomicrotome-cut sections (10 µm) were collected on poly-lysine slides and stored at – 80°C before processing.

Sections were co-incubated overnight with rabbit anti-mouse Iba1 (1:1000, Wako 019-19741), rat anti-mouse CD68 (1:800, Abcam 53444), rat anti-mouse Ly6G (1:500, clone 1A8, StemCell 60031), goat anti-mouse type-IV Collagen (1:1000, SouthernBiotech 1340), rabbit anti-mouse CD3 (1:25, Abcam 5690), rat anti-mouse CD4 (1:25, eBiosciences 14-0042-86), rabbit anti-mouse Laminin (1:1000, Abcam 14055-50), sheep anti-mouse Fibrinogen (1:10000). Primary antibodies were revealed by using Fab'2 fragments of Donkey anti-rabbit linked to FITC, anti-sheep linked to FITC, anti-rat linked to Cy3, anti-rabbit linked to Cy5, anti-goat IgG linked to Cy5 (1:600, Jackson ImmunoResearch, West Grove, USA). Washed sections were coverslipped with antifade medium containing DAPI and images were digitally captured using a Leica DM6000

epifluorescence microscope-coupled coolsnap camera and visualized with Leica MM AF 2.2.0 software (Molecular Devices, USA) and further processed using ImageJ 1.51k software.

#### *Quantitative PCR analyses*

Terminally anesthetized mice (n=6/group) were transcardially perfused with cold heparinized saline (15 mL) and brains were excised. Cortex were dissected and maintained at -80 °C until messenger RNA (mRNA) extraction. Tissues were dissociated in TRI reagent (Sigma; Lyon, France), and RNA was isolated by the addition of chloroform. Total RNA was washed by ethanol and treated with TURBO DNase (Ambion; Saint Aubin, France). Total RNA was quantified by spectrophotometry (NanoDrop Technologies; Wilmington, USA). Reverse transcription from 1 µg of total RNA (or water as an internal control) was performed with the iScript Select cDNA Synthesis kit (Bio-Rad; Marnes-la-Coquette, France) in a total volume of 20 µL with the following cycle conditions: 42 °C (90 min); 85 °C (5 min). The cDNA products were then stored at -20 °C until their use.

Quantitative PCR was performed with 1 µL of 1:20 diluted cDNA, water and the RT-qPCR internal control), that were analyzed in 15 µL total of a 1× solution of iQ SYBR Green Supermix (Bio-Rad; Marnes-la-Coquette, France) containing 200 nM of each primer. Based on mRNA coding sequences ([www.ensembl.org](http://www.ensembl.org)), mouse-specific primers were designed by using the Primer3Plus software (<http://www.bioinformatics.nl/cgi-bin/primer3plus/primer3plus.cgi>) Gene sequences are specified in Supplementary table 1. Two housekeeping genes (Hmbs and Ppib) were used. Assays were run in triplicate on the CFX96 real-time system c1000 thermal cycler (Bio-Rad; Marnes-la-Coquette, France), with the following cycle conditions: 95 °C (3 min); [95 °C (2 s), 60 °C (20 s)] × 39; 70 °C (30 s).

#### *Statistical analyses*

Results are the mean  $\pm$  SEM. Statistical analyses were performed using the Statview software. The Wilcoxon test was used to compare values between ipsi- and contralateral cortex; the Mann-Whitney test was used to compare between the different time points.

## **Results**

### *Characterization of thrombin-induced vascular occlusion*

Using T2-weighted MRI sequences, we revealed ischemic brain lesions 6 hours after surgery ( $5.93 \pm 0.91 \text{ mm}^2$ ), extending at 24 hours ( $15.01 \pm 2.75 \text{ mm}^2$ ;  $p < 0.05$  vs 6 hours), stabilizing at 48 hours ( $17.17 \pm 5.24 \text{ mm}^2$ ;  $p < 0.05$  vs 6 hours) and apparently reducing in size after 5 days ( $9.77 \pm 2.74 \text{ mm}^2$ ) (Fig. 1a-1c;  $n=4-6$  mice/group). Hemorrhagic transformation was not detected in any of the mice (data not shown). Similar to human stroke, in this experimental model clots are progressively and spontaneously fibrinolysed: 24 hours after MCAo 72% of mice show a partial (score 2) or total (score 3) recanalization of the MCA (Fig. 1d, 1e). These angiographic analyses were obtained from an independent series of mice ( $n=18$ ).

### *Microglial recruitment*

The macroscopic profile of microglia/macrophage responses after MCAo has been schematized in Fig. 2a. The shape of microglia, and the characteristic staining of Iba1 and CD68 markers are shown in Fig. 2b.

Six hours after ischemic stroke onset, the number of microglial cells (total Iba1<sup>+</sup> staining; Fig. 2c) increased in the ipsilateral cortex (peri-infarct zone  $191.73 \pm 10.96 \text{ cells/mm}^2$ , +176% vs before; core =  $202.26 \pm 15.65 \text{ cells/mm}^2$ , +185%), and this number considerably increased 5 days after stroke onset. The number of total CD68<sup>+</sup> cells (Fig. 2d), a lysosomal marker present in activated microglial cells and macrophages, also continuously increased from six hours (peri-infarct zone  $144.98 \pm 0.69 \text{ cells/mm}^2$ , +161% vs basal; core  $156.97 \pm 7.39 \text{ cells/mm}^2$ , +174%) to 5 days after stroke onset (peri-infarct zone  $334.57 \pm 25.23 \text{ cells/mm}^2$ , +371% vs basal; core  $1638.99 \pm 90.63 \text{ cells/mm}^2$ , +1818%).

### *Macrophage recruitment*

Furthermore, we also counted the number of CD68<sup>+</sup>Iba1<sup>-</sup> cells (which we considered as infiltrated) (Fig. 3a). The number of CD68<sup>+</sup>Iba1<sup>-</sup> cells increased from six hours (peri-infarct zone  $12.01 \pm 1.08$  cells/mm<sup>2</sup>, +177% vs basal; core  $16.28 \pm 2.25$  cells/mm<sup>2</sup>, +240%) to 48 hours (peri-infarct zone  $10.47 \pm 1.81$  cells/mm<sup>2</sup>, +154% vs basal; core  $28.95 \pm 6.69$  cells/mm<sup>2</sup>, +427%) after stroke onset. This number markedly increased 5 days after stroke onset in the core of the lesion (peri-infarct zone  $13.79 \pm 1.23$  cells/mm<sup>2</sup>, +203% vs basal; core  $1011.23 \pm 187.02$  cells/mm<sup>2</sup>, +14906%). Furthermore, 3D-T2\* acquisitions allowed the specific detection of hyposignals corresponding to phagocytized-MPIOs by macrophages (Fig. 3b-3c). Hyposignals were discrete at 24 and 48 hours after stroke onset and markedly increased at 5 days (Fig. 3d-3e).

#### *Fibrin(ogen) deposits*

Fibrin(ogen) deposits associated to blood-brain barrier (BBB) leakage were not detected before 48 hours post-stroke (Fig. 3f). Slight signals were found at 48 hours, and clear fibrin(ogen) deposits were found at the lesion core 5 days after stroke onset (Fig. 3f). No quantification has been performed on these photomicrographs.

#### *Neutrophils and lymphocytes*

A small number of Ly6G<sup>+</sup> neutrophils (Fig. 4a) was found at 48 hours after stroke onset (peri-infarct zone  $2.39 \pm 0.78$  cells/mm<sup>2</sup>; core  $29.58 \pm 3.88$  cells/mm<sup>2</sup>; Fig. 4b-4c). The number of neutrophils markedly increased at 5 days after stroke onset on the core as well as on the peri-infarct zone of the lesion (peri-infarct zone  $46.72 \pm 15.86$  cells/mm<sup>2</sup>; core  $54.85 \pm 17.66$  cells/mm<sup>2</sup>; Fig. 4b-4c). In both time points, neutrophils were found beside blood vessels and within the brain parenchyma (Fig. 4a). No neutrophils were found before stroke.

CD3<sup>+</sup> and CD4<sup>+</sup> lymphocytes (Fig. 4d) were only found in the brain only at 5 days after stroke onset (Fig. 4e). Lymphocytes were found in the peri-infarct zone (CD3<sup>+</sup> cells:  $85.55 \pm 17.88$  cells/mm<sup>2</sup>; Fig. 4f) (CD4<sup>+</sup> cells:  $17.61 \pm 1.25$  cells/mm<sup>2</sup>; Fig. 4g) and in the core of the lesion CD3<sup>+</sup>

cells:  $213.53 \pm 31.71$  cells/mm<sup>2</sup>; Fig. 4f) (CD4<sup>+</sup> cells:  $79.91 \pm 9.2$  cells/mm<sup>2</sup>; Fig. 4g). In both cases, lymphocytes were found beside blood vessels and within the brain parenchyma. No lymphocytes were found before stroke.

#### *Gene expression of inflammatory markers*

We have studied the levels of inflammatory markers gene expression in the brain during the first 24 hours after stroke. We found an early and marked increase of the pro-inflammatory cytokines IL-1b and TNF, which rapidly returned to basal levels in the ipsilateral cortex (Supplementary Fig. 2). Expression of the Toll-like receptor (TLR) 4 significantly increased at 24 hours post stroke onset (Supplementary Fig. 2). In accordance to the double role as an inflammatory mediator during the acute phase and as a neurotrophic mediator between the subacute and prolonged phases [17], IL-6 shows an early but more sustained increase in the ipsilateral cortex from 6 hours after stroke (Supplementary Fig. 2). The anti-inflammatory cytokine TGF $\beta$  significantly increased at 24 hours post stroke onset (Supplementary Fig. 2).

## **Discussion**

This study has been designed to describe the time-course of the inflammatory responses triggered in an experimental model of thromboembolic stroke consisting in the injection of thrombin directly into the MCA, which provokes the *in situ* formation of a fibrin-rich clot. This experimental model is clinically relevant, since it shows two important similarities to the human pathology: (i) the early administration of tPA is beneficial and reduces lesion size [3,10,16], and (ii) **more than 70% of mice progressively and spontaneously recanalize within the first 24 hours after MCAo.**

Our study shows that in this thromboembolic stroke model (TESM), the inflammatory response is characterized by a marked, long-lasting microglial response beginning early after stroke onset (from 6 hours). Neutrophils start to infiltrate at 48 hours, whereas lymphocytes and monocyte-derived macrophages arrive later on (after 48 hours). Given that, in our hands, the volume of the infarcted area is maximal at 24-48 hours, our data suggest that **only the inflammatory responses within the first 48 hours (notably microglial response) could play a role on the establishment of the final lesion.** Upon these data, immunomodulatory therapies aiming at reducing lesion volume by blocking leukocyte infiltration are doomed to failure, but therapies targeting microglia might be able to reduce lesion volume. Recently, experimental studies have focused on the switch of microglial cell phenotype from pro- to anti-inflammatory as a potential target to improve stroke outcome, by administering IL-33 [18] or IL-4 [19]. In addition, mice selectively depleted for microglia show an increased lesion volume after experimental stroke [20], and the selective elimination of proliferating microglial cells exacerbates ischemic injury in the brain [21]. One of the future challenges in stroke therapy will be the effective administration of specific microglia-modulating therapies in clinical practice. From the clinical side, the antibiotic minocycline, by inhibiting microglial activation among other mechanisms, has shown promising results in two

phase II clinical trials [22,23]. However, a third pilot study performed in a small sample of acute stroke patients has shown that minocycline administration was safe but not efficacious [24]. Larger clinical trials are thus needed to study the effect of minocycline in stroke patients.

We show here that 5 days after MCAo, blood-derived macrophage and lymphocyte infiltration are accompanied by fibrin(ogen) deposits at the lesion core. Fibrinogen is a central blood coagulation protein deposited in the CNS after blood–brain barrier (BBB) disruption. In the context of multiple sclerosis, fibrinogen induces microglial activation, encephalitogenic adaptive immune responses and peripheral macrophage recruitment into the CNS leading to demyelination [25,26]. The fibrin(ogen) deposits found in our study are the result of both the passage from the vasculature due to BBB leakage and an insufficient parenchymal fibrinolysis. In view of the simultaneous presence of fibrin(ogen), lymphocytes and macrophages 5 days after MCAo in our study, additional studies are needed to understand (i) whether fibrin(ogen) deposition is cause or consequence of lymphocyte and blood-derived macrophage infiltration in the context of stroke, and (ii) whether the modulation of fibrin(ogen) deposit can modulate leukocyte recruitment and/or neurological outcome.

Our results show that the inflammatory responses triggered by the TESM are globally similar those occurring after the permanent MCAo by electrocoagulation (EC) described by Zhou and colleagues [7] (see comparative schema in Fig. 5). This observation suggests that **the timing of immune responses is independent of the recanalization of the artery**, since in the TESM mice spontaneously recanalize within 24 hours after MCAo, in contrast with the permanent EC model [27]. It has been recently suggested that the transendothelial route could not be the primary route of leukocyte infiltration after stroke. Instead, leukocyte would infiltrate the ischemic region via the choroid plexus [28] and the perivascular spaces. This could explain **how immune cells arrive to**

**the lesion site even after the permanent occlusion of the MCA**, as well as the failure of the blockade of the transendothelial migration of leukocytes in stroke clinical trials. The final location of neutrophils in the ischemic tissue is still debated. Some studies have reported that neutrophils cross the vessel wall but stay at the perivascular space [29]. In our hands, neutrophil reach the brain parenchyma, in accordance with other studies [30].

The vast majority of preclinical data on experimental models of ischemic stroke has been obtained on transient mechanical vascular occlusion (TMVO) models, in which recanalization occurs too but provoke ischemia/reperfusion injury, thromboinflammation and secondary microthrombosis. Secondary microthrombosis is a major pathophysiologic mechanism leading to brain damage, which does not occur in other models based on clot-induced ischemic stroke like the TESM [6]. Interestingly, the time-course immune response induced by the TESM model and EC models of stroke substantially differs from the TMVO models reported in the past [7,8]. Notably, microglial response is practically absent after 30 or 90 minutes of TMVO, and neutrophil infiltration occur earlier and is maximal at 24 hours after MCAo. Immunomodulatory agents that have clearly shown beneficial effects on TMVO models of stroke could actually be targeting thromboinflammation and secondary microthrombosis. Since it is unclear whether thromboinflammation is a universal pathophysiological mechanism of human stroke, immunomodulatory drugs need to be evaluated or re-evaluated in experimental stroke models not inducing secondary thromboinflammation before trying to apply them in clinical practice.

Although it is clear that ischemic stroke triggers a series of inflammatory responses at the lesion site, **it is less clear whether these inflammatory responses, especially leukocyte infiltration to the ischemic area, actually contribute to the propagation of ischemic lesions and to the final lesion volume**. The reasons of this controversy are sustained by (i) the lack of beneficial effects of

immunomodulatory therapies in stroke patients, (ii) contradictory pre-clinical results testing leukocyte recruitment obtained in different models of stroke, (iii) the fact that the timing of leukocyte infiltration does not match with the establishment of the final lesion (at least in preclinical studies), and (iv) pre-clinical data showing similar infarct volumes despite decreased or increased leukocyte infiltration after stroke [28,31].

Interestingly, it has been described that **leukocyte infiltration may influence neurological outcome independently of the final lesion volume** [28,31], **but the mechanisms mediating this effect are poorly understood and need to be elucidated.** It is possible that the modulation of the sub-acute and late inflammatory responses after stroke (notably leukocyte infiltration to the tissue) could have an impact on the neurological outcome. Given the time-course responses observed here, and the absence of a clear beneficial effect on the clinical trials on the use of immunomodulatory therapies blocking leukocyte infiltration when administered early after stroke onset, it is maybe time to reconsider a later administration in clinical practice.

It is important to note that the results presented here have been obtained in young, healthy mice, and we acknowledge that immune responses can substantially vary in time and intensity in co-morbid conditions like hypertension or ageing.

## **Summary/Conclusions**

Taken together, our data show that this thromboembolic model of stroke (TESM) by the *in situ* injection of thrombin provokes immune responses, such as microglial activation and leukocyte recruitment. The timeline of cell infiltration is similar to the permanent model of electrocoagulation, suggesting that the immune responses triggered after ischemic stroke are independent of recanalization. Given the timeline of the immune responses found in this study,

immunomodulatory drugs targeting leukocyte infiltration after stroke may influence neurological outcome, but not lesion volume. This clinically relevant TESM should be used to test immunomodulatory drugs before the translation to clinical trials.

**Acknowledgments:**

**Sources of Funding:** This work was funded by INSERM (Institut National de la Santé et de la Recherche Médicale), the French ministry of higher education and research, the University of Caen Basse-Normandie.

**Disclosures:** None

## **References:**

1. Rha J-H, Saver JL. The impact of recanalization on ischemic stroke outcome: a meta-analysis. *Stroke*. 2007;38:967–73.
2. Dirnagl U, Iadecola C, Moskowitz MA. Pathobiology of ischaemic stroke: an integrated view. *Trends Neurosci*. 1999;22:391–7.
3. Carpenter CR, Keim SM, Milne WK, Meurer WJ, Barsan WG, Best Evidence in Emergency Medicine Investigator Group. Thrombolytic therapy for acute ischemic stroke beyond three hours. *J Emerg Med*. 2011;40:82–92.
4. Nogueira RG, Jadhav AP, Haussen DC, Bonafe A, Budzik RF, Bhuva P, et al. Thrombectomy 6 to 24 Hours after Stroke with a Mismatch between Deficit and Infarct. *N Engl J Med*. 2018;378:11–21.
5. Drieu A, Levard D, Vivien D, Rubio M. Anti-inflammatory treatments for stroke: from bench to bedside. *Ther Adv Neurol Disord*. 2018;11:1756286418789854.
6. Gauberti M, Martinez de Lizarrondo S, Orset C, Vivien D. Lack of secondary microthrombosis after thrombin-induced stroke in mice and non-human primates. *J Thromb Haemost*. 2014;12:409–14.
7. Zhou W, Liesz A, Bauer H, Sommer C, Lahrmann B, Valous N, et al. Postischemic brain infiltration of leukocyte subpopulations differs among murine permanent and transient focal cerebral ischemia models. *Brain Pathol*. 2013;23:34–44.
8. Gelderblom M, Leypoldt F, Steinbach K, Behrens D, Choe C-U, Siler DA, et al. Temporal and Spatial Dynamics of Cerebral Immune Cell Accumulation in Stroke. *Stroke*. 2009;40:1849–57.
9. Chu HX, Kim HA, Lee S, Moore JP, Chan CT, Vinh A, et al. Immune cell infiltration in malignant middle cerebral artery infarction: comparison with transient cerebral ischemia. *J Cereb Blood Flow Metab*. 2014;34:450–9.
10. Orset C, Macrez R, Young AR, Panthou D, Angles-Cano E, Maubert E, et al. Mouse model of in situ thromboembolic stroke and reperfusion. *Stroke*. 2007;38:2771–8.
11. Le Behot A, Gauberti M, Martinez De Lizarrondo S, Montagne A, Lemarchand E, Repesse Y, et al. GpIba-VWF blockade restores vessel patency by dissolving platelet aggregates formed under very high shear rate in mice. *Blood*. 2014;123:3354–63.
12. Kimura K, Sakamoto Y, Iguchi Y, Shibasaki K. Serial changes in ischemic lesion volume and neurological recovery after t-PA therapy. *J Neurol Sci*. 2011;304:35–9.
13. Pialat J-B, Wiart M, Nighoghossian N, Adeleine P, Derex L, Hermier M, et al. Evolution of lesion volume in acute stroke treated by intravenous t-PA. *J Magn Reson Imaging*. 2005;22:23–8.

14. Effect of intravenous recombinant tissue plasminogen activator on ischemic stroke lesion size measured by computed tomography. NINDS; The National Institute of Neurological Disorders and Stroke (NINDS) rt-PA Stroke Study Group. *Stroke*. 2000;31:2912–9.
15. Orset C, Haelewyn B, Allan SM, Ansar S, Campos F, Cho TH, et al. Efficacy of Alteplase in a Mouse Model of Acute Ischemic Stroke: A Retrospective Pooled Analysis. *Stroke*. 2016;47:1312–8.
16. Macrez R, Obiang P, Gauberti M, Roussel B, Baron A, Parcq J, et al. Antibodies preventing the interaction of tissue-type plasminogen activator with N-methyl-D-aspartate receptors reduce stroke damages and extend the therapeutic window of thrombolysis. *Stroke*. 2011;42:2315–22.
17. Suzuki S, Tanaka K, Suzuki N. Ambivalent aspects of interleukin-6 in cerebral ischemia: inflammatory versus neurotrophic aspects. *J Cereb Blood Flow Metab*. 2009;29:464–79.
18. Yang Y, Liu H, Zhang H, Ye Q, Wang J, Yang B, et al. ST2/IL-33-Dependent Microglial Response Limits Acute Ischemic Brain Injury. *J Neurosci*. 2017;37:4692–704.
19. Liu X, Liu J, Zhao S, Zhang H, Cai W, Cai M, et al. Interleukin-4 Is Essential for Microglia/Macrophage M2 Polarization and Long-Term Recovery After Cerebral Ischemia. *Stroke*. 2016;47:498–504.
20. Szalay G, Martinecz B, Lénárt N, Környei Z, Orsolits B, Judák L, et al. Microglia protect against brain injury and their selective elimination dysregulates neuronal network activity after stroke. *Nature Communications*. 2016;7:11499.
21. Lalancette-Hébert M, Gowing G, Simard A, Weng YC, Kriz J. Selective ablation of proliferating microglial cells exacerbates ischemic injury in the brain. *J Neurosci*. 2007;27:2596–605.
22. Lampl Y, Boaz M, Gilad R, Lorberboym M, Dabby R, Rapoport A, et al. Minocycline treatment in acute stroke: an open-label, evaluator-blinded study. *Neurology*. 2007;69:1404–10.
23. Padma Srivastava MV, Bhasin A, Bhatia R, Garg A, Gaikwad S, Prasad K, et al. Efficacy of minocycline in acute ischemic stroke: a single-blinded, placebo-controlled trial. *Neurol India*. 2012;60:23–8.
24. Kohler E, Prentice DA, Bates TR, Hankey GJ, Claxton A, van Heerden J, et al. Intravenous minocycline in acute stroke: a randomized, controlled pilot study and meta-analysis. *Stroke*. 2013;44:2493–9.
25. Davalos D, Ryu JK, Merlini M, Baeten KM, Le Moan N, Petersen MA, et al. Fibrinogen-induced perivascular microglial clustering is required for the development of axonal damage in neuroinflammation. *Nat Commun*. 2012;3:1227.
26. Ryu JK, Petersen MA, Murray SG, Baeten KM, Meyer-Franke A, Chan JP, et al. Blood coagulation protein fibrinogen promotes autoimmunity and demyelination via chemokine release and antigen presentation. *Nat Commun*. 2015;6:8164.

27. Gauberti M, Montagne A, Marcos-Contreras OA, Le Béhot A, Maubert E, Vivien D. Ultra-sensitive molecular MRI of vascular cell adhesion molecule-1 reveals a dynamic inflammatory penumbra after strokes. *Stroke*. 2013;44:1988–96.
28. Llovera G, Benakis C, Enzmann G, Cai R, Arzberger T, Ghasemigharagoz A, et al. The choroid plexus is a key cerebral invasion route for T cells after stroke. *Acta Neuropathologica*. 2017;134:851–68.
29. Enzmann G, Mysiorek C, Gorina R, Cheng Y-J, Ghavampour S, Hannocks M-J, et al. The neurovascular unit as a selective barrier to polymorphonuclear granulocyte (PMN) infiltration into the brain after ischemic injury. *Acta Neuropathol*. 2013;125:395–412.
30. Perez-de-Puig I, Miró-Mur F, Ferrer-Ferrer M, Gelpí E, Pedragosa J, Justicia C, et al. Neutrophil recruitment to the brain in mouse and human ischemic stroke. *Acta Neuropathol*. 2015;129:239–57.
31. Pedragosa J, Salas-Perdomo A, Gallizoli M, Cugota R, Miró-Mur F, Briansó F, et al. CNS-border associated macrophages respond to acute ischemic stroke attracting granulocytes and promoting vascular leakage. *Acta Neuropathol Commun*. 2018;6:76.

## **Figure legends**

**Fig. 1. Murine model of thromboembolic stroke.** (a) MCA occlusion (MCAo) model (adapted from Orset et al., 2007). One  $\mu$ l of thrombin is directly injected into the MCA by using a glass micropipette. (b) Representative T2-weighted MRI scans at different time points before and after MCAo. (c) Quantification of the lesion volume at different time points. N=3-5 mice per group, \* $p<0.05$  vs 6 hours, Mann Whitney test. (d) Representative angiographies showing the complete occlusion of the MCA 1 hour after the occlusion and its spontaneous recanalization after 24 hours. (e) Percentage of angiographic scores 24 hours after the MCAo. Score 0 = complete occlusion; score 1 = incomplete filling of the distal bed; score 2 = almost complete filling of the distal territory; score 3 = complete filling of the distal bed. (f) Identification of the studied zones by immunohistochemistry: contralateral cortex (CTL), peri-infarct zone (PI) and ischemic core (IC).

**Fig. 2. Quantification of total microglia, activated microglia/macrophages and macrophages at different time points after thromboembolic stroke.** (a) Schematic representation of the immunostainings found in the ipsilateral cortex, superposed on a T2w MRI scan: total microglia (green), activated microglia (yellow) and macrophages (red). (b) Characteristic shape of microglia, and the characteristic staining of Iba1 and CD68 markers in the ipsilateral cortex. Quantification of (c) total microglia (Iba1+cells), (d) activated microglia/macrophages (CD68+ cells) (N=3-5 mice per group).

**Fig. 3. Quantification of macrophage and fibrinogen infiltration after thromboembolic stroke.** (a) Quantification of macrophages (Iba1-CD68+cells) (N=3-5 mice per group). (b) Schema of the experimental design to detect specifically blood-derived macrophage infiltration after stroke. (c) Representative T2w and T2\*w MRI images from mice injected with nude MPIO (iv) 1 day before stroke. (d) Quantification of MPIO signal at each time point. N=6 mice per group, \* $p<0.05$ ,

Mann-Whitney test. Scale bar: 10 $\mu$ m. (e) Representative photomicrographs of infiltrated macrophages positive for CD68 and containing MPIO 5 days after MCAo, (f) Representative photomicrographs of fibrinogen deposits (Fibrinogen $^+$ , green) and macrophages (CD68 $^+$ , red) in the ischemic lesion 6 hours, 24 hours, 48 hours and 5 days after MCAo. Scale bar: 100  $\mu$ m.

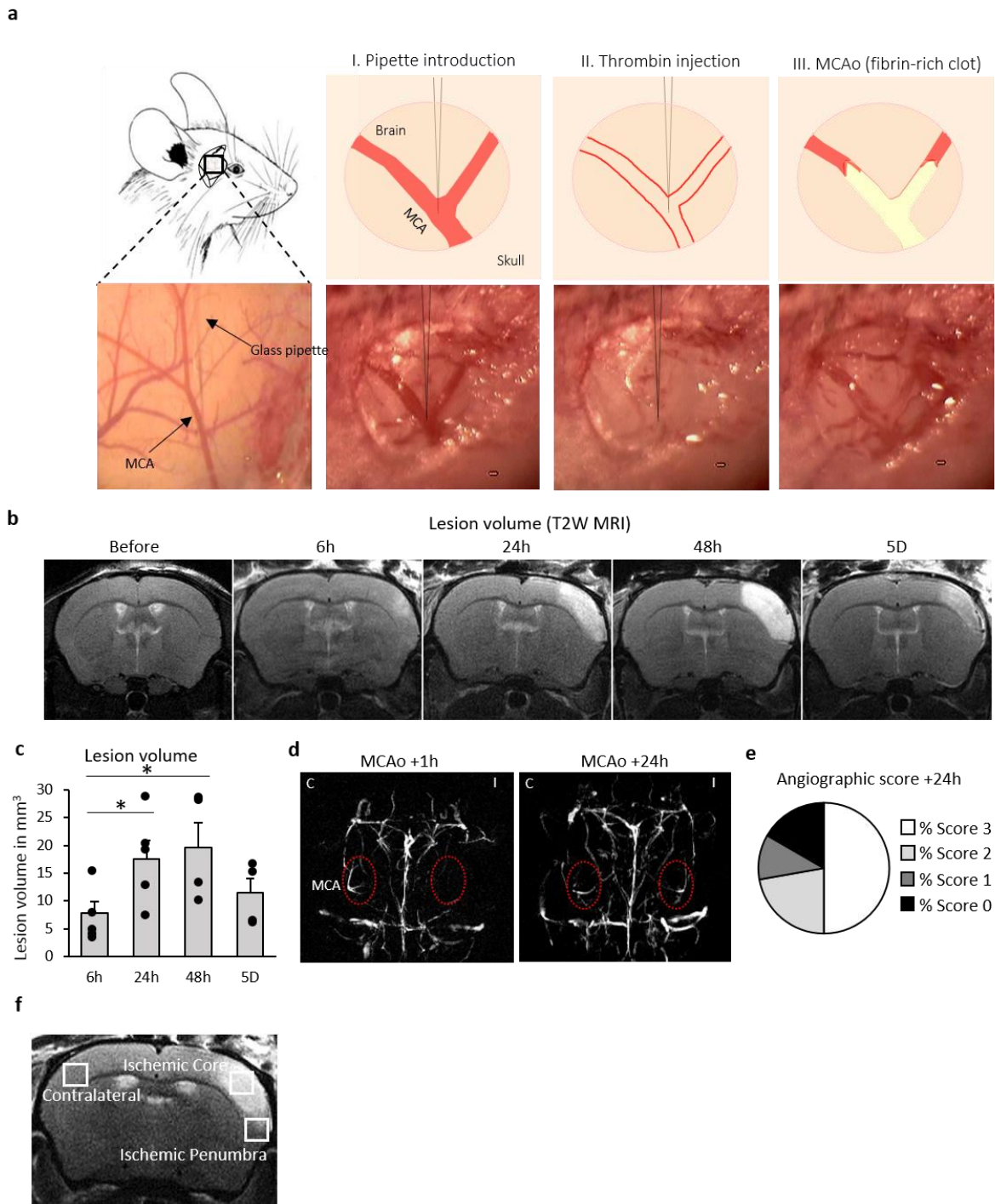
**Fig. 4. Quantification of neutrophil and lymphocyte infiltration after thromboembolic stroke.**

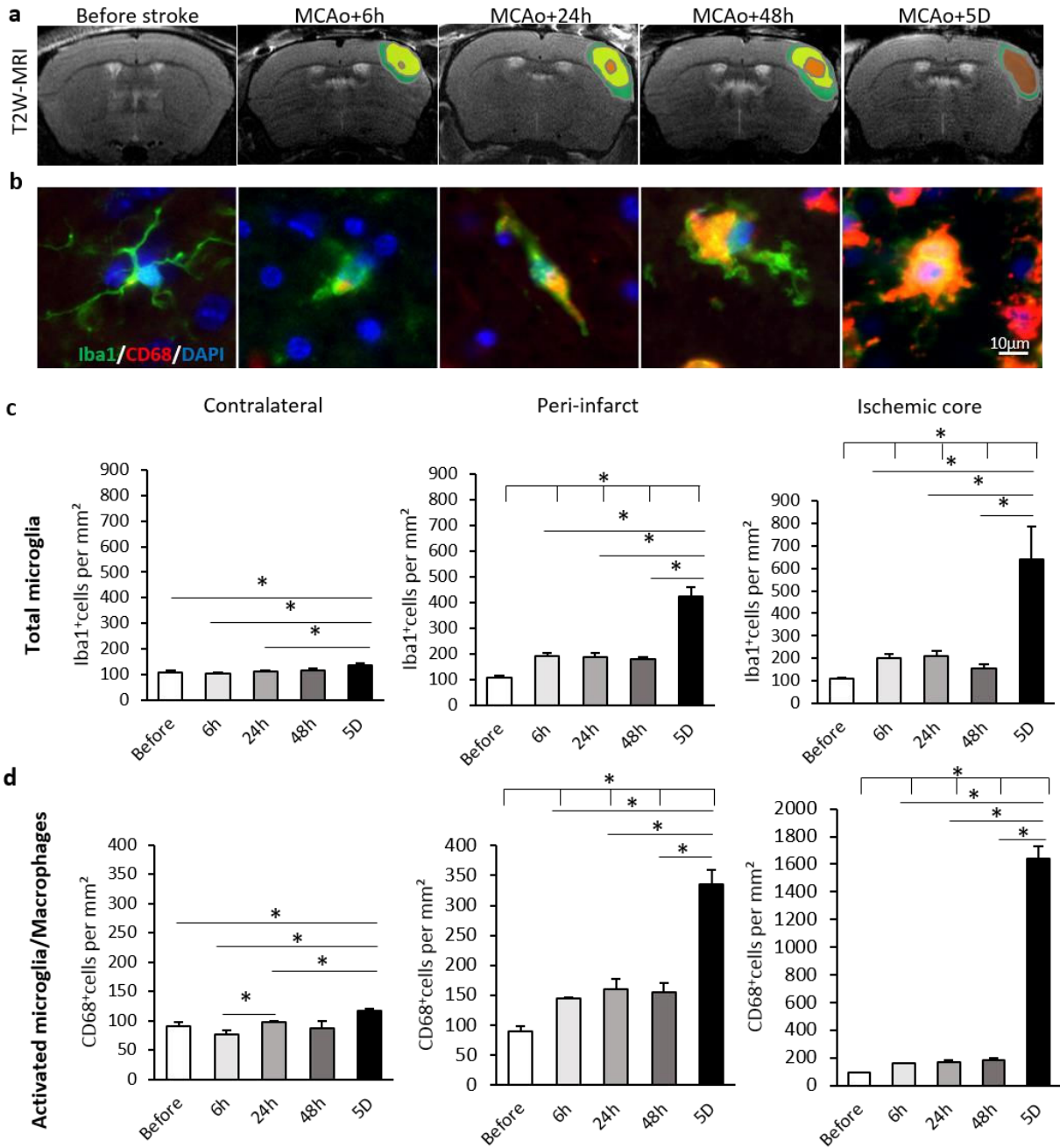
(a) Representative photomicrographs obtained by epifluorescence microscopy of neutrophil (Ly6G $^+$  cells) infiltration on the ischemic core 5 days after thromboembolic stroke. Note the absence of Ly6G $^+$  cells at 6 and 24 hours after MCAo. (b) Illustration of the distribution of Ly6G $^+$  cells 48 hours and 5 days after MCAo. (c) Quantification of neutrophils on the contralateral cortex, peri-infarct zone and the ischemic core at 6, 24, 48 hours and 5 days after MCAo. N=3-5 mice per group, \*p<0.05, Mann-Whitney test. Scale bar: 50 $\mu$ m. (d) Representative photomicrographs of lymphocytes on the ischemic core 5 days after thromboembolic stroke. Note the absence of CD3 $^+$  and CD4 $^+$  cells at 6, 24 and 48 hours after MCA occlusion. (e) Illustration of the distribution of lymphocytes 5 days after MCA occlusion. (f) Quantification of total lymphocytes (CD3 $^+$  cells). (g) Quantification of CD4 $^+$  lymphocytes. All the quantifications were done on contralateral cortex, peri-infarct zone and core of the lesion at 6, 24, 48 hours and 5 days after MCAo. N=3-5 mice per group, \*p<0.05, Mann-Whitney test. Scale bar: 50 $\mu$ m.

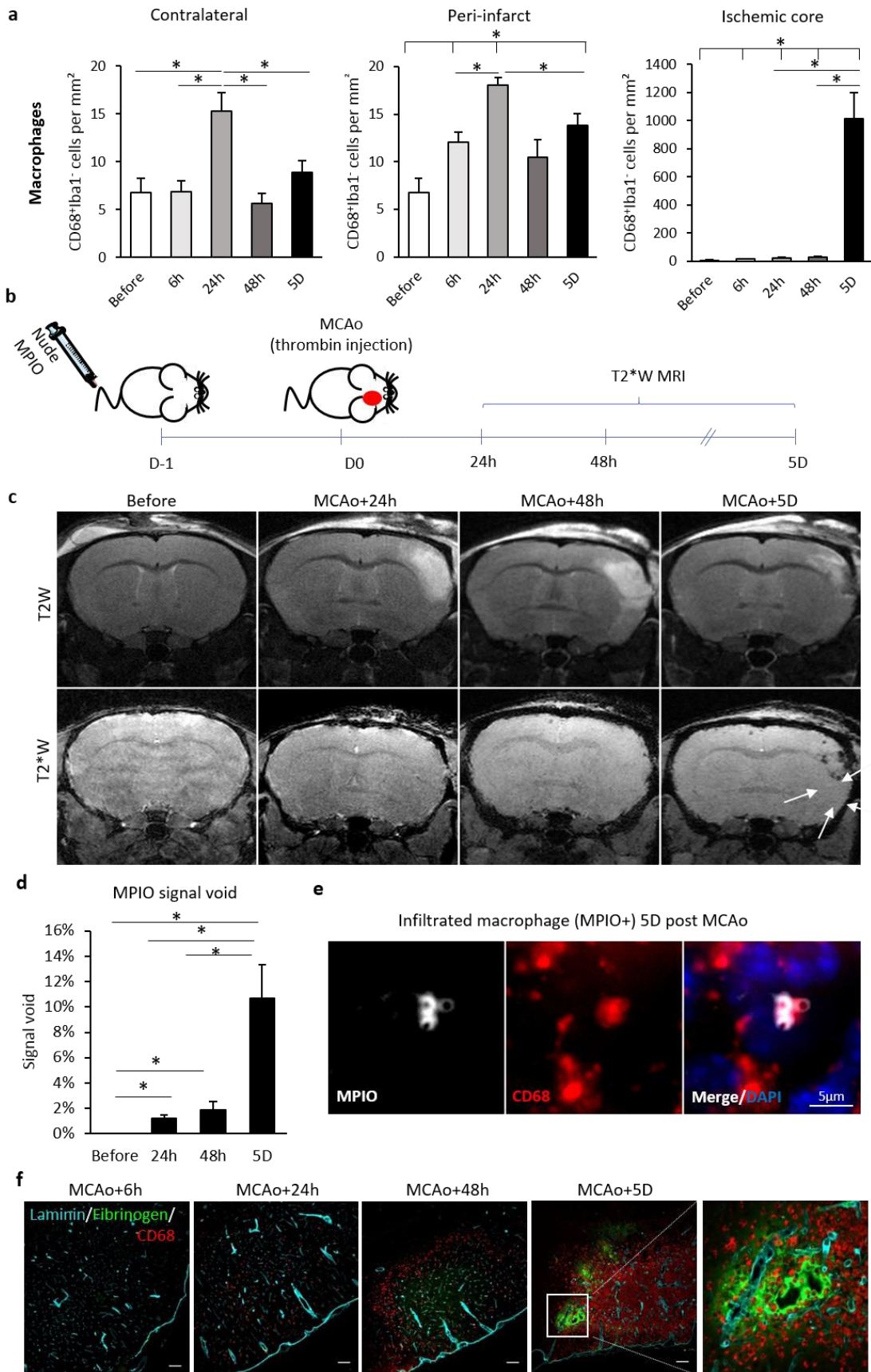
**Fig 5. Schematic representation of the temporal profile of the stroke-induced immune responses at the ipsilateral cortex in different experimental models of stroke.**

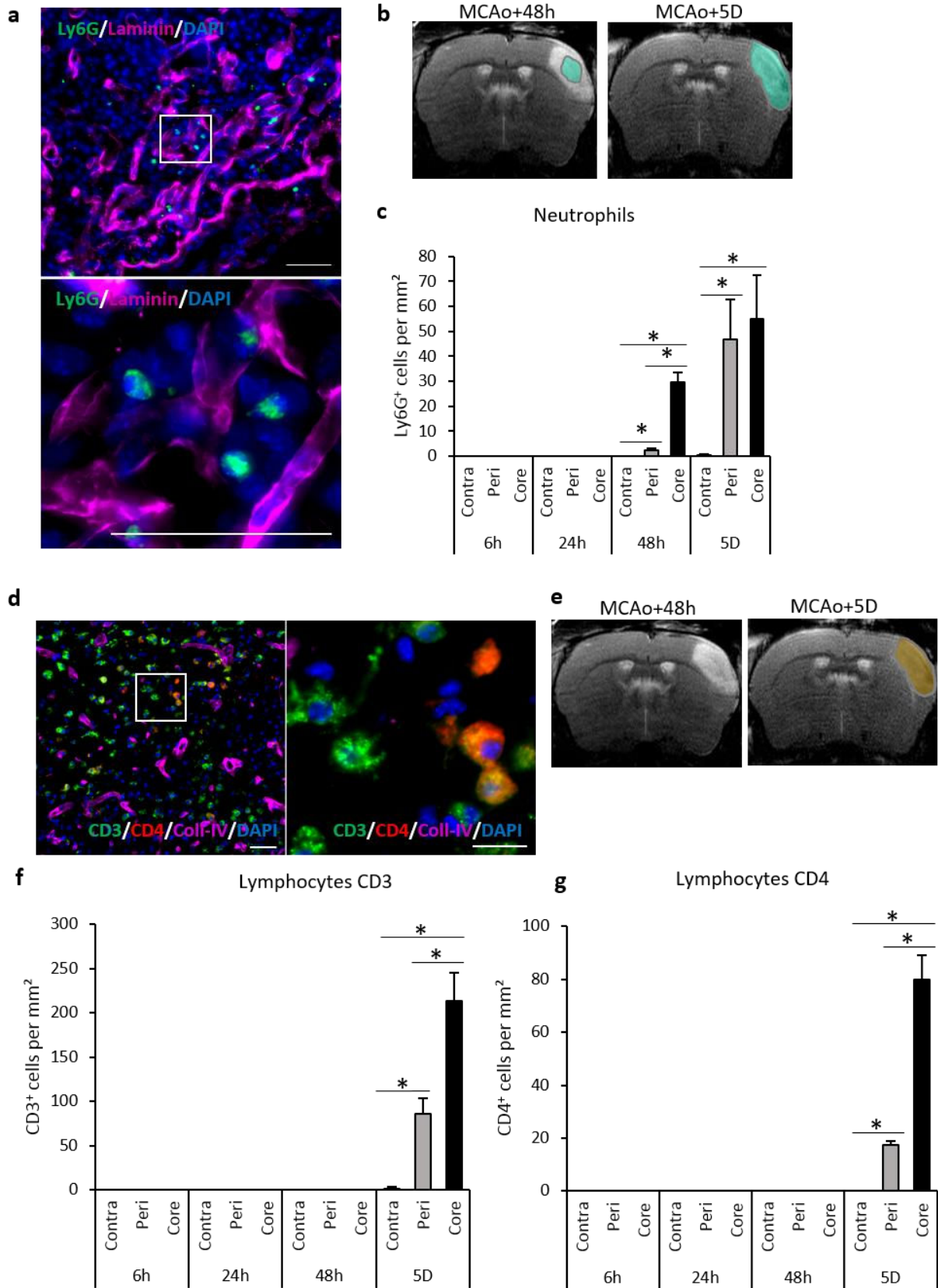
**Supplementary Fig. 1. Quantification of the gene expression of inflammatory markers in the brain before and after thromboembolic stroke.** N=5-6 mice per group, \*p<0.05, Mann-Whitney test.

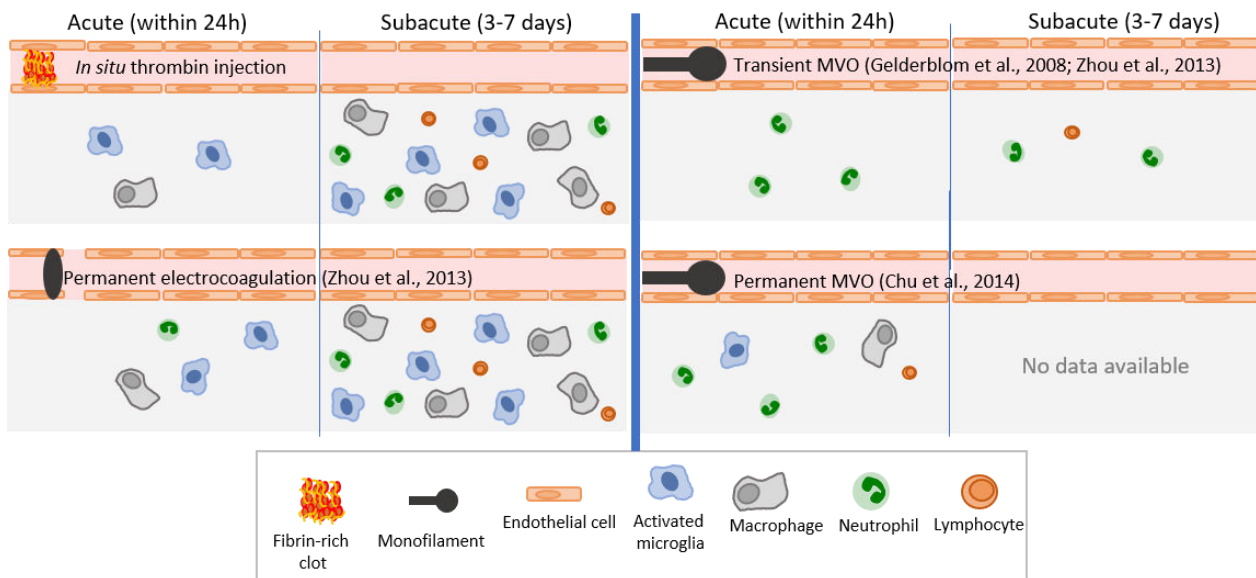
**Supplementary Table 1.** Primers used for qPCR analyses.

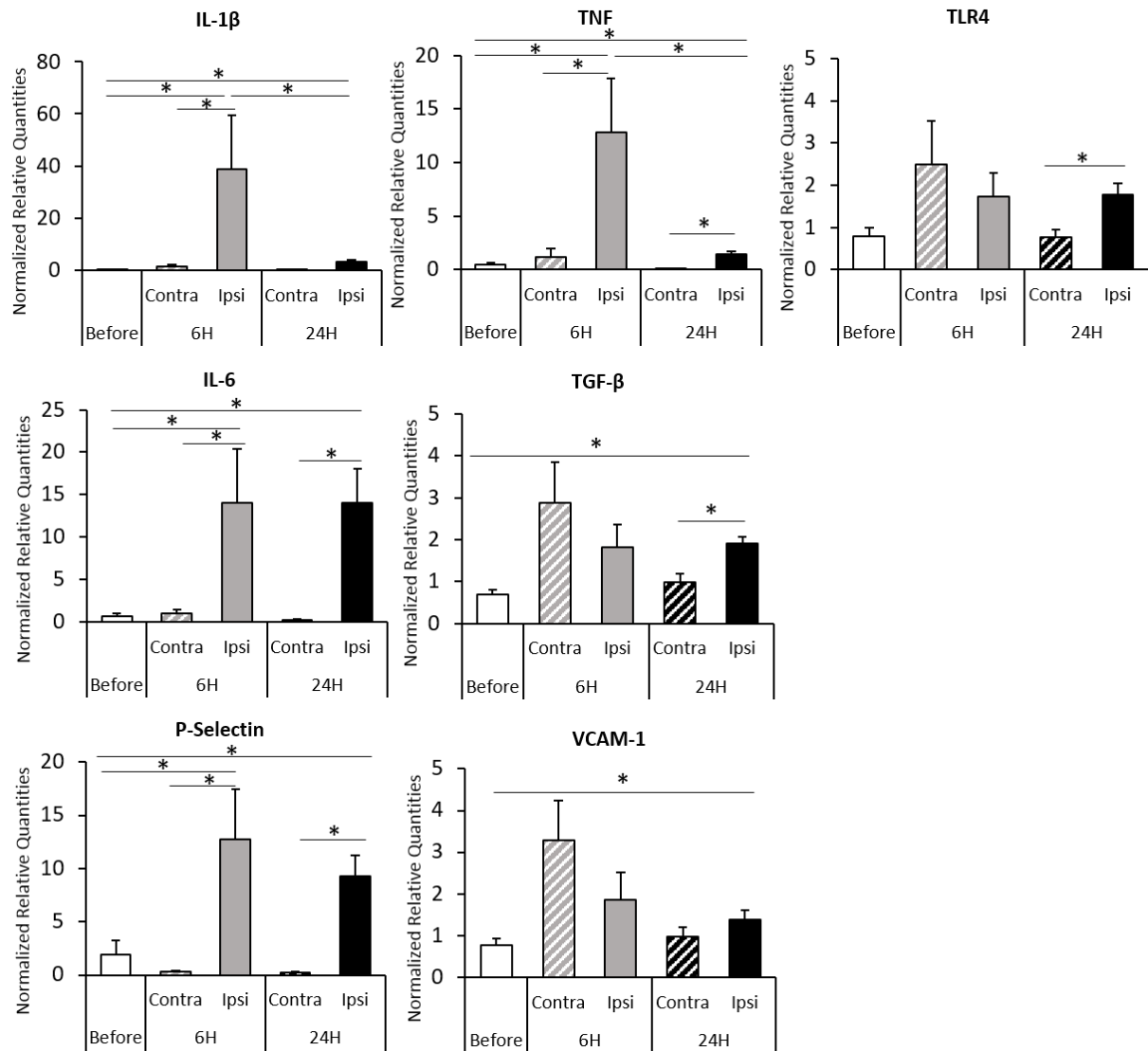












Gene	Forward sequence	Reverse sequence
TNF $\alpha$	TCTACTGAACCTCGGGGTGA	AGGGTCTGGGCCATAGAACT
IL-1 $\beta$	GACCTTCCAGGATGAGGACA	AGGCCACAGGTATTTGTCG
IL-6	GACAAAGCCAGAGTCCTTCAG	GCCACTCCTCTGTGACTCC
TGF $\beta$	GGCTACCATGCCAACTTCTG	TGGTTGTAGAGGGCAAGGAC
VCAM-1	GAACCCAAACAGAGGCAGAG	TGAGCAGGTCAGGTTCACAG
ICAM	AGGGCTGGCATTGTTCTTA	CTTGGAATGGTAGCTGGAA
P-selectin	GGCAAGTCCAATGATGAACC	CCATAGAAGCCTGGTAGCA
Hmbs	GAAATCATTGCTATGTCCACCA	GGGTTTCTAGCTCCTGGTAA
Ppib	CAAGACCTCCTGGCTAGACG	TTCTCCACCTCCGTACCAC

## 2. Study 2: Review of the literature of anti-inflammatory treatments in stroke

Therapeutic choices for stroke treatment are limited nowadays to tPA-induced thrombolysis and/or mechanical thrombectomy. Moreover, only about 5% of patients can benefit from tPA-induced thrombolysis because of the short therapeutic window (within 4.5 hours after stroke onset). Although mechanical thrombectomy has substantially enlarged stroke therapeutic window, this neuroradiological approach can be performed exclusively in patients with large diameter vessels occlusion. It is therefore necessary to find new therapeutic targets for the large majority of untreated patients.

Inflammation plays an important role in the pathophysiology of stroke (Iadecola and Anrather, 2011). It has been shown in experimental stroke models that strategies to modulate the inflammatory response were beneficial in the evolution of lesion volume (Lalancette-Hébert et al., 2007; Liesz et al., 2009; Matsuo et al., 1994; Szalay et al., 2016). However, these strategies have not shown a beneficial effect in clinical practice. **The purpose of this review is to identify key players in brain inflammation, as well as to review the preclinical and clinical therapeutic strategies used to modulate the post-stroke inflammatory response.**



# Anti-inflammatory treatments for stroke: from bench to bedside

Antoine Drieu, Damien Levard, Denis Vivien and Marina Rubio 

*Ther Adv Neurol Disord*

2018, Vol. 11: 1–15

DOI: 10.1177/  
1756286418789854

© The Author(s), 2018.  
Reprints and permissions:  
<http://www.sagepub.co.uk/journalsPermissions.nav>

**Abstract:** So far, intravenous tissue-type plasminogen activator (tPA) and mechanical removal of arterial blood clot (thrombectomy) are the only available treatments for acute ischemic stroke. However, the short therapeutic window and the lack of specialized stroke unit care make the overall availability of both treatments limited. Additional agents to combine with tPA administration or thrombectomy to enhance efficacy and improve outcomes associated with stroke are needed. Stroke-induced inflammatory processes are a response to the tissue damage due to the absence of blood supply but have been proposed also as key contributors to all the stages of the ischemic stroke pathophysiology. Despite promising results in experimental studies, inflammation-modulating treatments have not yet been translated successfully into the clinical setting. This review will (a) describe the timing of the stroke immune pathophysiology; (b) detail the immune responses to stroke sift-through cell type; and (c) discuss the pitfalls on the translation from experimental studies to clinical trials testing the therapeutic pertinence of immune modulators.

**Keywords:** clinical trial, immunomodulatory drugs, inflammation, stroke models, translation

Received: 23 March 2018; revised manuscript accepted: 19 June 2018.

## Introduction

Every year, 15 million people worldwide suffer a stroke. Of these, 5 million die and another 5 million are left permanently disabled, placing a burden on family and community ([http://www.who.int/cardiovascular\\_diseases/en/cvd\\_atlas\\_15\\_burden\\_stroke.pdf?ua=1](http://www.who.int/cardiovascular_diseases/en/cvd_atlas_15_burden_stroke.pdf?ua=1)). In the United States a stroke event happens every 40 seconds, and every 4 minutes, someone dies of stroke (American Stroke Association). Ischemic stroke is provoked by an arterial occlusion in the brain that leads to the rapid death of the brain tissue irrigated by that particular artery. So far, intravenous tissue-type plasminogen activator (tPA) is the only available pharmacological agent for acute ischemic stroke, but this agent is frequently underutilized due to its limited therapeutic window (4.5 h) and increased risk of intracerebral hemorrhage. Recently, mechanical thrombectomy has demonstrated beneficial effects on ischemic stroke in selected patients<sup>1</sup> and has become the standard of care for patients with large-vessel occlusion up to 24 h of stroke onset.<sup>2,3</sup> Additional agents to combine with tPA administration or thrombectomy to

improve efficacy and ameliorate outcomes associated with stroke are needed, in particular, for those patients not eligible for thrombolysis or thrombectomy, or with no access to specialized stroke unit care. Easily administrable agents reducing tissue damage even modestly would drastically decrease the burden of stroke on society and would ameliorate patient outcomes and quality of life.<sup>4</sup>

Stroke-induced inflammatory processes, which include mechanisms of innate and adaptive immunity, are a response to tissue damage due to the absence of blood supply but have also been proposed as key contributors to all the stages of the ischemic stroke pathophysiology.<sup>5</sup> However, despite promising results in experimental studies, inflammation-modulating treatments have not yet been translated successfully into the clinical setting. This review will focus on the innate and adaptive immune responses participating in ischemic brain injury and their impact on tissue damage and repair in both experimental models of stroke and available clinical data. It has been

Correspondence to:  
**Marina Rubio**  
Pathophysiology and Imaging of Neurological Disorders, Normandy University, Boulevard Henri Becquerel BP 5229, Caen Cedex, 14000, France  
[rubio@cyceron.fr](mailto:rubio@cyceron.fr)

**Antoine Drieu**  
**Damien Levard**  
Pathophysiology and Imaging of Neurological Disorders, Normandy University, Caen, France

**Denis Vivien**  
Pathophysiology and Imaging of Neurological Disorders, Normandy University, Caen, France  
Pathophysiology and Imaging of Neurological Disorders, Centre Hospitalier Universitaire de Caen, Caen, France



structured in three parts: a first part describing the timing of the stroke pathophysiology from an immunological point of view (Figure 1); a second part detailing the immune responses to stroke sift-through cell type; and a third part discussing the pitfalls on the translation from preclinical to clinical stroke research of immunomodulating therapeutic agents.

### **Timeline of inflammatory events after stroke**

Basically, inflammatory responses after stroke can be decomposed in three phases.<sup>5</sup> The acute phase (first hours after stroke onset) corresponds to the clearing of dead cells mainly by resident phagocytic cells such as microglia/macrophages and a first entry of leukocytes, mainly neutrophils. The subacute phase (first days after stroke) corresponds to resolution of inflammation. The late phase (days and weeks after stroke) corresponds to tissue repair by astrocytes and microglia (glial scar).

#### *The acute phase of stroke: tissue injury, microglial and endothelial activation*

The arterial occlusion at the origin of ischemic stroke leads to deprivation of oxygen and nutrients that are essential for neuronal survival, leading to rapid neuronal death in the core of the lesion site only minutes after stroke onset. The absence of blood supply into the tissue is followed by a cascade of events starting with a reduction in cellular adenosine triphosphate (ATP) that is required to maintain ionic gradients. The disruption of ionic gradients leads to an influx of  $\text{Na}^+$  and  $\text{Ca}^{2+}$ , cellular depolarization and release of neurotransmitters, including the excitatory neurotransmitter glutamate.<sup>6</sup> As energy-dependent removal of glutamate is impaired, glutamate accumulation leads to overactivation and opening of monovalent ion channels followed by water influx, thus resulting in cellular swelling and death.<sup>7</sup> Dying neurons at the core of the lesion express free radicals, damage-associated molecular patterns (DAMPs) and high-mobility group box 1 (HMGB1) protein that lead to inflammatory reactivity by microglia. Edaravone, a free radical scavenger, has shown beneficial properties in stroke patients with large-vessel occlusion, especially when combined with recombinant tissue-type plasminogen activator, but not in combination with thrombectomy.<sup>8</sup> Activated microglia

adopt a pro-inflammatory status, expressing pro-inflammatory cytokines [interleukin 1 (IL-1), IL-6] that are released into blood circulation.<sup>9</sup>

Pro-inflammatory cytokines exacerbate endothelial cell (EC) activation contributing to leukocyte rolling, adhesion and infiltration in brain tissue. Leukocytes start to roll on the vessel wall with the help of selectins expressed by activated EC. After rolling, leukocytes strongly adhere to the vessel wall by strong links with intercellular adhesion molecule (ICAM-1) and vascular cell adhesion molecule (VCAM-1).<sup>10,11</sup> Into the brain, there is almost no way for leukocytes to pass through the blood-brain barrier (BBB) in nonpathological conditions.<sup>12</sup> However, the BBB integrity is disrupted after stroke onset and tight junctions between EC disappear, allowing leukocyte infiltration into the injured brain tissue.<sup>13</sup> Clinical data and experimental models of stroke have shown that neutrophils infiltrate within hours of stroke onset.<sup>14,15</sup>

#### *The subacute phase: resolution of inflammation*

In the first days after stroke, different leukocyte populations, including macrophages and lymphocytes, infiltrate the brain.<sup>14,15</sup> The infiltration of leukocyte subpopulations differs among murine permanent and transient mechanical focal cerebral ischemia models<sup>16</sup> and the inflammatory response seems to be more pronounced after permanent electrocoagulatory middle cerebral artery occlusion (MCAO) compared with 30-min and 90-min transient mechanical vascular occlusion (TMVO).<sup>16</sup> Descriptive data on the timeline inflammatory responses in thrombus-induced experimental stroke models are missing.

Preclinical studies performed on TMVO models of ischemic stroke have shown a secondary injury after reperfusion (i.e. cerebral ischemia/reperfusion injury). While mechanical thrombectomy also promotes rapid reperfusion, it does not seem to provoke such a secondary injury in patients with proximal middle-cerebral-artery or internal-carotid-artery occlusion and a penumbral region of tissue (i.e. a brain region that is ischemic but not infarcted yet, which is therefore salvageable). This is probably due to a better collateral circulation and slower infarct growth in these patients and is associated to a higher proportion of good functional outcomes at 3 months after stroke, compared with patients with little or no penumbra,

even when performed late (16–24 h) after stroke onset.<sup>2,3,17</sup> In the DEFUSE 2 study, patients with little or no penumbra had a greater lesion growth despite reperfusion. This greater lesion growth could be the result of reperfusion-related edema based on the larger infarct core volumes in the no penumbra group.<sup>17</sup>

#### *The late phase: tissue repair and glial scar*

Neuroinflammation is also considered necessary for the reparation phase that persists after the initial brain insult.<sup>18–20</sup> This phase aims at restoring tissue integrity and involves matrix remodeling, neurogenesis, axon sprouting, dendritogenesis and oligodendrogenesis.<sup>21</sup> All these processes are common to acute brain injuries (including ischemia, hemorrhage, and trauma), neuroinflammatory (including multiple sclerosis) and neurodegenerative disorders,<sup>22</sup> that initiate an extensive glial response known as reactive gliosis. Reactive gliosis involves an enhanced expression of specific markers, such as various extracellular matrix molecules (ECM) like chondroitin sulfate proteoglycans (CSPG) and glial fibrillary acidic protein (GFAP) for astrocytes. Glial scar formation is crucial for sealing the lesion site to remodel the injured tissue, in order to spatially and temporally control the local immune response and revascularization of blood capillaries. Nonetheless, the glial scar also acts as an obstacle to axon regeneration and thus avoids the recovery of central nervous system (CNS) function in the chronic phase after stroke. Experimental studies on the glial response to ischemic stroke have been performed in animal models using variations of permanent or focal transient MCAO and photothrombosis.<sup>23–25</sup> The human brain after ischemic injury seems to share similar properties to these experimental models of stroke.<sup>26</sup>

#### **Immunomodulating therapeutic strategies for stroke: sift-through cell type**

Clinical trials on stroke immunology have targeted both innate and adaptive immune responses, by reducing microglial activation, inhibiting leukocyte or lymphocyte migration to the brain parenchyma, and blocking the IL-1 receptor. The increasing number of immunomodulatory treatments that are already established for other indications in humans have provided a good opportunity to fast-track innovative proof-of-concept trials in stroke. However, and despite promising preclinical results,

immunomodulatory drugs have not shown clear benefits in large clinical trials on stroke. Another strategy has been the induction of hypothermia to reduce inflammatory responses and apoptosis triggered after stroke (among other mechanisms). Several trials have shown its safety and feasibility, alone or in combination with thrombolysis;<sup>27–30</sup> however, its efficacy in the treatment of ischemic stroke is still debatable, especially because of increased pneumonia incidence and mortality in the hypothermia group.<sup>31</sup> New clinical trials on the effects of the combination of thrombolysis/thrombectomy plus hypothermia are ongoing.<sup>32</sup> Figure 2 summarizes the results of clinical trials targeting the immune responses triggered after ischemic stroke.

#### *Microglial cells*

**Pathophysiology.** Microglial cells constitute 10–15% of the brain cells and are the resident mononuclear phagocytes of the brain parenchyma.<sup>33</sup> As aforementioned, microglial response is one of the first steps of the innate immune responses triggered after stroke. Microglial cells are in close contact with neurons and constantly survey the environment with their processes.<sup>34</sup> These cells can adopt a large spectrum of phenotypes ranging from pro-inflammatory to anti-inflammatory and neuroprotective. At the acute phase after stroke onset, microglial cells at the core of the lesion detect DAMPs and HMGB1 via their receptors mainly belonging to the Toll-like receptor (TLR) family.<sup>13,35–37</sup> This ligand–receptor link leads to internalization of nuclear factor of kappa light polypeptide gene enhancer in B-cells inhibitor (IkB) kinase into the nucleus and the subsequent activation of the nuclear factor of kappa light chain enhancer of activated B-cells (NF- $\kappa$ B) pathway and thus to the activation of microglial cells. Also, loss of the constitutively expressed neuronal ligand CX3CL1 (fractalkine) after neuronal death results in enhanced microglial activation through their receptors CX3CR1.<sup>38</sup> Experimental models of both transient and permanent ischemic stroke have shown an increase in the number of microglial cells on the ipsilateral cortex in the first 24 h after stroke onset.<sup>14,16</sup> Once activated, microglial cells express high levels of CD11b, CD45 and CD68 corresponding to a phagocytic phenotype responsible for the clearance of cellular debris,<sup>9</sup> as well as tumor necrosis factor and the pro-inflammatory interleukins IL-1 and IL-6 that are released into blood circulation.<sup>9</sup> IL-1 has been targeted to

reduce further cerebral injury mediated by inflammation. A meta-analysis showed that IL-1 receptor antagonist (IL-1Ra) administration was associated with a 38.2 % reduction in mean infarct volume across 16 published preclinical studies.<sup>39</sup> In a phase II clinical study, recombinant human IL-1Ra (rhIL-1Ra; anakinra) administered at hospital arrival has shown beneficial effects in patients with cortical infarcts, with better clinical outcomes after 3 months in the treated group.<sup>40</sup> However, the recently published results of a second phase II study on the effect of subcutaneous IL-1Ra administration (SCIL-STROKE) has shown that, in spite of a significant reduction in plasma inflammatory markers associated with a worse outcome after ischemic stroke, IL-1Ra treatment was not associated with a favorable outcome on modified Rankin Scale (mRS).<sup>41</sup>

Recently developed techniques of total microglial depletion have shown that microglia seem essential to the limitation of stroke damages, since microglia-depleted mice show larger infarct volumes than nondepleted mice.<sup>42</sup>

*Therapeutic strategies targeting microglia.* Minocycline, an anti-infective agent of the tetracycline family used for the treatment of infections caused by a wide range of organisms, has been tested for the treatment of stroke. It is highly lipophilic and crosses the blood-brain barrier. Minocycline, by acting through different pathways, is able to inhibit microglial activation, decrease migration of T cells, reduce neuronal apoptosis, block free radical production, decrease CNS expression of chemokines and their associated receptors, and inhibit matrix metalloproteinases, particularly matrix metalloproteinase-9.<sup>43-58</sup> In preclinical stroke studies, minocycline ameliorated behavioral function and decreased lesion volume and hemorrhagic transformation.<sup>44-47</sup> It did not alter the fibrinolytic effect of rtPA<sup>46</sup> and could enlarge the time window for thrombolysis.<sup>49</sup> Two phase II clinical trials have shown minocycline to be safe and potentially effective in acute ischemic stroke, alone or in combination with tPA, when administered in the first 24 h after stroke onset and for 5 days.<sup>59,60</sup> However, a third pilot study performed in a small sample of acute stroke patients has shown that minocycline administration in the first 24 h was safe but not efficacious.<sup>43</sup> The authors acknowledged that this third study was not powered to identify reliably or exclude a modest but clinically important treatment effect of minocycline.<sup>43</sup> Larger clinical trials

are thus needed to study the effect of minocycline in stroke patients.

Recently, preclinical studies have focused also on the switch of microglial cell phenotype from M1 to M2 as a potential target to improve stroke outcome, by administering IL-33<sup>61</sup> or IL-4.<sup>62</sup>

### *Endothelial cells*

*Pathophysiology.* In the brain, the functional unit formed by tightly joined ECs and astrocytic end-feet constitute the BBB, a strong protective blood-tissue barrier against pathogens. A few minutes after stroke onset, the BBB is disrupted, and local ECs are activated.<sup>63,64</sup> When activated, ECs express cellular adhesion molecules (CAMs) which allow leukocyte rolling and adhesion to the luminal side of the EC and eventually leukocyte transmigration toward the brain parenchyma.<sup>5</sup> After their activation, the first adhesion molecules expressed by ECs are the selectins (E- and P-selectins). They are constitutively produced by ECs and stored in Weibel-Palade bodies until EC activation. The initial adhesive interactions between leukocytes and selectins expressed on the luminal side of the venular endothelium are tethering (capture) and rolling. These low-affinity (weak) interactions are subsequently strengthened as a result of the sequential activation of different families of adhesion molecules that are located on the surface of leukocytes and ECs.<sup>65</sup> A few hours after stroke onset, ECs start to express the VCAM-1 and the ICAM-1,<sup>63,66</sup> allowing leukocytes to adhere and remain stationary on the vessel wall. Finally, ECs express the platelet endothelial cell adhesion molecule (PECAM-1), responsible for leukocyte transmigration into the brain parenchyma.<sup>11</sup>

*Therapeutic strategies targeting selectins.* Strategies for the blockade of CAMs through the intravenous injection of antibodies have failed in ameliorating stroke outcome both in clinical and preclinical trials.

Enlimomab, a murine ICAM-1 antibody, reduces leukocyte adhesion and infarct size in experimental stroke studies.<sup>67</sup> However, the clinical trial performed in stroke patients showed that the administration of enlimomab within 6 h after stroke onset is not an effective treatment for ischemic stroke and, indeed, significantly worsened stroke outcome and increased adverse events.<sup>68</sup> One of the possible explanations for this

failure is the murine origin of the injected antibody to stroke patients.<sup>69</sup>

Induction of mucosal tolerance to E-selectin to minimize inflammation and risk of further cerebral insult has been tested in a phase I clinical trial, but results have not been disclosed.<sup>70</sup>

L-selectin, a CAM located in the surface of leukocytes, has also been targeted in an experimental stroke model in rabbits by using a humanized monoclonal antibody (HuDREG200). This strategy, alone or in combination with alteplase, failed to significantly ameliorate stroke outcome.<sup>71</sup>

### *Neutrophils*

*Pathophysiology.* The principal role of neutrophils is to enhance leukocyte recruitment by degranulation of their content, rich in cytokines/chemokines, proteolytic enzymes and activated complement system.<sup>72</sup> The extent of neutrophil infiltration after stroke is still debated, being described either limited to the perivascular space or infiltrating the brain tissue in preclinical stroke models (permanent or mechanical transient occlusion of the MCA) and human postmortem samples.<sup>73–75</sup>

It was postulated that neutrophils could contribute to brain injury after ischemic stroke by obstructing microvessel circulation, damaging endothelial cells and ECM by hydrolytic enzymes and free radicals, promoting intravascular thrombus formation together with platelet activation, and releasing cytokines and chemotactic factors that could promote extension of the inflammatory response.<sup>76</sup>

*Therapeutic strategies targeting neutrophils.* Pre-clinical and clinical studies aiming at blocking neutrophil infiltration have targeted CD11/CD18 (LFA-1 for lymphocyte function-associated antigen 1), located at the surface of neutrophils, to prevent their adhesion to ICAM-1 (expressed at the luminal surface of ECs). Pre-clinical studies have shown that CD11/CD18 monoclonal antibodies are not beneficial in permanent stroke models,<sup>77,78</sup> but are beneficial on a transient mechanical ischemic stroke model.<sup>79</sup> In spite of this, two clinical trials have been performed to prevent neutrophil recruitment after stroke onset and have shown no beneficial effect. On the HALT phase III trial, the humanized antibody

Hu23F2G, administered twice daily, appeared to produce an improvement in mRS score in a phase II study. However, the sponsor terminated a subsequent phase III study when a ‘futility analysis’ advised that no benefit of the treatment would occur if the study was completed. No public information regarding the database, outcomes, safety issues, or relative number of adverse events has appeared.<sup>76</sup> On the ASTIN (Acute Stroke Therapy by Inhibition of Neutrophils) study, UK-279,276 (another CD18 antagonist) was administered within 6 h of stroke symptom onset, but, similar to the HALT study, the trial was stopped early due to futility.<sup>80</sup>

### *Lymphocytes*

*Pathophysiology.* Adaptive immunity also plays an important role during stroke. Lymphocytes consist of distinct subpopulations with diverse functions and can be subdivided into two groups: pro- and anti-inflammatory lymphocytes. The consequences of the adaptive immune response on ischemic stroke are still debated, as both beneficial and deleterious results have been reported depending on the type of T-helper (Th) immune response set in motion after the activation of lymphocytes.<sup>81–83</sup> Both transient (mechanical) and permanent experimental models of stroke have shown that lymphocyte infiltration into the ischemic tissue comes later after stroke onset (starting at 3 days).<sup>14,16</sup> Postmortem human samples have shown that lymphocyte infiltration into the ischemic area occur from day 3 and can be present up to 53 years after stroke.<sup>15</sup>

The choroid plexuses (CP) have recently been proposed as the preferential route for lymphocyte infiltration into the lesion site after experimental stroke. Indeed, CP infarction reduces lymphocyte infiltration after stroke onset; however, the ischemic volume is not modified in these mice, even if lymphocyte infiltration is actually reduced.<sup>84</sup> These intriguing results raise important questions about the role of lymphocytes on the development of the ischemic lesion.

*Therapeutic strategies targeting lymphocytes.* Therapeutic strategies targeting lymphocytes would be desirable because they focus the delayed phase of the injury and thus could have a particularly wide therapeutic window. Several pre-clinical studies have shown that pro-inflammatory lymphocytes, such as TH1, TH17, and  $\gamma\delta$  T

cells worsen stroke outcome, and that blocking of their brain invasion is neuroprotective.<sup>85–87</sup>

Contrary to pro-inflammatory lymphocytes, regulatory T cells (Treg) and B cells have been characterized as anti-inflammatory and as disease-limiting protective cells. Targeting Tregs as the endogenous orchestrators of the postischemic immune response has been proposed as a more effective therapy than blocking only a particular inflammatory pathway.<sup>5,13</sup> However, because of the complex function of regulatory cells in immune homeostasis and disease, as well as partially divergent findings using different stroke models, the pathophysiologic function of regulatory lymphocytes in stroke remains uncertain. As an example, among nine studies using Treg-depletion paradigms, three of the studies revealed an increase in infarct volume<sup>88–90</sup> whereas five studies did not detect any effect on stroke outcome<sup>88,89,91–93</sup> and one study even observed a reduction of infarct size in Treg-deficient mice.<sup>94</sup> To explain this, the experimental model used (permanent *versus* transient mechanical) and more particularly, the resulting volume of the ischemic lesion, has been proposed as a determinant on the overall effect of Treg depletion that seems to provide a benefit only on small lesion volumes provoked on the permanent stroke model.<sup>95</sup>

Another strategy for Treg modulation has been the administration of enhancers of Treg function by adoptive cell transfer of purified Treg to wild-type animals to increase circulating Treg numbers, or by the administration of a CD28 superagonist (CD28SA), which provokes *in vivo* expansion of Tregs and amplification of their suppressive function. However, the obtained results are again controversial, with some studies describing an improvement of stroke outcome<sup>96</sup> and other studies describing an increase of ischemic volume.<sup>97</sup> Once again, it has been proposed that stroke severity might predict the net biological effect of Tregs.<sup>95</sup>

It has been proposed that Tregs have a deleterious role on ischemic stroke not related to their established immunoregulatory characteristics but to a specific effect on microvascular thrombus formation in a model of transient mechanical occlusion.<sup>94</sup> Secondary microthrombosis arises within minutes after reperfusion in transient mechanical models of stroke once the occluding filament has been removed. It provokes delayed cerebral blood flow (CBF) reduction, secondary ischemia and

lesion growth, which is responsible for ~70% of the final ischemic lesion size.<sup>98</sup> However, clinical studies have shown that secondary ischemia and lesion growth are modest or nonexistent after reperfusion in selected patients,<sup>2,17,99,100</sup> and concerns have been raised about the clinical relevance of transient mechanical vascular occlusion stroke models.<sup>101</sup> For these reasons, it would be interesting to test the role of Tregs in nonmechanical models of ischemic stroke, where secondary microthrombosis is absent.<sup>102</sup>

To increase the complexity of this question, fingolimod (FTY720), an immunomodulatory drug currently approved by the US Food and Drug Administration for the treatment of multiple sclerosis that inhibits lymphocyte circulation and brain immigration, has been tested in models of permanent and transient mechanical ischemia. As in the case of the aforementioned CP infarction,<sup>84</sup> although a reduction of lymphocyte brain invasion was detected using fingolimod, no effect was observed on infarct volumes and behavioral dysfunction in any of the models. This lack of neuroprotection despite effective lymphopenia was attributed to a divergent impact of fingolimod on cytokine expression and possible activation of innate immune cells after brain ischemia.<sup>86</sup> A phase II clinical trial using fingolimod (administered within 6 h after the onset of symptoms) combined with alteplase and mechanical thrombectomy on ischemic stroke (FAMTAIS) is ongoing.<sup>103</sup>

Two clinical pilot studies have tested fingolimod, alone and later than 4.5 h after stroke onset for 3 days,<sup>104</sup> or in combination with tPA (thus before 4.5 h after stroke onset) for 3 days.<sup>105</sup> These two studies have shown a beneficial effect of the oral administration of fingolimod within 72 h of stroke onset, especially when combined with tPA, where patients who received the combination exhibited smaller lesion volumes, less hemorrhage, and a better recovery at day 90.

*Therapeutic strategies targeting global leukocyte infiltration.* The transendothelial migration of leukocytes through the interaction between the molecules VLA-4 (leukocyte very late antigen-4) (present at the surface of neutrophils, monocytes, and T and B lymphocytes among other blood cell types) and VCAM-1 (vascular cell adhesion molecule-1) has been targeted in several studies. Antibodies against the alpha chain of VLA-4 (anti-CD49d antibodies) have shown efficacy in several models of autoimmune diseases, and the

humanized antibody natalizumab is currently one of the most effective therapies for patients with multiple sclerosis.<sup>106</sup> However, preclinical data have shown conflicting results from four positive and one inconclusive studies on the use of anti-CD49d antibodies on ischemic stroke.<sup>86,107–110</sup> Recently, a preclinical randomized controlled multicenter trial highlighted the importance of testing new therapies in different experimental stroke models (discussed further on), since the administration of CD49d-antibodies reduced both leukocyte invasion and infarct volume after the permanent distal occlusion of the MCA (which causes a small cortical infarction), whereas it did not reduce leukocyte invasion or infarct volume after transient proximal mechanical occlusion of the MCA (which induces large lesions).<sup>111</sup> These results could suggest that the benefits of immune-targeted therapies may be dependent on infarct localization and severity.

The recently published results of the administration of one dose of natalizumab in patients with acute ischemic stroke (ACTION trial) have shown that natalizumab administered up to 9 h after stroke onset did not reduce infarct growth (primary endpoint of the study), but more patients in the natalizumab group than in the placebo group had mRS scores of 0 or 1 at day 30, although this beneficial effect disappeared 90 days after stroke.<sup>112</sup> These results reinforce the need of new studies to understand (a) how natalizumab exerts a positive effect on functional outcome without reducing the infarct volume at 30 days, and (b) why this beneficial effect on functional outcome is lost at 90 days. Additionally, the ACTION II trial has been recently completed. Its primary objective was to assess the effects of natalizumab on functional independence and activities of daily living.<sup>113</sup> Results have not been published yet.

### **Immunomodulating therapies in stroke: a gap between our expectations and reality**

The reasons for the failure of immunomodulatory therapies in clinical trials are multifactorial. As discussed, one of the main issues of the bench-to-bed translation of immunomodulatory therapies for stroke is the huge gap between human pathophysiology and the stroke models that have mainly been used to study stroke immunology. In experimental stroke models, preclinical stroke research nowadays disposes of a wide range of experimental models including permanent and transient arterial

occlusions. In addition to this, the origin of the occlusion may also vary from a transient mechanical occlusion to real blood clots located in the lumen of the artery. In the case of clot-induced stroke models, researchers can even adopt different strategies to determine the nature of clots (fibrin-rich or platelet-rich) and, consequently, clot susceptibility to thrombolytic agents<sup>114–116</sup> to mimic the heterogeneity of human thrombi subtypes. It is important to note that despite the variety of available stroke models, the vast majority of preclinical data on transient models of ischemic stroke has been obtained on mechanical occlusion models that provoke thromboinflammation and secondary microthrombosis. This secondary microthrombosis is a major pathophysiologic mechanism leading to brain damage which does not occur in other models based on clot-induced ischemic stroke like the thrombin-induced stroke model.<sup>102,116</sup> As in the aforementioned case of Treg-targeted drugs, immunomodulatory agents that have clearly shown beneficial effects on mechanical occlusion models of stroke could actually be targeting thromboinflammation and secondary microthrombosis. Since it is unclear whether thromboinflammation is a universal pathophysiological mechanism of human stroke, immunomodulatory drugs deserve to be evaluated or re-evaluated in experimental stroke models not inducing secondary thromboinflammation before trying to apply them in clinical practice.

Other reasons for the failure in the translation of immunomodulatory therapies from bench to bedside may include poorly designed preclinical and clinical studies, and underpowered clinical trials with overambitious and pathophysiologically irrelevant therapeutic windows.<sup>117,118</sup> In addition, a biased selection of substances for clinical testing may partially explain the slow progress in developing treatments.<sup>118</sup>

It is also possible that the positive results seen with immunomodulatory drugs in experimental studies are not transposable to the complexity and the variability of the immunologic response in human stroke, which may depend on different parameters including prestroke status of the patient and the natural history of the disease.<sup>63,93</sup> In most animal studies, complete occlusion is induced and is either maintained or followed by complete reperfusion. In human stroke, however, only a few patients are likely to experience both complete occlusion and complete reperfusion (excepting thrombectomized patients). The

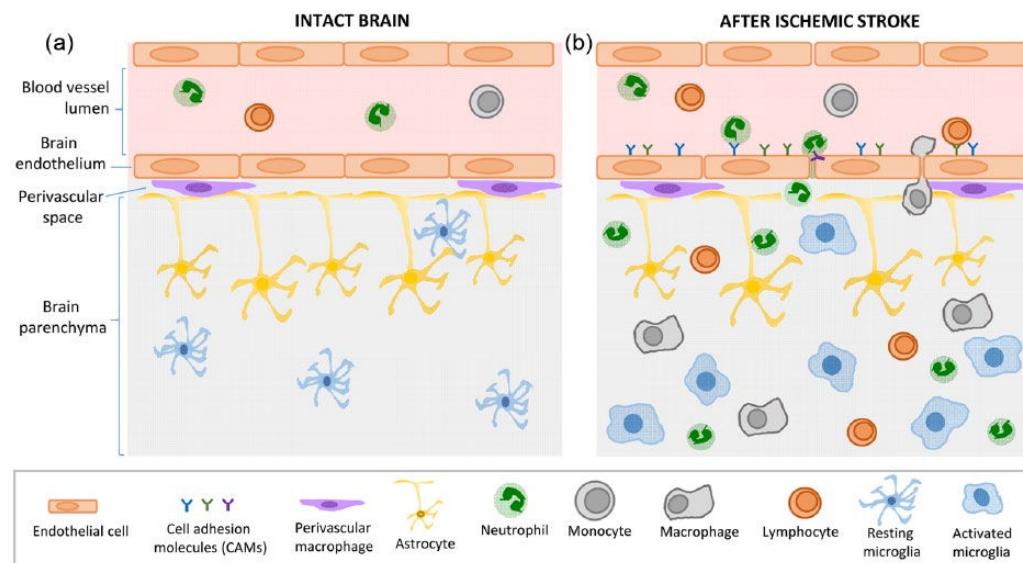


**Figure 1.** Immune reactions after ischemic stroke.

(a) In the intact brain, the functional unit formed by tightly jointed ECs and astrocytic endfeet constitute the BBB, a strong protective blood-tissue barrier from pathogens. Immune cells circulate freely in the blood, and in the brain parenchyma, resting microglia survey the environment with their processes. (b) A few minutes after stroke onset, the BBB is disrupted and local ECs are activated. The tight junctions between ECs disappear and activated ECs express CAMs. This allows white cell rolling and adhesion at the luminal side of the blood vessel and then transmigration from the vascular compartment to the brain parenchyma. Once infiltrated in the tissue, neutrophils secrete pro-inflammatory factors that will recruit monocytes/macrophages, and later lymphocytes to the parenchyma. After stroke, microglia switches from a resting form to an activated state, adopting a phagocytic phenotype and secreting pro-inflammatory factors.

BBB, blood-brain barrier; CAM, cellular adhesion molecule; EC, endothelial cell.

unlimited variety of outcomes seen in stroke patients suggests that stroke itself, as well as the body's response to ischemic stroke represents a seamless continuum of exigencies rather than the definitive scenario employed in animal studies.<sup>68</sup> In addition, stroke risk factors such as diet, smoking, aging, atherosclerosis, hypertension, alcohol consumption and stress cannot be replicated well in the laboratory; actually, most of the preclinical studies are performed in healthy mice. Moreover, although stroke remains the third cause of death in women,<sup>119</sup> most of the preclinical studies are performed on male animals. Inflammatory cells such as microglia, dendritic cells, neutrophils and lymphocytes show variations between sex, and so may play different roles in the pathophysiology of stroke.<sup>120–123</sup>

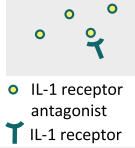
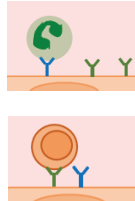
The failure of immunomodulatory drugs clinically tested on stroke to date may also indicate that the inflammatory response after stroke is an important aspect of the regenerative process triggered after stroke and only becomes detrimental when exaggerated, perhaps in relation to the severity of ischemic injury (as shown in preclinical stroke models) or to concomitant disease states or risk factors. However, many of the preclinical

studies examining immunomodulation were targeted at the acute phase, not during the phases where recovery is expected to occur. Thus, this hypothesis needs to be addressed in future studies.

Another important element to be considered when testing immunomodulatory drugs for stroke is that postischemic systemic immunomodulation and infectious complications are some of the main comorbidities after stroke. In experimental models, the systemic immune responses differ substantially among stroke models and infarct volume.<sup>89,124</sup> Translational studies of immunomodulatory therapies for stroke must account for this heterogeneity, especially in the case of drugs with long-term effects such as natalizumab, that blocks the  $\alpha$ -4 integrin for at least 4 weeks.<sup>125</sup>

## Conclusion

Factors contributing to the failure in the translation of therapies targeting stroke-induced immune responses to clinical practice include nonmodifiable factors (differences in the cerebrovascular system in humans and rodents, variability in the immune response in patients depending on their

	<b>Therapeutic strategies targeting IL-1-induced inflammation</b> <b>Recombinant human IL-1 receptor antagonist, rhIL1-Ra</b> Positive results in a Phase II clinical trial (intravenous administration) (Emsley et al., 2005) Not beneficial in a Phase II clinical trial (subcutaneous administration) ( <b>SCIL-STROKE</b> ) (Smith et al., 2018)
	<b>Therapeutic strategies targeting microglial activation</b> <b>Minocycline</b> Positive results in two Phase II clinical trials (Lampl et al., 2007; Padma Srivastava et al., 2012) Phase IV clinical trial stopped for futility ( <b>NeuMAST</b> ) (Kohler et al., 2013)
	<b>Therapeutic strategies targeting endothelial selectins</b> <b>Enlimomab</b> (mouse anti-ICAM-1) Worse stroke outcome in a Phase III clinical trial (Enlimomab Acute Stroke Trial Investigators, 2001) <b>E-selectin tolerance</b> Results from Phase II clinical trial not disclosed ( <a href="http://clinicaltrials.gov/show/NCT00012454">http://clinicaltrials.gov/show/NCT00012454</a> )
	<b>Therapeutic strategies targeting leukocyte infiltration</b> <b>UK-279, 276</b> (Recombinant neutrophil inhibitory factor, blocking its interaction with ICAM-1) ( <b>ASTIN</b> ) Phase II clinical trial stopped for futility (Krams et al., 2003) <b>Hu23F2G</b> (Humanized monoclonal antibody against neutrophil CD11/CD18, blocking its interaction with ICAM-1) ( <b>HALT</b> ) Phase III clinical trial stopped for futility (results not disclosed) (del Zoppo, 2010) <b>Fingolimod</b> (sphingosine-1-phosphate receptor on lymphocytes) Positive results in two pilot studies (Fu et al., 2014; Zhu et al., 2015) <b>Natalizumab</b> (humanized antibody against the VCAM-1 leukocyte ligand VLA-4) ( <b>ACTION</b> ) Not beneficial in a Phase II clinical trial (Elkins et al., 2017)

**Figure 2.** Summary of clinical trials targeting the immune responses triggered after ischemic stroke. CD11/CD18, LFA-1 for lymphocyte function-associated antigen 1; IL-1, interleukin 1; rhIL1-Ra, recombinant human interleukin 1 receptor antagonist; ICAM-1, intercellular adhesion molecule; VCAM-1, vascular cell adhesion molecule; VLA-4, leukocyte very late antigen-4.

prestroke inflammatory status, which is extremely difficult to mimic in animal models of stroke...) that need to be considered when interpreting results. However, most of these factors are modifiable and include, among others, the use of clinically relevant stroke models and therapeutic time windows, the comparison of a same molecule in different stroke models, the improvement in the experimental designs and the inclusion of females and comorbidities in preclinical studies.

Now that we are in the age of acute revascularization, one might wonder if we can do better than thrombectomy for patients with penumbra. If the answer is ‘no’ then there is probably no need for immunomodulatory treatments for these patients. If the answer is ‘yes,’ and also for all the other patients, immunomodulation will retain therapeutic interest. Preclinical studies should be conceived according to the targeted stroke subpopulation. In any case, a strictly linear bench-to-bedside

paradigm is probably not optimal for translating basic scientific findings into clinically effective stroke therapies, and a bedside-back-to-bench paradigm will help in this translation.

In spite of the limitations of experimental stroke models, our knowledge about the inflammatory responses triggered after stroke onset exponentially increases thanks to preclinical and clinical studies, and gives rise to novel therapeutic targets and improved strategies, with the hope of ameliorating stroke outcome in patients.

## Funding

This research received no specific grant from any funding agency in the public, commercial, or not-for-profit sectors.

## Conflict of interest statement

The authors declare that there is no conflict of interest.

**ORCID iD**

Marina Rubio  <https://orcid.org/0000-0002-6120-4053>

**References**

1. Jovin TG, Chamorro A, Cobo E, *et al.* Thrombectomy within 8 hours after symptom onset in ischemic stroke. *N Engl J Med* 2015; 372: 2296–2306.
2. Nogueira RG, Jadhav AP, Haussen DC, *et al.* Thrombectomy 6 to 24 hours after stroke with a mismatch between deficit and infarct. *N Engl J Med* 2018; 378: 11–21.
3. Albers GW, Marks MP, Kemp S, *et al.* Thrombectomy for stroke at 6 to 16 hours with selection by perfusion imaging. *N Engl J Med* 2018; 378: 708–718.
4. Fagan SC, Cronic LE and Hess DC. Minocycline development for acute ischemic stroke. *Transl Stroke Res.* 2011; 2: 202–208.
5. Iadecola C and Anrather J. The immunology of stroke: from mechanisms to translation. *Nat Med* 2011; 17: 796–808.
6. Choi DW. Glutamate neurotoxicity in cortical cell culture is calcium dependent. *Neurosci Lett* 1985; 58: 293–297.
7. Koistinaho M and Koistinaho J. Interactions between Alzheimer's disease and cerebral ischemia—focus on inflammation. *Brain Res Brain Res Rev* 2005; 48: 240–250.
8. Miyaji Y, Yoshimura S, Sakai N, *et al.* Effect of edaravone on favorable outcome in patients with acute cerebral large vessel occlusion: subanalysis of RESCUE-Japan Registry. *Neurol Med Chir (Tokyo)* 2015; 55: 241–247.
9. Perego C, Fumagalli S and De Simoni M-G. Temporal pattern of expression and colocalization of microglia/macrophage phenotype markers following brain ischemic injury in mice. *J Neuroinflammation* 2011; 8: 174.
10. Huang J, Upadhyay UM and Tamargo RJ. Inflammation in stroke and focal cerebral ischemia. *Surg Neurol* 2006; 66: 232–245.
11. Muller WA. Leukocyte-endothelial cell interactions in the inflammatory response. *Lab Investig J Tech Methods Pathol* 2002; 82: 521–533.
12. Engelhardt B and Ransohoff RM. The ins and outs of T-lymphocyte trafficking to the CNS: anatomical sites and molecular mechanisms. *Trends Immunol* 2005; 26: 485–495.
13. Eltzschig HK and Eckle T. Ischemia and reperfusion—from mechanism to translation. *Nat Med* 2011; 17: 1391–1401.
14. Gelderblom M, Leyboldt F, Steinbach K, *et al.* Temporal and spatial dynamics of cerebral immune cell accumulation in stroke. *Stroke* 2009; 40: 1849–1857.
15. Mena H, Cadavid D and Rushing EJ. Human cerebral infarct: a proposed histopathologic classification based on 137 cases. *Acta Neuropathol (Berl)* 2004; 108: 524–530.
16. Zhou W, Liesz A, Bauer H, *et al.* Postischemic brain infiltration of leukocyte subpopulations differs among murine permanent and transient focal cerebral ischemia models: infiltration differs among cerebral ischemia. *Brain Pathol* 2013; 23: 34–44.
17. Lansberg MG, Straka M, Kemp S, *et al.* MRI profile and response to endovascular reperfusion after stroke (DEFUSE 2): a prospective cohort study. *Lancet Neurol* 2012; 11: 860–867.
18. Kyritis N, Kizil C, Zocher S, *et al.* Acute inflammation initiates the regenerative response in the adult zebrafish brain. *Science* 2012; 338: 1353–1356.
19. Macrez R, Ali C, Toutirais O, *et al.* Stroke and the immune system: from pathophysiology to new therapeutic strategies. *Lancet Neurol* 2011; 10: 471–480.
20. Tobin MK, Bonds JA, Minshall RD, *et al.* Neurogenesis and inflammation after ischemic stroke: what is known and where we go from here. *J Cereb Blood Flow Metab Off J Int Soc Cereb Blood Flow Metab* 2014; 34: 1573–1584.
21. Peruzzotti-Jametti L, Donegá M, Giusto E, *et al.* The role of the immune system in central nervous system plasticity after acute injury. *Neuroscience* 2014; 283: 210–221.
22. Schwartz M, Kipnis J, Rivest S, *et al.* How do immune cells support and shape the brain in health, disease, and aging? *J Neurosci Off J Soc Neurosci* 2013; 33: 17587–17596.
23. Nowicka D, Rogozinska K, Aleksy M, *et al.* Spatiotemporal dynamics of astrogial and microglial responses after photothrombotic stroke in the rat brain. *Acta Neurobiol Exp (Warsz)* 2008; 68: 155–168.
24. Lively S, Moxon-Emre I and Schlichter LC. SC1/hevin and reactive gliosis after transient ischemic stroke in young and aged rats. *J Neuropathol Exp Neurol* 2011; 70: 913–929.
25. Morioka T, Kalehua AN and Streit WJ. Characterization of microglial reaction after

- middle cerebral artery occlusion in rat brain. *J Comp Neurol* 1993; 327: 123–132.
26. Huang L, Wu Z-B, Zhuge Q, et al. Glial scar formation occurs in the human brain after ischemic stroke. *Int J Med Sci* 2014; 11: 344–348.
  27. Krieger DW, Georgia MAD, Abou-Chebl A, et al. Cooling for Acute Ischemic Brain Damage (COOL AID): an open pilot study of induced hypothermia in acute ischemic stroke. *Stroke* 2001; 32: 1847–1854.
  28. De Georgia MA, Krieger DW, Abou-Chebl A, et al. Cooling for Acute Ischemic Brain Damage (COOL AID): a feasibility trial of endovascular cooling. *Neurology* 2004; 63: 312–317.
  29. Lyden PD, Allgren RL, Ng K, et al. Intravascular Cooling in the Treatment of Stroke (ICTuS): early clinical experience. *J Stroke Cerebrovasc Dis Off J Natl Stroke Assoc* 2005; 14: 107–114.
  30. Hemmen TM, Raman R, Guluma KZ, et al. Intravenous thrombolysis plus hypothermia for acute treatment of ischemic stroke (ICTuS-L): final results. *Stroke* 2010; 41: 2265–2270.
  31. Lyden P, Hemmen T, Grotta J, et al. Results of the ICTuS 2 trial (Intravascular Cooling in the Treatment of Stroke 2). *Stroke* 2016; 47: 2888–2895.
  32. van der Worp HB1, Macleod MR, Bath PM, et al. Trial of therapeutic cooling in patients with acute ischaemic stroke. *Int J Stroke* 2014; 9(5): 642–645. doi: 10.1111/ijjs.12294. <https://www.eurohyp1.eu/> (accessed 15 May 2018).
  33. Lawson LJ, Perry VH and Gordon S. Turnover of resident microglia in the normal adult mouse brain. *Neuroscience* 1992; 48: 405–415.
  34. Kettenmann H, Hanisch U-K, Noda M, et al. Physiology of microglia. *Physiol Rev* 2011; 91: 461–553.
  35. Chen GY and Nuñez G. Sterile inflammation: sensing and reacting to damage. *Nat Rev Immunol* 2010; 10: 826–837.
  36. Fernandez-Fernandez S, Almeida A and Bolaños JP. Antioxidant and bioenergetic coupling between neurons and astrocytes. *Biochem J* 2012; 443: 3–11.
  37. Fernandez-Lizarbe S, Pascual M and Guerri C. Critical role of TLR4 response in the activation of microglia induced by ethanol. *J Immunol* 2009; 183: 4733–4744.
  38. Cardona AE, Pioro EP, Sasse ME, et al. Control of microglial neurotoxicity by the fractalkine receptor. *Nat Neurosci* 2006; 9: 917–924.
  39. Banwell V, Sena ES and Macleod MR. Systematic review and stratified meta-analysis of the efficacy of interleukin-1 receptor antagonist in animal models of stroke. *J Stroke Cerebrovasc Dis Off J Natl Stroke Assoc* 2009; 18: 269–276.
  40. Emsley HCA, Smith CJ, Georgiou RF, et al. A randomised phase II study of interleukin-1 receptor antagonist in acute stroke patients. *J Neurol Neurosurg Psychiatry* 2005; 76: 1366–1372.
  41. Smith CJ, Hulme S, Vail A, et al. SCIL-STROKE (Subcutaneous Interleukin-1 Receptor Antagonist in Ischemic Stroke): a randomized controlled phase 2 trial. *Stroke* 2018; 49: 1210–1216.
  42. Szalay G, Martinecz B, Lénárt N, et al. Microglia protect against brain injury and their selective elimination dysregulates neuronal network activity after stroke. *Nat Commun* 2016; 7: 11499.
  43. Kohler E, Prentice DA, Bates TR, et al. Intravenous minocycline in acute stroke: a randomized, controlled pilot study and meta-analysis. *Stroke* 2013; 44: 2493–2499.
  44. Lapchak PA, Chapman DF and Zivin JA. Metalloproteinase inhibition reduces thrombolytic (tissue plasminogen activator)-induced hemorrhage after thromboembolic stroke. *Stroke* 2000; 31: 3034–3040.
  45. Lee CZ, Xue Z, Zhu Y, et al. Matrix metalloproteinase-9 inhibition attenuates vascular endothelial growth factor-induced intracerebral hemorrhage. *Stroke* 2007; 38: 2563–2568.
  46. Machado LS, Sazonova IY, Kozak A, et al. Minocycline and tissue-type plasminogen activator for stroke: assessment of interaction potential. *Stroke* 2009; 40: 3028–3033.
  47. Matsukawa N, Yasuhara T, Hara K, et al. Therapeutic targets and limits of minocycline neuroprotection in experimental ischemic stroke. *BMC Neurosci* 2009; 10: 126.
  48. Morimoto N, Shimazawa M, Yamashima T, et al. Minocycline inhibits oxidative stress and decreases in vitro and in vivo ischemic neuronal damage. *Brain Res* 2005; 1044: 8–15.
  49. Murata Y, Rosell A, Scannevin RH, et al. Extension of the thrombolytic time window with minocycline in experimental stroke. *Stroke* 2008; 39: 3372–3377.
  50. Plane JM, Shen Y, Pleasure DE, et al. Prospects for minocycline neuroprotection. *Arch Neurol* 2010; 67: 1442–1448.

51. Power C, Henry S, Del Bigio MR, et al. Intracerebral hemorrhage induces macrophage activation and matrix metalloproteinases. *Ann Neurol* 2003; 53: 731–742.
52. Sanchez Mejia RO, Ona VO, Li M, et al. Minocycline reduces traumatic brain injury-mediated caspase-1 activation, tissue damage, and neurological dysfunction. *Neurosurgery* 2001; 48: 1393–1399; discussion 1399–1401.
53. Stirling DP, Khodarahmi K, Liu J, et al. Minocycline treatment reduces delayed oligodendrocyte death, attenuates axonal dieback, and improves functional outcome after spinal cord injury. *J Neurosci Off J Soc Neurosci* 2004; 24: 2182–2190.
54. Teng YD, Choi H, Onario RC, et al. Minocycline inhibits contusion-triggered mitochondrial cytochrome c release and mitigates functional deficits after spinal cord injury. *Proc Natl Acad Sci U S A* 2004; 101: 3071–3076.
55. Wang CX, Yang T, Noor R, et al. Delayed minocycline but not delayed mild hypothermia protects against embolic stroke. *BMC Neurol* 2002; 2: 2.
56. Wells JEA, Hurlbert RJ, Fehlings MG, et al. Neuroprotection by minocycline facilitates significant recovery from spinal cord injury in mice. *Brain J Neurol* 2003; 126(Pt 7): 1628–1637.
57. Xu L, Fagan SC, Waller JL, et al. Low dose intravenous minocycline is neuroprotective after middle cerebral artery occlusion-reperfusion in rats. *BMC Neurol* 2004; 4: 7.
58. Yong VW, Wells J, Giuliani F, et al. The promise of minocycline in neurology. *Lancet Neurol* 2004; 3: 744–751.
59. Lampl Y, Boaz M, Gilad R, et al. Minocycline treatment in acute stroke: an open-label, evaluator-blinded study. *Neurology* 2007; 69: 1404–1410.
60. Padma Srivastava MV, Bhasin A, Bhatia R, et al. Efficacy of minocycline in acute ischemic stroke: a single-blinded, placebo-controlled trial. *Neurol India* 2012; 60: 23–28.
61. Yang Y, Liu H, Zhang H, et al. ST2/IL-33-dependent microglial response limits acute ischemic brain injury. *J Neurosci Off J Soc Neurosci* 2017; 37: 4692–4704.
62. Liu X, Liu J, Zhao S, et al. Interleukin-4 is essential for microglia/macrophage M2 polarization and long-term recovery after cerebral ischemia. *Stroke* 2016; 47: 498–504.
63. Gauberti M, Montagne A, Marcos-Contreras OA, et al. Ultra-sensitive molecular MRI of vascular cell adhesion molecule-1 reveals a dynamic inflammatory penumbra after strokes. *Stroke* 2013; 44: 1988–1996.
64. Montagne A, Gauberti M, Macrez R, et al. Ultra-sensitive molecular MRI of cerebrovascular cell activation enables early detection of chronic central nervous system disorders. *NeuroImage* 2012; 63: 760–770.
65. Granger DN and Senchenkova E. *Inflammation and the microcirculation*. San Rafael (CA): Morgan & Claypool Life Sciences, <http://www.ncbi.nlm.nih.gov/books/NBK53373/> (2010, accessed 12 March 2018).
66. Gauberti M, Fournier AP, Docagne F, et al. Molecular magnetic resonance imaging of endothelial activation in the central nervous system. *Theranostics* 2018; 8: 1195–1212.
67. Bowes MP, Rothlein R, Fagan SC, et al. Monoclonal antibodies preventing leukocyte activation reduce experimental neurologic injury and enhance efficacy of thrombolytic therapy. *Neurology* 1995; 45: 815–819.
68. Enlimomab Acute Stroke Trial Investigators. Use of anti-ICAM-1 therapy in ischemic stroke: results of the Enlimomab Acute Stroke Trial. *Neurology* 2001; 57: 1428–1434.
69. DeGraba TJ. The role of inflammation after acute stroke: utility of pursuing anti-adhesion molecule therapy. *Neurology* 1998; 51(3 Suppl 3): S62–S68.
70. Cayce Onks. *E-selectin nasal spray to prevent stroke recurrence*. <https://clinicaltrials.gov/ct2/show/NCT00012454> (accessed 22 March 2018).
71. Bednar M, Gross C, Russell S, et al. Humanized anti-L-selectin monoclonal antibody DREC200 therapy in acute thromboembolic stroke. *Neurol Res* 1998; 20: 403–408.
72. Nathan C. Neutrophils and immunity: challenges and opportunities. *Nat Rev Immunol* 2006; 6: 173–182.
73. Enzmann G, Mysiorek C, Gorina R, et al. The neurovascular unit as a selective barrier to polymorphonuclear granulocyte (PMN) infiltration into the brain after ischemic injury. *Acta Neuropathol (Berl)* 2013; 125: 395–412.
74. Chu HX, Kim HA, Lee S, et al. Immune cell infiltration in malignant middle cerebral artery infarction: comparison with transient cerebral

- ischemia. *J Cereb Blood Flow Metab Off J Int Soc Cereb Blood Flow Metab* 2014; 34: 450–459.
75. Perez-de-Puig I, Miró-Mur F, Ferrer-Ferrer M, et al. Neutrophil recruitment to the brain in mouse and human ischemic stroke. *Acta Neuropathol (Berl)* 2015; 129: 239–257.
  76. Del Zoppo GJ. Acute anti-inflammatory approaches to ischemic stroke. *Ann N Y Acad Sci* 2010; 1207: 143–148.
  77. Garcia JH, Liu KF and Bree MP. Effects of CD11b/18 monoclonal antibody on rats with permanent middle cerebral artery occlusion. *Am J Pathol* 1996; 148: 241–248.
  78. Jiang N, Chopp M and Chahwala S. Neutrophil inhibitory factor treatment of focal cerebral ischemia in the rat. *Brain Res* 1998; 788: 25–34.
  79. Prestigiacomo CJ, Kim SC, Connolly ES, et al. CD18-mediated neutrophil recruitment contributes to the pathogenesis of reperfused but not nonreperfused stroke. *Stroke* 1999; 30: 1110–1117.
  80. Krams M, Lees KR, Hacke W, et al. Acute Stroke Therapy by Inhibition of Neutrophils (ASTIN): an adaptive dose-response study of UK-279,276 in acute ischemic stroke. *Stroke* 2003; 34: 2543–2548.
  81. Gee JM, Kalil A, Shea C, et al. Lymphocytes: potential mediators of postischemic injury and neuroprotection. *Stroke* 2007; 38(2 Suppl): 783–788.
  82. Hallenbeck J, Del Zoppo G, Jacobs T, et al. Immunomodulation strategies for preventing vascular disease of the brain and heart: workshop summary. *Stroke* 2006; 37: 3035–3042.
  83. Schwartz M and Kipnis J. Autoimmunity on alert: naturally occurring regulatory CD4(+) CD25(+) T cells as part of the evolutionary compromise between a « need » and a « risk ». *Trends Immunol* 2002; 23: 530–534.
  84. Llovera G, Benakis C, Enzmann G, et al. The choroid plexus is a key cerebral invasion route for T cells after stroke. *Acta Neuropathol (Berl)* 2017; 134: 851–868.
  85. Gelderblom M, Weymar A, Bernreuther C, et al. Neutralization of the IL-17 axis diminishes neutrophil invasion and protects from ischemic stroke. *Blood* 2012; 120: 3793–3802.
  86. Liesz A, Zhou W, Mrácskó É, et al. Inhibition of lymphocyte trafficking shields the brain against deleterious neuroinflammation after stroke. *Brain J Neurol* 2011; 134(Pt 3): 704–720.
  87. Shichita T, Sugiyama Y, Ooboshi H, et al. Pivotal role of cerebral interleukin-17-producing gammadeltaT cells in the delayed phase of ischemic brain injury. *Nat Med* 2009; 15: 946–950.
  88. Liesz A, Zhou W, Na S-Y, et al. Boosting regulatory T cells limits neuroinflammation in permanent cortical stroke. *J Neurosci Off J Soc Neurosci* 2013; 33: 17350–17362.
  89. Liesz A, Suri-Payer E, Veltkamp C, et al. Regulatory T cells are key cerebroprotective immunomodulators in acute experimental stroke. *Nat Med* 2009; 15: 192–199.
  90. Xie L, Sun F, Wang J, et al. mTOR signaling inhibition modulates macrophage/microglia-mediated neuroinflammation and secondary injury via regulatory T cells after focal ischemia. *J Immunol Baltim Md 1950* 2014; 192: 6009–6019.
  91. Li P, Gan Y, Sun B-L, et al. Adoptive regulatory T-cell therapy protects against cerebral ischemia. *Ann Neurol* 2013; 74: 458–471.
  92. Ren X, Akiyoshi K, Vandebark AA, et al. CD4+FoxP3+ regulatory T-cells in cerebral ischemic stroke. *Metab Brain Dis* 2011; 26: 87–90.
  93. Stubbe T, Ebner F, Richter D, et al. Regulatory T cells accumulate and proliferate in the ischemic hemisphere for up to 30 days after MCAO. *J Cereb Blood Flow Metab Off J Int Soc Cereb Blood Flow Metab* 2013; 33: 37–47.
  94. Kleinschmitz C, Kraft P, Dreykluft A, et al. Regulatory T cells are strong promoters of acute ischemic stroke in mice by inducing dysfunction of the cerebral microvasculature. *Blood* 2013; 121: 679–691.
  95. Liesz A, Hu X, Kleinschmitz C, et al. Functional role of regulatory lymphocytes in stroke: facts and controversies. *Stroke* 2015; 46: 1422–1430.
  96. Na S-Y, Mrácsko E, Liesz A, et al. Amplification of regulatory T cells using a CD28 superagonist reduces brain damage after ischemic stroke in mice. *Stroke* 2015; 46: 212–220.
  97. Schuhmann MK, Kraft P, Stoll G, et al. CD28 superagonist-mediated boost of regulatory T cells increases thrombo-inflammation and ischemic neurodegeneration during the acute phase of experimental stroke. *J Cereb Blood Flow Metab Off J Int Soc Cereb Blood Flow Metab* 2015; 35: 6–10.

98. Pham M, Kleinschmitz C, Helluy X, et al. Enhanced cortical reperfusion protects coagulation factor XII-deficient mice from ischemic stroke as revealed by high-field MRI. *NeuroImage* 2010; 49: 2907–2914.
99. Davis SM, Donnan GA, Parsons MW, et al. Effects of alteplase beyond 3 h after stroke in the Echoplanar Imaging Thrombolytic Evaluation Trial (EPITHET): a placebo-controlled randomised trial. *Lancet Neurol* 2008; 7: 299–309.
100. Delgado-Mederos R, Rovira A, Alvarez-Sabín J, et al. Speed of tPA-induced clot lysis predicts DWI lesion evolution in acute stroke. *Stroke* 2007; 38: 955–960.
101. Gauberti M and Vivien D. Letter by Gauberti and Vivien regarding article, « amplification of regulatory T cells using a CD28 superagonist reduces brain damage after ischemic stroke in mice ». *Stroke* 2015; 46: e50–e51.
102. Gauberti M, Montagne A, Quenault A, et al. Molecular magnetic resonance imaging of brain-immune interactions. *Front Cell Neurosci* 2014; 8: 389.
103. Min Lou. *Combinating fingolimod with alteplase bridging with mechanical thrombectomy in acute ischemic stroke*, <https://clinicaltrials.gov/ct2/show/NCT02956200> (2016, accessed 15 May 2018).
104. Fu Y, Zhang N, Ren L, et al. Impact of an immune modulator fingolimod on acute ischemic stroke. *Proc Natl Acad Sci U S A*. 2014; 111: 18315–18320.
105. Zhu Z, Fu Y, Tian D, et al. Combination of the immune modulator fingolimod with alteplase in acute ischemic stroke: a pilot trial. *Circulation* 2015; 132: 1104–1112.
106. Rudick R, Polman C, Clifford D, et al. Natalizumab: bench to bedside and beyond. *JAMA Neurol* 2013; 70: 172–182.
107. Becker K, Kindrick D, Relton J, et al. Antibody to the alpha4 integrin decreases infarct size in transient focal cerebral ischemia in rats. *Stroke* 2001; 32: 206–211.
108. Langhauser F, Kraft P, Göb E, et al. Blocking of α4 integrin does not protect from acute ischemic stroke in mice. *Stroke* 2014; 45: 1799–1806.
109. Neumann J, Riek-Burchardt M, Herz J, et al. Very-late-antigen-4 (VLA-4)-mediated brain invasion by neutrophils leads to interactions with microglia, increased ischemic injury and impaired behavior in experimental stroke. *Acta Neuropathol (Berl)* 2015; 129: 259–277.
110. Relton JK, Sloan KE, Frew EM, et al. Inhibition of alpha4 integrin protects against transient focal cerebral ischemia in normotensive and hypertensive rats. *Stroke* 2001; 32: 199–205.
111. Llovera G, Hofmann K, Roth S, et al. Results of a preclinical randomized controlled multicenter trial (pRCT): anti-CD49d treatment for acute brain ischemia. *Sci Transl Med* 2015; 7: 299ra121.
112. Elkins J, Veltkamp R, Montaner J, et al. Safety and efficacy of natalizumab in patients with acute ischaemic stroke (ACTION): a randomised, placebo-controlled, double-blind phase 2 trial. *Lancet Neurol* 2017; 16: 217–226.
113. Jake Elkins. *Safety and efficacy of intravenous natalizumab in acute ischemic stroke*, <https://clinicaltrials.gov/ct2/show/NCT02730455> (accessed 31 May 2018.)
114. Martinez de Lizarrondo S, Gakuba C, Herbig BA, et al. Potent thrombolytic effect of n-acetylcysteine on arterial thrombi. *Circulation* 2017; 136: 646–660.
115. Orset C, Haelewyn B, Allan SM, et al. Efficacy of alteplase in a mouse model of acute ischemic stroke: a retrospective pooled analysis. *Stroke* 2016; 47: 1312–1318.
116. Orset C, Macrez R, Young AR, et al. Mouse model of in situ thromboembolic stroke and reperfusion. *Stroke* 2007; 38: 2771–2778.
117. Hossmann K-A. The two pathophysiolgies of focal brain ischemia: implications for translational stroke research. *J Cereb Blood Flow Metab Off J Int Soc Cereb Blood Flow Metab* 2012; 32: 1310–1316.
118. O'Collins VE, Macleod MR, Donnan GA, et al. 1,026 experimental treatments in acute stroke. *Ann Neurol* 2006; 59: 467–477.
119. Spychala MS, Honarpisheh P and McCullough LD. Sex differences in neuroinflammation and neuroprotection in ischemic stroke. *J Neurosci Res* 2017; 95(1–2): 462–471.
120. Ginhoux F, Greter M, Leboeuf M, et al. Fate mapping analysis reveals that adult microglia derive from primitive macrophages. *Science* 2010; 330: 841–845.
121. Yilmaz G and Granger DN. Leukocyte recruitment and ischemic brain injury. *Neuro Molecular Med* 2010; 12: 193–204.

122. Felger JC, Abe T, Kaunzner UW, et al. Brain dendritic cells in ischemic stroke: time course, activation state, and origin. *Brain Behav Immun* 2010; 24: 724–737.
123. Liu F and McCullough LD. Middle cerebral artery occlusion model in rodents: methods and potential pitfalls. *J Biomed Biotechnol* 2011; 2011: 464701.
124. Hug A, Dalpke A, Wieczorek N, et al. Infarct volume is a major determiner of post-stroke immune cell function and susceptibility to infection. *Stroke* 2009; 40: 3226–3232.
125. Veltkamp R and Gill D. Clinical trials of immunomodulation in ischemic stroke. *Neurother J Am Soc Exp Neurother* 2016; 13: 791–800.

Visit SAGE journals online  
[journals.sagepub.com/  
home/tan](http://journals.sagepub.com/home/tan)

 SAGE journals



### 3. Study 3: Impact of chronic alcohol consumption on ischemic stroke

Alcohol consumption triggers both systemic and cerebral inflammation. Due to the great heterogeneity of the type of consumption, interindividual effects, time of consumption as well as factors such as age or sex, the study of the physiopathological effects of alcohol are various and varied. Take for example the case of ischemic stroke. Alcohol is a risk factor for stroke, and, at low doses, alcohol consumption will reduce the risk of stroke (Sacco et al., 1999). Alcohol, administered downstream, can also improve recovery in stroke in mice (Wang et al., 2012). In addition, alcohol has neuroprotective properties and allows reduction of the lesion volume at low doses in rodents (Geng et al., 2013; McCarter et al., 2017), but can also exacerbate it (Lemarchand et al., 2015). In humans, it has been shown that heavy drinking have a deleterious effect of excessive alcohol consumption on stroke (Ducroquet et al., 2013), but it has also been found an absence of statistical difference in the severity of stroke between consumers and non-users alcohol (Gattringer et al., 2015).

In view of these controversial results, we carried out a translational study in collaboration with the Clinical Hospital of Santiago de Compostela (Spain). **We studied the impact of alcohol consumption on the severity and neurological outcome of ischemic stroke in 3,645 subjects, and we detected an aggravating effect of chronic alcohol consumption that is related to the inflammatory response.** To better understand the links between the inflammatory response and worsening neurological outcome in patients, we conducted a study in mice where we showed that **alcohol triggers an inflammatory priming at the cerebral level, which causes an exacerbated response to secondary brain damage such as stroke.**



1    **Neurovascular inflammatory priming induced by heavy drinking is associated with an**  
2    **aggravated ischemic stroke outcome**

3

4    **Authors:** Antoine Drieu<sup>1</sup>, Anastasia Lanquetin<sup>1</sup>, Francisco Campos, PhD<sup>2</sup>, Aurélien Quenault,  
5    PhD<sup>1</sup>, Eloïse Lemarchand, PhD<sup>1</sup>, Mikaël Naveau, PhD<sup>1</sup>, Anne Lise Pitel, PhD<sup>4</sup>, José Castillo,  
6    MD, PhD<sup>2</sup>, Denis Vivien, PhD<sup>5</sup>, Marina Rubio, PhD<sup>1\*</sup>

7

8    **Affiliations:**

9    <sup>1</sup> Normandie Univ, UNICAEN, INSERM, Physiopathology and Imaging of Neurological  
10   Disorders, 14000 Caen, France

11   <sup>2</sup> Clinical Neurosciences Research Laboratory, Department of Neurology, Stroke Unit,  
12   University Clinical Hospital, Health Research Institute of Santiago de Compostela (IDIS),  
13   Santiago de Compostela, Spain

14   <sup>4</sup> Normandie Univ, UNICAEN, INSERM, Neuropsychologie et Imagerie de la Mémoire  
15   Humaine, 14000 Caen, France

16   <sup>5</sup> Normandie Univ, UNICAEN, INSERM, CHU de Caen, Physiopathology and Imaging of  
17   Neurological Disorders, 14000 Caen, France

18   \*To whom correspondence should be addressed: rubio@cyceron.fr

19

20   **Running title:** Heavy drinking worsens stroke outcome

21

1    **Abstract**

2    Alcohol abuse is a major public health problem worldwide causing a wide range of preventable  
3    morbidity and mortality. In this translational study, we show that heavy drinking (HD) ( $\geq 6$   
4    standard drinks/day) is independently associated to a worse outcome of ischemic stroke  
5    patients. To study the underlying mechanisms of this deleterious effect of HD, we performed  
6    an extensive analysis of the brain inflammatory responses of mice exposed or not to 10%  
7    alcohol before and after stroke. Inflammatory responses were analyzed at the parenchymal,  
8    perivascular and vascular levels by using transcriptomic, immunohistochemical, *in vivo* two-  
9    photon microscopy and molecular MRI analyses. Alcohol-exposed mice show, in the absence  
10   of any other insult, a neurovascular inflammatory priming (i.e., an abnormal inflammatory  
11   status) associated to exacerbated inflammatory responses after a secondary insult (ischemic  
12   stroke or LPS challenge). Similar to our clinical data, alcohol-exposed mice showed larger  
13   ischemic lesions. This study opens new therapeutic avenues aiming at blocking alcohol-induced  
14   exacerbation of the neurovascular inflammatory responses triggered after ischemic stroke.

15

16    **Keywords:** stroke, inflammatory priming, alcohol, *in vivo* imaging, early neurological  
17   deterioration

18

**1    List of abbreviations used in the text:**

- 2    NIHSS: National Institute of Health Stroke Scale
- 3    mRS: modified Rankin Scale
- 4    END: Early Neurological Deterioration
- 5    HD: Heavy Drinking
- 6    DSM: Diagnostic and Statistical Manual of Mental Disorders
- 7    AUD: Alcohol Use Disorder
- 8    AUDIT: Alcohol Use Disorders Identification Test
- 9    STAI: State-Trait Anxiety Inventory scale
- 10   BMI: Body Mass Index
- 11   CRP: C-reactive protein
- 12   ARRIVE: Animal Research: Reporting of In Vivo Experiments
- 13   BAL: Blood Alcohol Levels
- 14   MCA: Middle Cerebral Artery
- 15   MCAo: Middle Cerebral Artery occlusion
- 16   LPS: lipopolysaccharide
- 17   MPIO: Micro Particles of Iron Oxide
- 18   PMT: Photomultiplier
- 19   OR: Odds Ratio
- 20   TOAST: Trial of ORG 10172 in Acute Stroke Treatment

1 TNF: Tumor Necrosis Factor

2 IL: Interleukin

3

1    **Introduction**

2    Alcohol abuse is a major public health problem worldwide causing a wide range of preventable  
3    morbidity and mortality. In the European Union 89% of men and 82% of women are current  
4    drinkers; among them, 15.3% of men and 3.4% of women are heavy drinkers (>6 drinks/day)  
5    [29]. In the United States, excessive alcohol use is known to kill about 88,000 people each year,  
6    and the cost of excessive alcohol use reached \$249 billion in 2010  
7    (<https://www.cdc.gov/features/costsofdrinking/>). Alcohol modifies the risk of stroke: light and  
8    moderate alcohol consumption (0-2 drinks/day) are associated with a lower risk of ischemic  
9    stroke, whereas higher doses of alcohol are associated with an increased risk [18]. Importantly,  
10   stroke risk associated with high and heavy drinking in midlife (<75 years) predominates over  
11   well-known stroke risk factors like hypertension and diabetes [17]. However, the impact of  
12   alcohol consumption on stroke outcome is less known. Current clinical studies are controversial  
13   and have described either an aggravating effect [7] or no effect of heavy drinking [9] on stroke  
14   severity. Preclinical reports have also described either a protective effect of low alcohol  
15   consumption on ischemic stroke [20, 32], or larger infarcts in rodents exposed to heavy drinking  
16   [19, 32]. The reasons for this aggravation are not well understood yet. Our previous results on  
17   the impact of heavy alcohol consumption on ischemic stroke, obtained in a clinically relevant  
18   thromboembolic model of stroke [22, 23], have shown that the aggravating effect of heavy  
19   drinking is not due to alcohol-induced changes in hemodynamic parameters (clot formation,  
20   stability or sensitivity to fibrinolysis) [19]. On the other hand, clinical and preclinical data have  
21   shown that heavy alcohol consumption may have an impact on inflammation [1, 11, 16]. Due  
22   to the role of inflammation on the pathophysiology of ischemic lesions [15], in this translational  
23   study we aimed to investigate the role of inflammation in the aggravating effect of heavy  
24   drinking on ischemic stroke.

1   **Materials and methods**

2   **Stroke cohort study population and patient characteristics**

3   We retrospectively analyzed a cohort of 3.645 ischemic stroke patients from the stroke registry  
4   of the Stroke Unit of the Neurology Department of the University Clinical Hospital of Santiago  
5   de Compostela (Spain) included from January 2010 to December 2016. The registry was  
6   approved by the Ethics Committee of Galicia (CEIC). Signed informed consent was obtained  
7   from patients or a relative before study inclusion. Acute management (diagnostic and treatment)  
8   of patients with stroke was performed according the protocol described by the European Stroke  
9   Organization.

10   **Stroke outcome variables**

11   To evaluate the influence of chronic, excessive alcohol consumption on the outcome of stroke  
12   patients, the following primary outcomes variables were considered: i) neurological stroke  
13   severity determined by the National Institute of Health Stroke Scale (NIHSS) at admission, 24  
14   and 48 hours, ii) early neurological deterioration (END) defined as increase of NIHSS in  $\geq 4$  in  
15   the first 48 hours after admission, iii) infarct volume determined by TC scan between the 4th  
16   and 7th day after admission, iv) degree of disability at 3 months assessed by modified Rankin  
17   Scale (mRS), and v) percentage of patients with good outcome at 3 months ( $mRS \leq 2$ ).

18   To determine the association between chronic alcohol consumption and inflammatory response,  
19   the following biological variables were included in the analysis: 1) leukocyte numbers, 2)  
20   fibrinogen, 3) C-reactive protein and 4) sedimentation rate. Axillary temperature  $>37.5$  °C at  
21   admission was also considered as a marker of inflammation.

22   History of arterial hypertension was considered when the blood pressure was  $>140/90$  mmHg  
23   at least two different days before stroke onset, if the patient was diagnosed for hypertension or  
24   when the patient was under antihypertensive treatment. History of diabetes disease was defined

1 as serum glucose levels  $\geq 7.0$  mmol/L, if the patient was diagnosed of diabetes or when the  
2 patients was under diabetic medication. Smoking patients were defined as those patients who  
3 presented smoking habits in the last 5 years. Heavy drinking (HD) habits were defined as a  
4 daily alcohol consumption  $\geq 6$  drinks/day in the last 5 years.

5 **Stroke cohort statistical analyses**

6 Results were expressed as percentages for categorical variables and as mean ( $\pm SD$ ) or median  
7 and range [25th and 75th percentiles] for continuous variables depending on whether their  
8 distribution was normal or not. The Kolmogorov-Smirnov test was used to assess normality.  
9 Proportions were compared using the chi-square or Fisher test, while the continuous variables  
10 between groups were compared with the Student's t or the Mann-Whitney test depending on  
11 whether their distribution was normal or not. Bivariate correlations were performed using  
12 Pearson's coefficient (normally distributed variables) or Spearman's coefficient (variables  
13 without normal distribution).

14 The association between heavy drinking and early neurological deterioration (END) was  
15 assessed using logistic regression analysis; the influence on infarct volume was assessed by  
16 multiple linear regression models. Both logistic regression analysis and multivariate linear  
17 regression models were adjusted for those variables which showed biological relevance for each  
18 endpoint in order to avoid spurious associations. Results were expressed as adjusted odds ratios  
19 (ORs) or B estimate with the corresponding 95% confidence intervals (95% CI). Statistical  
20 significance was set at  $P < 0.05$ . The statistical analysis was conducted in SPSS 20.0 (IBM,  
21 Chicago, IL, USA) for Mac.

22 **Analysis of inflammatory markers in heavy drinking (HD) patients without stroke**

23 We retrospectively analyzed data from an independent cohort including 34 patients with a  
24 DSM-V (Diagnostic and Statistical Manual of Mental Disorders - 5<sup>th</sup> edition) diagnostic of

1 Alcohol Use Disorder (AUD) (heavy drinking patients, HD) and 21 healthy control subjects.  
2 All the participants were informed about the study, approved by the local ethics committee  
3 (CPP Nord Ouest III, no. IDRCCB: 2011-A00495-36), and provided their written informed  
4 consent before their inclusion.

5 HD patients were recruited in the Addiction Unit of the University Hospital of Caen  
6 (Normandy, France) while they were receiving withdrawal treatment as inpatients. They all met  
7 alcohol-dependence criteria according to the DSM-IV and AUD according to the DSM-V for  
8 at least 5 years. Control subjects were interviewed with the Alcohol Use Disorders  
9 Identification Test (AUDIT; [8]), in order to verify that they were not at risk for alcohol misuse  
10 or alcohol dependence (score <6 for women and <7 for men). Participants were matched for  
11 age, sex and body mass index (BMI).

12 Exclusion criteria for all the participants were: neurological diseases, active infectious disease,  
13 cardiovascular or psychiatric diseases, cancer, depression [Beck questionnaire, [2]], anxiety  
14 [State-Trait Anxiety Inventory scale, STAI A et B parts, [31]], or misuse of any other substance  
15 than alcohol (excepting tobacco) [misuse and/or dependence measured by the Fagerström score  
16 [12]].

17 Blood samples were collected from fasted participants, either at inclusion (control subjects) or  
18 the day after admission to hospital (HD patients). Immune cell counts (leukocytes, neutrophils,  
19 eosinophils, basophils, lymphocytes and monocytes) were measured in all participants. C-  
20 reactive protein (CRP) levels were measured only in HD patients.

21 **HD cohort statistical analyses**

22 The normality of the distribution of the laboratory measures for the HD and control groups was  
23 examined using the Shapiro Wilk test. *Student's t* tests were used to compare the two groups  
24 for measures of immune cell counts and CRP.

1    **Experimental study design**

2    The goal of this study was to investigate the impact of heavy drinking on stroke outcome and  
3    describe the underlying mechanisms in an experimental model of ischemic stroke in mice.

4    Animals were randomized to treatment groups, and all analyses were performed by  
5    investigators blinded to group allocation. Unblinding was performed after completion of  
6    statistical analysis. All animal experiments were performed and reported in accordance with the  
7    Animal Research: Reporting of In Vivo Experiments (ARRIVE) guidelines  
8    (<http://www.nc3rs.org.uk>), with approval from the local ethical committee (agreement number  
9    3748).

10    **Animals**

11    Two months-old male Swiss mice (35-45g) (Centre Universitaire de Ressources Biologiques,  
12    Normandy University, Caen, France) were housed at 21° C in a 12 h light/dark cycle with food  
13    and water (control group) or a 10% (v/v) alcohol solution (alcohol group) with *ad libitum* free  
14    access for 6 weeks. All mice were checked daily for fluid consumption, health and abnormal  
15    behavior. The average daily liquid intake and weight gain were similar between both groups  
16    (~6 ml of liquid intake/mouse/day and a weight gain of ~6g between the beginning and the end  
17    of the alcohol exposure period (final weight ~40g in both groups). Blood alcohol levels (BAL)  
18    were measured at the pharmacology unit of Caen University Hospital in mice at the end of the  
19    6 weeks of alcohol exposure (n=10 mice). At the moment of the blood extraction, only 3 out of  
20    10 mice showed positive BAL values (0.39, 0.54 and 0.63 g/L), the rest of the mice showed  
21    non-detectable values (<0.1 g/L).

22    All the procedures needing anesthesia of the mice were performed by an initial exposure to 5%  
23    isoflurane followed by a maintaining phase of 1.5-2% isoflurane 30%O<sub>2</sub>/70%N<sub>2</sub>O.

24    **Thromboembolic Focal Cerebral Ischemia**

1 We used the *in situ* thromboembolic stroke model consisting in the injection of thrombin  
2 directly into the middle cerebral artery as described before [23]. Anesthetized mice were placed  
3 in a stereotaxic device, a small craniotomy was performed, the dura was excised, and the middle  
4 cerebral artery (MCA) was exposed. A pulled glass micropipette was introduced into the lumen  
5 of the MCA and 1 µL (1 UI/µL) of purified murine alpha-thrombin (Enzyme Research Labs,  
6 USA) was pneumatically injected to induce MCA occlusion (MCAo) by the *in situ* formation  
7 of a clot. Lesion volumes were quantified on Image J 24 hours after stroke onset by regular  
8 thionin staining. In order to mimic clinical conditions, alcohol solutions were changed by water  
9 after stroke onset and until killing.

10 **Intraperitoneal lipopolysaccharide (LPS) injection**

11 A subset of control and alcohol-exposed mice (n=5-6 mice per group) were intraperitoneally  
12 injected with a single dose of the bacterial endotoxin LPS (1 mg/kg) (Sigma-Aldrich, France)  
13 [21] and underwent two-photon imaging and molecular MRI 24 hours after the injection of  
14 LPS. Alcohol-exposed mice kept free access to the alcohol solution after LPS injection and  
15 until killing.

16 **Vascular adhesion molecular imaging**

17 Micro-sized particles of iron oxide (MPIOs) (diameter 1.08 mm) (Invitrogen) covalently  
18 conjugated to purified polyclonal goat anti-mouse antibodies for P-selectin (R&D Systems,  
19 clone AF737) were prepared as previously described [28]. The quality of conjugated MPIOs  
20 was systematically checked in a naive mouse, by stereotaxic injection of lipopolysaccharide  
21 (1µl, 1mg/kg) in the striatum (0.5mm anterior, 2.0mm lateral, -3mm ventral to the Bregma).  
22 Three-dimensional T2\*- weighted gradient echo imaging with flow compensation (spatial  
23 resolution of 70 mm x 70 mm x 70 mm interpolated to an isotropic resolution of 70 mm), TE/TR  
24 13.2ms/200 ms and a flip angle of 21° was performed to visualize MPIOs. MRI acquisitions  
25 started immediately after the intravenous injection of MPIOs (200 µl of 2 mg Fe/kg of

1 conjugated MPIOs). All T2\*-weighted images presented are minimum intensity projections of  
2 six consecutive slices. For the ischemic stroke study, signal void quantification on 3D T2\*-  
3 weighted images was measured by using automatic triangle threshold in ImageJ software and  
4 results presented as MPIOs-induced signal void on the contralateral cortex divided by the signal  
5 void on the structure of interest (in percent). For the lipopolysaccharide (LPS) study, only  
6 cortical blood vessels (which were identified as straight lines in hyposignal on T2\*-weighted  
7 images) were counted.

8 **Thin-skull cranial window**

9 Anesthetized mice used for two-photon experiments underwent thin-skull cranial window for  
10 the cortical *in vivo* detection of leukocyte rolling and adhesion. The head skin was opened to  
11 expose the skull and the right parietal bone was completely polished with a drill to leave only  
12 a thin layer of bone enabling the visualization of cortical cerebral blood vessels by transparency.  
13 The imaged area corresponds to the right somatosensory cortex (stroke peri-infarct area).

14 **Intravital two-photon microscopy**

15 Anesthetized mice were placed in a stereotaxic device and aqueous medium was deposited  
16 between the thin-skull window and the X25 immersive objective. One hundred  $\mu$ l of  
17 Rhodamine 6G (1mg/kg) and 100  $\mu$ l of 70kDa FITC-Dextran (5mg/ml) (Sigma Aldrich,  
18 France) were injected in the tail vein to stain circulating leukocytes and to visualize the lumen  
19 of blood vessels, respectively. Acquisitions were performed one day before stroke onset using  
20 a Leica TCS SP5 MP microscope at 840 nm two-photon excitation wavelength (Coherent  
21 Chameleon, USA). Leukocyte adhesion and rolling were measured with time-lapse acquisitions  
22 (2 minutes, 7.7 frames per second, 256x256 pixel resolution, 1000Hz frequency).  
23 Photomultiplier (PMT) 2 (recorded capacity: 500-550nm) was used to record FITC-Dextran  
24 signal (gain 850V; offset 0), and PMT3 (recorded capacity: 565-605nm) for Rhodamine-6G

1 signal (gain 850V; offset 0). The pulsing laser characteristics were: gain 23%; trans 17%; offset  
2 50%.

3 **Leukocyte rolling/adhesion counting**

4 For adherent leukocyte quantification, the images obtained by time-lapse were compiled and  
5 red spots, corresponding to adherent leukocytes, were counted for each group (n=3-5 mice per  
6 group). For rolling leukocytes, we used the Kymograph plugin on ImageJ software (developed  
7 by J. *Rietdorf* and A. *Seitz*) (line width perpendicular to vessel lumen: 10; size pixel<sup>2</sup> after  
8 threshold: (2-5)-infinity). Leukocytes that were too fast were considered as background and not  
9 counted as rolling leukocytes.

10 ***In vivo* microglial phagocytic capacity measurement**

11 The protocol was modified from Hughes et al. [14]. Briefly, 1µl of nonionic latex beads (6 µm)  
12 (1:50, Molecular Probes, Life Technologies, USA) were gently injected in the brain cortex (2.2  
13 mm lateral, -1.6 mm ventral to bregma) of anesthetized mice (n=4 mice/group) with a glass  
14 micropipette (angle 335°). The micropipette was left *in situ* for 2 min before slow withdrawal  
15 and then mice were sutured. Eight hours after the injection, mice were terminally anesthetized  
16 and prepared for immunohistochemical analyses. Alcohol-exposed mice kept free access to the  
17 alcohol solution after beads injection and until killing. The number of latex beads completely  
18 surrounded by Iba1<sup>+</sup> staining was counted in the ipsilateral cortex of control and alcohol-  
19 exposed mice. All beads forming clusters of more than 20 beads were omitted (tight clusters  
20 might prevent access of microglial cells to individual beads). The total number of beads  
21 phagocytosed was divided by the total not phagocytosed to calculate a ratio for each animal and  
22 these ratios were averaged for four animals in each treatment group.

23 **Quantitative PCR analyses**

1 Terminally anesthetized mice (n=6/group) were transcardially perfused with cold heparinized  
2 saline (15 mL) and brains were excised. Cortex were dissected and maintained at -80 °C until  
3 messenger RNA (mRNA) extraction. Tissues were dissociated in TRI reagent (Sigma; Lyon,  
4 France), and RNA was isolated by the addition of chloroform. Total RNA was washed by  
5 ethanol and treated with TURBO DNase (Ambion; Saint Aubin, France). Total RNA was  
6 quantified by spectrophotometry (NanoDrop Technologies; Wilmington, USA). Reverse  
7 transcription from 1 µg of total RNA (or water as an internal control) was performed with the  
8 iScript Select cDNA Synthesis kit (Bio-Rad; Marnes-la-Coquette, France) in a total volume of  
9 20 µL with the following cycle conditions: 42 °C (90 min); 85 °C (5 min). The cDNA products  
10 were then stored at -20 °C until their use.

11 Quantitative PCR was performed with 1 µL of 1:20 diluted cDNA, water and the RT-qPCR  
12 internal control), that were analyzed in 15 µL total of a 1× solution of iQ SYBR Green  
13 Supermix (Bio-Rad; Marnes-la-Coquette, France) containing 200 nM of each primer. Based on  
14 mRNA coding sequences ([www.ensembl.org](http://www.ensembl.org)), mouse-specific primers were designed by using  
15 the Primer3Plus software (<http://www.bioinformatics.nl/cgi-bin/primer3plus/primer3plus.cgi>)  
16 (Supplementary table 4). Two housekeeping genes (Hmbs and Ppib) were used. Assays were  
17 run in triplicate on the CFX96 real-time system c1000 thermal cycler (Bio-Rad; Marnes-la-  
18 Coquette, France), with the following cycle conditions: 95 °C (3 min); [95 °C (2 s), 60 °C (20  
19 s)] × 39; 70 °C (30 s).

20 **Immunohistochemistry**

21 Terminally anesthetized mice were transcardially perfused with cold heparinized saline (15 mL)  
22 and fixed with 100 mL of 2% paraformaldehyde and 0.2% picric acid phosphate buffer (pH  
23 7.4) (n=4 mice/group). Brains were post-fixed with 2% paraformaldehyde and 0.2% picric acid  
24 phosphate buffer (18 hours; 4°C) and cryoprotected (sucrose 20% in PBS; 24 hours; 4°C) before  
25 freezing in Tissue-Tek (Miles Scientific, Naperville, IL, USA). Cryostat-cut sections (10 µm

1 excepting latex beads experiment, where 20 µm sections were used) were collected on poly-  
2 lysine slides and stored at – 80°C before processing.

3 Sections were co-incubated overnight with rabbit anti-mouse Iba1 (1:1000, Wako 019-19741),  
4 rat anti-mouse CD68 (1:800, Abcam 53444), rat anti-mouse CD206 (1:200, Serotec, clone  
5 MR5D3), goat anti-mouse P-selectin (1:1000, RD System AF737), goat anti-mouse Collagen-  
6 IV (1:1000, SouthernBiotech 1340), rabbit anti-mouse Aquaporin 4 (sc 20812, Santa Cruz).

7 Primary antibodies were revealed by using Fab'2 fragments of Donkey anti-rabbit linked to  
8 FITC, anti-rat linked to Cy3, anti-goat IgG linked to Cy5 (1:600, Jackson ImmunoResearch,  
9 West Grove, USA). Washed sections (5 sections/mouse) were coverslipped with antifade  
10 medium containing DAPI. Epifluorescence images (~10 images/section) were digitally  
11 captured using a Leica DM6000 epifluorescence microscope-coupled coolsnap camera,  
12 visualized with Leica MM AF 2.2.0 software (Molecular Devices, USA) and further processed  
13 using ImageJ 1.51k software. Studied regions were always located at the brain cortex [ipsi (peri-  
14 infarct and core) and contralateral cortices for stroke experiments] (see supplementary fig.1).

15 Specificity controls were performed by not adding primary antibodies.

16 *Confocal microscopy analysis of microglial activation*

17 Microglial morphology and activation were analyzed on confocal images taken on a Leica TCS  
18 SP5 MP microscope. Using the X40 oil immersive objective, images were randomly taken  
19 using LAS AF Leica Software and analyses were performed using ImageJ 1.51k software. Iba1  
20 analyses allowed the quantification of microglial cell numbers, soma area and number of main  
21 processes starting from the soma. CD68 staining in Iba1<sup>+</sup> cells allowed the quantification of the  
22 activation of microglial cells. For this latter analysis, after thresholding CD68 and Iba1  
23 channels, we used the Image Calculator ImageJ plugin to collect the mask of CD68 only in  
24 Iba1<sup>+</sup> cells. After that, we measured the area of Iba1 mask cell per cell, and the area of CD68  
25 inside each cell in both groups (n=800-1000 cells/group; n=4 mice per group).

**1 Statistical analyses on pre-clinical data**

**2 Results are the mean  $\pm$  SEM. Statistical analyses were performed by the Mann-Whitney test  
3 using the Statview software.**

**4**

1    **Results**

2    *Heavy drinking (HD) stroke patients show higher stroke baseline severity and worse*  
3    *neurological outcome*

4    A total of 3.645 ischemic stroke patients were included in the retrospective analysis. HD stroke  
5    patients (n=424, 11.6%) were significantly younger, and more frequently men, presented  
6    history of hypertension and higher smoking habits than non HD stroke patients. In addition, HD  
7    stroke patients had more severe ischemic strokes, with a higher infarct volume, higher mortality  
8    during hospitalization, worse prognosis at 3 months and presented higher levels of markers  
9    associated with the inflammatory response. Mortality during hospitalization was significantly  
10   increased in HD stroke patients (11.7% vs 9.7%, p<0.0001; Table 1).

11   The National Institute of Health Stroke Scale (NIHSS) scores at admission, 24 hours and 48  
12   hours after stroke onset were significantly higher in HD stroke patients (Fig. 1A, Table 1).  
13   Interestingly, significantly more HD stroke patients presented early neurological deterioration  
14   (END) -defined as the increase of NIHSS in  $\geq 4$  in the first 48 hours after admission- (19,2% vs  
15   4,4%; Table 1, Fig. 1A).

16   *HD is independently associated with an increased risk of END*

17   Based on the first univariate analysis, END was used as the main variable to analyze the cohort  
18   of stroke patients included in this study (Table 2). In this second univariate analysis, a total  
19   3352 patients were included (3146 without END and 206 with END) (293 less patients than for  
20   the descriptive analysis since NIHSS data were not recorded or lost between the admission and  
21   the 48 hours). As expected, patients with END showed significantly higher hemorrhagic  
22   transformation, higher infarct volume and worse prognosis at 3 months. Moreover, patients  
23   with END presented higher inflammatory response at admission, characterized by higher

1 leukocyte numbers as well as C-reactive protein levels. Interestingly, significantly more END  
2 patients had HD habits (36.9% vs. 10.2%, p<0.0001; Table 2).

3 *The inflammatory response is associated with the risk of END in HD stroke patients*  
4 We then performed multivariate analysis of END adjusted by HD (Model A, Fig 1B,  
5 Supplementary Table 1) or by HD and inflammatory markers (Model B, Fig. 1C, and  
6 Supplementary Table 1). Model A showed that HD is independently associated with an  
7 increased risk of END (Odds Ratio (OR)=4.49; 95% CI: 2.94 - 6.86; p<0.0001) (Fig 1B,  
8 Supplementary table 1). When inflammatory markers [axillary temperature, leukocyte numbers  
9 and C-reactive protein (CRP)] were included in the analysis (Model B, Fig. 1C, Supplementary  
10 Table 1) the impact of HD on the END OR decreased from 4.49 (obtained on the Model A) to  
11 2.45 (OR=2.45; 95% CI: 1.01 – 5.91; p<0.0001), showing that the inflammatory response is  
12 associated with the risk of END in HD stroke patients.

13 Finally, we studied the effect of HD on infarct volume. After adjusting for those variables that  
14 can interfere with the variable “infarct volume” (age, sex, axillary temperature, leukocyte  
15 levels, fibrinogen levels, C-reactive protein levels, tPA treatment, thrombectomy, hemorrhagic  
16 transformation, NIHSS on admission, END, TOAST (Trial of ORG 10172 in Acute Stroke  
17 Treatment) classification and HD; Supplementary Table 2), linear regression analysis of infarct  
18 volume showed that the predictor value of HD was 19.66 (B=19.66; 95% CI: 8.03-31.30;  
19 p<0.001; Supplementary Table 3).

20 *HD patients without stroke show high levels of inflammatory markers*

21 Data from the independent cohort of HD patients without stroke showed that the levels of  
22 circulating monocytes are significantly increased compared to control healthy subjects ( $0.73 \pm$   
23  $0.27$  vs.  $0.2 \pm 0.17$  respectively, p=0.003) (Table 3). In addition to this, 61.8% of HD showed  
24 increased high sensitivity-CRP (hs-CRP) levels (Table 3).

1    *Alcohol exposure induces a neurovascular inflammatory priming in mice*

2    The first set of experiments aimed to analyze the parenchymal, perivascular and vascular  
3    inflammatory status in the brain of mice drinking 10% alcohol for 6 weeks (~5 g/kg/day), in  
4    the absence of any other insult. To study microglial cells, brain samples were stained with Iba1,  
5    a constitutive marker of microglial cells, and with the lysosomal marker CD68, characteristic  
6    of activated microglia [24]. We found that whereas the total number of activated microglial  
7    ( $\text{Iba1}^+\text{CD68}^+$ ) cells remained unchanged (Fig. 2A, Fig. 2C), the total area of  $\text{CD68}^+$  staining  
8    was significantly increased in alcohol-exposed mice ( $p<0.05$  vs. control; Fig. 2B, Fig. 2D),  
9    suggestive of an alcohol-induced increase in microglial activation. Alcohol exposure did not  
10   change microglial cell numbers (total number of  $\text{Iba1}^+$  cells) (Fig. 2A, Fig. 2E;  $n=4$   
11   mice/group). In terms of microglial morphology, alcohol exposure did not change neither the  
12   number of main processes (starting from the soma) (Fig. 2B, Fig. 2F) nor the mean area of  
13   microglial cells (Fig. 2B, Fig. 2G).

14   The alcohol-induced increase in microglial activation was demonstrated by an *in vivo* functional  
15   measurement of microglial phagocytosis after the injection of nonionic latex beads in the brain  
16   cortex of control and alcohol-exposed mice (Fig. 2H). Eight hours after the intracortical  
17   injection of the beads, alcohol-exposed mice showed significantly more phagocytized beads  
18   (surrounded by Iba1 positive staining) than control mice (Fig. 2I-2K;  $n=4$  mice/group;  $p<0.05$   
19   vs. control), demonstrating that microglia in alcohol-exposed mice is more prone for  
20   phagocytosis. These results show an alcohol-induced microglial priming characterized by a  
21   morphological “resting” state accompanied however by an increase in both microglial  
22   activation status and phagocytic capacity.

23   In addition to the microglial priming profile, alcohol-exposed mice also showed significantly  
24   increased numbers of brain perivascular macrophages (PVM), a sub-population of resident  
25   brain macrophages located at the perivascular level (Fig. 2L-2N;  $n=4$  mice/group;  $p<0.05$  vs

1 control). PVM are negative for Iba1 and can be stained with both CD68 (Fig. 2O, Fig. 2P) and  
2 CD206 antibodies (Fig. 2Q, Fig. 2R).

3 In this study, we also wanted to examine potential inflammatory effects of alcohol exposure on  
4 the brain vasculature triggered after stroke. For this reason, we analyzed the endothelial levels  
5 of the adhesion molecule P-selectin (CD62P marker), responsible of leukocyte tethering and  
6 rolling on the vessel wall. At the vascular level, alcohol-exposed mice showed significantly  
7 increased P-selectin positive blood vessels (+152% increase;  $1.03\pm0.31$  CD62P<sup>+</sup> blood  
8 vessels/mm<sup>2</sup>; n=4 mice/group; p<0.05 vs. control), whereas in control mice very low levels of  
9 P-selectin ( $0.31\pm0.11$  CD62P<sup>+</sup> blood vessels/mm<sup>2</sup>) were detected (Fig. 2S, Fig. 2T),  
10 demonstrating an alcohol-induced endothelial activation.

11 To determine the functional impact of the increase in P-selectin expression, we performed *in*  
12 *vivo* two-photon microscopy analyses to measure leukocyte adhesion and rolling in mice  
13 exposed or not to alcohol, after the intravenous injection of FITC-Dextran (allowing blood  
14 vessels visualization) and Rhodamine-6G (staining leukocytes). Alcohol-exposed mice showed  
15 significantly more adherent (Fig. 2U, Fig. 2V) and rolling (Fig. 2W, Fig. 2X) leukocytes  
16 compared to control mice (+317% and +724% increase respectively; n=6 mice/group; p<0.05  
17 vs. control).

18 Concerning mRNA expression of inflammatory markers, alcohol-exposed mice showed a  
19 significant increase in TGF $\square$  mRNA levels (p<0.05, n=6 mice/group) compared to control  
20 mice, that was not accompanied by changes in pro-inflammatory cytokines such as interleukin  
21 (IL)-1 $\beta$ , tumor necrosis factor (TNF), IL-6, P-Selectin, TLR4, or VCAM1 (Table 4).

22 Concerning blood-brain barrier (BBB) integrity and the potential alcohol-induced neuronal  
23 death, we did not find any fibrin(ogen) deposit (Supplementary Fig. 1A, n=4 mice/group) or

1 fluorojade C positive staining (Supplementary Fig. 1B, n=4 mice/group) on brain tissue in any  
2 of the groups.

3 *Alcohol exposure exacerbates brain neurovascular inflammatory reactions after an acute*  
4 *systemic insult*

5 Alcohol-exposed mice showed a global exacerbated inflammatory response in the brain 24  
6 hours after an acute intraperitoneal injection of LPS compared to control mice. At the  
7 parenchymal level, alcohol-exposed mice receiving LPS showed a significant increase in (i)  
8 total microglial cells (Iba1<sup>+</sup> cells) (Fig. 3A, Fig. 3B; n=5 mice/group; p<0.05 vs. control), (ii)  
9 activated microglia (Iba1<sup>+</sup>CD68<sup>+</sup> cells) (Fig. 3A, Fig. 3C; n=5 mice/group; p<0.05 vs. control)  
10 and (iii) CD68<sup>+</sup>Iba1<sup>-</sup> cells (Fig. 3A, Fig. 3D) compared to LPS-injected control mice.

11 At the vascular level, P-selectin immunostaining (Fig. 3E, Fig. 3F) was significantly increased  
12 in alcohol-exposed mice receiving LPS compared to control mice (n=5 mice/group; p<0.05 vs  
13 control). Molecular MRI also showed significantly increased number of P-selectin-coupled  
14 MPIO<sup>+</sup> blood vessels in alcohol-exposed mice receiving LPS (Fig. 3G, Fig. 3H; n=5  
15 mice/group; p<0.05 vs control). Consequently, leukocyte adhesion (Fig. 3I, Fig. 3J) and rolling  
16 (Fig. 3K, Fig. 3L), measured by intravital two-photon microscopy, were significantly increased  
17 in alcohol-exposed mice receiving LPS compared to control mice (n=5 mice/group; p<0.05 vs  
18 control).

19 *Alcohol exposure aggravates stroke lesions and exacerbates neurovascular inflammatory*  
20 *responses after ischemic stroke in mice.*

21 Alcohol-exposed mice showed significantly larger ischemic lesions than control mice (drinking  
22 only water) 24 hours after stroke onset (Fig. 4A, Fig. 4B; n=7-8 mice/group; p<0.05 vs control,  
23 [19]). These data on lesion volume are part of a previously published figure [19]. No  
24 hemorrhagic transformation was detected in any mice (data not shown).

1 Microglial reaction after stroke (Fig. 4C-4I) was exacerbated in the ipsilateral cortex of alcohol-  
2 exposed mice, with significant increases in (i) the number of total microglial cells (Iba1<sup>+</sup>  
3 staining) in the peri-infarct area (Fig. 4E; n=3 mice/group; p<0.05 vs control), (ii) the number  
4 of CD68<sup>+</sup> microglial cells in the peri-infarct area and the ischemic core (Fig. 4F; n=3  
5 mice/group; p<0.05 vs control), and (iii) the area of CD68 staining on microglial cells in the  
6 ipsilateral hemisphere (Fig. 4G; n=3 mice/group; p<0.05 vs control). The number of processes  
7 starting from the soma was significantly decreased in the ipsilateral cortex of alcohol-exposed  
8 mice (Fig. 4H; n=3 mice/group; p<0.05 vs control), suggestive of an increased microglial  
9 phagocytic phenotype. Whole cell area of microglial cells remained unchanged between groups  
10 (Fig. 4I; n=3 mice/group).

11 At the perivascular level, the number of CD68<sup>+</sup>Iba1<sup>-</sup> cells was significantly increased in the  
12 peri-infarct area of alcohol-exposed mice 24 hours after stroke onset (Fig. 4J; n=3 mice/group;  
13 p<0.05 vs control).

14 Vascular activation was exacerbated in alcohol-exposed mice after stroke (Fig. 4K-4P). The  
15 area of P-selectin in blood vessels was significantly increased in alcohol-exposed mice 24 hours  
16 after stroke onset (Fig. 4M; n=3 mice/group; p<0.05 vs control), although the number of P-  
17 selectin<sup>+</sup> blood vessels showed no changes between groups (Fig. 4L). Similarly, molecular MRI  
18 (Fig. 4N-4P) showed significantly increased hypo-signals corresponding to P-selectin-coupled  
19 MPIOs adhering to blood vessels in the ipsilateral cortex of alcohol-exposed mice 24 hours  
20 after stroke onset (Fig. 4P; n=5-6 mice/group; p<0.05 vs control), with no changes in the total  
21 number of P-selectin MPIO positive blood vessels (Fig. 4O).

22 Leukocyte adhesion (Fig. 4Q, Fig. 4R) and rolling (Fig. 4S, Fig. 4T) were both significantly  
23 increased in alcohol-exposed mice compared to control mice (+317% and +724% increase  
24 respectively; n=6 mice/group; p<0.05 vs control) 24 hours after stroke.

1 mRNA levels of IL1 $\beta$ , P-selectin and TNF were significantly increased in alcohol-exposed  
2 mice in the ipsilateral cortex 24 hours after stroke onset compared to control mice ( $p<0.05$ ,  $n=6$   
3 mice/group; Table 4).

1    **Discussion**

2    We have performed here a translational study to investigate the effects of chronic, excessive  
3    alcohol consumption on ischemic stroke outcome. Our clinical results show that heavy drinking  
4    ( $\geq 6$  drinks/day in the last 5 years) is independently associated (i) to early neurological  
5    deterioration (END, defined as the increase of NIHSS in  $\geq 4$  in the first 48 hours after  
6    admission), (ii) to stroke severity baseline, and (iii) to higher infarct volume in stroke patients.

7    The baseline characteristics of the study population, and outcomes at 3 months, were similar to  
8    those of large multicenter registries, suggesting good external validity of the results [6].

9    Our results show that the inflammatory response is associated with the risk of END in heavy  
10   drinking (HD) stroke patients. In order to elucidate the role of inflammation on the deleterious  
11   effect of heavy drinking after stroke, we performed pre-clinical experiments in mice exposed  
12   to 10% ethanol in drinking water during 6 weeks. Our pre-clinical findings show that chronic,  
13   excessive alcohol consumption by itself provokes a neurovascular inflammatory priming. The  
14   term “priming” is used to describe the propensity of a particular cell type to make an  
15   exaggerated response to a secondary stimulus [13] such as intracerebral or systemic LPS  
16   injection [5]. Microglial priming was first described in the ME7 model of prion disease [25] but  
17   has been replicated in other models of chronic neuroinflammatory pathologies including  
18   Alzheimer’s disease [30] and Parkinson’s disease [10].

19   To our knowledge, this is the first study defining a neurovascular inflammatory priming induced  
20   by chronic, excessive alcohol consumption. This alcohol-driven priming affects the brain  
21   parenchyma as well as the perivascular and vascular compartments. In the parenchyma, it is  
22   characterized by (i) an unconventional activation profile of microglial cells, in accordance with  
23   results described by Cruz et al. [3]; and (ii) an increase in the expression of TGF $\beta$  mRNA not  
24   accompanied by changes in pro-inflammatory cytokines, thus following a similar profile as in

1 priming-driving diseases such as prion disease [4]. At the brain perivascular compartment,  
2 alcohol provokes an increase in the number of perivascular macrophages (PVM). Finally, at the  
3 vascular level, alcohol-induced priming is characterized by increased levels of P-selectin at the  
4 endothelial surface, accompanied by an increase in the number of adherent and rolling  
5 leukocytes in the brain blood vessels.

6 We demonstrate here that alcohol provokes a brain inflammatory priming in mice by using two  
7 different approaches. First, we intracortically injected inert latex beads to control and alcohol-  
8 exposed mice. Eight hours after the injection, alcohol-exposed mice showed significantly more  
9 phagocytized beads than control mice, thus demonstrating that chronic alcohol exposure makes  
10 microglia more prone to phagocytosis. Second, we systemically injected a single dose of LPS  
11 to control and alcohol-exposed mice and studied the subsequent parenchymal, perivascular and  
12 vascular inflammatory responses 24 hours later. In accordance with our priming hypothesis,  
13 mice exposed to alcohol showed increased total microglial and activated microglial cell  
14 numbers, increased levels of P-selectin in the brain vasculature, characteristic of increased  
15 endothelial activation, as well as significantly increased rolling and adhering leukocyte  
16 numbers after the injection of LPS. Previous studies have reported that the exposure of  
17 C57BL/6 mice to 10 daily doses of ethanol followed by a LPS or Poly I:C challenge resulted in  
18 a sustained increase of proinflammatory cytokines in the brain compared with control-  
19 challenged animals [26, 27].

20 In accordance with our inflammatory priming hypothesis, our data show that inflammatory  
21 responses at the parenchymal, perivascular and vascular levels are exacerbated in alcohol-  
22 exposed mice also after stroke. More precisely, microglial numbers and phagocytic capacity,  
23 brain perivascular macrophages (PVM)/infiltrated macrophages numbers, P-selectin levels at  
24 the brain endothelium, as well as leukocyte rolling and adhesion to brain vasculature are all  
25 exacerbated in alcohol-exposed mice after stroke. Inflammatory responses participate in the

1 progression of ischemic lesions [15], but the causality or consequence relationship between the  
2 exacerbation of inflammatory responses and the increased lesion volume is difficult to  
3 determine. For this reason, our data on the inflammatory status prior to the ischemic injury are  
4 crucial and show that, even in the absence of stroke, heavy drinking alters the inflammatory  
5 status in both humans and mice. It has been proposed that inflammatory priming could have  
6 significant implications for acute sterile inflammatory insults such as stroke and traumatic brain  
7 injury occurring on a background of aging or neurodegeneration [13]. Our data show that  
8 chronic heavy drinking triggers a similar generalized heightened inflammatory sensitivity than  
9 in the aforementioned models of neurodegenerative diseases, and that alcohol-induced  
10 inflammatory priming has extremely deleterious consequences in stroke, not only in mice, but  
11 also in humans.

12 A potential limitation of this study is that we cannot exclude an impact of alcohol withdrawal  
13 on the outcome worsening of HD stroke patients and mice. Alcohol-withdrawn neurons are  
14 more sensitive to excitotoxic injuries (Rubio et al., 2009) characteristic of early phases of  
15 ischemic stroke. Indeed, we cannot exclude that this mechanism also participates to the  
16 aggravation of stroke lesions observed in our study, making the exacerbated inflammatory  
17 responses observed after stroke the consequence and not the cause of the aggravated stroke  
18 outcome. However, our preclinical data on intracortical latex beads-injected mice and on  
19 systemic LPS-injected mice, which were performed in mice not subjected to alcohol  
20 withdrawal, demonstrate that the exacerbated inflammatory response to both latex beads and  
21 acute LPS is present even in the absence of alcohol withdrawal. Other mechanisms that could  
22 contribute to the aggravation of stroke severity could be an endothelial dysfunction induced by  
23 chronic alcohol consumption (Sun et al., 2001 Am J Physiol Heart Circ Physiol// Mayhan et  
24 al., 1992 Am J Physiol), and further studies are needed to elucidate this issue.

1 Interestingly, our new data and the recently published data on the beneficial effect of low-dose  
2 alcohol consumption on inflammation following transient focal cerebral ischemia in rats [20]  
3 suggest that, similarly to the biphasic effects of alcohol on the risk of ischemic stroke [18],  
4 alcohol consumption also seems to have a biphasic effect on the consequences of ischemic  
5 stroke. These data thus help to better understand the apparently controversial clinical results  
6 found on the impact of alcohol consumption on stroke [7, 9].

7 In conclusion, we show that chronic, excessive alcohol consumption in both humans and mice  
8 provokes by itself a neurovascular inflammatory priming. We experimentally demonstrate that  
9 this priming leads to the exacerbation of the inflammatory responses after a secondary insult  
10 such as a systemic infection and stroke. These exacerbated inflammatory responses are  
11 associated to a worsened ischemic stroke outcome in both humans and mice. Our study opens  
12 new avenues for the study of strategies targeting the alcohol-induced inflammatory priming  
13 prior to any neurological insult, in order to prevent a worsened neurological outcome in heavy  
14 drinkers.

1    **Acknowledgements**

2    The authors are grateful to Dr Carine Ali and Dr Fabian Docagne for their valuable scientific  
3    suggestions, Dr Laurent Coulbaut for the analyses of human samples from the ALCOBRAIN  
4    cohort.

5    **Funding**

6    This study was funded by the Fondation pour la Recherche en Alcoologie (MR), the AXA  
7    Research Found (MR), INSERM, Caen-Normandy University, the Regional Council of  
8    Normandy, the ANR grant RHU MARVELOUS (ANR-16-RHUS-0009) (DV), ANR “Retour  
9    jeune chercheur” (ALP), the BALATON project (M. Rubio and A. Denes, #38601ZM).

10    **Author contributions**

- 11    -    Study design, coordination of the study: MR
- 12    -    Stroke model surgeries: MR
- 13    -    Histological and transcriptional analyses, *in vivo* functional analyses of microglial  
14    phagocytosis: AD
- 15    -    Molecular MRI: AD, AQ and EL
- 16    -    Two-photon microscopy: AD and MR
- 17    -    Analyses of immunohistochemical samples: AD and MN
- 18    -    Analyses of data from the ALCOBRAIN cohort of HD patients: AL and ALP
- 19    -    Analyses of data and writing of results from the stroke cohort of patients: FC and JC
- 20    -    Supervision of the study: DV
- 21    -    Manuscript writing: MR with the revision and approval of all authors

22    **Competing interests**

23    The authors declare no competing financial interests.

1      **References**

- 2      1. Alho H, Sillanaukee P, Kalela A, Jaakkola O, Laine S, Nikkari ST (2004) Alcohol  
3      Misuse Increases Serum Antibodies to Oxidizes LDL and C-Reactive Protein. *Alcohol*  
4      *Alcohol* 39:312–315. doi: 10.1093/alcalc/agh059
- 5      2. Beck AT, Steer RA (1987) BDI, Beck depression inventory: manual. Psychological  
6      Corp.; Harcourt Brace Jovanovich, San Antonio, Tex.; New York
- 7      3. Cruz SA, Hari A, Qin Z, Couture P, Huang H, Lagace DC, Stewart AFR, Chen H-H  
8      (2017) Loss of IRF2BP2 in Microglia Increases Inflammation and Functional Deficits  
9      after Focal Ischemic Brain Injury. *Frontiers in Cellular Neuroscience* 11:201. doi:  
10      10.3389/fncel.2017.00201
- 11      4. Cunningham C, Boche D, Perry VH (2002) Transforming growth factor  $\beta$ 1, the  
12      dominant cytokine in murine prion disease: influence on inflammatory cytokine  
13      synthesis and alteration of vascular extracellular matrix. *Neuropathology and Applied*  
14      *Neurobiology* 28:107–119. doi: 10.1046/j.1365-2990.2002.00383.x
- 15      5. Cunningham C, Wilcockson DC, Campion S, Lunnon K, Perry VH (2005) Central and  
16      Systemic Endotoxin Challenges Exacerbate the Local Inflammatory Response and  
17      Increase Neuronal Death during Chronic Neurodegeneration. *J Neurosci* 25:9275–9284.  
18      doi: 10.1523/JNEUROSCI.2614-05.2005
- 19      6. Dávalos A, Alvarez-Sabín J, Castillo J, Díez-Tejedor E, Ferro J, Martínez-Vila E, Serena  
20      J, Segura T, Cruz VT, Masjuan J, Cobo E, Secades JJ (2012) Citalopram in the treatment  
21      of acute ischaemic stroke: an international, randomised, multicentre, placebo-controlled  
22      study (ICTUS trial). *The Lancet* 380:349–357. doi: 10.1016/S0140-6736(12)60813-7
- 23      7. Ducroquet A, Leys D, Saabi AA, Richard F, Cordonnier C, Girot M, Deplanque D,  
24      Casolla B, Allorge D, Bordet R (2013) Influence of Chronic Ethanol Consumption on  
25      the Neurological Severity in Patients With Acute Cerebral Ischemia. *Stroke* 44:2324–  
26      2326. doi: 10.1161/STROKEAHA.113.001355
- 27      8. Gache P, Michaud P, Landry U, Accietto C, Arfaoui S, Wenger O, Daepen J-B (2005)  
28      The Alcohol Use Disorders Identification Test (AUDIT) as a screening tool for  
29      excessive drinking in primary care: reliability and validity of a French version. *Alcohol*  
30      *Clin Exp Res* 29:2001–2007
- 31      9. Gattringer T, Enzinger C, Fischer R, Seyfang L, Niederkorn K, Khalil M, Ferrari J, Lang  
32      W, Brainin M, Willeit J, Fazekas F (2015) IV thrombolysis in patients with ischemic  
33      stroke and alcohol abuse. *Neurology* 85:1592. doi: 10.1212/WNL.0000000000002078
- 34      10. Godoy MCP, Tarelli R, Ferrari CC, Sarchi MI, Pitossi FJ (2008) Central and systemic  
35      IL-1 exacerbates neurodegeneration and motor symptoms in a model of Parkinson's  
36      disease. *Brain* 131:1880–1894. doi: 10.1093/brain/awn101
- 37      11. He J, Crews FT (2008) Increased MCP-1 and Microglia in Various Regions of the  
38      Human Alcoholic Brain. *Exp Neurol* 210:349–358. doi:  
39      10.1016/j.expneurol.2007.11.017

- 1       12. Heatherton TF, Kozlowski LT, Frecker RC, Fagerström KO (1991) The Fagerström Test  
2       for Nicotine Dependence: a revision of the Fagerström Tolerance Questionnaire. *Br J*  
3       Addict
- 4       13. Hennessy E, Griffin ÉW, Cunningham C (2015) Astrocytes Are Primed by Chronic  
5       Neurodegeneration to Produce Exaggerated Chemokine and Cell Infiltration Responses  
6       to Acute Stimulation with the Cytokines IL-1 $\beta$  and TNF- $\alpha$ . *J Neurosci* 35:8411–8422.  
7       doi: 10.1523/JNEUROSCI.2745-14.2015
- 8       14. Hughes MM, Field RH, Perry VH, Murray CL, Cunningham C (2010) Microglia in the  
9       degenerating brain are capable of phagocytosis of beads and of apoptotic cells, but do  
10      not efficiently remove PrPSc, even upon LPS stimulation. *Glia* 58:2017–2030. doi:  
11      10.1002/glia.21070
- 12      15. Iadecola C, Anrather J (2011) The immunology of stroke: from mechanisms to  
13      translation. *Nat Med* 17:796–808. doi: 10.1038/nm.2399
- 14      16. Imhof A, Froehlich M, Brenner H, Boeing H, Pepys MB, Koenig W (2001) Effect of  
15      alcohol consumption on systemic markers of inflammation. *The Lancet* 357:763–767.  
16      doi: 10.1016/S0140-6736(00)04170-2
- 17      17. Kadlecová P, Andel R, Mikulík R, Handing EP, Pedersen NL (2015) Alcohol  
18      Consumption at Midlife and Risk of Stroke During 43 Years of Follow-Up: Cohort and  
19      Twin Analyses. *Stroke* 46:627–633. doi: 10.1161/STROKEAHA.114.006724
- 20      18. Larsson SC, Wallin A, Wolk A, Markus HS (2016) Differing association of alcohol  
21      consumption with different stroke types: a systematic review and meta-analysis. *BMC*  
22      Medicine 14:178. doi: 10.1186/s12916-016-0721-4
- 23      19. Lemarchand E, Gauberti M, Lizarondo SM de, Villain H, Repessé Y, Montagne A,  
24      Vivien D, Ali C, Rubio M (2015) Impact of Alcohol Consumption on the Outcome of  
25      Ischemic Stroke and Thrombolysis: Role of the Hepatic Clearance of Tissue-Type  
26      Plasminogen Activator. *Stroke* 46:1641–1650. doi: 10.1161/STROKEAHA.114.007143
- 27      20. McCarter KD, Li C, Jiang Z, Lu W, Smith HC, Xu G, Mayhan WG, Sun H (2017) Effect  
28      of Low-Dose Alcohol Consumption on Inflammation Following Transient Focal  
29      Cerebral Ischemia in Rats. *Scientific Reports* 7:12547. doi: 10.1038/s41598-017-12720-  
30      w
- 31      21. Montagne A, Gauberti M, Macrez R, Jullienne A, Briens A, Raynaud J-S, Louin G,  
32      Buisson A, Haelewyn B, Docagne F, Defer G, Vivien D, Maubert E (2012) Ultra-  
33      sensitive molecular MRI of cerebrovascular cell activation enables early detection of  
34      chronic central nervous system disorders. *NeuroImage* 63:760–770. doi:  
35      10.1016/j.neuroimage.2012.07.018
- 36      22. Orset C, Haelewyn B, Allan SM, Ansar S, Campos F, Cho TH, Durand A, El Amki M,  
37      Fatar M, Garcia-Yébenes I, Gauberti M, Grudzenski S, Lizasoain I, Lo E, Macrez R,  
38      Margail I, Maysami S, Meairs S, Nighoghossian N, Orbe J, Paramo JA, Pariente J-J,  
39      Rothwell NJ, Rubio M, Waeber C, Young AR, Touzé E, Vivien D (2016) Efficacy of  
40      Alteplase® in a mouse model of acute ischemic stroke: a retrospective pooled analysis.  
41      *Stroke* 47:1312–1318. doi: 10.1161/STROKEAHA.116.012238

- 1       23. Orset C, Macrez R, Young AR, Panthou D, Angles-Cano E, Maubert E, Agin V, Vivien  
2           D (2007) Mouse Model of In Situ Thromboembolic Stroke and Reperfusion. *Stroke*  
3           38:2771–2778. doi: 10.1161/STROKEAHA.107.487520
- 4       24. Perego C, Fumagalli S, De Simoni M-G (2011) Temporal pattern of expression and  
5           colocalization of microglia/macrophage phenotype markers following brain ischemic  
6           injury in mice. *J Neuroinflammation* 8:174. doi: 10.1186/1742-2094-8-174
- 7       25. Perry VH, Cunningham C, Boche D (2002) Atypical inflammation in the central nervous  
8           system in prion disease. *Curr Opin Neurol* 15:349–354
- 9       26. Qin L, Crews FT (2012) Chronic ethanol increases systemic TLR3 agonist-induced  
10           neuroinflammation and neurodegeneration. *J Neuroinflammation* 9:130. doi:  
11           10.1186/1742-2094-9-130
- 12       27. Qin L, He J, Hanes RN, Pluzarev O, Hong J-S, Crews FT (2008) Increased systemic and  
13           brain cytokine production and neuroinflammation by endotoxin following ethanol  
14           treatment. *Journal of Neuroinflammation* 5:10. doi: 10.1186/1742-2094-5-10
- 15       28. Quenault A, Martinez de Lizarrondo S, Etard O, Gauberti M, Orset C, Haelewyn B,  
16           Segal HC, Rothwell PM, Vivien D, Touzé E, Ali C (2017) Molecular magnetic  
17           resonance imaging discloses endothelial activation after transient ischaemic attack. *Brain*  
18           140:146–157. doi: 10.1093/brain/aww260
- 19       29. Rehm J, Marmet S, Anderson P, Gual A, Kraus L, Nutt DJ, Room R, Samokhvalov AV,  
20           Scafato E, Trapencieris M, Wiers RW, Gmel G (2013) Defining Substance Use  
21           Disorders: Do We Really Need More Than Heavy Use? *Alcohol Alcohol* 48:633–640.  
22           doi: 10.1093/alcalc/agt127
- 23       30. Sly LM, Krzesicki RF, Brashler JR, Buhl AE, McKinley DD, Carter DB, Chin JE (2001)  
24           Endogenous brain cytokine mRNA and inflammatory responses to lipopolysaccharide  
25           are elevated in the Tg2576 transgenic mouse model of Alzheimer's disease. *Brain*  
26           Research Bulletin 56:581–588. doi: 10.1016/S0361-9230(01)00730-4
- 27       31. Spielberger CD (1983) Manual for the State-Trait Anxiety Inventory STAI (Form Y)  
28           ("self evaluation questionnaire). Consulting Psychologists Press
- 29       32. Zhao H, Mayhan WG, Arrick DM, Xiong W, Sun H (2011) Dose-Related Influence of  
30           Chronic Alcohol Consumption on Cerebral Ischemia/Reperfusion Injury. *Alcohol Clin*  
31           Exp Res 35:1265–1269. doi: 10.1111/j.1530-0277.2011.01461.x
- 32
- 33

1    **Figure legends**

2    **Fig 1. Heavy drinking (HD) aggravates ischemic stroke baseline severity and outcome,**  
3    **and increases early neurological deterioration (END) risk. Inflammatory markers are**  
4    **independently associated to the alcohol-induced increased risk of END.** A) Representation  
5    of neurological stroke severity determined by the National Institute of Health Stroke Scale  
6    (NIHSS) at admission, 24 and 48 hours in stroke patients with and without heavy drinking  
7    habits. Early neurological deterioration (END) is defined as an increase of NIHSS in  $\geq 4$  points  
8    in the first 48 hours after admission. B) Forest plot of the multivariate analysis including  
9    variables predicting END such as hemorrhagic transformation, infarct volume, NIHSS on  
10   admission and heavy drinking habits (Model A). C) Forest plot of the multivariate analysis of  
11   the variables included in the Model A and inflammatory biomarkers (axillary temperature,  
12   number of leukocytes levels and C-reactive protein levels) (Model B).

13   **Fig 2. Alcohol exposure provokes a neurovascular priming affecting microglia,**  
14   **perivascular macrophages (PVM) numbers and brain endothelium in mice.** (A)  
15   Representative photomicrographs of microglial cells stained with Iba1 and CD68. Scale bar:  
16   100 $\mu$ m. (B) High magnification- representative photomicrographs of microglial cells in control  
17   and alcohol-exposed mice. (C) Quantification of Iba1 and CD68 double-positive cells. (D)  
18   Quantification of CD68 area on Iba1<sup>+</sup> microglial cells. (E) Quantification of Iba1<sup>+</sup> cells. (F)  
19   Quantification of the number of processes starting from the soma. (G) Quantification of the area  
20   of microglial cells. (H) Schema of the *in vivo* test of microglial phagocytic capacity: 1  $\mu$ l of  
21   latex beads were injected in the cortex of control and alcohol-exposed mice. Eight hours after,  
22   phagocytosed latex beads were quantified by immunohistochemical analyses. (I)  
23   Representative photomicrographs of Iba1<sup>+</sup> microglial cells and latex beads. (J) Detail of a latex  
24   bead phagocytosed by a microglial cell in an alcohol-exposed mouse. Note the lysosomal  
25   activation (CD68, red) at the apex of microglial process. (K) Quantification of phagocytosed

1 latex beads/total number of beads. N=4 mice per group, \*p<0.05 vs Control, Mann-Whitney  
2 test. Scale bar: 20 $\mu$ m. (L) Representative photomicrographs of CD68<sup>+</sup>Iba1<sup>-</sup> cells (arrows)  
3 surrounding blood vessels (dotted lines), corresponding to perivascular macrophages (PVM).  
4 Scale bar: 100 $\mu$ m. (M) PVM are also positive for the marker CD206. Representative  
5 photomicrographs of brain CD206<sup>+</sup>Iba1<sup>-</sup> (arrows) cells. Scale bar: 20 $\mu$ m. (N) Quantification of  
6 CD68<sup>+</sup>Iba1<sup>-</sup> and CD206<sup>+</sup>Iba1<sup>-</sup> cells (N=4 mice per group, p<0.05 vs control, Mann-Whitney  
7 test). (O) Higher magnification of a PVM located between the endothelium (Coll-IV) and an  
8 astrocytic endfeet (AQP4). Scale bar: 20 $\mu$ m. (P) 3D reconstruction of the blood vessel selected  
9 in O. Scale bar: 10 $\mu$ m. (Q) Detail of a blood vessel with a PVM. (R) Detail of a PVM on the  
10 wall of a blood vessel. Scale bar: 10 $\mu$ m. (S) Representative photomicrographs of P-selectin  
11 positive vessels in control and alcohol-exposed mice (note the absence of positive staining in  
12 control mice). Dotted lines represent the lumen (L) of the blood vessel. Scale bar: 20 $\mu$ m. (T)  
13 Quantification of P-selectin signal in the brain cortex of control and alcohol-exposed mice. (U)  
14 Compilation of *in vivo* time-lapse images obtained by two-photon microscopy showing  
15 Rhodamine 6G (R6G)<sup>+</sup> leukocyte adhesion (arrows) in control and alcohol-exposed mice. Scale  
16 bar: 50 $\mu$ m. (V) Quantification of adherent leukocytes. (W) Representative time-lapse images  
17 of leukocyte rolling (green circles). Scale bar: 50 $\mu$ m. (X) Quantification of rolling leukocytes  
18 per second.

19 **Fig. 3: Alcohol exposure exacerbates brain neurovascular inflammatory reactions after**  
20 **an acute systemic insult in mice.** (A) Representative photomicrographs of the brain cortex of  
21 control and alcohol-exposed mice 24 hours after the acute systemic injection of LPS. Scale bar:  
22 100 $\mu$ m. (B) Quantification of total microglia (Iba1<sup>+</sup> cells). (C) Quantification of activated  
23 microglia (Iba1<sup>+</sup>/CD68<sup>+</sup> cells). Scale bar: 100 $\mu$ m. (D) Quantification of PVM (CD68<sup>+</sup>Iba1<sup>-</sup>  
24 cells). (E) Representative photomicrographs of P-selectin staining. (F) Quantification of the  
25 number of P-selectin<sup>+</sup> blood vessels. (G) Representative T2\*-weighted images showing P-

1 selectin-coupled MPIO *in vivo* accumulation in the brain of control and alcohol-exposed mice  
2 after the acute injection of LPS. (H) Quantification of MPIO<sup>+</sup> blood vessels. (I) Compilation of  
3 time-lapse images showing representative *in vivo* leukocyte adhesion (arrows) obtained by two-  
4 photon microscopy. Scale bar: 50μm. (J) Quantification of leukocyte adhesion. (K)  
5 Representative time-lapse images of *in vivo* leukocyte rolling (see also Movies S1 and S2).  
6 Scale bar: 50μm. (L) Quantification of rolling leukocytes per second.

7 **Fig. 4. Alcohol exposure increases lesion volume and inflammatory responses after**  
8 **ischemic stroke in mice.** (A) Representative brain lesions and (B) corresponding  
9 quantifications in control and alcohol-exposed mice 24 hours after stroke onset (n=7-8  
10 mice/group). (C) Representative photomicrographs of microglial cells and infiltrated  
11 macrophages in the ipsilateral cortex 24 hours after stroke onset. Scale bar: 100μm. n=4  
12 mice/group. (D) High magnification- photomicrographs of microglial cells. Scale bar: 20μm.  
13 (E) Quantification of microglial cells (Iba1<sup>+</sup>) (F) Quantification of CD68<sup>+</sup> microglial cells  
14 (Iba1<sup>+</sup>/CD68<sup>+</sup>). (G) Quantification of CD68 area in microglial cells. (H) Quantification of the  
15 number of processes starting from the soma. (I) Quantification of the mean whole cell area of  
16 microglial cells. (J) Quantification of CD68<sup>+</sup>Iba1<sup>-</sup> cells. (K) Representative photomicrographs  
17 of P-selectin immunostaining. Scale bar: 50μm. (L) Quantification of the number of P-selectin<sup>+</sup>  
18 vessels. (M) Quantification of P-selectin<sup>+</sup> immunostaining area. (N) Representative T2\*-  
19 weighted images of *in vivo* P-selectin molecular imaging. Arrows show MPIO<sup>+</sup> blood vessels  
20 (N=5-6 mice/group). (O) Quantification of MPIO<sup>+</sup> blood vessels. (P) Quantification of MPIO<sup>+</sup>  
21 signal. (Q) Compilation of representative time-lapse images showing *in vivo* leukocyte  
22 adhesion (arrows) obtained by two-photon microscopy. Scale bar: 50μm. (R) Quantification of  
23 leukocyte adhesion. (S) Representative time-lapse images of *in vivo* leukocyte rolling. Scale  
24 bar: 50μm. (T) Quantification of leukocyte rolling (see also Movies S3 and S4). n=4  
25 mice/group. \*p<0.05 vs control.

**Table 2: Univariate analysis of stroke patients with and without early neurological deterioration (END).**

Early neurological deterioration			
	No	Yes	
	n = 3146	n = 206	
Age (years)	72.1 ± 13.4	73.8 ± 11.9	0.977
Men (%)	54.7	59.2	0.219
History of hypertension (%)	62.8	62.6	0.509
History of diabetes (%)	24.5	23.3	0.384
History of smoking (%)	17.4	20.2	0.193
History of dyslipemia (%)	33.8	35.4	0.339
History of ischemic heart disease (%)	11.3	14.1	0.135
Axillary temperature at admission (°C)	36.3 ± 0.6	36.4 ± 0.8	0.005
Leukocytes on admission ( $\times 10^3/\text{mL}$ )	8.9 ± 3.3	10.4 ± 4.2	0.019
Fibrinogen on admission (mg/dL)	426.7 ± 102.8	422.8 ± 120.5	0.255
C-reactive protein on admission (mg/L)	3.2 ± 4.3	4.6 ± 4.9	< 0.0001
Sedimentation rate (mm)	27.7 ± 25.6	28.5 ± 26.1	0.695
tPA treatment (%)	23.5	22.3	0.389
Trombectomy (%)	2.7	3.9	0.210
Hemorrhagic transformation (%)	9.4	17.1	< 0.0001

Infarct volume (mL)	$50.3 \pm 77.1$	$107.7 \pm 107.8$	< 0.0001
NIHSS at admission	12 [7,17]	13 [8,15]	0.017
mRS at 3 months	3 [1,4]	5 [3,6]	< 0.0001
Poor outcome at 3 months (%)	51.0	81.2	< 0.0001
TOAST			0.613
Atherothrombotic (%)	24.3	25.2	
Cardioembolic (%)	35.8	38.3	
Small vessel disease (%)	7.2	4.4	
Indeterminate (%)	31.6	31.1	
Others (%)	1.1	1.0	
Heavy drinking (%)	10.2	36.9	< 0.0001

**Table 3. Heavy drinkers have higher levels of inflammatory markers, in the absence of any other injury.**

Demographic and clinical characteristics, leukocyte cell counting and C-reactive Protein (CRP) levels in an independent cohort of healthy control participants and heavy drinkers recruited in the Addiction Unit of the University Hospital of Caen (Normandy, France) while they were receiving withdrawal treatment as inpatients. Data are expressed as mean+/-Standard Deviation; parenthesis data correspond to interval.

	<b>Control subjects</b>	<b>Heavy drinkers</b>	<b>P</b>
	<b>n=21</b>	<b>n=34</b>	
Age	43.8 ± 7.4 (29-55)	45.7 ± 9.2 (33-66)	0.29
Women/Men Ratio	5/21	9/34	0.83
BMI (*2 missing data)	25.3 ± 4.4* (19.5-35.5)	23.9 ± 4.4 (17.3-39.8)	0.32
AUDIT	2.9 ± 1.6 (0-6)	28.9 ± 7.7 (4-40)	<0.001
Leucocytes (g/L)	6.4 ± 1.7 (3.7-9.7)	7.0 ± 2.1 (3.5-12.3)	0.24
Neutrophils (g/L)	3.6 ± 1.4 (1.7-7.2)	4.1 ± 1.7 (1.7-8.6)	0.28
Eosinophils (g/L)	0.17 ± 0.08 (0.04-0.31)	0.18 ± 0.13 (0-0.53)	0.80
Basophils (g/L)	0.03 ± 0.02 (0.01-0.07)	0.04 ± 0.02 (0.01-0.1)	0.09
Lymphocytes (g/L)	1.95 ± 0.72 (1.03-3.85)	1.93 ± 0.75 (0.93-3.88)	0.96
Monocytes (g/L)	0.52 ± 0.17 (0.27-0.99)	0.73 ± 0.27 (0.11-1.42)	0.003

---

C Reactive protein >3 mg/L 61.8% (21/34)

---

BMI, Body Mass Index; AUDIT, Alcohol Use Disorders Identification Test.

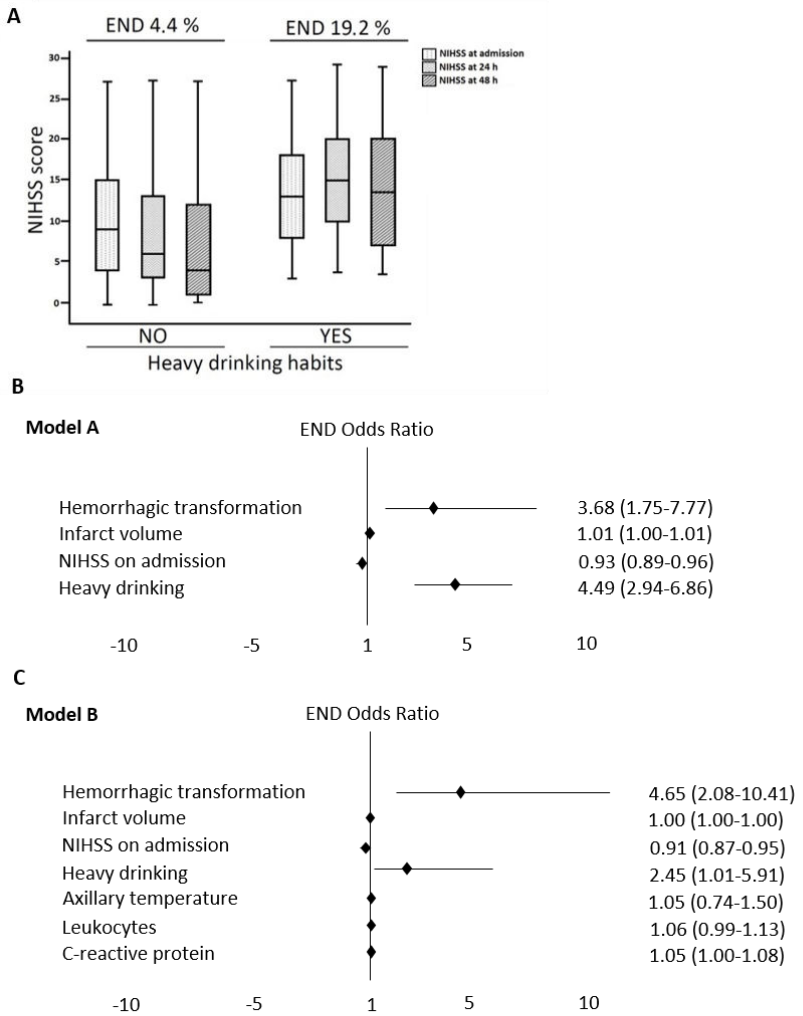


Figure 1

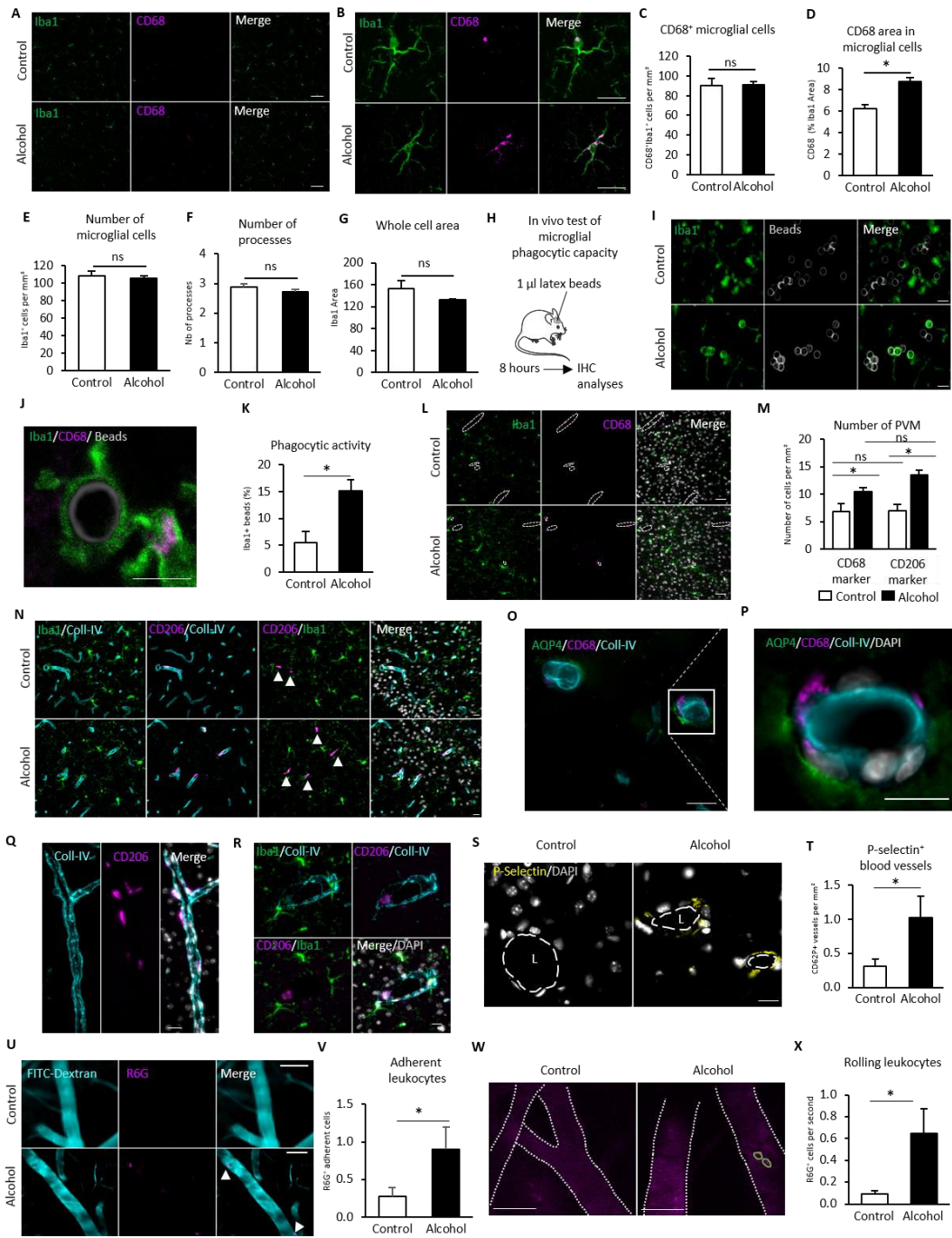


Figure 2

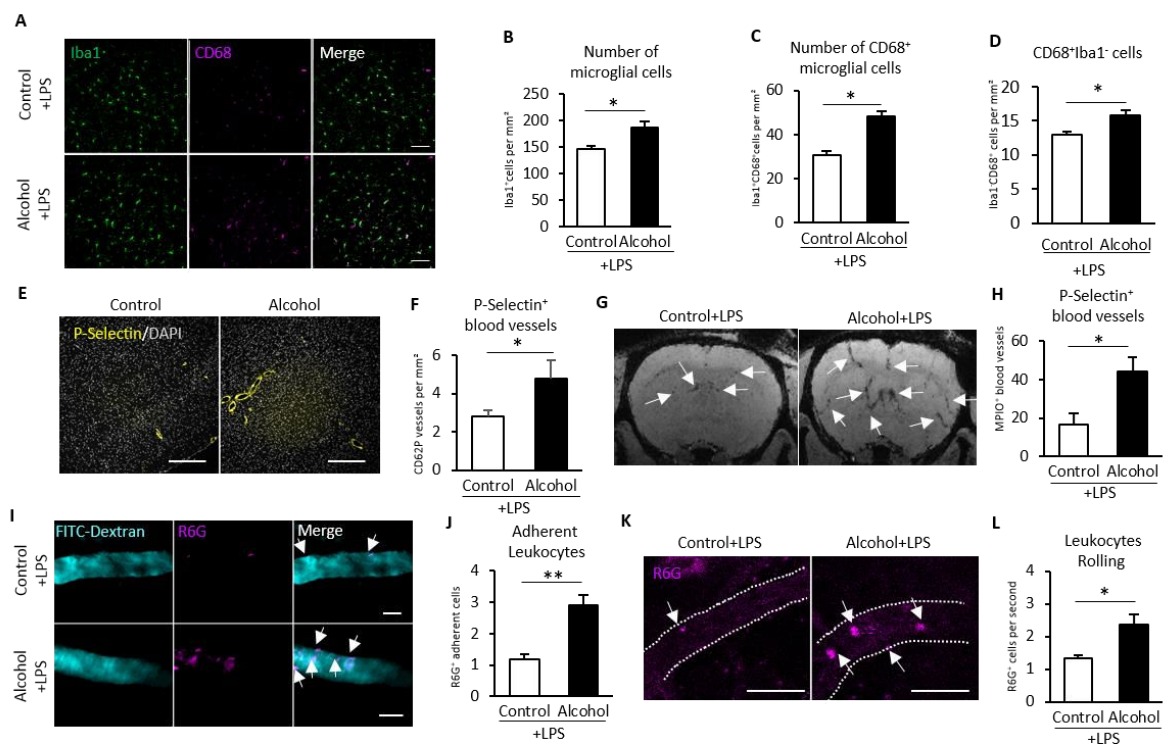


Figure 3

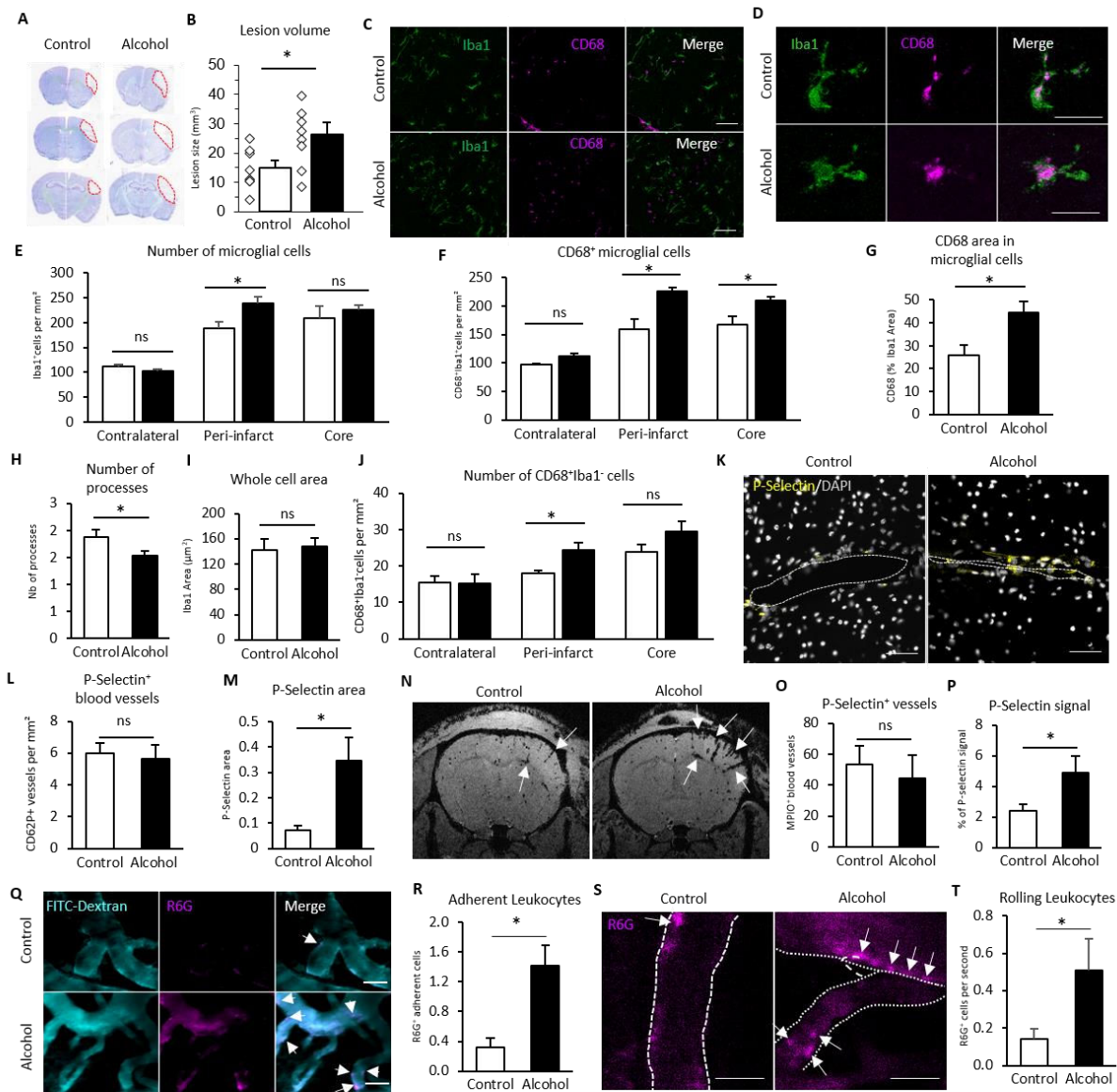
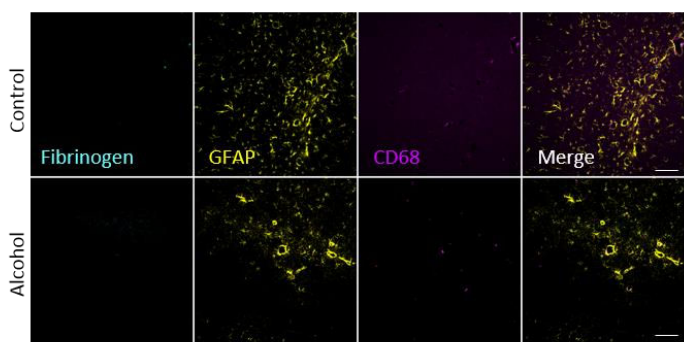
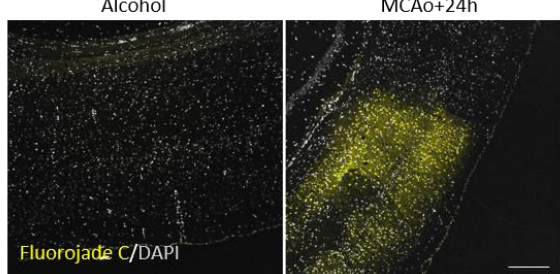


Figure 4

**A**



**B**



Supplementary Figure 1

## 4. Study 4: Perivascular macrophages mediate the aggravating effect of inflammatory priming on ischemic stroke

We have demonstrated in the previous study that chronic alcohol exposure induces, in mice, a neurovascular inflammatory priming (i) associated to more severe ischemic lesions and (ii) responsible of the exacerbation of the inflammatory responses after stroke. **This alcohol-induced inflammatory priming includes a dramatic increase of brain perivascular macrophages (PVM).** Because of the strategic location of PVM between the brain parenchyma and the cerebral blood vessels, in this study **we have studied the role of PVM on ischemic stroke outcome in naïve and primed (alcohol-exposed) mice.**

To do this, we have selectively depleted PVMs by intraventricularly injecting liposomes containing clodronate, a pro-apoptotic substance. This method has already been used in the context of multiple sclerosis (Polfliet et al., 2002), Alzheimer's disease (Park et al., 2017), chronic hypertension (Faraco et al., 2016), and recently stroke (Pedragosa et al., 2018). **Our study i) confirms that PVMs do not influence the ischemic lesion volume in naïve mice as in the study by Pedragosa et al. (2018), but (ii) shows that PVM do influence lesion volume in primed mice: the aggravating effect of chronic alcohol exposure is prevented in PVM-depleted mice. This study is still ongoing: future studies on naïve and primed mice are planned to better understand (i) if and how PVM can influence inflammatory responses from surrounding cells (notably microglia and endothelial cells), and (ii) the influence of PVM phenotype on secondary inflammatory responses.**



# **Perivascular macrophages mediate the aggravating effect of inflammatory priming on ischemic stroke**

## **Introduction**

Two subgroups of myeloid cells reside in the central nervous system (CNS): microglial cells and border-associated macrophages (BAMs). Among BAMs, three populations can be distinguished: (i) choroid plexus macrophages (cpM), located in the choroid plexus; (ii) meningeal macrophages (mM), located in the lateral ventricles and meninges (Goldmann et al., 2016); and (iii) perivascular macrophages (PVM), that surround large brain blood vessels and are located at the perivascular space (Goldmann et al., 2016; He et al., 2016). In physiological conditions, BAMs have scavenger functions, revealing a role of clearing debris from the CNS (Kida et al., 1993; Mendes-Jorge et al., 2009) and can also present antigens to lymphocytes (Fabriek et al., 2005). However, their roles in pathological conditions are less known. In the CNS, PVM were identified as modulators of neurovascular coupling in models of chronic hypertension (Faraco et al., 2016), and Alzheimer disease (Park et al., 2017). It has been demonstrated that PVM can produce reactive oxygen species and cytokines, linking them to the inflammatory response (Faraco et al., 2016). Outside the CNS, PVM mediate leukocyte recruitment in the case of skin infection (Abtin et al., 2014).

Stroke is the leading cause of permanent disability and the second cause of death worldwide. In the past few years, much attention has focused on the immune response to stroke. Key inflammatory processes after stroke include the activation of resident glial cells as well as the invasion of circulating leukocytes, but the role of PVM on stroke outcome has been barely studied. A recent study has shown a role of BAMs on granulocyte infiltration and blood-brain barrier integrity after stroke (Pedragosa et al., 2018).

Ninety percent of strokes are caused by ten potentially modifiable risk factors, such as chronic arterial hypertension, diabetes, or heavy drinking (O'Donnell et al., 2010). However, the stroke-induced inflammatory responses (including BAMs role in stroke) have been principally studied in young, healthy animals. In the **study n°3** we have experimentally showed that chronic alcohol exposure induces a neurovascular inflammatory priming which provokes the aggravation of

ischemic lesions and the exacerbation of inflammatory responses to stroke. This alcohol-induced inflammatory priming includes a marked increase of PVM numbers. Thus, the goal of this **4th study** was to investigate the role of PVM on stroke outcome in naïve mice and primed mice (chronically exposed to alcohol).

## **Material and methods**

### **Animals**

Two months-old male Swiss mice (35-45g) (Centre Universitaire de Ressources Biologiques, Normandy University, Caen, France) were housed at 21° C in a 12 h light/dark cycle with food and water (naive group) *ad libitum*. Another group of mice was forced to drink 10% (v/v) alcohol solution (primed group) with free access for 6 weeks. All mice were checked daily for fluid consumption, health and abnormal behavior. For intravital two-photon imaging, male C57/BL6J CX3CR1-GFP<sup>+/−</sup> mice were used.

All the procedures needing anesthesia were performed by an initial exposure to 5% isoflurane followed by a maintaining phase of 1.5-2% isoflurane 30%O<sub>2</sub>/70%N<sub>2</sub>O during experiments.

### **Depletion of perivascular macrophages (PVM)**

Anesthetized mice were placed in a stereotaxic device. Then the skin was removed and a small craniotomy was performed (coordinates: -0.2mm anteroposterior; +1mm lateral; -2mm depth from the Bregma). A glass micropipette containing 10µl PBS-liposomes (PBS group) or clodronate (a pro-apoptotic drug)-encapsulated liposomes (CLO group) was inserted and the product was gently injected in the left lateral ventricle during 20 minutes.

### **PVM labelling**

Three days after the injection of liposomes, a glass micropipette was inserted at the aforementioned coordinates and 3µl of TRITC-Dextran (4.400 kDa, Sigma Aldrich, France) were gently injected.

### **Thromboembolic stroke**

We used the *in situ* thromboembolic stroke model consisting in the injection of thrombin directly into the middle cerebral artery as described before (Orset et al., 2007, 2016, **study n°1**). Briefly, anesthetized mice were placed in a stereotaxic device, a small craniotomy was performed, the dura was excised, and the middle cerebral artery (MCA) was exposed. A pulled glass micropipette was introduced into the lumen of the MCA and 1 µL (1 UI/µl for Swiss mice or 1.5 UI/µl for C57/BL6J CX3CR1-GFP<sup>+/−</sup> mice) of purified murine alpha-thrombin (Enzyme Research Labs, USA) was pneumatically injected to induce MCA occlusion (MCAo) by the *in situ* formation of a clot. Lesion

volumes were quantified by Magnetic Resonance Imaging (MRI) on Image J software 24 hours after stroke onset.

### **Intravital two-photon microscopy**

Anesthetized mice were placed in a stereotaxic device and an aqueous medium was deposited between the thin-skull window and the X25 immersive objective. All the acquisitions were performed using a Leica TCS SP5 MP microscope (Coherent Chameleon, USA). A first acquisition at 840 nm two-photon excitation wavelength was made two days after PBS/CLO-containing liposomes to check (i) PVM depletion and (ii) GFP signal detection emitted by microglial cells (n=6 mice per group). Noise fluorescence is present in the meninges and interfere with specific fluorescence from PVM and microglia. For this reason, we acquired images only from submeningeal regions and voluntarily avoided any fluorescent signal coming from the meninges.

A second acquisition at 840 $\mu$ m was performed after the intravenous injection of 100  $\mu$ l of Rhodamine 6G (1mg/kg) and 100  $\mu$ l of 70kDa FITC-Dextran (5mg/ml) (Sigma Aldrich, France) to stain circulating leukocytes and visualize the lumen of blood vessels, respectively (n= 5-6 mice per group). Leukocyte adhesion and rolling were measured with time-lapse acquisitions (2 minutes, 7.7 frames per second, 256x256 pixel resolution, 1000Hz frequency). Photomultiplier (PMT) 2 (recorded capacity: 500-550nm; gain 850V; offset 0) and PMT3 (recorded capacity: 565-605nm; gain 850V; offset 0) were used. The pulsing laser characteristics were: gain 23%; trans 17%; offset 50%.

The quantification of leukocyte rolling and adhesion was performed using the Kymograph plugin. Briefly, a stack image was obtained by 2-photon videos, and adherent leukocytes were counted as spots located onto blood vessel wall. For rolling leukocytes, the video was uploaded then a line (arbitrary units: 10 thickness) was placed perpendicularly to the vessels. The Kymograph detected the number of leukocytes passing through the line the time of video duration (2mins). Circulating leukocytes that were too fast were considered as background and were not counted.

### **Magnetic Resonance Imaging**

T2-weighted images were acquired in anesthetized mice 24 hours after MCAo using a multislice multiecho sequence (TE/TR 33 ms/2500 ms) on a Pharmascan 7T (Bruker, Germany) (n= 4-7 mice

per group). Lesion sizes were quantified on these images using ImageJ software. T2\*-weighted sequences were used to detect hemorrhagic events (TE/TR 8.7064ms/500ms).

### **Molecular Imaging of P-Selectin**

Micro-sized particles of iron oxide (MPIOs) (diameter 1.08 mm) (Invitrogen) covalently conjugated to purified polyclonal goat anti-mouse antibodies for P-selectin (R&D Systems, clone AF737) were prepared as previously described. The quality of conjugated MPIOs was systematically checked in a naive mouse, by stereotaxic injection of lipopolysaccharide (1 $\mu$ l, 1mg/kg) in the striatum (0.5mm anterior, 2.0mm lateral, -3mm ventral to the Bregma).

Three-dimensional T2\*- weighted gradient echo imaging with flow compensation (spatial resolution of 70 mm x 70 mm x 70 mm interpolated to an isotropic resolution of 70 mm), TE/TR 13.2ms/200 ms and a flip angle of 21° was performed to visualize MPIOs. MRI acquisitions started immediately after the intravenous injection of MPIOs (200  $\mu$ l of 2 mg Fe/kg of conjugated MPIOs). All T2\*-weighted images presented are minimum intensity projections of six consecutive slices. The signal void quantification of MPIOs on 3D T2\*-weighted images was measured by using automatic triangle threshold in ImageJ software and results presented as MPIOs-induced signal void on the contralateral cortex divided by the signal void on the structure of interest (in percent) (n= 4-7 mice per group).

### **Isolated brain vessels**

Terminally anesthetized mice were transcardially perfused with cold heparinized saline (15 mL/min). Brain were then dissociated in a solution of HEPES and HBSS and then centrifuged at 2000g at 4°C during 10 min. Most of myelin is eliminated at this step, and vessels form a pellet. The pellet was then suspended in a solution of HEPES/HBSS and Dextran (Dextran from Leuconostoc spp. Mr ~70,000 kDa, Sigma-Aldrich) and centrifuged at 4400g at 4°C during 15 min. Remaining myelin is eliminated here. Vessels were then suspended in a solution of HEPES/HBSS and BSA 1% and filtrated on a 20 $\mu$ m mesh filter. After that, vessels stay on the filter. Vessels were then detached from the filter in a PBS solution. Vessels were then put on a poly-lysine coated slides, cryoprotected overnight in a 20% sucrose PBS solution and fixated during 15 min with PBS 0.1 M. pH 7.4 containing 2% paraformaldehyde and 0.2% picric acid. Slide were stored at -80°C before processing.

## **Immunohistochemistry**

Terminally anesthetized mice were transcardially perfused with cold heparinized saline (15 mL/min) and fixed with 100 mL of 2% paraformaldehyde and 0.2% picric acid phosphate buffer (pH 7.4) (n=4 mice/group). Brains were post-fixed with 2% paraformaldehyde and 0.2% picric acid phosphate buffer (18 hours; 4°C) and cryoprotected (sucrose 20% in PBS; 24 hours; 4°C) before freezing in Tissue-Tek (Miles Scientific, Naperville, IL, USA). Cryostat-cut sections (10 µm) were collected on poly-lysine slides and stored at – 80°C before processing.

Sections were co-incubated overnight with rabbit anti-mouse Iba1 (1:1000, Wako 019-19741), rat anti-mouse CD68 (1:800, Abcam 53444), rat anti-mouse CD206 (1:200, Serotec, clone MR5D3), goat anti-mouse P-selectin (1:1000, RD System AF737), goat anti-mouse Collagen-IV (1:1000, SouthernBiotech 1340), rabbit anti-mouse Aquaporin 4 (sc 20812, Santa Cruz), rabbit anti-mouse Laminin (1:1500, Abcam 11575), rat anti-mouse VCAM-1 (1:1000, 553330, BP Pharmingen), and rabbit anti-mouse neutrophil elastase (1:500, Abcam 21595). Primary antibodies were revealed by using Fab'2 fragments of Donkey anti-rabbit linked to FITC, anti-rat linked to Cy3, anti-goat IgG linked to Cy5 (1:600, Jackson ImmunoResearch, West Grove, USA). Washed sections were coverslipped with antifade medium containing DAPI. Epifluorescence images were digitally captured using a Leica DM6000 epifluorescence microscope-coupled coolsnap camera, visualized with Leica MM AF 2.2.0 software (Molecular Devices, USA) and further processed using ImageJ 1.52k software.

## **Statistical analyses**

Results are the mean ± SEM. Statistical analyses were performed using the Statview software. Mann-Whitney test was used when independent experiments were compared between groups. Wilcoxon test was used when CD68 and CD206 cell numbers were compared on the same group.

## Results

### **Perivascular macrophage (PVM) depletion prevents the aggravating effect of chronic alcohol consumption on ischemic stroke, but has no impact in naïve mice**

As described in figure 2 of the **study n°3**, alcohol exposure for 6 weeks provoked an inflammatory priming at the parenchymal, perivascular and vascular levels, including a marked increase of PVM numbers (CD206<sup>+</sup> cells) compared to control mice (Figures 1A, B; p<0.05 vs PBS, n=4 mice per group). In this study, we aimed at determine the specific role of PVM on ischemic stroke outcome in both healthy (naïve) and primed mice (chronically exposed to alcohol). To do this, we depleted PVM by intracerebroventricular (icv) injection of clodronate (CLO)-encapsulated liposomes to mice exposed or not to 10% ethanol for 6 weeks (see schema in figure 1C).

As mentioned in the methods section, we focused our IHC and *in vivo* imaging experiments exclusively on PVM, and measured only sub-meningeal signals. PVM are positive for the scavenger receptor CD206 and very low positive for Iba1, whereas microglial cells are positive for Iba1 and negative for CD206 in naive conditions (Suppl Figures 1A-F, H, I, n=4 mice per group). PVM are located along cerebral blood vessels (Suppl Figure 1B), both in arteries ( $\alpha$ SMA<sup>+</sup>), and veins ( $\alpha$ SMA<sup>-</sup>) (Suppl Figure 1C). PVM are located at the perivascular space, a space delimited by the basal lamina of the brain endothelium (Coll-IV<sup>+</sup>), and the glia limitans formed by astrocytic endfeet (AQP4<sup>+</sup>) (Suppl Figure 1D). PVM can also be stained with the lysosomal marker CD68, characteristic of phagocytosis (Suppl Figure 1E-F). CD68<sup>+</sup> lysosomes are autofluorescent, and this property allows the *in vivo* PVM detection by 2-photon (2P) microscopy without the need for additional fluorophore injection (Suppl Figure 2, n=4 mice per group). Otherwise, PVM can be also detected *in vivo* by using their phagocytic capacity and taking profit of the cerebrospinal fluid (CSF) circulation, through the intracerebroventricular (icv) injection of TRITC-dextran. Twenty-four hours after this icv injection, PVM can be detected around brain blood vessels (Suppl Figure 1G, arrows). The phagocytosis of TRITC-dextran by PVM was confirmed by immunohistochemistry: the TRITC dextran-positive cells were all co-stained with CD206 (Suppl Figure 1H-I).

By using CX3CR1-GFP<sup>+/−</sup> mice, PVM can be distinguished *in vivo* from GFP-positive microglial cells 4 days after the icv injection of TRITC-dextran (Suppl Figure 2A, n=6 mice per group), since PVM are very low positive for GFP (Suppl Figures 1B, D). We observed *in vivo* that the icv

injection of CLO depleted 87% of PVM (Suppl Figure 2B, C, p<0.01 vs PBS), without altering microglial cell numbers or morphology (Suppl Figures 2D-E).

In accordance to the results described in the **study n°3**, we observed an aggravating effect of chronic alcohol exposure on ischemic lesion volume (Figure 1D, E; p<0.05 vs PBS naïve, n=5-6 mice per group). Interestingly, whereas CLO treatment did not modify ischemic lesions in naïve mice (Figure 1D, E), CLO treatment prevented the aggravating effect of chronic alcohol exposure on ischemic lesion volume (Figure 1D, E; p<0.05 vs PBS).

### **PVM depletion exacerbates cellular immune responses after stroke in naïve mice, but not in primed mice**

In order to explore the mechanisms of the beneficial effect of PVM depletion on stroke in primed mice, we studied the cellular immune responses triggered 24 hours after stroke (n=4 mice per group). We analyzed microglial cell numbers (total Iba1<sup>+</sup> staining, Figure 2A, B), total number of macrophages (CD68<sup>+</sup>/Iba1<sup>-</sup> staining, Figures 2A, C) and neutrophil infiltration (Figures 2D, E) at the ischemic core, the peri-infarct zone and the contralateral hemisphere in PBS- and CLO-injected mice exposed or not to alcohol. No differences between groups were found in any of these cell counts at the contralateral hemisphere, excepting CD68<sup>+</sup>/Iba1<sup>-</sup> cell numbers, which were significantly decreased due to PVM depletion by CLO in both naïve and primed mice (data not shown).

In accordance to the results described in the **study n°3**, microglial and macrophage numbers were significantly increased after stroke in PBS-alcohol-exposed mice compared to naïve mice (Figures 2A-C; p<0.05 vs PBS-treated naïve mice).

All the stroke-induced immune responses measured here were exacerbated in CLO-treated naïve mice, but were not altered in CLO-treated primed mice. CLO-treated naïve mice showed significantly more microglial cells (Figure 2B, p<0.05 vs naïve PBS) and macrophages (Figure 2C, p<0.05 vs naïve PBS) at the peri-infarct area, as well as more neutrophils (Figure 2E, p<0.05 vs naïve PBS) at the core of the lesion compared to PBS-treated naïve mice. Opposite to naïve mice, PVM depletion by CLO treatment had no impact on any of the cellular immune responses triggered after stroke in primed mice.

## **PVM depletion exacerbates stroke-induced endothelial activation in naïve mice, but not in primed mice**

In order to study the role of PVM on endothelial activation after ischemic stroke, we performed molecular imaging ( $n=4-7$  mice per group) and immunohistochemical analyses of P-selectin (responsible of leukocyte rolling on the vessel wall) and VCAM (responsible of leukocyte adhesion to the vessel wall) ( $n=4$  mice per group).

In accordance to the results described in the **study n°3**, P-selectin levels were significantly increased after stroke in PBS primed mice (Figures 3A-F;  $p<0.05$  vs PBS-treated naïve mice).

Similar to microglial, macrophage and neutrophil cell counts, MPIO signal also increased significantly after CLO treatment in naïve mice (Figure 3C;  $p<0.05$  vs PBS-treated naïve mice), and again CLO treatment had no impact on MPIO signal in primed mice (Figure 3A-C). Immunohistochemical analyses slightly differed from MPIO data, since we did not find any difference on P-selectin<sup>+</sup> blood vessels between PBS- and CLO-treated naïve mice (Figure 3F). By contrast, CLO-treated primed mice expressed significantly less P-selectin than PBS-treated primed mice (Figure 3F,  $p<0.05$  vs PBS-treated primed mice).

Alcohol exposure also provoked an increase of VCAM-1 expression in the peri-infarct zone (Figure 3H,  $p<0.05$  vs PBS-treated naïve mice).

Again, CLO treatment provoked *per se* an increase of VCAM-1 levels in naïve mice compared to PBS-treated naïve mice (Figure 3H,  $p<0.05$  vs PBS-treated mice), which was not present in primed mice.

## **PVM determine leukocyte adhesion to the vessel wall**

By intravital 2P microscopy, we observed a significant decrease of leukocyte adhesion to the vessel wall in CLO-treated mice compared to PBS-treated mice, both in naïve and primed mice 24 hours after stroke (Figures 4A, B, D, E;  $p<0.05$  vs PBS,  $n=4$  mice per group). This effect was specific of leukocyte adhesion, since no difference was detected in the number of rolling or circulating leukocytes in any of the groups (Figures 4C, 4F).

## Discussion

As aforementioned, 90% of strokes are caused by ten potentially modifiable risk factors, (O'Donnell et al., 2010). Furthermore, some of these risk factors such as arterial hypertension (Möller et al., 2015) or chronic alcohol consumption (Ducroquet et al., 2013; Lemarchand et al., 2015, **study n°3**) can aggravate stroke outcome. In this ongoing study, we have focused on the role of PVM on the aggravating effect of chronic alcohol consumption in ischemic stroke outcome, since chronic alcohol exposure provokes the increase of PVM numbers. Our results show that clodronate (CLO) treatment, which provokes the **specific depletion of perivascular macrophages (PVM)** and, in general, border-associated macrophages (BAMs) in the brain, **prevents the aggravating effect of inflammatory priming on lesion volume**. This preventive effect does not seem to be mediated by a reduction of the inflammatory responses triggered after ischemic stroke, since PBS- and CLO-treated primed (alcohol-exposed) mice show globally the same inflammatory responses to stroke. The beneficial effect of PVM depletion on lesion volume **is exclusive of primed mice, since naïve mice show similar lesion volumes independently of the presence or the absence of PVM**.

**Our data show that PVM depletion exacerbates *per se* the inflammatory responses triggered after ischemic stroke in naïve mice**, at both the parenchymal (microglia, macrophages and neutrophil infiltration) and vascular (endothelial activation and expression of the adhesion molecules P-selectin and VCAM-1) compartments. Interestingly, this exacerbation is only present in naïve mice, and not in primed mice. The significant increase of infiltrated neutrophils found in PVM-depleted (CLO) naïve mice can be explained because PVMs can release NO, which has been associated with the inhibition of leukocyte infiltration in case of systemic infection (Olivera et al., 2016).

Surprisingly, **the exacerbation of the inflammatory responses found in CLO-treated naïve mice has no impact on lesion volume**. Pedragosa and colleagues (2018), have also shown that lesion volume remains unchanged after PVM depletion in naïve mice, despite the reduction of leukocyte infiltration in CLO-treated naïve mice (Pedragosa et al., 2018). These results are in accordance with previous studies showing no impact of leukocyte recruitment on ischemic stroke volume (Harris et al., 2005; Schmidt et al., 2017). As mentioned in this manuscript, leukocyte infiltration has been proposed as a key part of stroke progression (Neumann et al., 2015). For this

reason, research on anti-inflammatory strategies for stroke has focused on limiting the transendothelial migration of peripheral immune cells from the compromised vasculature into the brain parenchyma. However, trials testing the blockage of cerebral leukocyte infiltration in patients reported inconsistent results. To explain this, alternative cerebral infiltration routes for leukocytes, including the meninges and the choroid plexus, have been proposed. Nevertheless, a recent study on lymphocyte infiltration in a model of permanent occlusion of the MCA by electrocoagulation has shown that the reduction of lymphocyte infiltration after stroke is not related with a decrease of the ischemic size (Llovera et al. 2017).

In support of an alternative entry route for leukocytes into the brain parenchyma, our data show that PVM depletion by CLO treatment diminishes leukocyte adhesion to the blood vessel wall in both naïve mice and primed mice. In spite of a decreased leukocyte adhesion, infiltration of neutrophils to the ischemic site is significantly increased in PVM-depleted naïve mice, **suggestive of an alternative entry route other than the transendothelial pathway**. Also, **further investigations of other CAMs (notably, PECAM-1, which is responsible of leukocyte transmigration) after PVM depletion are needed** to explain the paradoxical impaired leukocyte adhesion and increased leukocyte infiltration after stroke in naïve mice.

In any case, our data suggest that **lesion volume does not seem to directly depend on the studied immune responses**, since (i) naïve mice show exacerbated immune responses after CLO treatment, but PBS and CLO-treated naïve mice show similar lesion volumes, whereas (ii) PBS and CLO-treated primed mice show similar immune responses but CLO-treated mice have smaller lesion volumes.

In view of the global effects of CLO in naïve mice, another hypothesis to be taken into account is that **CLO could have pro-inflammatory effects *per se***. In other words, the globally exacerbated inflammatory responses observed in naïve mice could be due to a pro-inflammatory effect of CLO and not (or not only) to PVM depletion. This hypothesis is supported by the neutrophil accumulation in the choroid plexus (CP) of CLO-treated mice (Suppl Figure 3). If this is the case, then an intriguing question arises: **why the pro-inflammatory effects of CLO are not present after chronic alcohol consumption?** A possible explanation is that **alcohol exposure (as it has been proposed in other pathological conditions like MS (Polfliet et al. 2002) or VIH infection (Filipowicz et al., 2016) could provoke not only an increase in PVM numbers, but could also**

**shift PVM phenotype and function from a scavenger, “buffer” cell (Kida et al., 1993; Mendes-Jorge et al., 2009) to a pro-inflammatory cell in pathological conditions.** This could explain why PVM depletion is only beneficial in primed mice and not in naïve mice, and strengthens the idea that pre-clinical stroke research should be performed in co-morbid conditions like chronic alcohol consumption or hypertension, instead of being performed in healthy mice. The phenotype of PVM must be further characterized to better understand their roles in case of chronic neuroinflammation, as they seem to be potential therapeutic targets for limiting the aggravating effects of such risk factors on stroke outcome.

Taken together, we demonstrate here that **PVM participate in the aggravating effect of inflammatory priming on ischemic stroke.** Surprisingly, PVM depletion has no effect on lesion volume in naïve mice, although it decreased leukocyte adhesion and exacerbated immune responses to stroke. This latter finding arises the question of what is the real impact of immune responses on determining ischemic lesion volume? **PVMs, and more generally BAMs, could be potential targets on stroke outcome only in case of previous chronic neuroinflammatory status, or associated comorbidity.**

## References

- Abtin, A., Jain, R., Mitchell, A.J., Roediger, B., Brzoska, A.J., Tikoo, S., Cheng, Q., Ng, L.G., Cavanagh, L.L., von Andrian, U.H., et al. (2014). Perivascular macrophages mediate neutrophil recruitment during bacterial skin infection. *Nat Immunol* 15, 45–53.
- Fabriek, B.O., Van Haastert, E.S., Galea, I., Polfliet, M.M.J., Döpp, E.D., Van Den Heuvel, M.M., Van Den Berg, T.K., De Groot, C.J.A., Van Der Valk, P., and Dijkstra, C.D. (2005). CD163-positive perivascular macrophages in the human CNS express molecules for antigen recognition and presentation. *Glia* 51, 297–305.
- Faraco, G., Sugiyama, Y., Lane, D., Garcia-Bonilla, L., Chang, H., Santisteban, M.M., Racchumi, G., Murphy, M., Van Rooijen, N., Anrather, J., et al. (2016). Perivascular macrophages mediate the neurovascular and cognitive dysfunction associated with hypertension. *Journal of Clinical Investigation* 126, 4674–4689.
- Filipowicz, A.R., McGary, C.M., Holder, G.E., Lindgren, A.A., Johnson, E.M., Sugimoto, C., Kuroda, M.J., and Kim, W.-K. (2016). Proliferation of Perivascular Macrophages Contributes to the Development of Encephalitic Lesions in HIV-Infected Humans and in SIV-Infected Macaques. *Scientific Reports* 6.
- Goldmann, T., Wieghofer, P., Jordão, M.J.C., Prutek, F., Hagemeyer, N., Frenzel, K., Amann, L., Staszewski, O., Kierdorf, K., Krueger, M., et al. (2016). Origin, fate and dynamics of macrophages at central nervous system interfaces. *Nature Immunology* 17, 797–805.
- Harris, A.K., Ergul, A., Kozak, A., Machado, L.S., Johnson, M.H., and Fagan, S.C. (2005). Effect of neutrophil depletion on gelatinase expression, edema formation and hemorrhagic transformation after focal ischemic stroke. *BMC Neurosci* 6, 49.
- He, H., Mack, J.J., Güç, E., Warren, C.M., Squadrito, M.L., Kilarski, W.W., Baer, C., Freshman, R.D., McDonald, A.I., Ziyad, S., et al. (2016). Perivascular Macrophages Limit Permeability. *Arterioscler. Thromb. Vasc. Biol.* 36, 2203–2212.
- Kida, S., Steart, P.V., Zhang, E.T., and Weller, R.O. (1993). Perivascular cells act as scavengers in the cerebral perivascular spaces and remain distinct from pericytes, microglia and macrophages. *Acta Neuropathol.* 85, 646–652.
- Lemarchand, E., Gauberti, M., Martinez de Lizarrondo, S., Villain, H., Repessé, Y., Montagne, A., Vivien, D., Ali, C., and Rubio, M. (2015). Impact of alcohol consumption on the outcome of ischemic stroke and thrombolysis: role of the hepatic clearance of tissue-type plasminogen activator. *Stroke* 46, 1641–1650.
- Mendes-Jorge, L., Ramos, D., Luppo, M., Llombart, C., Alexandre-Pires, G., Nacher, V., Melgarejo, V., Correia, M., Navarro, M., Carretero, A., et al. (2009). Scavenger function of resident autofluorescent perivascular macrophages and their contribution to the maintenance of the blood-retinal barrier. *Invest. Ophthalmol. Vis. Sci.* 50, 5997–6005.

Möller, K., Pösel, C., Kranz, A., Schulz, I., Scheibe, J., Didwischus, N., Boltze, J., Weise, G., and Wagner, D.-C. (2015). Arterial Hypertension Aggravates Innate Immune Responses after Experimental Stroke. *Front Cell Neurosci* *9*, 461.

Neumann, J., Riek-Burchardt, M., Herz, J., Doeppner, T.R., König, R., Hütten, H., Etemire, E., Männ, L., Klingberg, A., Fischer, T., et al. (2015). Very-late-antigen-4 (VLA-4)-mediated brain invasion by neutrophils leads to interactions with microglia, increased ischemic injury and impaired behavior in experimental stroke. *Acta Neuropathol.* *129*, 259–277.

O'Donnell, M.J., Xavier, D., Liu, L., Zhang, H., Chin, S.L., Rao-Melacini, P., Rangarajan, S., Islam, S., Pais, P., McQueen, M.J., et al. (2010). Risk factors for ischaemic and intracerebral haemorrhagic stroke in 22 countries (the INTERSTROKE study): a case-control study. *Lancet* *376*, 112–123.

Olivera, G.C., Ren, X., Vodnala, S.K., Lu, J., Coppo, L., Leepiyasakulchai, C., Holmgren, A., Kristensson, K., and Rottenberg, M.E. (2016). Nitric Oxide Protects against Infection-Induced Neuroinflammation by Preserving the Stability of the Blood-Brain Barrier. *PLOS Pathogens* *12*, e1005442.

Orset, C., Macrez, R., Young, A.R., Panthou, D., Angles-Cano, E., Maubert, E., Agin, V., and Vivien, D. (2007). Mouse model of in situ thromboembolic stroke and reperfusion. *Stroke* *38*, 2771–2778.

Orset, C., Haelewyn, B., Allan, S.M., Ansar, S., Campos, F., Cho, T.H., Durand, A., El Amki, M., Fatar, M., Garcia-Yébenes, I., et al. (2016). Efficacy of Alteplase in a Mouse Model of Acute Ischemic Stroke: A Retrospective Pooled Analysis. *Stroke* *47*, 1312–1318.

Park, L., Uekawa, K., Garcia-Bonilla, L., Koizumi, K., Murphy, M., Pistik, R., Younkin, L., Younkin, S., Zhou, P., Carlson, G., et al. (2017). Brain Perivascular Macrophages Initiate the Neurovascular Dysfunction of Alzheimer A $\beta$  Peptides. *Circ. Res.* *121*, 258–269.

Pedragosa, J., Salas-Perdomo, A., Gallizioli, M., Cugota, R., Miró-Mur, F., Briansó, F., Justicia, C., Pérez-Asensio, F., Marquez-Kisinousky, L., Urra, X., et al. (2018). CNS-border associated macrophages respond to acute ischemic stroke attracting granulocytes and promoting vascular leakage. *Acta Neuropathol Commun* *6*, 76.

Quenault, A., Martinez de Lizarrondo, S., Etard, O., Gauberti, M., Orset, C., Haelewyn, B., Segal, H.C., Rothwell, P.M., Vivien, D., Touzé, E., et al. (2017). Molecular magnetic resonance imaging discloses endothelial activation after transient ischaemic attack. *Brain* *140*, 146–157.

Schmidt, A., Strecker, J.-K., Hucke, S., Bruckmann, N.-M., Herold, M., Mack, M., Diederich, K., Schäbitz, W.-R., Wiendl, H., Klotz, L., et al. (2017). Targeting Different Monocyte/Macrophage Subsets Has No Impact on Outcome in Experimental Stroke. *Stroke* *48*, 1061–1069.

**Figure 1. PVMs mediate the aggravating effect of inflammatory priming on ischemic stroke.**

(A) Representative photomicrographs obtained by epifluorescence microscopy of perivascular macrophages (PVM) CD206<sup>+</sup> (in magenta) in control and primed (alcohol-exposed) mice. (B) Quantification of CD206<sup>+</sup> cells. N=4 mice per group, p<0.05 vs control, Mann-Whitney test. (C) Study design. (D) Representative T2-weighted MRI images showing ischemic lesions in PBS- and clodronate (CLO)-treated naïve and primed mice 24 hours after stroke onset. (E) Quantification of lesion volumes. N=5-6 mice per group; p<0.05 vs PBS, Mann-Whitney test.

**Figure 2. PVM modulate cellular immune responses to stroke in naïve mice but not in primed mice.** (A) Representative photomicrographs of microglial cells (Iba1<sup>+</sup>) and macrophages (CD68<sup>+</sup>Iba1<sup>-</sup>) in the peri-infarct area 24 hours after stroke onset in PBS- and CLO-treated mice. (B) Quantification of microglial cells. (C) Quantification of macrophages. (D) Representative photomicrographs of neutrophils at the core of the lesion. (E) Quantification of neutrophil numbers. N=4 mice per group, p<0.05 vs PBS, Mann-Whitney test.

**Figure 3. PVM mediate endothelial activation in naïve mice, but not in primed mice.** (A) Representative T2\*-GEFC acquisitions showing MPIO/αP-selectin accumulation in the ipsilateral cortex of mice after stroke. (B) Quantification of MPIO/αP-selectin positive blood vessels. (C) Quantification of MPIO/αP-selectin signal void vs contralateral cortex. (D) Representative photomicrographs of P-selectin staining 24 hours after stroke onset. (E) High magnification of a P-selectin positive cerebral blood vessel with juxtaposed MPIO/αP-selectin. (F) Quantification of P-selectin positive blood vessels. (G) Representative photomicrograph of VCAM-1 positive blood vessel 24 hours after stroke onset. (H) Quantification of VCAM-1 positive blood vessels. N=4-7 mice/group for in vivo molecular imaging. N=4 mice/group for immunohistochemical studies. \*p<0.05 vs control PBS or alcohol PBS, Mann-Whitney test.

**Figure 4. PVM mediate leukocyte adhesion to the blood vessel wall in both naïve mice and primed mice.** (F) Representative photomicrographs obtained by 2-photon microscopy of leukocytes (in magenta, Rhodamine 6G) in PBS- and CLO-treated primed mice 24 hours after stroke onset. (G) Quantification of adherent leukocytes. (H) Quantification of circulating/rolling leukocytes. N=4 mice per group, p<0.05 vs PBS, Mann-Whitney test.

**Suppl. Figure 1.** Characterization of PVMs in the mouse brain. (A) PVMs are negative or very low positive for Iba1, a common marker of microglial cells. (B) PVMs are located near blood

vessels, (C) both on arteries (stained with  $\alpha$ SMA in yellow) and veins (total blood vessels are stained with Coll-IV). (D) Isolated vessel technique showing PVM location between the blood vessel (cyan, Coll-IV) and astrocytic endfeet (yellow, AQP4). (E) PVMs can be stained with both CD206 and CD68. (F) Quantification of CD68 $^{+}$  or CD206 $^{+}$  cells. N=5 mice per group, Wilcoxon test. (G) PVM can be labelled with intracerebroventricular injection of TRITC-dextran, and then observed on intravital 2-photon microscopy (arrows). (H) Colocalization of CD206 and TRITC-dextran in the same mouse. (I) 3D visualization of a double positive PVM for TRITC-dextran and CD206.

**Suppl. Figure 2. PVMs can be detected by autofluorescence.** (A) Study design. (B) *In vivo* images obtained by 2P microscopy before and after 24 hours after electrocoagulation of the MCA. Brain blood vessels are visible after the intravenous injection of FITC-dextran (cyan). (C) Quantification of *in vivo*-detected autofluorescent cells. N=4 mice per group, \*p<0.05, Mann-Whitney test. (D) Representative photomicrographs obtained by epifluorescence microscopy of CD68 $^{+}$ Iba1 $^{-}$  PVM (in magenta, arrows) before and 24 hours after electrocoagulation of the MCA. Note that, under physiological conditions, CD68 $^{+}$  autofluorescent lysosomes are almost exclusive present in PVM. However, after stroke, CD68 $^{+}$  lysosomes are also present in activated microglial cells. (E) Quantification of CD68 $^{+}$ Iba1 $^{-}$  cells by IHC. N=4 mice per group, p<0.05, Mann-Whitney test. (F) and (G) Representative microphotographs obtained by confocal microscopy of a naive mouse brain before (top panels) and after (F) CD206 and (G) CD68 stainings (arrows).

**Suppl. Figure 3. PVM depletion by CLO-encapsulated liposomes.** (A) Study design. (B) CX3CR1-GFP $^{+/}$  mice were injected (icv) with PBS/CLO before *in vivo* 2-photon microscopy imaging. (C) Quantification of TRITC-Dextran $^{+}$  cells. (D-E) CLO treatment has no effect on microglial cells. (D) Representative photomicrographs of GFP $^{+}$  microglial cells and CD206 $^{+}$ PVMs in PBS- and CLO-treated mice. (E) Quantification of GFP $^{+}$  cells. N=6 mice per group, p<0.05, Mann-Whitney test.

**Suppl Figure 4. CLO-treated mice are inflammed in the choroid plexus.** (A) Representative T2\*-GEFC MRI acquisition of a CLO-treated control mouse with a clear MPIO/ $\alpha$ P-selectin signal in the ventricles. (B) Representative photomicrograph of MPIO/ $\alpha$ P-selectin on the same mouse brain. (C) Representative microphotographs of neutrophil invasion in the choroid plexus of PBS- and

CLO-treated mice 24 hours after stroke onset. **(D)** Representative photomicrographs of VCAM1 and neutrophil recruitment in a CLO-exposed mouse 24 hours after stroke onset.

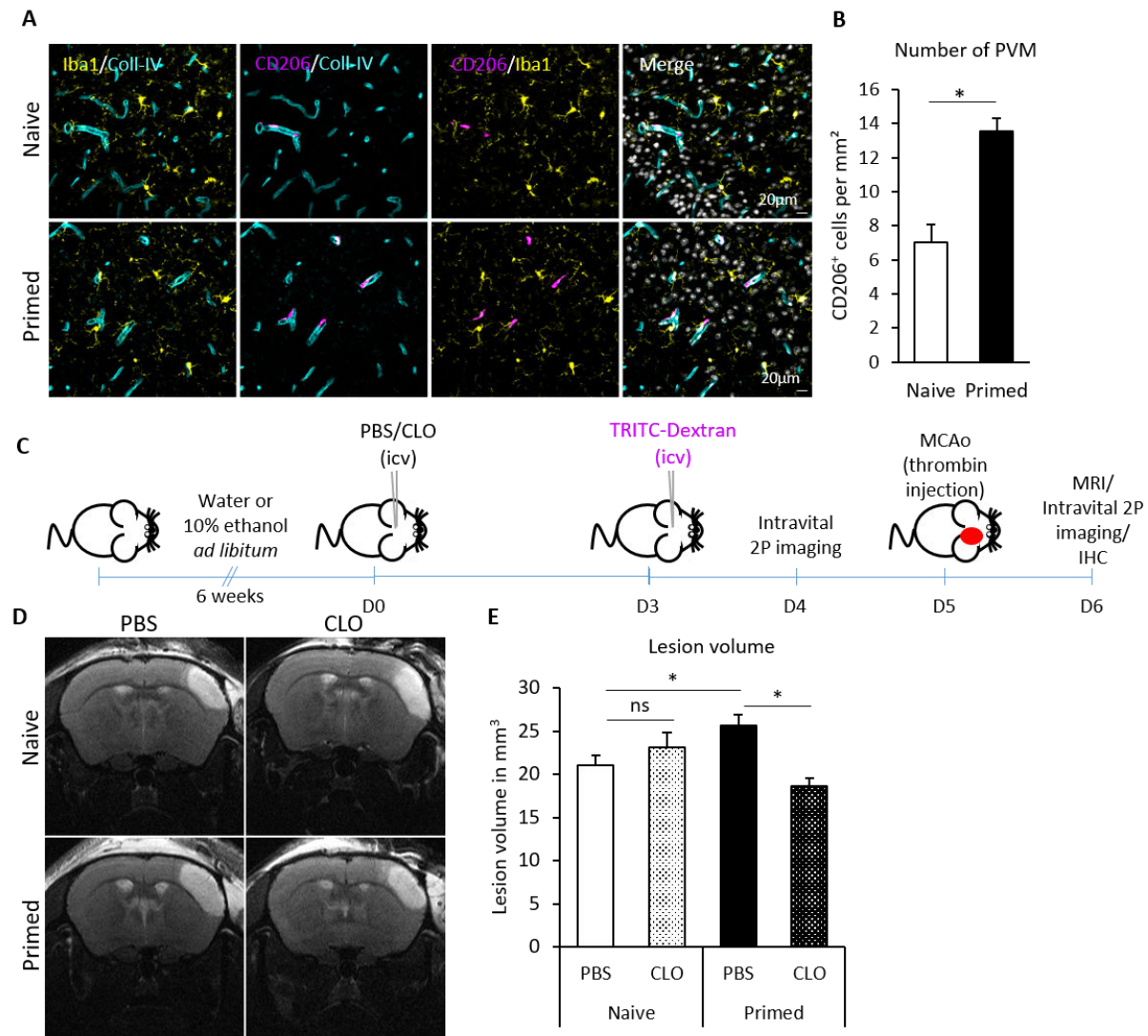


Figure 1

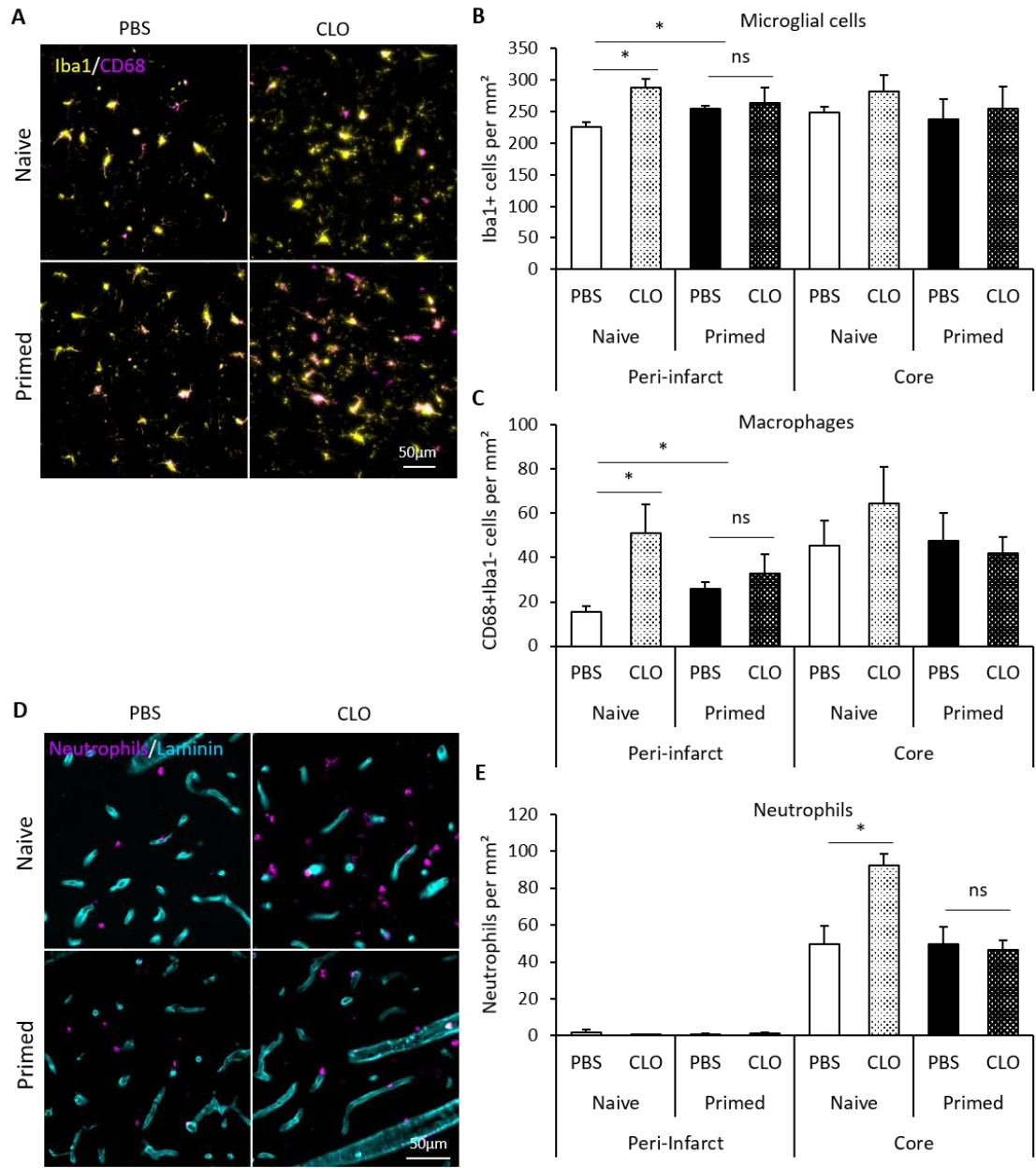


Figure 2

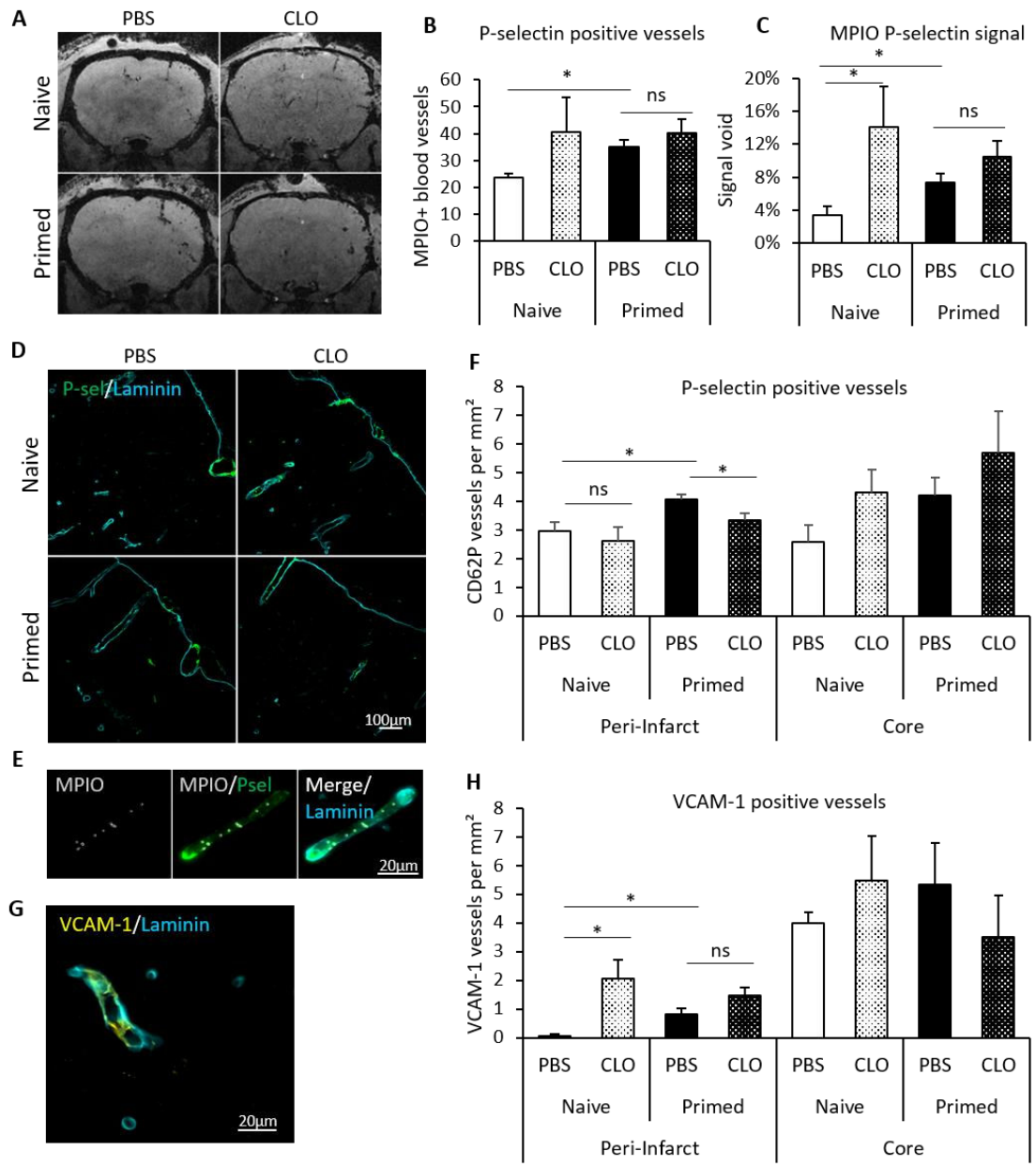


Figure 3

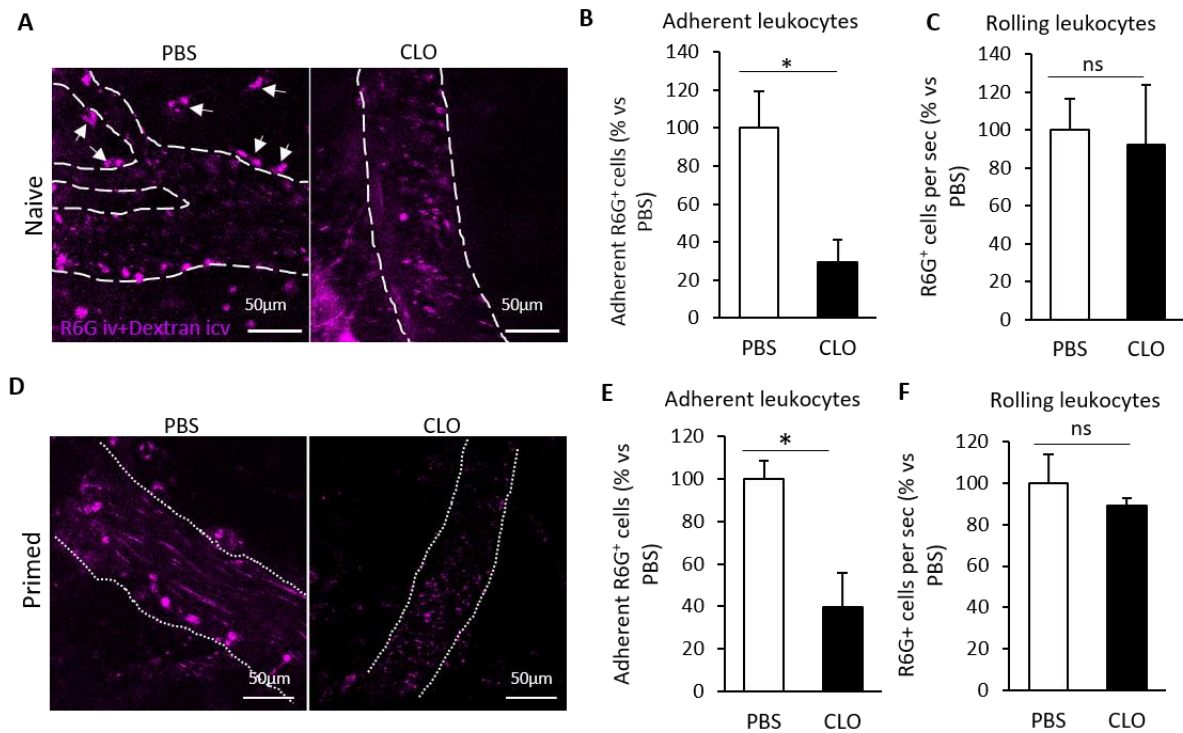
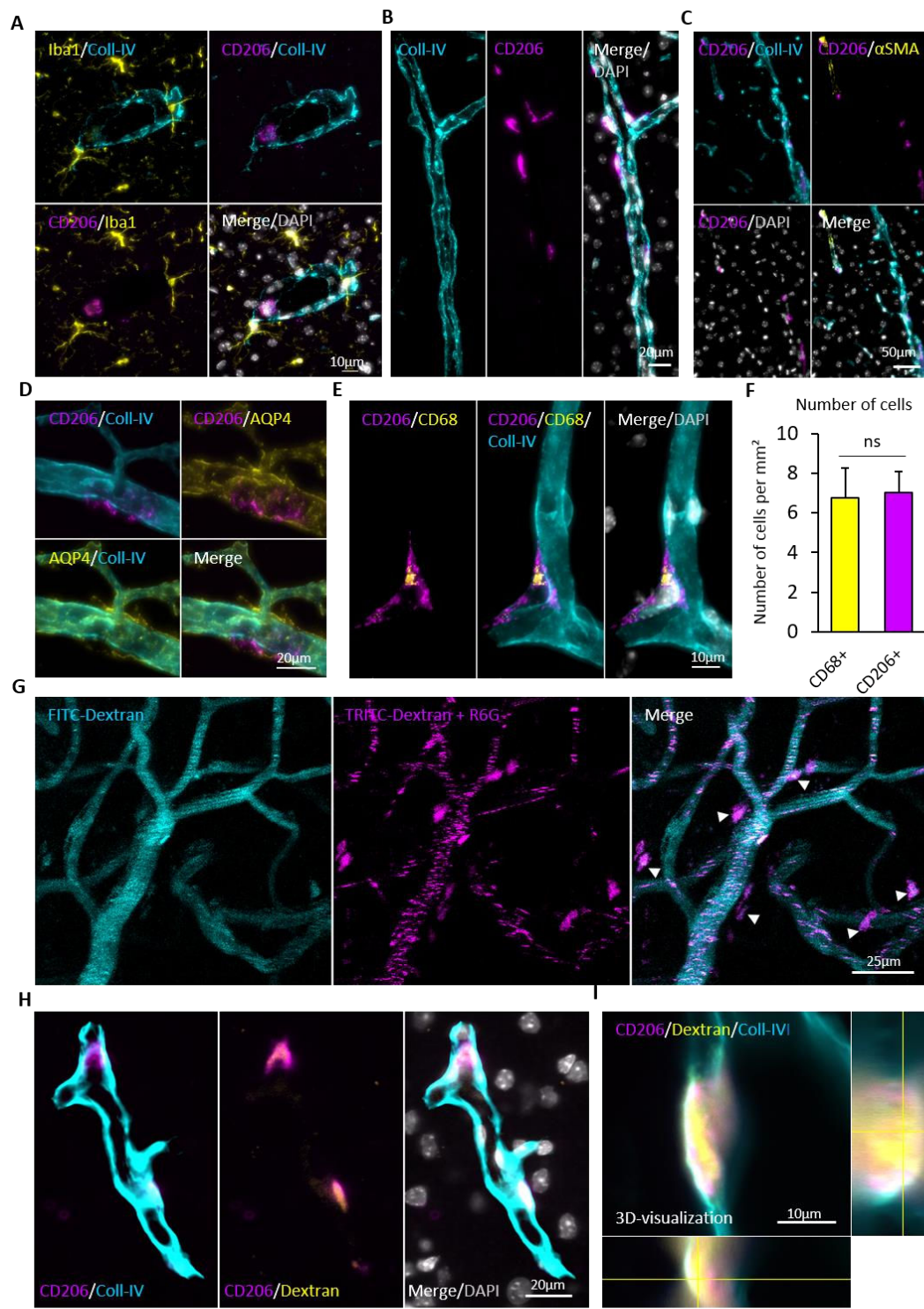
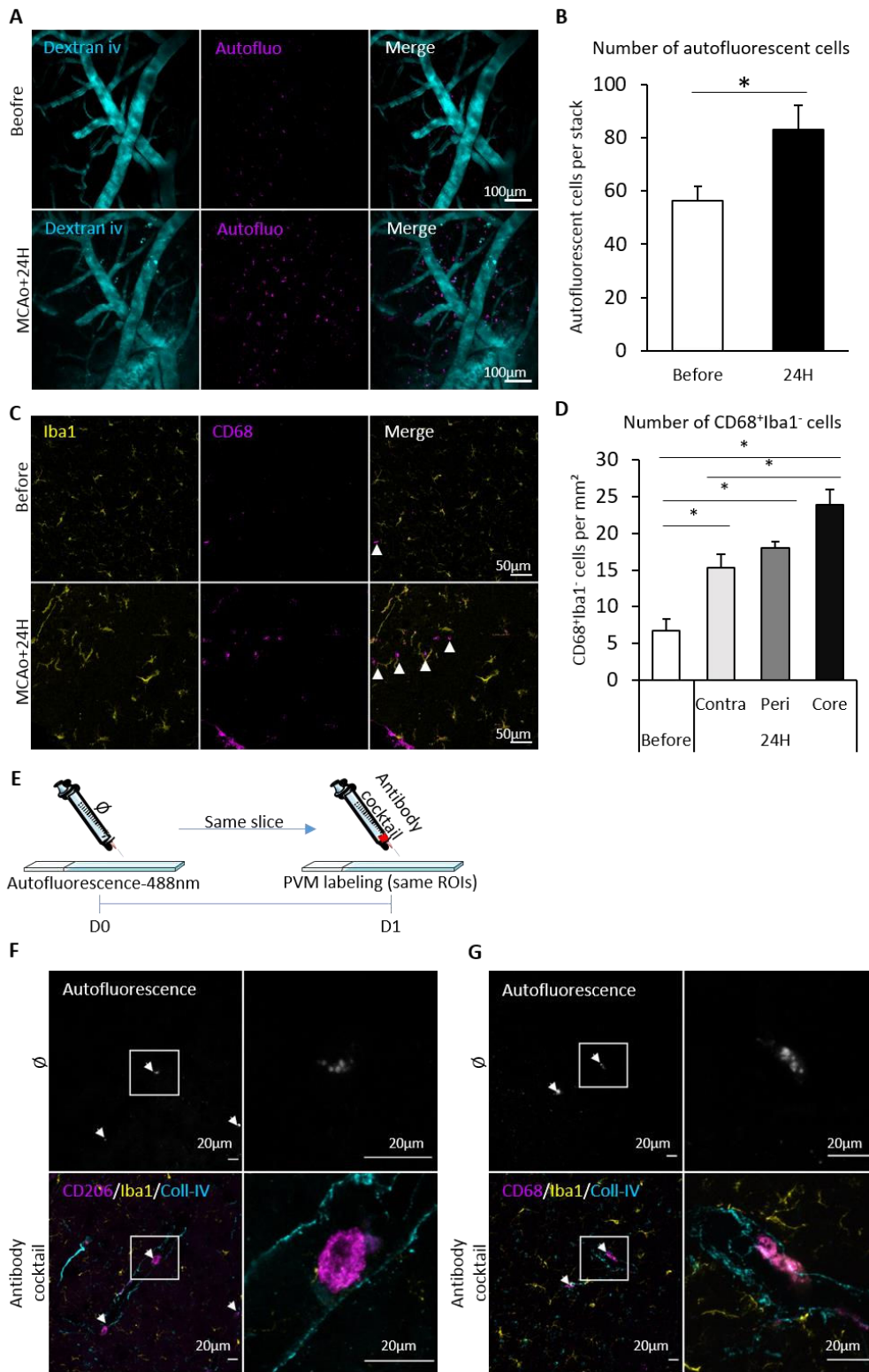


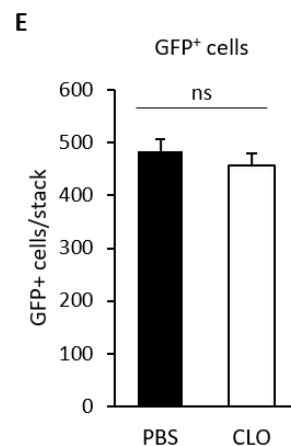
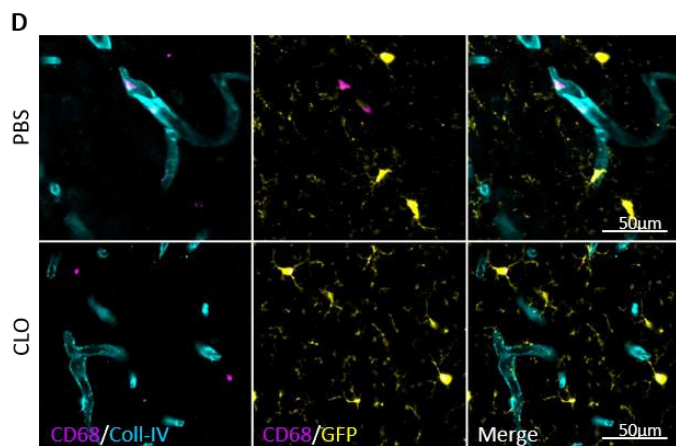
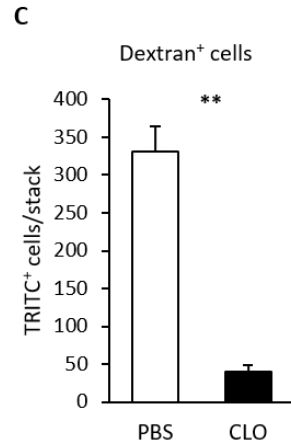
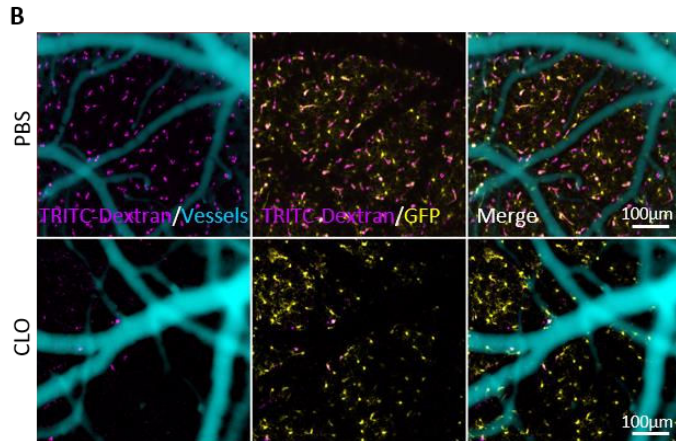
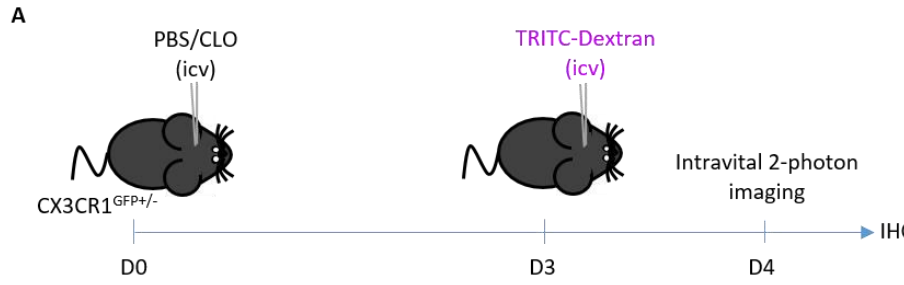
Figure 4



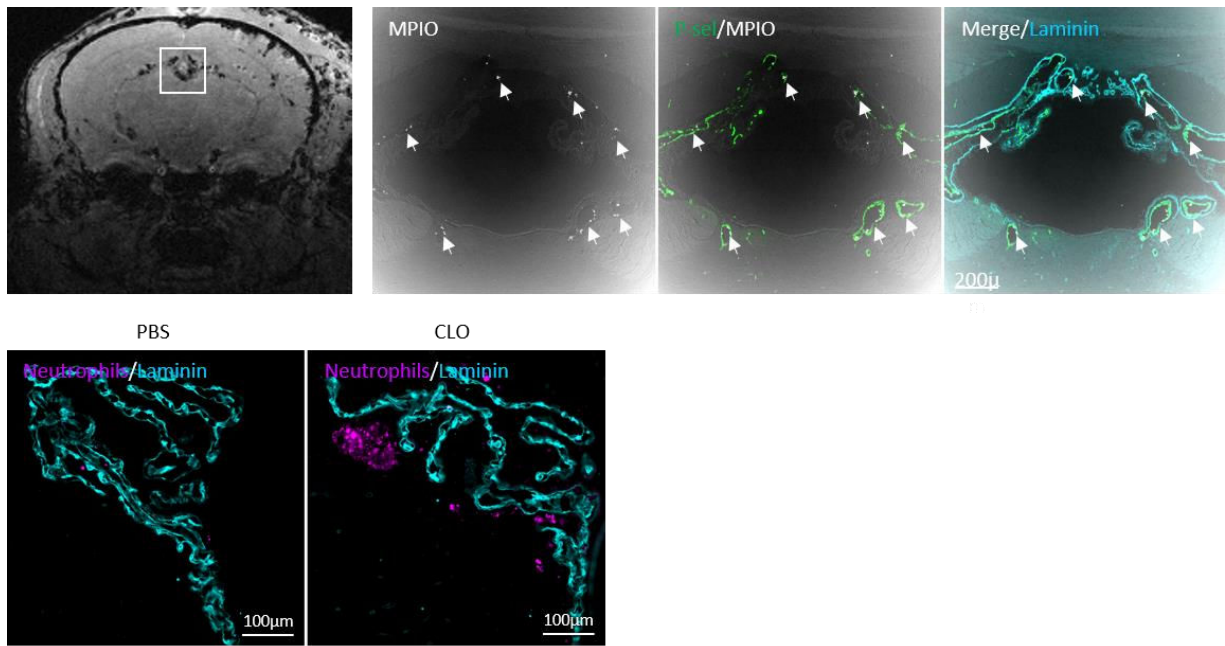
Suppl Figure 1



Suppl Figure 2



### Suppl Figure 3



Suppl Figure 4



## 5. Study 5: How to detect invisible lesion induced by a single mTBI

After **mild traumatic brain injury (mTBI)**, there may be no immediate major disorders or brain imaging injury (when performed). However, 30 to 60% of patients with mTBI develop medium or long-term brain deficits. It is therefore important for these patients to be able to objectify the existence of a real brain suffering, potentially at the origin of these disorders at a distance.

The objective of this ongoing study supported by the UNAFTC (Union Nationale des Associations de Familles de Traumatisés Crâniens et Cérébro-lésés) was to develop new imaging techniques to make visible the brain damage caused by mTBI which are today invisible. **In this study we have**  
**(i) implemented a new mouse model of mTBI without apparent lesion in conventional imaging,**  
**(ii) detected and characterized the inflammatory processes caused by the occurrence of mTBI.**

In this new model of mTBI, the mice have behavioral deficits in the absence of a visible lesion by conventional MRI imaging.

These results lead us to believe that disorders experienced by mTBI patients may come from the inflammatory reaction caused by the shock. **Moreover, our results obtained by autoradiography suggest that this mTBI-induced inflammation could be potentially imaged *in vivo* by positron emission tomography (PET) examination**, an innovative and advanced technique that would allow patients to objectify their suffering.

[\*\*This study was also the subject of a communication in the UNAFTC journal "Résurgences" \(No. 55, June 2017\).\*\*](#)



**Relevance of sensitive imaging of neuro-inflammation to explain neurological deficits after mild traumatic brain injury in mice.**

Antoine Drieu<sup>1</sup>, Anastasia Lanquetin<sup>1</sup>, Zuhal Gulhan<sup>2</sup>, Gloria Vegliante<sup>3</sup>, Marina Rubio<sup>1</sup>, Elisa R. Zanier<sup>3</sup>, Sylvie Chalon<sup>2</sup>, Denis Vivien<sup>1</sup>, Carine Ali<sup>1</sup>

<sup>1</sup> Normandie Univ, UNICAEN, INSERM, INSERM UMR-S U1237, Physiopathology and Imaging of Neurological Disorders, Cyceron, Caen, 14000, France.

<sup>2</sup> UMR 1253, iBrain, Université de Tours, Inserm, Tours, France.

<sup>3</sup> Department of Neuroscience, IRCCS-Istituto di Ricerche Farmacologiche Mario Negri, Milan, Italy.

Corresponding author: Pr C. Ali

INserm U1237, GIP Cyceron, boulevard Becquerel, 14074 Caen, France.

Tel: +33231470265; Email: ali@cyceron.fr

**Abstract:**

Traumatic brain injury (TBI) is a leading cause of disability worldwide. Most of the time, TBI is considered as a mild event, with no evidence of brain damage on conventional imaging. However, secondary injuries may well provoke long term disabilities. For these patients, it is thus crucial to provide biomarkers linking the initial event to the deficits they complain about.

By varying the depth of impact in a model of closed-head cortical-controlled impact, we found that despite no evidence of infarction or bleeding on conventional MRI (T2 and T2\* sequences), mice developed neurological deficits (Y-maze, open field)), thus recapitulating features of mild TBI in the clinical situation. Based on encouraging recent developments in the field of brain imaging, we first sought to detect cerebrovascular inflammation in these animals. However, molecular MRI for P-selectin, a key adhesion molecule, failed to reveal any sign of endothelial activation after mild TBI, which concords with immunohistochemical analyses. Interestingly, these latter analyses showed a robust parenchymal inflammatory response: astrogliosis and microgliosis were evident at the cortical level, but also deeper in the brain, in the hippocampus. Cortical inflammation increased markedly at least up to 3 weeks post-injury, while hippocampal inflammation peaked at one week but remained strong after 3 weeks. Importantly, these spatio-temporal profiles of inflammation could be confirmed by autoradiography using the TSPO ligand [<sup>3</sup>H]-DPA14. In conclusion, position emission tomography studies should be considered to provide objective evidence that patients with mild TBI indeed develop tissue damages that likely explain long term deficits.

**Abbreviations:**

CCI: controlled-cortical impact

CSF: cerebrospinal fluid

GFAP: glial fibrillary acid protein

Iba1: Iodonized calcium-binding adapter molecule-1

LPS: lipopolysaccharide

MPIO: Microparticle of iron oxide; PET: positron emission tomography

MRI: magnetic resonance imaging

MSME: multi-spin multi-echo

mTBI: mild traumatic brain injury

PET: positon emission tomography

SPECT: single photon emission computed tomography

TBI: traumatic brain injury

TSPO: translocator protein

USPIO: ultra-small particles of iron oxide

VCAM-1: vascular cell adhesion molecule-1

## **Introduction:**

Traumatic brain injury (TBI) is a leading cause of mortality and morbidity worldwide. Each year, 69 million people suffer a TBI (Dewan *et al.*, 2018). Various triggers (penetrating objects, blast injury or mechanical impact) can induce TBI, of which short-term functional consequences can result in hospitalization. In the clinical setting, TBI is classified as being mild, moderate or severe. Practice guidelines include structural imaging and neurological scoring, including the 15-point Glasgow Coma Scale, in their criteria for classifying injury severity. Patients with a score of 3-8 are classified as severe, 9-12 as moderate, and those between 13-15 as mild TBI (Teasdale and Jennett, 1974). Mild TBIs are by far the most frequent type of TBI, although their real incidence can only be estimated, since many patients do not present to hospital (Gardner and Yaffe, 2015).

After the initial mechanical damage, TBI induces a progressive secondary injury, which can lead to long term neurological and neuropsychiatric sequelae (Gardner and Yaffe, 2015; Perry *et al.*, 2016; Cruz-Haces *et al.*, 2017). Thus, cumulative epidemiological evidence show that moderate or severe TBI, and very likely mild TBI, are important risk factors for neurodegenerative diseases such as Alzheimer's disease, Parkinson's disease and amyotrophic lateral sclerosis. Around 30% of patients with mild TBI have persistent symptoms. It can thus be important to predict who are these 30% patients at risk. Imaging, or multimodal imaging is likely a key to success for this goal, which is part of the objectives of the Enigma consortium.

Inflammation is a hallmark of most neurological disorders. Thus, monitoring (neuro)inflammatory responses could have major diagnostic/prognostic implications for CNS pathological conditions, including mild TBI. Inflammation is undoubtedly an important marker/player of TBI (Donat *et al.*, 2017). Beside plasma/CSF biomarkers, molecular magnetic resonance imaging (MRI) to study endothelial activation has recently emerged as a promising axis of research (Gauberti *et al.*, 2018). Currently, only nuclear medicine technology (single photon emission computed tomography (SPECT) or positron emission tomography (PET)) is performed in humans. For instance, highly sensitive imaging of neuroinflammation using translocator protein (TSPO) ligands (TSPO is mostly described as a marker of active microglia) and PET, can be performed in stroke, Alzheimer's disease and multiple sclerosis. Higher TSPO signals have been reported in National Football League (NFL) players, a population of patients likely subjected to repeated mild TBI (Coughlin *et al.*, 2015) and also long after single events of moderate and severe TBI (Folkersma *et al.*, 2011;

Ramlackhansingh *et al.*, 2011). To our knowledge, no data is available for patients after a single mild TBI. TSPO imaging (with radiolabeled PK11195, DPA-714, fluoroethyl-DAA1106 or CLINDE) has also been used to show microglial activation in several animal models of moderate and severe TBI, but is less documented in mild TBI models (Venneti *et al.*, 2007; Cao *et al.*, 2012; Grossman *et al.*, 2012; Donat *et al.*, 2016; Israel *et al.*, 2016).

Molecular MRI may have some advantages over nuclear medicine modalities, although it has remained limited to proof-of-concept studies in animal models. The recently developed contrast agents called micro-sized particles of iron oxide (MPIO) has significantly improved molecular MRI sensitivity and specificity, compared to the historical intraparenchymal imaging of myeloperoxidase or of extravasation of targeted ultra-small particles of iron oxide (USPIO). MPIOs harboring antibodies against adhesion molecules recruited at the endothelial luminal membrane (including VCAM-1 and P-selectin), have proven as highly relevant MRI tools to detect neuroinflammation in various conditions, including stroke, ageing, multiple sclerosis (McAteer *et al.*, 2010; Montagne *et al.*, 2012; Gauberti *et al.*, 2013; Fournier *et al.*, 2017; Quenault *et al.*, 2017). Interestingly, we have previously found in a model of transient ischemic attack that MPIOs targeted against P-selectin can detect an area of neuroinflammation, while conventional MRI shows no evidence of brain infarction (Quenault *et al.*, 2017).

Recently, it has been confirmed that mild TBI is a serious condition: patients with mild TBI are at risk to commit suicide (with an adjusted incidence rate ratio of 1.8; (Madsen *et al.*, 2018)). It is thus critical to increase awareness on mild TBI, the so-called “silent epidemic”. Here, we sought to identify objective and translatable imaging evidence of post-mild TBI sequelae, in a mouse model, the closed-head controlled cortical impact procedure. This model has the advantage to preserve the skull and the dura (Siebold *et al.*, 2018).

## **Material and Methods:**

### ***Animals***

Experiments were performed on two months-old male Swiss mice (35-45g; Centre Universitaire de Ressources Biologiques, Normandy University, Caen, France). Animals were housed at 21°C in a 12 h light/dark cycle with food and water with *ad libitum* free access. All experiments were performed and reported in accordance with the Animal Research: Reporting of In Vivo Experiments (ARRIVE) guidelines (<http://www.nc3rs.org.uk>), in accordance with French laws (act no. 87–848; Ministère de l’Agriculture et de la Forêt) and European Communities Council Directives of November 24, 1986 (86/609/EEC) guidelines, and have been approved by the ethical committee (affiliation number #15301). None of the experimental procedures induced mortality. Mice weight was monitored before every behavioural assessment, the day and the day after the surgical procedure.

### ***Surgical procedure for mild traumatic brain injury***

For surgeries, mice were anesthetized with isoflurane 5% and maintained under anaesthesia with 1.5-2.5% isoflurane in a 70%/30% gas mixture (N<sub>2</sub>O/O<sub>2</sub>). The rectal temperature was maintained at 37±0.5°C throughout using a feedback-regulated heating system. Breathing was constantly checked and adjusted with anesthesia level. A sagittal incision (not midline to avoid major bleeding) was made to discover the skull. Then, the left parietal skull was cleaned with a cotton bud. Close-head controlled cortical impact (CCI) was performed thanks to an electromagnetic device Impactor (Leica; (Brody *et al.*, 2007) between the bregma and lambda of the left skull (depth of the impact: 1.5 mm for mild TBI and 2 mm for moderate-to-severe TBI; angle: 20°; velocity: 5.0 m/s ; time of impact: 0.2 s, tip diameter: 3 mm). Mice were sutured and placed in a recovery box until recovery (ie: restoration of a normal gait).

### ***MRI of brain lesions***

Mice were deeply anesthetized with 5% isoflurane in 30/70% O<sub>2</sub>/N<sub>2</sub>O and then maintained under anaesthesia during all the experiment with 1.5-2.5% anaesthesia in 30/70% O<sub>2</sub>/N<sub>2</sub>O. Imaging was carried out on a Pharmascan 7 T/12 cm system using surface coils (Bruker, Germany; (Gauberti *et al.*, 2013)). T2-weighted images to visualize oedema formation were acquired 24h, 1

week and 3 weeks post-TBI using MSME sequences (multi-spin multi-echo): TE/TR: 51ms/2500ms TE/TR 33 ms/2500 ms with a 70 $\mu$ m\*70 $\mu$ m\*500 $\mu$ m spatial resolution. Haemorrhage was assessed on T2\* imaging (TE/TR: 7.7ms/500ms TE/TR 8.7064ms/500ms) was performed. Lesion size was using the Image J (v1.452k, NIH).

### ***Behavioural assessments***

#### **Place recognition test.**

Spatial memory was tested 1 week before and 1 and 3 weeks after mild (n=12) or severe TBI (n=11 since 1 animal died after surgery), in a white plastic Y-maze with three identical arms (34 x 7 x 14.5 cm). Mice were tested after a two-session procedure with a 2h30 intersession interval, as previously described (Obiang *et al.*, 2012). During the acquisition session, one arm was randomly closed with a guillotine door. The position of the closed arm was chosen randomly among the three arms. Each mouse was placed in one of the two other arms (arms 1 and 2, with its head facing away from the center of the maze) and allowed to visit the two accessible arms for 5 min. Mice were then returned to their home cage for 2h30, before being subjected to the retention test, in which they had free access to all three arms for 5 min. The number of visits to each arm (considered only when the mouse passed two-thirds of the arm) was recorded for each session. Spatial memory was assessed through the comparison of the percentage of visits in each arm for the 5 min of the retention test.

#### **Open field**

General activity was evaluated 1 week before and 1 and 3 weeks after mild (n=12) or severe TBI (n=11), in a squared box (31.5 x 31.5 cm) during 10 minutes as previously described (Pruvost *et al.*, 2017). Animals were videotracked (DMK 21AF04, The Imaging Source®) and distance and velocity analysed with EthoVision XT 11.5 (Noldus. Additionally, a central region of 15 x 15 cm was defined in order to measure anxiety-like behavior. Rodents typically spend more time exploring the periphery of the arena by walking along the walls (thigmotaxis) than the center area (Prut & Belzung, 2003). Therefore, the percentage of time spent in the center area was measured.

#### ***Targeting-moiety conjugation to MPIOs and molecular imaging***

Microparticles of iron oxide (MPIOs; diameter 1.08 µm) with p-toluenesulphonyl reactive surface groups (Invitrogen) were used for peptide conjugation (Montagne *et al.*, 2012). Purified polyclonal goat anti-mouse antibodies for P-selectin (R&D Systems, clone AF737) were covalently conjugated to MPIOs in borate buffer with ammonium sulphate (pH 9.5), by incubation at 37°C for 48 h. The specificity of these MPIOs targeting P-selectin has been previously published (Quenault *et al.*, 2017). MPIOs were then washed in phosphate buffered saline (PBS) containing 0.5% bovine serum albumin (BSA) at 4°C and incubated for 24 h at room temperature, to block the remaining active groups. MPIOs were rinsed in PBS (0.1% BSA) and stored at 4°C.

Three-dimensional T2\*- weighted gradient echo imaging with flow compensation (spatial resolution of 70 mm x 70 mm x 70 mm interpolated to an isotropic resolution of 70 mm), TE/TR 13.2ms/200 ms and a flip angle of 21° was performed to visualize MPIOs. MRI acquisitions started immediately after the intravenous injection of MPIOs (200 µl of 2 mg Fe/kg of conjugated MPIOs). The quality of conjugated MPIOs was systematically checked in a naive mouse, by stereotaxic injection of lipopolysaccharide (1µl, 1mg/kg) in the striatum (0.5mm anterior, 2.0mm lateral, -3mm ventral to the Bregma).

### **[<sup>3</sup>H] DPA 714 autoradiography**

One week (n=7) or 3 weeks (n=6) after mTBI, brains were harvested, frozen in isopentane cooled at -35°C and stored at -80°C. Coronal brain sections 20-µm thick (coordinates: Bregma -2.30 mm according to Franklin & Paxinos) were sliced using a cryostat at -20°C (CM 3050S™, Leica, Germany), dropped off on gelatinized slides and stored at -80°C for at least 4 days. The density of TSPO binding sites was measured by *in vitro* autoradiographic experiments using [<sup>3</sup>H]DPA-714 (Specific Activity 2.01 GBq/µmol; provided by F. Dollé, CEA, Institut des Sciences du Vivant Frédéric Joliot, SHFJ, Université Paris Saclay, Orsay, France) according to the method used in Foucault-Fruchard and colleagues (Foucault-Fruchard *et al.*, 2017). Brain sections were allowed to equilibrate at RT for 3 hours and then incubated with 1 nmol/L of [<sup>3</sup>H]DPA-714 in 50 mmol/L Tris-HCl buffer pH 7.4 at RT for 60 minutes. The non-specific binding was measured in the presence of 1 µmol/L PK-11195 (Sigma Aldrich, Lyon, France). Sections were rinsed twice in ice cold buffer (4°C) for 5 minutes, then briefly in distilled water at 4°C and dried at RT. Acquisitions were compiled over a period of 4 hours using the β-imager™ 2000 (Biospace Lab, Paris, France). Four sections were analyzed per mouse. ROIs were manually drawn on the hippocampus and

frontal cortex in the intact and lesioned sides of the brain. The level of bound radioactivity was directly determined by counting the number of  $\beta$ -particles emitted from the delineated area using the  $\beta$ -vision software (Biospace Lab, France). The radioligand signal in the ROIs was expressed as counts per minute per square millimeter ( $\text{cpm}/\text{mm}^2$ ). Specific binding was determined by subtracting nonspecific binding from total binding.

### ***Immunohistochemistry***

One or 3 weeks post-TBI, deeply anesthetized mice were transcardially perfused with cold heparinized saline (15 mL) and fixed with 100 mL of 2% paraformaldehyde and 0.2% picric acid phosphate buffer (pH 7.4) (n=6 mice/group). Brains were post-fixed with 2% paraformaldehyde and 0.2% picric acid phosphate buffer (18 hours; 4°C) and cryoprotected (sucrose 20% in PBS; 24 hours; 4°C) before freezing in Tissue-Tek (Miles Scientific, Naperville, IL, USA). Cryostat-cut sections (10  $\mu\text{m}$ ) were collected on poly-lysine slides and stored at – 80°C before processing.

Sections were co-incubated overnight with rabbit polyclonal anti-mouse Iba1 (1:1000, Wako 019-19741), rat polyclonal anti-mouse CD68 (1:1000, Abcam 53444), goat polyclonal anti-mouse P-selectin (1:1000, RD System AF737), chicken polyclonal anti-mouse GFAP (1:2000, Abcam 4674) and rabbit polyclonal anti-mouse Laminin (1:1500, Abcam 11575). Primary antibodies were revealed by using Fab'2 fragments of Donkey anti-rabbit linked to FITC or Cy5, anti-rat linked to Cy3, anti-goat IgG linked to FITC (1:600, Jackson ImmunoResearch, West Grove, USA). Washed sections were coverslipped with antifade medium containing DAPI. Epifluorescence images were digitally captured using a Leica DM6000 epifluorescence microscope-coupled coolsnap camera, visualized with Leica MM AF 2.2.0 software (Molecular Devices, USA) and further processed using ImageJ 1.52k software.

### ***Statistical analyses***

Results are the mean  $\pm$  SEM. Because quantifications of cell numbers in the ipsilateral regions were compared to contralateral region, statistical analyses were performed by the Wilcoxon test (Statview software). For autoradiography, comparisons between the binding both sides were performed using the 2-way ANOVA and Bonferroni post-hoc test. The level of significance was  $p<0.05$  (GraphPad Prism software v. 5, San Diego, Calif., USA).



## Results

### ***mTBI does not induce brain damage***

We first intended to demonstrate that like in the clinical setting, our model of mild TBI does not induce brain infarction on conventional MRI. Two depths of CCI (Figure 1A) were compared by 7T MRI performed after 24h (Figure 1B). As expected, CCI at 1.5 mm did not induce skull fracture and did not translate into measurable infarction or bleeding on MRI (Figure 1C-1D). By contrast, CCI at 2.0 mm provoked skull fractures, blood expansion in the brain, as well as a 6 mm<sup>3</sup> edematous lesion (n=12 mice/group; Figure 1C-1D). We thus selected CCI at 1.5 mm as a model of mild TBI (mTBI) and CCI at 2.0 mm as a model of moderate-severe TBI (sTBI). In both groups, mice lost weight 24h after surgical procedure. Interestingly, mTBI mice recovered their weight at 1 week, while sTBI mice did not.

### ***mTBI induces functional deficits***

Spatial memory was evaluated using Y maze in mild and severe TBI mice before and 1 and 3 weeks after surgery (Figure 2A). Both groups were initially able to differentiate the new arm (Figure 2B). However, neither mTBI nor sTBI mice were able to recognize the new arm one week after TBI (Figure 2B). Three weeks after surgery, only mTBI mice were able to discriminate the new arm (Figure 2B).

We also evaluated the general activity of mice using the Open field test (Figure 2C). There was no difference between groups before the injury, but we found an important decrease in the velocity and distance in mTBI animals 1 and 3 weeks after surgery (Figure 2D, 2F). Surprisingly, these deficits were not found in sTBI animals (Figure 2D, 2F). We did not detect anxiety behavior in both groups (Figure 2G).

### ***mTBI does not induce cerebrovascular inflammation***

Patients with mTBI experience long term functional deficits, despite no evidence of brain damage. Microscopic tissue alterations likely explain these deficits. In a previous study, we found in a mouse model of transient ischemic attack, that while conventional MRI detects no damage, molecular MRI, using MPIOs targeting the adhesion molecule P-selectin allows a sensitive detection of an area of cerebrovascular inflammation (Quenault *et al.*, 2017). We postulated that mTBI could as well induce an activation of the endothelium, and thus transposed molecular

imaging of P-selectin to our model, 1 or 3 weeks post-injury (Figure 3A). MPIOs coated with antibodies against P-selectin (Figure 3B; n=5 per time) were indeed able to bind the endothelium challenged by LPS-induced inflammation (Figure 2C for immunohistochemistry and Figure 3D for molecular MRI). However, mTBI did not induce any positive signal on MRI 1 nor 3 weeks post-injury (Figure 3E). This was comforted by an immunohistochemistry analysis, showing no immunostaining in brain vessels after mTBI (Figure 3F; n=6 per time).

### ***mTBI induces cortical neuroinflammation***

We also performed immunohistochemical analyses 1 and 3 weeks post-injury to assess glial activation as an index of neuro-inflammation (Figure 4, n=6 mice per group). We first checked astrocytic reactivity by GFAP staining (Figure 4A, 3C) and found, in the ipsilateral cortex, an increase in the number of astrocytes 1 week after mTBI (Figure 4B), which was even more pronounced 3 weeks after mTBI (Figure 4D).

Regarding microglia/macrophage activation (Figure 4E-3N), the number of microglial cell increased 1 week after mTBI in the ipsilateral cortex (Figure 4E, 4G), as did the number of activated microglial cells (Iba1 and CD68 positive, Figure 4F, 4H). We also found an increased number of CD68 positive and Iba1 negative cells, which we identified as macrophages/perivascular macrophages (Figure 4I). Interestingly, microgliosis and microglial activation (Figure 4K-4M) as well as the proportion of macrophages/perivascular macrophages (Figure 3M) markedly increased 3 weeks after mTBI (Figure 4J-4N).

### ***mTBI induces hippocampal neuroinflammation***

Interestingly, we found evidence of neuroinflammation at distance compared to the impact. There was a massive astrocytic reactivity in the hippocampus of mice 1 week after mTBI (see dotted rectangles in Figure 5A, 5B). Hippocampal astrocyte numbers also increased 3 weeks after mTBI, but less than 1 week after mTBI (Figure 5C-5D).

Microglial cell number also markedly increased 1 week after mTBI in the ipsilateral hippocampus (Figure 5E-4F), as well as activated microglia (Figure 5G) and macrophages/perivascular macrophages (Figure 5H). This increase persisted 3 weeks after mTBI, but generally less important than at 1 week for all cell types (Figure 5I-5L).

### ***Proof of concept that PET imaging of TSPO is relevant to mTBI patients***

Again, as we were interested in providing a detection tool that can be transferred to the clinic, we took advantage of the development of radiolabeled ligands of TSPO, a marker of microglial activation. Autoradiography was thus performed with [<sup>3</sup>H]DPA-714 (Figure 6A). In the cortex, a significantly higher specific binding of [<sup>3</sup>H]DPA-714 was measured in the ipsilateral vs contralateral hemisphere both at 1 week and 3 weeks after mTBI (Figure 6B). In the hippocampus, a significantly higher specific binding of [<sup>3</sup>H]DPA-714 was measured in the ipsilateral vs contralateral hemisphere both at 1 week and 3 weeks after mTBI (Figure 6C).

## **Discussion:**

Secondary injury following traumatic brain injury can be detrimental to patients even several years after injury (Cassidy *et al.*, 2004). In the clinical setting, almost 90% of TBI are considered as being mild cases, which are defined as a short period of unconsciousness, or a loss of memory lasting less than 24h. For patients suffering from mTBI, there is limited medical intervention, for both diagnosis and therapy. The most studied populations of patients with mild TBI are pediatric individuals, soldiers and sports players, who can all be exposed to repeated mild TBI. There is compelling evidence showing that these patients develop brain abnormalities that likely explain long term deficits (Fehily and Fitzgerald, 2017). A better knowledge of potential pathogenic mechanisms after a single event of mTBI is mandatory for patients, but clinical observations are sparse and animal models not always relevant to the clinical situation. We thus chose to investigate pathogenic mechanisms in a murine model of mTBI, the closed-head controlled cortical impact.

This model has several advantages, including preservation of the skull and dura, and the fact that injury severity can be graded by adjusting impact depth and/or velocity (Ren *et al.*, 2013). Accordingly, we show that under a specific threshold of impact depth, conventional MRI detects neither infarction nor bleeding. Yet, animals in this case acutely lost weight post-trauma, but more importantly, exhibited deficits in spatial memory and in general activity after 1 week. This highlights the importance of considering patients with mTBI as patients with potentially invalidating disabilities later in life.

We thus sought to adopt a problem solving approach, in which translatable imaging modalities could provide evidence of tissue damage in mTBI patients. Formerly, we found that in experimental transient ischemic attack, a condition with no infarction on conventional imaging, molecular MRI targeting endothelial activation can uncover an area of inflammation, with a high sensitivity (Quenault *et al.*, 2017). However, such a strategy has not proven efficiency in the present model of mTBI, concordant with immunohistological analyses. Although disappointing, these findings suggest that therapeutic interventions focusing on leukocyte recruitment may not be adequate in mTBI patients.

By contrast, we found a marked parenchymal inflammatory response, which concerned all glial cell types enrolled in inflammation (astrocytes, microglia and macrophages). It has already been described that microglial cells can adopt a silent inflammatory status, which is called inflammatory

*priming* (Hughes *et al.*, 2010; Ramaglia *et al.*, 2012; Norden *et al.*, 2015). In our study, microglial cells seemed to develop an inflammatory *priming*, since their morphology is not fully amoeboid, and their activation status is long lasting. Furthermore, the macrophage infiltration we observed is restricted to the perivascular space. This is also observed in *primed* brains in case of neurodegenerative diseases (Perry and Holmes, 2014). Finally, studies have also described a *primed* phenotype in astrocytes (Henn *et al.*, 2011; Hennessy *et al.*, 2015).

Interestingly, this inflammatory response to mTBI occurred not only at the vicinity of the impact (ie at the cortical level), but also deeper in the brain, in the hippocampus, a structure well-known to control key mnemonic processes. The inflammatory response peaked at 1 week in the hippocampus, but increased for at least 3 weeks in the cortex. It is reasonable to associate this long lasting and expanded parenchymal inflammation to functional deficits, since inflammation has already been associated with cognitive deficits in obesity (Miller and Spencer, 2014), Alzheimer's disease (Bettcher and Kramer, 2014), sepsis (Schwalm *et al.*, 2014) and depression (Hermida *et al.*, 2012).

Relevant to the clinical setting, autoradiographic studies with the TSPO ligand DPA14 successfully corroborated the immunohistological analyses and confirmed the spatio-temporal development of parenchymal inflammation after mTBI.

In conclusion, we provide a solid proof of concept that one single mild TBI can provoke a tremendous inflammatory response, despite any visible lesion detectable by conventional imaging techniques. PET-scan should be considered for patients with mild TBI, as it may give objective evidence that troubles these patients complain about long after their injury are indeed associated to real brain sequelae. Our study adds to other research efforts towards introduction of new imaging modalities for patients with mTBI, such as sensitive diffusion (Sollmann *et al.*, 2018), free water imaging (Kikinis *et al.*, 2017), MR spectroscopy, PET for TAU (with flortaucipir).

## **Funding and acknowledgements:**

This work was supported by Institut National de la Santé Et de la Recherche Médicale (INSERM), Caen Normandy University (UNICAEN), Institut pour la Recherche sur la Moelle épinière et l'Encéphale (IRME), Union Nationale des Associations de Familles de Traumatisés crâniens et de Cérébro-lésés (UNAFTC), and by Labex IRON (ANR-11-LABX-18-01).

We are grateful to Julie Busson for technical assistance.

## **References:**

- Bettcher BM, Kramer JH. Longitudinal inflammation, cognitive decline, and Alzheimer's disease: a mini-review. *Clin. Pharmacol. Ther.* 2014; 96: 464–469.
- Brody DL, Mac Donald C, Kessens CC, Yuede C, Parsadanian M, Spinner M, et al. Electromagnetic controlled cortical impact device for precise, graded experimental traumatic brain injury. *J. Neurotrauma* 2007; 24: 657–673.
- Cao T, Thomas TC, Ziebell JM, Pauly JR, Lifshitz J. Morphological and genetic activation of microglia after diffuse traumatic brain injury in the rat. *Neuroscience* 2012; 225: 65–75.
- Cassidy JD, Carroll LJ, Peloso PM, Borg J, von Holst H, Holm L, et al. Incidence, risk factors and prevention of mild traumatic brain injury: results of the WHO Collaborating Centre Task Force on Mild Traumatic Brain Injury. *J Rehabil Med* 2004; 28–60.
- Coughlin JM, Wang Y, Munro CA, Ma S, Yue C, Chen S, et al. Neuroinflammation and brain atrophy in former NFL players: An in vivo multimodal imaging pilot study. *Neurobiol. Dis.* 2015; 74: 58–65.
- Cruz-Haces M, Tang J, Acosta G, Fernandez J, Shi R. Pathological correlations between traumatic brain injury and chronic neurodegenerative diseases. *Transl Neurodegener* 2017; 6: 20.
- Dewan MC, Rattani A, Gupta S, Baticulon RE, Hung Y-C, Punchak M, et al. Estimating the global incidence of traumatic brain injury. *J. Neurosurg.* 2018; 1–18.
- Donat CK, Gaber K, Meixensberger J, Brust P, Pinborg LH, Hansen HH, et al. Changes in Binding of [(123)I]CLINDE, a High-Affinity Translocator Protein 18 kDa (TSPO) Selective Radioligand in a Rat Model of Traumatic Brain Injury. *Neuromolecular Med.* 2016; 18: 158–169.
- Donat CK, Scott G, Gentleman SM, Sastre M. Microglial Activation in Traumatic Brain Injury. *Front Aging Neurosci* 2017; 9: 208.
- Fehily B, Fitzgerald M. Repeated Mild Traumatic Brain Injury: Potential Mechanisms of Damage. *Cell Transplant* 2017; 26: 1131–1155.
- Folkersma H, Boellaard R, Yaqub M, Kloet RW, Windhorst AD, Lammertsma AA, et al. Widespread and prolonged increase in (R)-(11)C-PK11195 binding after traumatic brain injury. *J. Nucl. Med.* 2011; 52: 1235–1239.

Foucault-Fruchard L, Doméné A, Page G, Windsor M, Emond P, Rodrigues N, et al. Neuroprotective effect of the alpha 7 nicotinic receptor agonist PHA 543613 in an in vivo excitotoxic adult rat model. *Neuroscience* 2017; 356: 52–63.

Fournier AP, Quenault A, Martinez de Lizarrondo S, Gauberti M, Defer G, Vivien D, et al. Prediction of disease activity in models of multiple sclerosis by molecular magnetic resonance imaging of P-selectin. *Proc. Natl. Acad. Sci. U.S.A.* 2017; 114: 6116–6121.

Gardner RC, Yaffe K. Epidemiology of mild traumatic brain injury and neurodegenerative disease. *Mol. Cell. Neurosci.* 2015; 66: 75–80.

Gauberti M, Fournier AP, Docagne F, Vivien D, Martinez de Lizarrondo S. Molecular Magnetic Resonance Imaging of Endothelial Activation in the Central Nervous System. *Theranostics* 2018; 8: 1195–1212.

Gauberti M, Montagne A, Marcos-Contreras OA, Le Béhot A, Maubert E, Vivien D. Ultra-sensitive molecular MRI of vascular cell adhesion molecule-1 reveals a dynamic inflammatory penumbra after strokes. *Stroke* 2013; 44: 1988–1996.

Grossman R, Paden CM, Fry PA, Rhodes RS, Biegton A. Persistent region-dependent neuroinflammation, NMDA receptor loss and atrophy in an animal model of penetrating brain injury. *Future Neurol* 2012; 7: 329–339.

Henn A, Kirner S, Leist M. TLR2 hypersensitivity of astrocytes as functional consequence of previous inflammatory episodes. *J. Immunol.* 2011; 186: 3237–3247.

Hennessy E, Griffin ÉW, Cunningham C. Astrocytes Are Primed by Chronic Neurodegeneration to Produce Exaggerated Chemokine and Cell Infiltration Responses to Acute Stimulation with the Cytokines IL-1 $\beta$  and TNF- $\alpha$ . *J. Neurosci.* 2015; 35: 8411–8422.

Hermida AP, McDonald WM, Steenland K, Levey A. The association between late-life depression, mild cognitive impairment and dementia: is inflammation the missing link? *Expert Rev Neurother* 2012; 12: 1339–1350.

Hughes MM, Field RH, Perry VH, Murray CL, Cunningham C. Microglia in the degenerating brain are capable of phagocytosis of beads and of apoptotic cells, but do not efficiently remove PrPSc, even upon LPS stimulation. *Glia* 2010; 58: 2017–2030.

Israel I, Ohsiek A, Al-Momani E, Albert-Weissenberger C, Stetter C, Mencl S, et al. Combined [(18)F]DPA-714 micro-positron emission tomography and autoradiography imaging of microglia activation after closed head injury in mice. *J Neuroinflammation* 2016; 13: 140.

Kikinis Z, Muehlmann M, Pasternak O, Peled S, Kulkarni P, Ferris C, et al. Diffusion imaging of mild traumatic brain injury in the impact accelerated rodent model: A pilot study. *Brain Inj* 2017; 31: 1376–1381.

Madsen T, Erlangsen A, Orlovska S, Mofaddy R, Nordentoft M, Benros ME. Association Between Traumatic Brain Injury and Risk of Suicide. *JAMA* 2018; 320: 580–588.

McAtee MA, Akhtar AM, von Zur Muhlen C, Choudhury RP. An approach to molecular imaging of atherosclerosis, thrombosis, and vascular inflammation using microparticles of iron oxide. *Atherosclerosis* 2010; 209: 18–27.

Miller AA, Spencer SJ. Obesity and neuroinflammation: a pathway to cognitive impairment. *Brain Behav. Immun.* 2014; 42: 10–21.

Montagne A, Gauberti M, Macrez R, Jullienne A, Briens A, Raynaud J-S, et al. Ultra-sensitive molecular MRI of cerebrovascular cell activation enables early detection of chronic central nervous system disorders. *NeuroImage* 2012; 63: 760–770.

Norden DM, Muccigrosso MM, Godbout JP. Microglial priming and enhanced reactivity to secondary insult in aging, and traumatic CNS injury, and neurodegenerative disease. *Neuropharmacology* 2015; 96: 29–41.

Obiang P, Macrez R, Jullienne A, Bertrand T, Lesept F, Ali C, et al. GluN2D subunit-containing NMDA receptors control tissue plasminogen activator-mediated spatial memory. *J. Neurosci.* 2012; 32: 12726–12734.

Perry DC, Sturm VE, Peterson MJ, Pieper CF, Bullock T, Boeve BF, et al. Association of traumatic brain injury with subsequent neurological and psychiatric disease: a meta-analysis. *J. Neurosurg.* 2016; 124: 511–526.

Perry VH, Holmes C. Microglial priming in neurodegenerative disease. *Nat Rev Neurol* 2014; 10: 217–224.

Pruvost M, Lépine M, Leonetti C, Etard O, Naveau M, Agin V, et al. ADAMTS-4 in oligodendrocytes contributes to myelination with an impact on motor function. *Glia* 2017; 65: 1961–1975.

Quenault A, Martinez de Lizarrondo S, Etard O, Gauberti M, Orset C, Haelewyn B, et al. Molecular magnetic resonance imaging discloses endothelial activation after transient ischaemic attack. *Brain* 2017; 140: 146–157.

Ramaglia V, Hughes TR, Donev RM, Ruseva MM, Wu X, Huitinga I, et al. C3-dependent mechanism of microglial priming relevant to multiple sclerosis. *Proc. Natl. Acad. Sci. U.S.A.* 2012; 109: 965–970.

Ramlackhansingh AF, Brooks DJ, Greenwood RJ, Bose SK, Turkheimer FE, Kinnunen KM, et al. Inflammation after trauma: microglial activation and traumatic brain injury. *Ann. Neurol.* 2011; 70: 374–383.

Schwalm MT, Pasquali M, Miguel SP, Dos Santos JPA, Vuolo F, Comim CM, et al. Acute brain inflammation and oxidative damage are related to long-term cognitive deficits and markers of neurodegeneration in sepsis-survivor rats. *Mol. Neurobiol.* 2014; 49: 380–385.

Siebold L, Obenaus A, Goyal R. Criteria to define mild, moderate, and severe traumatic brain injury in the mouse controlled cortical impact model. *Exp. Neurol.* 2018; 310: 48–57.

Sollmann N, Echlin PS, Schultz V, Viher PV, Lyall AE, Tripodis Y, et al. Sex differences in white matter alterations following repetitive subconcussive head impacts in collegiate ice hockey players. *Neuroimage Clin* 2018; 17: 642–649.

Teasdale G, Jennett B. Assessment of coma and impaired consciousness. A practical scale. *Lancet* 1974; 2: 81–84.

Venneti S, Wagner AK, Wang G, Slagel SL, Chen X, Lopresti BJ, et al. The high affinity peripheral benzodiazepine receptor ligand DAA1106 binds specifically to microglia in a rat model of traumatic brain injury: implications for PET imaging. *Exp. Neurol.* 2007; 207: 118–127.

### **Figure legends:**

**Figure 1.** mTBI does not induce brain damage, compared to sTBI. (A) Experimental design. (B) Representative T2-weighted (left panels) and T2\*-weighted (right panels) MRI acquisitions in mTBI (upper panels) and sTBI (bottom panels). (C) Quantification of lesion volume measured with T2/weighted MRI acquisitions. (D) Quantification of hemorrhage volume measured with T2\*-weighted acquisitions. (E) Measure of weight in m- and sTBI. N=12 mice per group, p<0.05 vs mTBI; \*\*p<0.01 vs mTBI; \*\*\*p<0.001 vs mTBI, Mann-Whitney test; # p<0.05 vs d0; ## p<0.01 vs d0, Wilcoxon test.

**Figure 2.** mTBI does induce brain deficits. (A) Schematic representation of Y maze behavioural test. (B) Quantification of the percentage of entries in the new arm 7 days before and 1 and 3 weeks after mild or severe TBI. (C) Representative sample traces of mild (upper panels) and severe TBI mice (bottom panels) 7 days before and 1 and 3 weeks after injury. (D) Quantification of the velocity (in m/s). (E) Quantification of total distance moved (in cm). (F) Quantification of time in movement. (G) Quantification of time staying in the center. N=10 mice per group, £p<0.05 vs d-7, Student t-test; \*\*p<0.01 vs mTBI d7, Wilcoxon test; #p<0.05 vs mTBI d-7, Mann-Whitney test.

**Figure 3.** mTBI does not induce vascular inflammation. (A) Experimental design. (B) Schematic representation of a MPIO. (C) Representative photomicrographs of MPIOS (arrows) along P-selectin positive (green) brain blood vessels stained with laminin (cyan). (D) Representative T2\*-GEFC MPIO/αP-selectin acquisition in a mouse subjected to an intrastriatal injection of LPS 24h before. (E) Representative T2\*-GEFC MPIO/αP-selectin acquisitions 1 week (upper panel) and 3 weeks after mTBI. (F) Representative photomicrographs of P-selectin staining 1 and 3 weeks after mTBI.

**Figure 4.** mTBI provokes a long lasting cortical inflammation. (A) GFAP positive astrocytes were found in the cortical layer 1 week after mTBI. (B) Quantification astrocyte numbers 1 week after mTBI. (C) Astrocytes were found abundantly in the cortex 3 weeks after mTBI. (D) Quantification of astrocyte numbers 3 weeks after mTBI. (E) Representative photomicrographs of microglial cells,

as well as activated microglia and macrophages in the cortex 1 week after mTBI. (F) High magnification of an activated microglial cell, expressing both Iba1 and CD68. (G-I) Quantification of (G) total microglial cell numbers, (H) activated microglia and (I) macrophages 1 week after mTBI. (J) Representative photomicrographs of microglial cells, as well as activated microglia and macrophages in the cortex 3 weeks after mTBI. (K) High magnification of an activated microglial cell, expressing both Iba1 and CD68. (L-N) Quantification of (L) total microglial cell numbers, (M) activated microglia and (N) macrophages 1 week after mTBI. N=6 mice per group, p<0.05 vs contralateral cortex, Wilcoxon test.

**Figure 5.** mTBI provokes a long lasting hippocampal inflammation. (A) GFAP positive astrocytes were found abundantly in the hippocampus 1 week after mTBI. (B) Quantification astrocyte numbers 1 week after mTBI. (C) Astrocytes were found in the hippocampus 3 weeks after mTBI. (D) Quantification of astrocyte numbers 3 weeks after mTBI. (E) Representative photomicrographs of microglial cells, as well as activated microglia and macrophages in the hippocampus 1 week after mTBI. (F-H) Quantification of (F) total microglial cell numbers, (G) activated microglia and (H) macrophages 1 week after mTBI. (I) Representative photomicrographs of microglial cells, as well as activated microglia and macrophages in the hippocampus 3 weeks after mTBI. (J-L) Quantification of (J) total microglial cell numbers, (K) activated microglia and (L) macrophages 1 week after mTBI. N=6 mice per group, p<0.05 vs contralateral hippocampus, Wilcoxon test.

**Figure 6.** [<sup>3</sup>H]-DPA14 autoradiography allows inflammatory detection after mTBI. (A) Representative brain sections 1 week (left panel) and 3 weeks (right panel) after mTBI. (B) Quantification of [<sup>3</sup>H]-DPA14 binding in the contralateral and ipsilateral cortex 1 and 3 weeks after mTBI. (C) Quantification of [<sup>3</sup>H]-DPA14 binding in the contralateral and ipsilateral hippocampi 1 and 3 weeks after mTBI. N=6-7 mice per group, \*\*\*p<0.001 vs contralateral, 2 way ANOVA test.

Fig 1.

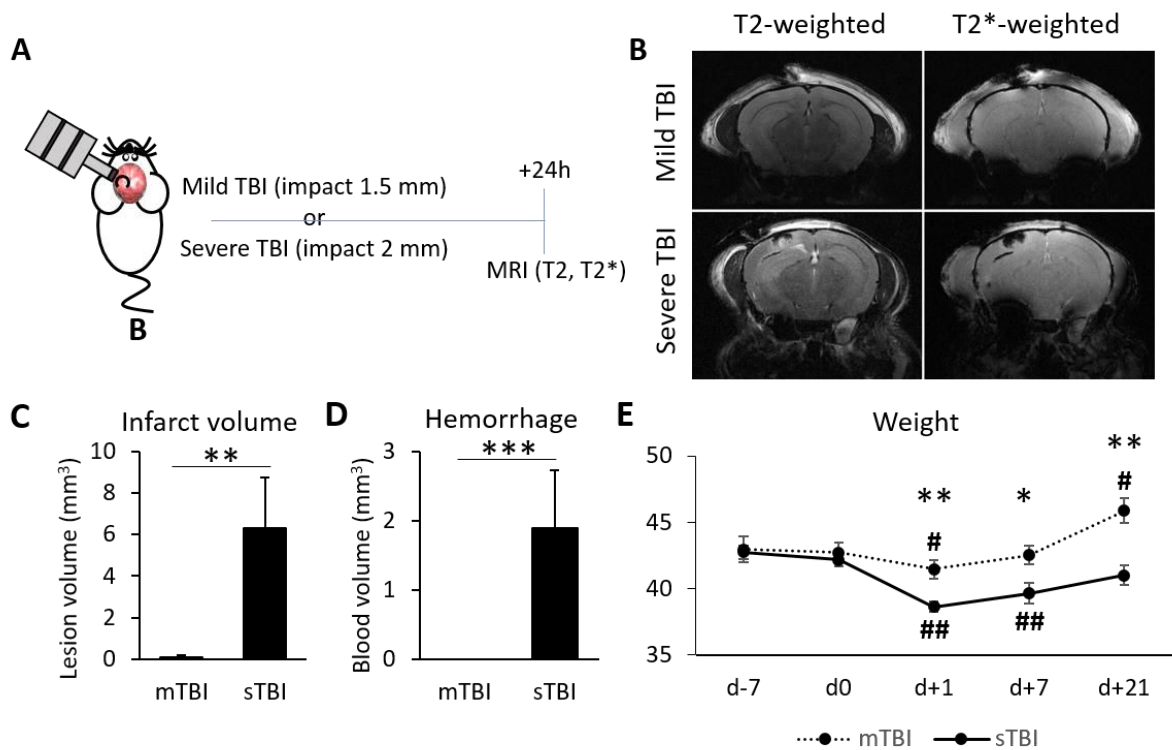


Fig 2.

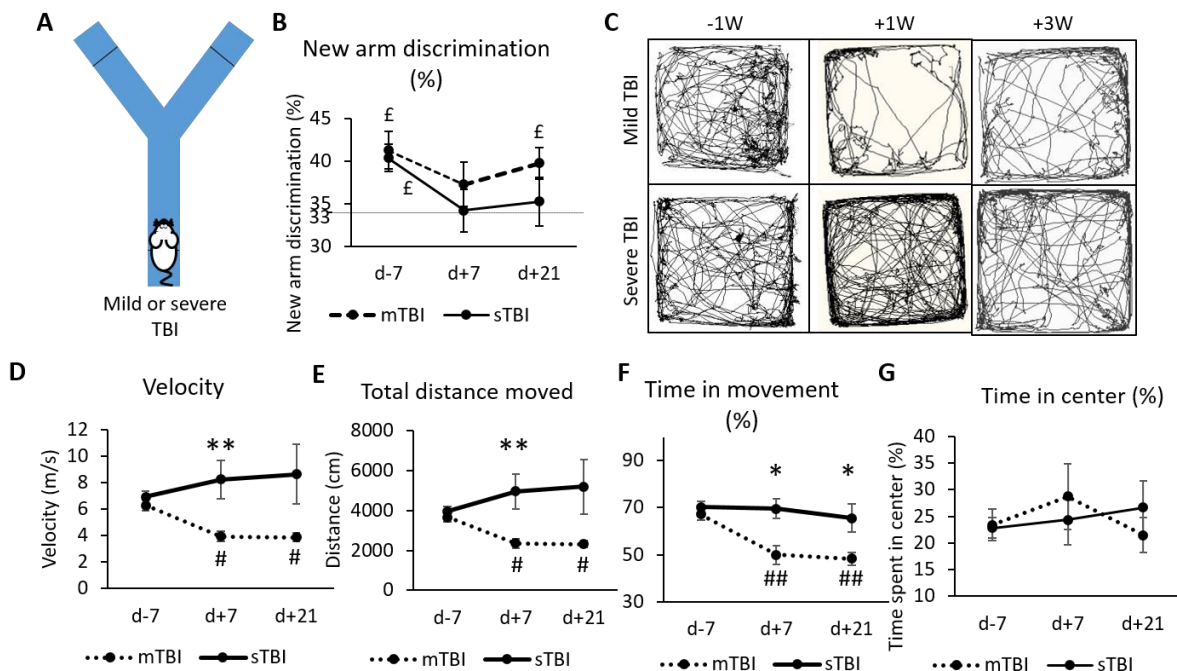


Fig 3.

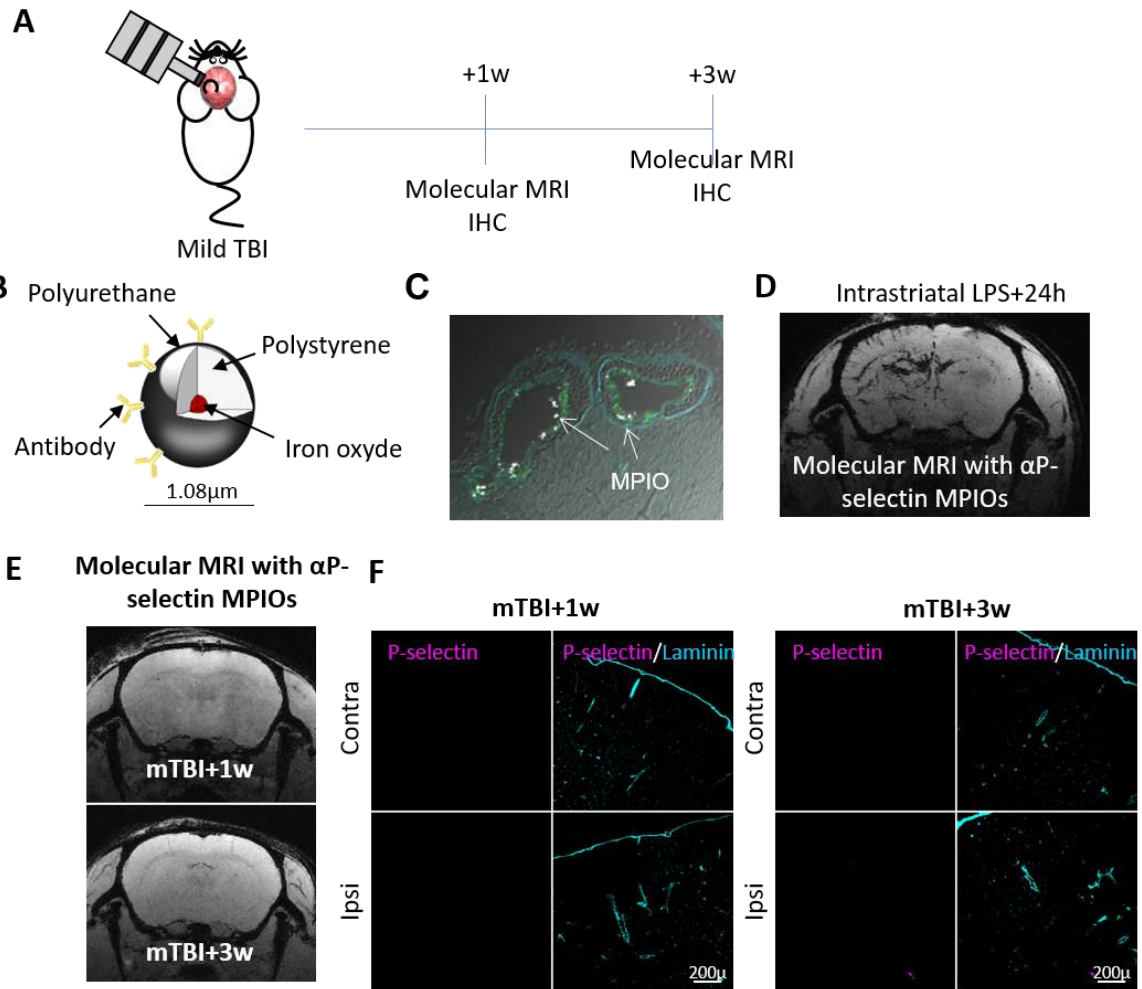
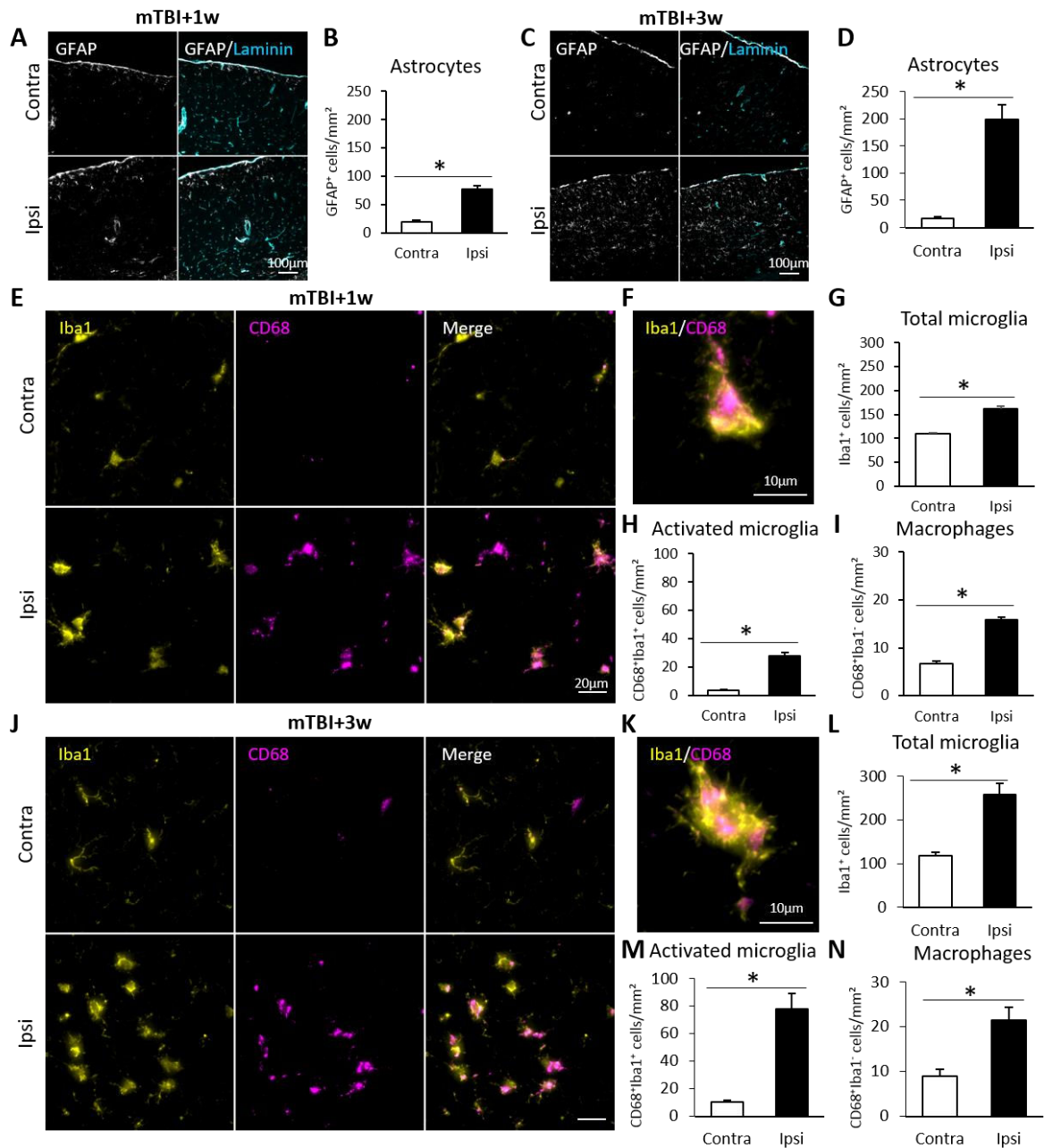


Fig 4.



**Fig 5.**

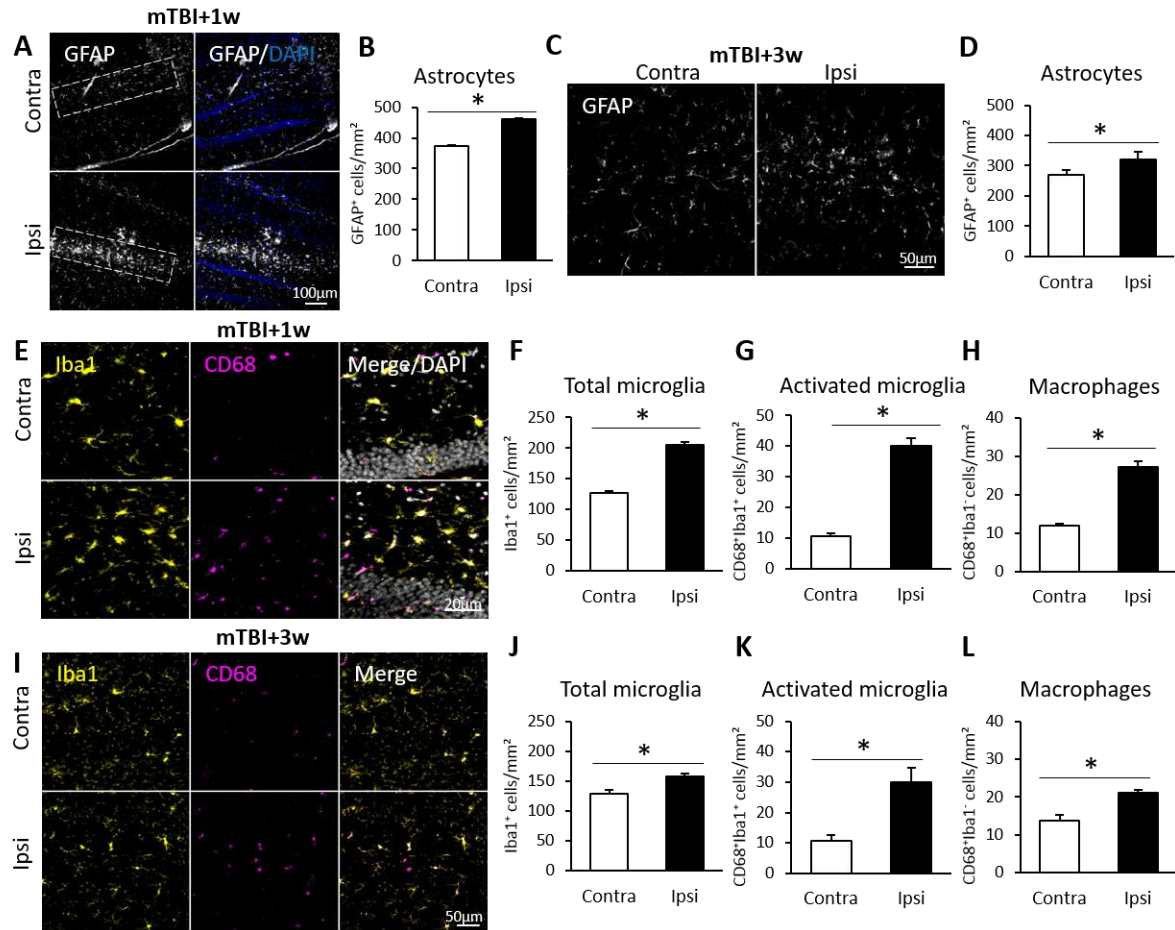
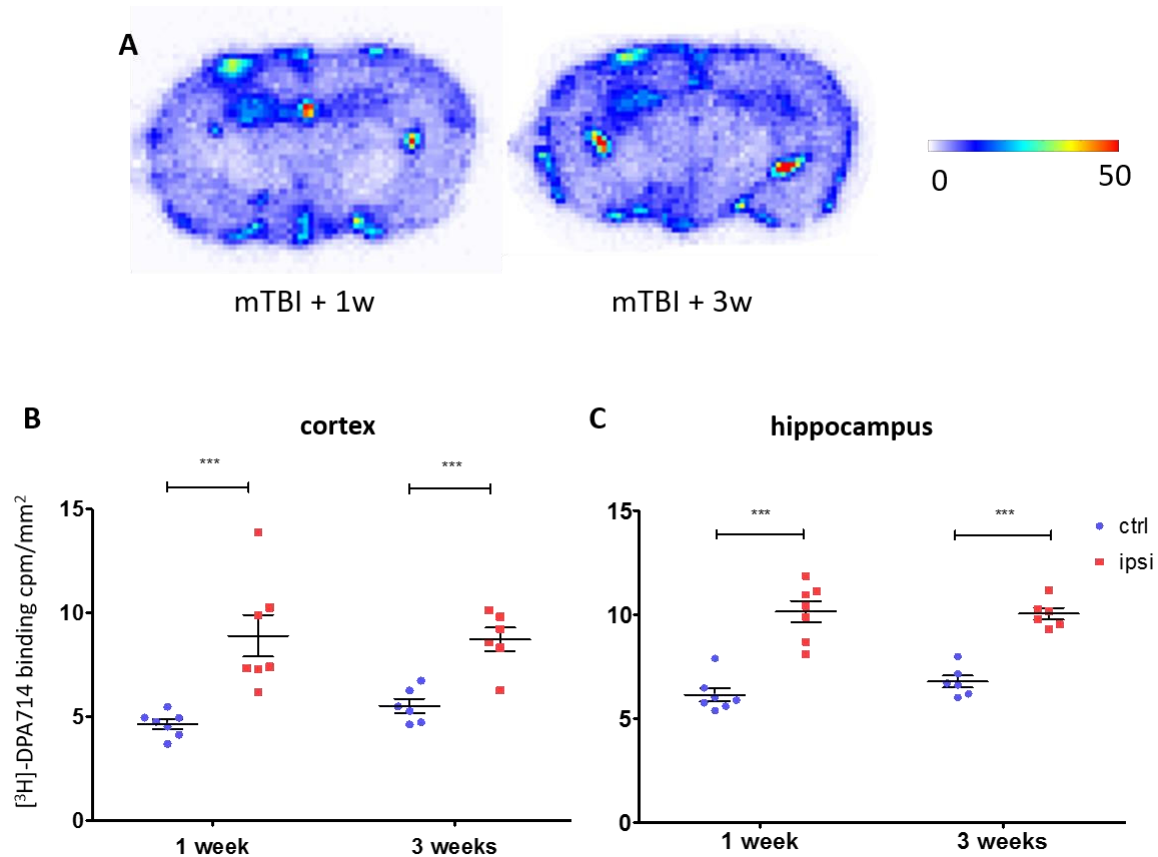


Fig 6.





# DISCUSSION



## I. What is the role of the inflammatory response after stroke?

As previously described in the introduction part, **although inflammation has an important place in the pathophysiology of stroke, therapy targeting the inflammatory response has never shown any clinical benefit to date**. One of the possible reasons is that targets that have already shown beneficial effects were identified in the experimental model of monofilament, which does not seem to be the most representative model of clinical reality. This model i) does not induce generation of a clot, ii) most likely causes significant vascular damage when inserting the monofilament, iii) the lesion size is much larger (proportionally) than the majority of brain lesions found in patients, and (iv) does not respond to the only clinically approved pharmacological treatment (tPA).

**It therefore seems appropriate to combine experimental models of cerebral ischemia that are more adapted to clinical reality** (such as thromboembolic model by thrombin injection). Moreover, these more "physiological" models (while taking into account their limitations) could **provide innovative strategies to identify new therapeutic targets (and / or re-test the previous ones) modulating the inflammatory reaction after stroke.**

## II. Does leukocyte infiltration determine lesion volume?

We have shown in our **study 4** that perivascular macrophages (PVM) were able to modulate the inflammatory response caused by stroke. Specifically, we have shown that PVM can modulate the inflammatory response on the vascular and parenchymal side:

- On the vascular side, PVM i) favor the adhesion of leukocytes to the blood vessel wall, whereas ii) they appear to temper the expression of adhesion molecules (P-selectin and VCAM-1);
- On the parenchymal side, they moderate the infiltration of neutrophils and monocytes, as well as microglial activation.

**In this context, we found that the number of leukocytes that infiltrate the brain parenchyma following a stroke has no influence on the fate of lesion volume in naive animals.** This result is in agreement with results recently published by Pedragosa and colleagues on naive animals depleted in border associated macrophages (BAM) (Pedragosa et al., 2018). Also, results from Llovera and colleagues showed that a decrease in lymphocyte infiltration - by photothrombosis of choroid plexus - also has no effect on lesion volume (Llovera et al., 2017).

Other studies have focused on the **depletion of immune cell types to reduce lesion volume after stroke onset, with very heterogeneous results.** One study showed a decrease in lesion volume in the transient monofilament model in animals depleted in neutrophils (Matsuo et al., 1994). However, this finding has not been confirmed in other studies since they do not show any beneficial effect of neutrophil depletion in the same experimental model (Harris et al., 2005; Herz et al., 2015). The depletion of circulating monocytes does not induce a change in lesion volume either (Schmidt et al., 2017). However, depletion of regulatory lymphocytes has been shown to exacerbate lesion volume in permanent electrocoagulation and transient occlusion with monofilament models (Liesz et al., 2009).

**Leukocyte depletion, however, appears to be beneficial on the outcome of ischemic injury in case of associated comorbidities.** Depletion of neutrophils has indeed shown a beneficial effect on the lesion volume in a model of hyperlipidemia in mice (Herz et al., 2015), and in spontaneous hypertensive rats (Gautier et al., 2009). **These experiments would support an important role of the inflammatory status preceding stroke onset.**

### III. Inflammatory priming, a status to be taken into account

The results of our **studies 3 and 4** indicate that the activation state of microglia may play a role in stroke outcome. However, what could be the consequences of an activated state of microglia before stroke onset? In our study, **we have shown that prolonged exposure to alcohol induces microglial priming (study 3).** Microglial priming has already been described in aging, Alzheimer's disease, head trauma (Norden et al., 2015), prion disease (Hughes et al., 2010) and multiple sclerosis (Ramaglia et al., 2012). Moreover, in experimental models, it has been proven that aging

(Zhu et al., 2017) as well as Alzheimer's disease (Bi et al., 2017; Tuo et al., 2017) could participate in the aggravation of the lesion volume. **We have also shown that prolonged exposure to alcohol exacerbates stroke outcome and the associated inflammatory response.** Several interpretations are possible to explain the worsening of the ischemic lesion in mice chronically exposed to alcohol:

- Inflammatory priming due to prolonged exposure to alcohol is responsible for the exacerbation of the inflammatory response, and the volume of lesion;
- The ischemic lesion is more important in alcohol-exposed mice and the associated inflammatory response is just proportional to the lesion volume;
- The mice exposed to alcohol are withdrawn after stroke onset (this choice was made to mimic the clinical condition of stroke patients). It is conceivable that the exacerbation of the inflammatory reaction, or even the final lesion volume, could be the consequences of alcohol withdrawal. This hypothesis seems less pertinent, given that animals chronically exposed to alcohol intracortically injected with latex beads, as well as animals injected intraperitoneally with LPS have intentionally not been withdrawn and still showed an exacerbated inflammatory response compared to control mice. **These results demonstrate that animals chronically exposed to alcohol have exacerbated inflammatory reactions, regardless of alcohol withdrawal.**

Recent studies suggest that microglial cells could be neuroprotective after stroke. On the one side, studies have shown that microglial cell depletion exacerbates the lesion volume in the transient monofilament model (Jin et al., 2017; Lalancette-Hébert et al., 2007; Szalay et al., 2016). On the other side, the orientation of the microglial phenotype could also play a role in the fate of lesion volume. Indeed, treatment with minocycline would orientate microglial phenotype to an anti-inflammatory state (characterized by increased expression of Ym1, IL-10 and TGF- $\beta$ ), resulting in decreased lesion volume up to 4 weeks after stroke onset (Yang et al., 2015) (Figure 46). It should be noted, however, that this study was performed in spontaneous hypertensive rats. Another study also showed a beneficial effect of low doses (20mg/kg) of minocycline on

lesion volume (Matsukawa et al., 2009). Finally, a low dose (10 mg/kg) of minocycline treatment repeated daily for 14 days improved functional recovery after stroke, accompanied by decreased microglial activation (Hayakawa et al., 2008).

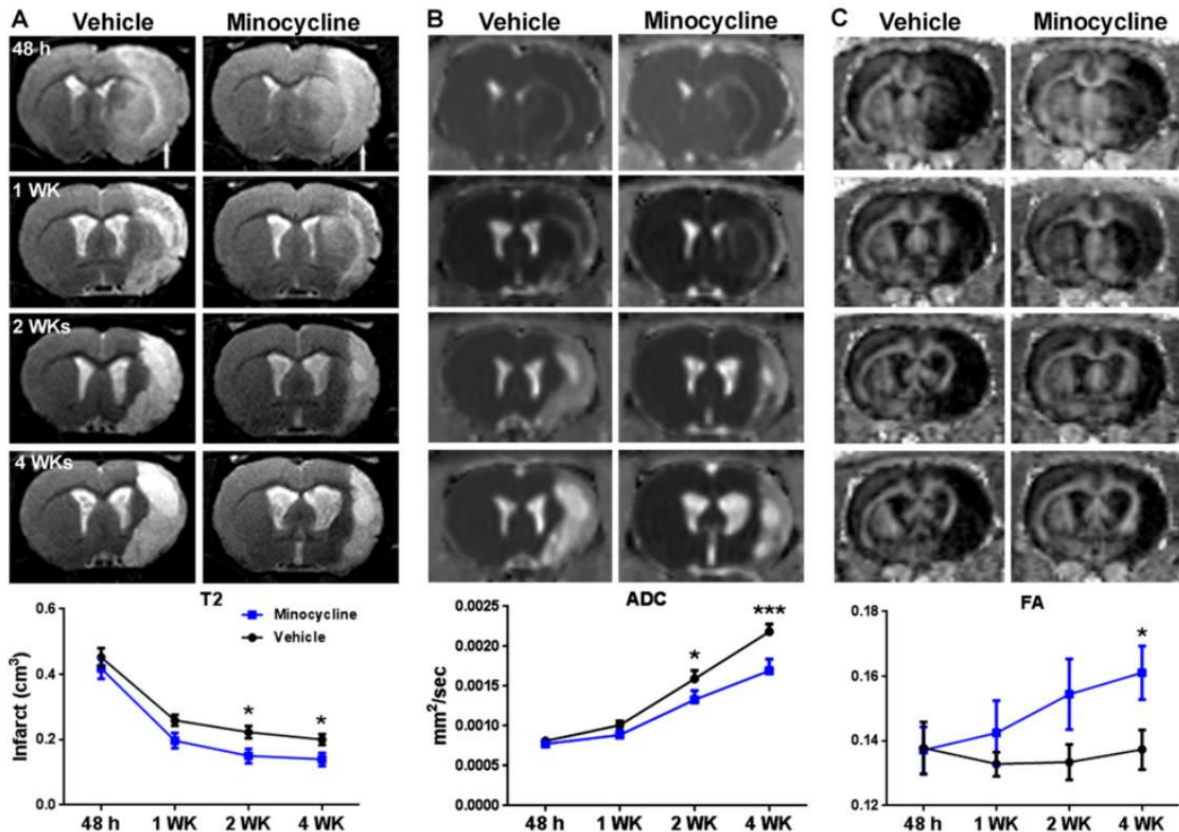


*Figure 46 : Minocycline is neuroprotective, as observed on (A) lesion volume (B and C) diffusion imaging (ADC = apparent diffusion coefficient ; FA = fractional anisotropy). In the same study, minocycline also decreases microglial activation up to 4 weeks after stroke onset (Yang et al., 2015).*

In the **study 3**, alcohol induced an inflammatory priming consisted not only in an altered microglial activation state and increased leukocyte rolling and adhesion, **we also detected a significant increase in the number of PVM**. Moreover, in our **study 4**, we showed that the stroke lesions are reduced in mice exposed to alcohol that were depleted in PVM compared to non-depleted alcohol-exposed mice. This confirms that:

- **PVM, in the context of acute stress such as stroke, modulate the inflammatory response, but this does not affect the fate of the lesion:** other phenomena could compensate (for instance, microglial or endothelial activation);
- **PVM, in the context of inflammatory priming, are able to modulate the inflammatory reaction and to worsen stroke lesion volume,** since their depletion annihilates the exacerbation of the inflammatory reaction, and the lesion volume is reduced.

It has been proposed that in pathological conditions, and especially in chronic diseases (multiple sclerosis, Alzheimer's disease or arterial hypertension), that PVM are able to diversify their roles, in order to harmonize the homeostatic balance (Faraco et al., 2017). ). It has already been described that other peripheral pathologies are able to influence the number or activation of PVM, while these pathologies are not cerebral. This is the case, for example, of myocardial infection (Yu et al., 2010), or HIV exposition (Filipowicz et al., 2016; Holder et al., 2014). Finally, some diseases, as is the example of chronic alcohol consumption (alcoholism is a disease recognized by the WHO since 1978), seem to influence the activity of PVM themselves: their action seems indeed deleterious on stroke, since their absence decreases the lesion volume (**study 4**). **Determining the phenotype of PVM could anticipate a future exacerbation of the cerebral inflammatory response and associated brain damages.**

## 1. Visualization methods

**During my thesis I have described an inflammatory priming in two distinct brain disorders: chronic alcohol consumption (**study 3**) and mild traumatic brain injury (mTBI) (**study 5**)** (Figure 47). TBI represents around 150,000 persons per year in France 90% of these TBI are considered to be mild. Worldwide, about 200 people per 100,000 inhabitants per year suffer a TBI, representing around 15 million persons per year.

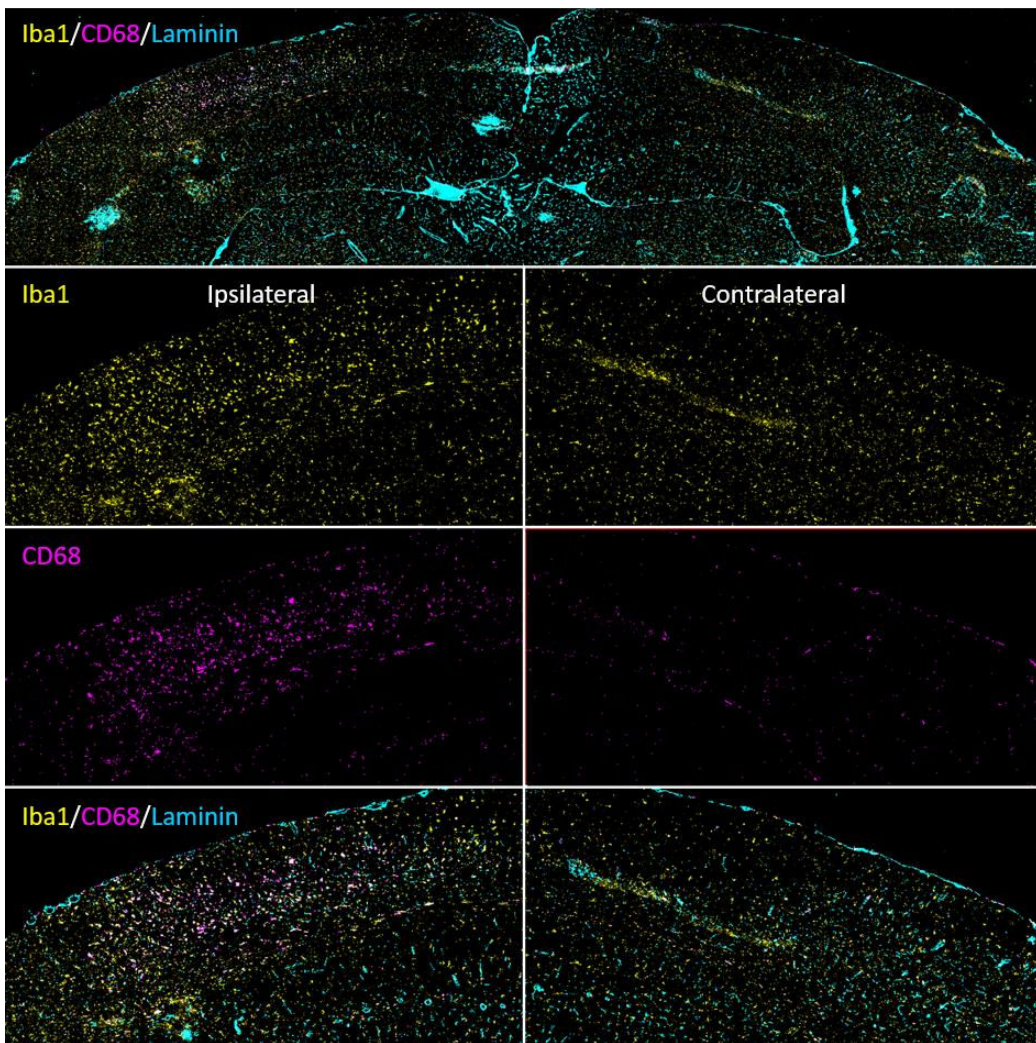
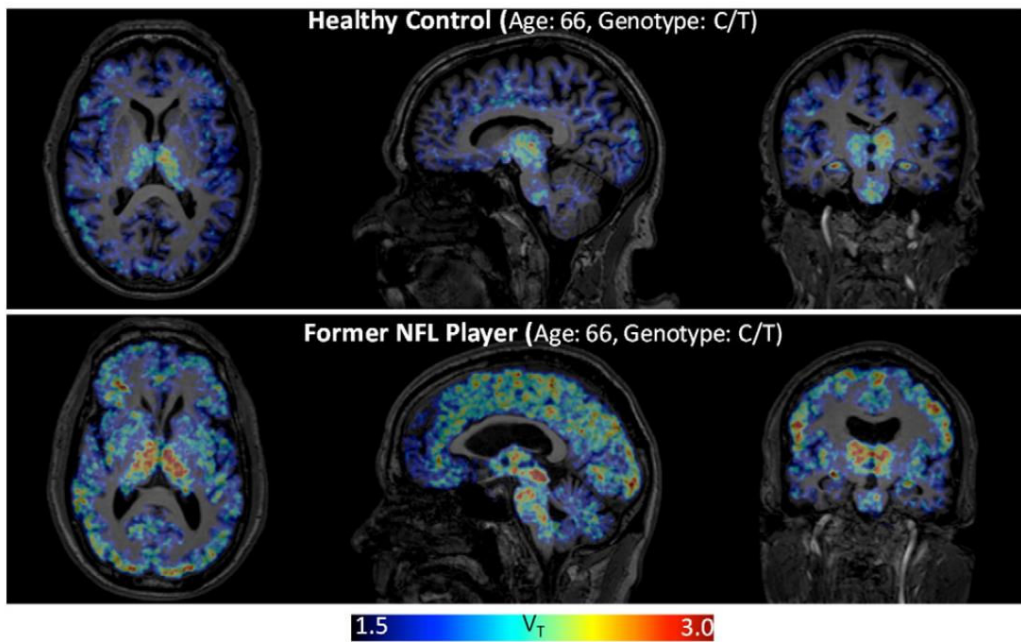


Figure 47 : Microglial priming 3 weeks after mTBI onset. Drieu et al., *in preparation*.

**In the context of mTBI, microglial priming appears to be different from alcohol-induced priming, since i) microglial cell numbers increase, ii) the Iba1 and CD68 labeling are increased, and iii) the area covered by primed microglial cells is only restricted to the level of the impact zone (Figure 47) (study 5).** In the context of TBI, we have detected microglial priming also by autoradiography by using [<sup>18</sup>F]-DPA, a ligand specific for the translocator protein (TSPO) which is specifically expressed by activated microglial cells. The prospective of this study is already scheduled: in collaboration with an INSERM team of Tours university (France), we will perform a positron emission tomography (PET) study with [<sup>18</sup>F]-DPA in mice 3 weeks after mTBI onset. If our results are positive, PET imaging could help to the diagnostic of TBI-induced neuroinflammatory priming, in the absence of classic lesion on MRI that could be underlying cognitive disorders (memory

loss, vertigo, locomotor problems) in patients. In support of this hypothesis, it has already been shown in retired National Football League (NFL) subjects that these individuals had positive PET signals for  $[^{11}\text{C}]$ -DPA (Coughlin et al., 2015) (Figure 48).



*Figure 48 : PET-scan using radioligand  $[^{11}\text{C}]$ -DPA on a control subject (upper panel) and former NFL player (bottom panel) (Coughlin et al., 2015).*

However, subjects on the study by Coughlin and colleagues have been suffered from repetitive TBI over several years. **We have shown in our study that after a single impact in mice, inflammatory disorders were found at the cortical and hippocampal level, in the absence of fracture, and persisting in time (study 4, 5).** It is important to note the difficulty to get PET exams into clinical practice. Indeed, there are very few machines (114 in France in 2012 in 107 centers, against 664 MRI), and even fewer cyclotrons, which are needed for the synthesis of radioligands. In addition, given the scarcity of devices, the price of a PET exam is expensive. Therefore, research should be directed towards new strategies to detect priming, or at least in the case of TBI, to assess its severity by means other than PET.

## 2. New approaches

Despite being an invasive approach, CSF sampling may be a good indicator of brain damage (Sharma and Laskowitz, 2012). **A much simpler and especially less invasive strategy that could be easily applicable in clinic would be to find a biomarker of priming in the bloodstream.** In our cohort of heavy drinker subjects, C-reactive protein (an indicator of inflammation) was detected in the blood in 62% of subjects, compared to zero non-alcoholic subjects. In addition, the number of circulating monocytes was also increased. In mice, we observed an increase of vascular inflammatory reaction by i) an increase in the number of circulating and adherent leukocytes and by ii) an increase in the expression of P-selectin in mice chronically exposed to alcohol.

**Interestingly, no vascular inflammatory reaction was detected after mTBI: the inflammatory response is restricted to brain tissue.** However, studies have focused on TBI blood markers. In fact, significant levels of S100 $\beta$ , GFAP and NSE (neuron specific enolase) have been detected in the blood of mice after TBI (Plog et al., 2015). In our experimental model, we observed an increase in the number of astrocytes (GFAP positive) 1 and 3 weeks after mTBI in the cortex and hippocampus ([study 5](#)). It would therefore be interesting to quantify the level of circulating GFAP or S100 $\beta$  in this model, even if we did not observe inflammation at the vascular level.

A blood marker of priming could be also detected in our model of prolonged exposure to alcohol: indeed, a study reports an increase in the number of GFAP positive cells following prolonged exposure to alcohol (Fontes-Júnior et al., 2016). In addition, another study showed that mice chronically exposed to alcohol expressed significantly more CCL2 (for chemokine ligand 2, also called MCP-1 for monocyte chemoattractant protein 1) than naive mice (Kane et al., 2014). Interestingly, in the same study, levels of TNF and IL6 did not vary between groups, indicating a specific link between CCL2 and alcohol consumption. CCL2 has also been associated with priming, since it is strongly expressed by astrocytes in prion disease (Hennessy et al., 2015). Overexpression of CCL2 has also been attributed to microglial cells and PVM in the context of status epilepticus (Varvel et al., 2016). In humans, significant levels of CCL2, as well as microglial activation, have been found in the brains of heavy drinker subjects (He and Crews, 2008). **All these data lead us to believe that CCL2 could be a key player in inflammatory priming that we**

observed after chronic alcohol consumption ([study 3](#)), and could be the subject of future investigations.

#### IV. PVM as priming regulators?

In our [study 4](#) we show that PVM depletion was sufficient to alleviate the aggravating effect of priming on stroke outcome. **There is reason to believe that PVM plays an important role in inflammatory priming.** Indeed, their number is increased in the two priming studies (alcohol consumption and mTBI) during my thesis, as well as in an experimental model of multiple sclerosis (Polfliet et al., 2002), of chronic arterial hypertension, aging (Liu et al., 1994), and HIV infection (Filipowicz et al., 2016). The origin of the increased number of PVM is still unknown: a study proposes that a specific population of monocytes, the rod-shaped monocytes, would permanently monitor the CNS and differentiate into PVM under the influence of an inflammatory event (Audoy-Rémus et al., 2008) (Figure 49).

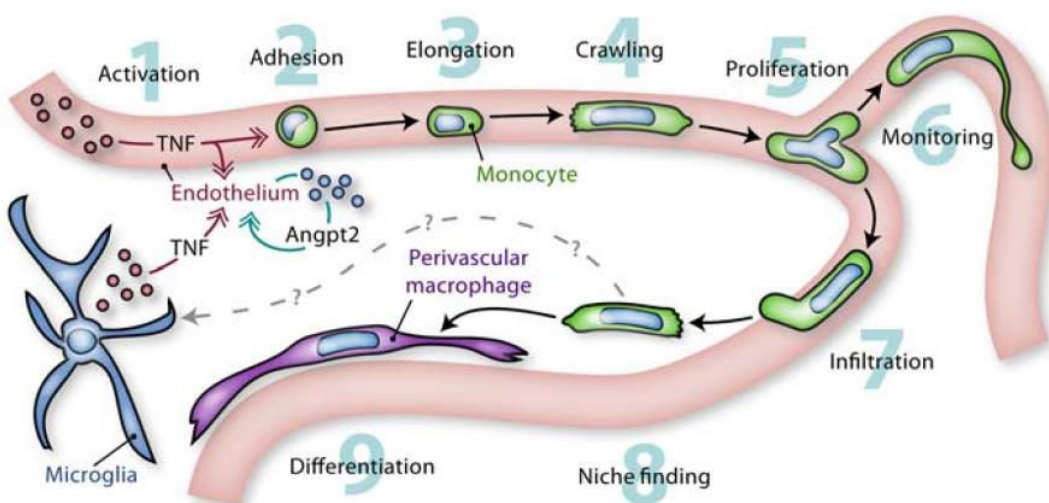


*Figure 49 : Possible mechanism explaining the recruitment of PVM in a context of systemic inflammation. Rod-shaped monocytes survey brain blood vessels in naïve condition. Following systemic inflammation, Rod-shaped monocytes can reach perivascular spaces and become PVM (Audoy-Rémus et al., 2008).*

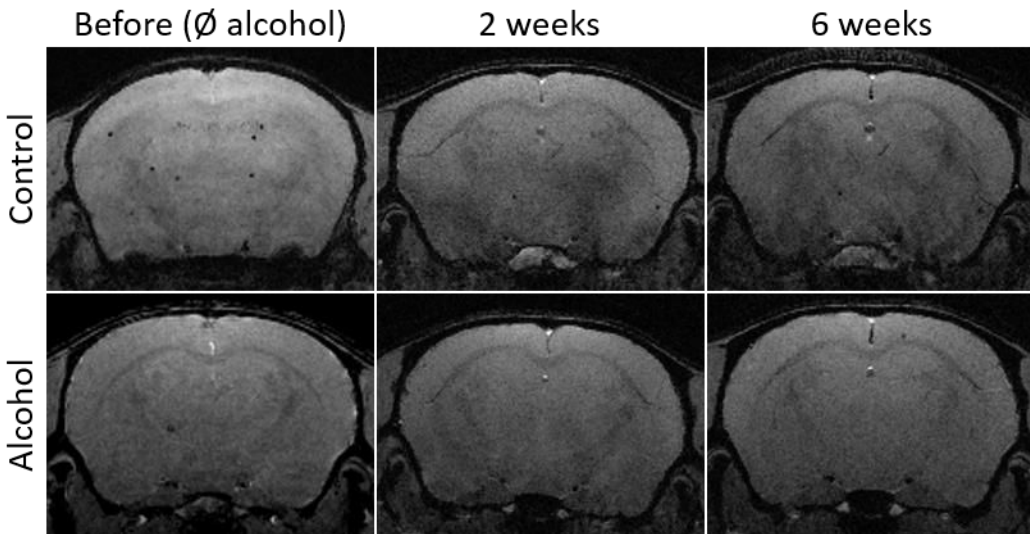


*Figure 50: PVM does not seem to migrate from the circulation. Nude MPIOs were injected in mice, then half of mice were continuously exposed to alcohol. T2\*-weighted sequences were not able to detect any MPIO positive macrophages. Work in process.*

### 1. Role of PVM on leukocyte infiltration

The mechanism linking leukocyte infiltration and PVM is poorly understood. **In our study, we found that PVM clearly have a role on leukocyte adhesion to the wall of cerebral blood vessels following stroke.** Nevertheless, even if the adhesion of leukocytes is decreased in the absence of PVM, leukocyte infiltration is more important ([study 4](#)). One hypothesis to explain this phenomenon is that PVM can produce nitric oxide (NO) when stimulated by inducible nitric oxide synthase (iNOS) released from endothelial cells. NO production is associated with loss of sensitivity to TNF and inhibition of leukocyte infiltration (Olivera et al., 2016). In iNOS-deficient mice, TNF production and leukocyte infiltration are increased, suggesting that PVM could play a pivotal role in this process. In our [study 4](#), we found that PVM depletion lead to increased leukocyte infiltration in naive mice after stroke. It would be interesting to measure the levels of iNOS, NO and TNF produced in this study.

## 2. Prospects

### a. *Scavenger role of PVM in brain pathologies*

As aforementioned, PVM have a physiological role of scavenger. **A side project performed during my thesis shows that PVM could influence the normal functioning of the glymphatic system under physiological conditions** (Figure 51).

The glymphatic system has been proposed as a pathway of liquid exchanges through the CNS parenchyma, whose primary purpose would be to clear the CNS from cellular debris. This system involves two liquids: the CSF and interstitial fluid. The hypothetic route of the glymphatic system is that the CSF, via the peri-arterial perivascular spaces, diffuses into the cerebral parenchyma, interacts with the interstitial fluid, and then transport the brain debris into the perivascular spaces. This system has been well described in the context of Alzheimer's disease: it would be beneficial to drive the  $\beta$ -amyloid peptide to the perivascular spaces in order to facilitate its degradation (Iliff et al., 2012). Interestingly, it has recently been shown that PVM participate in neurovascular dysfunctions induced by  $\beta$ -amyloid peptide in Alzheimer's disease (Park et al., 2017). PVM would phagocytose the  $\beta$ -amyloid peptide leading to the production of reactive oxygen species by PVM and neurovascular dysfunctions (Park et al., 2017).

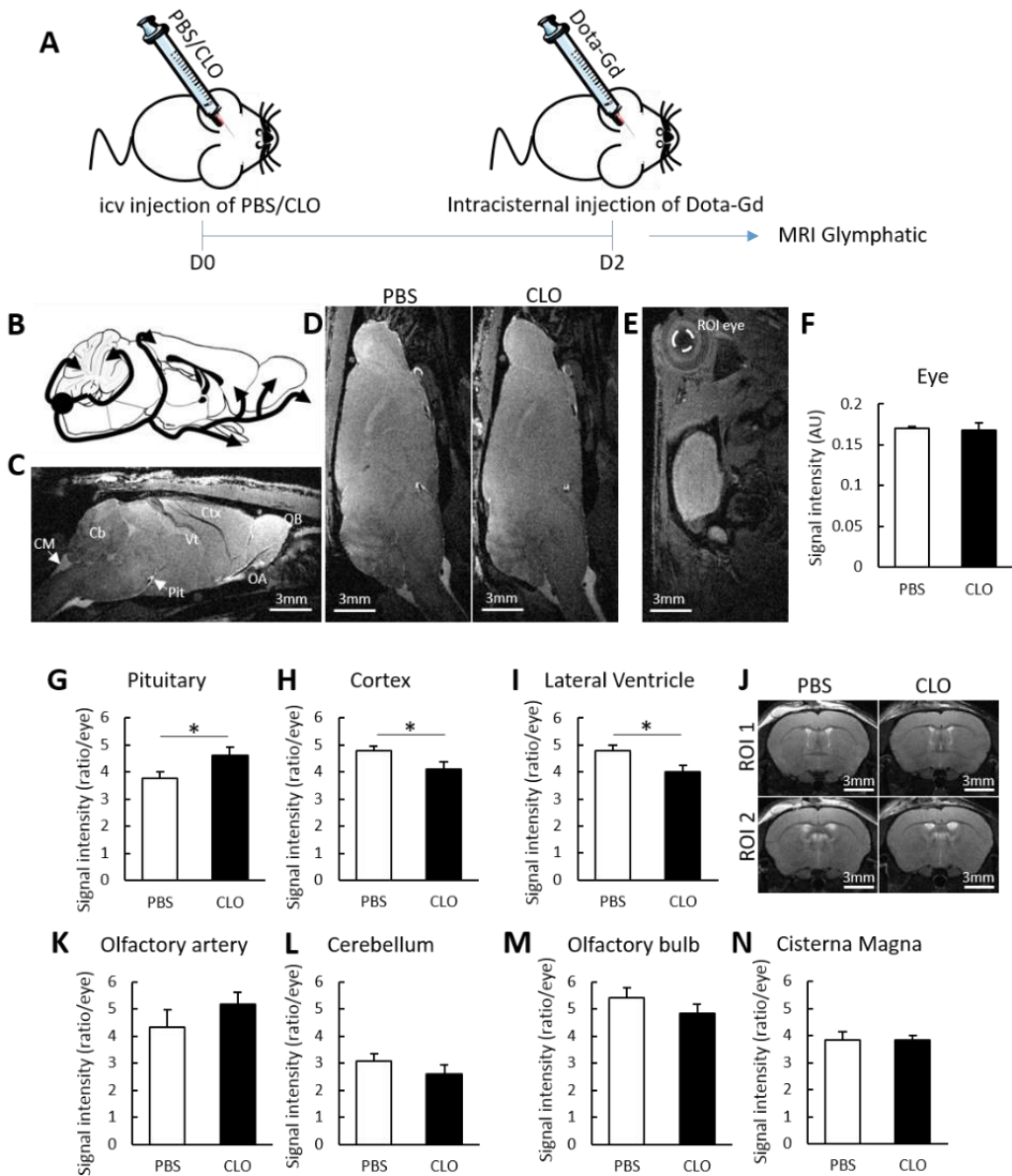


**Figure 51 : PVM participate on the good functioning of the glymphatic system. (A) Experimental design. (B) CSF circulation design. (C) T2-weighted MRI sequence showing regions of interest (ROI). CM = cisterna magna ; Cb = cerebellum ; Pit = pituitary gland ; OA = olfactory artery; OB = olfactory bulb ; Ctx = cortex ; Vt = ventricle. (D) T1-FLASH 3D MRI sequences on PBS- or Clodronate (CLO)-treated mice. (E) We selected the eye to calculate intensity ratio (dotted circle). (F) Quantification of signal intensity in the eye. (G-I) Quantification of the ratio (G) pit, (H) ctx and (I) lateral Vt compared to the signal obtained in the eye. (J) We did not find any difference in the size of ventricles between groups. (K-N) Quantification of the ratio (K) OA, (L) Cb, (M) OB and (N) cisterna magna compared to the signal obtained in the eye. N=4 mice per group,  $p<0.05$  vs PBS, Mann-Whitney test. Work in process.**

The glymphatic system also seems to be impaired in the context of alcohol consumption. In fact, a study by Lundgaard and colleagues showed that moderate chronic alcohol consumption appeared to improve the performance of the blood system, while severe chronic consumption decreased glymphatic activity via deregulation of aquaporin-4 channel expression on the surface of the astrocytic feet lining the wall of the cerebral blood vessels (Lundgaard et al., 2018) (Figure 52).

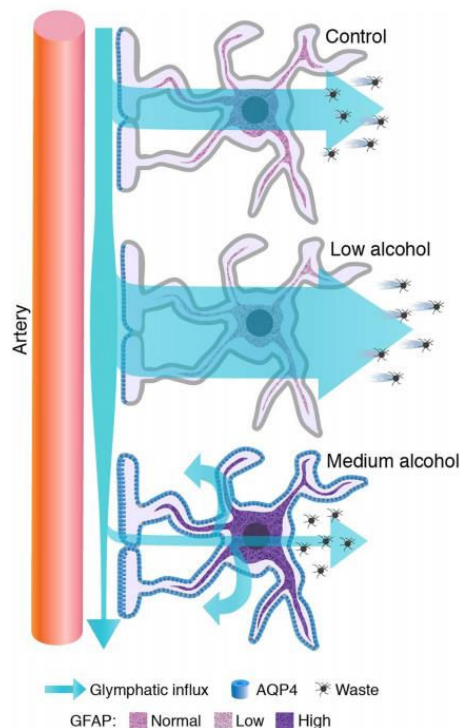


Figure 52 : Influence of alcohol consumption on the glymphatic system. Low doses of alcohol (0,5mg/kg daily for 30 days) ameliorate glymphatic system performances, since a stronger chronic consumption (1,5mg/kg daily for 30 days) worsens the glymphatic system performances (Lundgaard et al., 2018).

We could in future studies measure the activity of the glymphatic system in our experimental model of chronic alcohol exposure in mice, since i) PVM participate in the good functioning of the glymphatic system and ii) the number of PVM is abnormally important in mice chronically exposed to alcohol.

b. Role of PVM on leukocyte infiltration in other brain pathologies

In our **study 4**, we showed that PVM can modulate leukocyte infiltration in the context of **stroke**. We have also investigated the activity of PVM in other neuroinflammatory conditions by injecting LPS directly into the cortex of mice treated with liposomes containing PBS or clodronate. **We show that PVM also modulate the inflammatory response in the context of a cerebral infection.** We first have shown an increase of MPIO signal in the cortex of LPS-treated mice, corresponding to an infiltration of macrophages having previously phagocytized the MPIOs. Interestingly, macrophages having phagocytized MPIOs were systematically found at the edge of blood vessels (Figure 53).

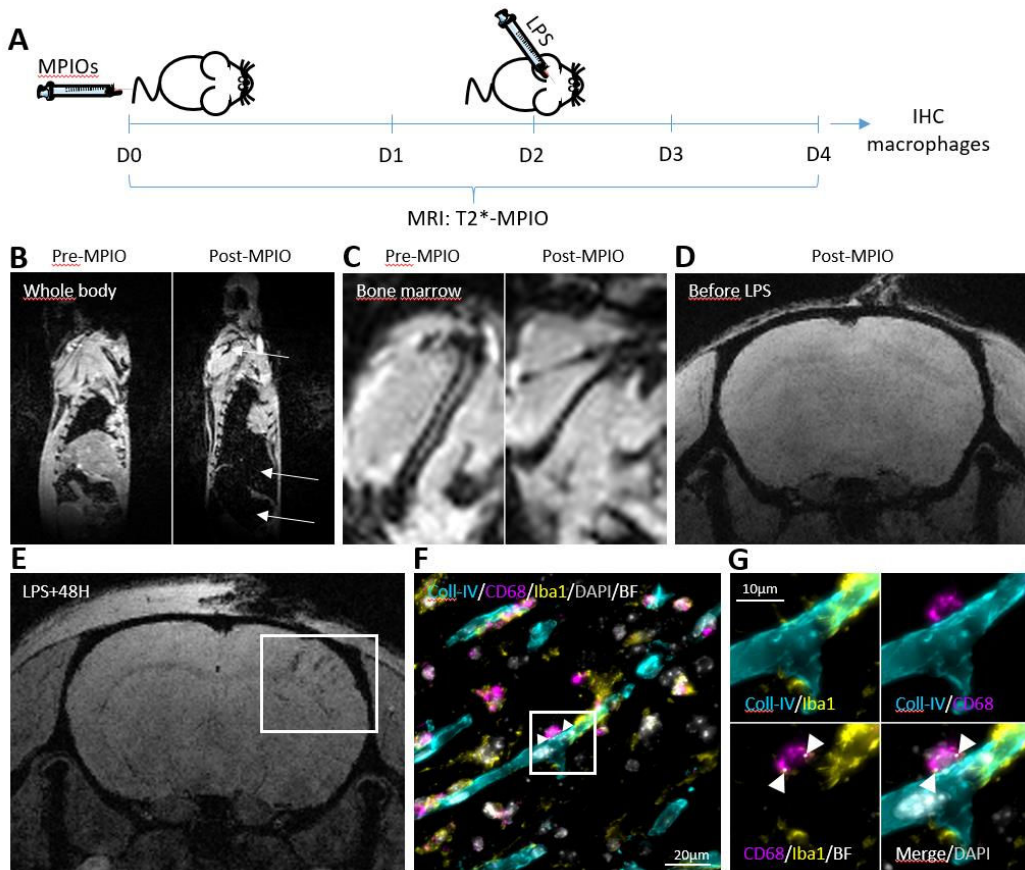


Figure 53 : MPIO-labelled macrophages are recruited after brain infection. (A) Experimental design. (B and C) Whole body MRI sequences allowing the visualization of MPIO accumulated on (B) liver and spleen (arrows) and (C) bone marrow. (D et E) Representative T2\*-weighted MRI sequences. (D) Any MPIO were detected before intracortical LPS injection (E) but hiposignals were detected on the ipsilateral cortex 48h after LPS injection. (F) Representative photomicrograph obtained by epifluorescence microscopy of a macrophage (CD68 positive) which phagocytized MPIOs and located along a blood vessel. (G) High magnification of (F). Work in process.

We therefore performed an intracerebroventricular injection of liposomes containing PBS or clodronate in order to deplete PVM. We observed a significant decrease in the infiltration of immune cells, both CD45 positive (corresponding to all of the myeloid cells) and MPO positive (corresponding to neutrophils) in PVM-depleted mice (Figure 54).

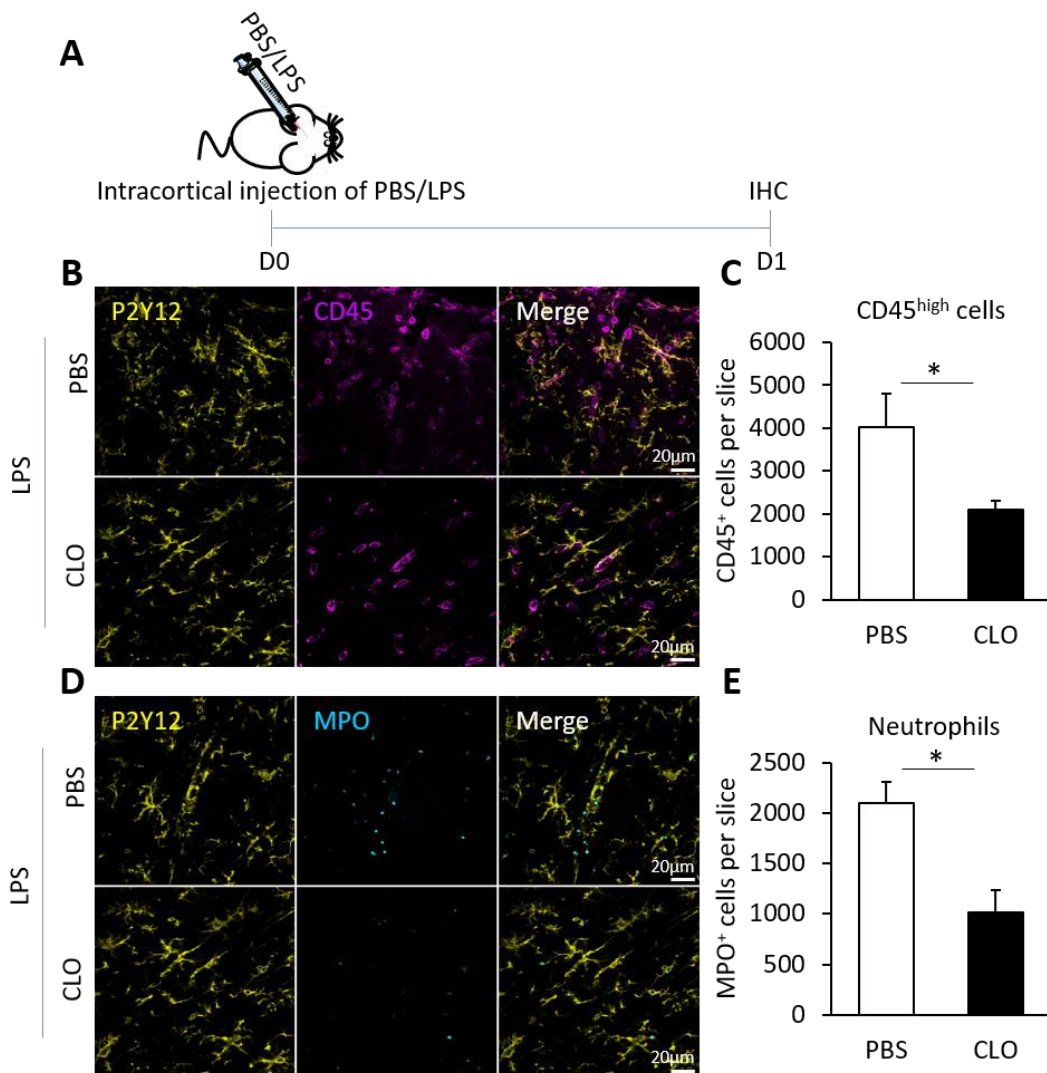


Figure 54 : PVM mediate leukocyte recruitment after brain infection. (A) Experimental design. (B-E) Representative images are obtained only on LPS-treated mice. (B) Representative photomicrographs of CD45 positive cells (magenta). (C) Quantification of CD45 positive cells. (D) Representative photomicrographs of MPO positive cells. (E) Quantification of MPO positive cells. N=4-5 mice per group, p<0.05 vs PBS, Mann-Whitney test. Work in process.

Interestingly, we do not observe the same effect of PVM depletion as in the context of stroke. Our results show, in the context of stroke and in naive conditions, that the **PVM seem rather to play a role of moderator of the infiltration of immune cells, whereas they seem to play the role**

**of mediators in a case of brain infection.** By contrast, the study conducted by Pedragosa and colleagues describes a decrease of MPO positive cells (neutrophils) 24 hours after stroke onset (Pedragosa et al., 2018). This again shows the variability of the inflammatory response according to the experimental model used.

## V. General conclusion

The inflammatory response can be induced by a wide variety of stimuli, ranging from infection to injury. This response is very heterogeneous in terms of cell types and molecular mediators involved. Furthermore, this response can be acute or chronic, local or systemic. This variety of inflammatory responses are in some cases difficult to detect and diagnose, particularly at the CNS level. The goal of my PhD work was to detect and describe the inflammatory reactions induced by an acute CNS injury (ischemic stroke); a chronic central and systemic injury (provoked by chronic alcohol consumption); and a chronic CNS injury (mild traumatic brain injury).

During this work, we show that:

- (i) the thromboembolic model of stroke consisting of the *in situ* formation of a fibrin-rich clot directly into the MCA, appears to be a relevant and clinically relevant experimental model for studying the pathophysiology of stroke and for testing immunomodulatory treatments.
- (ii) chronic alcohol consumption provokes an inflammatory priming at the parenchymal, perivascular and endothelial levels in the brain. This neurovascular priming exacerbates the inflammatory response and could aggravate stroke lesions. These data have an important clinical relevance, since we have also shown in patients an aggravation of stroke lesion volume in heavy drinker stroke patients.
- (iii) perivascular macrophages (PVM) mediate the exacerbated inflammatory response induced by excessive alcohol consumption.
- (iv) a single mild acute TBI may also induce brain inflammatory priming, detectable with TSPO radioligand. PET (positron emission tomography) imaging could become a clinical diagnostic tool for the detection of priming.

# Références bibliographiques



Alfonso-Loeches, S., Pascual-Lucas, M., Blanco, A.M., Sanchez-Vera, I., and Guerri, C. (2010). Pivotal Role of TLR4 Receptors in Alcohol-Induced Neuroinflammation and Brain Damage. *Journal of Neuroscience* 30, 8285–8295.

Anthony, I.C., Crawford, D.H., and Bell, J.E. (2003). B lymphocytes in the normal brain: contrasts with HIV-associated lymphoid infiltrates and lymphomas. *Brain* 126, 1058–1067.

Arac, A., Grimaldeston, M.A., Nepomuceno, A.R.B., Olayiwola, O., Pereira, M.P., Nishiyama, Y., Tsykin, A., Goodall, G.J., Schlecht, U., Vogel, H., et al. (2014). Evidence that Meningeal Mast Cells Can Worsen Stroke Pathology in Mice. *The American Journal of Pathology* 184, 2493–2504.

Armstrong, R.C., Mierzwa, A.J., Marion, C.M., and Sullivan, G.M. (2016). White matter involvement after TBI: Clues to axon and myelin repair capacity. *Exp. Neurol.* 275 Pt 3, 328–333.

Attella, M.J., Nattinville, A., and Stein, D.G. (1987). Hormonal state affects recovery from frontal cortex lesions in adult female rats. *Behav. Neural Biol.* 48, 352–367.

Audoy-Rémus, J., Richard, J.-F., Soulet, D., Zhou, H., Kubes, P., and Vallières, L. (2008). Rod-Shaped monocytes patrol the brain vasculature and give rise to perivascular macrophages under the influence of proinflammatory cytokines and angiopoietin-2. *J. Neurosci.* 28, 10187–10199.

Bachstetter, A.D., Xing, B., de Almeida, L., Dimayuga, E.R., Watterson, D.M., and Van Eldik, L.J. (2011). Microglial p38 $\alpha$  MAPK is a key regulator of proinflammatory cytokine up-regulation induced by toll-like receptor (TLR) ligands or beta-amyloid (A $\beta$ ). *Journal of Neuroinflammation* 8, 79.

Bachstetter, A.D., Rowe, R.K., Kaneko, M., Goulding, D., Lifshitz, J., and Eldik, L.J.V. (2013). The p38 $\alpha$  MAPK Regulates Microglial Responsiveness to Diffuse Traumatic Brain Injury. *J. Neurosci.* 33, 6143–6153.

Banwell, V., Sena, E.S., and Macleod, M.R. (2009). Systematic review and stratified meta-analysis of the efficacy of interleukin-1 receptor antagonist in animal models of stroke. *J Stroke Cerebrovasc Dis* 18, 269–276.

Bechmann, I., Kwidzinski, E., Kovac, A.D., Simbürger, E., Horvath, T., Gimsa, U., Dirnagl, U., Priller, J., and Nitsch, R. (2001a). Turnover of Rat Brain Perivascular Cells. *Experimental Neurology* 168, 242–249.

Bechmann, I., Priller, J., Kovac, A., Böntert, M., Wehner, T., Klett, F.F., Bohsung, J., Stuschke, M., Dirnagl, U., and Nitsch, R. (2001b). Immune surveillance of mouse brain perivascular spaces by blood-borne macrophages. *Eur. J. Neurosci.* 14, 1651–1658.

Becker, K., Kindrick, D., Relton, J., Harlan, J., and Winn, R. (2001). Antibody to the alpha4 integrin decreases infarct size in transient focal cerebral ischemia in rats. *Stroke* 32, 206–211.

Beier, J.I., and McClain, C.J. (2010). Mechanisms and cell signaling in alcoholic liver disease. *Biological Chemistry* 391.

Benakis, C., Garcia-Bonilla, L., Iadecola, C., and Anrather, J. (2015). The role of microglia and myeloid immune cells in acute cerebral ischemia. *Frontiers in Cellular Neuroscience* 8.

Bi, M., Gladbach, A., van Eersel, J., Ittner, A., Przybyla, M., van Hummel, A., Chua, S.W., van der Hoven, J., Lee, W.S., Müller, J., et al. (2017). Tau exacerbates excitotoxic brain damage in an animal model of stroke. *Nature Communications* 8.

Blinzinger, K., and Kreutzberg, G. (1968). Displacement of synaptic terminals from regenerating motoneurons by microglial cells. *Zeitschrift Für Zellforschung Und Mikroskopische Anatomie* 85, 145–157.

Blumbergs, P.C., Scott, G., Vis, J.M., Wainwright, H., Simpson, D.A., and McLEAN, A.J. (1995). Topography of Axonal Injury as Defined by Amyloid Precursor Protein and the Sector Scoring Method in Mild and Severe Closed Head Injury. *Journal of Neurotrauma* 12, 565–572.

Bombardier, C.H., Fann, J.R., Temkin, N.R., Esselman, P.C., Barber, J., and Dikmen, S.S. (2010). Rates of major depressive disorder and clinical outcomes following traumatic brain injury. *JAMA* 303, 1938–1945.

Bonnard, T., and Hagemeyer, C.E. (2015). Ferric Chloride-induced Thrombosis Mouse Model on Carotid Artery and Mesentery Vessel. *J Vis Exp* e52838.

Bowes, M.P., Rothlein, R., Fagan, S.C., and Zivin, J.A. (1995). Monoclonal antibodies preventing leukocyte activation reduce experimental neurologic injury and enhance efficacy of thrombolytic therapy. *Neurology* 45, 815–819.

Bowman, C.L., Ding, J.-P., Sachs, F., and Sokabe, M. (1992). Mechanotransducing ion channels in astrocytes. *Brain Research* 584, 272–286.

Bracard, S., Ducrocq, X., Mas, J.L., Soudant, M., Oppenheim, C., Moulin, T., Guillemin, F., and THRACE investigators (2016). Mechanical thrombectomy after intravenous alteplase versus alteplase alone after stroke (THRACE): a randomised controlled trial. *Lancet Neurol* 15, 1138–1147.

Brown, G.C., and Neher, J.J. (2014). Microglial phagocytosis of live neurons. *Nat. Rev. Neurosci.* 15, 209–216.

Browne, K.D., Chen, X.-H., Meaney, D.F., and Smith, D.H. (2011). Mild traumatic brain injury and diffuse axonal injury in swine. *J. Neurotrauma* 28, 1747–1755.

Burda, J.E., Bernstein, A.M., and Sofroniew, M.V. (2016). Astrocyte roles in traumatic brain injury. *Exp. Neurol.* 275 Pt 3, 305–315.

Bush, T.G., Puvanachandra, N., Horner, C.H., Polito, A., Ostenfeld, T., Svendsen, C.N., Mucke, L., Johnson, M.H., and Sofroniew, M.V. (1999). Leukocyte Infiltration, Neuronal Degeneration, and Neurite Outgrowth after Ablation of Scar-Forming, Reactive Astrocytes in Adult Transgenic Mice. *Neuron* 23, 297–308.

Caravagna, C., Jaouën, A., Desplat-Jégo, S., Fenrich, K.K., Bergot, E., Luche, H., Grenot, P., Rougon, G., Malissen, M., and Debarbieux, F. (2018). Diversity of innate immune cell subsets across spatial and temporal scales in an EAE mouse model. *Sci Rep* 8, 5146.

Cardona, A.E., Pioro, E.P., Sasse, M.E., Kostenko, V., Cardona, S.M., Dijkstra, I.M., Huang, D., Kidd, G., Dombrowski, S., Dutta, R., et al. (2006). Control of microglial neurotoxicity by the fractalkine receptor. *Nature Neuroscience* 9, 917–924.

Carlos, T.M., Clark, R.S., Franicola-Higgins, D., Schidling, J.K., and Kochanek, P.M. (1997). Expression of endothelial adhesion molecules and recruitment of neutrophils after traumatic brain injury in rats. *J. Leukoc. Biol.* 61, 279–285.

Chen, G., Zhang, S., Shi, J., Ai, J., Qi, M., and Hang, C. (2009). Simvastatin reduces secondary brain injury caused by cortical contusion in rats: possible involvement of TLR4/NF- $\kappa$ B pathway. *Exp. Neurol.* 216, 398–406.

Chen, S.-F., Hung, T.-H., Chen, C.-C., Lin, K.-H., Huang, Y.-N., Tsai, H.-C., and Wang, J.-Y. (2007). Lovastatin improves histological and functional outcomes and reduces inflammation after experimental traumatic brain injury. *Life Sci.* 81, 288–298.

Chinnery, H.R., Ruitenberg, M.J., and McMenamin, P.G. (2010). Novel characterization of monocyte-derived cell populations in the meninges and choroid plexus and their rates of replenishment in bone marrow chimeric mice. *J. Neuropathol. Exp. Neurol.* 69, 896–909.

Chu, H.X., Kim, H.A., Lee, S., Moore, J.P., Chan, C.T., Vinh, A., Gelderblom, M., Arumugam, T.V., Broughton, B.R.S., Drummond, G.R., et al. (2014). Immune cell infiltration in malignant middle cerebral artery infarction: comparison with transient cerebral ischemia. *J. Cereb. Blood Flow Metab.* 34, 450–459.

Cobb, M.I.-P.H., Bruce, D.J., Graffagnino, C., and Hauck, E.F. (2017). Symbiotic relationship of IV-tPA and mechanical thrombectomy in a case of acute tandem ICA-MCA occlusion. *J Clin Neurosci* 38, 68–71.

Coughlin, J.M., Wang, Y., Munro, C.A., Ma, S., Yue, C., Chen, S., Airan, R., Kim, P.K., Adams, A.V., Garcia, C., et al. (2015). Neuroinflammation and brain atrophy in former NFL players: An in vivo multimodal imaging pilot study. *Neurobiol. Dis.* 74, 58–65.

Cunningham, A.S., Salvador, R., Coles, J.P., Chatfield, D.A., Bradley, P.G., Johnston, A.J., Steiner, L.A., Fryer, T.D., Aigbirhio, F.I., Smielewski, P., et al. (2005). Physiological thresholds for irreversible tissue damage in contusional regions following traumatic brain injury. *Brain* 128, 1931–1942.

Cunningham, C., Boche, D., and Perry, V.H. (2002). Transforming growth factor beta1, the dominant cytokine in murine prion disease: influence on inflammatory cytokine synthesis and alteration of vascular extracellular matrix. *Neuropathol. Appl. Neurobiol.* 28, 107–119.

D'Agostino, P.M., Gottfried-Blackmore, A., Anandasabapathy, N., and Bulloch, K. (2012). Brain dendritic cells: biology and pathology. *Acta Neuropathol.* 124, 599–614.

Daly, S., Thorpe, M., Rockswold, S., Hubbard, M., Bergman, T., Samadani, U., and Rockswold, G. (2018). Hyperbaric Oxygen Therapy in the Treatment of Acute Severe Traumatic Brain Injury: A Systematic Review. *J. Neurotrauma* 35, 623–629.

Deczkowska, A., Baruch, K., and Schwartz, M. (2016). Type I/II Interferon Balance in the Regulation of Brain Physiology and Pathology. *Trends in Immunology* 37, 181–192.

Deddens, L.H., van Tilborg, G.A.F., van der Marel, K., Hunt, H., van der Toorn, A., Viergever, M.A., de Vries, H.E., and Dijkhuizen, R.M. (2017). In Vivo Molecular MRI of ICAM-1 Expression on Endothelium and Leukocytes from Subacute to Chronic Stages After Experimental Stroke. *Transl Stroke Res.*

Denes, A., Vidyasagar, R., Feng, J., Narvainen, J., McColl, B.W., Kauppinen, R.A., and Allan, S.M. (2007). Proliferating resident microglia after focal cerebral ischaemia in mice. *J. Cereb. Blood Flow Metab.* 27, 1941–1953.

Deoke, A., Deoke, S., Saoji, A., and Hajare, S. (2012). Profile of Modifiable and Non-Modifiable Risk Factors in Stroke in a Rural Based Tertiary Care Hospital – A Case Control Study. *Glob J Health Sci* 4, 158–163.

DeWitt, D.S., and Prough, D.S. (2009). Blast-induced brain injury and posttraumatic hypotension and hypoxemia. *J. Neurotrauma* 26, 877–887.

Dirnagl, U., Iadecola, C., and Moskowitz, M.A. (1999). Pathobiology of ischaemic stroke: an integrated view. *Trends Neurosci.* 22, 391–397.

D'Mello, C., and Swain, M.G. (2017). Immune-to-Brain Communication Pathways in Inflammation-Associated Sickness and Depression. *Curr Top Behav Neurosci* 31, 73–94.

D'Mello, C., Le, T., and Swain, M.G. (2009). Cerebral Microglia Recruit Monocytes into the Brain in Response to Tumor Necrosis Factor Signaling during Peripheral Organ Inflammation. *Journal of Neuroscience* 29, 2089–2102.

D'Mello, C., Riazi, K., Le, T., Stevens, K.M., Wang, A., McKay, D.M., Pittman, Q.J., and Swain, M.G. (2013). P-selectin-mediated monocyte-cerebral endothelium adhesive interactions link peripheral organ inflammation to sickness behaviors. *J. Neurosci.* 33, 14878–14888.

Dobrovolskaia, M.A., and Vogel, S.N. (2002). Toll receptors, CD14, and macrophage activation and deactivation by LPS. *Microbes and Infection* 4, 903–914.

Doyle, K.P., Quach, L.N., Sole, M., Axtell, R.C., Nguyen, T.-V.V., Soler-Llavina, G.J., Jurado, S., Han, J., Steinman, L., Longo, F.M., et al. (2015). B-Lymphocyte-Mediated Delayed Cognitive Impairment following Stroke. *Journal of Neuroscience* 35, 2133–2145.

Dreier, J.P., Reiffurth, C., Woitzik, J., Hartings, J.A., Drenckhahn, C., Windler, C., Friedman, A., MacVicar, B., Herreras, O., and COSBID study group (2015). How spreading depolarization can be the pathophysiological correlate of both migraine aura and stroke. *Acta Neurochir. Suppl.* 120, 137–140.

Drieu, A., Martinez de Lizarrondo, S., and Rubio, M. (2017). Stopping Inflammation in Stroke: Role of ST2/IL-33 Signaling. *J. Neurosci.* 37, 9614–9616.

Drieu, A., Levard, D., Vivien, D., and Rubio, M. (2018). Anti-inflammatory treatments for stroke: from bench to bedside. *Ther Adv Neurol Disord* 11, 1756286418789854.

Drouin-Ouellet, J., Sawiak, S.J., Cisbani, G., Lagacé, M., Kuan, W.-L., Saint-Pierre, M., Dury, R.J., Alata, W., St-Amour, I., Mason, S.L., et al. (2015). Cerebrovascular and blood-brain barrier impairments in Huntington's disease: Potential implications for its pathophysiology. *Ann. Neurol.* 78, 160–177.

- Ducroquet, A., Leys, D., Al Saabi, A., Richard, F., Cordonnier, C., Girot, M., Deplanque, D., Casolla, B., Allorge, D., and Bordet, R. (2013). Influence of chronic ethanol consumption on the neurological severity in patients with acute cerebral ischemia. *Stroke* 44, 2324–2326.
- Durrant, W.E., and Dong, X. (2004). Systemic acquired resistance. *Annu Rev Phytopathol* 42, 185–209.
- Engelhardt, B., and Ransohoff, R.M. (2005). The ins and outs of T-lymphocyte trafficking to the CNS: anatomical sites and molecular mechanisms. *Trends Immunol.* 26, 485–495.
- Enlimomab Acute Stroke Trial Investigators (2001). Use of anti-ICAM-1 therapy in ischemic stroke: results of the Enlimomab Acute Stroke Trial. *Neurology* 57, 1428–1434.
- Enzmann, G., Mysiorek, C., Gorina, R., Cheng, Y.-J., Ghavampour, S., Hannocks, M.-J., Prinz, V., Dirnagl, U., Endres, M., Prinz, M., et al. (2013). The neurovascular unit as a selective barrier to polymorphonuclear granulocyte (PMN) infiltration into the brain after ischemic injury. *Acta Neuropathol.* 125, 395–412.
- Enzmann, G.U., Pavlidou, S., Vaas, M., Klohs, J., and Engelhardt, B. (2018). ICAM-1null C57BL/6 Mice Are Not Protected from Experimental Ischemic Stroke. *Transl Stroke Res.*
- Essani, N.A., McGuire, G.M., Manning, A.M., and Jaeschke, H. (1995). Differential induction of mRNA for ICAM-1 and selectins in hepatocytes, Kupffer cells and endothelial cells during endotoxemia. *Biochem. Biophys. Res. Commun.* 211, 74–82.
- Faraco, G., Sugiyama, Y., Lane, D., Garcia-Bonilla, L., Chang, H., Santisteban, M.M., Racchumi, G., Murphy, M., Van Rooijen, N., Anrather, J., et al. (2016). Perivascular macrophages mediate the neurovascular and cognitive dysfunction associated with hypertension. *Journal of Clinical Investigation* 126, 4674–4689.
- Faraco, G., Park, L., Anrather, J., and Iadecola, C. (2017). Brain perivascular macrophages: characterization and functional roles in health and disease. *Journal of Molecular Medicine* 95, 1143–1152.
- Farkas, A., and Kemény, L. (2013). Alcohol, liver, systemic inflammation and skin: a focus on patients with psoriasis. *Skin Pharmacol Physiol* 26, 119–126.
- Feeney, D.M., Boyeson, M.G., Linn, R.T., Murray, H.M., and Dail, W.G. (1981). Responses to cortical injury: I. Methodology and local effects of contusions in the rat. *Brain Res.* 211, 67–77.
- Felipo, V. (2013). Hepatic encephalopathy: effects of liver failure on brain function. *Nature Reviews Neuroscience* 14, 851–858.
- Feng, Y., Liao, S., Wei, C., Jia, D., Wood, K., Liu, Q., Wang, X., Shi, F.-D., and Jin, W.-N. (2017). Infiltration and persistence of lymphocytes during late-stage cerebral ischemia in middle cerebral artery occlusion and photothrombotic stroke models. *J Neuroinflammation* 14, 248.
- Fenn, A.M., Gensel, J.C., Huang, Y., Popovich, P.G., Lifshitz, J., and Godbout, J.P. (2014). Immune activation promotes depression 1 month after diffuse brain injury: a role for primed microglia. *Biol. Psychiatry* 76, 575–584.

Filipowicz, A.R., McGary, C.M., Holder, G.E., Lindgren, A.A., Johnson, E.M., Sugimoto, C., Kuroda, M.J., and Kim, W.-K. (2016). Proliferation of Perivascular Macrophages Contributes to the Development of Encephalitic Lesions in HIV-Infected Humans and in SIV-Infected Macaques. *Scientific Reports* 6.

Fleischhauer, K. (1964). [ON FLUORESCENCE OF PERIVASCULAR CELLS IN THE CAT BRAIN]. *Z Zellforsch Mikrosk Anat* 64, 140–152.

Floyd, C.L., Gorin, F.A., and Lyeth, B.G. Mechanical strain injury increases intracellular sodium and reverses Na<sup>+</sup>/Ca<sup>2+</sup> exchange in cortical astrocytes. *Glia* 51, 35–46.

Flygt, J., Djupsjö, A., Lenne, F., and Marklund, N. Myelin loss and oligodendrocyte pathology in white matter tracts following traumatic brain injury in the rat. *European Journal of Neuroscience* 38, 2153–2165.

Fontes-Júnior, E.A., Maia, C.S.F., Fernandes, L.M.P., Gomes-Leal, W., Costa-Malaquias, A., Lima, R.R., Prediger, R.D., and Crespo-López, M.E. (2016). Chronic Alcohol Intoxication and Cortical Ischemia: Study of Their Comorbidity and the Protective Effects of Minocycline. *Oxid Med Cell Longev* 2016.

Galea, I., Palin, K., Newman, T.A., Van Rooijen, N., Perry, V.H., and Boche, D. (2005). Mannose receptor expression specifically reveals perivascular macrophages in normal, injured, and diseased mouse brain. *Glia* 49, 375–384.

Garcia, J.H., Liu, K.F., and Bree, M.P. (1996). Effects of CD11b/18 monoclonal antibody on rats with permanent middle cerebral artery occlusion. *Am. J. Pathol.* 148, 241–248.

Garcia-Bonilla, L., Faraco, G., Moore, J., Murphy, M., Racchumi, G., Srinivasan, J., Brea, D., Iadecola, C., and Anrather, J. (2016). Spatio-temporal profile, phenotypic diversity, and fate of recruited monocytes into the post-ischemic brain. *Journal of Neuroinflammation* 13.

Garcia-Bonilla, L., Brea, D., Benakis, C., Lane, D., Murphy, M., Moore, J., Racchumi, G., Jiang, X., Iadecola, C., and Anrather, J. (2018). Endogenous protection from ischemic brain injury by preconditioned monocytes. *J. Neurosci.*

Gardiner, C.M., and Mills, K.H.G. (2016). The cells that mediate innate immune memory and their functional significance in inflammatory and infectious diseases. *Semin. Immunol.* 28, 343–350.

Gauberti, M., Montagne, A., Marcos-Contreras, O.A., Le Béhot, A., Maubert, E., and Vivien, D. (2013). Ultra-sensitive molecular MRI of vascular cell adhesion molecule-1 reveals a dynamic inflammatory penumbra after strokes. *Stroke* 44, 1988–1996.

Gauberti, M., Martinez de Lizarrondo, S., Orset, C., and Vivien, D. (2014). Lack of secondary microthrombosis after thrombin-induced stroke in mice and non-human primates. *J. Thromb. Haemost.* 12, 409–414.

Gauberti, M., Fournier, A.P., Docagne, F., Vivien, D., and Martinez de Lizarrondo, S. (2018). Molecular Magnetic Resonance Imaging of Endothelial Activation in the Central Nervous System. *Theranostics* 8, 1195–1212.

- Gautier, S., Ouk, T., Petrault, O., Caron, J., and Bordet, R. (2009). Neutrophils contribute to intracerebral haemorrhages after treatment with recombinant tissue plasminogen activator following cerebral ischaemia. *Br. J. Pharmacol.* *156*, 673–679.
- Gelderblom, M., Leypoldt, F., Steinbach, K., Behrens, D., Choe, C.-U., Siler, D.A., Arumugam, T.V., Orthey, E., Gerloff, C., Tolosa, E., et al. (2009). Temporal and Spatial Dynamics of Cerebral Immune Cell Accumulation in Stroke. *Stroke* *40*, 1849–1857.
- Girard, S., Brough, D., Lopez-Castejon, G., Giles, J., Rothwell, N.J., and Allan, S.M. (2013). Microglia and macrophages differentially modulate cell death after brain injury caused by oxygen-glucose deprivation in organotypic brain slices: Microglial Phenotype and Brain Injury. *Glia* *61*, 813–824.
- Goldmann, T., Wieghofer, P., Jordão, M.J.C., Prutek, F., Hagemeyer, N., Frenzel, K., Amann, L., Staszewski, O., Kierdorf, K., Krueger, M., et al. (2016). Origin, fate and dynamics of macrophages at central nervous system interfaces. *Nature Immunology* *17*, 797–805.
- Goldstein, L.B. (2016). IV tPA for acute ischemic stroke. 2.
- Gomez-Nicola, D., and Perry, V.H. (2015). Microglial dynamics and role in the healthy and diseased brain: a paradigm of functional plasticity. *Neuroscientist* *21*, 169–184.
- Gorina, R., Font-Nieves, M., Márquez-Kisinousky, L., Santalucia, T., and Planas, A.M. Astrocyte TLR4 activation induces a proinflammatory environment through the interplay between MyD88-dependent NF $\kappa$ B signaling, MAPK, and Jak1/Stat1 pathways. *Glia* *59*, 242–255.
- Gottfried-Blackmore, A., Kaunzner, U.W., Idoyaga, J., Felger, J.C., McEwen, B.S., and Bulloch, K. (2009). Acute in vivo exposure to interferon- $\gamma$  enables resident brain dendritic cells to become effective antigen presenting cells. *PNAS* *106*, 20918–20923.
- Graeber, M.B., Streit, W.J., and Kreutzberg, G.W. (1989). Identity of ED2-positive perivascular cells in rat brain. *J. Neurosci. Res.* *22*, 103–106.
- Greter, M., Lelios, I., and Croxford, A.L. (2015). Microglia Versus Myeloid Cell Nomenclature during Brain Inflammation. *Front. Immunol.* *6*.
- Griffith, J.W., Sokol, C.L., and Luster, A.D. (2014). Chemokines and Chemokine Receptors: Positioning Cells for Host Defense and Immunity. *Annual Review of Immunology* *32*, 659–702.
- Hachinski, V.C., Lassen, N.A., and Marshall, J. (1974). Multi-infarct dementia. A cause of mental deterioration in the elderly. *Lancet* *2*, 207–210.
- Hailer, N.P., Bechmann, I., Heizmann, S., and Nitsch, R. (1997). Adhesion molecule expression on phagocytic microglial cells following anterograde degeneration of perforant path axons. *Hippocampus* *7*, 341–349.
- Hall, E.D., Sullivan, P.G., Gibson, T.R., Pavel, K.M., Thompson, B.M., and Scheff, S.W. (2005). Spatial and temporal characteristics of neurodegeneration after controlled cortical impact in mice: more than a focal brain injury. *J. Neurotrauma* *22*, 252–265.

- Hanisch, U.-K., and Kettenmann, H. (2007). Microglia: active sensor and versatile effector cells in the normal and pathologic brain. *Nature Neuroscience* *10*, 1387–1394.
- Harris, A.K., Ergul, A., Kozak, A., Machado, L.S., Johnson, M.H., and Fagan, S.C. (2005). Effect of neutrophil depletion on gelatinase expression, edema formation and hemorrhagic transformation after focal ischemic stroke. *BMC Neurosci* *6*, 49.
- Hayakawa, K., Mishima, K., Nozako, M., Hazekawa, M., Mishima, S., Fujioka, M., Orito, K., Egashira, N., Iwasaki, K., and Fujiwara, M. (2008). Delayed treatment with minocycline ameliorates neurologic impairment through activated microglia expressing a high-mobility group box1-inhibiting mechanism. *Stroke* *39*, 951–958.
- Hayashi, T., Nagai, S., Fujii, H., Baba, Y., Ikeda, E., Kawase, T., and Koyasu, S. (2009). Critical roles of NK and CD8+ T cells in central nervous system listeriosis. *J. Immunol.* *182*, 6360–6368.
- He, J., and Crews, F.T. (2008). Increased MCP-1 and microglia in various regions of the human alcoholic brain. *Experimental Neurology* *210*, 349–358.
- Hennessy, E., Griffin, É.W., and Cunningham, C. (2015). Astrocytes Are Primed by Chronic Neurodegeneration to Produce Exaggerated Chemokine and Cell Infiltration Responses to Acute Stimulation with the Cytokines IL-1 $\beta$  and TNF- $\alpha$ . *J. Neurosci.* *35*, 8411–8422.
- Herz, J., Sabellek, P., Lane, T.E., Gunzer, M., Hermann, D.M., and Doeppner, T.R. (2015). Role of Neutrophils in Exacerbation of Brain Injury After Focal Cerebral Ischemia in Hyperlipidemic Mice. *Stroke* *46*, 2916–2925.
- Hickey, W.F., and Kimura, H. (1988). Perivascular microglial cells of the CNS are bone marrow-derived and present antigen in vivo. *Science* *239*, 290–292.
- Holder, G.E., McGary, C.M., Johnson, E.M., Zheng, R., John, V.T., Sugimoto, C., Kuroda, M.J., and Kim, W.-K. (2014). Expression of the Mannose Receptor CD206 in HIV and SIV Encephalitis: A Phenotypic Switch of Brain Perivascular Macrophages with Virus Infection. *Journal of Neuroimmune Pharmacology* *9*, 716–726.
- Homsi, S., Piaggio, T., Croci, N., Noble, F., Plotkine, M., Marchand-Leroux, C., and Jafarian-Tehrani, M. (2010). Blockade of Acute Microglial Activation by Minocycline Promotes Neuroprotection and Reduces Locomotor Hyperactivity after Closed Head Injury in Mice: A Twelve-Week Follow-Up Study. *Journal of Neurotrauma* *27*, 911–921.
- Hotchkiss, R.S., Monneret, G., and Payen, D. (2013). Sepsis-induced immunosuppression: from cellular dysfunctions to immunotherapy. *Nature Reviews Immunology* *13*, 862–874.
- Hughes, M.M., Field, R.H., Perry, V.H., Murray, C.L., and Cunningham, C. (2010). Microglia in the degenerating brain are capable of phagocytosis of beads and of apoptotic cells, but do not efficiently remove PrPSc, even upon LPS stimulation. *Glia* *58*, 2017–2030.
- Iadecola, C. (2013). The Pathobiology of Vascular Dementia. *Neuron* *80*, 844–866.

Iadecola, C., and Anrather, J. (2011). The immunology of stroke: from mechanisms to translation. *Nat. Med.* 17, 796–808.

Iliff, J.J., Wang, M., Liao, Y., Plogg, B.A., Peng, W., Gundersen, G.A., Benveniste, H., Vates, G.E., Deane, R., Goldman, S.A., et al. (2012). A paravascular pathway facilitates CSF flow through the brain parenchyma and the clearance of interstitial solutes, including amyloid  $\beta$ . *Sci Transl Med* 4, 147ra111.

Janelins, M.C., Mastrangelo, M.A., Park, K.M., Sudol, K.L., Narrow, W.C., Oddo, S., LaFerla, F.M., Callahan, L.M., Federoff, H.J., and Bowers, W.J. (2008). Chronic Neuron-Specific Tumor Necrosis Factor-Alpha Expression Enhances the Local Inflammatory Environment Ultimately Leading to Neuronal Death in 3xTg-AD Mice. *Am J Pathol* 173, 1768–1782.

Jiang, N., Chopp, M., and Chahwala, S. (1998). Neutrophil inhibitory factor treatment of focal cerebral ischemia in the rat. *Brain Res.* 788, 25–34.

Jin, A.Y., Tuor, U.I., Rushforth, D., Kaur, J., Muller, R.N., Petterson, J.L., Boutry, S., and Barber, P.A. (2010). Reduced blood brain barrier breakdown in P-selectin deficient mice following transient ischemic stroke: a future therapeutic target for treatment of stroke. *BMC Neurosci* 11, 12.

Jin, W.-N., Shi, S.X.-Y., Li, Z., Li, M., Wood, K., Gonzales, R.J., and Liu, Q. (2017). Depletion of microglia exacerbates postischemic inflammation and brain injury. *J Cereb Blood Flow Metab* 37, 2224–2236.

Kadlecová, P., Andel, R., Mikulík, R., Handing, E.P., and Pedersen, N.L. (2015a). Alcohol consumption at midlife and risk of stroke during 43 years of follow-up: cohort and twin analyses. *Stroke* 46, 627–633.

Kadlecová, P., Andel, R., Mikulík, R., Handing, E.P., and Pedersen, N.L. (2015b). Alcohol consumption at midlife and risk of stroke during 43 years of follow-up: cohort and twin analyses. *Stroke* 46, 627–633.

Kane, C.J.M., and Drew, P.D. (2016). Inflammatory responses to alcohol in the CNS: nuclear receptors as potential therapeutics for alcohol-induced neuropathologies. *J. Leukoc. Biol.* 100, 951–959.

Kane, C.J.M., Phelan, K.D., Douglas, J.C., Wagoner, G., Johnson, J.W., Xu, J., Phelan, P.S., and Drew, P.D. (2014). Effects of Ethanol on Immune Response in the Brain: Region-Specific Changes in Adolescent Versus Adult Mice. *Alcoholism: Clinical and Experimental Research* 38, 384–391.

Karatas, H., Erdener, S.E., Gursoy-Ozdemir, Y., Gurer, G., Soylemezoglu, F., Dunn, A.K., and Dalkara, T. (2011). Thrombotic distal middle cerebral artery occlusion produced by topical FeCl(3) application: a novel model suitable for intravital microscopy and thrombolysis studies. *J. Cereb. Blood Flow Metab.* 31, 1452–1460.

Kaunzner, U.W., Miller, M.M., Gottfried-Blackmore, A., Gal-Toth, J., Felger, J.C., McEwen, B.S., and Bulloch, K. (2012). Accumulation of resident and peripheral dendritic cells in the aging CNS. *Neurobiol. Aging* 33, 681–693.e1.

Kawai, T., and Akira, S. (2010). The role of pattern-recognition receptors in innate immunity: update on Toll-like receptors. *Nature Immunology* 11, 373–384.

Keaney, J., and Campbell, M. (2015). The dynamic blood-brain barrier. *FEBS Journal* 282, 4067–4079.

- Keskin, I., Gunal, M.Y., Ayturk, N., Kilic, U., Ozansoy, M., and Kilic, E. (2017). Dose-dependent neuroprotective effect of enoxaparin on cold-induced traumatic brain injury. *Neural Regen Res* 12, 761–764.
- Kisler, K., Nelson, A.R., Rege, S.V., Ramanathan, A., Wang, Y., Ahuja, A., Lazic, D., Tsai, P.S., Zhao, Z., Zhou, Y., et al. (2017). Pericyte degeneration leads to neurovascular uncoupling and limits oxygen supply to brain. *Nat. Neurosci.* 20, 406–416.
- Kleine, T.O. (2015). Cellular immune surveillance of central nervous system bypasses blood–brain barrier and blood–cerebrospinal–fluid barrier: Revealed with the New Marburg cerebrospinal–fluid model in healthy humans. *Cytometry Part A* 87, 227–243.
- Kleinschnitz, C., Kraft, P., Dreykluft, A., Hagedorn, I., Göbel, K., Schuhmann, M.K., Langhauser, F., Helluy, X., Schwarz, T., Bittner, S., et al. (2013). Regulatory T cells are strong promoters of acute ischemic stroke in mice by inducing dysfunction of the cerebral microvasculature. *Blood* 121, 679–691.
- Kohler, E., Prentice, D.A., Bates, T.R., Hankey, G.J., Claxton, A., van Heerden, J., and Blacker, D. (2013). Intravenous minocycline in acute stroke: a randomized, controlled pilot study and meta-analysis. *Stroke* 44, 2493–2499.
- Kolakowsky-Hayner, S.A., Gourley, E.V., Kreutzer, J.S., Marwitz, J.H., Cifu, D.X., and McKinley, W.O. (1999). Pre-injury substance abuse among persons with brain injury and persons with spinal cord injury. *Brain Inj* 13, 571–581.
- Korcyn, A.D. (2015). Vascular parkinsonism—characteristics, pathogenesis and treatment. *Nature Reviews Neurology* 11, 319–326.
- Kostulas, N., Li, H.-L., Xiao, B.-G., Huang, Y.-M., Kostulas, V., and Link, H. (2002). Dendritic cells are present in ischemic brain after permanent middle cerebral artery occlusion in the rat. *Stroke* 33, 1129–1134.
- Kovesdi, E., Kamnaksh, A., Wingo, D., Ahmed, F., Grunberg, N.E., Long, J.B., Kasper, C.E., and Agoston, D.V. (2012). Acute minocycline treatment mitigates the symptoms of mild blast-induced traumatic brain injury. *Front Neurol* 3, 111.
- Krabbe, G., Minami, S.S., Etchegaray, J.I., Taneja, P., Djukic, B., Davalos, D., Le, D., Lo, I., Zhan, L., Reichert, M.C., et al. (2017). Microglial NF $\kappa$ B-TNF $\alpha$  hyperactivation induces obsessive-compulsive behavior in mouse models of progranulin-deficient frontotemporal dementia. *PNAS* 201700477.
- Kristián, T., and Siesjö, B.K. (1996). Calcium-related damage in ischemia. *Life Sciences* 59, 357–367.
- Kumasaka, K., Marks, J.A., Eisenstadt, R., Murcy, M.A., Samadi, D., Li, S., Johnson, V., Browne, K.D., Smith, D.H., Schwab, C.W., et al. (2014). In vivo leukocyte-mediated brain microcirculatory inflammation: a comparison of osmotherapies and progesterone in severe traumatic brain injury. *Am. J. Surg.* 208, 961–968; discussion 967–968.
- Labat-gest, V., and Tomasi, S. (2013). Photothrombotic ischemia: a minimally invasive and reproducible photochemical cortical lesion model for mouse stroke studies. *J Vis Exp.*

Lacy, P. (2006). Mechanisms of degranulation in neutrophils. *Allergy Asthma Clin Immunol* 2, 98–108.

Lalancette-Hébert, M., Gowing, G., Simard, A., Weng, Y.C., and Kriz, J. (2007). Selective ablation of proliferating microglial cells exacerbates ischemic injury in the brain. *J. Neurosci.* 27, 2596–2605.

Lampl, Y., Boaz, M., Gilad, R., Lorberboym, M., Dabby, R., Rapoport, A., Anca-Hershkowitz, M., and Sadeh, M. (2007). Minocycline treatment in acute stroke: an open-label, evaluator-blinded study. *Neurology* 69, 1404–1410.

Langlois, J.A., Rutland-Brown, W., and Wald, M.M. (2006). The epidemiology and impact of traumatic brain injury: a brief overview. *J Head Trauma Rehabil* 21, 375–378.

Lapergue, B., Labreuche, J., Blanc, R., Barreau, X., Berge, J., Consoli, A., Rodesch, G., Saleme, S., Costalat, V., Bracard, S., et al. (2018). First-line use of contact aspiration for thrombectomy versus a stent retriever for recanalization in acute cerebral infarction: The randomized ASTER study protocol. *Int J Stroke* 13, 87–95.

Lawrence, T. (2016). Coordinated Regulation of Signaling Pathways during Macrophage Activation. *Microbiol Spectr* 4.

Lawrence, T., Willoughby, D.A., and Gilroy, D.W. (2002). Anti-inflammatory lipid mediators and insights into the resolution of inflammation. *Nat. Rev. Immunol.* 2, 787–795.

Lawson, L.J., Perry, V.H., and Gordon, S. (1992). Turnover of resident microglia in the normal adult mouse brain. *Neuroscience* 48, 405–415.

Le Behot, A., Gauberti, M., Martinez De Lizarrondo, S., Montagne, A., Lemarchand, E., Repesse, Y., Guillou, S., Denis, C.V., Maubert, E., Orset, C., et al. (2014). GpIba $\alpha$ -VWF blockade restores vessel patency by dissolving platelet aggregates formed under very high shear rate in mice. *Blood* 123, 3354–3363.

Leclercq, S., De Saeger, C., Delzenne, N., de Timary, P., and Stärkel, P. (2014). Role of Inflammatory Pathways, Blood Mononuclear Cells, and Gut-Derived Bacterial Products in Alcohol Dependence. *Biological Psychiatry* 76, 725–733.

Lehmann, J., Härtig, W., Seidel, A., Füldner, C., Hobohm, C., Grosche, J., Krueger, M., and Michalski, D. (2014). Inflammatory cell recruitment after experimental thromboembolic stroke in rats. *Neuroscience* 279, 139–154.

Lemarchand, E., Gauberti, M., Martinez de Lizarrondo, S., Villain, H., Repessé, Y., Montagne, A., Vivien, D., Ali, C., and Rubio, M. (2015). Impact of alcohol consumption on the outcome of ischemic stroke and thrombolysis: role of the hepatic clearance of tissue-type plasminogen activator. *Stroke* 46, 1641–1650.

Li, Y., and Chopp, M. (1999). Temporal profile of nestin expression after focal cerebral ischemia in adult rat. *Brain Research* 838, 1–10.

Liddelow, S.A. (2011). Fluids and barriers of the CNS: a historical viewpoint. *Fluids Barriers CNS* 8, 2.

Liesz, A., Suri-Payer, E., Veltkamp, C., Doerr, H., Sommer, C., Rivest, S., Giese, T., and Veltkamp, R. (2009). Regulatory T cells are key cerebroprotective immunomodulators in acute experimental stroke. *Nat. Med.* 15, 192–199.

Liesz, A., Zhou, W., Mracskó, É., Karcher, S., Bauer, H., Schwarting, S., Sun, L., Bruder, D., Stegemann, S., Cerwenka, A., et al. (2011). Inhibition of lymphocyte trafficking shields the brain against deleterious neuroinflammation after stroke. *Brain* 134, 704–720.

Liesz, A., Zhou, W., Na, S.-Y., Hämmерling, G.J., Garbi, N., Karcher, S., Mracsko, E., Backs, J., Rivest, S., and Veltkamp, R. (2013). Boosting regulatory T cells limits neuroinflammation in permanent cortical stroke. *J. Neurosci.* 33, 17350–17362.

Lin, J.W., Tsai, J.T., Lee, L.M., Lin, C.M., Hung, C.C., Hung, K.S., Chen, W.Y., Wei, L., Ko, C.P., Su, Y.K., et al. (2008). Effect of hyperbaric oxygen on patients with traumatic brain injury. *Acta Neurochir. Suppl.* 101, 145–149.

Lippai, D., Bala, S., Csak, T., Kurt-Jones, E.A., and Szabo, G. (2013a). Chronic Alcohol-Induced microRNA-155 Contributes to Neuroinflammation in a TLR4-Dependent Manner in Mice. *PLoS ONE* 8, e70945.

Lippai, D., Bala, S., Petrasek, J., Csak, T., Levin, I., Kurt-Jones, E.A., and Szabo, G. (2013b). Alcohol-induced IL-1 $\beta$  in the brain is mediated by NLRP3/ASC inflammasome activation that amplifies neuroinflammation. *J. Leukoc. Biol.* 94, 171–182.

Lipton, M.L., Gellella, E., Lo, C., Gold, T., Ardekani, B.A., Shifteh, K., Bello, J.A., and Branch, C.A. (2008). Multifocal white matter ultrastructural abnormalities in mild traumatic brain injury with cognitive disability: a voxel-wise analysis of diffusion tensor imaging. *J. Neurotrauma* 25, 1335–1342.

Liu, C., Wu, C., Yang, Q., Gao, J., Li, L., Yang, D., and Luo, L. (2016). Macrophages Mediate the Repair of Brain Vascular Rupture through Direct Physical Adhesion and Mechanical Traction. *Immunity* 44, 1162–1176.

Liu, G.-J., Middleton, R.J., Hatty, C.R., Kam, W.W.-Y., Chan, R., Pham, T., Harrison-Brown, M., Dodson, E., Veale, K., and Banati, R.B. (2014). The 18 kDa Translocator Protein, Microglia and Neuroinflammation: TSPO, Microglia and Neuroinflammation. *Brain Pathology* 24, 631–653.

Liu, Y., Jacobowitz, D.M., Barone, F., McCarron, R., Spatz, M., Feuerstein, G., Hallenbeck, J.M., and Sirén, A.-L. (1994). Quantitation of Perivascular Monocytes and Macrophages around Cerebral Blood Vessels of Hypertensive and Aged Rats. *Journal of Cerebral Blood Flow & Metabolism* 14, 348–352.

Liu, Z., Li, Y., Cui, Y., Roberts, C., Lu, M., Wilhelmsson, U., Pekny, M., and Chopp, M. Beneficial effects of gfap/vimentin reactive astrocytes for axonal remodeling and motor behavioral recovery in mice after stroke. *Glia* 62, 2022–2033.

Llovera, G., Benakis, C., Enzmann, G., Cai, R., Arzberger, T., Ghasemigharagoz, A., Mao, X., Malik, R., Lazarevic, I., Liebscher, S., et al. (2017). The choroid plexus is a key cerebral invasion route for T cells after stroke. *Acta Neuropathologica* 134, 851–868.

Loane, D.J., and Faden, A.I. (2010). Neuroprotection for traumatic brain injury: translational challenges and emerging therapeutic strategies. *Trends Pharmacol. Sci.* 31, 596–604.

- Loane, D.J., Kumar, A., Stoica, B.A., Cabatbat, R., and Faden, A.I. (2014). Progressive neurodegeneration after experimental brain trauma: association with chronic microglial activation. *J. Neuropathol. Exp. Neurol.* *73*, 14–29.
- Lobsien, D., Gawlitza, M., Schaudinn, A., Schob, S., Hobohm, C., Fritzsch, D., Quäschling, U., Hoffmann, K.-T., and Friedrich, B. (2016). Mechanical thrombectomy versus systemic thrombolysis in MCA stroke: a distance to thrombus-based outcome analysis. *Journal of NeuroInterventional Surgery* *8*, 878–882.
- Loftis, J.M., Huckans, M., Ruimy, S., Hinrichs, D.J., and Hauser, P. (2008). Depressive symptoms in patients with chronic hepatitis C are correlated with elevated plasma levels of interleukin-1beta and tumor necrosis factor-alpha. *Neurosci. Lett.* *430*, 264–268.
- Louvet, A., and Mathurin, P. (2015). Alcoholic liver disease: mechanisms of injury and targeted treatment. *Nat Rev Gastroenterol Hepatol* *12*, 231–242.
- Lu, D., Goussev, A., Chen, J., Pannu, P., Li, Y., Mahmood, A., and Chopp, M. (2004). Atorvastatin reduces neurological deficit and increases synaptogenesis, angiogenesis, and neuronal survival in rats subjected to traumatic brain injury. *J. Neurotrauma* *21*, 21–32.
- Lundgaard, I., Wang, W., Eberhardt, A., Vinitsky, H.S., Reeves, B.C., Peng, S., Lou, N., Hussain, R., and Nedergaard, M. (2018). Beneficial effects of low alcohol exposure, but adverse effects of high alcohol intake on glymphatic function. *Sci Rep* *8*, 2246.
- Macrez, R., Ali, C., Toutirais, O., Le Mauff, B., Defer, G., Dirnagl, U., and Vivien, D. (2011). Stroke and the immune system: from pathophysiology to new therapeutic strategies. *Lancet Neurol* *10*, 471–480.
- Marelli-Berg, F.M., Clement, M., Mauro, C., and Caligiuri, G. (2013). An immunologist's guide to CD31 function in T-cells. *J Cell Sci* *126*, 2343–2352.
- Margulies, S., Hicks, R., and Combination Therapies for Traumatic Brain Injury Workshop Leaders (2009). Combination therapies for traumatic brain injury: prospective considerations. *J. Neurotrauma* *26*, 925–939.
- Marmarou, A., Foda, M.A., van den Brink, W., Campbell, J., Kita, H., and Demetriadou, K. (1994). A new model of diffuse brain injury in rats. Part I: Pathophysiology and biomechanics. *J. Neurosurg.* *80*, 291–300.
- Mato, M., Ookawara, S., and Kurihara, K. (1980). Uptake of exogenous substances and marked infoldings of the fluorescent granular pericyte in cerebral fine vessels. *Am. J. Anat.* *157*, 329–332.
- Matsukawa, N., Yasuhara, T., Hara, K., Xu, L., Maki, M., Yu, G., Kaneko, Y., Ojika, K., Hess, D.C., and Borlongan, C.V. (2009). Therapeutic targets and limits of minocycline neuroprotection in experimental ischemic stroke. *BMC Neurosci* *10*, 126.
- Matsuo, Y., Onodera, H., Shiga, Y., Nakamura, M., Ninomiya, M., Kihara, T., and Kogure, K. (1994). Correlation between myeloperoxidase-quantified neutrophil accumulation and ischemic brain injury in the rat. Effects of neutrophil depletion. *Stroke* *25*, 1469–1475.

- Mazzeo, A.T., Alves, O.L., Gilman, C.B., Hayes, R.L., Tolias, C., Niki Kunene, K., and Ross Bullock, M. (2008). Brain metabolic and hemodynamic effects of cyclosporin A after human severe traumatic brain injury: a microdialysis study. *Acta Neurochir (Wien)* *150*, 1019–1031; discussion 1031.
- McIntosh, T.K., Vink, R., Noble, L., Yamakami, I., Fernyak, S., Soares, H., and Faden, A.L. (1989). Traumatic brain injury in the rat: characterization of a lateral fluid-percussion model. *Neuroscience* *28*, 233–244.
- McMenamin, P.G. (1999). Distribution and phenotype of dendritic cells and resident tissue macrophages in the dura mater, leptomeninges, and choroid plexus of the rat brain as demonstrated in wholemount preparations. *J. Comp. Neurol.* *405*, 553–562.
- Mierzwa, A.J., Marion, C.M., Sullivan, G.M., McDaniel, D.P., and Armstrong, R.C. (2015). Components of myelin damage and repair in the progression of white matter pathology after mild traumatic brain injury. *J. Neuropathol. Exp. Neurol.* *74*, 218–232.
- Miller, S.I., Ernst, R.K., and Bader, M.W. (2005). LPS, TLR4 and infectious disease diversity. *Nature Reviews Microbiology* *3*, 36–46.
- Mistry, E.A., Mistry, A.M., Nakawah, M.O., Chitale, R.V., James, R.F., Volpi, J.J., and Fusco, M.R. (2017). Mechanical Thrombectomy Outcomes With and Without Intravenous Thrombolysis in Stroke Patients: A Meta-Analysis. *Stroke* *48*, 2450–2456.
- Montagne, A., Gauberti, M., Macrez, R., Jullienne, A., Briens, A., Raynaud, J.-S., Louin, G., Buisson, A., Haelewyn, B., Docagne, F., et al. (2012). Ultra-sensitive molecular MRI of cerebrovascular cell activation enables early detection of chronic central nervous system disorders. *NeuroImage* *63*, 760–770.
- Morelli, N., Rota, E., Michieletti, E., and Guidetti, D. (2017). Mechanical thrombectomy after intravenous thrombolysis for acute ischaemic stroke. *The Lancet Neurology* *16*, 103–104.
- Mori, S., and Leblond, C.P. (1969). Identification of microglia in light and electron microscopy. *J. Comp. Neurol.* *135*, 57–80.
- Morimoto, N., Shimazawa, M., Yamashima, T., Nagai, H., and Hara, H. (2005). Minocycline inhibits oxidative stress and decreases in vitro and in vivo ischemic neuronal damage. *Brain Res.* *1044*, 8–15.
- Muccigrosso, M.M., Ford, J., Benner, B., Moussa, D., Burnsides, C., Fenn, A.M., Popovich, P.G., Lifshitz, J., Walker, F.R., Eiferman, D.S., et al. (2016). Cognitive deficits develop 1month after diffuse brain injury and are exaggerated by microglia-associated reactivity to peripheral immune challenge. *Brain Behav. Immun.* *54*, 95–109.
- Muller, W.A. (2002). Leukocyte-endothelial cell interactions in the inflammatory response. *Lab. Invest.* *82*, 521–533.
- Murray, P.J., Allen, J.E., Biswas, S.K., Fisher, E.A., Gilroy, D.W., Goerdt, S., Gordon, S., Hamilton, J.A., Ivashkiv, L.B., Lawrence, T., et al. (2014). Macrophage activation and polarization: nomenclature and experimental guidelines. *Immunity* *41*, 14–20.
- Napoli, I., and Neumann, H. (2009). Microglial clearance function in health and disease. *Neuroscience* *158*, 1030–1038.

- National Institute of Neurological Disorders and Stroke rt-PA Stroke Study Group (1995). Tissue plasminogen activator for acute ischemic stroke. *N. Engl. J. Med.* **333**, 1581–1587.
- Neary, J.T., Kang, Y., Tran, M., and Feld, J. (2005). Traumatic Injury Activates Protein Kinase B/Akt in Cultured Astrocytes: Role of Extracellular ATP and P2 Purinergic Receptors. *Journal of Neurotrauma* **22**, 491–500.
- Netea, M.G., Joosten, L.A.B., Latz, E., Mills, K.H.G., Natoli, G., Stunnenberg, H.G., O'Neill, L.A.J., and Xavier, R.J. (2016). Trained immunity: A program of innate immune memory in health and disease. *Science* **352**, aaf1098.
- Neumann, J., Riek-Burchardt, M., Herz, J., Doeppner, T.R., König, R., Hütten, H., Etemire, E., Männ, L., Klingberg, A., Fischer, T., et al. (2015). Very-late-antigen-4 (VLA-4)-mediated brain invasion by neutrophils leads to interactions with microglia, increased ischemic injury and impaired behavior in experimental stroke. *Acta Neuropathol.* **129**, 259–277.
- Niogi, S.N., Mukherjee, P., Ghajar, J., Johnson, C., Kolster, R.A., Sarkar, R., Lee, H., Meeker, M., Zimmerman, R.D., Manley, G.T., et al. (2008). Extent of microstructural white matter injury in postconcussive syndrome correlates with impaired cognitive reaction time: a 3T diffusion tensor imaging study of mild traumatic brain injury. *AJNR Am J Neuroradiol* **29**, 967–973.
- Norden, D.M., and Godbout, J.P. (2013). Review: microglia of the aged brain: primed to be activated and resistant to regulation. *Neuropathol. Appl. Neurobiol.* **39**, 19–34.
- Norden, D.M., Muccigrosso, M.M., and Godbout, J.P. (2015). Microglial priming and enhanced reactivity to secondary insult in aging, and traumatic CNS injury, and neurodegenerative disease. *Neuropharmacology* **96**, 29–41.
- O'Donnell, M.J., Xavier, D., Liu, L., Zhang, H., Chin, S.L., Rao-Melacini, P., Rangarajan, S., Islam, S., Pais, P., McQueen, M.J., et al. (2010). Risk factors for ischaemic and intracerebral haemorrhagic stroke in 22 countries (the INTERSTROKE study): a case-control study. *Lancet* **376**, 112–123.
- O'Leary, J.G., Goodarzi, M., Drayton, D.L., and von Andrian, U.H. (2006). T cell- and B cell-independent adaptive immunity mediated by natural killer cells. *Nat. Immunol.* **7**, 507–516.
- Olivera, G.C., Ren, X., Vodnala, S.K., Lu, J., Coppo, L., Leepiyasakulchai, C., Holmgren, A., Kristensson, K., and Rottenberg, M.E. (2016). Nitric Oxide Protects against Infection-Induced Neuroinflammation by Preserving the Stability of the Blood-Brain Barrier. *PLOS Pathogens* **12**, e1005442.
- Onofre, G., Kolácková, M., Jankovicová, K., and Krejsek, J. (2009). Scavenger receptor CD163 and its biological functions. *Acta Medica (Hradec Kralove)* **52**, 57–61.
- Orset, C., Macrez, R., Young, A.R., Panthou, D., Angles-Cano, E., Maubert, E., Agin, V., and Vivien, D. (2007). Mouse model of in situ thromboembolic stroke and reperfusion. *Stroke* **38**, 2771–2778.
- Orset, C., Haelewyn, B., Allan, S.M., Ansar, S., Campos, F., Cho, T.H., Durand, A., El Amki, M., Fatar, M., Garcia-Yébenes, I., et al. (2016). Efficacy of Alteplase in a Mouse Model of Acute Ischemic Stroke: A Retrospective Pooled Analysis. *Stroke* **47**, 1312–1318.

Ostrow, L.W., Suchyna, T.M., and Sachs, F. (2011). Stretch induced endothelin-1 secretion by adult rat astrocytes involves calcium influx via stretch-activated ion channels (SACs). *Biochemical and Biophysical Research Communications* *410*, 81–86.

Oude Engberink, R.D., Blezer, E.L., Hoff, E.I., van der Pol, S.M., van der Toorn, A., Dijkhuizen, R.M., and de Vries, H.E. (2008). MRI of monocyte infiltration in an animal model of neuroinflammation using SPIO-labeled monocytes or free USPIO. *J. Cereb. Blood Flow Metab.* *28*, 841–851.

Padma Srivastava, M.V., Bhasin, A., Bhatia, R., Garg, A., Gaikwad, S., Prasad, K., Singh, M.B., and Tripathi, M. (2012). Efficacy of minocycline in acute ischemic stroke: a single-blinded, placebo-controlled trial. *Neurol India* *60*, 23–28.

Park, L., Uekawa, K., Garcia-Bonilla, L., Koizumi, K., Murphy, M., Pistik, R., Younkin, L., Younkin, S., Zhou, P., Carlson, G., et al. (2017). Brain Perivascular Macrophages Initiate the Neurovascular Dysfunction of Alzheimer A $\beta$  Peptides. *Circ. Res.* *121*, 258–269.

Pedragosa, J., Salas-Perdomo, A., Gallizioli, M., Cugota, R., Miró-Mur, F., Briansó, F., Justicia, C., Pérez-Asensio, F., Marquez-Kisinousky, L., Urra, X., et al. (2018). CNS-border associated macrophages respond to acute ischemic stroke attracting granulocytes and promoting vascular leakage. *Acta Neuropathol Commun* *6*, 76.

Perego, C., Fumagalli, S., and De Simoni, M.-G. (2011). Temporal pattern of expression and colocalization of microglia/macrophage phenotype markers following brain ischemic injury in mice. *J Neuroinflammation* *8*, 174.

Perez-de-Puig, I., Miró-Mur, F., Ferrer-Ferrer, M., Gelpi, E., Pedragosa, J., Justicia, C., Urra, X., Chamorro, A., and Planas, A.M. (2015). Neutrophil recruitment to the brain in mouse and human ischemic stroke. *Acta Neuropathol.* *129*, 239–257.

Perry, V.H., and Holmes, C. (2014). Microglial priming in neurodegenerative disease. *Nature Reviews Neurology* *10*, 217–224.

Perry, V.H., Nicoll, J.A.R., and Holmes, C. (2010). Microglia in neurodegenerative disease. *Nature Reviews Neurology* *6*, 193–201.

Peruzzotti-Jametti, L., Donegá, M., Giusto, E., Mallucci, G., Marchetti, B., and Pluchino, S. (2014). The role of the immune system in central nervous system plasticity after acute injury. *Neuroscience* *283*, 210–221.

Pham, M., Kleinschmitz, C., Helluy, X., Bartsch, A.J., Austinat, M., Behr, V.C., Renné, T., Nieswandt, B., Stoll, G., and Bendszus, M. (2010). Enhanced cortical reperfusion protects coagulation factor XII-deficient mice from ischemic stroke as revealed by high-field MRI. *Neuroimage* *49*, 2907–2914.

Pisanu, A., Lecca, D., Mulas, G., Wardas, J., Simbula, G., Spiga, S., and Carta, A.R. (2014). Dynamic changes in pro- and anti-inflammatory cytokines in microglia after PPAR- $\gamma$  agonist neuroprotective treatment in the MPTP mouse model of progressive Parkinson's disease. *Neurobiol. Dis.* *71*, 280–291.

- Plog, B.A., Dashnaw, M.L., Hitomi, E., Peng, W., Liao, Y., Lou, N., Deane, R., and Nedergaard, M. (2015). Biomarkers of Traumatic Injury Are Transported from Brain to Blood via the Glymphatic System. *Journal of Neuroscience* *35*, 518–526.
- Polfliet, M.M., Goede, P.H., van Kesteren-Hendrikx, E.M., van Rooijen, N., Dijkstra, C.D., and van den Berg, T.K. (2001). A method for the selective depletion of perivascular and meningeal macrophages in the central nervous system. *J. Neuroimmunol.* *116*, 188–195.
- Polfliet, M.M.J., van de Veerdonk, F., Döpp, E.A., van Kesteren-Hendrikx, E.M.L., van Rooijen, N., Dijkstra, C.D., and van den Berg, T.K. (2002). The role of perivascular and meningeal macrophages in experimental allergic encephalomyelitis. *J. Neuroimmunol.* *122*, 1–8.
- Pradier, B., Erxlebe, E., Markert, A., and Rácz, I. (2018). Microglial IL-1 $\beta$  progressively increases with duration of alcohol consumption. *Naunyn Schmiedebergs Arch. Pharmacol.* *391*, 455–461.
- Prakash, A., Parekh, S.V., Oak, S.N., Gupta, R.K., Sanghvi, B.V., Bachani, M., and Patil, R. (2012). Role of hyperbaric oxygen therapy in severe head injury in children. *J Pediatr Neurosci* *7*, 4–8.
- Prestigiacomo, C.J., Kim, S.C., Connolly, E.S., Liao, H., Yan, S.-F., and Pinsky, D.J. (1999). CD18-mediated neutrophil recruitment contributes to the pathogenesis of reperfused but not nonreperfused stroke. *Stroke* *30*, 1110–1117.
- Price, C.J.S., Wang, D., Menon, D.K., Guadagno, J.V., Cleij, M., Fryer, T., Aigbirhio, F., Baron, J.-C., and Warburton, E.A. (2006). Intrinsic activated microglia map to the peri-infarct zone in the subacute phase of ischemic stroke. *Stroke* *37*, 1749–1753.
- Prinz, M., Erny, D., and Hagemeyer, N. (2017). Ontogeny and homeostasis of CNS myeloid cells. *Nat. Immunol.* *18*, 385–392.
- Proost, P., Wuyts, A., and van Damme, J. (1996). The role of chemokines in inflammation. *Int. J. Clin. Lab. Res.* *26*, 211–223.
- Qin, L., Wu, X., Block, M.L., Liu, Y., Breese, G.R., Hong, J.-S., Knapp, D.J., and Crews, F.T. (2007). Systemic LPS causes chronic neuroinflammation and progressive neurodegeneration. *Glia* *55*, 453–462.
- Quintin, J., Saeed, S., Martens, J.H.A., Giamparellos-Bourboulis, E.J., Ifrim, D.C., Logie, C., Jacobs, L., Jansen, T., Kullberg, B.-J., Wijmenga, C., et al. (2012). Candida albicans infection affords protection against reinfection via functional reprogramming of monocytes. *Cell Host Microbe* *12*, 223–232.
- Ramaglia, V., Hughes, T.R., Donev, R.M., Ruseva, M.M., Wu, X., Huitinga, I., Baas, F., Neal, J.W., and Morgan, B.P. (2012). C3-dependent mechanism of microglial priming relevant to multiple sclerosis. *Proc. Natl. Acad. Sci. U.S.A.* *109*, 965–970.
- Raychev, R., and Saver, J.L. (2012). Mechanical thrombectomy devices for treatment of stroke. *Neurol Clin Pract* *2*, 231–235.
- Reneer, D.V., Hisel, R.D., Hoffman, J.M., Kryscio, R.J., Lusk, B.T., and Geddes, J.W. (2011). A multi-mode shock tube for investigation of blast-induced traumatic brain injury. *J. Neurotrauma* *28*, 95–104.

Reshef, R., Kudryavitskaya, E., Shani-Narkiss, H., Isaacson, B., Rimmerman, N., Mizrahi, A., and Yirmiya, R. (2017). The role of microglia and their CX3CR1 signaling in adult neurogenesis in the olfactory bulb. *Elife* 6.

Rice, R.A., Spangenberg, E.E., Yamate-Morgan, H., Lee, R.J., Arora, R.P.S., Hernandez, M.X., Tenner, A.J., West, B.L., and Green, K.N. (2015). Elimination of Microglia Improves Functional Outcomes Following Extensive Neuronal Loss in the Hippocampus. *J. Neurosci.* 35, 9977–9989.

Ricklin, D., Mastellos, D.C., Reis, E.S., and Lambris, J.D. (2018). The renaissance of complement therapeutics. *Nat Rev Nephrol* 14, 26–47.

Rocha e Silva, M. (1978). A brief survey of the history of inflammation. *Agents Actions* 8, 45–49.

Rockswold, G.L., Ford, S.E., Anderson, D.C., Bergman, T.A., and Sherman, R.E. (1992). Results of a prospective randomized trial for treatment of severely brain-injured patients with hyperbaric oxygen. *J. Neurosurg.* 76, 929–934.

Rockswold, S.B., Rockswold, G.L., Vargo, J.M., Erickson, C.A., Sutton, R.L., Bergman, T.A., and Biros, M.H. (2001). Effects of hyperbaric oxygenation therapy on cerebral metabolism and intracranial pressure in severely brain injured patients. *J. Neurosurg.* 94, 403–411.

Rockswold, S.B., Rockswold, G.L., Zaun, D.A., Zhang, X., Cerra, C.E., Bergman, T.A., and Liu, J. (2010). A prospective, randomized clinical trial to compare the effect of hyperbaric to normobaric hyperoxia on cerebral metabolism, intracranial pressure, and oxygen toxicity in severe traumatic brain injury. *J. Neurosurg.* 112, 1080–1094.

Rockswold, S.B., Rockswold, G.L., Zaun, D.A., and Liu, J. (2013). A prospective, randomized Phase II clinical trial to evaluate the effect of combined hyperbaric and normobaric hyperoxia on cerebral metabolism, intracranial pressure, oxygen toxicity, and clinical outcome in severe traumatic brain injury. *J. Neurosurg.* 118, 1317–1328.

Rodhe, J., Burguillos, M.A., de Pablos, R.M., Kavanagh, E., Persson, A., Englund, E., Deierborg, T., Venero, J.L., and Joseph, B. (2016). Spatio-temporal activation of caspase-8 in myeloid cells upon ischemic stroke. *Acta Neuropathologica Communications* 4, 92.

Romani, L. (2004). Immunity to fungal infections. *Nat. Rev. Immunol.* 4, 1–23.

Rubovitch, V., Ten-Bosch, M., Zohar, O., Harrison, C.R., Tempel-Brami, C., Stein, E., Hoffer, B.J., Balaban, C.D., Schreiber, S., Chiu, W.-T., et al. (2011). A mouse model of blast-induced mild traumatic brain injury. *Exp. Neurol.* 232, 280–289.

Sacco, R.L., Elkind, M., Boden-Albala, B., Lin, I.F., Kargman, D.E., Hauser, W.A., Shea, S., and Paik, M.C. (1999). The protective effect of moderate alcohol consumption on ischemic stroke. *JAMA* 281, 53–60.

Saeed, S., Quintin, J., Kerstens, H.H.D., Rao, N.A., Aghajanirefah, A., Matarese, F., Cheng, S.-C., Ratter, J., Berentsen, K., Ent, M.A. van der, et al. (2014). Epigenetic programming of monocyte-to-macrophage differentiation and trained innate immunity. *Science* 345, 1251086.

Saijo, K., and Glass, C.K. (2011). Microglial cell origin and phenotypes in health and disease. *Nature Reviews Immunology* 11, 775–787.

Santos, E., Schöll, M., Sánchez-Porras, R., Dahlem, M.A., Silos, H., Unterberg, A., Dickhaus, H., and Sakowitz, O.W. (2014). Radial, spiral and reverberating waves of spreading depolarization occur in the gyrencephalic brain. *NeuroImage* 99, 244–255.

Saunders, N.R., Dreifuss, J.-J., Dziegielewska, K.M., Johansson, P.A., Habgood, M.D., Møllgård, K., and Bauer, H.-C. (2014). The rights and wrongs of blood-brain barrier permeability studies: a walk through 100 years of history. *Front Neurosci* 8, 404.

Schilling, M., Besselmann, M., Müller, M., Strecker, J.K., Ringelstein, E.B., and Kiefer, R. (2005). Predominant phagocytic activity of resident microglia over hematogenous macrophages following transient focal cerebral ischemia: an investigation using green fluorescent protein transgenic bone marrow chimeric mice. *Exp. Neurol.* 196, 290–297.

Schmidt, A., Strecker, J.-K., Hucke, S., Bruckmann, N.-M., Herold, M., Mack, M., Diederich, K., Schäbitz, W.-R., Wiendl, H., Klotz, L., et al. (2017). Targeting Different Monocyte/Macrophage Subsets Has No Impact on Outcome in Experimental Stroke. *Stroke* 48, 1061–1069.

Schouten, J.W. (2007). Neuroprotection in traumatic brain injury: a complex struggle against the biology of nature. *Curr Opin Crit Care* 13, 134–142.

Scott, G., Zetterberg, H., Jolly, A., Cole, J.H., De Simoni, S., Jenkins, P.O., Feeney, C., Owen, D.R., Lingford-Hughes, A., Howes, O., et al. (2018). Minocycline reduces chronic microglial activation after brain trauma but increases neurodegeneration. *Brain* 141, 459–471.

Sharma, R., and Laskowitz, D.T. (2012). Biomarkers in traumatic brain injury. *Curr Neurol Neurosci Rep* 12, 560–569.

Shear, D.A., Lu, X.-C.M., Bombard, M.C., Pedersen, R., Chen, Z., Davis, A., and Tortella, F.C. (2010). Longitudinal characterization of motor and cognitive deficits in a model of penetrating ballistic-like brain injury. *J. Neurotrauma* 27, 1911–1923.

Shear, D.A., Lu, X.-C.M., Pedersen, R., Wei, G., Chen, Z., Davis, A., Yao, C., Dave, J., and Tortella, F.C. (2011). Severity profile of penetrating ballistic-like brain injury on neurofunctional outcome, blood-brain barrier permeability, and brain edema formation. *J. Neurotrauma* 28, 2185–2195.

Shi, D.-W., Zhang, J., Jiang, H.-N., Tong, C.-Y., Gu, G.-R., Ji, Y., Summah, H., and Qu, J.-M. (2011). LPS pretreatment ameliorates multiple organ injuries and improves survival in a murine model of polymicrobial sepsis. *Inflamm. Res.* 60, 841–849.

Siegler, J.E., Boehme, A.K., Kumar, A.D., Gillette, M.A., Albright, K.C., Beasley, T.M., and Martin-Schild, S. (2013). Identification of modifiable and non-modifiable risk factors for neurological deterioration following acute ischemic stroke. *J Stroke Cerebrovasc Dis* 22, e207–e213.

Silver, J., and Miller, J.H. (2004). Regeneration beyond the glial scar. *Nat. Rev. Neurosci.* 5, 146–156.

Simon, N., Buschmann, K., Pflaum, J., Hudalla, H., Koch, L., Ryschich, E., Poeschl, J., and Frommhold, D. (2014). Anti-Inflammatory Functions of Protein C Require RAGE and ICAM-1 in a Stimulus-Dependent Manner. *Mediators of Inflammation* 2014, 743678.

Singh, A.K., Jiang, Y., Gupta, S., and Benhabib, E. (2007). Effects of chronic ethanol drinking on the blood brain barrier and ensuing neuronal toxicity in alcohol-preferring rats subjected to intraperitoneal LPS injection. *Alcohol Alcohol.* 42, 385–399.

Skolnick, B.E., Maas, A.I., Narayan, R.K., van der Hoop, R.G., MacAllister, T., Ward, J.D., Nelson, N.R., Stocchetti, N., and SYNAPSE Trial Investigators (2014). A clinical trial of progesterone for severe traumatic brain injury. *N. Engl. J. Med.* 371, 2467–2476.

Sly, L.M., Krzesicki, R.F., Brashler, J.R., Buhl, A.E., McKinley, D.D., Carter, D.B., and Chin, J.E. (2001). Endogenous brain cytokine mRNA and inflammatory responses to lipopolysaccharide are elevated in the Tg2576 transgenic mouse model of Alzheimer's disease. *Brain Res. Bull.* 56, 581–588.

Smith, C.J., Hulme, S., Vail, A., Heal, C., Parry-Jones, A.R., Scarth, S., Hopkins, K., Hoadley, M., Allan, S.M., Rothwell, N.J., et al. (2018). SCIL-STROKE (Subcutaneous Interleukin-1 Receptor Antagonist in Ischemic Stroke): A Randomized Controlled Phase 2 Trial. *Stroke STROKEAHA.* 118.020750.

Sokol, C.L., and Luster, A.D. (2015). The Chemokine System in Innate Immunity. *Cold Spring Harb Perspect Biol* a016303.

Soulas, C., Donahue, R.E., Dunbar, C.E., Persons, D.A., Alvarez, X., and Williams, K.C. (2009). Genetically Modified CD34+ Hematopoietic Stem Cells Contribute to Turnover of Brain Perivascular Macrophages in Long-Term Repopulated Primates. *The American Journal of Pathology* 174, 1808–1817.

Sullivan, P.G., Thompson, M., and Scheff, S.W. (2000). Continuous infusion of cyclosporin A postinjury significantly ameliorates cortical damage following traumatic brain injury. *Exp. Neurol.* 161, 631–637.

Sweeney, M.D., Sagare, A.P., and Zlokovic, B.V. (2015). Cerebrospinal Fluid Biomarkers of Neurovascular Dysfunction in Mild Dementia and Alzheimer's Disease. *J Cereb Blood Flow Metab* 35, 1055–1068.

Szabo, G. (2015). Gut–Liver Axis in Alcoholic Liver Disease. *Gastroenterology* 148, 30–36.

Szalay, G., Martinecz, B., Lénárt, N., Környei, Z., Orsolits, B., Judák, L., Császár, E., Fekete, R., West, B.L., Katona, G., et al. (2016). Microglia protect against brain injury and their selective elimination dysregulates neuronal network activity after stroke. *Nature Communications* 7, 11499.

Szmydynger-Chodobska, J., Strazielle, N., Gandy, J.R., Keefe, T.H., Zink, B.J., Ghersi-Egea, J.-F., and Chodobksi, A. (2012). Posttraumatic invasion of monocytes across the blood-cerebrospinal fluid barrier. *J. Cereb. Blood Flow Metab.* 32, 93–104.

Tajiri, N., Kellogg, S.L., Shimizu, T., Arendash, G.W., and Borlongan, C.V. (2013). Traumatic brain injury precipitates cognitive impairment and extracellular Aβ aggregation in Alzheimer's disease transgenic mice. *PLoS ONE* 8, e78851.

Tapia-Perez, J.H., Sanchez-Aguilar, M., Torres-Corzo, J.G., Gordillo-Moscoso, A., Martinez-Perez, P., Madeville, P., de la Cruz-Mendoza, E., and Chalita-Williams, J. (2008). Effect of rosuvastatin on amnesia and disorientation after traumatic brain injury (NCT003229758). *J. Neurotrauma* 25, 1011–1017.

Taylor, A., Verhagen, J., Blaser, K., Akdis, M., and Akdis, C.A. (2006). Mechanisms of immune suppression by interleukin-10 and transforming growth factor-beta: the role of T regulatory cells. *Immunology* 117, 433–442.

Thiel, A., and Heiss, W.-D. (2011). Imaging of Microglia Activation in Stroke. *Stroke* 42, 507–512.

Thompson, R.D., Noble, K.E., Larbi, K.Y., Dewar, A., Duncan, G.S., Mak, T.W., and Nourshargh, S. (2001). Platelet-endothelial cell adhesion molecule-1 (PECAM-1)-deficient mice demonstrate a transient and cytokine-specific role for PECAM-1 in leukocyte migration through the perivascular basement membrane. *Blood* 97, 1854–1860.

Tinianow, C.L., Tinianow, T.K., and Wilcox, M. (2000). Effects of hyperbaric oxygen on focal brain contusions. *Biomed Sci Instrum* 36, 275–281.

Tuo, Q.-Z., Lei, P., Jackman, K., Li, X.-L., Xiong, H., Liuyang, Z.-Y., Roisman, L., Zhang, S.-T., Ayton, S., Wang, Q., et al. (2017). Tau-mediated iron export prevents ferroptotic damage after ischemic stroke. *Molecular Psychiatry* 22.

Turner, M.D., Nedjai, B., Hurst, T., and Pennington, D.J. (2014). Cytokines and chemokines: At the crossroads of cell signalling and inflammatory disease. *Biochimica et Biophysica Acta (BBA) - Molecular Cell Research* 1843, 2563–2582.

Varvel, N.H., Neher, J.J., Bosch, A., Wang, W., Ransohoff, R.M., Miller, R.J., and Dingledine, R. (2016). Infiltrating monocytes promote brain inflammation and exacerbate neuronal damage after status epilepticus. *Proc. Natl. Acad. Sci. U.S.A.* 113, E5665–5674.

Vestweber, D. (2015). How leukocytes cross the vascular endothelium. *Nature Reviews Immunology* 15, 692–704.

Vidale, S., Longoni, M., Valvassori, L., and Agostoni, E. (2018). Mechanical Thrombectomy in Strokes with Large-Vessel Occlusion Beyond 6 Hours: A Pooled Analysis of Randomized Trials. *J Clin Neurol* 14, 407–412.

Von Bernhardi, R., Eugenin-von Bernhardi, L., and Eugenin, J. (2015). Microglial cell dysregulation in Brain Aging and Neurodegeneration. *Front. Aging Neurosci.* 7.

Wang, H.J. (2010). Alcohol, inflammation, and gut-liver-brain interactions in tissue damage and disease development. *World Journal of Gastroenterology* 16, 1304.

Wang, C.X., Yang, T., Noor, R., and Shuaib, A. (2002). Delayed minocycline but not delayed mild hypothermia protects against embolic stroke. *BMC Neurol* 2, 2.

Wang, G., Zhang, J., Hu, X., Zhang, L., Mao, L., Jiang, X., Liou, A.K.-F., Leak, R.K., Gao, Y., and Chen, J. (2013). Microglia/macrophage polarization dynamics in white matter after traumatic brain injury. *J. Cereb. Blood Flow Metab.* 33, 1864–1874.

- Wang, Y.F., Tsirka, S.E., Strickland, S., Stieg, P.E., Soriano, S.G., and Lipton, S.A. (1998). Tissue plasminogen activator (tPA) increases neuronal damage after focal cerebral ischemia in wild-type and tPA-deficient mice. *Nat. Med.* 4, 228–231.
- Wanner, I.B., Anderson, M.A., Song, B., Levine, J., Fernandez, A., Gray-Thompson, Z., Ao, Y., and Sofroniew, M.V. (2013). Glial Scar Borders Are Formed by Newly Proliferated, Elongated Astrocytes That Interact to Corral Inflammatory and Fibrotic Cells via STAT3-Dependent Mechanisms after Spinal Cord Injury. *J. Neurosci.* 33, 12870–12886.
- Wattananit, S., Tornero, D., Graubardt, N., Memanishvili, T., Monni, E., Tatarishvili, J., Miskinyte, G., Ge, R., Ahlenius, H., Lindvall, O., et al. (2016). Monocyte-Derived Macrophages Contribute to Spontaneous Long-Term Functional Recovery after Stroke in Mice. *J. Neurosci.* 36, 4182–4195.
- Wei, J., and Xiao, G. (2013). The neuroprotective effects of progesterone on traumatic brain injury: current status and future prospects. *Acta Pharmacol. Sin.* 34, 1485–1490.
- Weinstein, J.R., Koerner, I.P., and Möller, T. (2010). Microglia in ischemic brain injury. *Future Neurol* 5, 227–246.
- Werner, C., and Engelhard, K. (2007). Pathophysiology of traumatic brain injury. *Br J Anaesth* 99, 4–9.
- Wernersson, S., and Pejler, G. (2014). Mast cell secretory granules: armed for battle. *Nat. Rev. Immunol.* 14, 478–494.
- Whitnall, L., McMillan, T.M., Murray, G.D., and Teasdale, G.M. (2006). Disability in young people and adults after head injury: 5-7 year follow up of a prospective cohort study. *J. Neurol. Neurosurg. Psychiatry* 77, 640–645.
- Winkler, E.A., Sengillo, J.D., Sullivan, J.S., Henkel, J.S., Appel, S.H., and Zlokovic, B.V. (2013). Blood–spinal cord barrier breakdown and pericyte reductions in amyotrophic lateral sclerosis. *Acta Neuropathol* 125, 111–120.
- Wright, D.W., Kellermann, A.L., Hertzberg, V.S., Clark, P.L., Frankel, M., Goldstein, F.C., Salomone, J.P., Dent, L.L., Harris, O.A., Ander, D.S., et al. (2007). ProTECT: a randomized clinical trial of progesterone for acute traumatic brain injury. *Ann Emerg Med* 49, 391–402, 402.e1–2.
- Wright, D.W., Yeatts, S.D., Silbergliet, R., Palesch, Y.Y., Hertzberg, V.S., Frankel, M., Goldstein, F.C., Caveney, A.F., Howlett-Smith, H., Bengelink, E.M., et al. (2014). Very early administration of progesterone for acute traumatic brain injury. *N. Engl. J. Med.* 371, 2457–2466.
- Xiao, G., Wei, J., Yan, W., Wang, W., and Lu, Z. (2008). Improved outcomes from the administration of progesterone for patients with acute severe traumatic brain injury: a randomized controlled trial. *Crit Care* 12, R61.
- Xiong, Y., Mahmood, A., and Chopp, M. (2013). Animal models of traumatic brain injury. *Nat. Rev. Neurosci.* 14, 128–142.

- Xu, L., Fagan, S.C., Waller, J.L., Edwards, D., Borlongan, C.V., Zheng, J., Hill, W.D., Feuerstein, G., and Hess, D.C. (2004). Low dose intravenous minocycline is neuroprotective after middle cerebral artery occlusion-reperfusion in rats. *BMC Neurol* 4, 7.
- Xue, J., Schmidt, S.V., Sander, J., Draffehn, A., Krebs, W., Quester, I., De Nardo, D., Gohel, T.D., Emde, M., Schmidleithner, L., et al. (2014). Transcriptome-based network analysis reveals a spectrum model of human macrophage activation. *Immunity* 40, 274–288.
- Yan, A.W., Fouts, D.E., Brandl, J., Stärkel, P., Torralba, M., Schott, E., Tsukamoto, H., Nelson, K.E., Brenner, D.A., and Schnabl, B. (2011). Enteric dysbiosis associated with a mouse model of alcoholic liver disease. *Hepatology* 53, 96–105.
- Yang, J., Hirata, T., Croce, K., Merrill-Skoloff, G., Tchernychev, B., Williams, E., Flaumenhaft, R., and C. Furie, B. (2000). Targeted Gene Disruption Demonstrates That P-Selectin Glycoprotein Ligand 1 (Psgl-1) Is Required for P-Selectin–Mediated but Not E-Selectin–Mediated Neutrophil Rolling and Migration. *The Journal of Experimental Medicine* 190, 1769–1782.
- Yang, Y., Salayandia, V.M., Thompson, J.F., Yang, L.Y., Estrada, E.Y., and Yang, Y. (2015). Attenuation of acute stroke injury in rat brain by minocycline promotes blood–brain barrier remodeling and alternative microglia/macrophage activation during recovery. *Journal of Neuroinflammation* 12, 26.
- Yang, Y., Liu, H., Zhang, H., Ye, Q., Wang, J., Yang, B., Mao, L., Zhu, W., Leak, R.K., Xiao, B., et al. (2017). ST2/IL-33-Dependent Microglial Response Limits Acute Ischemic Brain Injury. *J. Neurosci.* 37, 4692–4704.
- Yu, Y., Zhang, Z.-H., Wei, S.-G., Serrats, J., Weiss, R.M., and Felder, R.B. (2010). Brain Perivascular Macrophages and the Sympathetic Response to Inflammation in Rats After Myocardial Infarction. *Hypertension* 55, 652–659.
- Zetterberg, H., and Blennow, K. (2016). Fluid biomarkers for mild traumatic brain injury and related conditions. *Nature Reviews Neurology* 12, 563–574.
- Zhang, Z., Zhang, Z.-Y., Wu, Y., and Schluesener, H.J. (2012). Lesional accumulation of CD163+ macrophages/microglia in rat traumatic brain injury. *Brain Res.* 1461, 102–110.
- Zhao, Z., Nelson, A.R., Betsholtz, C., and Zlokovic, B.V. (2015). Establishment and Dysfunction of the Blood-Brain Barrier. *Cell* 163, 1064–1078.
- Zhou, W., Liesz, A., Bauer, H., Sommer, C., Lahrmann, B., Valous, N., Grabe, N., and Veltkamp, R. (2013). Postischemic brain infiltration of leukocyte subpopulations differs among murine permanent and transient focal cerebral ischemia models. *Brain Pathol.* 23, 34–44.
- Zhu, X., Fréchou, M., Liere, P., Zhang, S., Pianos, A., Fernandez, N., Denier, C., Mattern, C., Schumacher, M., and Guennoun, R. (2017). A Role of Endogenous Progesterone in Stroke Cerebroprotection Revealed by the Neural-Specific Deletion of Its Intracellular Receptors. *The Journal of Neuroscience* 37, 10998–11020.
- Zhu, Z., Fu, Y., Tian, D., Sun, N., Han, W., Chang, G., Dong, Y., Xu, X., Liu, Q., Huang, D., et al. (2015). Combination of the Immune Modulator Fingolimod With Alteplase in Acute Ischemic Stroke: A Pilot Trial. *Circulation* 132, 1104–1112.

Ziebell, J.M., Taylor, S.E., Cao, T., Harrison, J.L., and Lifshitz, J. (2012). Rod microglia: elongation, alignment, and coupling to form trains across the somatosensory cortex after experimental diffuse brain injury. *J Neuroinflammation* 9, 247.

Ziebell, J.M., Ray-Jones, H., and Lifshitz, J. (2017). Nogo presence is inversely associated with shifts in cortical microglial morphology following experimental diffuse brain injury. *Neuroscience* 359, 209–223.

Ziv, Y., Ron, N., Butovsky, O., Landa, G., Sudai, E., Greenberg, N., Cohen, H., Kipnis, J., and Schwartz, M. (2006). Immune cells contribute to the maintenance of neurogenesis and spatial learning abilities in adulthood. *Nat. Neurosci.* 9, 268–275.

Zwadlo, G., Voegeli, R., Schulze Osthoff, K., and Sorg, C. (1987). A monoclonal antibody to a novel differentiation antigen on human macrophages associated with the down-regulatory phase of the inflammatory process. *Exp. Cell Biol.* 55, 295–304.





# Annexes



PERSONAL INFORMATION Antoine DRIEU

📍 INSERM UMR-S U1237 (PhIND) - GIP Cyceron - Bd Henri Becquerel,  
14074 Caen (France)

☎ (+33) 231 47 01 68 ☎ (+33) 635 46 47 65

✉ drieu@cyceron.fr

🌐 <http://www.phind.fr/index.php/en/>

Date of birth 08/07/1991 | Nationality French

POSITION PhD student

WORK EXPERIENCE

2015–Present PhD student

**PhIND unit - INSERM Unit 1237**, Caen (France)

“Invisible neuroinflammation in acute and chronic brain disorders”

- Stage at **MTA Institute of Experimental Medicine (Adam Denes' lab)** (1 month in 2017)

2012–2015 MSc student

PhIND unit - INSERM Unit 1237, Caen (France)

Project title: “The liver-brain axis: inflammatory responses after alcohol consumption”

EDUCATION AND TRAINING

June 2015 MSc degree

University of Caen Normandy (France)

Title: Neuroscience and behavioural sciences

June 2013 Bachelor degree

University of Caen Normandy (France)

Title: Cellular and Molecular Biology

ADDITIONAL INFORMATION

- Honours and awards**
- First award oral communication, “Normandy doctoral day”, Caen 2016.
  - IRME (Institut de Recherches sur la Moelle épinière et l’Encéphale) PhD grant (2015-2018).
  - UNAFTC (Union Nationale des Associations de Familles de Traumatisés Crâniens et Cérébro-lésés) PhD grant (2015-2018).
  - FRA (Fondation pour la Recherche en Alcoolologie) travel grant, New Orleans 2016.
- Other trainings**
- University diploma in animal experimentation for biomedical research, June 2017
  - “Innovative surgical techniques in rodents”, Rouen, May 2017
  - “Small animal imaging”, Bordeaux, October 2016
  - “Good practices and skills for MRI and animal physiology”, Caen, May 2016
  - ImageJ software, Caen, December 2015
  - Metamorph software (Leica), Caen, February 2015
- Meetings**
- Society for Neuroscience, Washington DC, 2017: “Alcohol-induced inflammatory priming worsens outcome after ischemic stroke”. Drieu A, Naveau M, Vivien D and Rubio M. **Poster presentation**.
  - 1<sup>st</sup> joint meeting of GFHT and CoMETH, Caen, 2017: “Key role of perivascular macrophages in the deleterious effects of chronic alcohol consumption during ischemic stroke. Drieu A, Naveau M, Vivien D and Rubio M. **Poster presentation**.
  - 39<sup>th</sup> annual RSA scientific meeting, New Orleans, 2016. “Alcohol consumption alters the central and systemic inflammatory responses after stroke”. Drieu A, Lemarchand E, Quenault A, Vivien D and Rubio M. **Poster presentation**.
  - 9<sup>th</sup> international symposium on neuroprotection and neurorepair, Leipzig, 2016: “Alcohol consumption alters the central and systemic inflammatory responses after stroke”. Drieu A, Lemarchand E, Quenault A, Vivien D and Rubio M. **Poster presentation**.
  - Normandy doctoral days, Caen, 2016: “Alcohol consumption alters the central and systemic inflammatory responses after stroke”. Drieu A, Lemarchand E, Quenault A, Vivien D and Rubio M. **Oral presentation. First price**.
  - French meeting of neuroimmunology, Paris, 2015. The liver-brain axis: inflammatory responses after alcohol consumption. Drieu A, Lemarchand E, Quenault A, Vivien D and Rubio M. **Oral presentation**.
  - Alcohol research foundation meeting, Paris, 2015. Drieu A, Lemarchand E,

Quenault A, Vivien D and Rubio M. **Poster presentation.**

**Publications**

- 1.** Goulay R\*, **Drieu A\***, Di Palma C, Pro Sistigia P, Delcroix N, Chazalviel L, Saulnier R, Gakuba C, Goursaud S, Young AR, Gauberti M, Emery E, Vivien D and Gaberel T. Modification of apparent intracerebral hematoma volume on T2\*-weighted images during normobaric oxygen therapy may contribute to false diagnosis. *J Clin Neurosci.* 2018 Jun;52:105-108.
- 2.** **Drieu A**, Martinez de Lizarondo S, Rubio M. Stopping Inflammation in Stroke: Role of ST2/IL-33 Signaling. *J Neurosci.* 2017 Oct 4;37(40):9614-9616. *Journal Club.*
- 3.** **Drieu A**, Levard D, Vivien D, Rubio M. Anti-inflammatory treatments for stroke: from bench to bedside. *Ther Adv Neurol Disord.* 2018. Jul 30;11:1756286418789854. *Review.*
- 4.** **Drieu A**, Lanquetin A, Campos F, Quenault A, Lemarchand E, Naveau M, Pitel AL, Castillo J, Vivien D, Rubio M. Neurovascular inflammatory priming induced by heavy drinking worsens ischemic stroke outcome. *Submitted.*
- 5.** Anfray A, **Drieu A**, Hingot V, Yetim M, Rubio M, Tanter M, Vivien D and Orset C. The activation of endothelial NMDA receptor by the circulating Tissue type Plasminogen Activator contributes to neurovascular coupling. *Submitted.*
  - **Drieu A**, Vivien D and Rubio M. Perivascular macrophages mediate the aggravating effect of inflammatory priming on ischemic stroke. *In preparation*
  - **Drieu A**, Brodin C, Levard D, Vivien D, Rubio M. Spatio-temporal profile of inflammatory responses in a thromboembolic stroke model. *In preparation*.
  - **Drieu A**, Lanquetin A, Gulhan Z, Vegliante G, Rubio M, Zanier ER, Chalon S, Vivien D, Ali C. Relevance of sensitive imaging of neuro-inflammation to explain neurological deficits after mild traumatic brain injury in mice. *In preparation.*

## Journal Club

**Editor's Note:** These short reviews of recent *JNeurosci* articles, written exclusively by students or postdoctoral fellows, summarize the important findings of the paper and provide additional insight and commentary. If the authors of the highlighted article have written a response to the Journal Club, the response can be found by viewing the Journal Club at [www.jneurosci.org](http://www.jneurosci.org). For more information on the format, review process, and purpose of Journal Club articles, please see <http://jneurosci.org/content/preparing-manuscript#journalclub>.

## Stopping Inflammation in Stroke: Role of ST2/IL-33 Signaling

Antoine Drieu,<sup>1</sup> Sara Martinez de Lizarrondo,<sup>1</sup> and Marina Rubio<sup>1,2</sup>

<sup>1</sup>Normandie Univ, UNICAEN, INSERM, INSERM UMR-S U1237, Physiopathology and Imaging of Neurological Disorders (PhIND), Cyceron, 14000 Caen, France, and <sup>2</sup>Délégation Recherche Clinique et Innovation (DRCI), Caen University Hospital CHU Côte de Nacre, 14000 Caen, France

Review of Yang et al.

Ischemic stroke is the second leading cause of death worldwide, according to data from the World Health Organization. It results from interruption of blood flow caused by *in situ* thrombus (blood clot) formation or embolization. Along with other mechanisms involved in the pathogenesis of stroke, postischemic inflammation accounts for brain cell death in the acute and subacute stages (Dirnagl et al., 1999). Over the past 20 years, many studies have focused on inflammatory responses triggered after ischemic stroke, with the aim of ameliorating stroke outcome. However, initial attempts to use anti-inflammatory treatments in acute ischemic stroke failed (del Zoppo, 2010). These failures may be explained by the nature of immune cells in stroke: on the one hand, they participate in the progression of postischemic injury; on the other hand, they mediate poststroke repair and regeneration.

The dual nature of the immune response to stroke is exemplified by microglia, the resident macrophages in the brain

parenchyma. Microglia actively survey the surrounding environment by protruding and retracting their processes; and after acute brain injury, they undergo dramatic morphological and phenotypic changes. Specifically, when activated by injury-associated molecules, microglial cells change from having branched processes to becoming amoeboid phagocytic cells, which express novel surface antigens and produce mediators that orchestrate the inflammatory response of the brain (Perego et al., 2011). Individual microglial cells can adopt a large spectrum of activated phenotypes ranging from proinflammatory (M1 phenotype) to anti-inflammatory and neuroprotective (M2). Although microglial cells can encompass a broad spectrum of phenotypes between the M1 and M2 extremes, the M1–M2 dichotomy is generally considered as a useful framework to understand and manipulate the functional status of microglial cells.

The mechanisms driving phenotypic changes of microglia remain poorly understood and represent a potential therapeutic target to both limit brain injury and promote brain repair. Clues about this regulation might come from the study of peripheral macrophages that also adopt a range of phenotypes. One such regulatory molecule is the cytokine IL-33, a member of the interleukin-1 (IL-1) cytokine family. IL-33 exerts a neuroprotective role by

promoting the shift of macrophage polarization from M1- to M2-type, reducing the levels of proinflammatory mediators and increasing the secretion of anti-inflammatory cytokines, such as IL-4 and IL-1 (Jiang et al., 2012; Pomeshchik et al., 2015). IL-33 binds to its specific receptor ST2. Although several papers have reported the neuroprotective role of IL-33 in stroke (Korhonen et al., 2015; Pomeshchik et al., 2015), the importance of IL-33/ST2 signaling cascade on microglial phenotype had never been addressed before.

Yang et al. (2017) investigated the potential beneficial effects of the activation of ST2 receptors via IL-33 in the switch of microglial cell phenotype from a proinflammatory to anti-inflammatory phenotype after ischemic stroke and asked whether activation of this pathway decreases the ischemic lesion volume. To do so, they used ST2 knock-out mice subjected to two different models of stroke. In both models, ST2-deficient mice had larger lesion volumes than wild-type mice. This deleterious effect was accompanied by neurobehavioral deficits (neuroscore and sensorimotor tests; e.g., rotarod, adhesive removal, and cylinder tests) at different times after stroke onset.

To identify the cells involved in the protective effects of ST2, the authors investigated which cells expressed this receptor and which secreted its ligand, IL-

Received July 3, 2017; revised Aug. 22, 2017; accepted Aug. 28, 2017.

The authors declare no competing financial interests.

Correspondence should be addressed to Dr. Marina Rubio, Institut National de la Santé et de la Recherche Médicale U1237, Physiopathology and Imaging for Neurological Disorders, GIP Cyceron, Bd Henri Becquerel, BP5229, 14074 Caen, France. E-mail: rubio@cyeron.fr.

DOI:10.1523/JNEUROSCI.1863-17.2017

Copyright © 2017 the authors 0270-6474/17/379614-03\$15.00/0

33. Immunohistological analyses showed that astrocytes and oligodendrocytes produce IL-33 after stroke onset. Flow cytometry and immunohistological analyses showed that ST2 receptors were expressed by astrocytes and microglial cells under physiological conditions. In addition, ST2 receptor levels were dramatically increased in these two populations after stroke. The number of ST2-positive infiltrated macrophages and neutrophils was also robustly elevated after stroke. The next step of their work was to assess the direct effects of IL-33 on microglia. *In vitro* (microglia-enriched cultures subjected to oxygen/glucose deprivation) and *in vivo* (ST2-deficient, stroke mice) data showed that the ST2/IL-33 pathway is implicated in the shift from a microglial “M1” to a “M2”-neuroprotective phenotype, by inducing the expression of M2 markers and inhibiting the expression of M1 markers (analyzed by immunohistological analyses and/or RT-PCR). Finally, the authors demonstrate, by *in vitro* and *in vivo* studies, that the neuroprotective effects of the ST2/IL-33 signaling pathway were mediated by IL-10 produced by microglial cells. *In vivo* experiments showed that the neuroprotective effects of IL-33 were abrogated in IL-10-deficient mice 3 d after stroke onset, whereas wild-type mice showed decreased lesion volumes when exposed to IL-33.

The discovery by Yang et al. (2017) links IL-33/ST2 signaling to the IL-10 pathway, for which downstream effects are known. IL-10 is one of the best studied anti-inflammatory cytokines produced by immune cells after brain injury (Iadecola and Anrather, 2011). IL-10 production impairs proinflammatory reactions by inhibiting cytokine production, downregulating MHC-II antigens, and decreasing NF- $\kappa$ B activity. In addition, IL-10 production may upregulate B-cell proliferation and antibody production (de Waal Malefyt et al., 1992). In stroke, many immune cells (including regulatory T and regulatory B cells) exert neuroprotective actions through IL-10 release (Liesz et al., 2009; Ren et al., 2011).

In contrast to previous data by Korhonen et al. (2015), Yang et al. (2017) did not observe any effect on the expression of IL-4 after IL-33 stroke-induced upregulation or *in vitro* IL-33 administration. IL-4 is another anti-inflammatory cytokine that has been largely reported to exert neuroprotection after stroke (Xiong et al., 2015; Liu et al., 2016). These differing findings suggest that the ST2/IL-33 signaling pathway in microglia is not at

the origin of IL-4 secretion because, in the work of Yang et al. (2017), IL-33-treated microglia did not express IL-4. In agreement with this hypothesis, Zhao et al. (2015) have suggested that IL-4 released from neurons and IL-33 coming from glial cells could promote a synergistic effect and exert neuroprotective effects after stroke.

To examine the temporal profile of ST2/IL-33 signaling after stroke, Yang et al. (2017) analyzed the expression of IL-33 at 1, 3, 7, and 14 d. They detected a significant increase of IL-33 in astrocytes and oligodendrocytes exclusively 1 d after stroke, after which IL-33 expression returned to basal levels. In contrast, ST2 expression was analyzed exclusively 3 d after stroke onset. At this time, expression of ST2 was significantly elevated in microglia and astrocytes. It would have been valuable to analyze the same time points for ST2 as for IL-33, especially 1 d after stroke onset, to link the expression pattern of both molecules and to explain the discrepant expression patterns of IL-33 and ST2 3 d after stroke onset.

Astrocytes have previously been shown to participate in neuroinflammatory responses (Dong and Benveniste, 2001) and can become activated (reactive) in response to many CNS pathologies, including stroke (Pekny and Nilsson, 2005). In the study by Yang et al. (2017), astrocytes were one of the sources of IL-33 1 d after stroke onset; and, like microglia, astrocytes showed an increased expression of ST2 receptors 3 d after stroke. These results suggest that astrocytes could also contribute to the beneficial effects of IL-33 and ST2-mediated signaling after stroke. This topic deserves additional studies.

Last, the results obtained by Yang et al. (2017) are in accordance with clinical findings obtained in stroke patients (Korhonen et al., 2015). Korhonen et al. (2015) studied the plasma concentration of the soluble form of ST2 (sST2), a secreted isoform generated by alternative splicing that inhibits IL-33 signaling (Hayakawa et al., 2007). Stroke patients with high plasma levels of sST2 had greater neurological deficits 3 months after stroke, suggesting that stronger inhibition of IL-33 was associated with poorer stroke outcome (Korhonen et al., 2015).

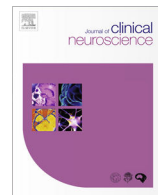
In conclusion, the results observed by Yang et al. (2017) open new venues targeting IL-33/ST2 signaling pathways for ischemic stroke treatment. To date, there is no specific therapeutic approach available to target poststroke microglial immune responses, although some candidates have

been investigated only in preclinical studies. Although some of them have been applied in other disorders, exploratory research for effective agents that regulate ischemic microglial activation is still in the early stages. Given the dual function of microglial cells after stroke, therapeutic strategies targeting microglia should be fine-tuned to selectively suppress the proinflammatory responses and/or promote anti-inflammatory effects. ST2 agonist injection might be a promising target to promote microglial beneficial responses in stroke if an effective and innocuous administration mechanism is found for stroke patients.

## References

- de Waal Malefyt R, Yssel H, Roncarolo MG, Spits H, de Vries JE (1992) Interleukin-10. *Curr Opin Immunol* 4:314–320. CrossRef Medline
- del Zoppo GJ (2010) Acute anti-inflammatory approaches to ischemic stroke. *Ann N Y Acad Sci* 1207:143–148. CrossRef Medline
- Dirnagl U, Iadecola C, Moskowitz MA (1999) Pathobiology of ischaemic stroke: an integrated view. *Trends Neurosci* 22:391–397. CrossRef Medline
- Dong Y, Benveniste EN (2001) Immune function of astrocytes. *Glia* 36:180–190. CrossRef Medline
- Hayakawa H, Hayakawa M, Kume A, Tominaga S (2007) Soluble ST2 blocks interleukin-33 signaling in allergic airway inflammation. *J Biol Chem* 282:26369–26380. CrossRef Medline
- Iadecola C, Anrather J (2011) The immunology of stroke: from mechanisms to translation. *Nat Med* 17:796–808. CrossRef Medline
- Jiang HR, Milovanović M, Allan D, Niedbala W, Besnard AG, Fukada SY, Alves-Filho JC, Togbe D, Goodyear CS, Linington C, Xu D, Lukic ML, Liew FY (2012) IL-33 attenuates EAE by suppressing IL-17 and IFN-gamma production and inducing alternatively activated macrophages. *Eur J Immunol* 42:1804–1814. CrossRef Medline
- Korhonen P, Kanninen KM, Lehtonen Š, Lemmarchant S, Puttonen KA, Oksanen M, Dhungana H, Loppi S, Pollari E, Wojciechowski S, Kidin I, García-Berrocuso T, Giralt D, Montaner J, Koistinaho J, Malm T (2015) Immunomodulation by interleukin-33 is protective in stroke through modulation of inflammation. *Brain Behav Immun* 49:322–336. CrossRef Medline
- Liesz A, Suri-Payer E, Veltkamp C, Doerr H, Sommer C, Rivest S, Giese T, Veltkamp R (2009) Regulatory T cells are key cerebroprotective immunomodulators in acute experimental stroke. *Nat Med* 15:192–199. CrossRef Medline
- Liu X, Liu J, Zhao S, Zhang H, Cai W, Cai M, Ji X, Leak RK, Gao Y, Chen J, Hu X (2016) Interleukin-4 is essential for microglia/macrophage M2 polarization and long-term recovery after cerebral ischemia. *Stroke* 47:498–504. CrossRef Medline

- Pekny M, Nilsson M (2005) Astrocyte activation and reactive gliosis. *Glia* 50:427–434. CrossRef Medline
- Perego C, Fumagalli S, De Simoni MG (2011) Temporal pattern of expression and colocalization of microglia/macrophage phenotype markers following brain ischemic injury in mice. *J Neuroinflammation* 8:174. CrossRef Medline
- Pomeshchik Y, Kidin I, Korhonen P, Savchenko E, Jaronen M, Lehtonen S, Wojciechowski S, Kanninen K, Koistinaho J, Malm T (2015) Interleukin-33 treatment reduces secondary injury and improves functional recovery after contusion spinal cord injury. *Brain Behav Immun* 44:68–81. CrossRef Medline
- Ren X, Akiyoshi K, Dziennis S, Vandembark AA, Herson PS, Hurn PD, Offner H (2011) Regulatory B cells limit CNS inflammation and neurologic deficits in murine experimental stroke. *J Neurosci* 31:8556–8563. CrossRef Medline
- Xiong X, Xu L, Wei L, White RE, Ouyang YB, Giffard RG (2015) IL-4 is required for sex differences in vulnerability to focal ischemia in mice. *Stroke* 46:2271–2276. CrossRef Medline
- Yang Y, Liu H, Zhang H, Ye Q, Wang J, Yang B, Mao L, Zhu W, Leak RK, Xiao B, Lu B, Chen J, Hu X (2017) ST2/IL-33-dependent microglial response limits acute ischemic brain injury. *J Neurosci* 37:4692–4704. CrossRef Medline
- Zhao X, Wang H, Sun G, Zhang J, Edwards NJ, Aronowski J (2015) Neuronal interleukin-4 as a modulator of microglial pathways and ischemic brain damage. *Neuroscience* 35:11281–11291. CrossRef Medline



## Short communication

## Modification of apparent intracerebral hematoma volume on T2\*-weighted images during normobaric oxygen therapy may contribute to false diagnosis

Romain Goulay <sup>a,1</sup>, Antoine Drieu <sup>a,1</sup>, Camille Di Palma <sup>a,b</sup>, Palma Pro-Sistiaga <sup>c</sup>, Nicolas Delcroix <sup>c</sup>, Laurent Chazalviel <sup>d</sup>, Romaric Saulnier <sup>c</sup>, Clément Gakuba <sup>a,e</sup>, Suzanne Goursaud <sup>a,e</sup>, Allan R. Young <sup>a</sup>, Maxime Gauberti <sup>a,f</sup>, Cyrille Orset <sup>a</sup>, Evelyne Emery <sup>a,b</sup>, Denis Vivien <sup>a,d,\*</sup>, Thomas Gaberel <sup>a,b</sup>

<sup>a</sup> INSERM, UMR-S U1237, Pathophysiology and Imaging of Neurological Disorders, University Caen-Normandy, CHU Caen, GIP Cyceron, Bd Henri Becquerel, Caen, France

<sup>b</sup> Department of Neurosurgery, Caen University Hospital, Avenue de la côte de Nacre, Caen, France

<sup>c</sup> UMS 3408, UNICAEN, CNRS, GIP Cyceron, Bd Henri Becquerel, Caen, France

<sup>d</sup> UMR6301-ISTCT, CNRS, CERVOXy Group, GIP Cyceron, Bd Henri Becquerel, Caen, France

<sup>e</sup> Department of Anesthesiology and Critical Care Medicine, Caen University Hospital, Avenue de la côte de Nacre, Caen, France

<sup>f</sup> Department of Radiology, Caen University Hospital, Avenue de la côte de Nacre, Caen, France

## ARTICLE INFO

## Article history:

Received 24 July 2017

Accepted 8 January 2018

Available online xxxx

## Keywords:

Diagnostic errors

Intracerebral hemorrhage

Magnetic resonance imaging

Oxygen inhalation therapy

## ABSTRACT

It was previously reported that normobaric oxygen therapy (NBO) significantly affected T2\*-weighted imaging in a mouse model of intracerebral hemorrhage (ICH). However, it is unclear whether a similar phenomenon exists in large volume ICH as seen in human pathology. We investigated the effects of NBO on T2\*-weighted images in a pig model of ICH. Our data show that NBO makes disappear a peripheral crown of the hematoma, which in turn decreases the apparent volume of ICH by 18%. We hypothesized that this result could be translated to ICH in human, and subsequently could lead to inaccurate diagnostic.

© 2018 Elsevier Ltd. All rights reserved.

Magnetic resonance imaging (MRI) is the most recommended modalities to evaluate hemorrhagic and ischemic stroke patients [1]. As an important part of these patients requires normobaric oxygen therapy (NBO) [1], the MRI related NBO impact has to be investigated. It was reported that NBO dramatically decreased the sensibility of T2\*-weighted imaging to detect intracranial hemorrhage (ICH) in a rodent model [2]. However, ICH volume in mice is very limited, so the generalization of this finding to human pathology was not possible. In the present study, we investigated the effects of NBO on standard T2\*-weighted imaging in a pig model of ICH. The report was carried out in accordance with the ARRIVE guidelines, the European Directives and the French Legislation on Animal Experimentation, and also approved by the local ethic committee (#7754 CENOMEXA, N°51, 2657–01). A total of 13 Langrâce pigs (35–40 kg) were included. During the surgical and imaging procedures, anesthesia was maintained with propofol

(80–120 µg/kg/min) and sevoflurane (1.5–2.0%). For ICH induction, a 3-mm burr hole was drilled at +2.4 cm anterior and +0.6 cm to the right of the bregma, and the dura mater was opened. The tip of a Fogarty catheter was introduced into the right frontal lobe and the balloon was inflated for 1 min. A catheter was then inserted into the preformed cavity and five ml of autologous arterial blood were injected (1.5 ml/min). The catheter was then removed and the wound closed [3].

Pigs were first exposed to normoxia (fraction of inspired oxygen,  $\text{FiO}_2 = 20\%$ ) during ICH induction and for an additional 30 min. A first MRI acquisition was performed, then pigs were exposed to NBO ( $\text{FiO}_2 = 100\%$ , NBO group,  $n = 7$ ) or normoxia (CTRL group,  $n = 6$ ) during 30 min. A second set of MRI acquisition was then performed. At each stage,  $\text{O}_2$ ,  $\text{CO}_2$  and pH arterial blood levels were measured using an automatic gas analyzer (Rapidlab, Siemens) (Fig. 1A). Experiments were performed in a 3 T scanner with the R3.2.3 release (Achieva quasar dual, Philips Healthcare; Amsterdam; The Netherlands) using small two elements flexible surface coil (FlexS, Philips Healthcare; Amsterdam; The Netherlands). The protocol consisted of a T2-weighted FFE sequence with these following sequence parameters: TR = 828.530 ms; TE = 16.1 ms; matrix size = 288 × 227; FOV = 230 × 182 × 71 mm;

\* Corresponding author at: Inserm, UMR-S U1237, Pathophysiology and Imaging of Neurological Disorders, University Caen-Normandy, CHU Caen, GIP Cyceron, Bd Henri Becquerel, Caen, France.

E-mail address: [vivien@cyceron.fr](mailto:vivien@cyceron.fr) (D. Vivien).

<sup>1</sup> Author with an equal contribution.

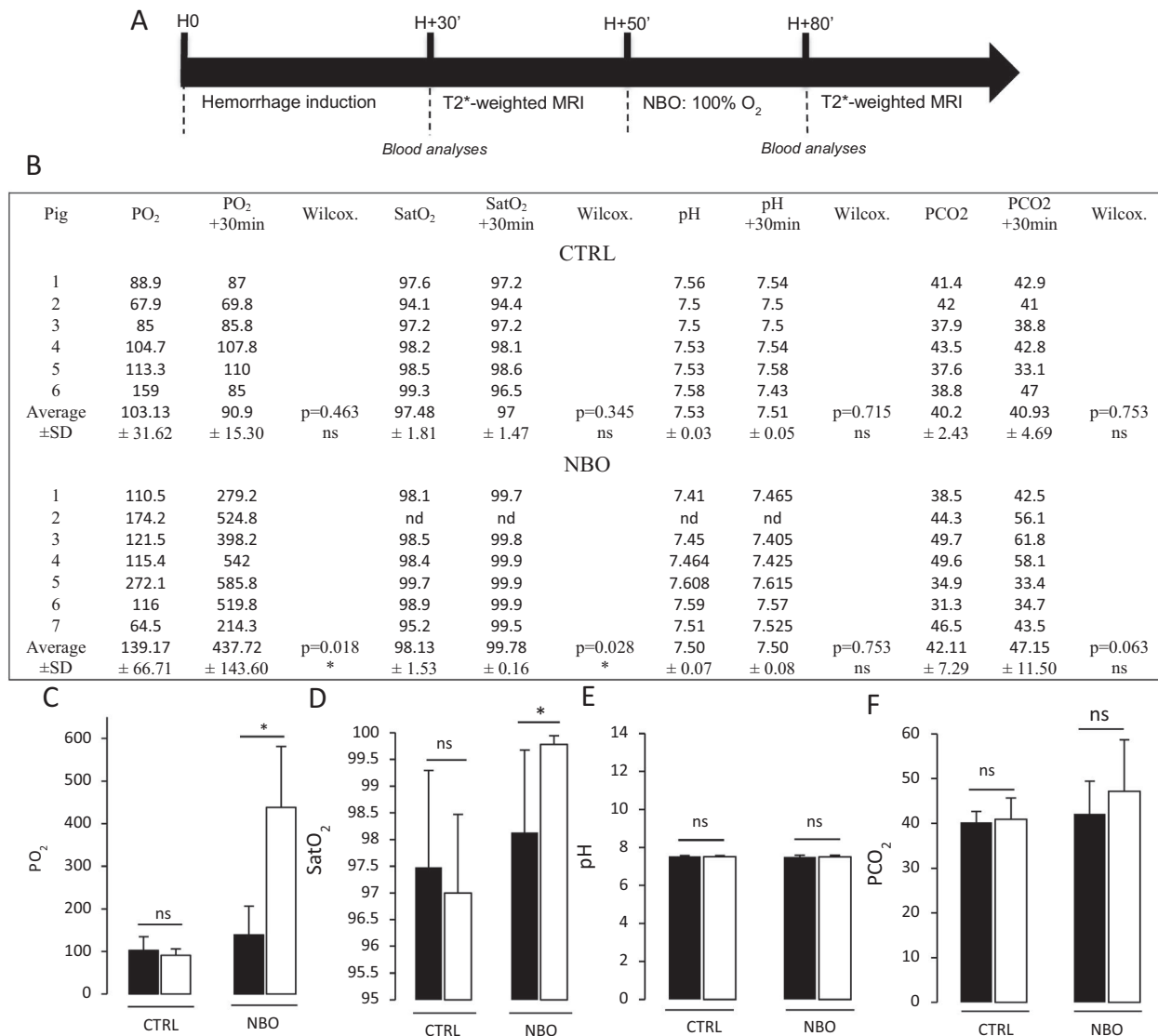


**Fig. 1.** NBO increases blood O<sub>2</sub> concentration. (A) Timeline of the performed experiments. (B) All the data are presented in the table. In comparison with CTRL group, NBO challenge increases (C) arterial blood PO<sub>2</sub> ( $139.17 \pm 66.7$  vs  $437.72 \pm 143.60$ ,  $p = 0.018$ ) and (D) SatO<sub>2</sub> ( $98.13 \pm 1.53$  vs  $99.78 \pm 0.16$ ,  $p = 0.028$ ). In both NBO and CTRL group, no significant changes were noticed for (E) pH and (F) PCO<sub>2</sub>. "nd" means no data available. Wilcoxon signed rank test, \*  $p < 0.05$ .

measurement time 151 s for 24 slices. Hemorrhagic volumes were then blindly quantified before and after normoxia or NBO challenge, using MRIcron 6.6 (2013) software [4]. Wilcoxon signed rank tests were performed with the SYSTAT 13 software package.

Although not modified after 30 min of normoxia, PO<sub>2</sub> was 3 times higher after NBO ( $p = 0.018$ ) (Fig. 1B, C) and the blood O<sub>2</sub> saturation significantly increased ( $p = 0.028$ ) (Fig. 1B–D). General pH (Fig. 1B–E) and PCO<sub>2</sub> (Fig. 1B–F) did not differ after both conditions. Evolution of the hematoma volumes (Fig. 2A, B) revealed an 18% decrease of the apparent hematoma volume after 30 min of NBO ( $-18\%$ ,  $p = 0.028$ ), although the apparent hematoma volume slightly increased in normoxia (+22%,  $p = 0.249$ ) (Fig. 2C).

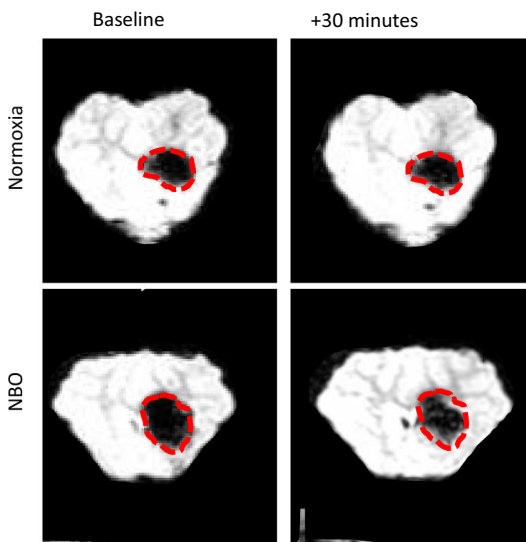
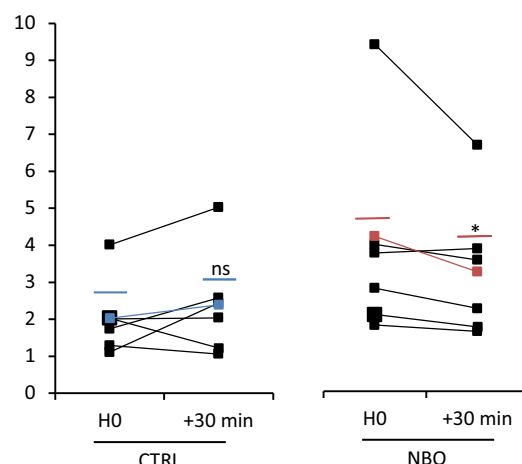
These data provide evidence in a large animal model that ICH signal on T2\*-weighted imaging is significantly affected by NBO, which confirm our previous work in mice [2]. This phenomenon can be explained by the transformation of deoxyhemoglobin (paramagnetic) to oxyhemoglobin (diamagnetic) due to a higher increased tissue concentration of O<sub>2</sub> induced by NBO, leading to normalization of the tissue magnetic susceptibility and therefore to an increase in magnetic resonance signal on T2\*-weighted images in hemorrhagic areas [5]. Interestingly, apparent hema-

toma volume in the normoxia group slightly increases. We hypothesized that this phenomenon is related to the transformation of oxyhemoglobin, present in the freshly induced hematoma, to deoxyhemoglobin. These results have several implications in preclinical studies. First, preclinical studies performed under anesthesia, involving measurement of hematoma volumes by T2\*-weighted imaging, should be considered with caution, and the PO<sub>2</sub> should be carefully monitored and reported as previously recommended [6,7]. We also unveil potential pitfalls of NBO therapy for T2\*-weighted imaging in patients, as our results suggest that T2\*-weighted imaging could 1) underestimate by about 18% the hematoma volume in patients treated by NBO and 2) fail to identify hematoma growth, which is a major risk factor of poor outcome. This would be particularly relevant for patients requiring respiratory support which are frequently ventilated with 100% O<sub>2</sub> during transport to the MRI facilities.

Nevertheless, since NBO is safe after ICH [8], identification of the underlying cause which remains a radiological challenge, may benefit from NBO preparation for revealing the brain parenchyma at the periphery of the hematoma. However, we must discuss

**A**

Pig	Lesion size (cm <sup>3</sup> )	Lesion size + 30 min (cm <sup>3</sup> )	Wilcox.	% evolution
<b>CTRL</b>				
1	1.74	2.58		48.27 +
2	1.29	1.06		17.82 -
3	1.11	2.44		119.81 +
4	2.03	1.22		39.903 -
5	2.01	2.04		1.49 +
6	4.01	5.03		25.43 +
Average	2.03	2.39	p=0.249	22.88 +
±SD	± 1.03	± 1.43	ns	± 56.75 +
<b>NBO</b>				
1	2.18	1.83		16.05 -
2	4.17	3.73		10.55 -
3	3.93	4.05		3.05 +
4	2.93	2.35		19.79 -
5	5.86	3.09		47.26 -
6	1.88	1.7		9.57 -
7	9.85	6.99		29.03 -
Average	4.4	3.39	p=0.028	18.46 -
±SD	± 2.75	± 1.82	*	± 16.09 -

**B****C**

**Fig. 2.** NBO decreases the apparent hematoma volume on T2\*-weighted imaging. (A) All the volume of the lesion and their evolution are presented in the table. These data are calculated from (B) representative T2\*-weighted images under normoxia or NBO following ICH. Hypo-intensity related to hemoglobin presence partially disappears after NBO. (C) Absolute individual values of hematoma volume before and after normoxia (CTRL) or NBO challenge show a significant decrease of the hematoma visualization after NBO ( $4.40 \pm 2.75$  vs  $3.39 \pm 1.82$ ,  $p = 0.028$ , Orange ligne) but not after normoxia ( $2.03 \pm 1.03$  vs  $2.39 \pm 1.43$ ,  $p = 0.249$ , Blue ligne). Wilcoxon signed rank test; \* =  $p < 0.05$ .

some limits of the present data. We investigated the effects of NBO therapy only 30 min after ICH onset. The efficiency of NBO preparation to induce disappearance of ICH on T2\*-weighted imaging later after ICH appearance remains to be investigated [9]. Finally, the clinical implications of our findings remain elusive and deserve to be adequately confirmed by human studies.

#### Author contribution statement

JP, DV, CO, RG and TG designed the experiments. TG, RG, AD, CDP, SG, LC, RS, CG, and PPS performed the experiments. PPS, ND, RG, AD acquired and analyzed the data. TG, RG, AD, PPS and DV wrote the manuscript.

#### Disclosure/conflicts of interest

The authors declare that they have no competing interest

#### Acknowledgements

This work was supported by the Institut National de la Santé Et de la Recherche Médicale, the French Ministry of Research and Technology. We thank Anthony LEVILLY, Severine LEVILLAIN and Claudine FAUCHON for their valuable technical support.

#### Appendix A. Supplementary data

Supplementary data associated with this article can be found, in the online version, at <https://doi.org/10.1016/j.jocn.2018.01.046>.

#### References

- [1] Jauch EC, Saver JL, Adams HP, Bruno A, Connors JJB, Demaerschalk BM. Guidelines for the early management of patients with acute ischemic stroke: a guideline for healthcare professionals from the American Heart Association/American Stroke Association. *Stroke* 2013;44(3):870–947.

- [2] Gaberel T, Gakuba C, Hebert M, Montagne A, Agin V, Rubio M. Intracerebral hematomas disappear on T2\*-weighted images during normobaric oxygen therapy. *Stroke* 2013;44(12):3482–9.
- [3] Rohde V, Rohde I, Thiex R, Ince A, Jung A, Dückers G. Fibrinolysis therapy achieved with tissue plasminogen activator and aspiration of the liquefied clot after experimental intracerebral hemorrhage: rapid reduction in hematoma volume but intensification of delayed edema formation. *J Neurosurg* 2002;97(4):954–62.
- [4] Rorden C, Karnath H-O, Bonilha L. Improving lesion-symptom mapping. *J Cogn Neurosci* 2007;19(7):1081–8.
- [5] Thulborn KR, Waterton JC, Matthews PM, Radda GK. Oxygenation dependence of the transverse relaxation time of water protons in whole blood at high field. *Biochim Biophys Acta* 1982;714(2):265–70.
- [6] Dirnagl U. Bench to bedside: the quest for quality in experimental stroke research. *J Cereb Blood Flow Metab* 2006;26(12):1465–78.
- [7] Sudduth TL, Powell DK, Smith CD, Greenstein A, Wilcock DM. Induction of hyperhomocysteinemia models vascular dementia by induction of cerebral microhemorrhages and neuroinflammation. *J Cereb Blood Flow Metab* 2013;33(5):708–15.
- [8] Fujiwara N, Mandeville ET, Geng X, Luo Y, Arai K, Wang X. Effect of normobaric oxygen therapy in a rat model of intracerebral hemorrhage. *Stroke* 2011;42(5):1469–72.
- [9] Linfante I, Llinas RH, Caplan LR, Warach S. MRI features of intracerebral hemorrhage within 2 hours from symptom onset. *Stroke* 1999;30(11):2263–7.

**THE ACTIVATION OF ENDOTHELIAL NMDA RECEPTOR BY THE CIRCULATING  
TISSUE TYPE PLASMINOGEN ACTIVATOR CONTRIBUTES TO  
NEUROVASCULAR COUPLING.**

Antoine ANFRAY<sup>1</sup>, Antoine DRIEU<sup>1</sup>, Vincent HINGOT<sup>3</sup>, Mervé YETIM<sup>1</sup>, Marina RUBIO<sup>1</sup>,  
Mikael TANTER<sup>3</sup>, Cyrille ORSET<sup>1,✉</sup> and Denis VIVIEN<sup>1,2✉,\*</sup>

1. Normandie Univ, UNICAEN, INSERM, UMR-S U1237, Physiopathology and Imaging of Neurological Disorders (PhIND), Caen, FRANCE.
2. CHU Caen, Department of Clinical Research, Caen University Hospital, Avenue de la Côte de Nacre, Caen, FRANCE.
3. Institut Langevin, ESPCI Paris, PSL Research University, CNRS UMR 7587, INSERM U979, Paris, FRANCE

<sup>✉</sup> These authors equally participated in the elaboration of the manuscript.

**\* Corresponding Author Information:**

Denis VIVIEN, PhD  
INSERM UMR-S U1237 “Physiopathology and Imaging of Neurological Disorders”, University Caen Normandie, GIP Cyceron, Bd Becquerel, BP5229, 14074 Caen, France.  
Phone, fax and e-mail: +33 2 31 47 01 66, +33 2 31 47 02 22, vivien@cyceron.fr

## **Abstract**

**Endothelial cells are centrally positioned to regulate key neurovascular functions of the brain.** Here, we postulated that endothelial cells may contribute to neurovascular coupling by a mechanism dependent of the tissue type Plasminogen Activator (tPA) present in the circulation. Thus, using pharmacological and genetic approaches to interfere with vascular tissue type Plasminogen Activator-dependent NMDA receptors signaling, combined with laser Doppler speckle flowmetry, intravital microscopy and fast ultrasound *in vivo* imaging, we demonstrate that the vascular tPA selectively increases the dilatation of large brain vessels, a mechanism elicited by a tPA-dependent activation of NMDA receptors expressed at the luminal part of endothelial cells. These data provide the first evidence that circulating molecules are capable to influence neurovascular coupling.

## **Introduction**

Regulation of the cerebral blood flow (CBF) plays a critical role in brain functions with its alteration as a cause or a consequence of several brain disorders, including stroke and Alzheimer's Disease. Therefore, understanding the cellular and molecular mechanisms underlying physiological and/or pathophysiological hemodynamic signals elicited by neuronal activation should lead to a better understanding of brain health and diseases. The control of the functional hyperemia, also known as neurovascular coupling (NVC)<sup>1</sup>, has been reported to involve almost all cells of the neurovascular unit (neurons, astrocytes, vascular smooth muscle cells, pericytes and endothelial cells)<sup>1-5</sup>, with mechanisms that may differ between arteries/arterioles and capillaries<sup>6-8</sup>.

Tissue type plasminogen activator (tPA) is a serine protease initially characterized for its role in fibrinolysis by its ability to convert plasminogen into plasmin<sup>9</sup>. Because of its beneficial properties against blood clot, tPA is currently used in the treatment of ischemic stroke either alone or combined with thrombectomy<sup>10,11</sup>. tPA was also described as a neuromodulator<sup>12,13</sup> and a gliotransmitter<sup>14</sup> implicated in various brain functions including learning and memory processes<sup>15,16</sup>, anxiety<sup>17,18</sup> or neuronal survival<sup>19</sup>. A number of its cerebral parenchymal effects are related to its ability to influence N-methyl-D-Aspartate receptor (NMDAR) signaling<sup>13,20,21</sup>. These data are in agreement with the previously proposed role of tPA in NVC via a mechanism involving neuronal NMDAR signaling<sup>22</sup>. However, the complete mechanism of action of tPA on NVC remains to be clarified since tPA may originate either from neurons<sup>23</sup> or endothelial cells<sup>24,25</sup> and NMDAR also being expressed on neurons and on endothelial cells<sup>26-29</sup>. When expressed on brain endothelial cells, NMDAR are involved in the maintenance of the integrity of

the blood–brain barrier (BBB)<sup>26,27</sup>, and their tPA-dependent modulations resulting in the passage of immune cells across the BBB in conditions of neuroinflammation<sup>30</sup>.

Whereas important studies have described signaling pathways in astrocytes, vascular smooth muscle cells, pericytes and endothelial cells involved in the control of hemodynamic signal induced by neuronal activity, some outstanding questions remain. As endothelial cells are localized at the interface between the circulation and the brain parenchyma, the question whether blood components are capable to influence NVC is still debated. Here, we hypothesized that vascular tPA may participate in hemodynamic responses induced by neuronal activation. To address this question, we took advantages of Doppler speckle, fast UltraSound (fUS) imaging and intravital imaging along with pharmacological and genetic approaches. We found that blood derived tPA, possibly released by endothelial cells, can potentiate the CBF increase evoked by activation of the mouse barrel cortex. Moreover, our study shows that this effect is mediated by a tPA-dependent activation of NMDAR expressed on endothelial cells of large vessels. Thus, while mechanisms reported so far to control NVC are centripetal (i.e. from the parenchyma to the vessels), we provide here the first evidences of a centrifugal mechanism in the control of NVC (i.e. from the blood stream to the endothelium).

## RESULTS

**Vascular tPA contributes to the full expression of functional hemodynamic signals.** We first performed a control study in which we compared CBF increase produced by whisker stimulation between mice with either an intact or a thinned skull (n = 3/4; **Suppl. Fig. 1a-c**). Briefly, the facial whiskers were mechanically stimulated in medetomidine anesthetized mice in which CBF was monitored on the whole brain surface by laser Doppler flowmetry, as described in the

methods section. As reported in the literature, whisker stimulation induced a 20% increased CBF in the thinned skull animals compared to a 10% increased CBF in the closed skull animals (**Suppl. Fig. 1b-c**). To avoid interferences due to the skull removal (integrity of the vessels, intracranial pressure, cerebrospinal fluid flows etc.) and to perform long term follow-up following genetic manipulations (see **Fig. 5**), we opted to use the closed skull model with each animal as its own control.

In a previous study by Park et al., (2008), it was proposed that the serine protease tPA contributes to the NVC. To further investigate the possible mechanisms of this action we examined the CBF increase produced by the activation of the whisker barrel cortex in 2-months old wild type (wt) versus tPA-deficient mice ( $tPA^{-/-}$ ) by using time lapse doppler speckle flowmetry. Using this procedure, we showed that the CBF increase evoked by whisker stimulation is significantly impaired in tPA deficient mice ( $tPA^{-/-}$ ) when compared to wt littermates (**Fig. 1a-c**; +7.29% of CBF increase for wt mice,  $n = 10$ , vs +5.45% for  $tPA^{-/-}$  mice,  $n = 10$ , i.e. -25.24% for  $tPA^{-/-}$  mice compared to tPAwt mice,  $p$ -value = 0.0042). There is no modification of the resting CBF either before or after whisker stimulation, neither heterogeneity of CBF increase in between the three stimulations performed prior and after treatments (**Suppl. Fig. 2**,  $n = 33$ ,  $p = 0.1577$ ).

Physiological parameters, including heart rate and arterial  $O_2$  saturation were not affected either by whisker stimulation nor by the phenotype of mice (**Suppl. Fig. 3a-b**). These data are in agreement with the literature<sup>22</sup>. Since tPA can be produced and released by both neurons<sup>23</sup> and endothelial cells<sup>24,25</sup>, we investigated in the absence of endogenous tPA expression whether exogenous tPA injected intravenously could rescue the phenotype observed in  $tPA^{-/-}$  mice.

Arginine free recombinant tPA (rtPA) was injected intravenously (10% in bolus and 90% in infusion for 15 minutes). The increase of the CBF in response to whisker stimulation was measured prior to and 10 minutes after the rtPA infusion, with each animal thus being its own

control (**Fig. 2a**). A control group injected with HEPES was also included. We found that intravenous rtPA infusion led to a significant increase of the hyperemia induced by whisker stimulation (**Fig. 2b-f**; CBF increase after whisker stimulation, compared before and after injections : HEPES injected tPA<sup>-/-</sup> mice, 6.60% vs 6.82%, i.e. +3.33% when normalized to the CBF increase before injection, *p*-value = 0.6953; rtPA injected tPA<sup>-/-</sup> mice, 6.57% vs 7.70%, i.e. +17.2% when normalized to the CBF increase before injection, *p*-value = 0.0117; n=11 in each group). These data demonstrate that the rtPA present in the blood stream contributes to the full expression of functional hyperemia. A similar set of experiments was performed using wild type animals instead of tPA<sup>-/-</sup> mice, in order to determine whether increasing the levels of circulating concentration tPA may promote NVC. Our data demonstrate that even in the presence of endogenous tPA, increasing rtPA levels in the blood stream leads to an increase of the hyperemia induced by whisker stimulation (**Suppl. Fig. 4**; CBF increase after whisker stimulation, compared before and after injections : HEPES injected tPAwt mice, 6.36% vs 6.24%, i.e. -1.89% when normalized to the CBF increase before injection, *p*-value = 0.8486; rtPA injected tPAwt mice, 6.45% vs 7.36%, i.e. +14.11% when normalized to the CBF increase before injection, *p*-value = 0.0093; n=11 for HEPES group and n=12 for rtPA group). A pooled analysis comparing all tPA<sup>-/-</sup> mice (n = 38), treated with rtPA or non-treated (i.e. injected with HEPES) confirms that vascular tPA promotes CBF increase induced by whisker stimulation (**Fig. 2b-f**; CBF increase after whisker stimulation, compared before and after injections : HEPES injected tPA<sup>-/-</sup> mice, 6.27% vs 6.31%, i.e. +0.64% when normalized to the CBF increase before injection, *p*-value = 0.8443; rtPA injected tPA<sup>-/-</sup> mice, 6.05% vs 6.98%, i.e. +15.18% when normalized to the CBF increase before injection, *p*-value < 0.0001; n=38 in each group). We then used functional fUS *in vivo* imaging modalities to confirm the function of tPA on NVC (**Fig. 3 a-e**). As reported above, when injected intravenously, rtPA led to an increase of the hyperemia induced by whisker

stimulation in the corresponding barrel cortex (CBF increase after whisker stimulation, compared before and after injections +7.31% vs +11.91% for rtPA treated tPA<sup>-/-</sup> mice (n = 7), i.e. +62.93% when normalized to the CBF increase before injection, *p*-value = 0.0042, n = 7). Control experiments were performed by injecting rtPA<sup>Alexa555</sup> in the circulation (at the same concentration as used for the rest of the study, i.e. 10mg/kg) to determine whether vascular rtPA may reach the brain parenchyma within the same time frame as the observations made in our experiments (**Suppl. Fig. 6**). In these conditions, our data show that the vascular rtPA did not reach the brain parenchyma (somatosensorial cortex) when evaluated 10 minutes after intravenous injection, in agreement with a direct effect of the vascular tPA on the endothelium. A positive control shows the extravasation of vascular rtPA<sup>Alexa555</sup> in the median eminence, a zone with fenestrated vessels. Altogether, these multimodal data demonstrate that intravenous tPA triggers the full expression of NVC.

**Vascular tPA enhances whisker stimulation induced vasodilation, a phenomenon restricted to large vessels.** Next, we used intravital microscopy in tPA<sup>-/-</sup> mice with or without intravenous infusions of rtPA to examine responses of individual vessels separated according their diameter (d) as follows: d>25μm, 15< d<25 and d<15μm (**Fig. 4a**). All types of vessels showed a dilation in response to whisker stimulation (**Fig. 4b-d**; +5.46% for vessels of d>25μm; +10.45% for 15< d<25μm; +16.54% for d<15μm). We observed that rtPA treatment leads to a more pronounced dilation of the vessels in the barrel cortex during whisker stimulation (**Fig. 4b**). However, a differential effect of rtPA was observed according to the vessels diameter. Indeed, although rtPA treatment led to an increase of the dilation of the larger vessels, rtPA did not affect the dilation of small vessels (**Fig. 4c-e**; d>25μm, +4.9%, p=0.0195; 15< d<25μm, +3.5%, p=0.0195; d<15 μm, -0.4%, p = 0.6406; n=9 vessels in each group).

## **NMDAR expressed on endothelial cells mediates the tPA-dependent modulation of NVC.**

We then postulated that the tPA present in the bloodstream could influence the NVC by its ability to modulate NMDAR signaling on endothelial cells. In order to address this question, we used a set of molecular tools that we have previously generated and characterized : tPA-K2\*, a tPA mutated on the amino-acids in positions 254 of the Lysine Binding Site (LBS) containing kringle 2 domain which is not capable to bind and activate NMDAR<sup>31</sup>; Glunomab®, a monoclonal antibody targeting the binding site of tPA on the GluN1 subunit of NMDAR, used as a competitive antagonist of tPA on NMDAR<sup>30,32</sup>. We then proposed that a chronic overexpression of tPA by the liver cells and its subsequent release in the circulation may promote the increased CBF induced by whisker stimulation in tPA<sup>-/-</sup> mice. We used a set of expression vectors that we previously characterized<sup>33</sup> (pLIVE plasmids) encoding for either a wt tPA (tPAwt) or a tPA-K2\* driven by a liver-specific promoter (pLIVE-tPAwt, pLIVE-tPA-K2\*; **Fig. 5**). The liver was transfected in vivo by a hydrodynamic injection of pLIVE constructs. For this set of experiments, each animal was tested before and after hydrodynamic transfection, and was thus its own control (**Fig. 5a**). Then, we performed zymography assays from corresponding blood samples to measure tPAs expression and activity<sup>33</sup>. As expected, we detected tPA proteolytic activity in the plasma of tPA<sup>-/-</sup> mice transfected with pLIVE-tPAwt or pLIVE-tPA-K2\*, but not with pLIVE (**Fig. 5b**). Our data showed that although tPA wt expression promoted the CBF increase induced by whisker stimulation, the expression of tPA-K2\*, unable to bind NMDAR<sup>31</sup>, did not (**Fig. 5c-f**; CBF increase after whisker stimulation, compared before and after transfection : pLIVE transfected tPA<sup>-/-</sup> mice, 6.40% vs 6.60%, i.e. +3.13% when normalized to the CBF increase before transfection, *p*-value = 0.6523; pLIVE-tPAwt transfected tPA<sup>-/-</sup> mice, 6.18% vs 7.22%, i.e. +16.83% when normalized to the CBF increase before transfection, *p*-value = 0.0391; pLIVE-tPA-K2\* transfected tPA<sup>-/-</sup> mice, 5.72% vs 6.12%, i.e. +6.99% when normalized to the CBF

increase before transfection,  $p$ -value = 0.25; n = 9 for pLIVE group, n = 8 in pLIVE-tPAwt and pLIVE-tPA-K2\* groups). These data demonstrate that the circulating tPA can promote the CBF increase induced by whisker stimulation through a mechanism involving its K2 domain, suggesting a mechanism dependent on NMDAR.

However, mutation of the LBS within the kringle 2 domain of tPA may also interfere with NMDAR-independent functions of tPA. For this reason, we performed complementary experiments using Glunomab®, targeting not tPA itself, but directly the binding site of tPA on NMDAR specifically and thus blocking subsequent NMDAR signaling<sup>30,32</sup>. In agreement with the above data and our hypothesis that vascular tPA may contribute to NVC by acting on NMDAR expressed on endothelial cells, acute infusion of Glunomab® blocked the rtPA-induced increase of hyperemia during whisker stimulation (**Fig. 6**; CBF increase after whisker stimulation, compared before and after injections : rtPA + control IgG injected tPA<sup>-/-</sup> mice, 6.10% vs 6.96%, i.e. +14.09% when normalized to the CBF increase before injection,  $p$ -value = 0.0391; rtPA + Glunomab® injected tPA<sup>-/-</sup> mice, 6.35% vs 6.36%, i.e. +0.16% when normalized to the CBF increase before injection,  $p$ -value = 0.8438; n=9 in each group). For all these experiments, each animal was its own control. A corresponding T-map analysis confirmed the rtPA mediated increase of hyperemia induced by whisker stimulation, an effect prevented by the co-infusion with Glunomab® (**Suppl. Fig. 7**; tPA<sup>-/-</sup> + tPA group, n = 12; tPA<sup>-/-</sup> + tPA + Glunomab® group, n = 9).

Furthermore, these data were confirmed by using common NMDAR antagonists: MK-801 (Dizocilpine), a competitive antagonist of NMDAR, and D-2-amino-5-phosphonopentanoate (AP5), a non-competitive NMDAR antagonist (**Fig. 7**). Both MK-801 and AP5 blocked the rtPA effect on the CBF increase induced by whisker stimulation (CBF increase after whisker stimulation, compared before and after injections: rtPA + saline injected tPA<sup>-/-</sup> mice, 5.23% vs

5.83%, i.e. +11.47% when normalized to the CBF increase before injection, *p*-value = 0.0078; rtPA + MK801 injected tPA<sup>-/-</sup> mice, 5.44% vs 5.61%, i.e. +3.13% when normalized to the CBF increase before injection, *p*-value = 0.8438; rtPA + AP5 injected tPA<sup>-/-</sup> mice, 6.05% vs 6.17%, i.e. +1.98% when normalized to the CBF increase before injection, *p*-value = 0.7422; n = 9 for rtPA + saline group, n = 10 for rtPA + MK801 group, n = 8 for rtPA + AP5 group). Altogether, these data demonstrate that the vascular tPA triggers NVC through a mechanism dependent of its ability to activate the NMDAR present at the surface of endothelial cells.

In order to understand why the dilation of only larger vessels is affected by rtPA, we sought to investigate the distribution of NMDAR in brain vessels. To do so, we performed immunostaining for GluN1-containing NMDAR from isolated brain vessels. Vessels were discriminated by positive or negative immunostaining for alpha-SMA (smooth muscle antigen; **Fig. 8a**). In agreement with the above data, immunostainings revealed the presence of NMDAR only on large and alpha-SMA positive vessels, i.e. arteries and arterioles (**Fig. 8b-e**; n = 34 for alpha-SMA positive vessels, n = 29 for alpha-SMA negative vessels, *p*-value = 0.011).

Overall, we demonstrate here for the first time that the vascular tPA presents in the circulation triggers the full expression of NVC by promoting the signaling of the NMDAR expressed on the lumen of endothelial cells, a phenomenon restricted to larger vessels (arteries and arterioles).

## DISCUSSION

CBF increases quickly in response to neural activation, a phenomenon termed functional hyperemia or NVC which triggers local supply of substrates and energy of corresponding neurons<sup>1</sup>. Many different molecules are involved in NVC, and their mechanisms of action are not yet completely understood. Among them, it was reported that NMDAR activation contributes to

this process<sup>1,2</sup>. Indeed, an important part of the vascular response is mediated by the activation of post-synaptic NMDAR. NMDAR are associated through the scaffolding postsynaptic density-95 protein (PSD-95) to the neuronal NO synthase (nNOS)<sup>34,35</sup>, a Ca<sup>2+</sup> calmodulin-dependent enzyme whose activation leads to the production and release of the vasodilator nitric oxide (NO)<sup>36</sup>.

Accordingly, NMDAR can regulate nNOS activity by increasing intra-cellular Ca<sup>2+</sup> concentration and regulating the phosphorylation of the nNOS<sup>37–40</sup>.

Other small molecules such as extracellular potassium, cyclooxygenase metabolites and adenosine have also been suggested to be involved in NVC<sup>2</sup>. More recently, a larger molecule, the serine protease tPA (69 kDa) was proposed as an actor of NVC<sup>10</sup> for its ability to influence NMDAR signaling<sup>11</sup>. Thus, in addition to its role in fibrinolysis<sup>12</sup>, tPA has more recently emerged as a pleiotropic neuromodulator implicated in various aspects of brain functions<sup>13,14</sup>. The evidence that tPA has a role in normal NVC was first reported by Park *et al* by using a mouse model of whisker stimulation<sup>10</sup>. Compared with wild-type mice, CBF in the corresponding barrel cortex of tPA deficient mice showed a sustained attenuation after whisker stimulation. In this pioneer publication, administration of rtPA (on the surface of the brain parenchyma) to tPA deficient mice restored NVC with NMDAR and activation of NOS implicated as mediators of this response<sup>10</sup>. Our present data confirm the role of tPA in NVC, providing in addition the demonstration that beyond its role at the synapse level, circulating tPA plays a significant role. Indeed, although tPA deficient mice showed an impaired CBF increase induced by whisker stimulation (**Fig. 1**, -25.24% when compared to wt mice, p = 0.0042), this lack of response is rescued after intravenous injection of rtPA (**Fig. 2**, +17.2% when compared to tPA<sup>-/-</sup> mice before injection, p = 0.0117). Increasing the amount of circulating tPA in wt mice also led to an increase of the hyperemia induced by whisker stimulation (**Suppl. Fig. 4**, +14.11%, p = 0.0093). Altogether, these data argue for a dose dependent role of circulating tPA on NVC.

NVC consists of coordinated series of vasomotor events, including dilation of penetrating arterioles and capillaries<sup>1</sup>. Despite evidence that the endothelium is an important contributor to brain hyperemia, the nature of how it contributes to the dialogue between neurons, smooth muscle cells and astrocytes in NVC remains unknown. Both centripetal (from the brain parenchyma to the endothelium) or centrifugal (from the endothelium) signaling are considered. Although centripetal pathways are largely described in the literature<sup>1,2</sup>, emerging evidence suggest an important role of endothelial cells in NVC. Endothelial cells would indeed be the support of the propagation of a retrograde activity-induced signal that triggered the dilation of larger vessels upstream of the activated area<sup>1,5,46</sup>. Furthermore, the presence of NMDAR on endothelial cells was reported by several groups<sup>25–28</sup> with roles in the control of the homeostasis of the BBB on healthy and injured brains<sup>47</sup>. NMDAR were also reported to act on the cerebral blood vessel tone<sup>48,49</sup>. Particularly, several studies have showed that NMDAR expressed on endothelial cells were involved in the dilation mechanism of middle cerebral arteries isolated from mice<sup>50</sup>, necessitating the co-activation by glutamate and D-serine. The activation of endothelial NMDAR elicited by astrocytes thus leads to the production of NO by the eNOS and to the dilation of brain vessels<sup>51,52</sup>.

Accordingly, vascular tPA was also reported to have vasodilation properties on peripheral vessels and to reduce the brain vessels reactivity<sup>53–55</sup>, cerebral vascular resistance and systemic blood pressure<sup>56</sup>, suggesting that tPA may modulate cerebrovascular tone during functional hyperemia. It is also interesting to note that an inactive tPA variant (tPA-S481A) was capable of preventing the impairment of autoregulation when administered 30 minutes after fluid percussion injury through the inhibition of the NMDAR over-activation<sup>57</sup>. Similarly, a tPA variant tPA-(A296-299), characterized to prevent the binding of endogenous tPA to NMDAR, was reported to prevent impairment of cerebral autoregulation and necrosis of hippocampal neurons after

stroke<sup>58</sup>. Here we made the hypothesis that vascular tPA could act on endothelial NMDAR to promote brain vessels dilation during functional hyperemia. Thus, deletion and rescue experiments were performed using a mutation of tPA, tPA-K2\* previously reported to not bind with NMDAR and thus to not promote their signaling (**Fig. 5**)<sup>41</sup>, and a monoclonal antibody (Glunomab®) characterized as an antagonist of tPA on NMDAR signaling (**Fig. 6**)<sup>42</sup>. Our data were also confirmed by using different modalities of *in vivo* imaging including the largely used Doppler speckle imaging (**Fig. 1, 2, , 5, 6, 7**) and intravital microscopy imaging (**Fig. 4**), in addition to the more recent promising methodology of fUS (**Fig. 3**)<sup>59–61</sup>.

In addition, it is interesting to note that tPA was previously reported to influence NO and ROS production on endothelial cells by a mechanism dependent of NMDAR<sup>26</sup>. This is to be compared with the study of LeMaistre et al., 2012, which shows that the dilation of the middle cerebral artery mediated by the activation of NMDAR required an intact endothelium and the presence of eNOS, supporting the hypothesis of on action of tPA directly on the vessel.

Our data show that the NMDAR exhibited on the luminal part of endothelial cells are involved in the control of NVC. Other receptors also expressed on endothelial cells have been shown to be involved in autoregulation<sup>62</sup>. It is the case for the Low density lipoprotein Receptor Protein (LRP-1), a receptor of tPA also known to interfere with the tPA-dependent NMDAR signaling<sup>63</sup>.

Traditionally, regulation of CBF was thought to occur at the level of arterioles<sup>48</sup>. However, capillaries in the brain are also wrapped by contractile cells called pericytes<sup>49</sup>, which can respond to neuronal activity and control blood flow. Our data confirm the dilation of large vessels (>15 μm of diameter) and small vessels (<15 μm of diameter) in response to whisker stimulation.

However, rtPA only promotes vasodilation of larger vessels of at least 15 μm of diameter (**Fig. 4c-e**). It is thus interesting to note that expression of NMDAR is restricted to these large vessels (**Fig. 8**). Accordingly, tPA has also been reported to be primarily associated with precapillary

arterioles in the CNS<sup>64</sup>. Furthermore, it should be noted that tPA deficiency in mice is possibly associated with abnormal cerebral vascularization, including a reduction in the amount of large diameter vessels<sup>65</sup>. However, injection of rtPA in the blood circulation of both tPA wt and tPA deficient mice leads to an increase in the vascular response to whisker stimulation thus supporting an effect of tPA on NVC independent of a possible abnormal vascularization.

Although NVC is the basis of blood oxygen level dependent (BOLD) functional magnetic resonance imaging (fMRI), our understanding of the underlying signaling mechanisms is still incomplete. Our study provides important information to understand the complexity of fMRI, with the demonstration that a vascular molecule such as tPA may contribute to NVC by interacting with NMDAR expressed on the luminal side of endothelial cells. The finding that tPA modulates functional hyperemia raises the possibility that levels of vascular tPA may contribute to the alterations in NVC that occur in aging<sup>66-69</sup> or brain pathologies such as Alzheimer's disease or ischemic stroke<sup>1,70</sup>. Indeed, the levels of the principal inhibitor of tPA in the blood stream, PAI-1, increased with Alzheimer Disease<sup>71</sup>, raise the possibility that this increased tPA inhibition in the circulation could participate in the impairment of NVC. Moreover, stroke leads to a profound alteration in NVC in the acute phase after the ischemic event, worsening cerebral perfusion and promoting brain damages<sup>70</sup>, an effect which could be explained by alterations of the vascular levels of active tPA.

Our study reports for the first time that a molecule present in the circulation (here tPA) contributes to the full expression of functional hemodynamic signals. We found that vascular tPA, potentially released in the blood circulation by endothelial cells during neuronal activity, can interact with endothelial NMDAR and promote the dilation of large vessels surrounded by SMC. Vascular tPA is thus necessary for the full expression of functional hyperemia.

## **Materials and Methods**

**Animals.** All experiments were performed on male tPA wt, tPA<sup>-/-</sup> or C57BL/6 aged from 8 to 12 weeks. tPA wt and tPA<sup>-/-</sup> were produced at the Centre Universitaire de Ressources Biologiques (Caen, France), and C57BL/6 mice came from Janvier labs (Le Genest-Saint-Isle, France). Mice were housed in plastic cages on a 12h light cycle with ad libitum access to water and food. During experiments, body temperature was maintained with electric heating pads with thermal feedback, and heart rate and blood O<sub>2</sub> saturation were monitored using the MouseOx+ device (Starr Life Sciences Corporation). All experiments and analysis were randomized and performed blind. All procedures were approved by the.....

**Animals preparation.** Anesthetized was initially induced using 5% isoflurane (Forene®, AbbVie) in 70% N<sub>2</sub>O / 30% O<sub>2</sub> and then maintained using 2% isoflurane in 70% N<sub>2</sub>O / 30% O<sub>2</sub>. Mice were intubated, placed under mechanical ventilation, and fixed in a stereotaxic frame. The skull was exposed, and lidocaine (Xylocaine 5% spray®, AstraZeneca) was applied. Whiskers on the left side of the mouse were cut to let only about 1 cm. A catheter was placed in the tail vein, to allow further IV injection. Anesthesia was then switched to medetomidine (Domitor®, Pfizer, 0.1mg/kg). Isoflurane, N<sub>2</sub>O and O<sub>2</sub> were stopped 10 min after the bolus injection. A waiting time of at least 20 min was then respected, to allow the stabilization of the CBF. Preliminary experiments were performed in order to evaluate physiological parameters, especially blood pCO<sub>2</sub> and pH, in mice placed in experimental conditions. These experiments revealed normal values for these parameters in our conditions. These controls were repeated regularly.

**Pharmacology.** During experiments, different treatments were injected through the tail vein of the mice. The total volume injected was 300µL as follows: a bolus of 150µL, 10 minutes before the beginning of the CBF response measurement, followed by an infusion (10µL/min). Dosages

were as follows: rtPA = 10mg/kg; AP5 (acide 2-amino-5-phosphonovalérique, noncompetitive antagonist of NMDARs) = 0.3mg/kg; MK-801 (competitive antagonist of NMDARs) = 0.3mg/kg; Glunomab® and control IgG = 5mg/kg. As a control, HEPES (0.3M) and saline (0.9%) were injected.

**rtPA preparation.** rtPA was prepared from Actilyse® (Boehringer Ingelheim). In order to eliminate the arginine buffer contained in the commercial solution, rtPA was dialyzed in HEPES buffer (4-(2-hydroxyethyl)-1-piperazineethanesulfonic acid, 0.3 M, pH 7.4, Sigma-Aldrich) using dialysis cassettes (Slide-A-Lyzer® 10K; ThermoScientific).

**Laser Doppler speckle flowmetry.** CBF responses to whisker stimulations in medetomidine anesthetized mice were determined using laser Doppler speckle flowmetry directly through the skull. Images were acquired using a Laser Speckle Contrast Imager (moorFLPI-2, Moor Instruments; Sample interval: 1 Hz, exposure time: 20 ms, FOV = 6 mm x 11.3 mm, images resolution752x580). Stimulation were performed by mechanically shaking (4-5Hz) mice whiskers on the left side over a period of 30 seconds, followed by a 90 seconds rest periods, three times (total time = 390s). Images were analyzed using the moorFLPIReviewV40 software (moorFLPI-2, Moor Instruments). The average of the images obtained during rest were subtracted to the average of the images obtained during stimulation, revealing the area where the CBF had changed during the stimulation. The average CBF signal of this area was then extracted, and the percent of increase of the CBF was calculated based on the baseline signal during rest. Values of the 3 stimulations were then averaged.

**Intravital microscopy.** The day before the experiment, animals were anesthetized with isoflurane and placed in a stereotaxic frame. The skull was exposed, and the area above the S1bf cortex was thinned with a drill. Anesthesia and animal preparation was the same as for laser Doppler speckle flowmetry. Just before the imaging, an IV injection of FITC Dextran (100µl;

70.000 kDa; Sigma Aldrich) was performed. Stimulation was performed during a single 10 seconds period. Images were analyzed using ImageJ software (NIH). Images obtained during rest and during stimulation were averaged, and the diameter was measured perpendicularly to the vessel walls.

**Hydrodynamic transfection.** Hydrodynamic transfection were conducted as previously described<sup>33</sup>. Mice were injected with 100 µg of pLIVE plasmid alone, as a control, pLIVE plasmid encoding wild-type rat tPA (pLIVE-tPA) or tPA mutants (pLIVE-tPA-K2\*). Briefly, a large volume (10% of body weight) of plasmid-containing saline buffer (0.9% NaCl) was injected in the tail vein of the mice in less than 5 seconds. This approach with the pLIVE vector allows the constitutive hepatic expression of the insert during few days. Laser Doppler speckle flowmetry was realized before the transfection (see **Laser Doppler speckle flowmetry** section). At the end of this first measurement, mice received an intraperitoneal injection of atipamezole (0.5mg/kg, Antisedan®, Pfizer) to facilitate their wake up. 48 hours after the transfection, a second CBF measurement was realized (see **Laser Doppler speckle flowmetry** section). Right after, blood sampling was performed by retro-orbital puncture. Blood was anticoagulated using citrate. Blood samples were then subject to a 1500g centrifugation for 15 min, to separate cells from plasma. Supernatant was separated and subjected to a 10.000g centrifugation, to separate plasma from remaining platelets.

**Zymography.** The presence of free plasmatic tPA after hydrodynamic transfection was detected by direct fibrin autography following sodium dodecylsulphate polyacrylamide gel electrophoresis (SDS-PAGE) performed as previously described<sup>72</sup>. Plasma samples and reference tPA (0.25 nM, 10µL) were subjected to SDS electrophoresis (8% polyacrylamide gels, under non-reducing conditions). SDS was then exchanged with 2.5% Triton X-100. After washing off excess Triton X-100 with distilled water, the gel was carefully overlaid on a 1% agarose gel containing

1mg/mL bovine fibrinogen, 100 nM plasminogen and 0.2 NIH U/mL of bovine thrombin.

Zymograms were allowed to develop at 37°C for 12h and photographed at regular intervals using dark-ground illumination. Active proteins in plasma samples were identified by reference to the migration of known tPA.

**Functional ultrasound imaging.** Introduced in Macé *et al.*, 2011<sup>61</sup>, functional ultrasound (fUS) enables a fast tracking of hemodynamic changes in depth in animal brains submitted to an external stimulation. fUS sequences and parameters in the present study reproduce the methodology described in Tiran *et al.*, 2017<sup>60</sup> where fUS was applied to different models of rodents, especially in mice's and describe the response to whisker stimulation.

The day before the experiment, animals were anesthetized with isoflurane and placed in a stereotaxic frame. The skin was cut to expose the skull and the area above the S1bf cortex was thinned with a drill.

The animal preparation was then the same as for the Laser Doppler speckle flowmetry experiments (see **Laser Doppler speckle flowmetry section**), except that ultrasound gel was applied between the ultrasound probe and the mouse skull to ensure good acoustic coupling. The probe was positioned over the coronal plane corresponding to the somatosensory barrel field cortex (S1bf; bregma -1.5mm). Stimulations were performed the same way as for the Laser Doppler speckle flowmetry experiments (see **Laser Doppler speckle flowmetry section**).

Ultrafast Acquisition were performed using compound plane wave ultrasound sequence (11 angles from -10° to 10° by steps of 2°) and a 15 MHz ultrasonic probe (Vermon, France, 80 µm x 100 µm voxels, elevation focus 8 mm) with a frame rate of 500 Hz. 200 images were acquired every second for 390s. For each bloc of 200 images, blood signal was extracted from tissue signal using singular value decomposition filters and excluding the 60 most energetic singular values.

For each pixel, the correlation coefficient was calculated between the normalized Power Doppler (PD) intensity along time and a step function following the stimulation pattern. An activation map was reconstructed by keeping only pixels with a correlation coefficient higher than 0.2 and superimposing the corresponding pixels on the mean Doppler image. An artefact caused by the mechanical respirator was masked on the bottom left of the image, without significant impact on the activation in the cortex.

The activated area was determined as the pixels with a correlation coefficient higher than 0.2 corresponding to 2 times the spatial standard deviation of CBV baseline estimated in a non-activated area. The quantification of the relative PD increase is performed of the mean PD signal in the activated area.

**Immunohistochemistry on isolated brain vessels.** Brain vessels of C57BL/6 mice were isolated as previously described<sup>73</sup>. Deeply anesthetized mice were transcardially perfused with cold heparinized saline (15 mL/min). Brain were then dissociated in a solution of HEPES and HBSS and then centrifuged at 2000g at 4°C during 10 min. Most of myelin is eliminated at this step, and vessels form a pellet. The pellet was then suspended in a solution of HEPES/HBSS and Dextran (Dextran from Leuconostoc spp. Mr ~70,000, Sigma-Aldrich) and centrifuged at 4400g at 4°C during 15 min. Remaining myelin is eliminated here. Vessels were then suspended in a solution of HEPES/HBSS and BSA 1% and filtrated on a 20µm mesh filter. After that, vessels stay on the filter. Vessels were then detached from the filter in a PBS solution. Vessels were then put on a poly-lysine coated slides, cryoprotected overnight in a 20% sucrose PBS solution and fixated during 15 min with PBS 0.1 M. pH 7.4 containing 2% paraformaldehyde and 0.2% picric acid. Slide were stored at -80°C before processing. Vessels were then co-incubated overnight with rabbit anti-PDGF-R $\beta$  (1:1000, ab32570, Abcam) primary antibodies and FITC-conjugated mouse anti- $\alpha$ SMA (1:500, ab8211, Abcam) primary antibodies, or with goat anti-GluN1 (1:200, sc-

1467, Santa-Cruz) primary antibodies, FITC-conjugated mouse anti- $\alpha$ SMA (1:500, ab8211, Abcam) primary antibodies and rabbit anti-laminin (1:2000, ab11575, Abcam) primary antibodies. Primary antibodies were revealed using Fab'2 fragment anti rabbit and goat IgG linked to CY3 and Alexa Fluor 647 (1:600, Jackson ImmunoResearch) co-incubated 90 min at room temperature. Vessels were then coverslipped using mounting medium containing DAPI. Images were digitally captured using an epifluorescence microscope (Leica DM6000). Fluorescent intensity of the GluN1 staining in vessels were assessed using ImageJ software (NIH).

**rtPA extravasation.** Arginine content in Actilyse was removed by dialysis at 4°C overnight (see **rtPA preparation** section). Then, purified rtPA was mixed with the N-succinimidyl ester of Alexa<sup>555</sup> for 4 h at 4°C with continuous stirring. The resulting solution was dialyzed in bicarbonate buffer overnight at 4°C to remove unbound dyes. Afterward, tPA-Alexa<sup>555</sup> (tPA<sup>555</sup>) was frozen and stored at -80°C until further use. tPA<sup>555</sup> (50 $\mu$ g) was then intravenously injected in mice. 10 min after the injection, mice were deeply anesthetized and were transcardially perfused with cold heparinized saline (15 mL/min) followed by 75 mL of fixative (phosphate buffer 0.1M; pH 7.4; 4% paraformaldehyde). Brains were post-fixed (24 hours; 4°C) and cryoprotected (sucrose 20% in PBS buffer; 4°C) before freezing in embedding medium (Shandon<sup>TM</sup> Cryomatrix<sup>TM</sup>; Thermo Scientific). Cryomicrotome-cut sections (10  $\mu$ m) were collected on poly-lysine slides and stored at - 80°C before processing. Sections were incubated overnight with FITC-conjugated mouse anti- $\alpha$ SMA (1:500, ab8211, Abcam) primary antibodies. Sections were then coverslipped using mounting medium containing DAPI. Images were digitally captured using an epifluorescence microscope (Leica DM6000).

**Electrophoresis of tPA<sup>555</sup>.** Increasing doses (1, 5 and 10µg) were subjected to electrophoresis in SDS-PAGE (7.5%). tPA<sup>555</sup> was then visualized using ImageQuant LAS 4000 camera (GE Healthcare).

**Pooled analysis:** Data from the tPA<sup>-/-</sup> mice that have received control treatment from figures 2, 5 and 8 and tPA<sup>-/-</sup> mice that have received rtPA treatment from figures 2, 5, 8, and 7, either from IV injection or hydrodynamic transfection, were pooled together to perform a pooled statistical analysis of the effect of the presence of rtPA in the blood circulation. T-map were created using data from tPA<sup>-/-</sup> mice that have received the rtPA treatment from figure 2 or using data from tPA<sup>-/-</sup> mice that have received rtPA + GluN1ab® from the figure 7. For this analysis, the average of the images obtained during rest were subtracted to the average of images obtained during stimulation before the injection, and a t-test was performed to reveal area where the stimulation produced a significant increase in the CBF. The same process was applied for the images obtained after the injection. Images (before and after the injection) were subtracted, spatially aligned and averaged between all mice of the group, and a t-test was performed on the resulting image, to reveal area where the presence of the rtPA in the blood flow induced a significant promotion of the CBF increase during whisker stimulation.

**Statistical analysis.** Results are expressed as the mean ± the standard error of the mean (SEM). Statistical analysis were performed using Mann-Whitney test, Wilcoxon test or t-test with the Statistica software (Statsoft). For the GluN1 fluorescence intensity and the pool meta-analysis, normality was assessed using D'Agostino & Pearson normality test. Values were considered statistically different if probability value, p<0.05.

## Authors contributions

Study design: D.V., A.A. and C.O. Conducting experiments and acquiring data: A.A., A.D., V.H., C.O., M.R. and M.Y. Analyzing data: A.A and V.H. Writing the manuscript: D.V., A.A, and M.T.

### **Competing interests**

The authors declare no competing financial interests.

## Bibliographie

1. Iadecola, C. The Neurovascular Unit Coming of Age: A Journey through Neurovascular Coupling in Health and Disease. *Neuron* **96**, 17–42 (2017).
2. Attwell, D. *et al.* Glial and neuronal control of brain blood flow. *Nature* **468**, 232–243 (2010).
3. Otsu, Y. *et al.* Calcium dynamics in astrocyte processes during neurovascular coupling. *Nat. Neurosci.* **18**, 210–218 (2015).
4. Kisler, K. *et al.* Pericyte degeneration leads to neurovascular uncoupling and limits oxygen supply to brain. *Nat. Neurosci.* **20**, 406–416 (2017).
5. Chen, B. R., Kozberg, M. G., Bouchard, M. B., Shaik, M. A. & Hillman, E. M. C. A Critical Role for the Vascular Endothelium in Functional Neurovascular Coupling in the Brain. *J. Am. Heart Assoc.* **3**, e000787 (2014).
6. Hill, R. A. *et al.* Regional Blood Flow in the Normal and Ischemic Brain Is Controlled by Arteriolar Smooth Muscle Cell Contractility and Not by Capillary Pericytes. *Neuron* **87**, 95–110 (2015).
7. Hall, C. N. *et al.* Capillary pericytes regulate cerebral blood flow in health and disease. *Nature* **508**, 55–60 (2014).
8. Fernández-Klett, F., Offenhauser, N., Dirnagl, U., Priller, J. & Lindauer, U. Pericytes in capillaries are contractile in vivo, but arterioles mediate functional hyperemia in the mouse brain. *Proc. Natl. Acad. Sci.* **107**, 22290–22295 (2010).
9. Collen, D. & Lijnen, H. R. Basic and clinical aspects of fibrinolysis and thrombolysis. *Blood* **78**, 3114–3124 (1991).

10. Vivien, D., Gauberti, M., Montagne, A., Defer, G. & Touzé, E. Impact of tissue plasminogen activator on the neurovascular unit: from clinical data to experimental evidence. *J. Cereb. Blood Flow Metab. Off. J. Int. Soc. Cereb. Blood Flow Metab.* **31**, 2119–2134 (2011).
11. Alberts, M. J., Shang, T. & Magadan, A. Endovascular Therapy for Acute Ischemic Stroke: Dawn of a New Era. *JAMA Neurol.* **72**, 1101–1103 (2015).
12. Samson, A. L. & Medcalf, R. L. Tissue-type plasminogen activator: a multifaceted modulator of neurotransmission and synaptic plasticity. *Neuron* **50**, 673–678 (2006).
13. Nicole, O. *et al.* The proteolytic activity of tissue-plasminogen activator enhances NMDAR-mediated signaling. *Nat. Med.* **7**, 59–64 (2001).
14. Cassé, F. *et al.* Glutamate controls tPA recycling by astrocytes, which in turn influences glutamatergic signals. *J. Neurosci. Off. J. Soc. Neurosci.* **32**, 5186–5199 (2012).
15. Pawlak, R. *et al.* Rapid, specific and active site-catalyzed effect of tissue-plasminogen activator on hippocampus-dependent learning in mice. *Neuroscience* **113**, 995–1001 (2002).
16. Madani, R. *et al.* Enhanced hippocampal long-term potentiation and learning by increased neuronal expression of tissue-type plasminogen activator in transgenic mice. *EMBO J.* **18**, 3007–3012 (1999).
17. Pawlak, R., Magarinos, A. M., Melchor, J., McEwen, B. & Strickland, S. Tissue plasminogen activator in the amygdala is critical for stress-induced anxiety-like behavior. *Nat. Neurosci.* **6**, 168–174 (2003).
18. Matys, T. *et al.* Tissue plasminogen activator promotes the effects of corticotropin-releasing factor on the amygdala and anxiety-like behavior. *Proc. Natl. Acad. Sci. U. S. A.* **101**, 16345–16350 (2004).

19. Chevilly, A. *et al.* Impacts of tissue-type plasminogen activator (tPA) on neuronal survival. *Front. Cell. Neurosci.* **9**, (2015).
20. Parcq, J. *et al.* Unveiling an exceptional zymogen: the single-chain form of tPA is a selective activator of NMDAR-dependent signaling and neurotoxicity. *Cell Death Differ.* **19**, 1983–1991 (2012).
21. Hébert, M. *et al.* Distant Space Processing is Controlled by tPA-dependent NMDAR Signaling in the Entorhinal Cortex. *Cereb. Cortex* **27**, 4783–4796 (2017).
22. Park, L. *et al.* Key role of tissue plasminogen activator in neurovascular coupling. *Proc. Natl. Acad. Sci.* **105**, 1073–1078 (2008).
23. Lochner, J. E. *et al.* Activity-dependent release of tissue plasminogen activator from the dendritic spines of hippocampal neurons revealed by live-cell imaging. *J. Neurobiol.* **66**, 564–577 (2006).
24. Levin, E. G. & Loskutoff, D. J. Cultured bovine endothelial cells produce both urokinase and tissue-type plasminogen activators. *J. Cell Biol.* **94**, 631–636 (1982).
25. Angles-Cano, E. *et al.* Production of monoclonal antibodies to the high fibrin-affinity, tissue-type plasminogen activator of human plasma. Demonstration of its endothelial origin by immunolocalization. *Blood* **66**, 913–920 (1985).
26. András, I. E. *et al.* The NMDA and AMPA/KA Receptors are Involved in Glutamate-Induced Alterations of Occludin Expression and Phosphorylation in Brain Endothelial Cells. *J. Cereb. Blood Flow Metab.* **27**, 1431–1443 (2007).
27. Reijerkerk, A. *et al.* The NR1 subunit of NMDAR regulates monocyte transmigration through the brain endothelial cell barrier. *J. Neurochem.* **113**, 447–453 (2010).
28. Sharp, C. D. *et al.* Human Neuroepithelial Cells Express NMDARs. *BMC Neurosci.* **4**, 28 (2003).

29. Scott, G. S., Bowman, S. R., Smith, T., Flower, R. J. & Bolton, C. Glutamate-stimulated peroxynitrite production in a brain-derived endothelial cell line is dependent on N-methyl-D-aspartate (NMDA) receptor activation. *Biochem. Pharmacol.* **73**, 228–236 (2007).
30. Macrez, R. *et al.* Neuroendothelial NMDARs as therapeutic targets in experimental autoimmune encephalomyelitis. *Brain* **139**, 2406–2419 (2016).
31. Parcq, J. *et al.* Molecular requirements for safer generation of thrombolytics by bioengineering the tissue-type plasminogen activator A chain. *J. Thromb. Haemost. JTH* **11**, 539–546 (2013).
32. Macrez, R. *et al.* Antibodies Preventing the Interaction of Tissue-Type Plasminogen Activator With N-Methyl-d-Aspartate Receptors Reduce Stroke Damages and Extend the Therapeutic Window of Thrombolysis. *Stroke* **42**, 2315–2322 (2011).
33. Marcos-Contreras, O. A. *et al.* Hyperfibrinolysis increases blood-brain barrier permeability by a plasmin- and bradykinin-dependent mechanism. *Blood* **128**, 2423–2434 (2016).
34. Bredt, D. S. & Snyder, S. H. Isolation of nitric oxide synthetase, a calmodulin-requiring enzyme. *Proc. Natl. Acad. Sci.* **87**, 682–685 (1990).
35. Christopherson, K. S., Hillier, B. J., Lim, W. A. & Bredt, D. S. PSD-95 Assembles a Ternary Complex with the N-Methyl-d-aspartic Acid Receptor and a Bivalent Neuronal NO Synthase PDZ Domain. *J. Biol. Chem.* **274**, 27467–27473 (1999).
36. Busija, D. W., Bari, F., Domoki, F. & Louis, T. Mechanisms Involved in the Cerebrovascular Dilator Effects of N-methyl-D-aspartate in Cerebral Cortex. *Brain Res. Rev.* **56**, 89–100 (2007).
37. Bredt, D. S., Ferris, C. D. & Snyder, S. H. Nitric oxide synthase regulatory sites. Phosphorylation by cyclic AMP-dependent protein kinase, protein kinase C, and

- calcium/calmodulin protein kinase; identification of flavin and calmodulin binding sites. *J. Biol. Chem.* **267**, 10976–10981 (1992).
38. Hayashi, Y. *et al.* Regulation of Neuronal Nitric-oxide Synthase by Calmodulin Kinases. *J. Biol. Chem.* **274**, 20597–20602 (1999).
39. Rameau, G. A., Chiu, L.-Y. & Ziff, E. B. NMDAR regulation of nNOS phosphorylation and induction of neuron death. *Neurobiol. Aging* **24**, 1123–1133 (2003).
40. Rameau, G. A. *et al.* Biphasic Coupling of Neuronal Nitric Oxide Synthase Phosphorylation to the NMDAR Regulates AMPA Receptor Trafficking and Neuronal Cell Death. *J. Neurosci.* **27**, 3445–3455 (2007).
41. Gualandris, A., Jones, T. E., Strickland, S. & Tsirka, S. E. Membrane depolarization induces calcium-dependent secretion of tissue plasminogen activator. *J. Neurosci.* **16**, 2220–2225 (1996).
42. Pang, P. T. & Lu, B. Regulation of late-phase LTP and long-term memory in normal and aging hippocampus: role of secreted proteins tPA and BDNF. *Ageing Res. Rev.* **3**, 407–430 (2004).
43. Baranes, D. *et al.* Tissue Plasminogen Activator Contributes to the Late Phase of LTP and to Synaptic Growth in the Hippocampal Mossy Fiber Pathway. *Neuron* **21**, 813–825 (1998).
44. Schaefer, U., Machida, T., Vorlova, S., Strickland, S. & Levi, R. The plasminogen activator system modulates sympathetic nerve function. *J. Exp. Med.* **203**, 2191–2200 (2006).
45. Lemarchant, S. *et al.* tPA promotes ADAMTS-4-induced CSPG degradation, thereby enhancing neuroplasticity following spinal cord injury. *Neurobiol. Dis.* **66**, 28–42 (2014).
46. Segal, S. S. Integration and Modulation of Intercellular Signaling Underlying Blood Flow Control. *J. Vasc. Res.* **52**, 136–157 (2015).

47. Mehra, A., Ali, C., Parcq, J., Vivien, D. & Docagne, F. The plasminogen activation system in neuroinflammation. *Biochim. Biophys. Acta BBA - Mol. Basis Dis.* **1862**, 395–402 (2016).
48. Fiumana, E., Parfenova, H., Jaggar, J. H. & Leffler, C. W. Carbon monoxide mediates vasodilator effects of glutamate in isolated pressurized cerebral arterioles of newborn pigs. *Am. J. Physiol. - Heart Circ. Physiol.* **284**, H1073–H1079 (2003).
49. Parfenova, H., Fedinec, A. & Leffler, C. W. Ionotropic Glutamate Receptors in Cerebral Microvascular Endothelium are Functionally Linked to Heme Oxygenase. *J. Cereb. Blood Flow Metab.* **23**, 190–197 (2003).
50. LeMaistre, J. L. *et al.* Coactivation of NMDARs by Glutamate and d-Serine Induces Dilation of Isolated Middle Cerebral Arteries. *J. Cereb. Blood Flow Metab.* **32**, 537–547 (2012).
51. Lu, L. *et al.* Astrocytes drive cortical vasodilatory signaling by activating endothelial NMDARs. *J. Cereb. Blood Flow Metab.* 0271678X17734100 (2017).  
doi:10.1177/0271678X17734100
52. Stobart, J. L. L., Lu, L., Anderson, H. D. I., Mori, H. & Anderson, C. M. Astrocyte-induced cortical vasodilation is mediated by D-serine and endothelial nitric oxide synthase. *Proc. Natl. Acad. Sci. U. S. A.* **110**, 3149–3154 (2013).
53. Nassar, T. *et al.* In vitro and in vivo effects of tPA and PAI-1 on blood vessel tone. *Blood* **103**, 897–902 (2004).
54. Nassar, T. *et al.* Regulation of Airway Contractility by Plasminogen Activators through N-Methyl-D-Aspartate Receptor-1. *Am. J. Respir. Cell Mol. Biol.* **43**, 703–711 (2010).
55. Heyman, S. N. *et al.* The fibrinolytic system attenuates vascular tone: effects of tissue plasminogen activator (tPA) and aminocaproic acid on renal microcirculation. *Br. J. Pharmacol.* **141**, 971–978 (2004).

56. Cipolla, M. J., Lessov, N. & Clark, W. M. Postischemic Attenuation of Cerebral Artery Reactivity Is Increased in the Presence of Tissue Plasminogen Activator. *Stroke* **31**, 940–945 (2000).
57. Armstead, W. M. *et al.* tPA-S481A Prevents Impairment of Cerebrovascular Autoregulation by Endogenous tPA after Traumatic Brain Injury by Upregulating p38 MAPK and Inhibiting ET-1. *J. Neurotrauma* **30**, 1898–1907 (2013).
58. Armstead, W. M., Hekierski, H., Yarovoi, S., Higazi, A. A.-R. & Cines, D. B. tPA variant tPA-A296-299 prevents impairment of cerebral autoregulation and necrosis of hippocampal neurons after stroke by inhibiting upregulation of ET-1. *J. Neurosci. Res.* **96**, 128–137 (2018).
59. Errico, C. *et al.* Ultrafast ultrasound localization microscopy for deep super-resolution vascular imaging. *Nature* **527**, 499–502 (2015).
60. Tiran, E. *et al.* Transcranial Functional Ultrasound Imaging in Freely Moving Awake Mice and Anesthetized Young Rats without Contrast Agent. *Ultrasound Med. Biol.* **43**, 1679–1689 (2017).
61. Macé, E. *et al.* Functional ultrasound imaging of the brain. *Nat. Methods* **8**, 662–664 (2011).
62. Armstead, W. M., Riley, J., Kiessling, J. W., Cines, D. B. & Higazi, A. A.-R. Novel plasminogen activator inhibitor-1-derived peptide protects against impairment of cerebrovasodilation after photothrombosis through inhibition of JNK MAPK. *Am. J. Physiol.-Regul. Integr. Comp. Physiol.* **299**, R480–R485 (2010).
63. Martin, A. M. *et al.* The Functional Role of the Second NPXY Motif of the LRP1  $\beta$ -Chain in Tissue-type Plasminogen Activator-mediated Activation of N-Methyl-D-aspartate Receptors. *J. Biol. Chem.* **283**, 12004–12013 (2008).

64. Levin, E. G. & del Zoppo, G. J. Localization of tissue plasminogen activator in the endothelium of a limited number of vessels. *Am. J. Pathol.* **144**, 855–861 (1994).
65. Stefanitsch, C., Lawrence, A.-L. E., Olverling, A., Nilsson, I. & Fredriksson, L. tPA Deficiency in Mice Leads to Rearrangement in the Cerebrovascular Tree and Cerebroventricular Malformations. *Front. Cell. Neurosci.* **9**, 456 (2015).
66. Fabiani, M. *et al.* Neurovascular coupling in normal aging: A combined optical, ERP and fMRI study. *NeuroImage* **85**, 592–607 (2014).
67. Stefanova, I. *et al.* Age-related changes of blood-oxygen-level-dependent signal dynamics during optokinetic stimulation. *Neurobiol. Aging* **34**, 2277–2286 (2013).
68. Toth, P. *et al.* Resveratrol treatment rescues neurovascular coupling in aged mice: role of improved cerebromicrovascular endothelial function and downregulation of NADPH oxidase. *Am. J. Physiol. - Heart Circ. Physiol.* **306**, H299–H308 (2014).
69. Zaletel, M., Strucl, M., Pretnar-Oblak, J. & Zvan, B. Age-related changes in the relationship between visual evoked potentials and visually evoked cerebral blood flow velocity response. *Funct. Neurol.* **20**, 115–120 (2005).
70. Girouard, H. & Iadecola, C. Neurovascular coupling in the normal brain and in hypertension, stroke, and Alzheimer disease. *J. Appl. Physiol.* **100**, 328–335 (2006).
71. Wilkerson, W. R. & Sane, D. C. Aging and thrombosis. *Semin. Thromb. Hemost.* **28**, 555–568 (2002).
72. Gaussem, P., Grailhe, P. & Anglés-Cano, E. Sodium dodecyl sulfate-induced dissociation of complexes between human tissue plasminogen activator and its specific inhibitor. *J. Biol. Chem.* **268**, 12150–12155 (1993).
73. Boulay, A.-C., Saubaméa, B., Declèves, X. & Cohen-Salmon, M. Purification of Mouse Brain Vessels. *J. Vis. Exp. JoVE* e53208 (2015). doi:10.3791/53208

## Figure legends

**Figure 1: Functional hyperemia is reduced in tPA<sup>-/-</sup> mice.** (a) Pseudo colored representative subtraction maps of the CBF highlighting CBF change during whisker stimulation of tPA wt and tPA<sup>-/-</sup> mice. Maps were obtained by subtracting Doppler speckle images recorded during stimulation to images recorded during rest. Color intensity goes from blue (no change during stimulation) to red (strong CBF increase during stimulation). (b) Mean CBF signal traces from the S1bf during whisker stimulation of tPA wt (—) and tPA<sup>-/-</sup> (—) mice extracted from Doppler speckle images (curves in transparency define the SEM, n = 10 per group). (c) Quantification of the CBF increase during whisker stimulation in tPA wt and tPA<sup>-/-</sup> mice. Circles represent values for each mouse (Mean ± SEM, Mann-Whitney test, n = 10 per group).

**Figure 2: Vascular rtPA increases the functional hyperemia in tPA<sup>-/-</sup> mice.** (a) Schematic representation of the experimental timeline, including a first train of stimulations as a control followed by an IV injection and a second train of stimulations 10 minutes after the injection. (b) Pseudo colored representative subtraction maps of the CBF highlighting CBF change during whisker stimulation of tPA<sup>-/-</sup> mice before and after the injection of HEPES (200μl, 0.3M) or rtPA (200μl, 10mg/kg). Maps were obtained by subtracting Doppler speckle images recorded during stimulation to images recorded during rest. Color intensity goes from blue (no change during stimulations) to red (strong CBF increase during stimulation). (c) Quantification of the CBF increase during whisker stimulation in tPA<sup>-/-</sup> mice before (●) and after (●) IV injection of HEPES (200μl, 0.3M) or rtPA (200μl, 10mg/kg). Circles represent values for each mouse (Mean ± SEM, Wilcoxon test, n = 10 for the HEPES group, n = 12 for the rtPA group). (d) Mean CBF signal trace from the S1bf during whisker stimulation of tPA<sup>-/-</sup> mice before and after the injection of

HEPES (200 $\mu$ l, 0.3M; —) or rtPA (200 $\mu$ l, 10mg/kg; —) extracted from Doppler speckle images (curves in transparency define the SEM, n = 10 for the HEPES group, n = 12 for the rtPA group).

(e) Diagram showing the evolution of the hemodynamic response of each mouse between the control condition and after the IV injection of HEPES (200 $\mu$ l, 0.3M) or rtPA (200 $\mu$ l, 10mg/kg). Lines are colored according to whether the response is more than 5% higher (—), between +5% and -5% (—), or decreased for more than 5% (—) after the injection.

**Figure 3: The promotion of the functional hyperemia by rtPA is not restricted to the surface of the brain but involved the whole barrel cortex.** (a) Schematic representation of functional ultrasound acquisition. (b) Ultrasensitive Doppler image of the brain of a C57BL/6 mouse through a thinned skull window, revealing blood vessels, and particularly penetrating arterioles (white arrows). (c) Schematic representation of the experimental timeline, including a first train of stimulations as control followed by an IV injection of rtPA and a second train of stimulations 10 minutes after the injection. Bottom images represent an example of the activation maps when stimulating the left whiskers before and after the injection of rtPA. Colormap correspond to the correlation coefficient between the normalized PD intensity along time and a step function representing the stimulation pattern. (d) Quantification of the relative PD intensity increase in the activated area (seen in c) during whisker stimulation in tPA<sup>-/-</sup> mice. Circles represent values for each mouse (Mean ± SEM, Wilcoxon test, n = 7). (e) Relative augmentation of the Power Doppler in the activated area (seen in c) during whisker stimulation of tPA<sup>-/-</sup> mice before (—) or after (—) intravenous injection of rtPA (curves in transparency define the SEM, n = 7).

**Figure 4: Vascular rtPA promotes whisker stimulation induced dilation of large vessels.** (a) Intravital microscopy images of vessels of different diameters revealed by in IV injection of FITC dextran. Images obtained from the S1bf cortex of tPA<sup>-/-</sup> mice (scale bar = 50μm). (b) Left: Intravital microscopy images of a vessel from the S1bf cortex of a tPA<sup>-/-</sup> mouse (scale bar = 50μm). Vessels were labelled using an IV injection of FITC dextran. Right: line-scans of the same vessel during whisker stimulation before (top) and after (bottom) rtPA (10mg/kg) injection. (c) Representative diagram of the dilation of different vessels separated according to their diameters. Black lines represent the position of the vessel wall in basal condition, blue line and red line represent the relative position of the vessel wall during whisker stimulation without (—) or after rtPA (10mg/kg) injection (—). (d) Quantification from intravital microscopy images of the vessels dilation during whisker stimulation according to their diameters before (●) and after (●) rtPA (10mg/kg) injection. Circles represent values for each vessel (Mean ± SEM, Wilcoxon test, n = 9 for the Ø>25μm group, n = 9 for the 25μm>Ø>15μm group, and n = 8 for the Ø<15μm group from 4 different mice). (e) Schematic representation of the brain vascular tree in basal condition (●), and during vessel dilation without (●) or with (●+●) vascular rtPA.

**Figure 5: Chronic expression of tPA restrained to the blood circulation promotes functional hyperemia in tPA<sup>-/-</sup> mice.** (a) Schematic representation of the experimental timeline, including a first train of stimulations as control followed 24 h later by the hydrodynamic transfection, and by a second train of stimulations 48 h after the transfection; Three different plasmids were transfected: pLIVE (empty), pLIVE-tPA and pLIVE- tPA-K2\*. (b) Representative fibrin-agar

zymography assays performed from plasma of pLIVE, pLive-tPA and pLIVE-tPA-K2\* transfectected mice, which demonstrate the presence of free plasmatic tPA and tPA-K2\* after the transfection. rtPA was used as standard in the zymography assays. (c) Pseudo colored representative subtraction maps of the CBF highlighting CBF change during whisker stimulation of tPA<sup>-/-</sup> mice before and after the transfection. Maps were obtained by subtracting Doppler speckle images recorded during stimulation to images recorded during rest. Color intensity goes from blue (no change during stimulations) to red (strong CBF increase during stimulation). (d) Quantification of the CBF increase during whisker stimulation in tPA<sup>-/-</sup> mice before (●) and after (●) the transfection. Circles represent values for each mouse (Mean ± SEM, Wilcoxon test, n = 9 for the pLIVE group, n = 8 for the pLIVE-tPA group and n = 8 for the pLIVE-tPA-K2\* group). (e) Mean CBF signal trace from the S1bf during whisker stimulation of tPA<sup>-/-</sup> mice before (—) and after (—) the transfection extracted from Doppler speckle images (curves in transparency define the SEM, n = 9 for the pLIVE group, n = 8 for the pLIVE-tPA group and n = 8 for the pLIVE-tPA-K2\* group). (f) Diagram showing the evolution of the hemodynamic response of each mouse between the control condition and after transfection. Lines are colored according to whether the response is more than 5% higher (—), between +5% and -5% (—), or decreased for more than 5% (—) after the injection.

**Figure 6: Inhibition of the interaction between vascular rtPA and NMDARs prevents the rtPA-induced potentiation of functional hyperemia.** (a) Pseudo colored representative subtraction maps of the CBF highlighting CBF change during whisker stimulation of tPA<sup>-/-</sup> mice before and after the injection of rtPA (10mg/kg) and a control IgG (5mg/kg) or rtPA (10mg/kg) and Glunomab® (5mg/kg). Maps were obtained by subtracting Doppler speckle images recorded

during stimulation to images recorded during rest. Color intensity goes from blue (no change during stimulations) to red (strong CBF increase during stimulation). **(b)** Quantification of the CBF increase during whisker stimulation in tPA<sup>-/-</sup> mice before (●) and after (●) IV injection of rtPA (10mg/kg) and a control IgG (5mg/kg) or rtPA (10mg/kg) and Glunomab® (5mg/kg). Circles represent values for each mouse (Mean ± SEM, Wilcoxon test, n = 8 for the rtPA + IgG group, n = 9 for the rtPA + Glunomab® group). **(c)** Mean CBF signal trace from the S1bf during whisker stimulation of tPA<sup>-/-</sup> mice before (—) and after (—) the injection of rtPA (10mg/kg) and a control IgG (5mg/kg) or rtPA (10mg/kg) and Glunomab® (5mg/kg;) extracted from Doppler speckle images (curves in transparency define the SEM, n = 8 for the rtPA + IgG group, n = 9 for the rtPA + Glunomab® group). **(d)** Diagram showing the evolution of the hemodynamic response of each mouse between the control condition and after the IV injection of rtPA (10mg/kg) and a control IgG (5mg/kg) or rtPA (10mg/kg) and Glunomab® (5mg/kg). Lines are colored according to whether the response is more than 5% higher (—), between +5% and -5% (—), or decreased for more than 5% (—) after the injection.

**Figure 7: Blockage of NMDARs signaling prevents the rtPA-induced potentiation of functional hyperemia. (a)** Pseudo colored representative subtraction maps of the CBF highlighting CBF change during whisker stimulation of tPA<sup>-/-</sup> mice before and after the injection of rtPA (10mg/kg) and saline, HEPES (0.3M) and MK-801 (0.4mg/kg), rtPA (10mg/kg) and MK-801 (0.4mg/kg), HEPES (0.3M) and AP5 (0.4mg/kg), or rtPA (10mg/kg) and AP5 (0.4mg/kg). Maps were obtained by subtracting Doppler speckle images recorded during stimulation to images recorded during rest. Color intensity goes from blue (no change during stimulations) to red (strong CBF increase during stimulation). **(b)** Quantification of the CBF increase during

whisker stimulation in tPA<sup>-/-</sup> mice before (●) and after (●) IV injection of rtPA (10mg/kg) and saline, HEPES (0.3M) and MK-801 (0.4mg/kg), rtPA (10mg/kg) and MK-801 (0.4mg/kg), HEPES (0.3M) and AP5 (0.4mg/kg), or rtPA (10mg/kg) and AP5 (0.4mg/kg). Circles represent values for each mouse (Mean ± SEM, Wilcoxon test, n = 9 for the tPA + saline group, n = 10 for the HEPES + MK-801 group, n = 8 for the rtPA + MK-801 group, n = 9 for the HEPES + AP5 group and n = 8 for the rtPA + AP5 group). (c) Mean CBF signal trace from the S1bf during whisker stimulation of tPA<sup>-/-</sup> mice before (—) and after (—) the injection of rtPA (10mg/kg) and saline, HEPES (0.3M) and MK-801 (0.4mg/kg), rtPA (10mg/kg) and MK-801 (0.4mg/kg), HEPES (0.3M) and AP5 (0.4mg/kg), or rtPA (10mg/kg) and AP5 (0.4mg/kg) extracted from Doppler speckle images (curves in transparency define the SEM, n = 9 for the rtPA + saline group, n = 10 for the HEPES + MK-801 group, n = 8 for the rtPA + MK-801 group, n = 9 for the HEPES + AP5 group and n = 8 for the rtPA + AP5 group). (d) Diagram showing the evolution of the hemodynamic response of each mice between the control condition and after the IV injection of rtPA (10mg/kg) and saline, HEPES (0.3M) and MK-801 (0.4mg/kg), rtPA (10mg/kg) and MK-801 (0.4mg/kg), HEPES (0.3M) and AP5 (0.4mg/kg), or rtPA (10mg/kg) and AP5 (0.4mg/kg). Lines are colored according to whether the response is more than 5% higher (—), between +5% and -5% (—), or decreased for more than 5% (—) after the injection.

### **Figure 8: Expression of NMDARs is restricted to arteries and arterioles. (a-b)**

Epifluorescence images of isolated vessels from C57BL/6 mice brain revealing in a (scale bar = 50μm): PDGF-R<sub>β</sub> (red), α-SMA (green) and cells nuclei (blue). Only vessels over 10μm in diameter express α-SMA. In b (scale bar = 100μm), immunostainings reveal GluN1 subunit of the NMDAR (red), α-SMA (green), laminin (magenta) and cells nuclei (blue). (c) Quantification

method used to assess GluN1 subunit in brain vessel. GluN1 staining fluorescence intensity was measured in  $\alpha$ -SMA positive vessels (left) and in  $\alpha$ -SMA negative vessels (right) separately. (d) Quantification of the GluN1 staining fluorescence intensity in  $\alpha$ -SMA positive vessels and in  $\alpha$ -SMA negative vessels (Mean  $\pm$  SEM, ANOVA test, n = 34 for the  $\alpha$ -SMA + group and n = 29 for the  $\alpha$ -SMA – group, from 4 different mice). (e) Epifluorescence images of isolated vessels from C57BL/6 mice brain revealing GluN1 staining (red), Col IV (green) and cells nuclei (blue), and corresponding schematic representation.

**Supplementary figure 1: Doppler Laser speckle imaging allows measurement of the CBF directly through the intact skull.** (a) Representative images of a mouse skull, intact (bottom right) or thinned (top right) and corresponding laser Doppler speckle images. (b) Mean CBF signal trace from the S1bf during whisker stimulation of C57BL/6 mice with an intact skull (—) or a thinned skull (—) extracted from Doppler speckle images (curves in transparency define the SEM, n = 4 for the thinned skull group, n = 3 for the intact skull group). (c) Quantification of the CBF increase during whisker stimulation of C57BL/6 mice with an intact skull or a thinned skull. Circles represent values for each mouse (Mean  $\pm$  SEM, Mann-Whitney test, n = 4 for the thinned skull group, n = 3 for the intact skull group).

**Supplementary figure 2: Physiological parameters.** (a) Schematic representation of the set of physiological parameters monitored during experimental procedures. (b) Heart rate (left) and O<sub>2</sub> saturation (right) of mice during experiments. No change was observed during whisker stimulation.

**Supplementary figure 3: Paradigms of whisker stimulation.** (a) Schematic representation of the laser Speckle imaging experiments. CBF is recorded at the whole surface of the brain during whisker stimulation of the mice. (b) The stimulations paradigm consists in three 30 s periods of stimulations followed by a 90 s period of rest. Quantification of the CBF increase during whisker stimulation of tPA wt mice reveal no difference between the 3 stimulations periods. Circles represent values for each mouse (Mean ± SEM, ANOVA test, n = 33 per group).

**Supplementary figure 4: Increasing the concentration of vascular tPA promotes functional hyperemia.** (a) Pseudo colored representative subtraction maps of the CBF highlighting CBF change during whisker stimulation of tPA wt mice before and after the injection of HEPES (200 $\mu$ l, 0.3M) or rtPA (200 $\mu$ l, 10mg/kg). Maps were obtained by subtracting Doppler speckle images recorded during stimulation to images recorded during rest. Color intensity goes from blue (no change during stimulations) to red (strong CBF increase during stimulation). (b) Quantification of the CBF increase during whisker stimulation in tPAwt mice before (●) and after (●) IV injection of HEPES (200 $\mu$ l, 0.3M) or rtPA (200 $\mu$ l, 10mg/kg). Circles represent values for each mouse (Mean ± SEM, Wilcoxon test, n = 10 for the HEPES group, n = 12 for the rtPA group). (c) Mean CBF signal traces from the S1bf during whisker stimulation of tPA wt mice before and after the injection of HEPES (200 $\mu$ l, 0.3M; —) or rtPA (200 $\mu$ l, 10mg/kg; —) extracted from Doppler speckle images (curves in transparency define the SEM, n = 10 for the HEPES group, n = 12 for the rtPA group). (d) Diagram showing the evolution of the hemodynamic response of each mouse between the control condition and after the IV injection of HEPES (200 $\mu$ l, 0.3M) or rtPA (200 $\mu$ l, 10mg/kg). Lines are colored according to whether the response is

more than 5% higher (green), between +5% and -5% (orange), or decreased for more than 5% (red) after the injection.

**Supplementary figure 5: Pooled analysis.** (a) Distribution of the mean value of the CBF increase during whisker stimulation before (blue circle) and after (red circle) injection of control solution (left) or rtPA (right). (b) Quantification of the CBF increase during whisker stimulation in tPA<sup>-/-</sup> mice before (blue dot) and after (red dot) injection of control solution (HEPES) or rtPA (Mean ± SEM, paired t-test, n = 38).

**Supplementary figure 6: Vascular tPA does not cross the intact blood brain barrier in the S1bf cortex 10 min after its IV injection.** (a) Two areas were selected to assess the rtPA extravasation 10 min after its injection: a control one, the median eminence, where there is no BBB, and the somatosensorial cortex. (b) Electrophoresis of increasing doses of tPA<sup>555</sup>. (c) Epifluorescence images of mouse brain slice revealing the presence of tPA555 in the median eminence (red) but not in the somatosensorial cortex around α-SMA positive vessels (green; scale bar = 50μm).

**Supplementary figure 7: Graphical statistical analysis (t-map).** T-map of the brain of tPA<sup>-/-</sup> mice that have received the rtPA treatment from figure 2 (top) or from tPA<sup>-/-</sup> mice that have received rtPA + Glunomab® from the figure 7 (bottom), revealing areas where the CBF increase during whisker stimulation is statistically different after injection compared to before injection (paired t-test, n = 12 for the [tPA<sup>-/-</sup> + rtPA] group, n = 9 for the [tPA<sup>-/-</sup> + rtPA + Glunomab®] group).

figure 1

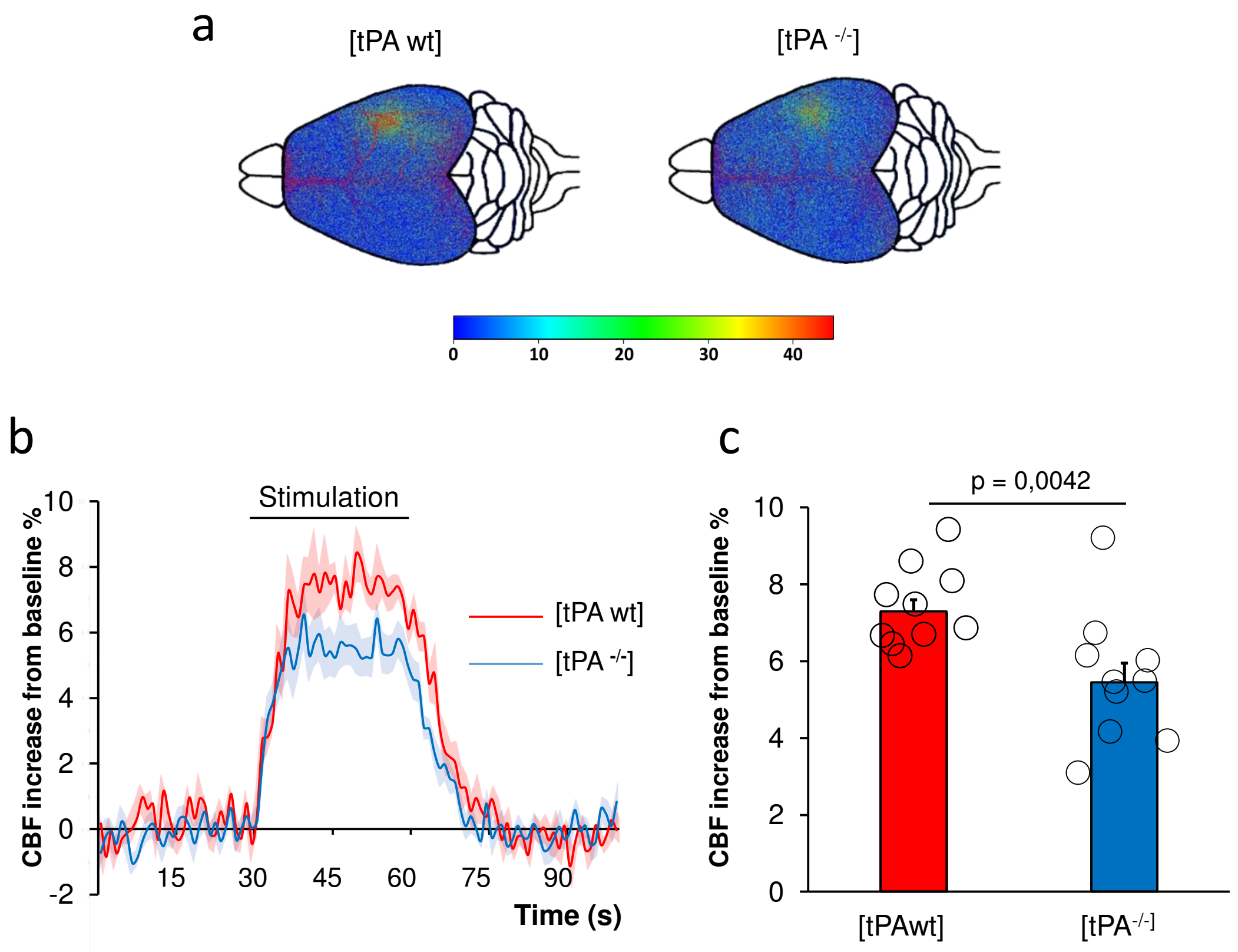
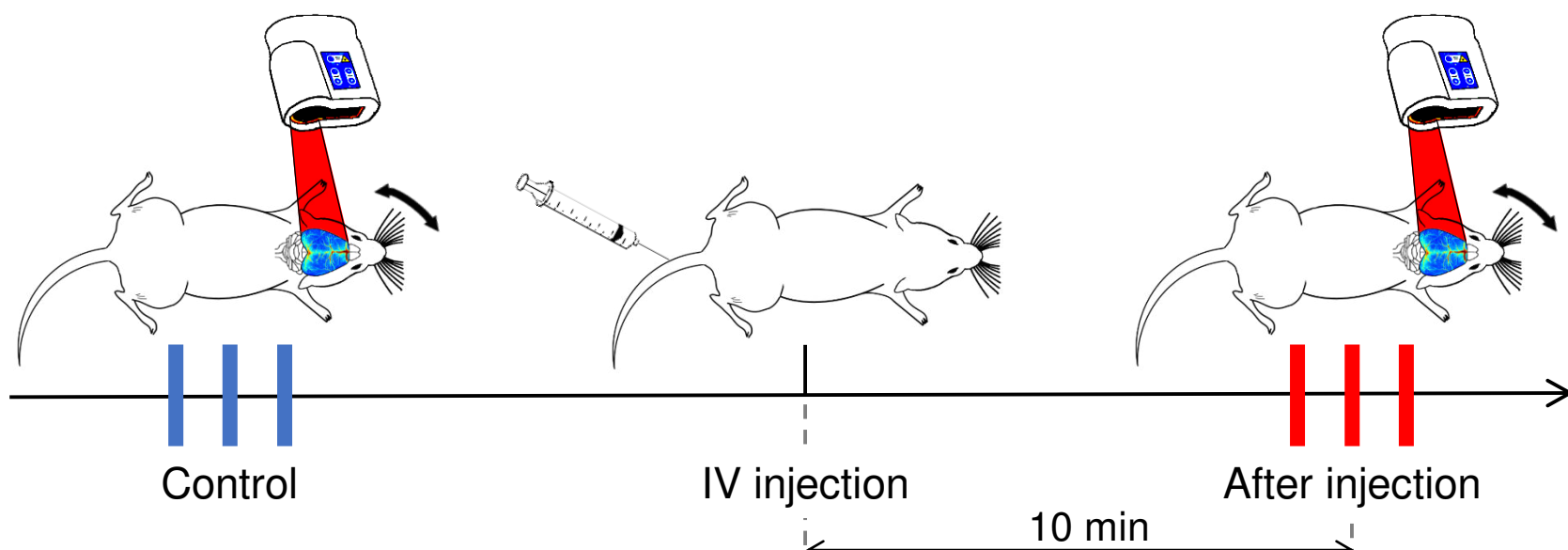
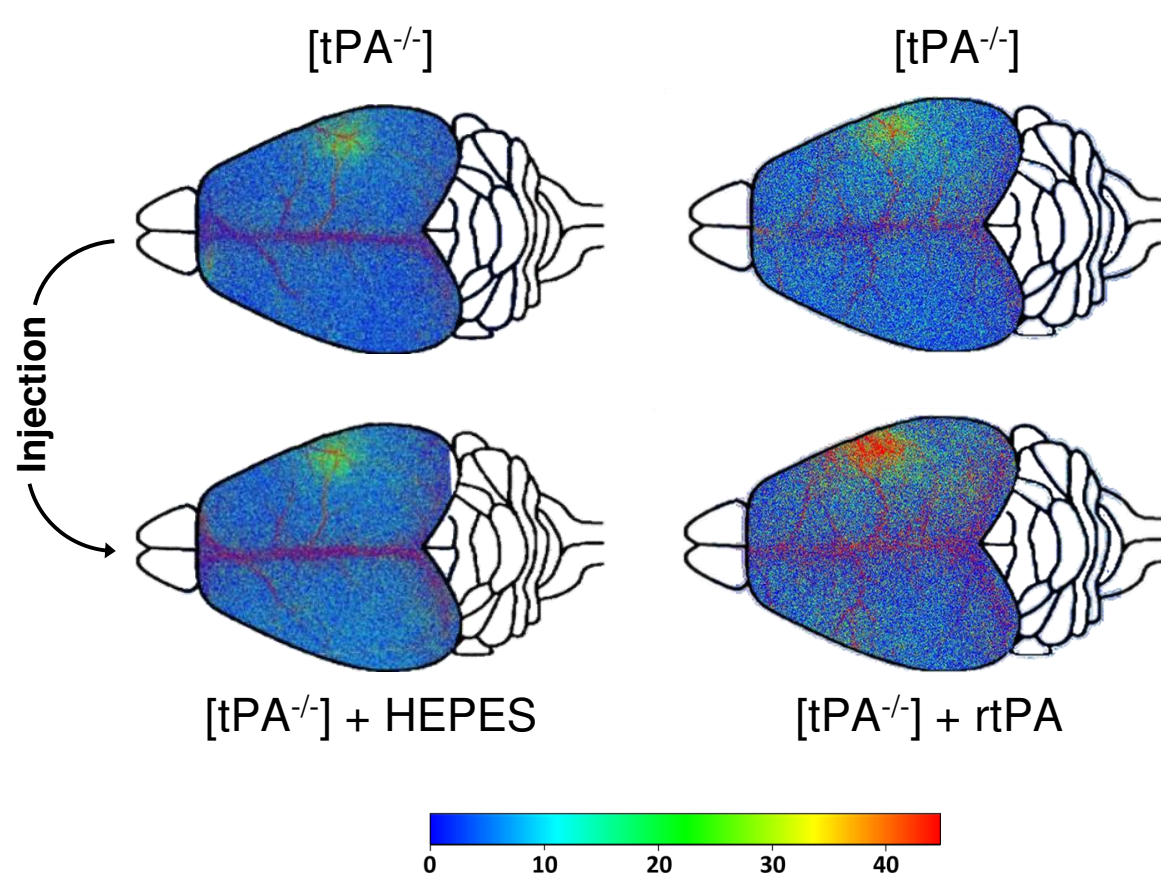


figure 2

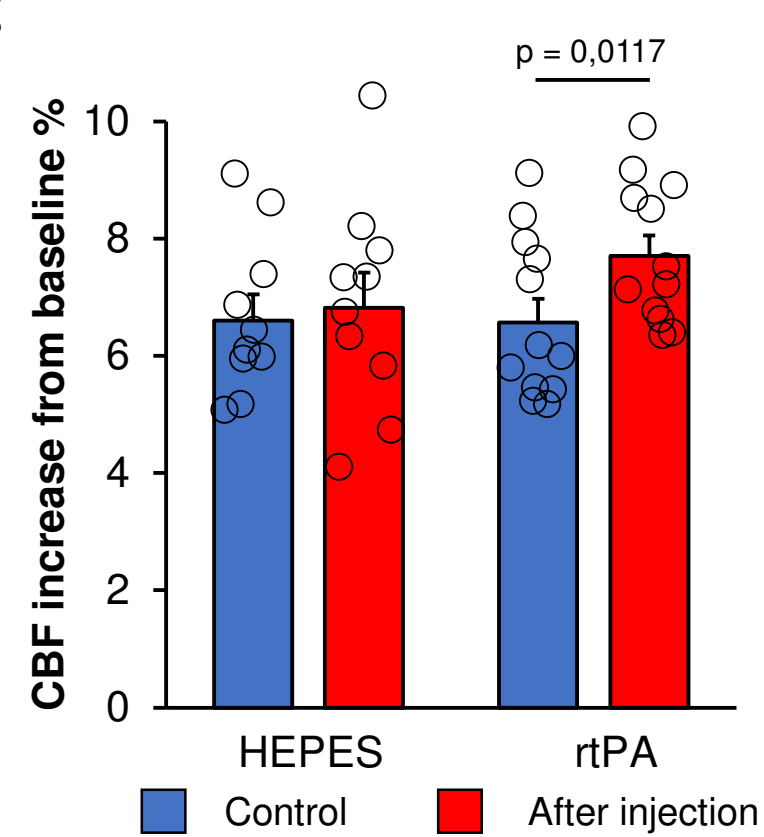
a



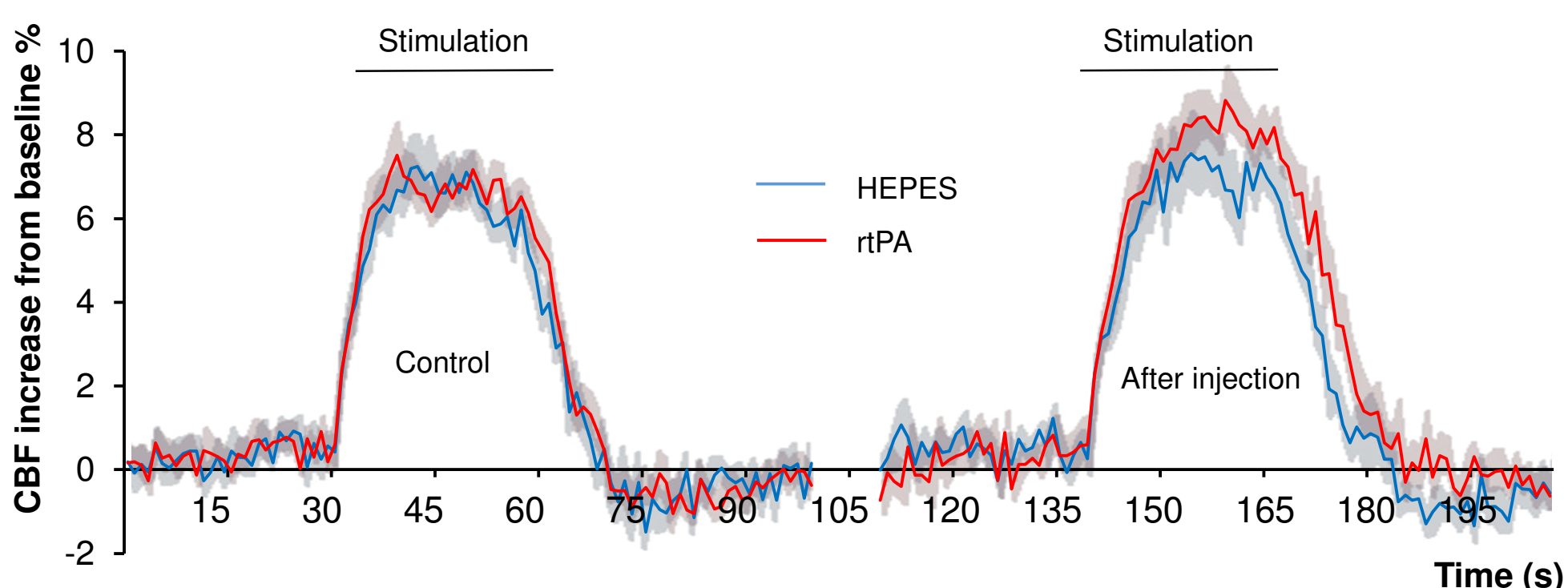
b



c



d



e

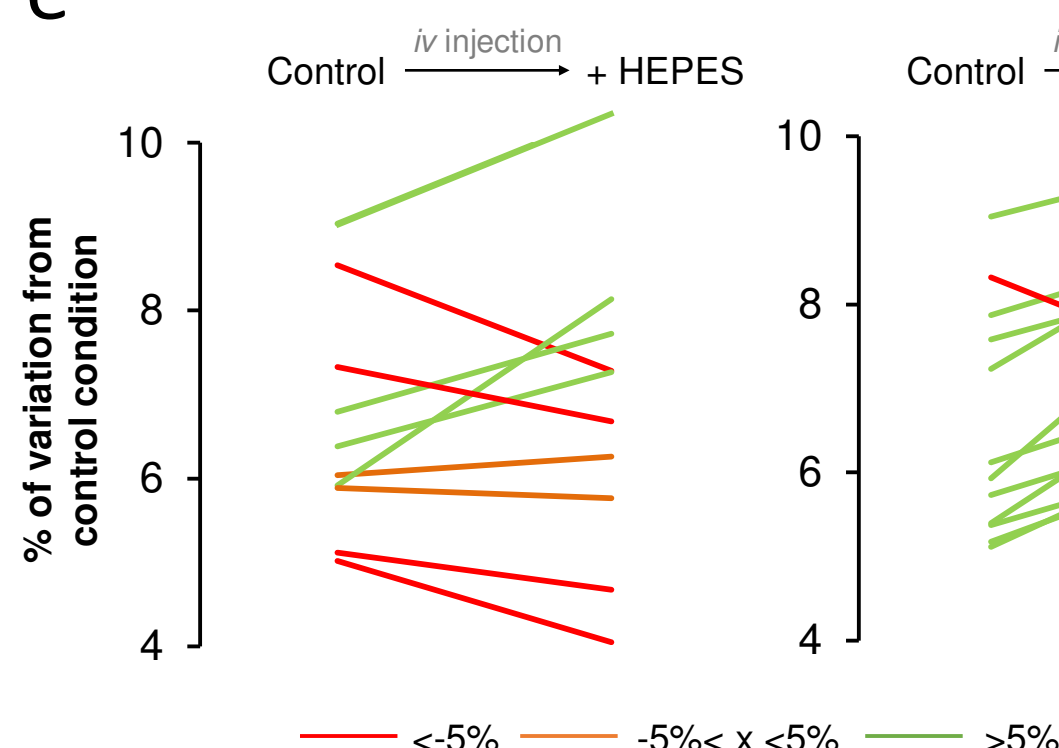


figure 3

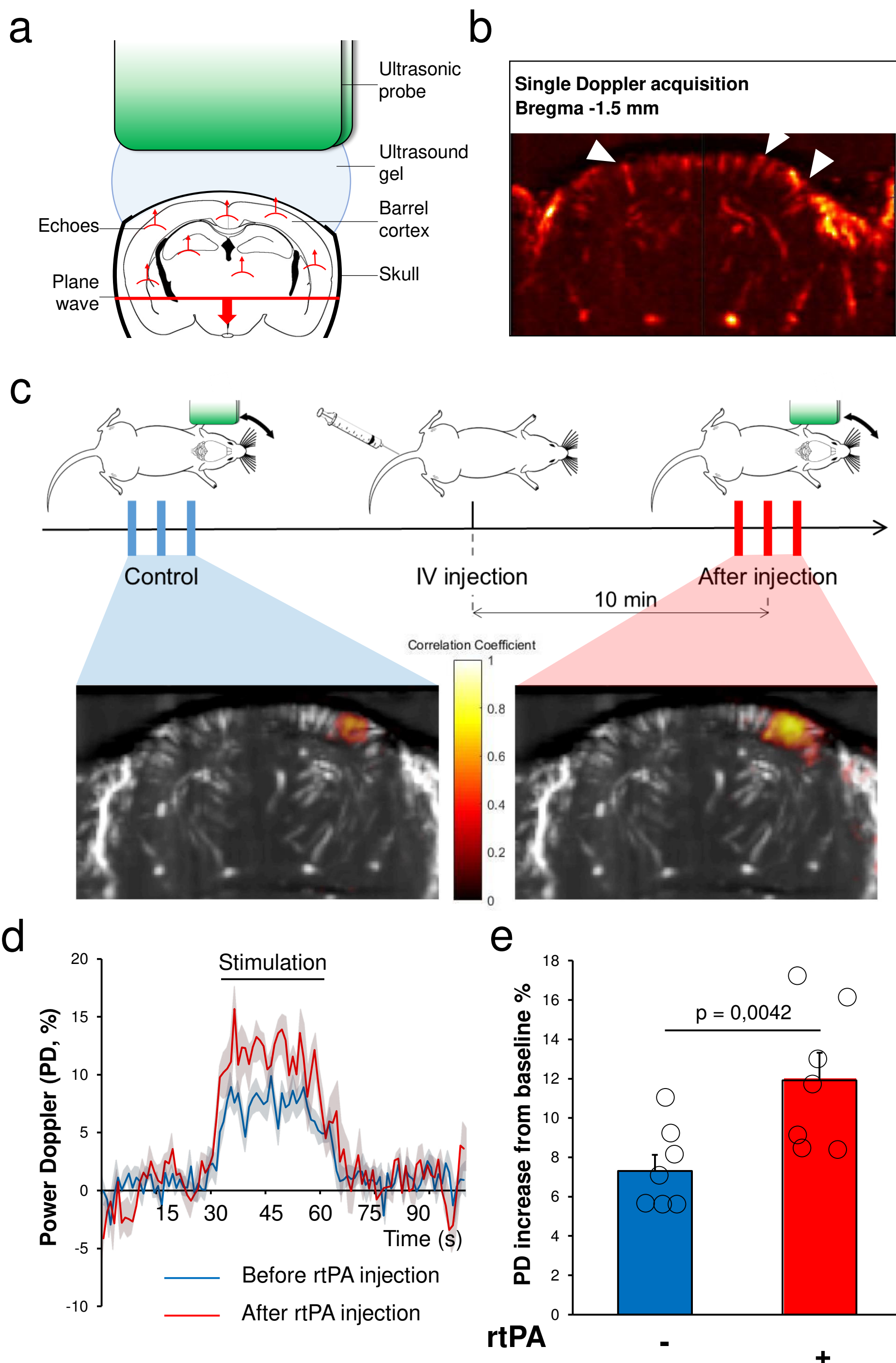


figure 4

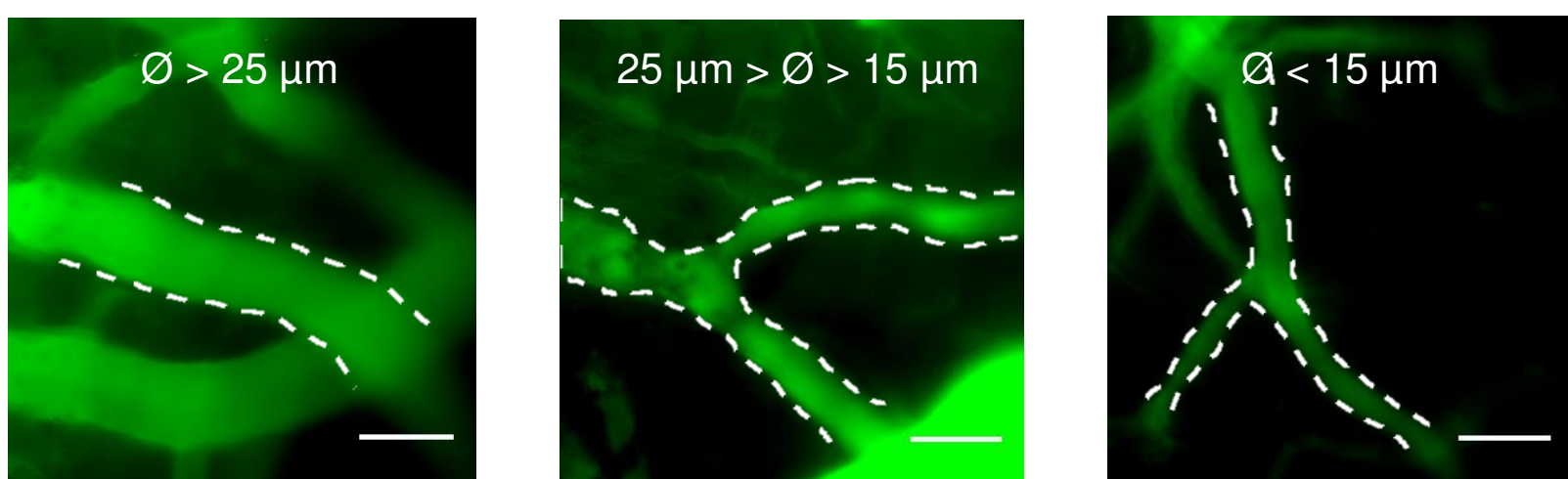
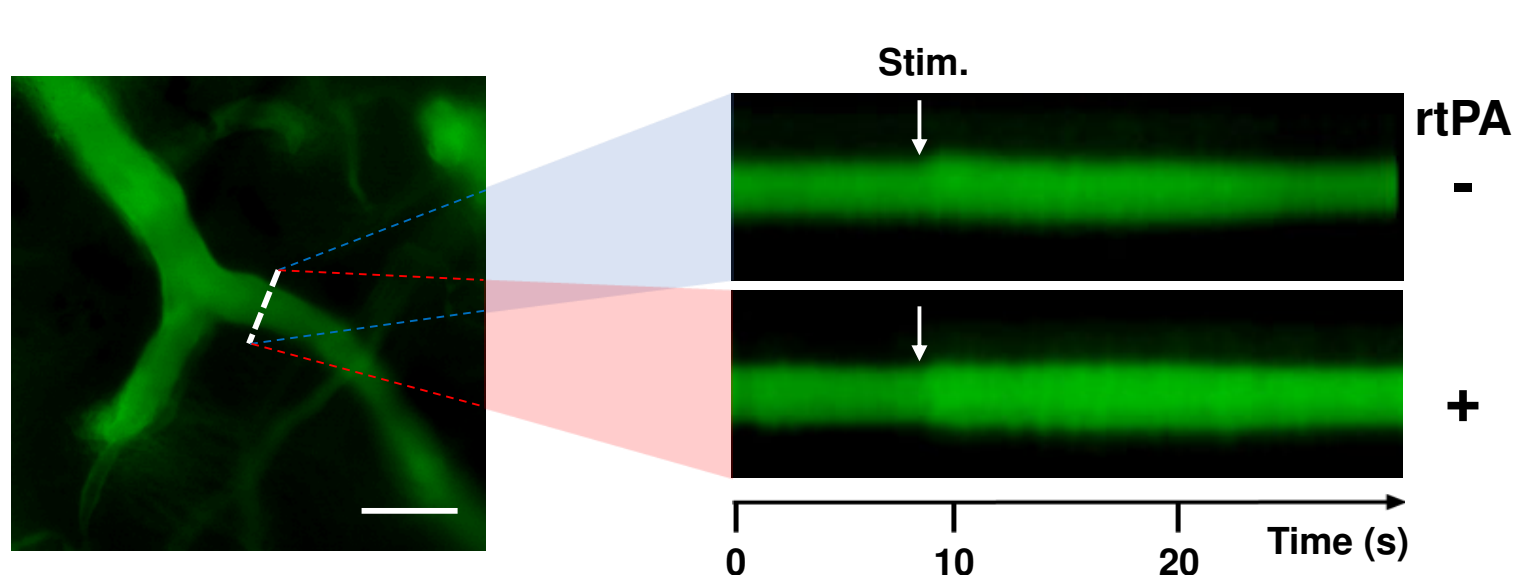
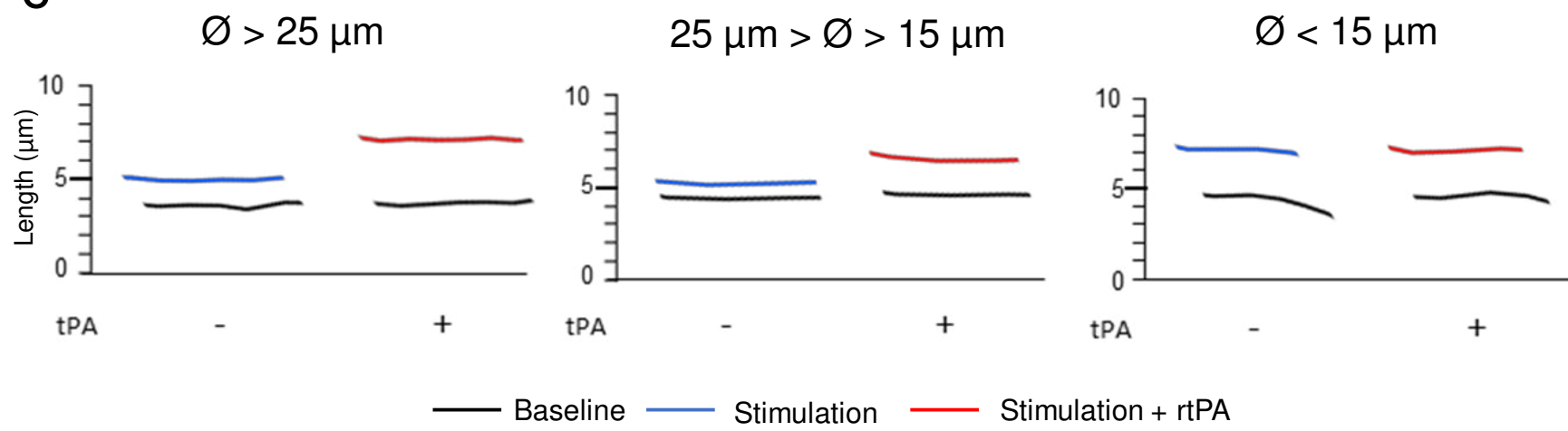
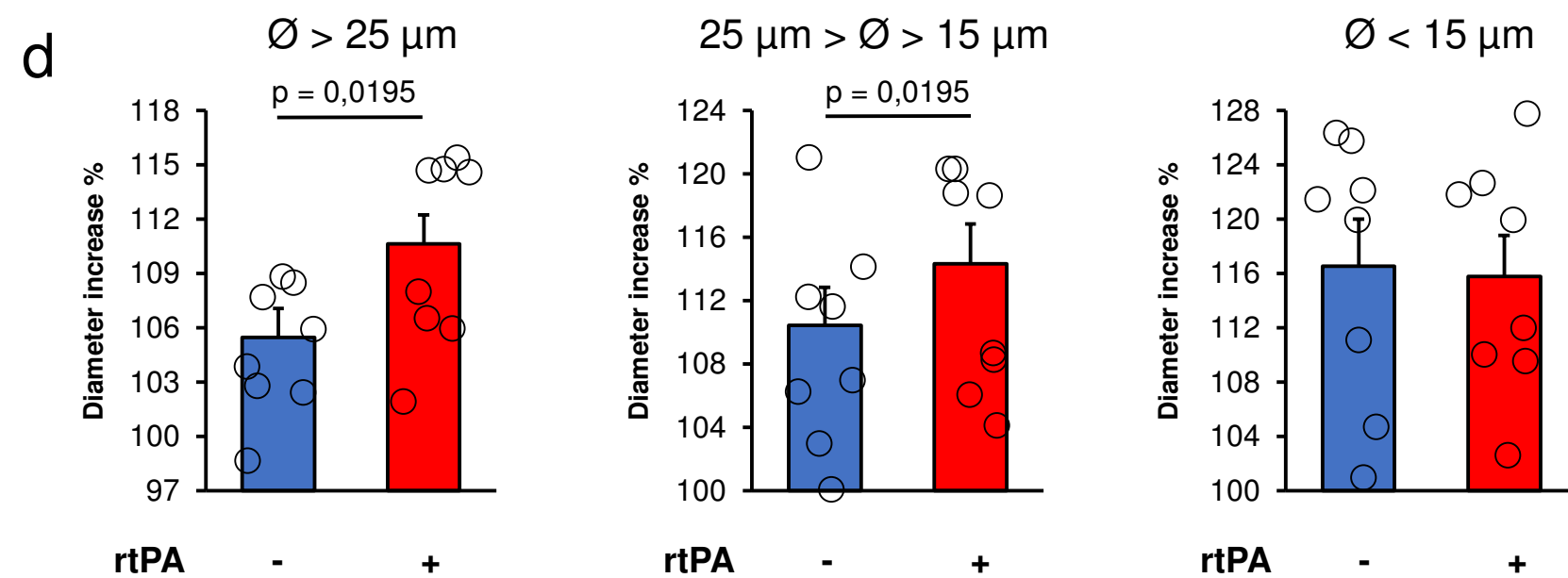
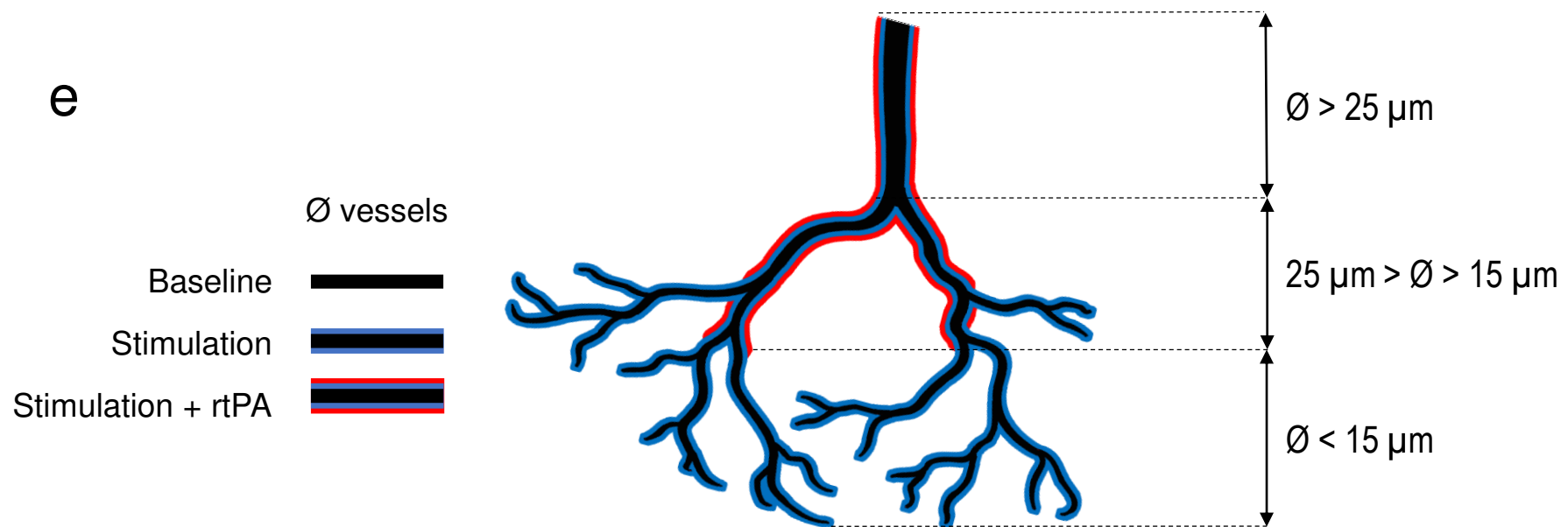
**a****b****c****d****e**

figure 5

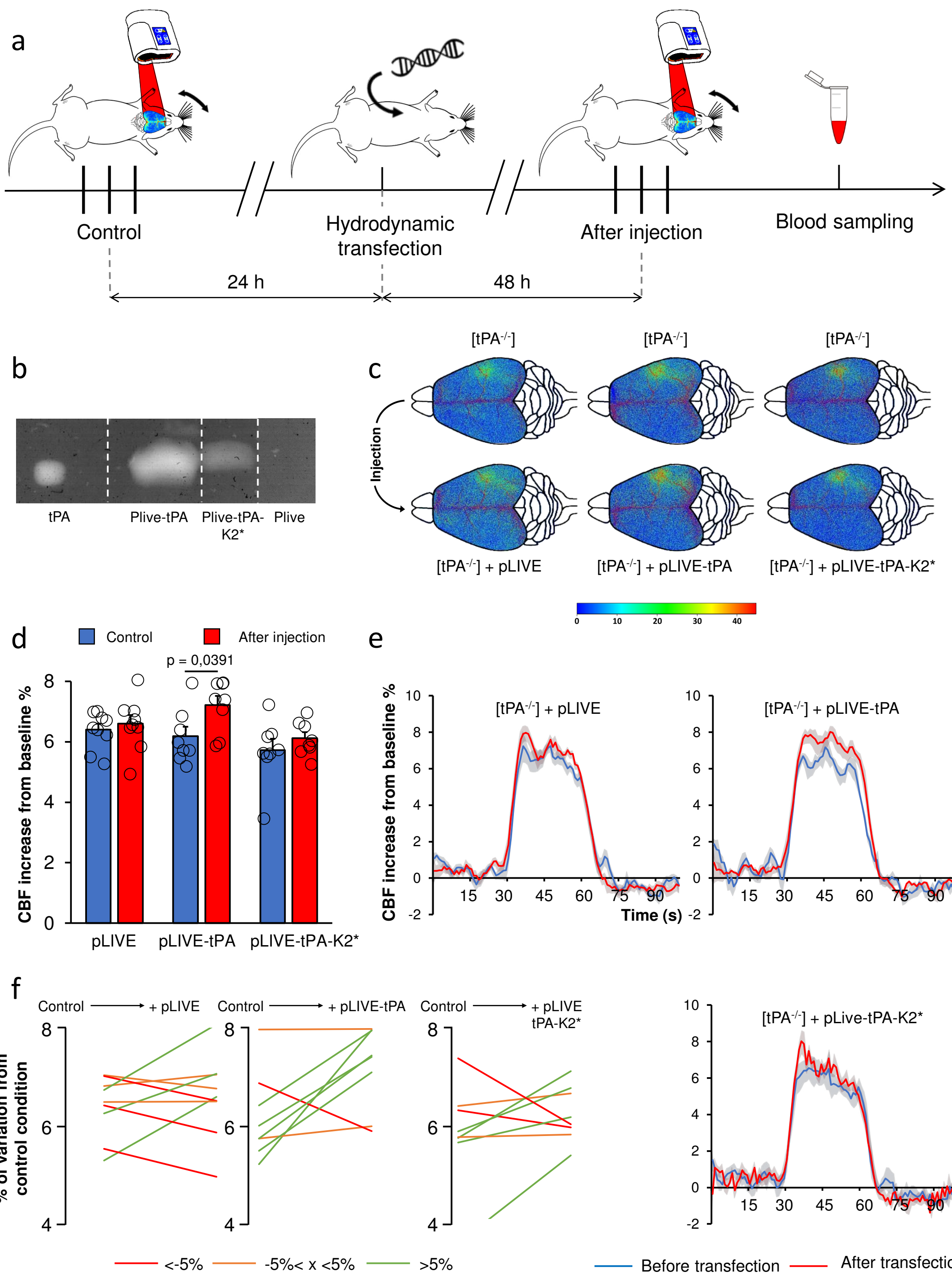


figure 6

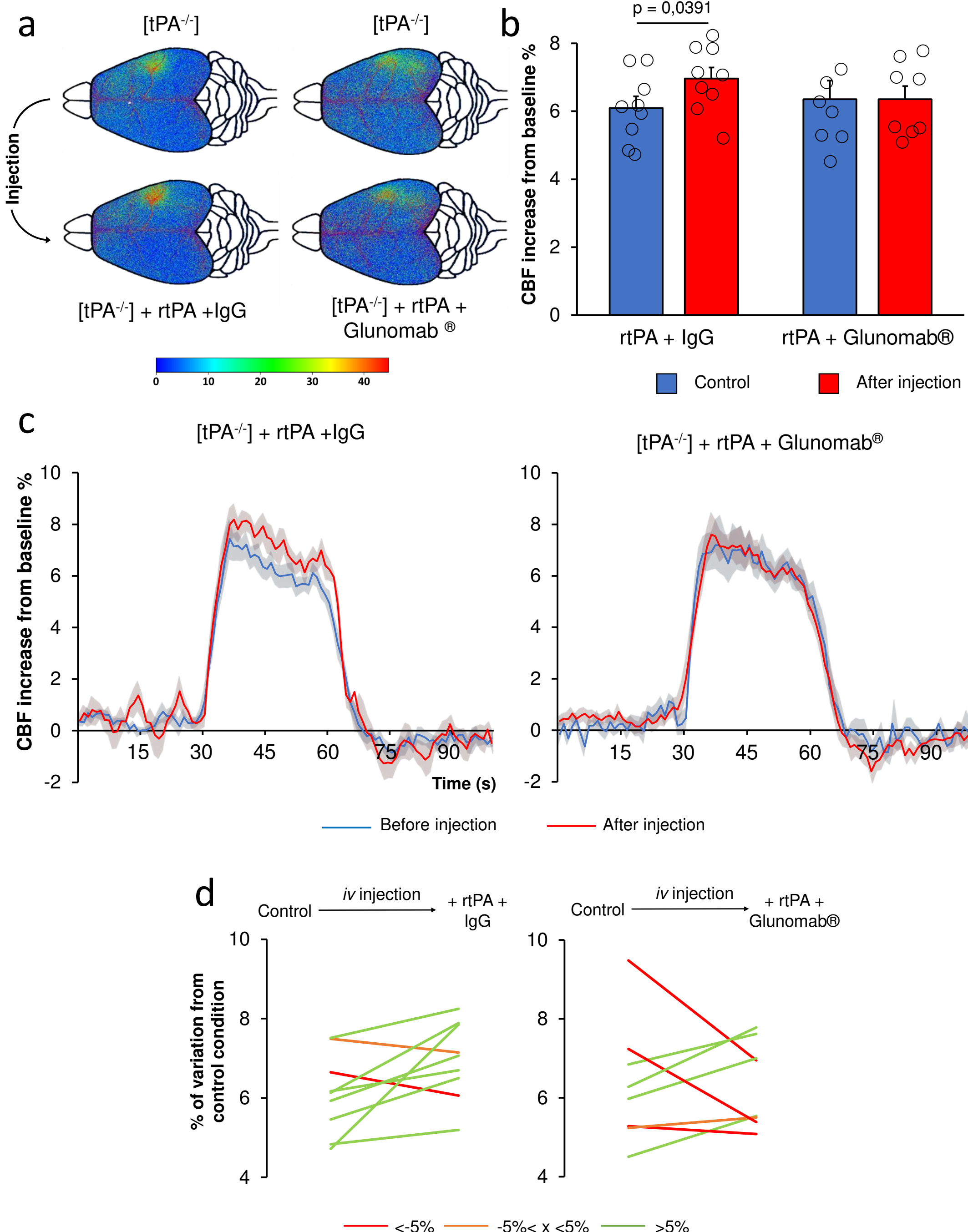


figure 7

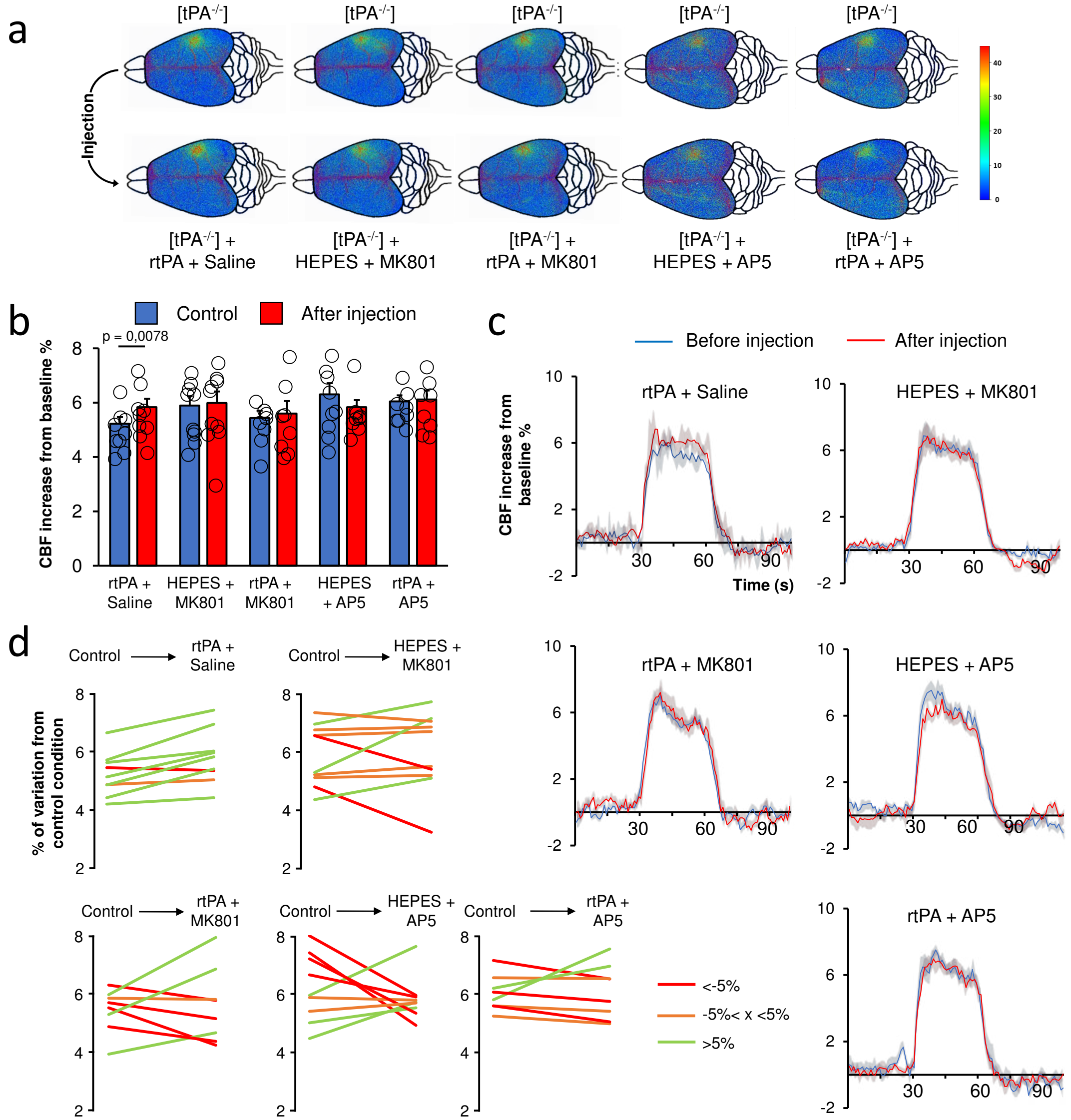
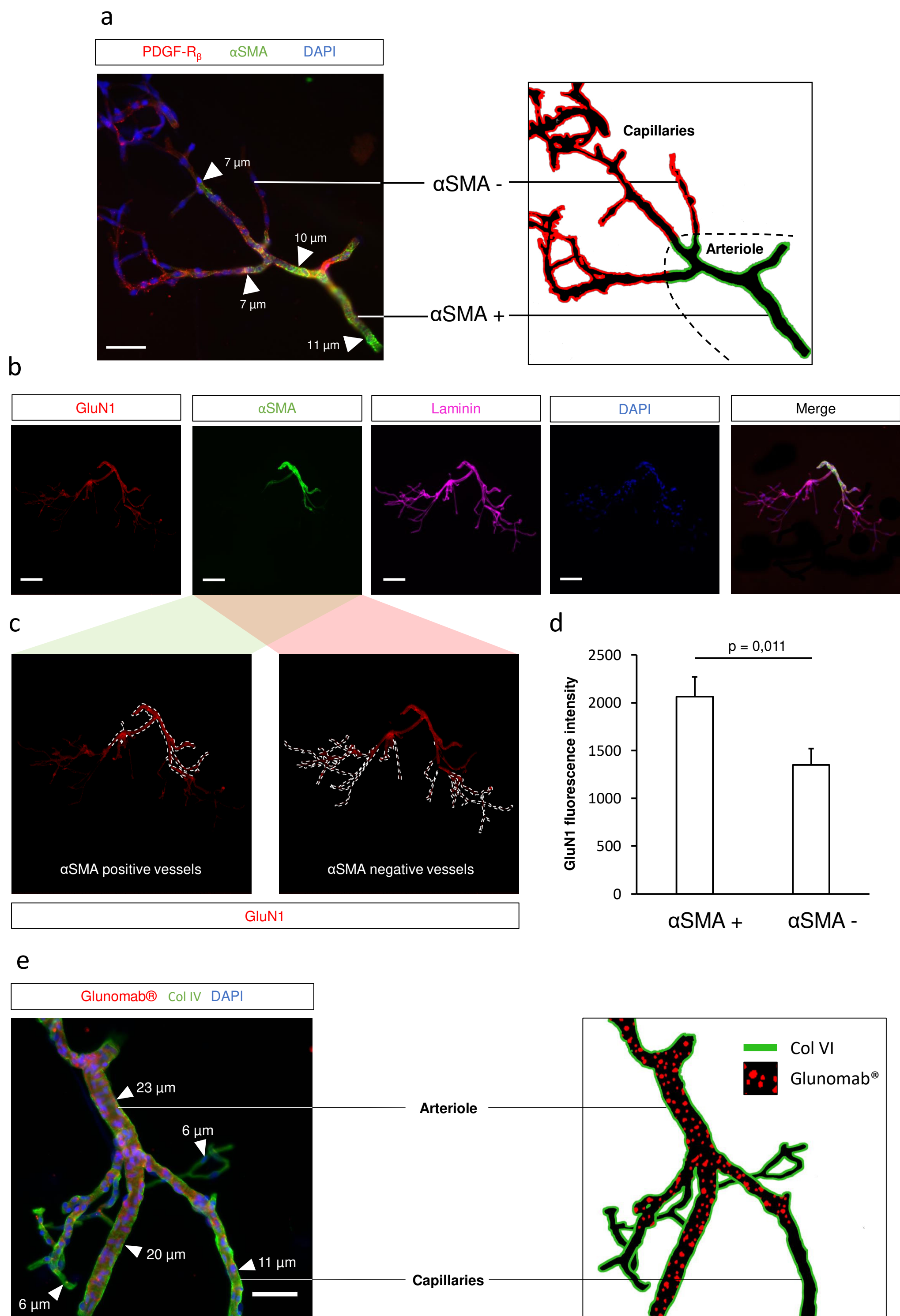
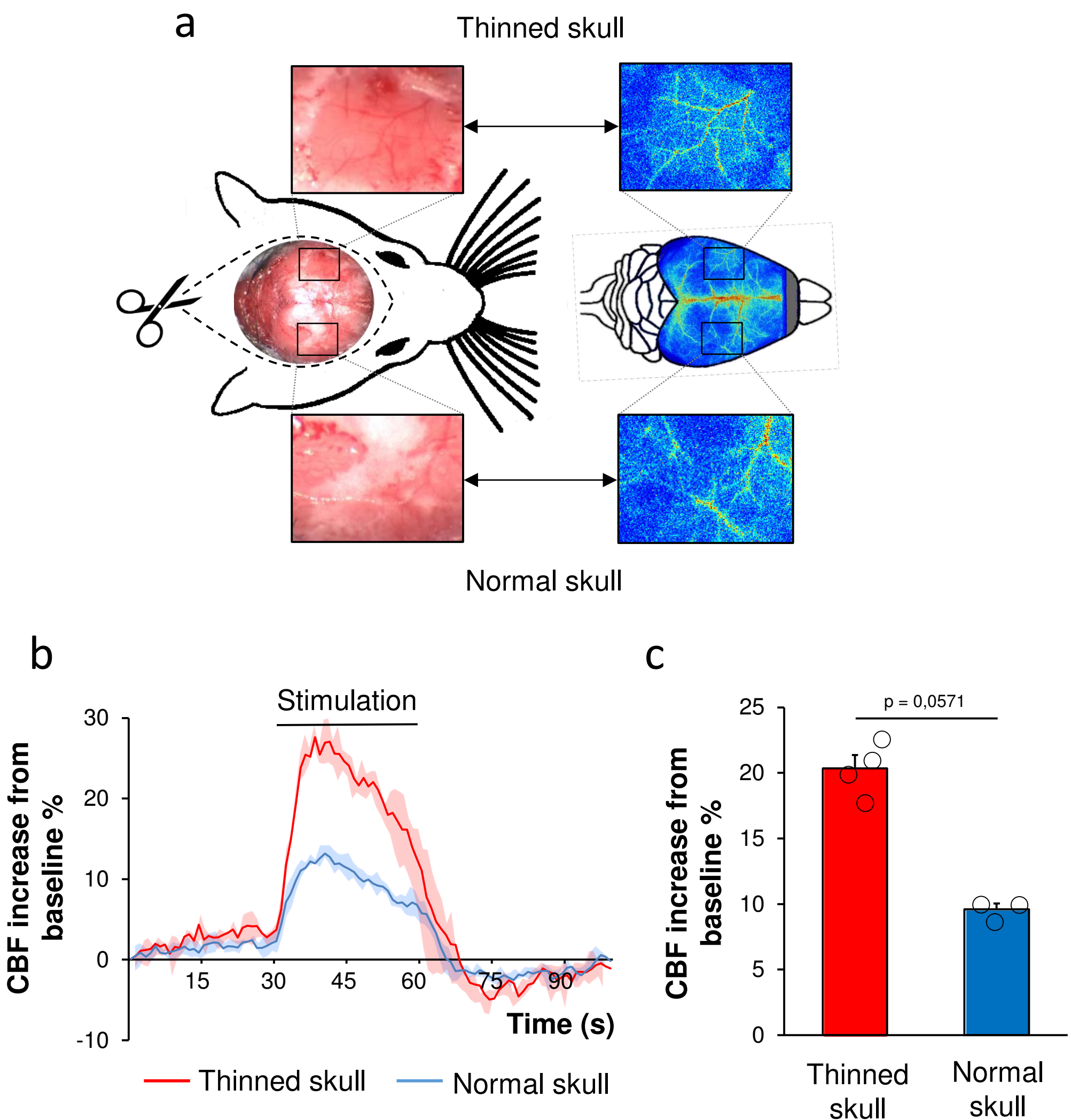


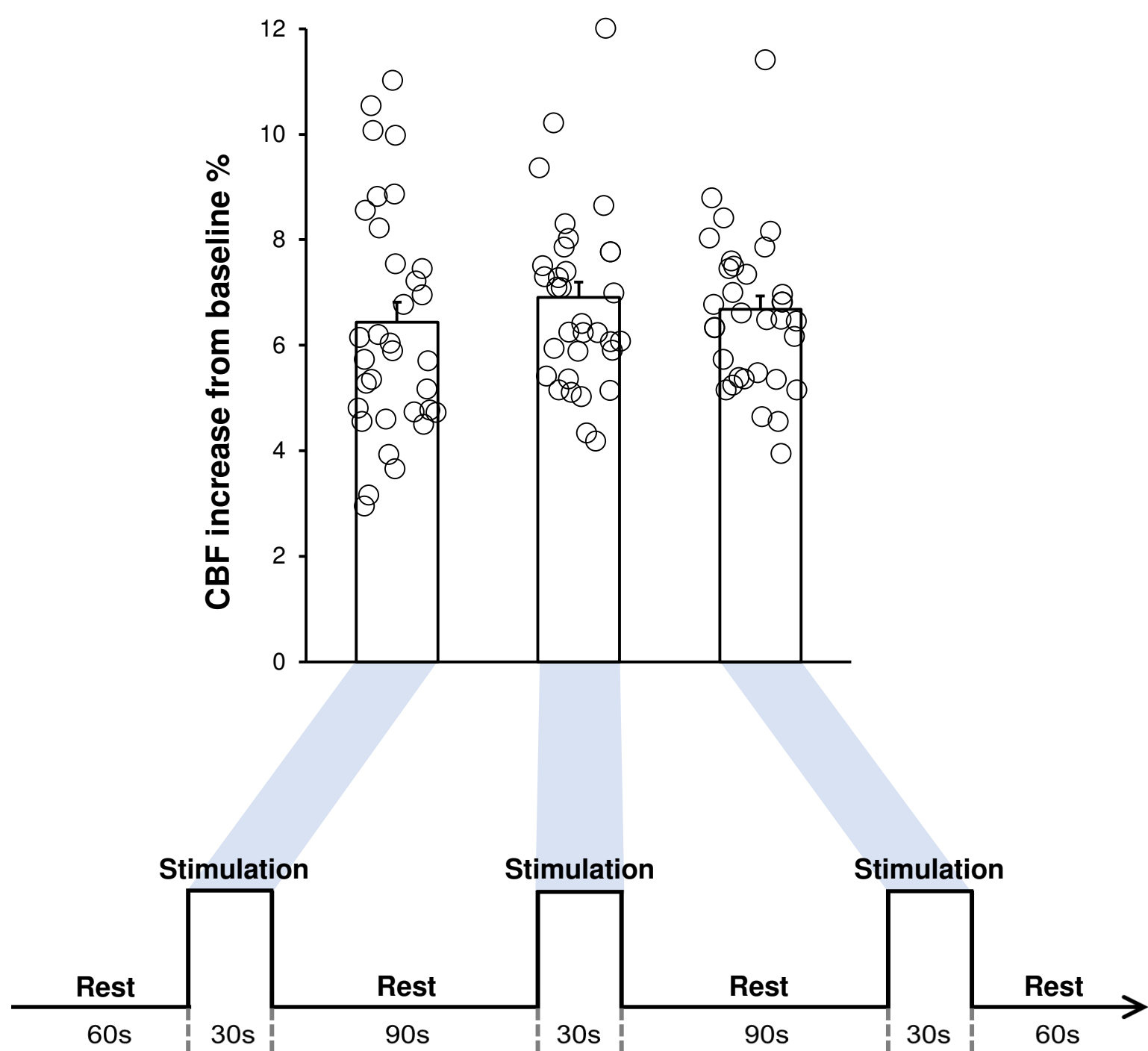
figure 8



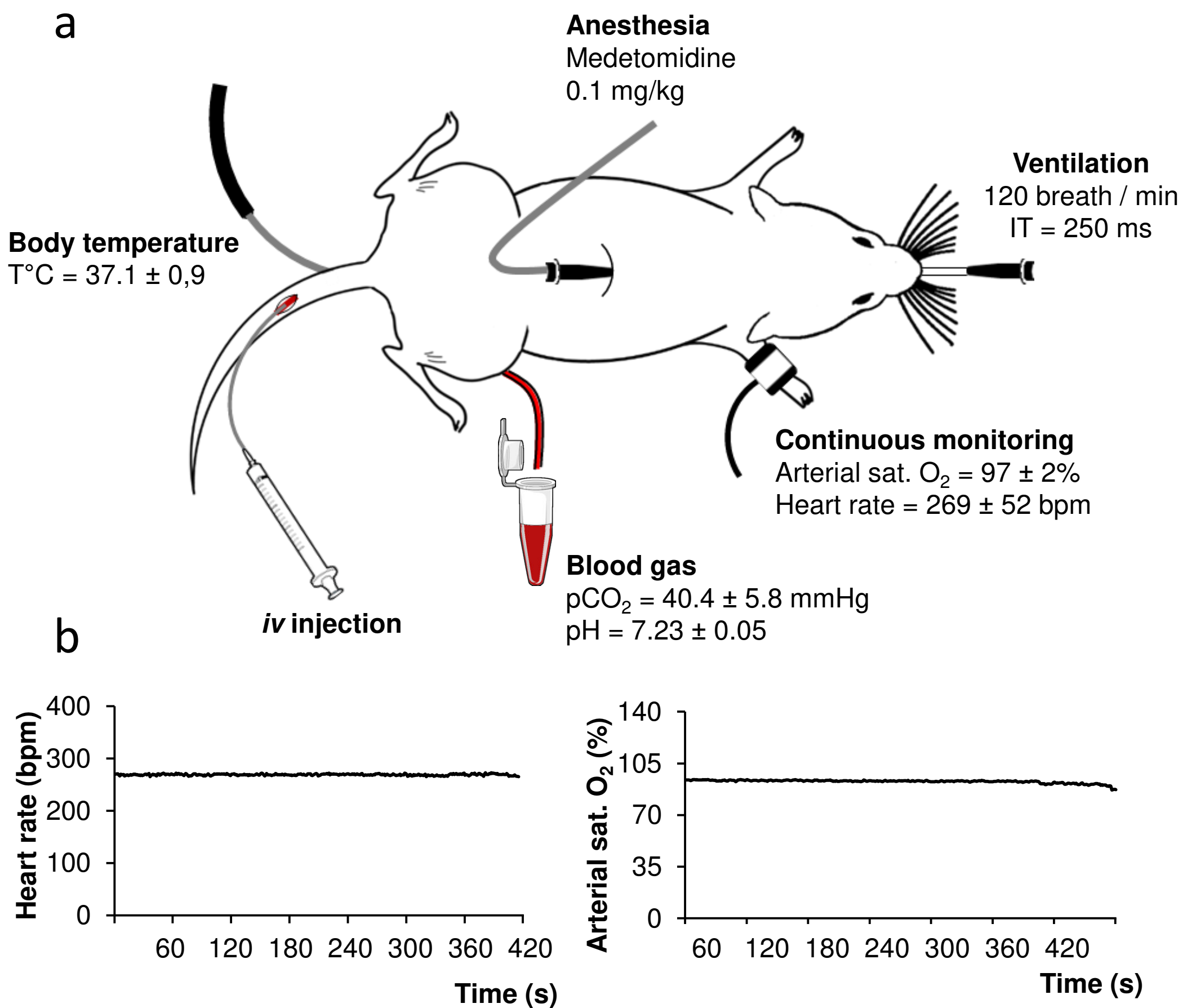
Supplementary figure 1



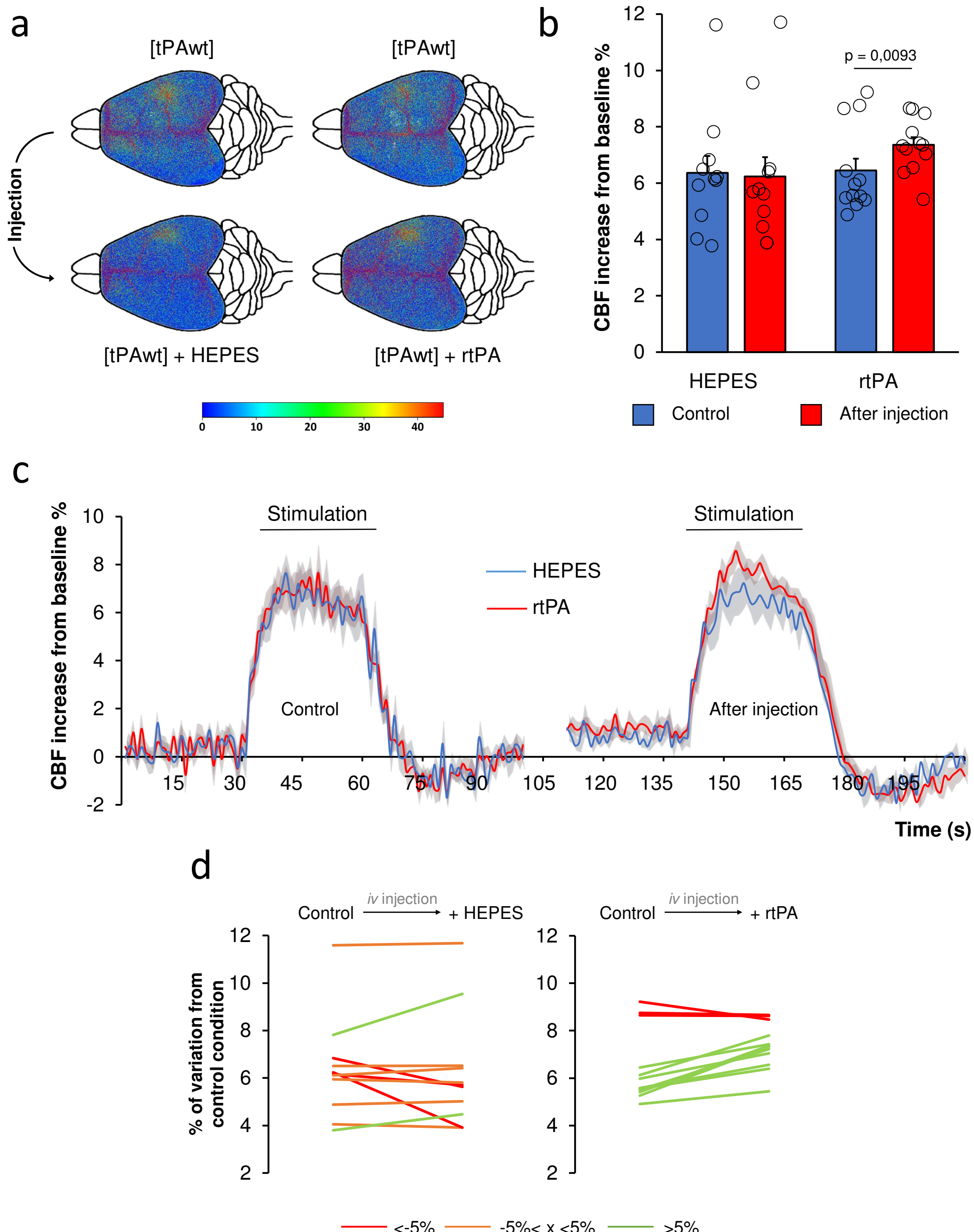
Supplementary figure 2



Supplementary figure 3



## Supplementary figure 4



1    **Acknowledgements**

2    The authors are grateful to Dr Carine Ali and Dr Fabian Docagne for their valuable scientific  
3    suggestions, Dr Laurent Coulbaut for the analyses of human samples from the ALCOBRAIN  
4    cohort.

5    **Funding**

6    This study was funded by the Fondation pour la Recherche en Alcoologie (MR), the AXA  
7    Research Found (MR), INSERM, Caen-Normandy University, the Regional Council of  
8    Normandy, the ANR grant RHU MARVELOUS (ANR-16-RHUS-0009) (DV), ANR “Retour  
9    jeune chercheur” (ALP), the BALATON project (M. Rubio and A. Denes, #38601ZM).

10    **Author contributions**

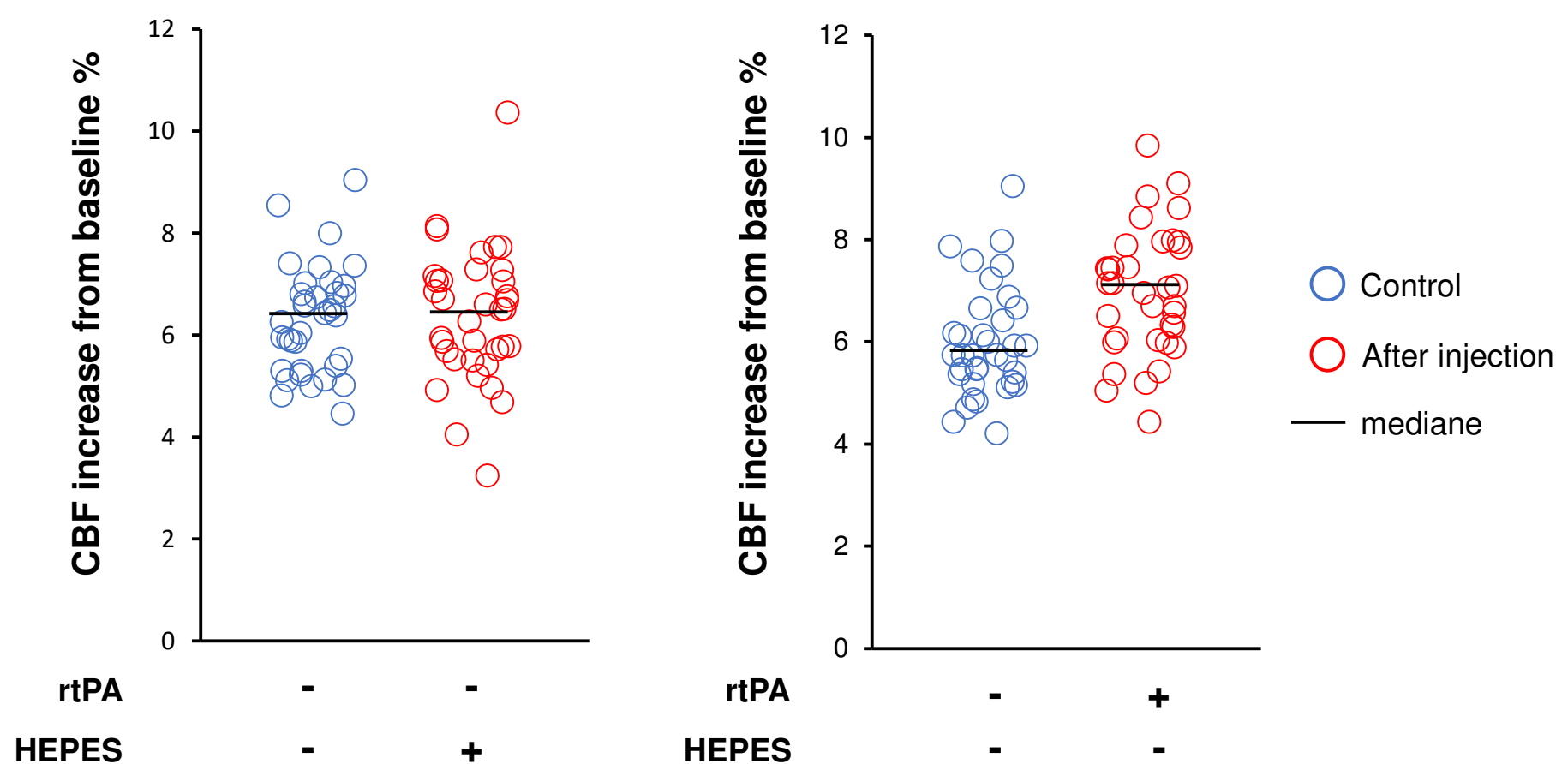
- 11    -    Study design, coordination of the study: MR
- 12    -    Stroke model surgeries: MR
- 13    -    Histological and transcriptional analyses, *in vivo* functional analyses of microglial  
14    phagocytosis: AD
- 15    -    Molecular MRI: AD, AQ and EL
- 16    -    Two-photon microscopy: AD and MR
- 17    -    Analyses of immunohistochemical samples: AD and MN
- 18    -    Analyses of data from the ALCOBRAIN cohort of HD patients: AL and ALP
- 19    -    Analyses of data and writing of results from the stroke cohort of patients: FC and JC
- 20    -    Supervision of the study: DV
- 21    -    Manuscript writing: MR with the revision and approval of all authors

22    **Competing interests**

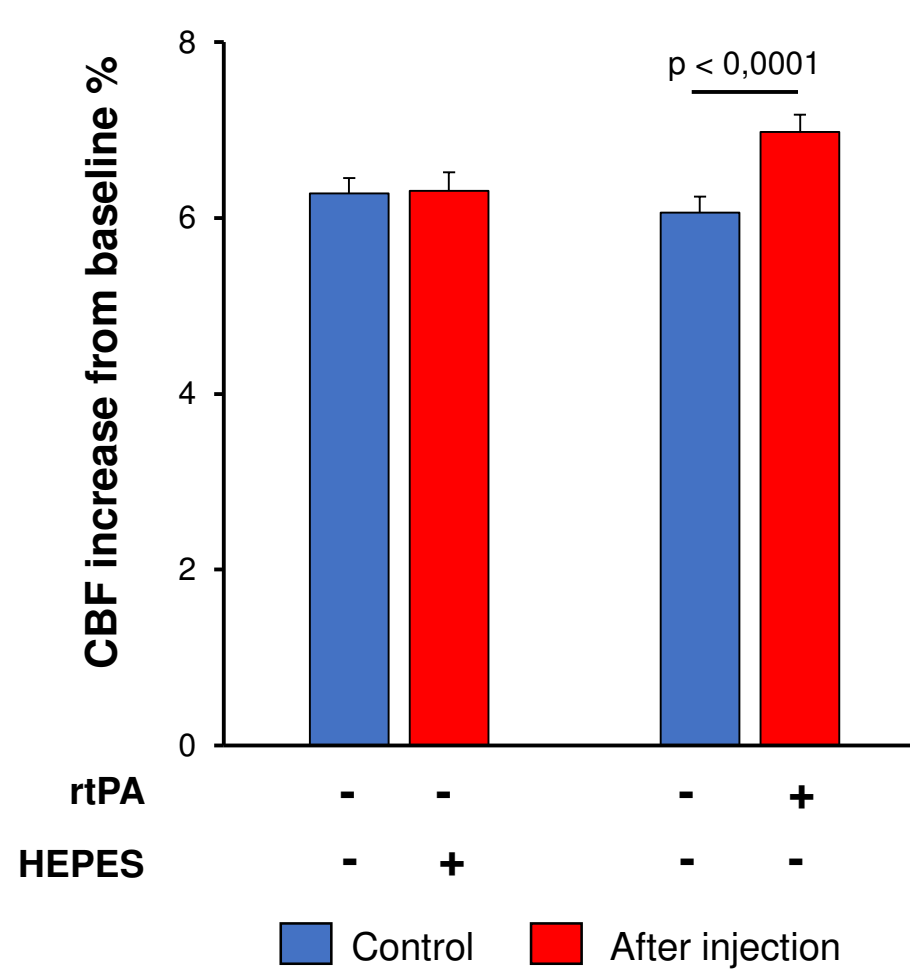
23    The authors declare no competing financial interests.

Supplementary figure 5

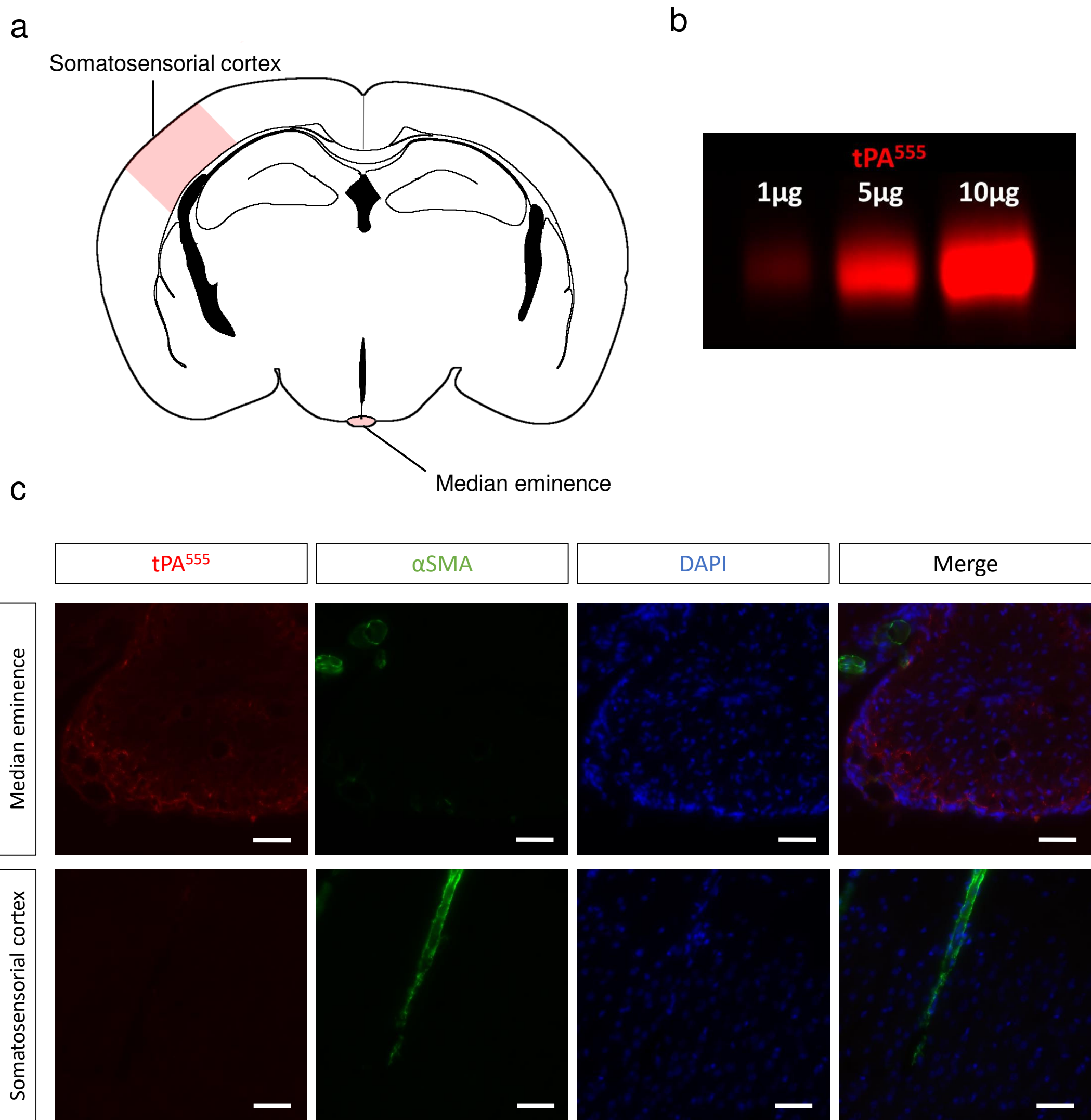
a



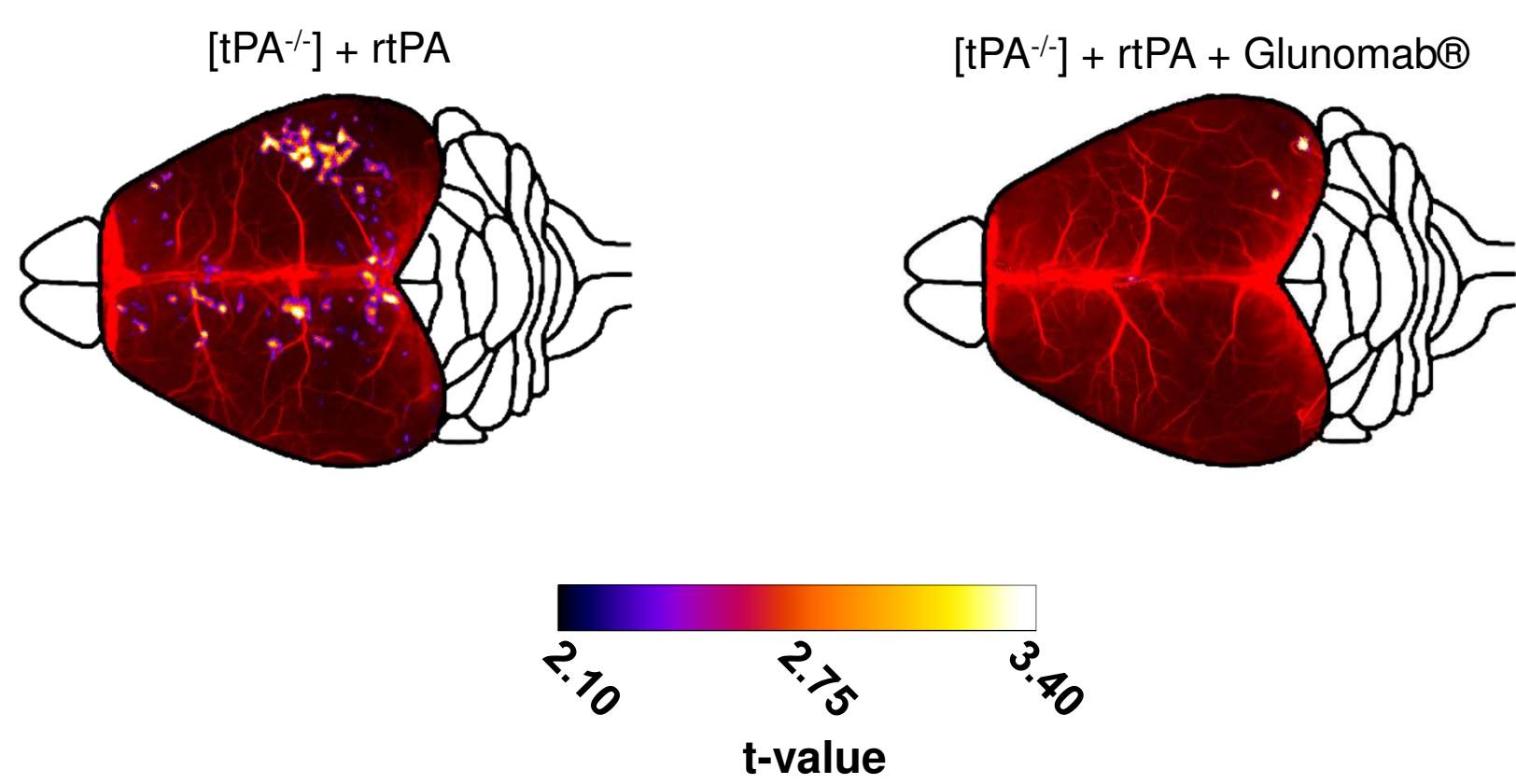
b



Supplementary figure 6



Supplementary figure 7





## Invisible inflammation in acute and brain disorders

### Résumé

L'inflammation est un processus essentiel à prendre en compte dans la pratique clinique. Nous avons montré durant cette thèse que le statut (neuro)inflammatoire précédant la survenue d'une pathologie cérébrale est à prendre en compte nécessairement puisqu'il modifie drastiquement la réponse inflammatoire suite à un deuxième stimulus comme la survenue d'un AVC. Il est d'autant plus important que 90% des AVC sont associés à des comorbidités comme l'hypertension artérielle, le diabète ou la consommation chronique d'alcool, qui ont d'ores et déjà été décrites comme des maladies avec une composante inflammatoire.

Nous avons caractérisé ce statut neuroinflammatoire silencieux, aussi appelé *priming*, dans le cadre de la consommation chronique d'alcool et dans le traumatisme crânien léger. De plus, nous avons identifié les macrophages périvasculaires comme participants à l'effet aggravateur du *priming* inflammatoire sur les lésions ischémiques. Ils semblent alors être une cible thérapeutique de choix et feront l'objet de futures études.

Il est donc nécessaire de trouver des techniques d'imagerie non invasives pour détecter le *priming*. L'autoradiographie ciblant le TSPO nous a permis de révéler le *priming* inflammatoire dans le cadre du traumatisme crânien léger. Nous proposons, au vu de nos résultats obtenus durant cette thèse, la tomographie par émission de positrons pour la détection de la neuroinflammation invisible dans les atteintes cérébrales aigüe(s) et chronique(s).

Mots-clés : inflammation, cerveau, AVC, traumatisme crânien léger, consommation d'alcool.

### Abstract

Inflammation is an essential process to be considered in clinical practice. We have shown during this thesis that the (neuro)inflammatory status preceding the occurrence of a cerebral pathology must necessarily be taken into account since it drastically modifies the inflammatory response following a second stimulus such as stroke. This is even more important given that 90% of strokes are associated with comorbidities such as chronic hypertension, diabetes or chronic alcohol consumption, for which inflammation is an important pathophysiological feature.

We have characterized this silent inflammatory status, also called priming, in the context of chronic alcohol consumption and in mild traumatic brain injury. We have identified perivascular macrophages (PVM) as mediators of the aggravating effect of inflammatory priming on ischemic stroke. PVM appear to be potential therapeutic targets and will be the subject of future investigations.

It is therefore necessary to find non-invasive imaging techniques to detect inflammatory priming. We show that autoradiography targeting TSPO reveals the inflammatory priming provoked by a single mild traumatic brain injury. We propose, in light of the results obtained during this thesis, the positron emission tomography imaging to detect the invisible neuroinflammation in acute and chronic brain diseases.

Key words: inflammation, brain, stroke, mild traumatic brain injury, chronic alcohol.